NOTE TO USERS

The original manuscript received by UMI contains pages with indistinct print. Pages were microfilmed as received.

This reproduction is the best copy available

UMI

University of Alberta

PETROGENESIS AND TECTONICS OF THE BASEMENT ROCKS OF THE APUSENI MOUNTAINS: SIGNIFICANCE FOR THE ALPINE TECTONICS OF THE CARPATHIAN - PANNONIAN REGION

by

DINU ION PANĂ ©

A thesis submitted to the Faculty of Graduate Studies and Research in partial fulfilment of the requirements for the degree of DOCTOR OF PHILOSOPHY

Department of Earth and Atmospheric Sciences
Edmonton, Alberta
Fall 1998

National Library of Canada
Acquisitions and Bibliographic Services
395 Wellington Street
Ottawa ON K1A 0N4
Canada

Bibliothèque nationale du Canada
Acquisitions et services bibliographiques
395, rue Wellington
Ottawa ON K1A 0N4
Canada

Your file Votre référence

Our file Notre référence

The author has granted a non-exclusive licence allowing the National Library of Canada to reproduce, loan, distribute or sell copies of this thesis in microform, paper or electronic formats.

L'auteur a accordé une licence non exclusive permettant à la Bibliothèque nationale du Canada de reproduire, prêter, distribuer ou vendre des copies de cette thèse sous la forme de microfiche/film, de reproduction sur papier ou sur format électronique.

The author retains ownership of the copyright in this thesis. Neither the thesis nor substantial extracts from it may be printed or otherwise reproduced without the author's permission.

L'auteur conserve la propriété du droit d'auteur qui protège cette thèse. Ni la thèse ni des extraits substantiels de celle-ci ne doivent être imprimés ou autrement reproduits sans son autorisation.

0-612-34818-0

Canadä

University of Alberta

Library Release Form

Name of the Author: DINU ION PANĂ

Title of Thesis: PETROGENESIS AND TECTONICS OF THE BASEMENT ROCKS OF THE APUSENI MOUNTAINS: SIGNIFICANCE FOR THE ALPINE TECTONICS OF THE CARPATHIAN - PANNONIAN REGION

Degree: DOCTOR OF PHILOSOPHY

Year this Degree Granted: 1998

Permission is hereby granted to the University of Alberta Library to reproduce single copies of this thesis and to lend or sell such copies for private, scholarly, or scientific research purposes only.

The author reserves all other publication and other rights in association with the copyright in the thesis, and except as hereinbefore provided, neither the thesis nor any substantial portion thereof may be printed or otherwise reproduced in any material form whatever without the author's prior written permission.

Dinu Ion Pană
#1, 10831-80 Ave
Edmonton, AB, T6E 1V9
CANADA

July 31, 1998

10
15
20
25
30
49
47
45
KIEV
BERDICHEV
LVOV
KATOWICE
ODESSA
Mouths of the Danube
SIN
COSTANTA
VARNA

UNIVERSITY OF ALBERTA

FACULTY OF GRADUATE STUDIES AND RESEARCH

The undersigned certify that they have read, and recommend to the Faculty of Graduate Studies and Research for acceptance, a thesis entitled PETROGENESIS AND TECTONICS OF THE BASEMENT ROCKS OF THE APUSENI MOUNTAINS: SIGNIFICANCE FOR THE ALPINE TECTONICS OF THE CARPATHIAN - PANNONIAN REGION submitted by DINU ION PANĂ in partial fulfilment of the requirements for the degree of DOCTOR OF PHILOSOPHY

Philippe Erdmer

Dr. P. Erdmer

Thomas Chacko

Dr. T. Chacko

Dr. R. Creaser

Larry Heaman

Dr. L. Heaman

D C Sego

Dr. D. C. Sego

March 24, 1998

E. L. Jackson

for Dr. J. Munoz i de la Fuente

ABSTRACT

Pre-Alpine basement units in the Apuseni Mountains and Romanian Carpathians consist of high- and medium-grade assemblages intruded by Paleozoic granitoids. Gneissic assemblages yielded relatively narrow ranges of $\varepsilon Nd_{(0)}$ and T_{DM} model age values which indicate high concentration of Precambrian crustal material and similar protoliths. Associated granitoid intrusions yielded $\varepsilon Nd_{(T)}$ and T_{DM} model age values suggesting variable assimilation of the gneissic crust. U-Pb zircon data for the granitoids of the Apuseni Mountains indicate Paleozoic magmatic events that correlate with those documented in Variscan Europe. $^{40}Ar/^{39}Ar$ dates from gneissic assemblages indicate mainly Variscan and Cretaceous cooling ages. Retrogressive low-grade assemblages define an anastomosing network more than 1000 km long of crustal-scale shear zones. $\varepsilon Nd_{(0)}$ values and T_{DM} model ages from phyllonites are similar to those from adjacent medium-grade or granitic rocks. $^{40}Ar/^{39}Ar$ direct dating of most phyllonites indicates Late Paleozoic and Cretaceous polyphase tectonism. Carbon and oxygen isotope data suggest the involvement of a juvenile-origin fluid in the development of carbonate layers which grew metasomatically during progressive exhumation and local involvement of cover strata in the crustal shear zones.

Low-grade shear zones accommodated most of the Early Alpine strain in the Carpathian-Pannonian region and record: I - tangential stretching of the Pre-Alpine basement at the southern boundary of ancestral Europe which resulted in two elongated flysch troughs floored by thinned continental crust with local mantle-derived material separating the Carpathians and the Apuseni-South Pannonian continental fragments. II - Cretaceous intra-continental tectonism dominated by transcurrent displacement with local uplift of the basement and gravitational emplacement of cover nappes in the peri-Carpathian basins; several "wildflysch" assemblages record strain concentration at shallow structural levels along the long-lived transcurrent shear zones.

Tertiary brittle strain varies from strike-parallel to thrust- and normal slip related to complex northeastward translation and rotation mainly accommodated by domains of thinned continental crust. The development of the Pannonian basins system accompanied by Neogene volcanic activity is consistent with crustal extension above a zone of mantle upwelling and contemporaneous tectonic loading of the surrounding European crust at the exterior of the Carpathian arc.

TO

Mike and Mara

ACKNOWLEDGMENTS

Dr. Philippe Erdmer is thanked for his friendly support and guidance throughout the course of my Ph.D. thesis. The members of my supervisory committee, Dr. Thomas Chacko, Dr. Larry Heaman, Dr. Robert Creaser and Dr. Karlis Muelenbachs are thanked for their guidance and relentless assistance during my Ph.D. Program.

Special thanks to Acad. Dan Rădulescu who encouraged and kindly assisted me in finding access to state-of-the-art instrumental facilities. I owe my involvement in the fantastic field of tectonics to the unique personality, work, and encouragements of Acad. Mircea Săndulescu. Dr. Ion Balintoni, Dr. Tudor Berza, Dr. Horst Hann, Dr. Gheorghe Mantea, Dr. Ion Hârtopanu, Dr. Ion Gheuca and Acad. Radu Dimitrescu generously sheared their encyclopedic knowledge on the Apuseni and Carpathians mountains and contributed to my understanding of the Alpine nappe concepts.

I am very thankful to Dr. Marin Şeclăman for passionate discussions on the petrogenesis of metamorphic rocks. His daring non-conventional ideas and his encouragements to search for alternative solutions strongly influenced my work. Discussions with Dr. Gheorghe Popescu and Dr. Marian Lupulescu helped clarify ideas and concepts. In the field, I enjoyed companionship and able assistance of by Dr. Calin Ricman and Dr. Mihai Tatu.

The help and friendship of my fellow graduate students at the University of Alberta made life away from home more enjoyable and bearable. I am thankful to Rob Stevens and Jochen Mezger for welcoming me to Edmonton and sheltering me on several occasions. I am grateful for the support, friendship and interesting discussions with Jochen Mezger, Karen Fallas, Steve Wetherup, Tarro Yamashita, Istvan Almasi and George Morris. Karen read parts of my thesis and kindly helped to improve my English.

I am also grateful for discussions with other geologists at various meetings. In particular, I would like to thank Dr. Clark Burchfiel (Massachusetts Institute of Technology), Dr. Paul Williams (University of New Brunswick), Dr. Bob Thompson and Dr. Burt Struik (Geological Survey of Canada).

I am very grateful for the moral and often financial support of my family who made this work possible: Cristina, Mimi, Mami, Gogu, and Bati. My wife Cristina and our kids Mihnea and Mara have heroically endured life with an always-too-busy husband and father.

This project was funded by NSERC operating grants to P. Erdmer and by the University of Alberta scholarships and the Geological Survey of Romania funding to the author. Dr. Udubaşa - General Manager of the GSR - personal involvement in solving logistical problems is highly appreciated. Employment by Halferdahl & Associates provided further financial support that helped to complete this project.

TABLE OF CONTENTS

CHAPTER 1.

INTRODUCTION.......1

1.1. Statement of Problem.......2
1.2. The Current Tectonic Model for the Carpathian Region.......5
    1.2.1. Pre-Alpine Evolution of the Basement Units from the Apuseni and Carpathians Mountains.......8
    1.2.2. Alpine Evolution.......8
1.3. The Model and the Real World.......13
1.4. New Results.......16
    1.4.1. Crustal evolution.......15
    1.4.2. Alpine evolution.......17
    References.......18

CHAPTER 2.

ALPINE CRUSTAL SHEAR ZONES AND PRE-ALPINE BASEMENT TERRANES IN THE ROMANIAN CARPATHIANS AND APUSENI MOUNTAINS.......24

2.1. Introduction.......25
2.2. Geologic Setting.......25
2.3. Reevaluation of Existing Data.......26
2.4. New Interpretation: Alpine Crustal Shear Zones.......28
    2.4.1. Basement Rocks.......28
    2.4.2. Greenschist Shear Zones.......29
2.5. Summary and Conclusions.......31
    References.......32

CHAPTER 3.

PRE-ALPINE TECTONIC FRAMEWORK OF THE APUSENI MOUNTAINS: CONSTRAINTS FROM A Sm-Nd AND U-Pb ISOTOPIC STUDY ON THE METAMORPHIC AND IGNEOUS BASEMENT ASSEMBLAGES.......37

3.1. Introduction.......38
3.2. Geological Units, Previous Isotope Data.......39
3.3. U-Pb Geochronology of Igneous Rocks.......43
3.4. Sm-Nd Analytical Data.......53
3.5. Summary and Comparison with Central-Western Europe.......60
    References.......66

CHAPTER 4.
TECTONOTHERMAL EVOLUTION OF THE APUSENI MOUNTAINS, ROMANIA: RESOLUTION OF VARISCAN VS. ALPINE EVENTS WITH ^{40}Ar/^{39}Ar AGES 71

- 4.1. Introduction 72
- 4.2. Geologic Setting, Previous Geochronology 74
- 4.3. Geological Units 77
- 4.4. Tectonothermal Evolution 78
- 4.5. Analytical Methods 81
- 4.6. Results 82
    - 4.6.1 Hornblende 82
    - 4.6.2 Muscovite 88
    - 4.6.3 Whole Rock 93
- 4.7. Significance 99
- 4.8. Conclusions 101
    - References 111

CHAPTER 5.
TECTONOTHERMAL EVOLUTION OF THE APUSENI MOUNTAINS, ROMANIA: IMPLICATIONS OF STRAIN PARTITIONING 106

- 5.1. Introduction 107
- 5.2. Regional Setting: Previous Work 109
- 5.3. Lithotectonic Assemblages: Distribution and Metamorphic Conditions 109
    - 5.3.1 Low-Grade Rocks 109
    - 5.3.2 Medium-Grade Rocks 132
- 5.4. Protolith Ages and Timing of Tectonism 139
- 5.5. Regional Orientation Data and Evidence of Strain Partitioning 141
- 5.6. Tectonic Evolution of the Northern Apuseni Sedimentary Basin 151
- 5.7. Tectonic Evolution of the Southern Apuseni Sedimentary Basin 151
- 5.8. Regional Correlations 154
- 5.9. Proposed Geodynamic Model 158
- 5.10. Conclusions 161
    - References 162

CHAPTER 6.
ALPINE STRAIN DISTRIBUTION AND LITHOLOGICAL CORRELATION OF BASEMENT ASSEMBLAGES IN THE CARPATHIAN-PANNONIAN REGION 169

- 6.1. Introduction 170
- 6.2. Basement Units of the Apuseni Mountains 170
- 6.3. Basement of the Neogene Pannonian Basin 176
- 6.4. Basement Units of the South Carpathians 178
- 6.5. Basement Units of the East Carpathians 190
- 6.6. Basement Units of the West Carpathians 199
- 6.7. Basement Units at the Junction of the West Carpathians and Eastern Alps 203
- 6.8. Basement Units of the Eastern Alps 204
- 6.9. Concluding remarks 208
    - 6.9.1. Lithotectonic Assemblages within the Orogenic Basement 208
    - 6.9.2. Oceanic Remnants in the Carpathian-Pannonian Region 210
- 6.10. Towards a New Tectonic Model For the Carpathian-Pannonian Region: Block Rotation and Orogen-Parallel Tectonics 212
    - References 221

APPENDIX I
OUTLINE OF THE MAJOR TECTONOSTRATIGRAPHIC UNITS OF THE CARPATHIANS - PANNONIAN SYSTEM AND OUTSTANDING PROBLEMS IN THE INTERPRETATION OF THE ALPINE EVOLUTION OF BASEMENT ASSEMBLAGES....233

I.1. Introduction....235
I.2. Eastern Alps....235
I.3. The Junction Region between the Eastern Alps and the West Carpathians....248
I.4. West Carpathians....251
I.5. East Carpathians....259
I.6. South Carpathians....270
I.7. Dinarides....281
I.8. Southern Alps....283
I.9. The Intra-Carpathian Region....285
  I.9.1. The North Pannonian Unit....287
  I.9.2. The South Pannonian Unit and Apuseni Mountains....292
I.10. Neogene to Quaternary Volcanism in the Carpathian-Pannonian Region....297
  References....300

APPENDIX II
Geochemical Data from Rocks of the Highis-Biharia Shear Zone, Apuseni Mountains....312

APPENDIX III
^{40}Ar/^{39}Ar Analytical Data....326

APPENDIX IV
Microprobe Data....326

LIST OF TABLES

CHAPTER 3

Table 3-1. Summary of U-Pb data on igneous rocks of the Apuseni Mountains........................ 45
Table 3-2. Nd and Sm concentrations and isotopic data for samples from the Apuseni Mountains........................ 54
Table 3-3. Nd and Sm concentrations and isotopic data for samples from the Romanian Carpathians........................ 54
Table 3-4. Summary of isotope data on granitoid samples from the Apuseni Mountains........... 62

CHAPTER 4

Table 4-1. Previous radiogenic data in the Apuseni Mountains (K-Ar neutron activation)........... 75
Table 4-2. ^{40}Ar/^{39}Ar sample localities and petrography........................ 83
Table 4-3. Summary of the ^{40}Ar/^{39}Ar plateau ages on rocks from the Apuseni Mountains........ 99

CHAPTER 5

Table 5-1. Summary of lithostratigraphic classification previously used for the metamorphic/magmatic basement of the Apuseni Mountains........................110
Table 5-2. Carbon and oxygen isotope data for carbonate lenses from the Apuseni Mountains........................127
Table 5-3. Oxygen isotope composition of silicate rocks within the Highis-Biharia shear zone........................130

APPENDIX I

Table I-1. Lithostratigraphic/tectonic units in the basement in Central and Eastern Alps...........239
Table I-2. Correlation of the main tectonic units in the Alpine-Carpathian transition zone..........250
Table I-3. Lithostratigraphic units of the West Carpathians basement........................253
Table I-4. Principal lithostratigraphic groups of Precambrian metamorphic rocks and their position in the main structural units of the East Carpathians........................262
Table I-5. Principal lithostratigraphic groups of Precambrian metamorphic rocks and their position in the main structural units of the South Carpathians....................272

APPENDIX II

Table II-1. Average compositions of rocks within Highiş unsheared igneous complex..............313
Table II-2. Chemical compositions of SiO$_2$ - rich rocks within Păiuşeni assemblage of the HBSZ........................314

Table II-3. Chemical composition of granitic rocks from HBSZ in the Biharia and Gilău mountains 315
Table II-4. Chemical composition of mafic rocks within Paiuseni assemblage of HBSZ, Highiş Mountains 316
Table II-5. Chemical compositions of the sheared mafic rocks from HBSZ in the Biharia and Gilău mountains 317
Table II-6. Chemical compositions of rocks within the "Black Series" 318

APPENDIX III

Table III-1. ^{40}Ar/^{39}Ar analytical data for incremental-heating experiments on hornblende concentrates from structural units comprising the Apuseni Mountains, Romania 327
Table III-2. ^{36}Ar/^{40}Ar vs. ^{40}Ar/^{39}Ar plateau isotope-correlations for hornblende concentrates from structural units comprising the Apuseni Mountains, Romania 331
Table III-3. ^{40}Ar/^{39}Ar analytical data for incremental-heating experiments on muscovite concentrates from structural units comprising the Apuseni Mountains, Romania 332
Table III-4. ^{40}Ar/^{39}Ar analytical data for incremental-heating experiments on whole-rock samples of slate/phyllite or phyllonite from structural units comprising the Apuseni Mountains, Romania 341

APPENDIX IV

Table IV-1. Carbonates 348

LIST OF FIGURES

CHAPTER 1

Figure 1-1. Simplified tectonic sketch of the Alpine Orogen.. 4

Figure 1-2. The configuration of three geosynclinal areas developed during the Precambrian and Paleozoic.. 6

Figure 1-3. Model representation of the metamorphic history of the basement rocks in the Carpathians.. 7

Figure 1-4. Reconstructed facies distribution and generalized cross-section for the middle Norian.. 9

Figure 1-5. Palinspastic sketch of the Carpathians.. 11

Figure 1-6. Palispastic reconstruction of the Apuseni - East Carpathians along Geotraverse V.. 12

CHAPTER 2

Figure 2-1. Sketch map of the distribution of basement rocks in the Romanian Carpathians and Apuseni Mountains showing the extent of proposed Alpine shear zones.........27

CHAPTER 3

Figure 3-1. Sketch map of the Apuseni Mountains with the sample locations (Sm-Nd and U-Pb samples).. 40

Figure 3-2. Microphotographs of zircon grains in granitoid samples from the Apuseni Mountains.. 48

Figure 3-3. Concordia diagrams for the granitoidic intrusions of the Highiş-Biharia Shear Zone.. 50

Figure 3-4. Concordia diagrams for the representative granitoidic intrusions within medium-grade assemblages of the Apuseni Mountains.. 51

Figure 3-5. Concordia diagram for the Săvârşin granitic intrusion within the "Tethys ophiolites".. 52

Figure 3-6. Nd isotopic characteristics of the gneissic assemblages and associated Paleozoic intrusions from the basement units of the Apuseni Mountains.. 56

Figure 3-7. Sketch map of the distribution of the metamorphic assemblage in the Apuseni and Romanian Carpathians mountains with the location of Sm-Nd samples......... 58

Figure 3-8. Evolution of εNd through time for the analysed samples from the Apuseni Mountains and Romanian Carpathians.. 59

CHAPTER 4

Figure 4-1. Structural map of the Apuseni Mountains.......... 73
Figure 4-2. Nappe stacking model for the Apuseni Mountains.......... 76
Figure 4-3. Generalized geologic-tectonic map of the Apuseni Mountains (with the locations of $^{40}Ar/^{39}Ar$ samples).......... 79
Figure 4-4. $^{40}Ar/^{39}Ar$ age and apparent K/Ca spectra for multigrain hornblende concentrates from the amphibolite collected within the Someş assemblage.......... 85
Figure 4-5. $^{40}Ar/^{39}Ar$ age and apparent K/Ca spectra for multigrain hornblende concentrates from the amphibolite collected within the Codru assemblage.......... 86
Figure 4-6. $^{40}Ar/^{39}Ar$ age and apparent K/Ca spectra for multigrain hornblende concentrates from the amphibolite collected within the Baia de Arieş assemblage.......... 87
Figure 4-7. $^{40}Ar/^{39}Ar$ age for multigrain muscovite concentrates from the gneiss collected within the Someş assemblage.......... 89
Figure 4-8. $^{40}Ar/^{39}Ar$ age for multigrain muscovite concentrates from the gneiss collected within the Codru assemblage.......... 91
Figure 4-9. $^{40}Ar/^{39}Ar$ age for multigrain muscovite concentrates from the gneiss collected within the Baia de Arieş assemblage.......... 91
Figure 4-10. $^{40}Ar/^{39}Ar$ age for multigrain muscovite concentrates from the phyllonite collected within the Highiş-Biharia shear zone.......... 92
Figure 4-11. $^{40}Ar/^{39}Ar$ age and apparent K/Ca spectra for a whole-rock sample of phyllonite collected within Triassic cover of the Codru assemblage.......... 94
Figure 4-12. $^{40}Ar/^{39}Ar$ age and apparent K/Ca spectra for a whole-rock sample of phyllonite collected within the Baia de Arieş assemblage.......... 96
Figure 4-12. (continued) $^{40}Ar/^{39}Ar$ age and apparent K/Ca spectra for a whole-rock sample of phyllonite collected within the Baia de Arieş assemblage.......... 97
Figure 4-13. $^{40}Ar/^{39}Ar$ age and apparent K/Ca spectra for a whole-rock sample of phyllonite collected within the Highiş-Biharia shear zone.......... 98

CHAPTER 5

Figure 5-1. European segments of the Alpine chain mentioned in the text; Main tectonic units of the Carpathians and Apuseni Mountains..........108
Figure 5-2. Structural map of the Apuseni Mountains..........111
Figure 5-3. Quartz-filled tension gashes in microgranite of the Păiuşeni assemblage..........113
Figure 5-4. Pseudo-metaconglomerate in the Păiuşeni assemblage..........116
Figure 5-5. Late granite intrusions in diorite within the Highiş igneous complex..........118
Figure 5-6. Centimetre-size veins of carbonate within igneous rocks affected by strain..........121
Figure 5-7. Carbonate nodules within phyllonite..........123

Figure 5-8. Massive replacement of diorite by carbonate....126
Figure 5-9. Stable isotope composition of the carbonate lenses in the Apuseni Mountains....128
Figure 5-9'. Oxygen isotope composition of silicate rocks within the Highiş-Biharia shear zone....130
Figure 5-10. Peak reequilibration temperatures recorded by carbonate rocks in the Apuseni Mountains....131
Figure 5-11. Pressure-temperature estimates for the eastern part of the Baia de Arieş assemblage....134
Figure 5-12. Pressure-temperature estimates for the central part of the Baia de Arieş assemblage....135
Figure 5-13. Temperature estimates for the easternmost exposures of the Someş and Baia de Arieş assemblages....136
Figure 5-14. Microphotographs of probed garnet grains....137
Figure 5-15. Proposed informal classification of the Apuseni Mountains metamorphic-magmatic basement rocks....140
Figure 5-16. Planar structures along the belt of low-grade rocks in the Apuseni Mountains....142
Figure 5-17. Linear structures along the belt of low-grade rocks in the Apuseni Mountains....143
Figure 5-18. Microscopic shear-sense indicators....146
Figure 5-19. Outcrop-scale kinematic indicators....148
Figure 5-19. (continued) Outcrop-scale kinematic indicators....150
Figure 5-20. Tectonic sketch of the Apuseni Mountains....153
Figure 5-21. Proposed correlation of the metamorphic assemblages from the Apuseni Mountains and southern Pannonian basement....157

CHAPTER 6

Figure 6-1. Stretching lineation within the Highiş-Biharia shear zone....173
Figure 6-2. Stretching lineation within the Baia de Arieş assemblage....175
Figure 6-3. Kinematic indicators along different segments of the shear zone through the Getic crust ("Supra Getic / Getic thrust contact")....181
Figure 6-4. Kinematic indicators along the Sibişel shear zone overprinting the Getic crust in the northern part of South Carpathians....183
Figure 6-5. Kinematic indicators in the northern Făgăraş Mountains....185
Figure 6-6. Kinematic indicators along the Corbu shear zone overprinting the Danubian crust in the southwestern part of the South Carpathians....187
Figure 6-7. Kinematic indicators along the contact between Getic and Danubian units in the southwestern part of the South Carpathians....189

Figure 6-8. Tectonic sketch with the major low-grade shear zones exposed in the East Carpathians 191
Figure 6-9. Kinematic indicators along the contact of the East Carpathians basement with the internal flysch unit 193
Figure 6-10. Stretching lineation within the Tulgheş shear zone 195
Figure 6-11. Tectonic sketch of the Rodna metamorphic core complex 196
Figure 6-12. Tectonic sketch of the Hăghimaş syncline on the eastern margin of the East Carpathians basement 198
Figure 6-13. Tectonic sketch of the basement units in the West Carpathians with the inferred transcurrent and normal shear zones 200
Figure 6-14. Late Cretaceous and Paleogene low-grade normal shear zones developed in the gneiss-granite core of the High Tatra metamorphic core complex 202
Figure 6-15. Simplified map of the Austro-Alpine basement units east of the Tauern Window with the existing ^{40}Ar/^{39}Ar data 206
Figure 6-16. Proposed kinematic model for the Alpine evolution of the Carpathian-Pannonian region 214
Figure 6-17. Proposed model of strain partitioning during oblique compression between the Carpathians and stable Europe 216
Figure 6-18. Major fractures significant for the Tertiary kinematics of the Apuseni and Carpathian crustal fragments 219

APPENDIX I

Figure I-1. Simplified tectonic sketch of the Carpathian-Pannonian system 234
Figure I-2. Legend of the lithostratigraphic columns compiled for the segments of the Alpine-Carpathian orogen discussed in text 236
Figure I-3. Simplified tectonic sketch of the Eastern Alps 237
Figure I-4. Simplified map of the Austro-Alpine basement units east of the Tauern Window 240
Figure I-5. Deep structure of the Alps 244
Figure I-6. Tomographic images of the upper mantle under the Alps 245
Figure I-6 (continued) Tomographic images of the upper mantle under the Dinarides ans Carpathians mountains 246
Figure I-7. Subsurface geology around the Rechnitz Window 249
Figure I-8. Simplified tectonic sketch of the West Carpathians 252
Figure I-9. Tectonic sketch of the main basement units in the West Carpathians 254
Figure I-10. Deep structure of the westernmost West Carpathians imaged by dep seismic reflection 257

Figure I-11. Deep structure of the central West Carpathians imaged by dep seismic reflection....258
Figure I-12. Simplified tectonic sketch of the East Carpathians....260
Figure I-13. Stratigraphic columns for the cover sequences which differenciate the postulated East Carpathians basement nappes....261
Figure I-14. The main Alpine nappes involving basement rocks in the East Carpathians....263
Figure I-15. Sr/Ca - Ba/Ca systematics of magmatic rocks from the Eastern Carpathians Volcanic Arc....265
Figure I-16. Deep structure of the East Carpathians as depicted by magnetotelluric data....268
Figure I-17. Deep structure of the East Carpathians along Geotraverse V as depicted by magnetotelluric data....269
Figure I-18. Simplified tectonic sketch of the South Carpathians....271
Figure I-19. Tectonometamorphic evolution of the medium- to high-grade rocks in the Getic Nappe....273
Figure I-20. The main Alpine nappes involving basement rocks in the South Carpathians....274
Figure I-21. Simplified tectonic sketch of the South Carpathians with the existing $^{40}Ar/^{39}Ar$ data....276
Figure I-22. Simplified tectonic sketch of the Dinarides....282
Figure I-23. Simplified tectonic sketch of the Southern Alps....284
Figure I-24. The main basement units of the Pannonian Basin....286
Figure I-25. Simplified tectonic sketch of the North Pannonian Unit....288
Figure I-26. Simplified tectonic sketch of the South Pannonian Unit....293
Figure I-27. Tectonic sketch of the Apuseni Mountains....296

APPENDIX II

Figure II-1. Major discrimination plots for the igneous and metamorphic rocks of the Highiş-Biharia Shear Zone....319
Figure II-2. General geochemical characteristics of the igneous and metamorphic rocks of the Highiş-Biharia Shear Zone....320
Figure II-3. Trace elements-tectonic discrimination plots for rocks of the Highiş-Biharia Shear Zone....321
Figure II-4. (continued) Trace elements-tectonic discrimination plots for rocks of the Highiş-Biharia Shear Zone....107

LIST OF PLATES (*in pocket*)

Geological Map of the Highis-Drocea Mountains, scale 1: 50 000
Geological Map of the central Apuseni Mountains, scale 1: 50 000

CHAPTER 1

INTRODUCTION

...une théorie, fût-elle séduisante,
ne résiste guère à l'épreuve du temps
si elle n'est pas fondée sur
des observations de terrain
nombreuses, précises et bien coordonées.
(Aubouin, 1970)

1.1. STATEMENT OF PROBLEM

The Carpathians orocline and the Apuseni Mountains belong to the central European belt of complex late Mesozoic and Cenozoic terrane accretion. Current tectonic models postulate that the kinematics of both the Carpathian and the Apuseni segments of the orogen are subduction-related. The present structural and isotopic study on basement rocks corroborated with existing geological and geophysical data, shows that subduction is either not required, or indeed, precluded. The thesis proposed here is that the geological evolution of the Carpathians and Apuseni mountains is the result of intra-continental tectonics.

The association of accretionary wedge-magmatic arc, similar to typical subduction zones, was initially emphasised in the East Carpathians (Rădulescu and Săndulescu, 1973; Bleahu et al., 1973). Regional synthesis extrapolated the subduction model to the entire Carpathian-Pannonian region (e.g., Săndulescu, 1975; 1984; Burchfiel, 1980; Balla, 1982; 1986; Debelmas and Săndulescu, 1987; Royden, 1988, Hamilton, 1990). In the Romanian segments of the orogen, two Mesozoic oceanic basins were postulated to have been consumed in west-dipping subduction zones, one beneath the Carpathians and a second beneath the Apuseni Mountains. Geologic evidence was presented as a drama in three acts that includes Middle-, and Late Cretaceous syn-subduction nappe stacking in the internal units along the entire orogen and Miocene syn-collision thrusts in the external units of the East Carpathians. The Cretaceous internal nappes are considered to be huge rigid basement nappes and scattered remnants of Mesozoic cover.

Although recent kinematic analysis (e.g., Royden and Burchfiel, 1989; Csontos et al., 1992; Ratschbacher et al., 1993; Linzer, 1995; Peresson and Decker, 1997) indicates that the Carpathians orocline resulted from complex Cenozoic tectonism, the original interpretation of Early Alpine evolution was never questioned. It is generally assumed that most of the evidence

Fig. 1-1. Simplified tectonic sketch of the Alpine Orogen (*compiled from* Debelmas et al., 1980,Burchfiel, 1980; Săndulescu, 1984; Kräutner, 1988). 1 to 7 - External zones of the European continental margin: 1 - Foreland; 2 - Molasse sequences of the northern foredeep; 3 - Helvetic units; 4 - Flysch units: a - Internal (Magura, Dragovo-Petrova; Rheno-Danubian), b - external (West - East Carpathians, Trojan, T; Kotel, K);
5 - Dacidic crustal fragment; 6 - Serbo-Macedonian Massif; 7 - Rhodope; 8 - Internal zones of the European continental margin: External and Median Pennine (Valais, Briancon, External Piedmont); 9 - Ophiolite suture (Internal Pennine, Transylvanides, Vardar); 10 to 14 - Southern continental border; 10 - Pieniny Klippen Belt; 11 - Austro-Alpine, Bukk, Tatric, Veporic, and Gemeric units; 12 - Bihor, Codru, and Biharia units; 13 - Inner Dinarides, Southern Alps; 14 - Outer Dinarides; 15 - Neogene volcanics; 16 - Neogene internal depressions; 17 - Upper Cretaceous and Paleogene.
E - Engadine Window; T - Tauern Window; Re - Rechnitz Window; W - West Carpathians; B - Bakony Mountains; M - Mecsek Mountains; V - Villany Mountains; LHP - Little Hungarian Plain; IB - Igal-Bükk zone; Bk - Bükk Mountains; GHP - Great Hungarian Plain; P - Pannonian Depression; A - Apuseni Mountains; Tr - Transylvanian Depression; E - East Carpathians; S - South Carpathians; PB - Prebalkan. SG - Sredna Gora; SP - Stara Planina; R - Rhodope Massif; SM - Serbo-Macedonian Massif.

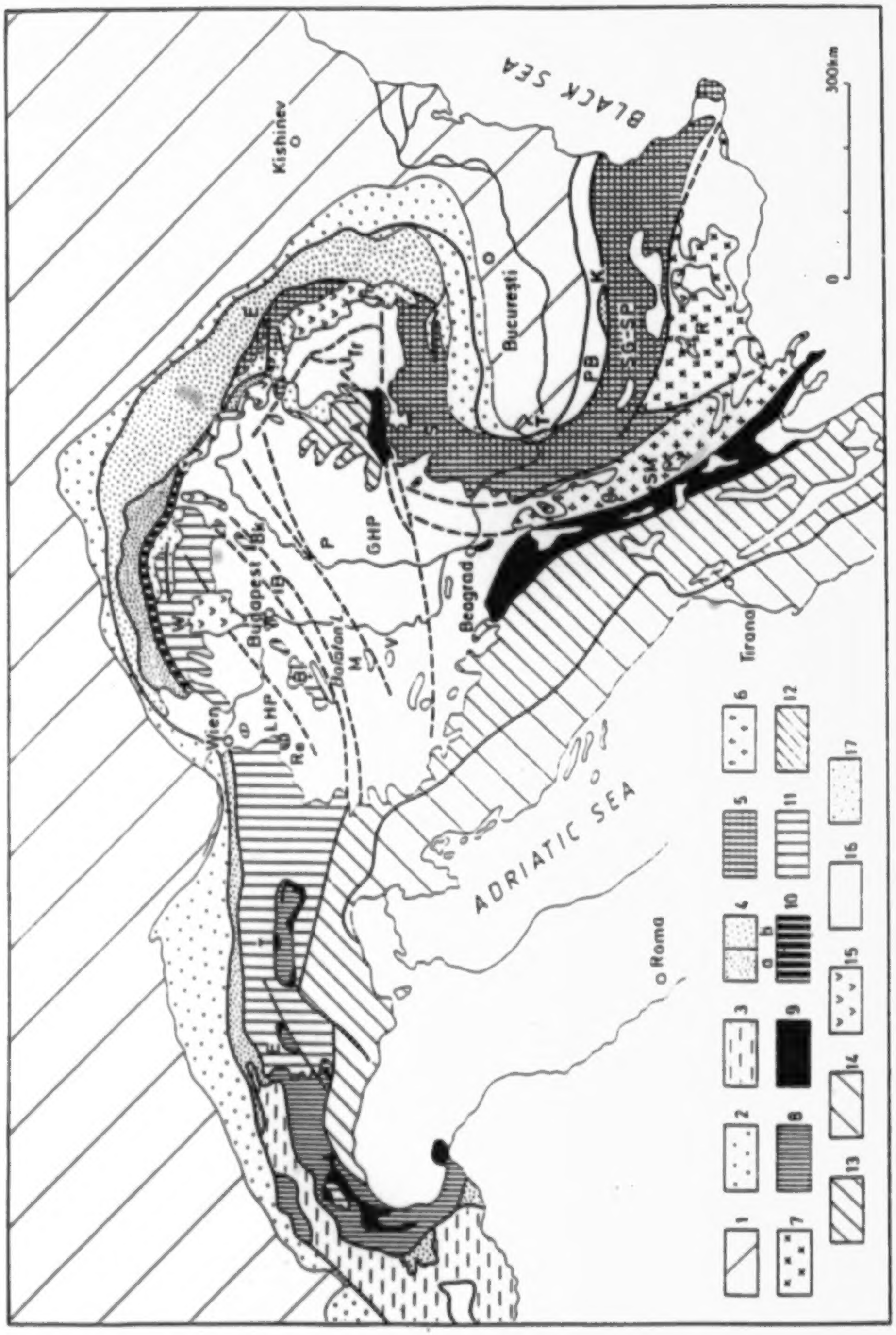
Kishinev
BLACK SEA
Bucureşti
PB
K
SG-SP
R
Sr
T
Tr
E
W
Wien
Budapest
Bk
IB
LHP
Re
Balaton
M
P
GHP
V
Beograd
Tirana
ADRIATIC SEA
Roma
0
300km
1
2
3
4
a
b
5
6
7
8
9
10
11
12
13
14
15
16
17

for early Alpine subduction and thrust tectonics was lost due to overprinting by subsequent widespread extension associated with the development of the Pannonian basin.

An increasing amount of data is inconsistent with the current interpretation of Early Alpine evolution and encourages alternative tectonic interpretations. No unambiguous evidence of Cretaceous subduction exists, the proposed Cretaceous stacking of far-travelled nappes is contradicted by kinematic indicators and isotope dating, the basement nappes supposed to be rigid and to preserve original stratigraphic successions show widespread internal strain consistent with Alpine kinematics.

The present study has investigated the relationships between internal strain observed in low-grade basement units of the Apuseni Mountains and Romanian Carpathians, and the Alpine tectonics. A three-part analysis has been undertaken in the case study area, the Apuseni Mountains:

- a detailed structural study aimed at deciphering the kinematic significance of the observed structures.
- the age of tectonism and the resolution of the Variscan versus Alpine tectonism were investigated using ^{40}Ar/^{39}Ar dating techniques.
- a stable (carbon and oxygen) and radiogenic isotope (Sm-Nd and U-Pb) study was undertaken to determine the origin and age of the protoliths of the metamorphic assemblages, and understand pre-Alpine tectonic framework of the region.

In addition, preliminary kinematic and isotopic data from the Carpathians Mountains, were collected and a first-order comparison with the basement units adjacent to the Apuseni Mountains crustal fragment was made. Representative traverses in the Carpathians were conducted in order to put kinematic and age constraints on major contacts involving basement rocks. Critical analysis of the existing data base followed by rejection of unreliable data and speculative interpretation was carried out in an attempt to develop an updated tectonic model. An outline of the major tectono-stratigraphic units of the Carpathian-Pannonian region and outstanding problems in the interpretation of the evolution of basement assemblages is presented in Appendix I.

1.2. THE CURRENT TECTONIC MODEL FOR THE CARPATHIAN REGION

The present anatomy of the Mesozoic-Cenozoic Carpathian orogen (Fig. 1-1) is interpreted to include an arcuate thrust-and-fold belt, basement units, and a volcanic arc. A complete record of the Variscan Orogeny is interpreted within basement units in the western segments of the Alpine orogen. In the Carpathians and Apuseni segments of the orogen, several superposed pre-Alpine orogenies have been inferred.

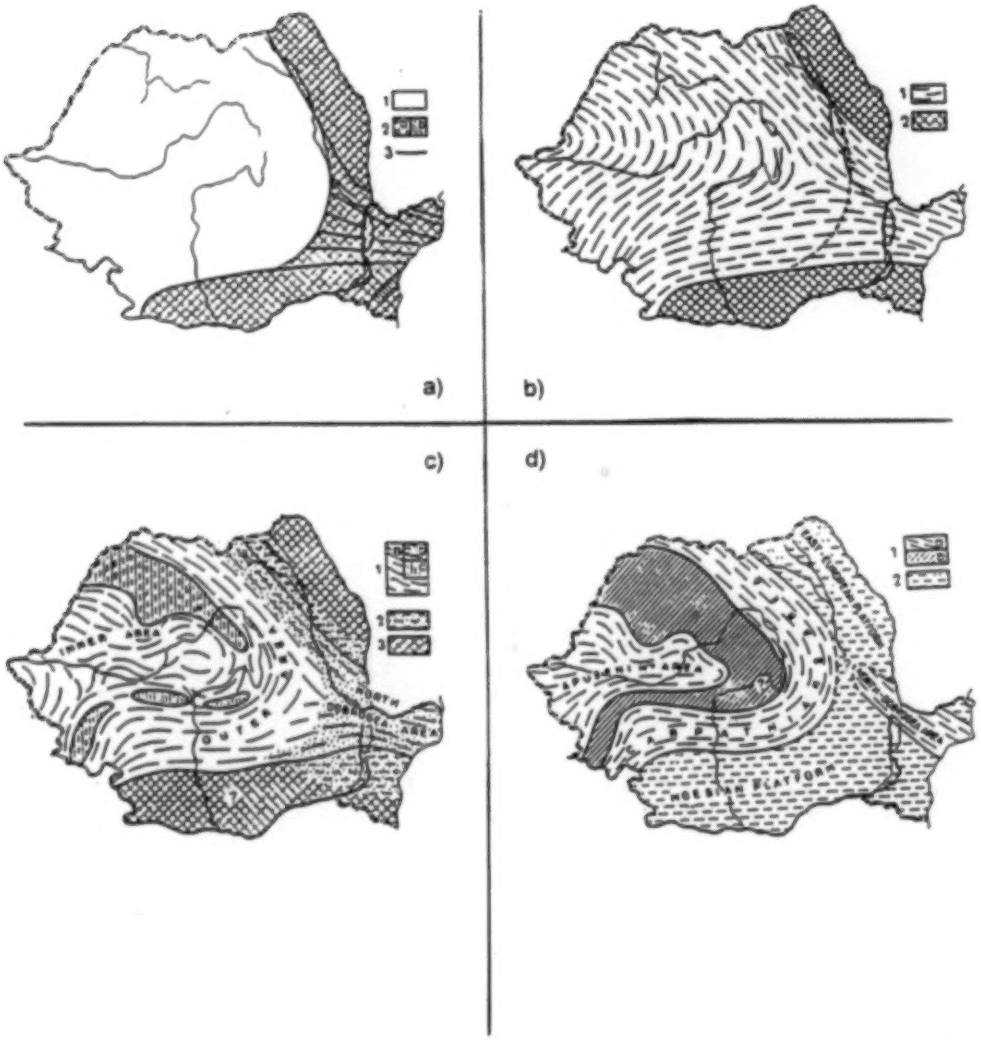
1
2
3
a)
1
2
b)
c)
1
2
3
INNER AREA
OUTER
NORTH
DOBROGEA AREA
d)
1
2
APUSENI AREA
CARPATHIAN
MOESIAN PLATFORM
EAST EUROPEAN PLATFORM

Fig. 1-2. The configuration of three geosynclinal areas developed during the Precambrian and Paleozoic (*after* Giuşcă et al., 1969). a) before the Pre-Baikalian cycle (Early Proterozoic ?): 1- oceanic zone; 2 - Pre-Karelian and Karelian shield rocks; 3 - deep-seated fractures; b) in the Pre-Baikalian (Middle Proterozoic?): 1- geosyncline area; 2 - shield; c) in the Baikalian (Late Proterozoic): 1 - geosyncline area; 1.a area of the metamorphic formations in the Carpathians; 1.b. - area of the green schist formation; 1.c - cordillera; 2 - area of the green schist formation overlying the shield; 3 - shield; d) in the Variscan cycle: 1 - geosyncline area; 1.a - submerged; 1.b - emerged; 2 - platform.

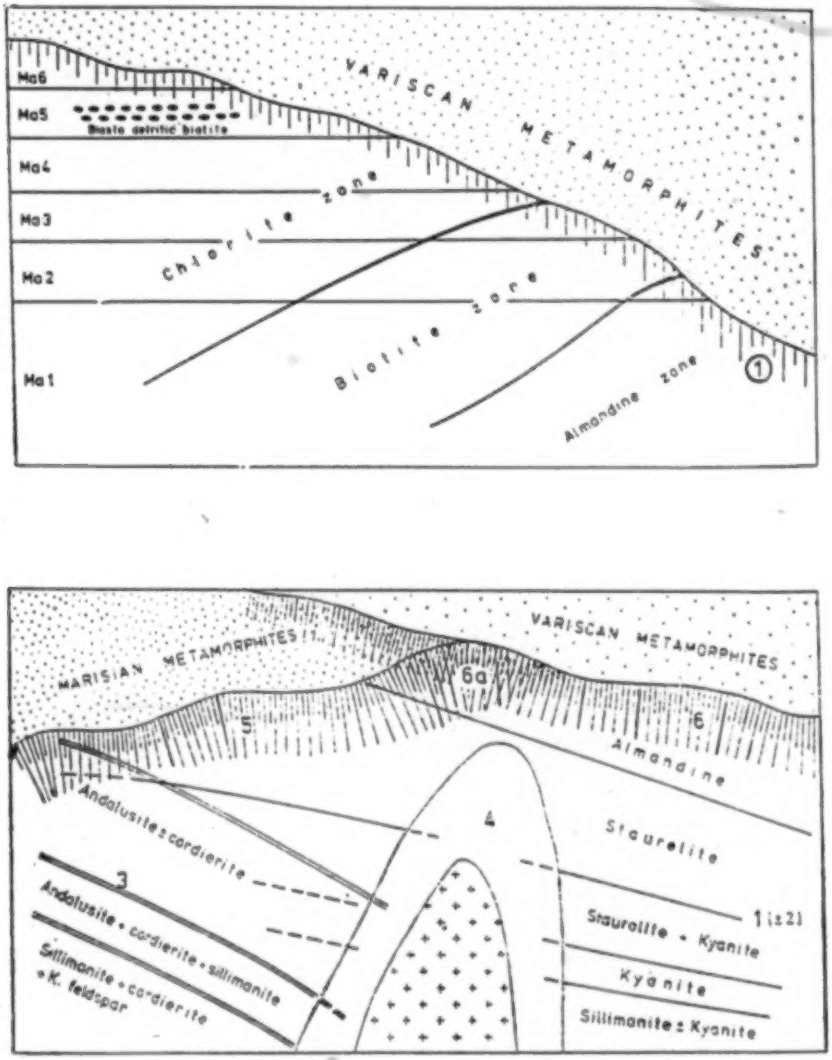
Ma6
Ma5
Blasto detritic biotite
Ma4
Ma3
Ma2
Ma1
VARISCAN METAMORPHITES
Chlorite zone
Biotite zone
Almandine zone
①
MARISIAN METAMORPHITES
VARISCAN METAMORPHITES
6a
5
6
Almandine
Andalusite ± cordierite
4
Staurolite
3
Andalusite + cordierite + sillimanite
Sillimanite + cordierite + K. feldspar
1 (±2)
Staurolite + Kyanite
Kyanite
Sillimanite ± Kyanite

Fig. 1-3. Model representation of the metamorphic history of the basement rocks in the Carpathians. Retrograde metamorphism would underlie stratigraphic unconformities postulated between sequences assigned to one of the three geosyncline cycles (*after* Kräutner, 1980).

1.2.1 Pre-Alpine evolution of the basement units

In the existing synthesis (Giuşcă et al., 1969; Kräutner, 1980; Dimitrescu, 1985; Kräutner, 1988), basement rocks in the Carpathians and Apuseni mountains are assigned to three geosynclinal cycles superposed in the same area (Fig. 1-2). Volcano-sedimentary sequences of Middle Proterozoic, Late Proterozoic-Cambrian, and Middle Paleozoic age were interpreted to have been metamorphosed under amphibolite, epidote-amphibolite and greenschist grade conditions, respectively. Stratigraphic and metamorphic discontinuities were postulated between the products of the three orogenic cycles (Fig.1-3). Retrogressive reactions documented in the greenschist rocks (e.g., Balintoni, 1969; Giuşcă et al., 1977) raised suspicions about the previous stratigraphy, but were accommodated in the model as re-hydrated stratigraphic units of the underlying older successions, and the boundary was moved up-section to the next lithologic unit without medium grade relics (e.g., Kräutner, 1980). Pre-Permian-Mesozoic basement sequences were interpreted to have been involved in a large number of Alpine and pre-Alpine nappes (e.g., Popescu-Voiteşti, 1942, Săndulescu, 1975; 1984; Bercia et al., 1976; Balintoni et al., 1983; 1989; Berza et al., 1994).

1.2.2 Alpine Evolution

In the late Paleozoic, the Alpine-Carpathian realm was part of Pangaea. From the east this continent was transgressed by Paleo-Tethys, an oceanic embayment of Panthalassa (Laubscher and Bernoulli, 1977). Paleo-Tethys was consumed in the Cimmerian - Indosinian suture zone interpreted in Bulgaria and Turkey, due to northward drift of Gondwanian microcontinents (Sengör et al., 1980). This northward drift of Gondwanian fragments created the space for a new oceanic domain called Neo-Tethys (Dercourt et al., 1986).

Throughout the Permian and Triassic, the southeastern Alpine-Carpathian area was increasingly dominated by marine facies, whereas to the west and north, the occurrence of terrestrial sediments (e.g., Verrucano) and detrital facies (e.g., Buntsandstein, Keuper) record epicontinental conditions (Tollmann, 1986). The north-westward propagation of Tethys sea is shown by the syn-tectonic progression of the deep-water sediments (Hallstatt facies): it reached Turkey in the Late Permian, the Dinarides in the Early Anisian, and the Alpine region in Middle to Late Anisian time (Bechstädt, 1978). In the Late Triassic, rifting ceased and a giant carbonate platform developed on the underlying thinned crust. The resulting distal (outer shelf) and proximal (inner shelf) facies zonation suggests a north-westward gulf-like embayment of Tethys, the Vardar Ocean (Haas et al., 1995) (Fig. 1-4). Paleomagnetic data from the African and Eurasian plates and the absence of island arc terranes in the western Alps constrain Tethys to being a relatively small embayment of a larger easterly ocean. The Triassic deep-water seaway was variously traced from the Central Alps (Austroalpine) to the inner West Carpathians into the

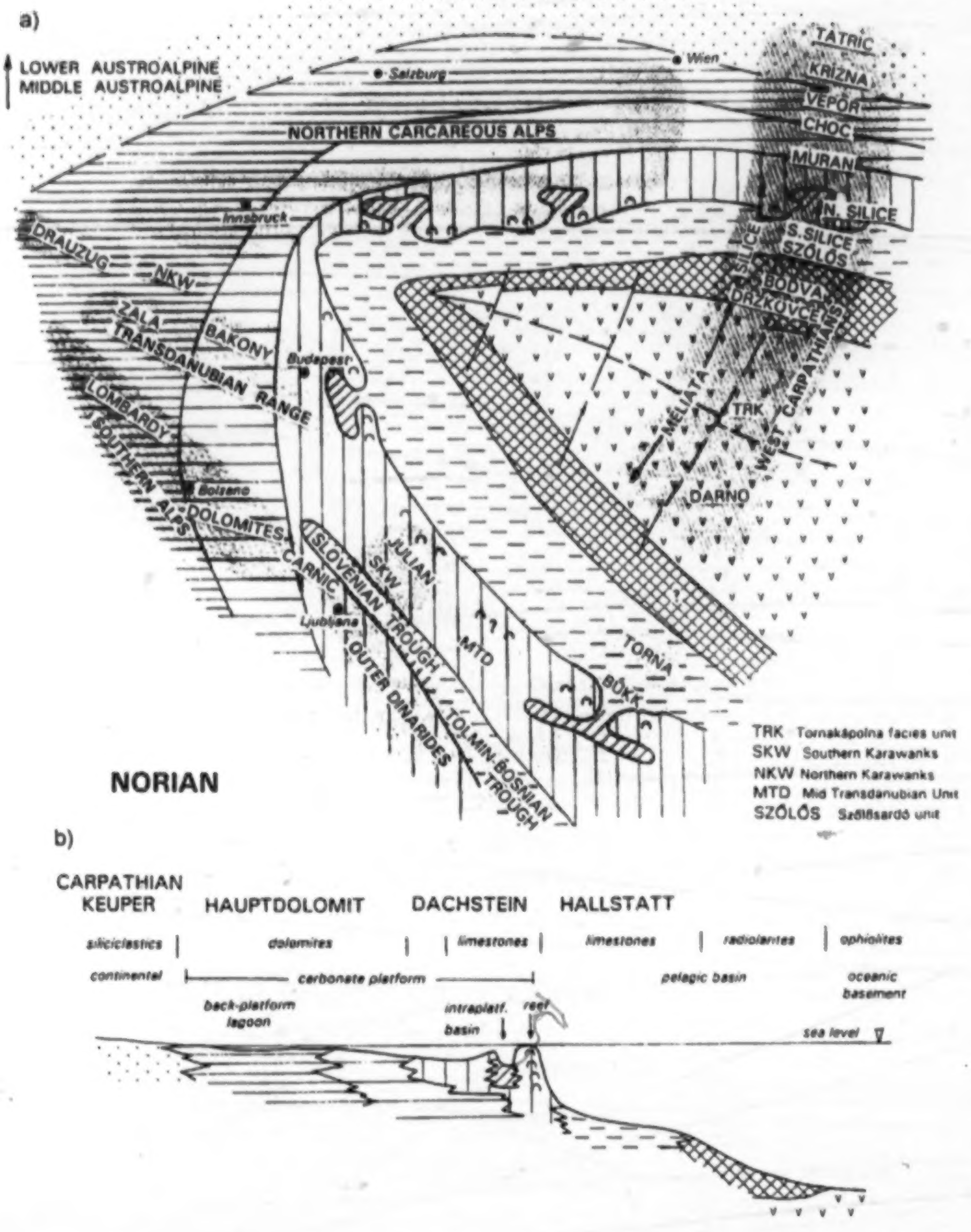
a)
LOWER AUSTROALPINE
MIDDLE AUSTROALPINE
Salzburg
Wien
TATRIC
KRIZNA
VEPOR
CHOC
MURAN
NORTHERN CARCAREOUS ALPS
Innsbruck
N. SILICE
S. SILICE
SZŐLŐS
SILICE
BODVA
DRZKOVCE
DRAUZUG
NKW
ZALA
BAKONY
TRANSDANUBIAN RANGE
Budapest
LOMBARDY
SOUTHERN ALPS
Bolzano
DOLOMITES
MELIATA
TRK
WEST CARPATHIANS
DARNO
CARNIC
SLOVENIAN TROUGH
SKW
JULIAN
MTD
Ljubljana
OUTER DINARIDES
TOLMIN-BOSNIAN TROUGH
TORNA
BÜKK
NORIAN
TRK Tornakápolna facies unit
SKW Southern Karawanks
NKW Northern Karawanks
MTD Mid Transdanubian Unit
SZŐLŐS Szőlősardó unit
b)
CARPATHIAN KEUPER
HAUPTDOLOMIT
DACHSTEIN
HALLSTATT
siliciclastics
dolomites
limestones
limestones
radiolarites
ophiolites
continental
carbonate platform
pelagic basin
oceanic basement
back-platform lagoon
intraplatf. basin
reef
sea level

Fig. 1-4. a) Reconstructed facies distribution and b) generalized cross-section for the middle Norian (*after* Haas et al., 1995) inner East Carpathians (Tollmann, 1969, 1990; Kovács, 1982; Săndulescu, 1984; Debelmas and Săndulescu, 1987). It was locally floored by oceanic crust as indicated by pillow lavas interfingered with Middle Triassic radiolarites in the Meliata unit of the inner West Carpathians, by basalts unconformably overlain by Carnian and/or Norian limestones in the Perşani Mountains (southern East Carpathians) and by mafic pebbles in Jurassic klippen within Senonian strata north of the Apuseni Mountains (Botiza). A Jurassic tholeiitic to calc-alkaline suite exposed in the southeastern Apuseni Mountains and inferred as basement of the Transylvanian Basin is currently interpreted to represent the main remnant of oceanic crust that traces Tethys from Vardar in the Dinarides to the south Penninic ocean in the Central Alps.

After Triassic-Jurassic spreading and local subduction of oceanic crust (e.g., Meliata), periods of relative stability seem to be separated by episodic, relatively rapid local plate migrations as a consequence of the motions of larger plates: 1. Middle to Late Jurassic brake-up of Pangea and the development of the Central Atlantic and Ligurian - Piemont (South Penninic) oceans; 2. Cretaceous opening of the South Atlantic accompanied by closure of Tethys. Motions of intra-Tethyan plates were primarily meridional, but eastward (Italy, Corsica, Sardinia, Carpathian) and westward (Alboran) arcs were also well established.

The Alps are a result of southward subduction of the Penninic ocean, followed by highly complex tectonism related to collision and thrusting of the Apulian promontory of the African plate onto the European shelf.

The Carpathians and the Inner Carpathian region resulted from the aggregation of several terranes, separated by sutures and/or major faults. Magmatic arc rocks, variously oceanic, continental, and hybrid in the Dinarides, Carpathians, and Aegean Sea, are interpreted to record major subductions. The main Tethyan suture is interpreted along the Transylvanides, would connect the Vardar Ocean to the Pieniny ocean, and farther to the Ligurian-Piemont ocean (Săndulescu, 1984). A second-order rift would have separated the Carpathians from stable Europe (Fig. 1-5a and 1-6).

As plates converged by subduction of intervening oceanic lithosphere, variably aggregated and deformed light crustal masses were brought together with offscrapings from subducted oceanic plates. (Figs. 1-5a and 1-6). Cretaceous compression resulted in closure of the Tethys Ocean partly by subduction and partly by bilateral obduction, to the west on the Apuseni fragment and to the east on the Carpathian fragment. Nappe emplacement would have prograded from the Tethys into the Carpathian crust and into the accretionary wedge during westward subduction of the oceanic or thinned continental crust that separated the Carpathians from Europe. Basement rocks have been involved as rigid slices in a large number of Cretaceous nappes (Appendix I), some of them of significant extent and displacement.

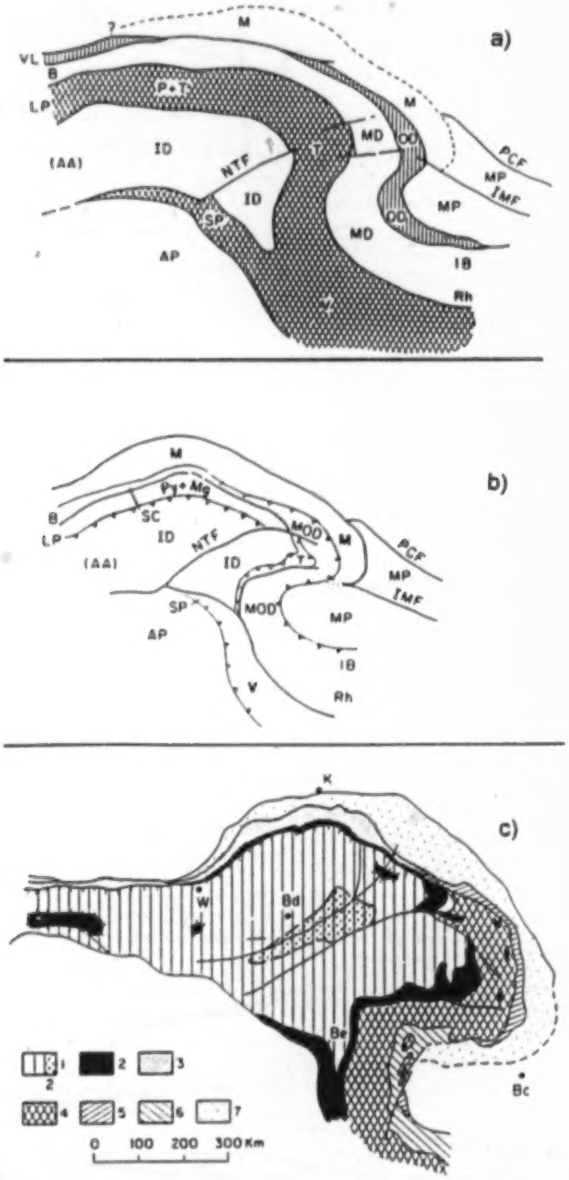
a)
?
M
VL
B
LP
P+T
(AA)
ID
NTF
T
MD
OD
M
PCF
MP
IMF
ID
SP
OD
MP
MD
AP
IB
Rh
V
b)
M
Py+Mg
B
SC
LP
ID
NTF
MOD
M
PCF
(AA)
ID
T
MP
IMF
SP
MOD
MP
AP
IB
V
Rh
c)
K
W
Bd
Be
Bc
1
2
3
4
5
6
7
0 100 200 300 Km

Fig. 1-5. a) Palinspastic sketch of the Carpathians at the end of the Mesozoic spreading and b) at the end of Cretaceous subduction. c) The major Tethyan suture in the Alpine-Carpathian orogen. 1-Austroalpine-Inner Dacides; 1b - Bükk Mountains and correlative units; 2 - Major Tethyan sutures (Vardar,V; South Pannonian, SP; Transylvanides, T; Pieniny Klippen Belt,P; Tauern, T and Rechnitz Windows); 3 - Flysch sequences of the Măgura Group; 4 - Middle Dacides, MD (Central East Carpathian nappes, Getic and Supragetic nappes); 5 - Flysch sequences of the Outer Dacides, OD; 6- marginal Dacides (Danubian); 7 - Moldavides, M; NTF - North Transylvanian Fault; IMF - Intra-Moesian Fault; Peceneaga-Camena Fault; Bc-Bucharest, Be-Beograd, Bd-Budapest; K-Krakow, W-Wien (*from* Săndulescu, 1988).

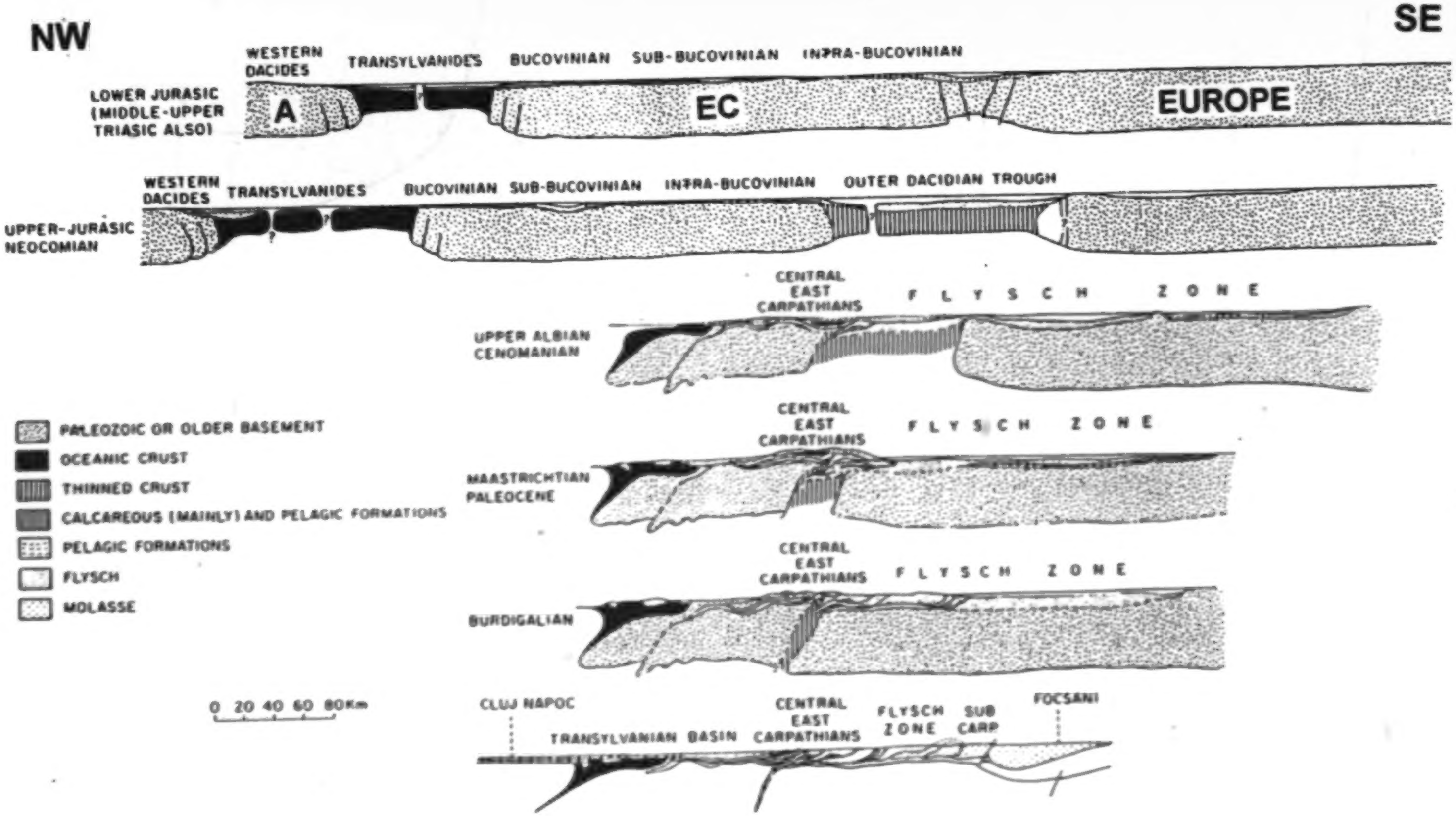
NW
SE
WESTERN DACIDES
TRANSYLVANIDES
BUCOVINIAN
SUB-BUCOVINIAN
INFRA-BUCOVINIAN
LOWER JURASIC (MIDDLE-UPPER TRIASIC ALSO)
A
EC
EUROPE
WESTERN DACIDES
TRANSYLVANIDES
BUCOVINIAN
SUB-BUCOVINIAN
INFRA-BUCOVINIAN
OUTER DACIDIAN TROUGH
UPPER-JURASIC NEOCOMIAN
CENTRAL EAST CARPATHIANS
FLYSCH ZONE
UPPER ALBIAN CENOMANIAN
CENTRAL EAST CARPATHIANS
FLYSCH ZONE
MAASTRICHTIAN PALEOCENE
CENTRAL EAST CARPATHIANS
FLYSCH ZONE
BURDIGALIAN
PALEOZOIC OR OLDER BASEMENT
OCEANIC CRUST
THINNED CRUST
CALCAREOUS (MAINLY) AND PELAGIC FORMATIONS
PELAGIC FORMATIONS
FLYSCH
MOLASSE
0 20 40 60 80Km
CLUJ NAPOC
TRANSYLVANIAN BASIN
CENTRAL EAST CARPATHIANS
FLYSCH ZONE
SUB CARP
FOCSANI

Figure 1-6. Palinspastic reconstruction of the Apuseni - East Carpathians crustal fragments (along Geotraverse V, Appendix I) (*from* Săndulescu, 1988). The generalized nappe interpretation of the East Carpathians (EC) required a shallow dipping suture zone beneath the Apuseni continental crust fragment (A).

In recent tectonic analysis, the Carpathian arc is thought to be the response to tectonic filling of what was, in Early Tertiary time, a westward-opening oceanic embayment. This filling is viewed in two different ways:

- a coherent continental plate pushed obliquely by north-moving plates, bounded and sliced by strike slip faults as needed to fit into this embayment (e.g., Tapponier, 1977; Royden et al., 1983), or
- the migration of the Carpathian arc and the complex suturing of various plates, some of them far-travelled in the inner Carpathians and intra-Carpathians (e.g., Balla, 1982; Hamilton, 1990)

Subduction magmatism started in the West Carpathians and Apuseni mountains during the Early Miocene and migrated to the East Carpathians. Continued subduction caused retro-arc crustal extension and formation of the Pannonian basin system. The arc migrated to the east and younger volcanism initiated in the southern East Carpathians. The older calc-alkaline volcanics were left behind in the southern Apuseni Mountains during development of the Transylvanian inter-arc basin (Bleahu et al., 1973). Progressive crustal extension of the Transylvanian basin is suggested by the Burdigalian strata accumulated within its centre, and expansion of the Sarmatian strata towards the peripheries.

Late Tertiary strike-slip faults are accompanied by Pliocene-Pleistocene alkali-basalts.

1.3. THE MODEL AND THE REAL WORLD

Recent overviews and tectonic syntheses tend to use a "self-explanatory" terminology. Although unavoidable in large scale generalizations, the self-explanatory terms are in some cases misleading. For example: a) an areally-limited complex of basalt, gabbro, pegmatoid quartz-diorite, granophyre, plagiogranite has been interpreted as a sheeted dyke complex with subvertical igneous contacts (Savu, 1984a), although the sub-vertical discontinuities are joints/cleavages consistent with the youngest Miocene tectonism in the southern Apuseni Mountains; b) strained agglomerates with tectonic enclaves from adjacent Jurassic strata were interpreted as Cretaceous "mélange" (Savu, 1984b), although they are located along an E-W lineament that projects into the south Transylvanian Late Tertiary strike-slip fault zone; c) volcanic rocks in the northeastern part of the Pannonian Basin were interpreted as a subduction arc related to northward subduction from K_2O/SiO_2 ratios (Balla, 1982) although significant uncertainties associated with K_2O zoning were known (e.g., Arculus and Johnson, 1978). Assimilated into regional tectonic synthesis the "self-explanatory" terms derived from suspect original interpretations resulted in evolutionary models that included wide oceans followed by subduction/obduction (e.g., Hamilton, 1990). Space and time inconsistencies exist and geochemical and geophysical data appear to have been disregarded.

1. Only the anatomy of the East Carpathian segment of the orogen resembles a subduction zone defined by the pair of accretionary wedge-magmatic arc. The local expression of the main Tethyan suture interpreted between the Apuseni and the Carpathians mountains bears no resemblance to a subduction zone. The original model (Rădulescu, Săndulescu, 1973) argued for Cretaceous subduction, and for the consumption of the oceanic crust in front of the Carpathians by Turonian time. For recent models, a remnant of Jurassic oceanic crust in Paleogene (eg., Royden et al., 1983; Linzer, 1995) or even Miocene time (Peresson and Decker, 1997) in front of the Carpathians is critical.

a) The only mafic rocks in front of the East Carpathians are intra-continental basalts interlayered in the most internal flysch units (Russo-Săndulescu, 1985). The Mesozoic igneous complex between the Apuseni Mountains and the Carpathians is dominated by calc-alkaline rocks with tholeiitic rocks restricted to its westernmost part. The source of sediments in flysch units is of continental origin (e.g., Winkler and Slaczka, 1992). There is no geological evidence for extensive Mesozoic oceanic crust in the region. The survival of oceanic crust until the Miocene is unlikely.

b) Deep water strata make a coherent thrust-and-fold belt only along the West and East Carpathians; it disappears in front of the South Carpathians, and reappears at the tip of the Moesian platform (Severin-Trojan flysch) and in front of the easternmost segment of the Balkans (as the Kotel flysch) (Fig. 1-1). The lack of continuity of deep water strata makes their interpretation as accretionary wedge suspect.

c) No volcanic arc associated with the assumed Cretaceous subduction zones can be traced: 1 - the belt of Late Cretaceous calc-alkaline intrusions stretching from the Balkans to the Apuseni Mountains, cuts the suture interpreted in the southern Apuseni Mountains, precluding a subduction zone/volcanic arc relationship for the main Tethyan suture; 2 - basaltic tuff and basaltic andesite (Savu et al., 1987) from the Turonian-Senonian "mélange" (Pop, 1973) overlying the external Danubian crust of the South Carpathians would record Cretaceous subduction in front of the Danubian domain and not between Danubian and Getic as postulated; 3 - andesitic tuffites interlayered in several Cenomanian flysch sequences of the East Carpathians were tentatively interpreted to record local subduction within the flysch basins (Rădulescu and Dimitrescu, 1982) because no contemporaneous andesitic tuff is known on the overriding East Carpathian plate.

d) The Neogene-Quaternary magmatic rocks cannot be matched with correlative sutures. The zone of igneous activity was diffuse and discontinuous, unlike most subduction-related magmatic arcs (Pécskay et al., 1995). Geochemical data are at variance with the notion of subduction-related volcanism (Seghedi and Szakács, 1995; Masson et al., 1996). The magmatic events do not show interpretable age progressions and chemical zoning, as proposed by subduction-related models.

The belt of Neogene magmatic rocks is generally interpreted to track the contour of the ~100 km isobath at the top of a subducting slab of oceanic crust (e.g., Royden, 1988) or delaminated lithosphere (Doglioni, 1993) along the West and East Carpathians orocline. A single, retreating subducted slab cannot explain the areal and temporal distribution of the calc-alkaline volcanism in the Carpathian-Pannonian region. While the Carpathians thrust-and-fold belt is strongly divergent, the volcanic "arc" consists in fact in lineaments that cut the internal units obliquely in the East Carpathians and transversely in the West Carpathians and Apuseni Mountains. Volcanoes within the Pieniny Klippen Belt, Magura and Sinaia flysch units are located forlandwards from the hinge of the postulated subduction. Moreover, there is a 100 My time gap between the first major subduction-related thrusts (Aptian), and over 60 My between the inferred complete consumption of the eastern oceanic basin (Turonian, Săndulescu, 1988), and the initiation of Miocene calc-alkaline volcanism. Along the South Carpathians segment, volcanic arc rocks are missing. The assumption that overriding did not proceed far onto the preexisting continental shelf (Hamilton, 1990) conflicts with current interpretation of the Getic (Murgoci, 1907) and the Supragetic (Streckeisen, 1934) basement nappe systems which are believed to have been thrust more than 100 kilometres onto the European foreland.

e) No geophysical evidence of fossil paleo-subduction zones exists. Magneto-telluric and seismic investigations of the contacts between the European, Carpathians, and Apuseni continental fragments show that shallow-dipping detachments in the upper crustal levels merge into vertical tectonic discontinuities at intermediate and deep crustal levels (e.g., Sollogub et al.,1973; 1986; Stănică and Stănică, 1993) (Appendix I). Horizontal seismic reflectors at the crust - mantle interface (e.g., Tomek, 1993) and the lack of any remnant of subducting slab underneath the West Carpathian (Spakman, 1990) and Apuseni mountains is interpreted as Moho rejuvenation via the gabbro-eclogite phase transition. The explanation is petrologically tenuous and at odds with the clear subduction geometry imaged under the Dinarides (Spakman, 1990). Several attempts to relate the subduction zone postulated beneath the East Carpathians to the seismically active Vrancea region (e.g., Roman, 1970; Royden, 1988; Linzer, 1995) invoke speculative models to explain the location of a vertically descending slab at the exterior of the "subducting wedge" under the stable European foreland, and its orientation perpendicular to the inferred subduction zone.

2. Cretaceous subduction is critical to the generalized nappe interpretation of the internal units. Strain associated with the Cretaceous subduction was implicitly considered to be regional-scale Cretaceous nappe stacking in the overriding plates. Thrusts inferred in different segments of the orogen long before the plate tectonics concept (e.g. the Getic nappe - Murgoci, 1907; the Supragetic nappes - Streckeisen, 1934; the Supragetic nappe - Codarcea et al., 1967; the Bucovinic and Transylvanian nappes - Uhlig, 1903) were correlated along the entire Carpathians

based on isolated exposures of Mesozoic cover strata reinterpreted as facies zones facing the postulated Tethys ocean (Săndulescu, 1975, 1984). All tectonic contacts involving basement rocks were interpreted as major Cretaceous (or older) overthrusts (e.g., Balintoni et al., 1983, 1989; Balintoni, 1994; Iancu, 1986; Hann and Szász, 1984; Berza et al., 1994). Although very popular, the assumed Cretaceous nappe stacking model is inconsistent with key evidence presented here: kinematic indicators and isotopic dating.

3. The stratigraphic interpretation of the metamorphic / magmatic assemblages (e.g., Codarcea, 1967, Kräutner, 1980, Dimitrescu, 1988) offered support to the nappe model: by postulating sedimentary protoliths in original stratigraphic succession, nappe contacts were justified by the omission of lithostratigraphic units. The age of sedimentary protoliths of greenschist to high-grade facies rocks were assigned on the basis of paleontological data (e.g., Codarcea and Iliescu, 1967; Visarion and Dimitrescu, 1971; Kräutner, 1980). A large number of K-Ar analyses were generally inconclusive.

1.4. NEW RESULTS

Detailed field and laboratory work on basement rocks of the Apuseni Mountains and selected regions of the Carpathians presented here shed new light on the crustal evolution and mode of involvement of basement units in Alpine tectonism.

1.4.1 Crustal evolution

Basement assemblages in the Apuseni and Carpathians mountains previously assigned to three superposed 'geosynclinals cycles' are inferred to be Precambrian crust variably reworked during subsequent tectonothermal events.

Medium-grade lithotectonic assemblages have yielded Early Proterozoic Sm-Nd crustal residence ages. U-Pb zircon data for granites previously assigned to the Middle Proterozoic tectonic-magmatic cycle have yielded Middle to Late Paleozoic ages. The Highiş igneous complex assigned to Variscan (e.g., Savu, 1965; Giuşcă, 1979) or Caledonian and Variscan igneous events (Balintoni, 1986) is of late Early Permian age. Corroborated with U-Pb zircon dates from associated pre- and post- tectonic granites, $^{40}Ar/^{39}Ar$ dates on metamorphic rocks are interpreted to indicate either rapid cooling following a metamorphic event or cooling during uplift.

Similar lithologies and isotopic compositions of basement units from the Apuseni and Carpathian mountains cast doubts upon their interpretation as distinct African and European crustal fragments, respectively. Sm-Nd isotopic data indicate that both crustal fragments started their evolution at about the same time in the Early Precambrian. U-Pb zircon data and $^{40}Ar/^{39}Ar$ data record Early and Late Variscan tectonothermal events, pointing to a similar Paleozoic evolution. It is highly unlikely that a crustal fragment detached and displaced during the opening of Tethys would have returned to its original location following ocean closure.

The low-grade assemblages show a large component of non-coaxial strain accompanied by retrogressive metamorphic reactions and are interpreted here as retrogressive Alpine shear zones overprinting basement units. Sm-Nd model ages are younger and $\varepsilon \mathrm{Nd}_{(0)}$ values less negative than those of medium-grade rocks; model ages are in the same range as Paleozoic granites variably contaminated during ascent through gneissic crust. Sm-Nd data suggest a stepwise evolution of the crust by repetitive addition of juvenile material followed by shearing and metamorphism. $^{40}\mathrm{Ar}/^{39}\mathrm{Ar}$ data for syn-kinematic muscovite, and whole rock samples from the belts of low-grade rocks indicate polyphase tectonism between Late Carboniferous and Late Cretaceous. The kinematics of these long-lived, tectonically active zones of weakness are integrated into a new regional geodynamic model below.

1.4.2 Alpine evolution

Crustal fragments at the southern margin of the European platform were repeatedly broken and re-welded during complex plate interaction dominated by large scale transcurrent shear zones. The Early Alpine extension of the European crust was dominated by tangential stretching rather than normal rifting. Mesozoic mafic rocks and deep water sediments are more likely related to local tracts than to a wide oceanic basin. Tithonian to Early Cretaceous flysch-like sequences developed in tectonically active troughs and are often accompanied by mantle-derived intrusions up to Albian.

Cretaceous to Recent compression resulted in diachronous phases of stress release and tectonic relaxation at fragment margins with distinct kinematics.

U-Pb zircon data on a calc-alkaline intrusion within the tholeiitic suite of the Southern Apuseni Mountains (Săvârşin granite) is inconsistent with the subduction/obduction model. The tholeiitic rocks were previously interpreted as a slab of oceanic crust obducted onto the Apuseni continental crust. The inherited grains of a uniform high-Th zircon population yielded a Callovian date (c. 155 Ma) for the tholeiitic substratum. No inheritance from continental crust has been found. The emplacement of the Săvârşin granite was previously inferred to be of Cretaceous age and related to Early Alpine subduction and nappe stacking. The youngest zircon population yielded a date of 55 Ma, suggesting Eocene emplacement instead.

Kinematic indicators along most contacts between postulated far-travelled Cretaceous basement nappes are orogen-parallel and oriented consistently with the internal strain within the adjacent metamorphic assemblages. The Alpine strain was gradually accommodated in wide retrogressive shear zones overprinting metamorphic and igneous basement and "wildflysch" assemblages in clastic cover strata. Although compressional structures including thrust faults are common, no evidence exists for a tectonic model that postulates hinterland nappes passing over frontal ones (eg., Getic, Supragetic, Bucovinic, Transylvanian nappes). The Cretaceous juxtaposition of crustal fragments resulted from transcurrent displacement and local oblique thrusts rather than from large overthrusts normal to a hypothetical subduction zones. During Cenozoic tectonism, the overridden crust in front of the East Carpathians is essentially thinned continental crust; the Moesian platform was not a passive promontory of Europe, but a relatively active west moving indenter. This view drastically limits the extent of the supposed Tertiary ocean embayment in the Carpathian area and the implied hundreds of kilometres of shortening by nappe stacking.

The Carpathian orocline is defined by a coherent thrust-and-fold belt along the Eastern Alps, West Carpathians, and East Carpathians (Fig. 1-1). Internal units however, are more discontinuously exposed, more deeply eroded, and have incomplete cover sequences. Their correlation is a matter of debate. The Apuseni Mountains, located between the Carpathians and the Dinarides branches of the Alpine orogen, are surrounded by Neogene fill of the Pannonian and Transylvanian basins. The correlation of lithologic assemblages from the Apuseni Mountains with isolated exposures along the orogen is tenuous. Paleo-geographic reconstruction and tectonic analysis based exclusively on Alpine (Permian to Recent) stratigraphy have resulted in contradictory interpretations. This study emphasises the Alpine kinematics recorded by basement lithologies relevant for regional correlations and tectonic interpretations.

REFERENCES

Arculus, R. J., and Johnson, R. W., 1978, Criticism of generalized models for magmatic evolution of arc-trench systems, Earth Planet. Sci. Lett., 39, 118-126.

Aubouin, J., and Celet, P., 1970, Introduction à la séance consacrée a la Géologie des Dinarides, Bull. Soc. Géol., de France, 7, XII, 6, p. 941-944.

Balla, Z., 1982, Development of the Pannonian Basin Basement through the Cretaceous-Cenozoic Collision: A New Synthesis, Tectonophysics, 88, 2, p. 61-102.

Balla, Z., 1985, The Carpathian Loop and the Pannonian Basin: a Kinematic Analysis, Geophys. Transactions, 30, 4, p. 313-353.

Balla, Z., 1986, Paleotectonic Reconstruction of the Central Alpine-Mediterranean Belt for the Neogene, Tectonophysics, 127, p. 213-243.

Balintoni, I., 1969, Asupra caracterului retromorf al paragneiselor biotitice cu clorit de pe Bâsca Groşetului (Făgăraş): Buletinul Societăţii Ştiinţifice de Geologie, XI, p. 275-281.

Balintoni, I., 1980, Date noi asupra poziţiei structurale a metamorfitelor din bazinul văii Putnei (Carpaţii Orientali): Dări de Seamă ale Institutului de Geologie şi Geofizică, LXVI, 5, p. 25-36.

Balintoni, I., 1986, Petrologic and Tectonic Features of the Highiş-Drocea Crystalline Massif, Dări de Seamă ale Institutului de Geologie şi Geofizică, 70-71, 5, p.5-21.

Balintoni, I., and Gheuca, I., 1977, Metamorphism progresiv, metamorphism regresiv şi tectonică în regiunea Zugreni-Barnar (Carpaţii Orientali): Dări de Seamă ale Institutului de Geologie şi Geofizică, LXIII/5, p.11-38.

Balintoni, I., Gheuca, I., and Vodă, Al., 1983, Alpine and Hercynian overthrust nappes from central and southern areas of the East Carpathian Crystalline-Mesozoic Zone: Anuarul Institutului de Geologie şi Geofizică, LX, p.15-22.

Balintoni, I., Berza, T., Hann, H.P., Iancu, V., Kräutner, H.G., and Udubaşa, G., 1989, Precambrian Metamorphics in the South Carpathians, Multilateral Cooperation of the Academies of Sciences of the Socialist Countries, Earth Crust Structure Evolution and Metallogeny, Guide to Excursions, 89 p.

Balintoni, I., 1994, Structure of the Apuseni Mountains, *in* Berza T. (Ed.): Geological evolution of the Alpine-Carpathian-Pannonian system, Rom. J. Tect. Reg. Geol., 75, 2, p. 51-58.

Bechstädt, T., 1978, Faziesanalyse permischer und triasicher Sedimente des Drauzuges als Hinweis auf eine grossraumige Lateralverschiebung Innerhalb des Ostalpins. Jb. Geol. B.-A., 121, p. 1-122.

Bercia, I., Kräutner, H.G., and Mureşan, M., 1976, Pre-Mesozoic Metamorphites of the East Carpathians: Anuarul Institutului de Geologie şi Geofizică, L, p. 37-70.

Berza, T., Balintoni, I., Iancu, V., Seghedi, A., and Hann, P. H., 1994, South Carpathians, *in* Berza T. (Ed.): Geological evolution of the Alpine-Carpathian-Pannonian system, Rom. J. Tect. Reg. Geol., 75, 2, p. 37-49.

Bleahu, M, D., Boccaletti, M., Manetti, P., and Peltz, S., 1973, Neogene Carpathian Arc: A Continental Arc Displaying the Features of an 'Island Arc', Journal of Geophysical Research, 78, 23, p. 5025-5031.

Burchfiel, B.C., 1980, Eastern European Alpine System and the Carpathian Orocline as an Example of Collision Tectonics: Tectonophysics, 63, p.31-61.

Codarcea, D., 1965, Studiul geologic şi petrografic al regiunii Răşinari-Cisnădioara-Sadu: Memorii -Institutul de Geologie, VI, 87p.

Codarcea, D., 1967, La division des massifs cristallophylliens préalpins des Carpates Roumaines: Rêvue Roumaine de Géologie Géophysique Géographie, Serie Géologie, Tome 12/1, p. 57-63.

Codarcea, D., and Iliescu, V., 1969, Noi date microfloristice asupra vîrstei complexului calcaros al seriei de Sibişel: Studii şi Cercetări de Geologie Geofizică Geografie, Geologie, Tom 14/1, p.279-282.

Codarcea, A., Lupu, M., Codarcea, D., and Lupu, D., 1967, Unitatea Supragetică în Carpaţii Meridionali, Studii şi Cercetări de Geologie Geofizică Geografie, 12, 2, p. 387-392.

Csontos, L., Nagymarosy, A., Horváth, F., and Kovác, M., 1992, Tertiary Evolution of the Intra-Carpathian Area: A Model, Tectonophysics, 208, p. 221-241.

Dallmeyer, R. D., and Neubauer, F., 1993, Variscan vs. Alpine tectonothermal evolution within the Southern Carpathians, Romania: evidence from ^{40}Ar/^{39}Ar mineral aes: GSA Annual Meeting, Boston, Mass., Abstract Volume, p. A-341.

Debelmas and Săndulescu, M., 1987, Transformante Nord-Penninique et Problemes de Correlation Palinspastique entre les Alpes et les Carpathes. Bull., Soc., Géol. France, 8, III, 2, p. 403-408.

Dercourt and 18 Co-Workers, 1986, Geological Evolution of the Tethys belt from the Atlantic to the Pamirs since the Lias, Tectonophysics, 123, p. 241-315.

Dimitrescu, R., 1963, Structura părţii centrale a Munţilor Făgăraşului: Carpatho-Balkan Geological Association, Congress V, 2, p. 17-25.

Dimitrescu, R., 1985, Early Caledonian Event in the Pre-Alpine Metamorphic Sequences of the Romanian Carpathians: Acta Mineralogica-Petrographica, XXVII, p. 59-70.

Dimitrescu, R., 1988, Apuseni Mountains, *in* Zoubek V., Cogné, J., Kozhoukharov, D., (Eds.): Precambrian in Younger Fold Belts, p. 665-674.

Doglioni, C., 1993, Comparison of subduction zones versus the global tectonic pattern: a possible explanation for the Alps-Carpathians system. Geophys. Trans., 37, p. 253-264

Gheuca, I., 1988, Versantul Sudic al Munţilor Făgăraş, Litostratigrafie şi tectonică: Dări de Seamă ale Institutului de Geologie şi Geofizică, v. LXXII-LXXIII/5, p. 93-117.

Giuşcă, D., 1979, Masivul Cristalin al Highişului, Studii şi Cercetări de Geologie Geofizică Geografie., 24, p. 14-43.

Giuşcă, D., Savu, H., Bercia, I., and Kräutner, H.G., 1969, Sequence of tectonomagmatic pre-Alpine cycles on the territory of Romania: Acta Geologica Academiae Scientiarum Hungaricae, 13, p.221-234.

Giuşcă, D., Anastasiu, N., Popescu, Gh., and Şeclăman, M., 1977, Observaţii asupra şisturilor cristaline din zona centrală a masivului Făgăraş (Cumpăna-Valea Cîrţişoara): Analele Universităţii Bucureşti, Geologie, v. XXVI, p. 3-17.

Haas, J., Kovács, S., Krysteyn, L., and Lein, R., 1995, Significance of Late Permian-Triassic facies zones in terrane reconstructions in the Alpine-North Pannonian domain:

Tectonophysics, 242, p. 19-40.

Hann, H. P., and Szász, L., 1984, Geological structure of the Olt Valley between Câineni and Brezoi (South Carpathians). Dări de Seamă ale Institutului de Geologie şi Geofizică,LXVIII, 5, p. 23-39.

Iancu, V., 1986, Unités structurales supragetique et infragetique de la partie Ouest des Carpathes Méridionales, Dări de Seamă ale Institutului de Geologie şi Geofizică, 70-71/5, p. 109-127.

Hamilton, W., B., 1990, On Terrane analysis, *in* Dewey, J. F., Gass, I., G., Şengor, A, M., C., (Eds.): Allochtonous Terranes, p. 55-66.

Ianovici, V., Borcoş, M., Bleahu, M., Patrulius, D., Lupu, M., Dimitrescu, R., and Savu, H., 1976, Geologia Munţilor Apuseni, Editura Academiei, 631p.

Kovács, 1982, Problems of the "Pannonian Median Massif" and the plate tectonic concept. Contribution based on the distribution of Late Paleozoic-Early Mesozoic isopic zones. Geol. Rundschau, 71, p. 617-640.

Kräutner, H.G., 1980, Lithostratigraphic Correlation of Precambrian in the Romanian Carpathians: Anuarul Institutului de Geologie şi Geofizică, v. LVII, p. 229-296.

Kräutner, H.G., 1988, Interregional Correlations, *in* Zoubek V., Cogné, J., Kozhoukharov, D., (Eds.): Precambrian in Younger Fold Belts, p. 853-862.

Laubscher, H.P., and Bernoulli, D., 1977, Mediterranean and Tethys, in A.E. Nairn, W.H. Kanes and F.G. Stehli (eds): The Ocean Basins and Margins, Plenum, p. 1-28,New York

Linzer, H-G., 1995, Kinematics of retreating subduction along the Carpathian Arc, Romania, Geology, 24, 2, p. 167-170.

Masson, P. R. D., Downes, H., Seghedi, I., Szakács, A., and Thirlwall, M. F., 1995, Low-pressure evolution of magmas from the Calimani, Gurghiu and Harghita Mountains, East Carpathians, Acta Vulcanologica, 7, 2, p. 43-52.

Murgoci, G.M., 1907, Sur l'existence d'une grande nappe de charriage des Carpates méridionales: Buletinul Societătii de Ştiinte Bucureşti, v. XVI, p. 52-54.

Peresson, H., and Decker, K., 1977, Far-field effects of Late Miocene subduction in the Eastern Carpathians: E-W compression and inversion of structures in the Alpine-Carpathian-Pannonian region, Tectonics, 16, 1, p.38-56.

Pécskay, Z., and 14 Co-authors, 1995, Space and time distribution of Neogene-Quaternary volcanism in the Carpatho-Pannonian Region, Acta Vulcanologica, 7, 2, p. 15-28.

Pop, 1973, Depozitele Mezozoice din Munţii Vâlcan, 155 p. Editura Academiei Române, Bucureşti.

Popescu-Voiteşti, I., 1942, Exposé synthétique sommaire sur la structure des régions carpathiques romaines. Bul. Soc. Rom. Geol., 3, 15-73.

Ratschbacher, L., Linzer, H.G., Moser, F., Strusievicz, R.O., Bedelean, H., Har, N., and Mogoş, P.A., 1993, Cretaceous to Miocene thrusting and wrenching along the central South Carpathians due to a corner effect during collision and orocline formation: Tectonics, v. 12, no. 4, p. 855-873.

Rădulescu, D., and Săndulescu, M., 1973, The Plate-Tectonics Concept and the Geological Structure of the Carpathians: Tectonophysics, v. 16, p.155-161.

Rădulescu, D., and Dimitrescu, R., 1982, Petrologia endogena a teritoriului R.S.Romania, Partea a III-a: Editura Universităţii Bucureşti, 120 p.

Rădulescu, D., Săndulescu, M., and Borcoş, M., 1993, Alpine Magmatogenetic Map of Romania: an Approach to the Systematization of the Igneous Activity, Rev. Roum., Géologie, 37, p. 3-8.

Roman, C., 1970, Seismicity in Romania-Evidence for the Sinking Lithosphere, Nature, 228, p. 1176-1178.

Royden, L., Horvath, F., and Rumpler, J., 1983, Evolution of the Pannonian Basin System: 1. Tectonics, Tectonics, 2, 1, p. 63-90.

Royden, L., 1988, Late Cenozoic Tectonics of the Pannonian Basin System, *in* Royden L., and Horváth (Eds.): The Pannonian Basin - A Study in Basin Evolution, AAPG Memoir, 45, p. 27-48.

Royden, L., and Báldi, T., 1988, Early Cenozoic Tectonics and Paleogeography of the Pannonian and Surrounding Regions, *in* Royden L., and Horváth (Eds.): The Pannonian Basin - A Study in Basin Evolution, AAPG Memoir, 45, p. 1-16.

Royden, L., and Burchfiel, B.C., 1989, Are systematic variations in thrust belt style related to plate boundary processes ? (The Western Alps versus the Carpathians), Tectonics, 8, 1, p. 51-61.

Russo-Săndulescu, D., and Bratosin, T., 1985, Caractères et signification du complexe basique de la nappe du Flysch Noir (Monts du Maramureş, Carpates Orientales): Carpatho-Balkan Geological Association, XIII Congress, Krakow, Abstract Volume, p. 112-115.

Savu, H., 1965, Masivul Eruptiv de la Bârzava (Munţii Drocei), Memorii, Comitetul Geologic, VIII, 148 p., Bucureşti.

Savu, H., 1970, Stratigrafia şi Izogradele de Metamorfism din Provincia Metamorfică Prebaikaliană din Munţii Semenic: Anuarul Institutului Geologic, v. XXXVIII, p. 223-311.

Savu, H., 1984a, The sheeted dike complex in the Mureş zone (Apuseni Mountains), Révue Roumaine de Géologie Géophysique Géographie, Serie Géologie, 28, p. 29-34.

Savu, H., 1984b, Melange-ul cu Matrice Piroclastica Asociat Arcului Insular Sudic al Zonei Mureş, Studii şi Cercetări de Geologie Geofizică Geografie, Geologie, 29, p. 36-43.

Savu, H., Udrescu, C., Lemne, M., Romanescu, O., Stoian., M., Neacşu, V., 1987, Island Arc Volcanics Related the Wildflysch on the Outer Margin of the Danubian Autochton (Southern Carpathians) and their Geotectonic Implications, Révue Roumaine de Géologie Géophysique Géographie, Serie Géologie, Tome 31, p 19-27.

Săndulescu, M., 1975, Essai de synthèse structurale des Carpathes, Bull. Soc. Géol. France, 7, XVII, 3, p. 299-358.

Săndulescu, M., 1984, Geotectonica României, Editura Tehnică, 323 p.

Săndulescu, M., 1988, Cenozoic Tectonic History of the Carpathians, *in* Royden L., and Horváth (Eds.): The Pannonian Basin - A Study in Basin Evolution, AAPG Memoir, 45, p. 17-25.

Săndulescu, M., Kräutner, H., Borcoş, M., Năstaseanu, S., Patrulius, D., Ştefănescu, M., Ghenea, C., Lupu, M., Savu, H., Bercia, I., and Marinescu, F., 1978, Geologic Map of Romania, Scale 1: 1000 000, Bucureşti.

Seghedi, I., Szakács, A., and Masson, P. R. D., 1995, Petrogenesis and magmatic evolution in the East Carpathian Neogene volcanic arc (Romania), Acta Vulcanologica, 7, 2, p. 135-143.

Şengör, A.M. C., Yilmaz, Y., and Ketin, I., 1980, Remnants of a pre-Late Jurassic ocean in northern Turkey: Fragments of Permian-Triassic Paleo-Tethys ?, Geol. Soc. of America Bull., 91, p. 599-609.

Sollogub, V. B., Prosen, D., and Co-Workers, 1973, Crustal Structure of Central and Southeastern Europe by Data of Explosion Seismology, Tectonophysics, 20, p. 1-33.

Sollogub, V. B., and Co-Workers, 1986, The Structure of the Lithosphere along Geotraverse V from Geological and Geophysical Data, Geophysical Journal, 7, 4, p. 417-440.

Spakman, W., 1990, Tomographic Images of the Upper Mantle below Central Europe and the Mediterranean, Terra Nova, 2, p. 542-553.

Stănică, D., and Stănică M., 1993, An electrical resistivity lithospheric model in the Carpathian Orogen from Romania, Physics of the Earth and Planetary Interiors, 81, p. 99-105.

Streckeisen, A., 1934, Sur la tectonique des Carpathes Méridionales. An. Inst. Geol. Rom., XVI, p. 327-417.

Tapponier, P., 1977, Évolution Tectonique du Système Alpin en Méditerranée: poinçonnement et écrasement rigide-plastique, Bull. Soc. Géol. France, 7, XIX, 3, p. 437-460.

Tollman, A., 1969, Die tektonisches Gliderung des Alpen-Karpaten Bogens, Geologie, 18, 10, p. 1131-1155.

CHAPTER 2*

ALPINE CRUSTAL SHEAR ZONES AND PRE - ALPINE BASEMENT TERRANES IN THE ROMANIAN CARPATHIANS AND APUSENI MOUNTAINS

---

* *This chapter contains an article published in Geology, 1994, 22, 9, p.807-810 by Dinu Pană and Philippe Erdmer*

2.1. INTRODUCTION

In the traditional interpretation of metamorphic basement rocks in the Carpathian Orogen, three superposed geosynclinal cycles of mid-Proterozoic, Late Proterozoic to Cambrian, and mid- to late-Paleozoic age resulted from the Dalradian, Cadomian/Caledonian, and Variscan orogenies, respectively (Codarcea, 1967; Giuşcă et al., 1969; Kräutner, 1980; Dimitrescu, *in* Rădulescu and Dimitrescu, 1982; Dimitrescu, 1985). The cycles were interpreted to have produced metamorphic sequences of amphibolite, epidote-amphibolite, and greenschist grade, respectively. Contacts between products of each cycle were inferred to be stratigraphic or metamorphic discontinuities.

Following a reexamination of metamorphic sequences in the orogen, we consider that some textures previously interpreted as metasedimentary and metavolcanic are pseudodepositional and are in fact polyphase blastomylonitic fabrics. For many epidote-amphibolite and greenschist grade sequences, we consider that the sense of the metamorphic reactions is retrograde and that rocks were involved during Alpine tectonism in wide retrograde shear zones that cut continental fragments on both sides of the Tethys suture. In addition, we consider that tectonic syntheses that highlight thrust faulting almost to the exclusion of other processes (e.g. Săndulescu, 1984; Balintoni et al., 1989) require revision to accommodate strike-slip displacements. We present the geologic setting, an evaluation of available data, and a new proposal for the style of Carpathian basement involvement in Alpine orogeny.

2.2. GEOLOGIC SETTING

Alpine evolution of the Carpathian orogen began with Triassic and Early Jurassic rifting and transform faulting. Mesozoic closure of the Tethys ocean and related rifts led to diachronous collision of continental fragments against the East European plate. Continental fragments have been considered as blocks locally rifted and rewelded during collision (the Internal and Median Dacides: Rădulescu and Săndulescu, 1973; Săndulescu, 1984), or as exotic fragments from more southern paleolatitudes (Apulian and Rhodopian continental fragments: Burchfiel, 1980). In the first interpretation, a recess-and-promontory rift geometry resulted in the inverse-S shape of the Carpathians (Fig. 2-1). In the second, initial northward-directed normal convergence was followed by eastward escape; the Moesian foreland promontory acted as a stress deviator during Paleogene compression (Ratschbacher et al., 1993), and Miocene back-arc extension in the hinterland (Transylvanian and Pannonian basins) was partly coeval with foreland thrusting (Royden and Burchfiel, 1989). Involvement of basement rocks in Alpine tectonism has been largely considered as being thrusting of rigid sheets. Strike-slip displacement and associated penetrative deformation during rifting (Săndulescu, 1984; Trümpy, 1988) or collision (Burchfiel, 1980) have been suggested, but not demonstrated.

2.3. REEVALUATION OF EXISTING DATA

As a result of different interpretations of the sense of metamorphic reactions, conflicting proposals were made for the evolution of the basement rocks. Barrovian zonation was initially interpreted (e.g. Dimitrescu, 1963; Savu, 1970; Streckeisen and Hunziker, 1975; Kräutner, 1980), but other researchers inferred that metamorphism in low-grade domains were retrograde, and that zonation is only apparent and resulted from retrograde metamorphism of medium- or high-grade crust (e.g., Balintoni, 1969; Popescu, 1974; Giuşcă et al., 1977; Hann and Sasz, 1984; Pană, 1990). The extent of reworking of metamorphic crust during Alpine orogeny is unclear. Basement rocks in the eastern Carpathians have been considered either as structurally rigid blocks unaffected by Alpine tectonism (eg.: Băncilă, 1965; Mutihac, 1974) or as slices involved in complex pre-Alpine and Alpine stacking (Săndulescu, 1984). In the southern Carpathians, continental crust originally interpreted as part of a single nappe (e.g., Murgoci, 1907) has also been interpreted as a stack of pre-Alpine and Alpine nappes (e.g., Balintoni et al., 1989).

In previous syntheses, the lithologic layering of metamorphic sequences was interpreted to be primary, foliations to be parallel to bedding, and metamorphic rocks to preserve primary structures (e.g. Codarcea, 1965; Kräutner, 1980; Dimitrescu et al., 1974). Lithostratigraphic "groups" with detailed stratigraphic columns were assigned to one of the three geosynclinal successions inferred to be separated by major depositional unconformities. Upon examination of these contacts, we were unable to locate basal conglomerates in several field localities in the southern Carpathians; rocks interpreted as basal arkosic transgressive beds are more likely brittlely deformed augen gneiss and granitic-microgranite. In the Apuseni Mountains, we interpret some horizons of metaconglomerate to be entirely tectonic in origin. Contacts interpreted as major thrusts by previous workers (e.g.: Hann and Sasz, 1984; Iancu, 1986; and even by one of us [Pană, 1990]) appear on reexamination to be slight lithologic contrasts or zones of slight retrograde metamorphic contrast, locally marked by faults.

We consider that domains mapped as Barrovian prograde zones or as distinct lithostratigraphic intervals are characterized instead by different intensities of retrograde metamorphism. Very-low-grade fault rocks are locally developed at domain margins; these rocks were previously considered as Carboniferous or Permian sedimentary deposits. We found them to range from gouge and cataclasite to tectonic breccia and conglomerate, and low-temperature mylonite.

Palynological data cited in support of lithostratigraphic models consist of microspores of Late Proterozoic or early to mid-Paleozoic age, reported from rocks considered to be simple prograde metamorphosed sedimentary strata (e.g. Codarcea and Iliescu, 1969; Olaru and Dimitrescu, 1990). The data are inconclusive, and may be suspect as most of the palynologically

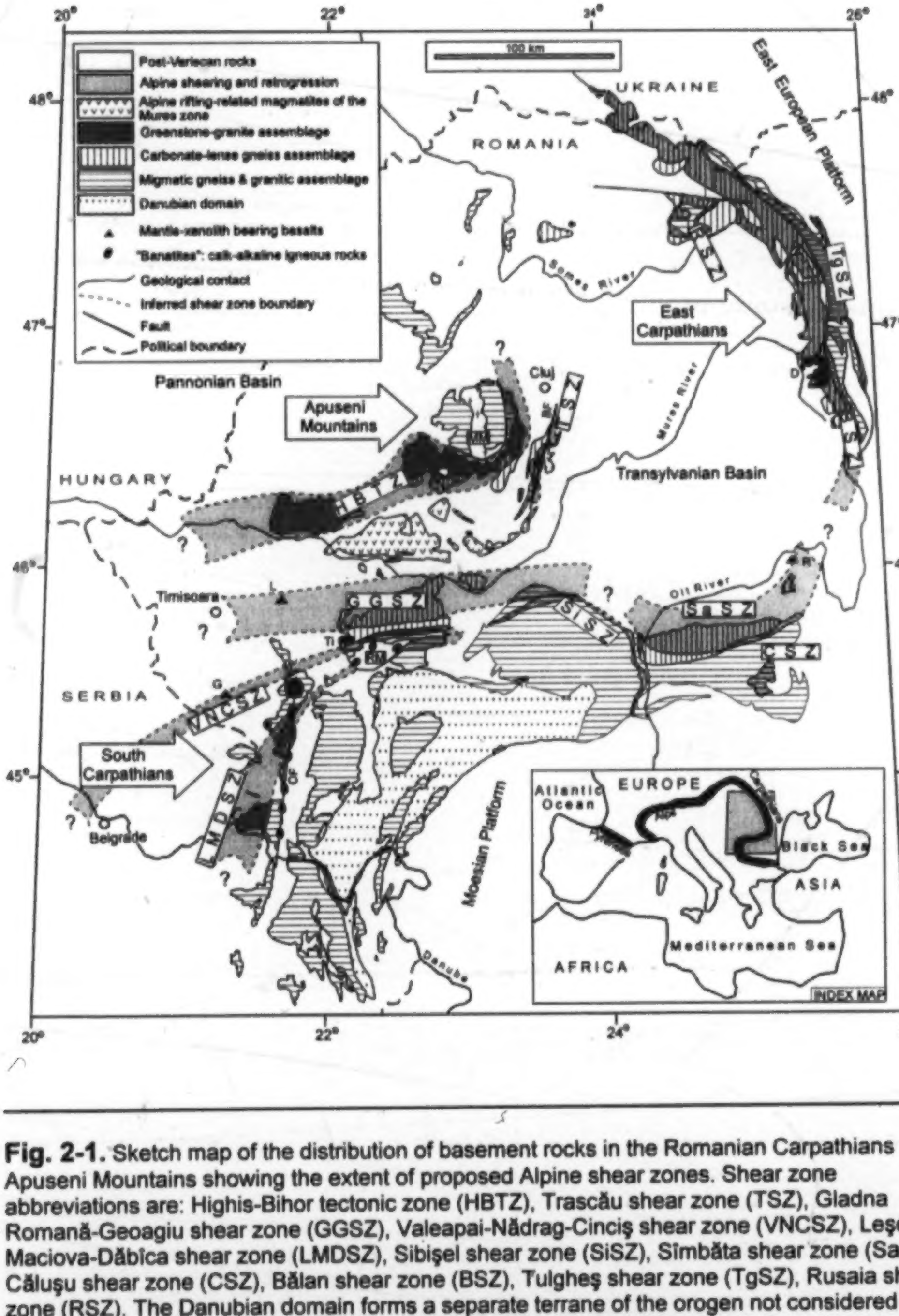
20°
22°
24°
26°
48°
47°
46°
45°
Post-Variscan rocks
Alpine shearing and retrogression
Alpine rifting-related magmatites of the Mures zone
Greenstone-granite assemblage
Carbonate-lense gneiss assemblage
Migmatic gneiss & granitic assemblage
Danubian domain
Mantle-xenolith bearing basalts
"Banatites": calk-alkaline igneous rocks
Geological contact
Inferred shear zone boundary
Fault
Political boundary
100 km
UKRAINE
ROMANIA
East European Platform
TgSZ
BSZ
Somes River
East Carpathians
Pannonian Basin
Apuseni Mountains
Cluj
TSZ
BF
MM
Mures River
Transylvanian Basin
D
RSZ
HUNGARY
HBTZ
Timisoara
L
GGSZ
SiSZ
Olt River
SaSZ
CSZ
R
T
Ti
RM
G
SERBIA
VNCSZ
South Carpathians
LMDSZ
OF
Belgrade
Moesian Platform
Danube
Atlantic Ocean
EUROPE
Alps
Black Sea
ASIA
AFRICA
Mediterranean Sea
INDEX MAP
?

Fig. 2-1. Sketch map of the distribution of basement rocks in the Romanian Carpathians and Apuseni Mountains showing the extent of proposed Alpine shear zones. Shear zone abbreviations are: Highis-Bihor tectonic zone (HBTZ), Trascău shear zone (TSZ), Gladna Romană-Geoagiu shear zone (GGSZ), Valeapai-Nădrag-Cinciş shear zone (VNCSZ), Leşcoviţa-Maciova-Dăbîca shear zone (LMDSZ), Sibişel shear zone (SiSZ), Sîmbăta shear zone (SaSZ), Căluşu shear zone (CSZ), Bălan shear zone (BSZ), Tulgheş shear zone (TgSZ), Rusaia shear zone (RSZ). The Danubian domain forms a separate terrane of the orogen not considered here. Open circles with letter abbreviation represent the following localities: D, Ditrău; L, Lucareţ; R, Racoş; T, Tomeşti. Named faults are OF, Oraviţa Fault; BF, Boerişte Fault. Other abbreviations: MM, Muntele Mare granite; Ti, Tincova Banatite; RM, Rusca Montană basin.

"dated" greenschist rocks have been later shown to be retrograded older metamorphic crust or even foliated igneous rocks (e.g. Hann and Sasz, 1984; Pană et al., 1991), suggesting the possibility of infiltration.

Isotopic age data are difficult to reconcile with proposed tectonic models. In medium- to high-grade metamorphic rocks, biotite yielded a Rb-Sr age of 840 Ma; in others, the oldest K-Ar mineral ages fall in the range 500-700 Ma, and K-Ar isochron ages are 850±50 Ma (cf. Kräutner, 1980); widespread mid-Cretaceous and younger K-Ar ages in low-grade rocks were originally interpreted to result from local resetting along faults, rather than from penetrative regional deformation (Soroiu et al., 1969; Kräutner, 1980). Recent $^{40}Ar/^{39}Ar$ analyses of medium- to high-grade metamorphic rocks in the South Carpathians yielded results of 294 to 309 Ma, and data from low grade rocks record two tectonothermal events, at 200 Ma and 118 Ma, respectively (Dallmeyer and Neubauer, 1993). These data hint that the last medium-grade metamorphic overprint is Variscan and show that the penetrative Alpine tectonism that affected at least some areas must be accommodated in regional interpretation.

2.4. NEW INTERPRETATION: ALPINE CRUSTAL SHEAR ZONES

2.4.1 Basement Rocks

Lithotype Associations. Using published data and preliminary results of field work, we have divided basement rocks into a sheared volcanic rock-gabbro-diorite and granite ("greenstone-granite") assemblage and two gneissic assemblages: type A, dominated by migmatitic gneiss and granitoid rocks with rare small eclogitic pods, and type B, dominated by large crystalline dolomitic and/or calcitic marble bodies and amphibolite. Original contact relations are masked by deformation and metamorphism.

Metamorphic History. The metamorphic history is best documented in the South Carpathians in type A crust, in where granulitic, eclogitic, and peridotitic bodies are preserved within medium-grade gneiss. Prograde medium-pressure mineral assemblages were variously overprinted by low pressure assemblages (Hârtopanu, 1975; Săbău et al., 1987). Şeclăman et al. (1987) proposed that nearly 80% of medium-grade metamorphic assemblages were retrograde. A discontinuous, cryptic blastomylonite zone hosting chloritoid is known (Hârtopanu et al., 1989). Wide areas of relict garnet ± kyanite ± staurolite in a greenschist matrix record shearing under chlorite-grade conditions (Pană, 1990; Stelea and Stelea, 1992). In the eastern Carpathians, medium-pressure parageneses overprinted by low-pressure assemblages have been reported (Balintoni and Gheuca, 1977) in type B crust, together with low-grade mylonitic reactivation.

2.4.2 Greenschist Shear Zones

We infer the existence of at least 10 discrete retrograde shear zones that may be part of an anastomosing network more than 1000 km long. These are (Fig. 2-1): the Highiş-Biharia tectonic zone (HBTZ), the Trascău , Gladna Română-Geoagiu, Valeapai-Nădrag-Cinciş, the Leşcoviţa-Maciova-Dăbîca, Sibişel, Sâmbăta, Căluşu, Bălan, Tulgheş, and the Rusaia shear zones. Although detailed study is needed to establish the outline of each shear zone and their interrelations, the zones have the following common features.

Extent, Orientation, Displacement. Greenschist rocks occupy in discontinuous linear domains between higher grade rocks. Their contacts are gradational and parallel to the local trend of the Carpathian orogen, except for the north-striking segment of the Sibişel shear zone, which cuts across regional strike. Although greenschist domains are dismembered along faults, locally juxtaposed, differentially exhumed, or buried beneath Tertiary deposits, most can be followed along strike for several tens of kilometres and some are continuously exposed for more than 200 km (Highiş-Biharia, Sibişel, Bălan, and Tulgheş shear zones). The Bălan shear zone correlates with a geophysically inferred fault (Socolescu et al., 1975), and the Valeapai-Nadrag-Cinciş shear zone coincides with a geophysical lineament that extends to Belgrade (Milan, 1989); both structures may exceed 500 km in length. The width of the zones varies from less than 1 Km (Sibişel, Trascău), to about 15 km (Highiş-Biharia, Gladna Română-Geoagiu, Tulgheş). A width of 3 km of completely reequilibrated rock is average.

Strike-slip displacement can be demonstrated for at least some of the shear zones: the offset of the Muntele Mare granite suggests a minimum of 20 km of sinistral displacement along the Highiş-Biharia shear zone and the geometry of the Rusca Montană basin (Săndulescu et al., 1978) suggests to us that it is a pull-apart, which implies about 30 km of late displacement along the Leşcoviţa-Maciova-Dăbâca shear zone; similarly, 40 to 50 km of dextral displacement along Sibişel shear zone is suggested by the outline of the Măgura-Cozia-Cumpăna augen-gneiss domain. On the basis of regional kinematic analysis, we suggest an initial left-lateral displacement for the Bălan and Tulgheş shear zones.

Metamorphic Conditions, Lithotectonic Assemblages. Reactions within the shear zones are retrograde. Shearing and fluid influx resulted in a symmetrical zonation about a relatively narrow axial zone where rehydration of medium-grade or magmatic parageneses commonly produced the assemblage chlorite + epidote + actinolite + albite + white mica + magnetite + quartz. The growth of chloritoid (in the Highiş-Biharia, Leşcoviţa-Maciova-Dăbâca, Sibişel, Bălan, and Rusaia shear zones), stilpnomelane (in the Leşcoviţa-Maciova-Dăbâca and Bălan shear zones), or margarite (in the Sibişel shear zone) may be the result of local strain rate variation. Domains of greenschist reequilibration are characterized by quartz-, carbonate-, and graphite-rich lenses of probable metasomatic origin. Although the size and proportions of quartzofeldspatic and mafic rock bodies vary widely at the outcrop scale, single or multiple layers of quartzite and/or carbonate schist to crystalline dolostone-limestone can be followed for tens of kilometres.

Rare gold, uranium, and sulphide occurrences are spatially and probably genetically related to the greenschist zones. Domains of albite schist several tens of square kilometers in area, some with higher-grade relict minerals, occur on both sides of the lowest-grade domains and indicate that fluids spread outside the axial zone. Lithotype and mineralogic assemblages in axial zones point to metamorphic conditions generally above the 400°C isotherm, but the range of retrograde metamorphism is wide. As indicated by the assemblage muscovite + margarite + quartz + fibrolite in garnet-kyanite micaschist within Sibişel shear zine (Stelea and Stelea, 1992), retrogression took place at high P-T conditions locally (500-520°C and 3.7-4.2 kb), and reequilibration temperatures as low as 280-250°C are indicated by calcite-dolomite geothermometry in carbonate lenses within the Highiş-Biharia shear zone (Pană, unpublished). Low-temperature fault-rocks such as breccia and gouge occur in many places.

Protoliths. Protoliths can be deduced from relations with adjacent prograde crust and from lithologic and mineralogic relicts. The Sâmbăta, Gladna Română-Geoagiu and Trascău shear zones are overprinted on mainly carbonate-lens gneiss crust, whereas the Tulgheş and Căluşu shear zones were developed mostly within granitic migmatitic-gneiss crust. Mylonitized granitoid bodies occur in the Tulgheş, Bălan, and Căluşu shear zones. The Rusaia and the Valeapai-Nădrag-Cinciş shear zones mark the general boundary between the two gneissic assemblages. The Highiş-Biharia and the Leşcoviţa-Maciova-Dăbâca shear zones are overprinted mainly on greenstone-granite assemblages; the Highiş-Biharia shear zone also affects the margin of the adjacent northern granitic gneiss terrane and of the southern carbonate-lens gneiss terrane. The Leşcoviţa-Maciova-Dăbâca shear zone affects adjacent granitic gneiss crust. Relict pods of gabbro-diorite and alkaline granite within the Highiş-Biharia (Pană et al., 1991) suggest a rift-like setting.

Ages of Shearing. The main retrogressive tectonism is sealed locally by unmetamorphosed cover as old as Permian(?)-Triassic (Highiş-Biharia, Sâmbăta, Bălan, and Tulgheş shear zones), or Jurassic (Căluşu and Trascău shear zones); basement-cover relations elsewhere are ambiguous. Contacts are commonly complicated by faults (Tulgheş, Bălan, and Sibişel shear zones) and unmetamorphosed pre-Late Cretaceous deposits do not overlie the axial parts of some shear zones (Highiş-Biharia, Trascău, Leşcoviţa-Maciova-Dăbâca, Sibişel). Greenschist belts mark crustal-scale discontinuities in which Alpine (Jurassic and Early to mid-Cretaceous) activity in at least some cases is indicated by K-Ar and $^{40}Ar/^{39}Ar$ isotopic data (Dallmeyer and Neubauer, 1993). Upper Cretaceous strata unconformably overlie parts of the belts and are affected locally by brittle strain and Late Cretaceous-Paleogene regional banatite (quartz diorite) intrusions follow the trend of the Oraviţa strike-slip fault (Fig. 2-1), slightly oblique to the Leşcoviţa-Maciova-Dăbâca shear zone. The Rusca Montană basin hosts Cretaceous-Paleogene clastic strata and coeval igneous rocks in a bend of the Leşcoviţa-Maciova-Dăbâca shear zone. The Tincova banatite is elongate parallel to the northern border of the Valeapai-Nădrag-Cinciş shear zone, and banatite intrusions and explosion breccias follow the trace of the Boerişte fault within the Trascău shear zone (Fig. 2-1). Undated small intrusions that may be coeval with the banatite suite occur along the east-trending segment of the Sibişel shear zone. Alpine doleritic sills are sheared and retrograde metamorphosed within Bălan shear zone (Popescu, 1974), but the 130 Ma-old Ditrău alkaline massif (Streckeisen and Hunziker, 1974) cuts that zone. Quaternary basalts hosting mantle xenoliths at Lucareţ and Racoş and Gătaia (Fig. 2-1) may pinpoint loci of extension along young faults overprinting the Gladna Română-Geoagiu and Sâmbăta zones, respectively. For all shear zones, isotopic ages and/or associated magmatism clearly indicate tectonic activity younger than inferred cover strata.

Internal Structure. Our reconnaissance data indicate that metamorphic rock units within the shear zones are tabular or linear, and contacts are gradational. Rock units display strong interfingering L-S shape fabric or random shape fabric, indicating polyphase deformation. Mesoscopic fold hinges are parallel or subparallel to the strike of the shear zones, and stretching lineations are everywhere parallel to fold hinges. Foliation is parallel to rock unit boundaries and ranges from steep to shallow dipping. We infer that a dominantly transpressional tectonic regime produced early steady-state ductile strain fabrics, and that brittle overprint at zone margins indicates strike-slip or thrust motion. Exceptions are the western part of the Highiş-Biharia tectonic zone, where we have observed top-to-the-northwest shear-sense indicators in southeast-dipping mylonite zones, and the Tulgheş shear zone, where a strike-parallel stretching lineation is overprinted by down-dip slickenlines indicating thrusting normal to the orogen. Isotopic age data show that the youngest medium-temperature fabrics are Variscan and the low-grade ones are Alpine.

2.5. SUMMARY AND CONCLUSIONS

We interpret the data to indicate that the Carpathian low-grade metamorphic belts are loci of repeated retrogressive metamorphism and deformation of higher grade polycyclic crust and associated igneous rocks. Basement rocks in continental fragments involved in Alpine tectonism in the Romanian Carpathians west of the former European platform consist of three Variscan lithotectonic assemblages: a "greenstone-granite" assemblage and two gneissic assemblages, one dominated by migmatic and granitoid rocks (type A) and the other by crystalline dolostone-limestone lenses (type B).

Early Alpine rifting (Triassic?- Jurassic) occurred within the type B crust; associated igneous activity is inferred to have occured in the Mureş zone (Fig. 2-1). Although the Mureş zone is traditionally interpreted as an oceanic remnant and the local expression of Tethys, the exposed magmatic suite is largely intermediate in composition. Because suturing juxtaposed the same (type B) lithologic assemblage on two relatively small "microplates", the ocean was probably not wide. We relate the geometry of most of the crustal-scale shear zones to tectonic inheritance from this early deformation phase. Shear-zone initiation could have been controlled by isostatic contrasts between crustal domains, but the locus of most intense strain likely migrated over time. Alpine strain concentration along at least some lineaments within the Variscan lithotectonic assemblages resulted in wide, generally steeply dipping tectonic discontinuities whose shallow parts are now exposed as greenschist belts. Reactivation in large strike-slip, transpressional, or extensional fault systems is recorded by igneous activity that follows the local strike of the zones. We propose that strain recorded by the greenschist belts accommodated most of the stress field in the Carpathian Orogen and is responsible for the Carpathian's double bend. The time when some of the shear zones began to form is probably Late Paleozoic, but Alpine activity is consistent with the present configuration of the Carpathian arc. Some zones were involved passively or actively in later deformation. Our observations strongly favor Burchfiel's (1980) suggestion that crustal fragments were repeatedly broken into smaller units and then welded and enlarged, so that their number and identity changed over time. On this basis, we consider unlikely the current interpretation of large rigid Cretaceous nappes involving basement rocks in the southern and eastern Carpathians. The extent and tectonic significance of the greenschist belts indicate that revisions to the interpretation of metamorphic rocks in the Romanian Carpathians and Apuseni Mountains must be made to accommodate Alpine tectonism.

REFERENCES

Balintoni, I., 1969, Asupra caracterului retromorf al paragneiselor biotitice cu clorit de pe Bîsca Groşetului (Făgăraş): Buletinul Societăţii Ştiinţifice de Geologie, v. XI, p. 275-281.

Balintoni, I., 1980, Date noi asupra poziţiei structurale a metamorfitelor din bazinul văii Putnei (Carpaţii Orientali): D.S. Institutul de Geologie si Geofizica, v. LXVI, 5, p. 25-36.

Balintoni, I., and Gheuca, I., 1977, Metamorphism progresiv, metamorphism regresiv şi tectonică în regiunea Zugreni-Barnar (Carpaţii Orientali): Dări de Seamă ale Institutului de Geologie şi Geofizică, v. LXIII/5, p.11-38.

Balintoni, I., Gheuca, I., and Vodă, Al., 1983, Alpine and Hercynian overthrust nappes from central and southern areas of the East Carpathian Crystalline-Mesozoic Zone: Anuarul Institutului de Geologie şi Geofizică, v. LX, p.15-22.

Balintoni, I., Berza, T., Hann, H.P., Iancu, V., Kräutner, H.G., and Udubaşa, G., 1989, Precambrian Metamorphics in the South Carpathians, Multilateral Cooperation of the Academies of Sciences of the Socialist Countries, Earth Crust Structure Evolution and Metallogeny, Guide to Excursions, 89 p.

Băncilă, I., 1965, Sur la tectonique des Carpathes Orientales: Carpatho-Balkan Geological Association, VII Congress, Sofia, Reports, Part I, p.257-266.

Bercia, I., Kräutner, H.G., and Mureşan, M., 1976, Pre-Mesozoic Metamorphites of the East Carpathians: Anuarul Institutului de Geologie şi Geofizică, v. L, p. 37-70.

Burchfiel, B.C., 1980, Eastern European Alpine System and the Carpathian Orocline as an Example of Collision Tectonics: Tectonophysics, v. 63, p.31-61.

Codarcea, D., 1965, Studiul geologic şi petrografic al regiunii Răşinari-Cisnădioara-Sadu: Memorii -Institutul de Geologie, v. VI, 87p.

Codarcea, D., 1967, La division des massifs cristallophylliens préalpins des Carpates Roumaines: Revue Roumaine de Géologie Géophysique Géographie, Serie Géologie, Tome 12/1, p. 57-63.

Codarcea, D., and Iliescu, V., 1969, Noi date microfloristice asupra vîrstei complexului calcaros al seriei de Sibişel: Studii şi Cercetări de Geologie Geofizică Geografie, Geologie, Tom 14/1, p.279-282.

Dallmeyer, R. D., and Neubauer, F., 1993, Variscan vs. Alpine tectonothermal evolution within the Southern Carpathians, Romania: evidence from ^{40}Ar/^{39}Ar mineral aes: GSA Annual Meeting, Boston, Mass., Abstract Volume, p. A-341.

Dimitrescu, R., 1963, Structura părţii centrale a Munţilor Făgăraşului: Carpato Balkan Geological Association, Congress V, v. 2, p. 17-25.

Dimitrescu, R., 1985, Early Caledonian Event in the Pre-Alpine Metamorphic Sequences of the Romanian Carpathians: Acta Mineralogica-Petrographica, v. XXVII, p. 59-70.

Dimitrescu, R., 1988, Elements structuraux préalpins dans le massif cristallin de Făgăraş: Dări de Seamă ale Institutului de Geologie şi Geofizică, v. VXXII-VXXIII/5, P. 59-68.

Dimitrescu, R., Bordea, J., and Bordea, S., 1974, Geologic Map of Romania 1: 50 000, Sheet 57c, Câmpeni, Institutul de Geologie şi Geofizică.

Gherasi, N., and Dimitrescu, R., 1964, Structura geologică a masivului Ezer-Păpuşa (Bazinul Râul Tîrgului): Dări de Seamă ale Comitetului Geologic, v. XLIX/1, p.13-25.

Gheuca, I., 1988, Versantul Sudic al Munţilor Făgăraş, Litostratigrafie şi tectonică: Dări de

Seamă ale Institutului de Geologie şi Geofizică, v. LXXII-LXXIII/5, p. 93-117.

Gluşcă, D., Savu, H., Bercia, I., and Kräutner, H.G., 1969, Sequence of tectonomagmatic pre-Alpine cycles on the territory of Romania: Acta Geologica Academiae Scientiarum Hungaricae, Tomus 13, p.221-234.

Gluşcă, D., Anastasiu, N., Popescu, Gh., and Şeclăman, M., 1977, Observaţii asupra şisturilor cristaline din zona centrală a masivului Făgăraş (Cumpăna-Valea Cîrţişoara): Analele Universităţii Bucureşti, Geologie, v. XXVI, p. 3-17.

Hann, H.P., and Sasz, L., 1984, Geological Structure of the Olt Valley between Cîineni and Brezoi (South Carpathians): Dări de Seamă ale Institutului de Geologie şi Geofizică, v. LXVIII/5, p. 23-37.

Hârtopanu, I., 1975, Le métamorphisme de basse pression dans les Monts Mehedinţi: Dări de Seamă ale Institutului de Geologie şi Geofizică, v. LXI/1, p. 217-238.

Hârtopanu, I., Conovici, M., Stelea, I., Săbău, G., 1989, Chloritoid bearing blastomylonites in the Cibin Mountains: Genetical and Structural Significances, Dări de Seamă ale Institutului de Geologie şi Geofizică, v. LXXIV, p. 209-228.

Iancu, V., 1986, Unités structurales supragétiques et infragétiques de la partie ouest des Carpathes Méridionales: Dări de Seamă ale Institutului de Geologie şi Geofizică, v. VXX-VXXI/5, p. 109-127.

Ianovici, V., Borcoş, M., Bleahu, M., Patrulius, D., Lupu, M., Dimitrescu, R., and Savu, H., 1976, Geologia Munţilor Apuseni, Editura Academiei, 631p.

Kräutner, H.G., 1980, Lithostratigraphic Correlation of Precambrian in the Romanian Carpathians: Anuarul Institutului de Geologie şi Geofizică, v. LVII, p. 229-296.

Kräutner, H.G., Năstaseanu, S., Berza, T., Stănoiu, I., and Iancu, V., 1981, Metamorphosed Paleozoic in the South Carpathians and its Relations with Pre-Paleozoic Basement: Carpatho-Balkan Geological Association, Congress XII, Guide to Excursion A 1, 116 p.

Milan, M.M., 1989, Extension of the ophiolitic belt in the basement of the Tertiary Pannonian basin: Carpatho-Balkan Geological Association, XIV Congress, Sofia, Abstracts Volume, p. 314-316.

Mureşan, M., Peltz, S., Seghedi, I., Szakacs, Al., Bandrabur, T., Kräutner, H.G., Săndulescu M., Mureşan, G., Peltz, M., and Kräutner, F., 1986, Geologic Map of Romania 1:50000, Sheet 62a, Voşlăbeni, Institutul de Geologie şi Geofizică.

Murgoci, G.M., 1907, Sur l'existence d'une grande nappe de charriage des Carpates méridionales: Buletinul Societătii de Ştiinte Bucureşti, v. XVI, p. 52-54.

Mutihac, V., 1974, Geologia Romaniei: Editura Tehnică Bucureşti, 646 p.

Olaru, L., and Dimitrescu, R., 1990, Contribuţii preliminare la cunoaşterea vîrstei seriei de

Păiuşeni din masivul cristalin Highiş: Romanian Journal of Stratigraphy, v. 1, p. 76-80.

Pană, D.I., 1990, Central and Northern Făgăraş-Lithological sequences and structure: Dări de Seamă ale Institutului de Geologie şi Geofizică, v.LXXIV/5, p. 81-99.

Pană, D.I., Balintoni, I., and Tatu, M., 1991, Low grade metamorphic series from the Arieş Valley (Apuseni Mountains). Studii şi Cercetări, Geologie, Academia Română, in press.

Popescu, Gh., 1974, Studiul formaţiunilor cristaline cu Sulfuri Metalice din Zona Bălan (Munţii Hăghimaş-Ciuc): Teză de doctorat, Universitatea Bucureşti, 114 p.

Ratschbacher, L., Linzer, H.G., Moser, F., Strusievicz, R.O., Bedelean, H., Har, N., and Mogos, P.A., 1993, Cretaceous to Miocene thrusting and wrenching along the central South Carpathians due to a corner effect during collision and orocline formation: Tectonics, v. 12, no. 4, p. 855-873.

Rădulescu, D., and Săndulescu, M., 1973, The Plate-Tectonics Concept and the Geological Structure of the Carpathians: Tectonophysics, v. 16, p.155-161.

Rădulescu, D., and Dimitrescu, R., 1982, Petrologia endogena a teritoriului R.S.Romania, Partea a III-a: Editura Universităţii Bucureşti, 120 p.

Reinhardt, M., 1909, Şisturile cristaline din Munţii Făgăraşului (clina română): Anuarul Institutului Geologic Roman, v. III, p. 165-265.

Royden, L., and Burchfiel, B.C., 1989, Are systematic variations in thrust belt style related to plate boundary processes? (The western Alps versus the Carpathians): Tectonics, v. 8, no. 1, p. 51-61.

Savu, H., 1970, Stratigrafia si izogradele de metamorfism din provincia metamorfică prebaikaliană din Munţii Semenic: Anuarul Institutului Geologic, v. XXXVIII, p. 223-311.

Savul, M., and Mastacan, G., 1952, Contribuţii la cunoaşterea gneiselor porfiroide din Carpaţii Orientali: Buletin ştiinţific al Academiei Republicii Populare Romane (Secţia biologie, agronomie, geologie, geografie), v. IV/2, p. 427-439.

Săbău, G., Bindea, G., Hann, H.P., Ricman, C., and Pană, D.I., 1987, The metamorphic evolution of the low pressure terrain in the central South Carpathians (Getic Nappe): Geologicky Zbornik, v. 38/6, p. 735-754.

Săndulescu, M., 1967, La nappe de Hăghimaş, une nouvelle nappe de décollement dans les Carpathes Orientales: Carpato-Balkan Geological Association, VIII Congress, Belgrade, Reports I, p. 179-185.

Săndulescu, M., Kräutner, H., Borcoş, M., Năstaseanu, S., Patrulius, D., Ştefăanescu, M., Ghenea, C., Lupu, M., Savu, H., Bercia, I., and Marinescu, F., 1978, Geologic Map of Romania, Scale 1: 1000 000.

Săndulescu, M., 1984, Geotectonica României, Editura Tehnică, 323 p.

Socolescu, M., Airinei, S., Ciocirdel, R., and Popescu, M., 1975, Fizica şi structura scoarţei terestre din Romania: Editura tehnică, Bucureşti.

Soroiu, Gh., Popescu, Gh., Kasper, U., and Dimitrescu, R., 1969, Contributions préliminaires à la géochronologie des massifs cristallins des Monts Apuseni: Anuarul Stiinţific al Universităţii "Al.I. Cuza" Iaşi, Secţiunea II,b (Geologie), v. XV, p. 25-33

Streckeisen, A., 1937, Le Mésozoïque de Tomeşti (Dep. de Ciuc, Carpates orientales): Comptes Rendus des Séances, Institut Géologique de Roumanie, v., p. 85-89.

Streckeisen, A., and Hunziker, J.C., 1974, On the Origin and Age of the Nepheline Syenite Massif of Ditro (Transylvania, Rumania): Schweizer Mineralogische Petrographische Mitteilungen, Bd. 54/1, p. 59-77.

Stelea, I., and Stelea, G., 1992, Margarite in Dynamically Metamorphosed Micaschists in the Cibin Mountains, South Carpathians: Romanian Journal of Mineralogy, v. 75, Supplement No.1, p. 41-42.

Şeclăman, M., Hîrtopanu, I., and Mărunţiu, M., 1987, Types of mineral reactions in the Carpathian metamorphic areas: Revue Roumaine de Géologie Géophysique, Géographie, Série Géologie, Tome 31, p. 29-38.

Trümpy, R., 1988, A possible Jurassic-Cretaceous transform system in the Alps and the Carpathians: Geological Society of America Special Paper, v. 218, p. 93-109.

CHAPTER 3*

PRE-ALPINE TECTONIC FRAMEWORK OF THE APUSENI MOUNTAINS: CONSTRAINTS FROM A Sm-Nd AND U-Pb ISOTOPIC STUDY ON THE METAMORPHIC AND IGNEOUS BASEMENT ASSEMBLAGES

---

* *A version of this chapter has been submitted to Journal of Geology by D. I. Pană, L. H. Heaman, R.C. Creaser, and P. Erdmer*

3.1. INTRODUCTION

The Apuseni Mountains represent the largest basement exposure between the Carpathians and Dinarides branches of the Alpine orogen. The Alpine evolution of the Apuseni Mountains has been debated in an impressive number of contributions, whilst the pre-Alpine evolution of the crust is largely speculative due to the lack of analytical data.

Recent geodynamic models agree to a certain degree upon the Cenozoic extent, nature of boundaries and geodynamic evolution of the Apuseni crustal fragment (e.g., Kovács et al., 1989; Márton and Mauritsch, 1990; Csontos et al., 1992; Haas et al., 1995). However, the Early Alpine evolution is controversial. In some reconstructions (e.g., Săndulescu, 1988) the Apuseni Mountains belong to a large crustal fragment that includes the Austroalpine units of the Alps and hence would have an African origin. In other reconstructions (e.g., Balla, 1982), the Apuseni fragment is interpreted as a slice of European crust.

The European Alpine belt is superposed on the wider Variscan belt. The Variscan orogen is currently interpreted as a collage of various tectono-stratigraphic units accreted along the northern margin of Gondwana during Early to Late Carboniferous transpressional collision (von Raumer and Neubauer, 1993). Extensive petrological and geochronological studies in the Alps and in the extra-Alpine Variscides have resulted in a relatively well constrained Late Proterozoic - Paleozoic evolutionary model. Attempts to integrate basement units from southeastern Europe into the model are based almost exclusively on lithostratigraphic correlations (e.g., Kräutner, 1988; Neubauer and Raumer, 1994). Precambrian and Paleozoic tectonothermal events have been inferred in the basement units of the Apuseni Mountains (e.g., Giuşcă et al., 1969; Kräutner, 1980; Dimitrescu, 1986). A widespread low-grade Alpine overprint affected the basement units of the Apuseni Mountains (Pană and Erdmer 1994). Alpine vs. Variscan tectonothermal evolution has been recently constrained by $^{40}Ar/^{39}Ar$ data on metamorphic rocks (Dallmeyer et al., 1998).

We present the first set of Sm-Nd and U-Pb data on representative lithotectonic assemblages and associated igneous rocks that constitute the Apuseni crustal fragment, in an attempt to reveal its ancient geological history and relationships to other Variscan terranes incorporated elsewhere as basement units in the Alpine orogen. Sm-Nd analysis on gneissic assemblages of the Apuseni and Carpathians mountains yielded similar Early Proterozoic crustal residence ages. The U-Pb zircon data indicate that several Paleozoic tectonomagmatic events documented in the Alps can be partly recognized in the basement rocks of the Apuseni Mountains. Low-grade assemblages traditionally attributed to the Variscan orogeny record in fact Alpine strain overprinting mainly Permian igneous rocks. However, further extensive petrological studies are needed to substantiate the appurtenance of a dated magmatic event to a certain pre-Alpine geotectonic setting in order to attempt the reconstruction of the Variscan orogen anatomy.

3.2. GEOLOGICAL UNITS, PREVIOUS ISOTOPE DATA

Amphibolite, epidote-amphibolite and greenschist facies assemblages were defined in the central and northern Apuseni Mountains (e.g., Giuşcă et al., 1968, Dimitrescu 1985). In the absence of reliable age data, the metamorphic rocks were traditionally assigned to either a Middle Proterozoic, a Late Proterozoic/Cambrian or Caledonian and a Variscan tectonomagmatic cycle, with the higher metamorphic grade rocks being the oldest. The age of the spatially associated igneous rocks were assigned assuming that they represent the magmatic activity during the tectonometamorphic event that affected the surrounding metamorphic assemblages. Stratigraphic and metamorphic unconformities were interpreted between rocks assigned to different tectonomagmatic cycles. Although the location and nature of these contacts are controversial (Balintoni, 1985; Dimitrescu, 1988) and the existing K-Ar data (Soroiu et al., 1969; Pavelescu et al., 1975) are inconsistent with the postulated evolutionary model, the stratigraphic systematics of the basement rocks is extensively used.

Recent recognition of a large component of non-coaxial strain and of the retrograde character of the metamorphic reactions in the low-grade assemblages (Pană and Erdmer, 1994) and systematic $^{40}Ar/^{39}Ar$ dating of low- and medium grade rocks (Dallmeyer et al., 1998) resulted in a different interpretation: the low-grade assemblages define a kilometre wide arcuate belt of polyphase Alpine strain concentration, the Highiş-Biharia Shear Zone (HBSZ). It can be traced across the Apuseni Mountains from the southern Pannonian Basin to the northern Transylvanian basin (Fig. 3-1). On either side, medium-grade rocks define distinct lithologies: to the north the Someş gneiss-granitic assemblage and the Codru amphibolite-granitoidic assemblage, and to the south the Baia de Arieş carbonate lenses gneissic assemblage.

The low-grade assemblages within the Alpine shear zone are defined by distinct lithologic and mineral relics, but have no stratigraphic connotation. In the axial zone of the belt the rocks are phyllonite and metre to kilometre size igneous pods. The igneous rocks show a range of chemical compositions and grain-sizes indicative for an upper crustal igneous complex. The protolith of the the HBSZ phyllonite is uncertain. Igneous textures are progressively obliterated towards the peripheries of the pods until completely losing their identity within the phyllonitic matrix which may indicate that most phyllonitic rock-types derived from igneous protoliths (Pană and Ricman, 1988). Partial overlapping between the field of igneous acidic rocks and that of the quartz-clast bearing schist ("metaconglomerate") samples suggest direct derivation of the schist from granitoids by shearing accompanied by loss of alkalies and relative enrichment in quartz (Appendix II, Figs. II-1 and II-2).

In the westernmost segment of the HBSZ, the Highiş Mountains expose an igneous complex, tens of square kilometres wide, wrapped in a mesh of phyllonite with undigested pods of gabbro-diorite-monzodiorite and tonalite-adamellite-granite (Appendix II, Fig. II-1). The

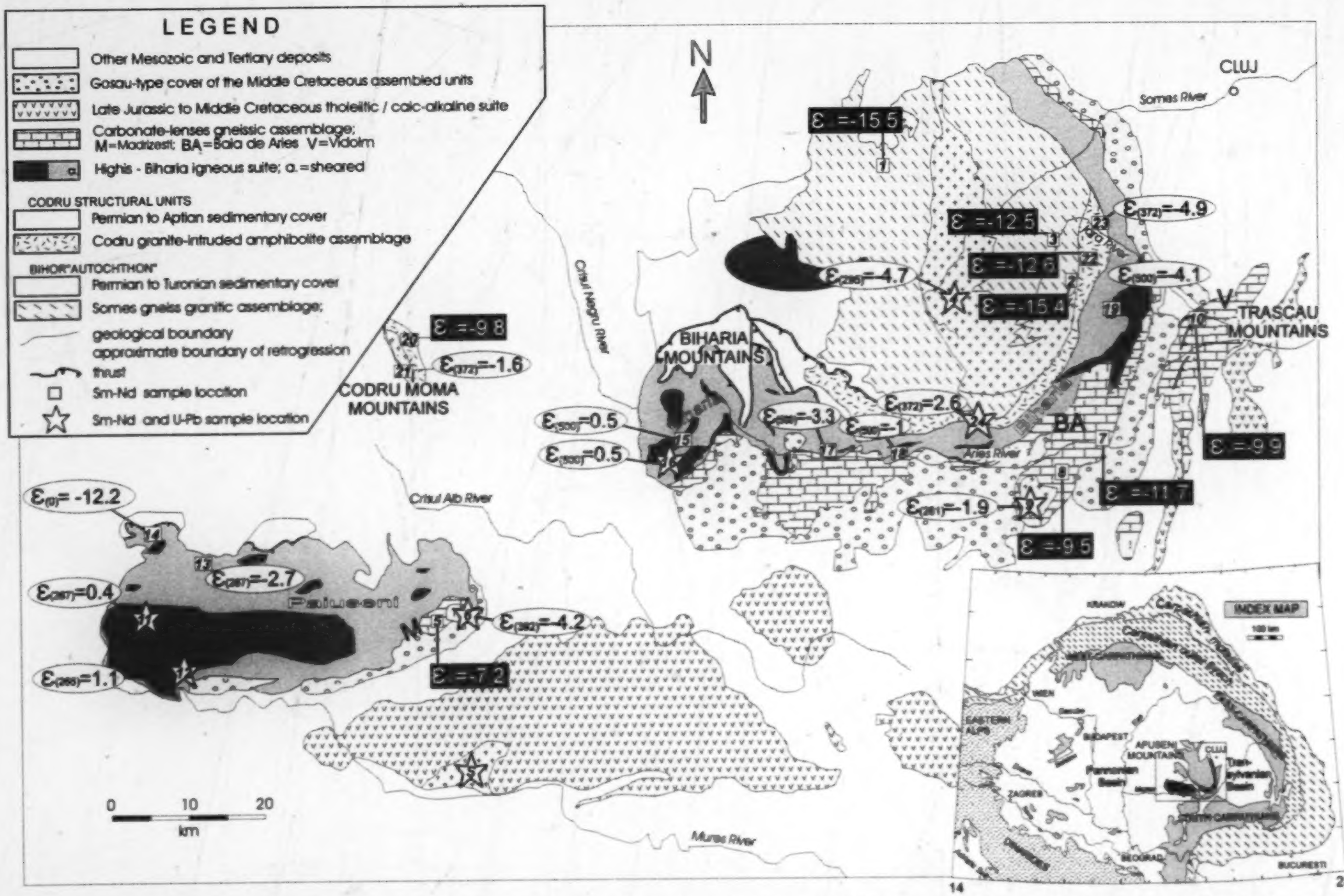
LEGEND
Other Mesozoic and Tertiary deposits
Gosau-type cover of the Middle Cretaceous assembled units
Late Jurassic to Middle Cretaceous tholeiitic / calc-alkaline suite
Carbonate-lenses gneissic assemblage; M=Madrizesti; BA=Baia de Aries V=Vidolm
Highis - Biharia igneous suite; a.=sheared
CODRU STRUCTURAL UNITS
Permian to Aptian sedimentary cover
Codru granite-intruded amphibolite assemblage
BIHOR"AUTOCHTHON"
Permian to Turonian sedimentary cover
Somes gneiss granitic assemblage;
geological boundary
approximate boundary of retrogression
thrust
Sm-Nd sample location
Sm-Nd and U-Pb sample location
N
CLUJ
Somes River
Crisul Negru River
Crisul Alb River
Aries River
Mures River
BIHARIA MOUNTAINS
CODRU MOMA MOUNTAINS
TRASCAU MOUNTAINS
BA
V
M
Pauseni
ε =-15.5
ε =-12.5
ε =-12.6
ε =-15.4
ε =-9.8
ε =-9.9
ε =-11.7
ε =-9.5
ε =-7.2
ε(372)=-4.9
ε(500)=-4.1
ε(290)=-4.7
ε(372)=-1.6
ε(500)=0.5
ε(500)=0.5
ε(290)=-3.3
ε(290)=-1
ε(372)=2.6
ε(261)=-1.9
ε(0)= -12.2
ε(287)=-2.7
ε(287)=0.4
ε(285)=1.1
ε(382)=-4.2
0 10 20
km
INDEX MAP
14
28
45
EASTERN ALPS
WIEN
BUDAPEST
APUSENI MOUNTAINS
CLUJ
Pannonian Basin
Transylvanian Basin
ZAGREB
BEOGRAD
BUCURESTI
SOUTH CARPATHIANS
KRAKOW

Fig. 3-1. Sketch map of the Apuseni Mountains with the sample locatinons; in ellipses - εNd$_{(t)}$ for granitoid rocks at the time of intrusion (known or inferred); in dark rectangles - εNd$_{(0)}$ for gneisses; numbers in white squares and stars are sample numbers as in Tables 3-1 and 3-2.

igneous rocks were previously interpreted to intrude a prograde greenschist facies assemblage and were consequently assigned to the Variscan event (e.g., Giuşcă et al. 1968). In a limited area near the western extremity of the Highiş Mountains, an association of black to gray massive rocks and their sheared equivalents, were initially mapped as black quartzite and shale (Giuşcă, 1979) and interpreted to represent a post-Variscan Carboniferous (Permian?) sedimentary cover named the "Black Series" (BS). Commonly, a very fine grained mesh of mica-quartz-albite-magnetite with epidote nests overprints and obscures the original texture. Similar rocks, later described from additional locations were shown to be low temperature hornfelses up to biotite isograde (Pană and Ricman, 1988), spatially and genetically related to basalt, quartz-latiandesite and trachyte of the Highiş igneous complex. Completely hornfelsed rocks plot in the latibasalt and trachyte fields and show a more alkali character than the associated igneous rocks (Appendix II, Figs. II-1 and II-2).

K-Ar age data ranging from 75 to 123 Ma (Soroiu, et al. 1969; Pavelescu et al., 1975) and ^{40}Ar/^{39}Ar plateau ages of 100-114 Ma on the low-grade rocks (Dallmeyer et al. 1997) indicate Early to Middle Cretaceous tectonism. A 350 Ma whole rock K-Ar age is the only isotope data reported so far on a granite sample from the Highiş Mountains (Giuşcă et al. 1968).

Along the HBSZ to the east, in the Biharia and Gilău mountains weakly to highly sheared gabbro-quartz diorite and granodiorite-tonalite (trondhjemite) units suggesting a bimodal magmatism (Appendix II, Fig. II-1c), are interlayered with subordinate phyllonite. Sheared and hydrated diorite bodies were previously interpreted as epidote-amphibolite facies clastic sediments and consequently assigned to the Caledonian event (e.g. Dimitrescu, 1985;1988). Balintoni (1986) interpreted the mafic rocks from Highiş and Biharia mountains to represent Caledonian ophiolitic crust and the granitic rocks to represent the Variscan magmatism. This model also assumes two metamorphic events contemporaneous with the intrusions, although the only available data were K-Ar ages ranging from 143 to 76 Ma (Pavelescu et al., 1975). An ^{40}Ar/^{39}Ar plateau age of c. 108 Ma and several Jurassic and Cretaceous Total Gas Ages were recently reported from the phyllonite in the Biharia Mountains (Dallmeyer et al. 1998).

Mafic rocks from the HBSZ show ambiguous chemical characteristics inconsistent with the classical patterns constrained for major tectonic settings. Same rocks plot within different fields in different discrimination diagrams or outside the defined fields (Appendix II, Figs. II-2 and II-3). Rocks from the eastern sector of the HBSZ (Highiş Mountains) with a more pronounced tholeiitic character plot in the "ocean floor" and "within plate" fields whilst rocks from the eastern segment (Biharia and Gilău mountains) show a calc-alkaline tendency and plot in the "ocean floor" and "island arc" fields (Appendix II). However, the initiation of magmatic activity with mafic intrusions along the entire HBSZ suggests a pre-Alpine rift-like setting with more advanced extension across the western segment. The pre-Alpine crustal thinning / weakness is also inferred from its overprinting by a wide Alpine shear zone.

Whereas no medium-grade relics exist within the axial zone of the belt, toward the peripheries, retrogressed medium-grade protoliths can be traced into the adjacent gneissic-amphibolitic assemblages.

To the north, HBSZ is bounded by the Codru assemblage which consists of a discontinuous belt of orthoamphibolite and their gabbroic protolith, invaded by multiple phases of diorite to granite intrusions. The cross-cutting relationships within individual exposures are difficult to correlate due to the limited size and variable chemistry of the granitoid bodies and widespread low-grade shearing. Two-mica gneisses are interlayered mainly in the western part and appear to be derived from two-mica granodiorite. K-Ar data on rocks assigned to the Codru assemblage range between 243-596 Ma (Giuşcă et al., 1968; Soroiu et al., 1969; Pavelescu, et al., 1975). Recent $^{40}Ar/^{39}Ar$ data on an hornblende concentrate from the orthoamphibolite and muscovite from gneiss samples yielded ages of c. 366 to 405 Ma and c. 335 to 340 Ma, respectively (Dallmeyer et al., 1998).

The lithology gradually changes northward into the Someş assemblage, dominated by monotonous micaceous gneisses, with interlayers of quartzofeldspathic gneisses and scarce amphibolite. The presence of garnet and staurolite zone followed by local sillimanite growth have been interpreted as evidence for a poly-metamorphic evolution (Hârtopanu and Hârtopanu, 1986). The Someş assemblage is intruded by the Muntele Mare granite. The contact is overprinted by a kilometre wide biotite to chlorite zone normal detachment. K-Ar data on the Someş assemblage yielded a wide range of values 77- 381 Ma (Soroiu et al., 1969; Pavelescu, et al., 1975). $^{40}Ar/^{39}Ar$ data on hornblende and muscovite concentrates yielded ages of c. 316-306 Ma and c. 303-314 Ma, respectively and were interpreted to date rapid cooling following the Variscan metamorphic event (Dallmeyer et al., 1998).

To the south, the low-grade assemblages of HBSZ are bounded by a gneissic assemblage dominated by kilometre-size lenses of variable dolomitic marble. The contact is gradational and often obscured by sheared granites of uncertain appurtenance. The gneiss-carbonate assemblage crops out in several isolated 'islands' along the southern margin of the Apuseni crustal fragment (Fig. 3-1). From west to east these are the Mădrigeşti, Baia de Arieş and Vidolm exposures of gneiss-carbonate assemblages. Unfortunately, detailed lithologic correlation is not possible, so different local names are still in use. However, a striking lithologic difference compared to the northern Someş assemblage is the presence of carbonate rocks with similar C-O isotopic signature (Pană et al., 1996) in all these relatively limited gneissic exposures south of HBSZ. The gneisses are intruded by concordant granite bodies up to several hundreds metres in size at Mădrigeşti and Surduc and by the Vinţa stock at Baia de Arieş. A polyphase tectonometamorphic evolution is indicated by metamorphic textures and

$^{40}Ar/^{39}Ar$ data. Different $^{40}Ar/^{39}Ar$ cooling ages in different 'islands' suggest heterochroneous Alpine tectonism along the now, southern margin of the Apuseni crustal fragment from Middle Jurassic (c. 156 Ma, Vidolm) to Early-Middle Cretaceous (c. 119-111 Ma, Baia de Arieş) (Dallmeyer et al., 1998).

3.3. U-Pb GEOCHRONOGY OF IGNEOUS ROCKS

The age of the intrusive units in the basement of the Apuseni Mountains was previously arbitrarily assigned based on the interpreted age of the associated metamorphic assemblages. We have selected seven granitoid samples from the most representative lithotectonic assemblages (Fig. 3-1) in order to constrain the pre-Alpine tectonomagmatic evolution of the region. A sample from the Savirsin granite intruding the supposed Tethyan suture in the southern Apuseni was analysed in order to constrain the Early Alpine evolution of the Apuseni fragment. Three to five zircon fractions have been analysed from each sample using the isotope dilution thermal ionization (TIMS) method.

Analytical procedure

10 to 15 kilograms of rock samples were pulverized to a fine powder with a jaw crusher and Bico mill and then passed over a Wilfley Table to obtain a heavy mineral concentrate. Zircon was separated from this concentrate using standard heavy liquid and magnetic mineral separation techniques outlined by Heaman and Machado (1992). Further zircon selection was made using a binocular microscope to avoid grains with cracks, alteration, inclusions or other imperfections. Multi-grain fractions were selected based on distinct optical features and grain quality for each sample. All the zircon fractions were abraded following the abrasion technique outlined by Krogh (1982) and washed prior to dissolution (Krogh, 1973; Heaman, 1986) The zircon fractions were spiked with a mixed ^{205}Pb-^{235}U tracer solution (Krogh and Davis, 1975). Sample dissolution and the extraction of Pb and U follows closely the procedure of Krogh (1973). Pb and U blanks measured during this study were progressively improved from 40 pg to 1.4 pg and from 0.36 pg to 0.06 pg, respectively.

Pb and U were loaded onto outgassed, single Re filaments in a silica gel-phosphoric acid mixture and analysed on a VG354 mass spectrometer. The Pb isotopic ratios were measured on a single Faraday cup collector and for a typical load of 10 ng of Pb the average beam intensity at mass 206 (1,450°C) was 0.5×10^{-11}A (10^{11}ohm resistor). All the Pb and U isotopic data were corrected for mass fractionation using factors of +0.088% /AMU for Pb and +0.155% /AMU for U (based on replicate analysis of the NBS-SRM 981common Pb and the NBS-SRM U 500 standards) and for isotopic ratios measured with a Daly photomultiplier detector, a Daly-Faraday empirical conversion factor of +0.13% / AMU was applied.

The errors associated with the Pb/U and $^{207}Pb/^{206}Pb$ ratios, are estimated to be 0.25 and

0.05% (1σ), respectively (numerical propagation of all known sources of error) based on the reproducibility of samples. The initial common Pb isotopic composition was calculated using the model proposed by Stacey and Kramers (1975). The regression lines and the errors associated with the age determinations (quoted at the 95% confidence level) were calculated using the ISOPLOT software (version 2.12 by K. Ludwig, USGS). The decay constants for ^{235}U (9.8485 x 10^{-10}yr^{-1}) and ^{238}U (1.55125 x 10^{-10}yr^{-1}) and the isotopic composition of uranium (137.88) used in this study are those recommended by Jaffey et al. (1971) and the IUGS Subcommission on Geochronology (Steiger and Jäger, 1977).

Results

U-Pb zircon data are summarized in Table 3-1.

Granitoid intrusions associated with the gneissic assemblages contain an invisible inherited radiogenic Pb component that is common for granitoids of anatectic origin. In contrast, the Codru granodiorite and two of the three analysed granitoids within the phyllonitic belt do not show radiogenic Pb inheritance consistent with a non-contaminated juvenile source.

Two samples from the Highiş igneous complex were selected in an attempt to bracket the age of the magmatism. Field relationships unequivocally indicate that crystallisation of mafic rocks was followed by granitoid intrusion and veining (Fig 5-5). An alkali-diorite (sample 11) previously assigned either to the initial phase of Variscan magmatism (Giuşcă, 1979; Savu, 1965) or to the Caledonian ophiolitic crust (Balintoni, 1986) was selected as a representative sample for the initiation of the igneous activity. Three multi-grain fractions of optically clean, euhedral zircons have been separated from the Cladova diorite. The first best fraction consisted in fluid inclusion-free, strongly abraded grains. The three near concordant analyses yield a discordia array with an upper intercept age of 267+/-4 Ma (Fig. 3-3a) which is interpreted as the emplacement age for the mafic rocks. A sample of porphyric microgranite (sample 12) was selected as the best estimate for the cessation of the igneous activity. Three fractions of tiny zircons yielded three points on a discordia array with an upper intercept age at 264+/-2 Ma (Fig. 3-3b). U-Pb zircon data on intrusive rocks from the Highiş Mountains indicate a relatively short lived (267-264 Ma) igneous event in late Early Permian and roll out the previous interpretations.

A weakly deformed granite from the Biharia Mountains (sample 16) was selected in order to investigate the assumed correlation of the igneous pods along the Alpine Highiş-Biharia Shear Zone. Under the microscope, a homogeneous population of tiny zircon grains show obvious core structure, interpreted as zircon inheritance (Fig. 3-2a). Two multi-grain fractions of tiny euhedral zircons yielded two data points 10% and 14% discordant, respectively. A regression line through origin and the two analysis intersect the concordia line at 516+/-8 Ma (Fig. 3-3c), and is tentatively interpreted as the best approximation of the emplacement age

Table 3-1. Summary of U-Pb zircon data on igneous rocks of the Apuseni Mountains

	Fr.	Weight	U	Pb rad	Th	TC Pb	206/204*	Atomic ratios**			Apparent age (Ma)			Discord.
		mg	*(ppm)*	*(ppm)*	*(ppm)*	*(pg)*		*206Pb/238Pb*	*207Pb/235Pb*	*207Pb/206Pb*	*206/238*	*207/235*	*207/206*	%
NORTHERN GNEISSIC ASSEMBLAGE														
4	1	0.134	1299	56	207	55.73	8828	0.04555; 15	0.32785; 109	0.05222; 4	**287**	**288**	**295**	*2.7*
Muntele	2	0.027	950	41	186	11.85	6152	0.04526; 14	0.32595; 107	0.05223; 5	**285**	**286**	**295**	*3.5*
Mare	3	0.064	902	30	137	41.86	3925	0.04537; 14	0.33210; 108	0.05309; 4	**286**	**291**	**332**	*14.3*
24	1	0.040	264	16	114	7.28	5415	0.06008; 20	0.44751; 158	0.05402; 6	**376**	**376**	**372**	*-1.2*
Codru	2	0.034	291	17	127	5.67	6254	0.05774; 19	0.43026; 148	0.05404; 5	**362**	**363**	**373**	*3.0*
	3	0.125	285	17	125	13.32	9610	0.05719; 14	0.42601; 133	0.05402; 4	**359**	**360**	**372**	*3.7*
	4	0.060	3325	19	155	12.20	5646	0.05614; 26	0.41810; 198	0.05401; 5	**352**	**355**	**372**	*5.4*
HIGHIS-BIHARIA IGNEOUS COMPLEX														
11	1	0.685	534	24	339	29.84	32274	0.04198; 24	0.29886; 175	0.05160; 3	**265**	**265**	**268**	*1.0*
Cladova	2	0.806	358	16	222	34.26	21783	0.04132; 14	0.29428; 100	0.05164; 3	**261**	**262**	**270**	*3.3*
	3	1.158	429	19	269	44.76	28780	0.04141; 16	0.29482; 118	0.05166; 3	**262**	**262**	**270**	*3.3*
12	1	0.124	1399	58	546	125.00	3597	0.04111; 26	0.29230; 169	0.05156; 5	**260**	**261**	**266**	*2.4*
Jernova	2	0.056	2301	96	1058	369.09	891	0.04026; 28	0.28683; 739	0.05157; 13	**253**	**256**	**267**	*4.6*
	3	0.050	1208	48	474	48.16	3070	0.03885; 16	0.27711; 424	0.05173; 6	**246**	**248**	**273**	*10.4*
16	1	0.025	219	17	69	14.83	1854	0.07820; 18	0.61803; 167	0.05732; 8	**485**	**489**	**504**	*3.8*
Leucii	2	0.075	240	18	75	31.48	2724	0.07551; 28	0.59480; 239	0.05713; 8	**469**	**474**	**497**	*5.7*
SOUTHERN GNEISS-CARBONATIC ASSEMBLAGE														
6	1	0.275	213	13	59	55.83	2942	0.05979; 35	0.44961; 162	0.05454; 7	**374**	**377**	**393**	*5.0*
Madrigesti	2	0.299	200	12	57	7.78	28256	0.05881; 15	0.44174; 141	0.05448; 4	**368**	**371**	**391**	*5.9*
	3	0.362	224	13	61	14.37	20934	0.05925; 23	0.46618; 181	0.05707; 7	**371**	**389**	**494**	*25.7*
9	1	0.039	726	29	38	264.19	241	0.03325; 11	0.23591; 205	0.05146; 41	**211**	**215**	**261**	*19.7*
Vinta	2	0.005	4610	176	228	199.78	327	0.03976; 11	0.36385; 182	0.06637; 27	**251**	**315**	**818**	*70.6*
	3	0.139	1013	43	46	997.35	397	0.04295; 12	0.45077; 186	0.07612; 23	**271**	**378**	**1098**	*76.9*
	4	0.024	336	18	37	24.57	1147	0.05431; 14	0.45585; 141	0.06088; 9	**341**	**381**	**635**	*47.5*
TRANSYLVANIAN IGNEOUS COMPLEX ("TETHYS")														
S	1	0.643	683	19	625	110.85	6062	0.02435; 13	0.16544; 89	0.04927; 4	**155**	**156**	**161**	*3.4*
Savarsin	2	0.093	573	16	497	11.32	7160	0.02422; 6	0.16461; 51	0.04930; 7	**154**	**155**	**162**	*4.8*
	3	0.189	270	3	245	10.95	2441	0.00830; 3	0.05389; 21	0.04721; 9	**53**	**53**	**55**	*3.4*

* Spike and fractionation corrected only

** Atomic ratios corrected for fractionation, blank, spike, initial common Pb; 1 sigma errors (inheritance can not be precluded). This Late Cambrian age for the granite sample from the Biharia Mountains contrasts significantly with the Permian age of the igneous complex from the Highiş Mountains. The heterochronous character of the igneous protolith within HBSZ indicates that geotectonic setting reconstructions based on geochemical data may be irrelevant unless the emplacement age of several other major intrusions along the magmatic arc are determined.

From the Codru assemblage, we have selected a representative two-mica granodiorite sample (sample 24). It shows no medium grade metamorphic record being only affected by localized low-grade shearing. Four multi-grain fractions of colourless, transparent, well abraded zircons (Fig. 3-2c) define a discordia array with an upper intercept age of 372+/-1 Ma (Fig. 3-4a). Under the microscope, the transparent, colourless, euhedral prismatic to needle-like zircon grains show no visible sign of disturbance or core structure. The upper intercept age is interpreted as emplacement age of the Codru granodiorite (Middle-Late Devonian). The amphibolite grade metamorphism is constrained to be pre-Late Devonian, and therefore can not be related to the Early Carboniferous main phase of Variscan collision/ metamorphism.

A granite sample from the central part of the Muntele Mare batholith (sample 4) was selected in order to put an upper limit on the last medium-grade overprint of the northern Someş gneissic assemblage. Two slightly discordant multi-grain fractions (1 and 2 in Fig. 3-4b) yielded $^{207}Pb/^{206}Pb$ ages of 295 Ma. The selected grains of fraction 1 were long prismatic, euhedral, transparent small zircon crystals whereas fraction 2 consisted of transparent fragments of larger prismatic crystals. The regression line through analysis 1, 2 and origin intersects the concordia line at 295+/-1 Ma. We interpret the upper intercept age as the minimum emplacement age of the Muntele Mare granite. A third multi-grain fraction with a significantly lower Th content (Table 3-1) yielded a 332 Ma $^{207}Pb/^{206}Pb$ age suggesting the presence of an inherited component. The inferred Late Carboniferous emplacement age represents the upper limit of the last medium-grade metamorphism that affected the main body of the Apuseni crustal fragment.

Two samples were selected from different granite intrusions in the carbonate-lenses bearing gneissic assemblages south of the HBSZ: one from a concordant granitic unit in the Mădrigeşti gneisses (sample 6), and the other from the Vinţa stock (sample 9) intruding the Baia de Arieş gneisses. Two fractions from the Mădrigeşti granite yielded two data points ca. 5% discordant with similar $^{207}Pb/^{206}Pb$ ages of 393 and 391 Ma, respectively. Both multi-grain fractions consisted of transparent, colourless euhedral well abraded zircon grains. The upper intercept age of ca. 392+/-6 Ma defined by the first two fractions (Fig. 3-4c) is interpreted to represent the emplacement age of the Mădrigeşti granite. A third multi-grain fraction yielded a $^{207}Pb/^{206}Pb$ age of 495 Ma which is similar to the age of the orthogneiss from the Biharia Mountains. The Mădrigeşti granitoids are decimeter to metre thick and up to few hundred metres long two-mica granite units interlayered with garnet-plagiogneiss. The last medium-grade

---

Fig. 3-2. Microphotographs of zircon grains in granitoid samples from the Apuseni Mountains; a) zircon grains separated from the Leucii granite slightly sheared and retrogressed within the Highiş-Biharia shear zone, Biharia Mountains, Leucii Creek: to the left unabraded grains, to the top selected best fraction and to the right best fraction after abrasion. b) zircon grains from the Vinţa granitic intrusion in the Baia de Aries carbonate lense gneissic assemblage, Hermeneasa Creek: centre left selected fragments of prismatic transparent grains; bottom left corner - the big grain that yielded the smallest discordance pointing to a late Paleozoic emplacement age. c) zircon grains from the Codru granodiorite, Neagu Creek; at the top selected first and second best fractions of intact bi-pyramidal transparent crystals and fragments, respectively; centre and right same fractions after abrasion; d) zircon grains from the Săvârşin granite, Arad-Deva highway at the Royal Castle in Săvârşin: yellow and larger grains yielded the late Middle Jurassic age and smaller colourless grains yielded the Eocene age.

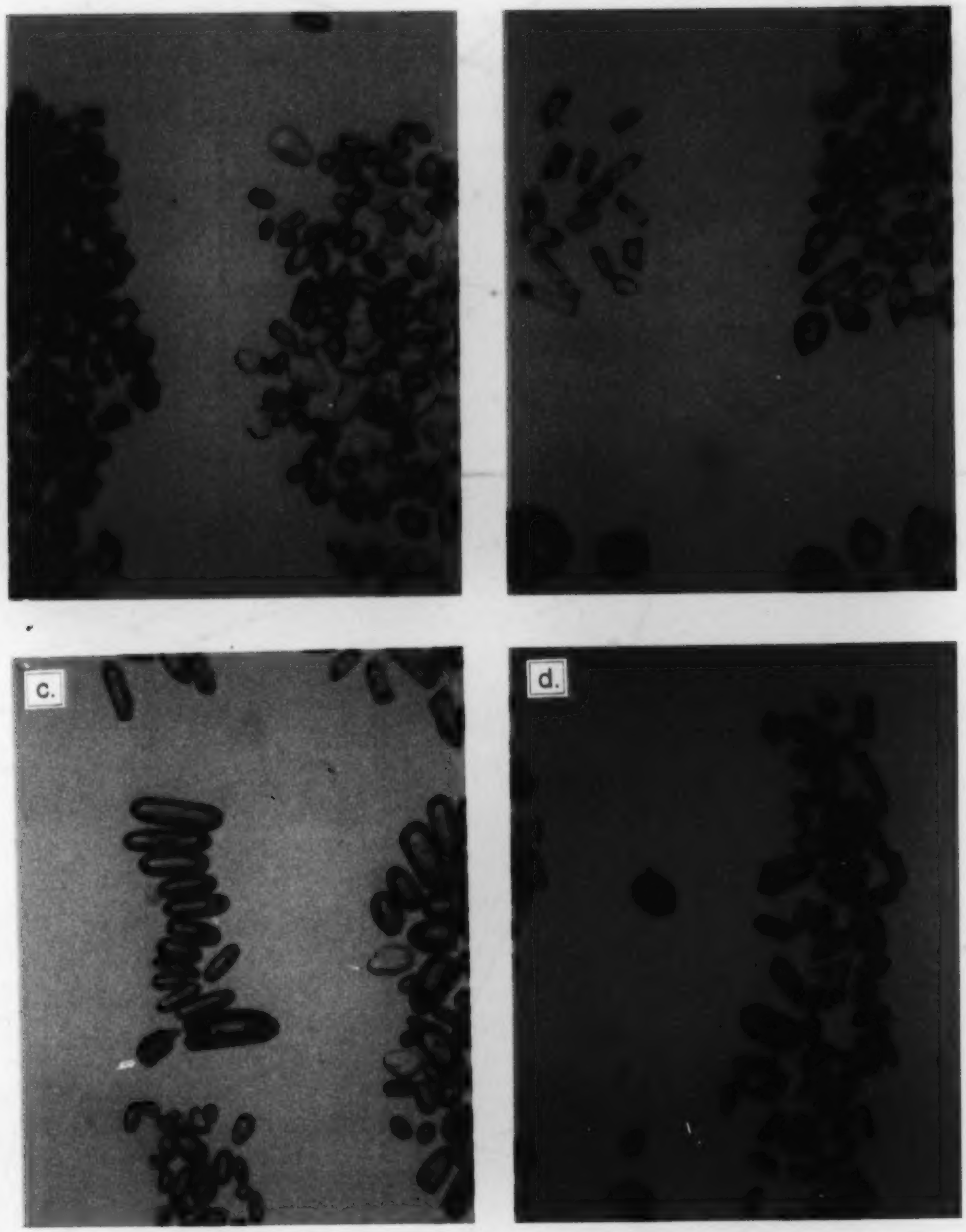
c.
d.

overprint recorded by the Mădrigeşti gneisses is thus constrained to be older than Early Devonian. U-Pb zircon data on the Vinţa granite (sample 9) yielded three highly discordant data points and a less discordant one that corresponds to a well abraded transparent zircon fragment (Fig. 3-2b and fraction 1 in Fig. 3-4d). The $^{207}Pb/^{206}Pb$ age of 261 Ma is therefore the best approximation of the emplacement age and roughly corresponds to the emplacement age of the Highiş igneous complex (c. 267-264 Ma). Fractions 1, 2 and 3 define a discordia array with an Early Proterozoic upper intercept age of c. 2365 Ma and a Late Triassic lower intercept age of c. 211 Ma. Both intercept ages may be geologically significant: Early Proterozoic zircon ages are reported in basement units of the Western Alps (Gebauer, 1993) and the 211 Ma age may be related to the Late Triassic - Early Jurassic tectonism that led to the development of Tethys. $^{40}Ar/^{39}Ar$ plateau ages between 216 Ma and 169 Ma at the margins of the HBSZ (Dallmeyer et al., 1998) support this interpretation. Fractions 1 and 4 define a poorly constrained discordia array with an upper intercept age of 980 Ma. Ages around 1000 Ma have been sporadically reported in central-western Europe (Pin, 1991). Although insufficiently well constrained, the U-Pb ages on zircon from the Vinţa intrusion suggests Precambrian inheritance in the Baia de Arieş gneiss-carbonate assemblage.

The age of the Săvârşin granite in the southern Apuseni Mountains is critical for the current interpretation of Alpine evolution of the region.

Two distinct population of zircon grains have been found in a sample from the Săvârşin granite (Fig. 3-2d). Most zircons are relatively large yellowish transparent zircon crystals and fragments with cracks and small fluid inclusions. A second group of smaller zircon grains are colourless, transparent incusion and cracks free. Two multi-grain fractions of the larger yellowish zircons yielded $^{207}Pb/^{206}Pb$ ages of 161 and 162 Ma, respectively. One fraction of colourless zircon crystals yielded a $^{207}Pb/^{206}Pb$ of 55 Ma. The yellowish zircon grains yielded a Callovian age. We interpret them as xenocrysts from the tholeiitic wall-rock. The Early Eocene age of the transparent colourless zircon grains is most likely the emplacement age of the Săvârşin granite. (Fig. 3-5).

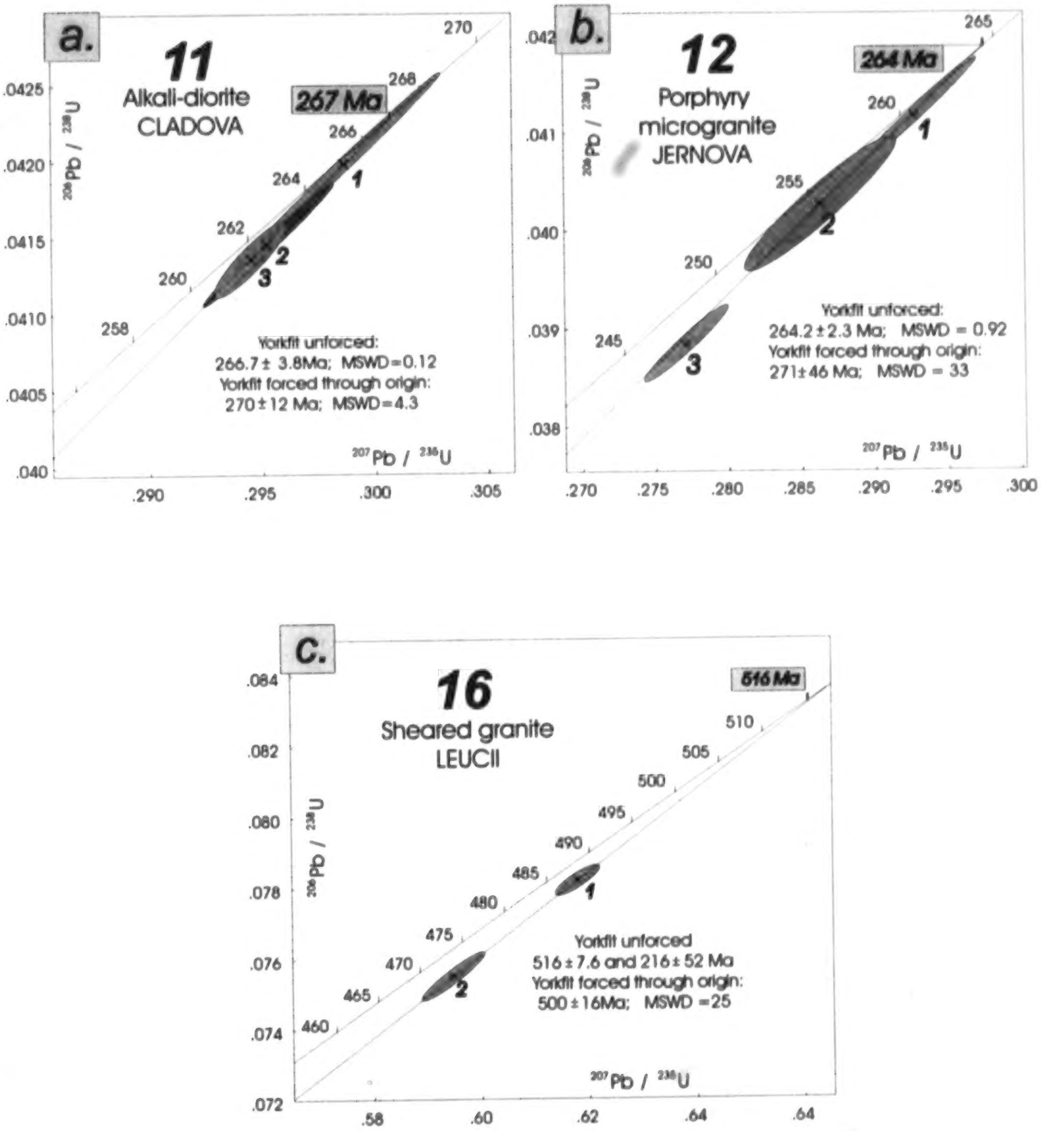

Fig. 3-3. Concordia diagrams for the granitoid intrusions of the Highis Biharia shear zone; sample and fraction numbers as in Tables 3-1 and 3-2.

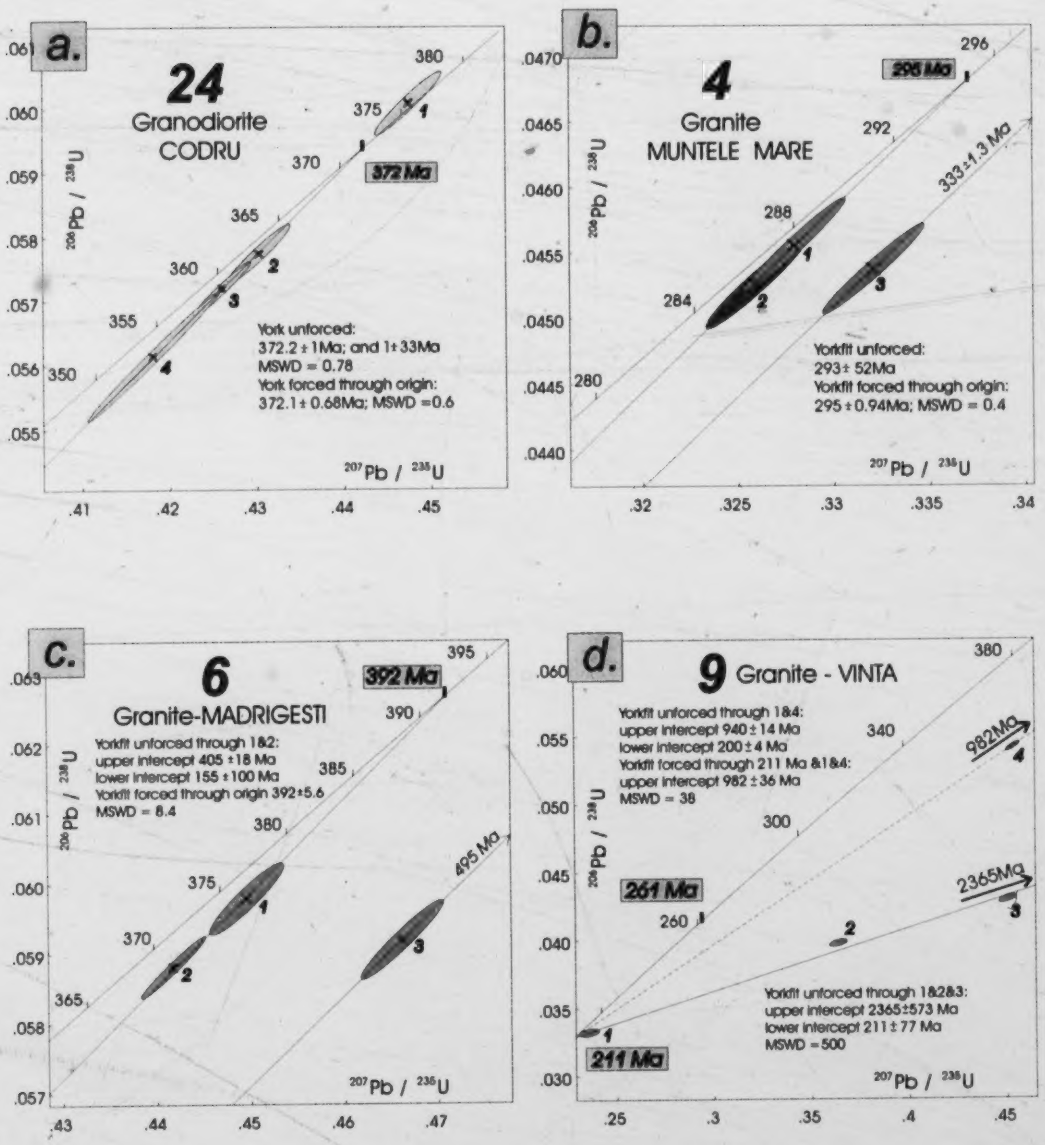

Fig. 3-4. Concordia diagrams for the representative granitoid intrusions within medium-grade assemblages of the Apuseni Mountains; sample and fraction numbers as in Tables 3-1 and 3-2.

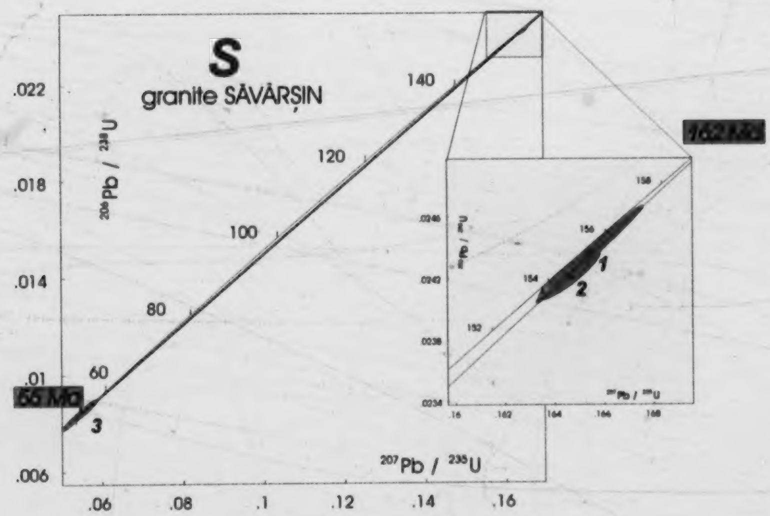

Fig. 3-5. Concordia diagram for the Săvârșin granitic intrusion within the Tethys "ophiolites".

3.4. Sm-Nd ANALYTICAL DATA

A suite of 31 samples of gneisses and granite of the basement units of the Apuseni and Carpathians mountains were analysed for their Nd isotopic signatures. For comparison, Sm-Nd data on 7 samples from the most representative basement assemblages of the Romanian Carpathians were also collected.

Analytical procedure

Samples were crushed to gravel size without direct contact with any metal surfaces, followed by final grinding to -35 microns. Neodymium isotopic analyses were performed at the University of Alberta. Sample powders were weighted, totally spiked with a tracer solution of ^{150}Nd and ^{149}Sm, and disolved in a 5:1 mix of vapour-distiled 24N HF and 16N HNO_3 in sealed teflon vessels at 160°C for 24 hours to dissolve flourides. This solution was evaporated and the residue taken up in HCl for separation of the rare earth elements as a group using standard cation chromatography, followed by separation of Nd from Sm using Di (2-ethylhexyl phosphate) chromatography (HDEHP). The purified Nd and Sm fractions were analyzed for isotopic composition using a VG354 mass spectrometer. Total procedural blanks for Nd and Sm are 0.5 ng. The ^{150}Nd - ^{149}Sm tracer solution was made from highly purified material; ^{150}Nd = 97.62 % and ^{149}Sm = 97.22 %. The concentrations of ^{150}Nd and ^{149}Sm in this solution were determined by direct calibration in triplicate against a mixed Sm/Nd normal solution (Wasserburg et al., 1981) with reproducibility of better than +/- 0.01 % for ^{150}Nd and +/-0.03% for ^{149}Sm. Isotopic analysis of Nd used a dynamic multicollector routine, correcting raw ratios both for variable mass-discrimination to ^{146}Nd/^{144}Nd = 0.7219 using an exponential law (Wasserburg et al., 1981) and for the effects of low abundance (non-^{150}Nd) tracer Nd isotopes. Sm was analysed in static multicollector mode and corrections made both for variable mass-discrimination to ^{152}Sm/^{154}Sm = 1.17537 using the exponential law (Wasserburg et al., 1981), and for the effects of low abundance (non-^{149}Sm) Sm tracer isotopes on ^{152}Sm/^{154}Sm.

Results

Sm-Nd data on basement assemblages from the Apuseni and Carpathians mountains are summarized in Table 3-2 and 3-3, respectively.

The Someş assemblage is characterized by the most depleted initial εNd(0) values ranging from ca. -12.5 to -15.5. A quartzofeldspathic layer (sample 1) in the northern, and a garnet-bearing plagiogneiss (sample 2) in the southeast Apuseni Mountains yielded very similar εNd(0) (-15.5 and -15.4, respectively) and crustal residence ages (1.90 and 1.87, respectively). A less negative εNd(0) value of -4.7 has been calculated for a kyanite-bearing micaceous plagiogneiss (sample 3), in an area interpreted to record two medium grade metamorphic events (Hârtopanu and Hârtopanu, 1986). However, all the three samples from the Someş assemblage

Table 3-2. Nd and Sm Concentrations and Isotopic Data for Samples from the Apuseni Mountains

Sample #	 Location	Rock Type	Nd ppm	Sm ppm	147Sm / 144Nd	143Nd / 144Nd	eNd(0)*	eNd(t)	TDM** (Ga)
SOMES GNEISS-GRANITIC ASSEMBLAGE								t=295	
1	Giurcuta	gneiss-Qz/F	30.84	5.52	0.1082	0.511846 +/-9	-15.5	-12.1	1.90
2	Boisoara	gneiss-Grt	54.66	9.70	0.1073	0.511850 +/-6	-15.4	-12.0	1.87
3	Iara	micaschist-Ky	36.47	6.80	0.1128	0.511996 +/-8	-12.5	-9.4	1.76
4	Muntele Mare	granite(295Ma)	33.99	7.27	0.1294	0.512266 +/-11	-7.3	-4.7	1.62
BAIA DE ARIES GNEISS-CARBONATIC ASSEMBLAGE									
	Highis Mountains							t=392Ma	
5	Madrigesti	gneiss	19.31	4.31	0.1351	0.512267 +/-16	-7.2	-4.2	1.73
6	Madrigesti	granite(392Ma)	18.81	4.45	0.1429	0.512346 +/-8	-5.7	-3.0	1.75
	Biharia-Gilau Mountains							t=261Ma	
7	Cioara Valley	gneiss-Grt	34.38	7.04	0.1238	0.512151 +/-10	-9.5	-7.1	1.71
8	Salciua Village	gneiss-Grt	32.73	6.48	0.1196	0.512036 +/-9	-11.7	-9.2	1.82
9	Vinta	granite(261Ma?)	11.07	2.73	0.1492	0.512460 +/-13	-3.5	-1.9	1.65
10	Surduc Village	gneiss-Grt	36.74	7.35	0.1209	0.512131 +/-12	-9.9	-7.4	1.69
HIGHIS-BIHARIA IGNEOUS COMPLEX									
	Highis Mountains							t=267	
11	Cladova Valley	diorite(267Ma)	40.52	9.87	0.1472	0.512574 +/-11	-1.3	0.4	1.35
12	Jernova Valley	granite(265Ma)	32.68	9.61	0.1779	0.512661 +/-8	0.5	1.1	2.12
13	Casoaia Valley	granite	20.89	5.43	0.1570	0.512432 +/-8	-4.0	-2.7	1.96
14	Siria Fortress	conglom.	10.03	1.82	0.1095	0.512011 +/-10	-12.2	-9.3	1.68
	Biharia-Gilau Mountains							t=516	
15	Leucii Valley	diorite	8.23	2.19	0.1609	0.512547 +/-10	-1.8	0.6	1.77
16	Leucii Valley	granite(516Ma)	20.65	5.12	0.1499	0.512508 +/-9	-2.5	0.6	1.56
17	Mihoiesti	granite	36.92	7.42	0.1215	0.512221 +/-8	-8.1	-3.2	1.55
18	Dobra Valley	granite	11.71	3.27	0.1687	0.512493 +/-14	-2.8	-1.0	2.26
19	Ocolisel Valley	granite	22.77	6.73	0.1786	0.512371 +/-11	-5.2	-4.0	3.40
CODRU ASSEMBLAGE								t=372	
20	Codru Moma	gneiss-Grt-And	30.90	5.98	0.1170	0.512136 +/-10	-9.8	-6.0	1.61
21	Codru Moma	granite	29.69	5.60	0.1141	0.512353 +/-8	-5.6	-1.6	1.24
22	Huzii Valley	fibrolite schist	182.57	31.53	0.1044	0.511993 +/-6	-12.6	-8.2	1.63
23	Iara Valley	granite	11.56	1.96	0.1025	0.512158 +/-10	-9.4	-4.9	1.38
24	Neagu Valley	granodiorite(372Ma)	33.75	6.94	0.1243	0.512597 +/-11	-0.8	2.6	0.96

Table 3-3. Nd and Sm Concentrations and Isotopic Data for Samples from the Romanian Carpathians

 #	Sample Location	Rock type	Nd ppm	Sm ppm	147Sm / 144Nd	143Nd / 144Nd	eNd(0)*	TDM** (Ga)
South Carpathians								
25	Sugag	pl-gneiss Grt-Ky Seb	26.20	4.92	0.1134	0.511893 +/-9	-14.5	1.92
26	Paltinis	pl-gneiss Grt Sebes	32.88	6.50	0.1195	0.511883 +/-9	-14.7	2.06
27	Bilea	schist Chl-Ser Suru	14.70	3.19	0.1311	0.512101 +/-9	-10.5	1.95
East Carpathians								
28	Balan	conglom Pangarati	37.09	6.81	0.1109	0.512092 +/-10	-10.7	1.58
29	Gheorghieni	pl-gneiss-Grt Bretila	18.88	3.68	0.1179	0.511888+/-11	-14.6	2.02
30	Gheorghieni	porphyroid Mandra	50.38	9.61	0.1154	0.512108+/-8	-10.3	1.63
31	Neagra	pl-gneiss-Grt-And Re	42.29	8.09	0.1156	0.511971+/-8	-13.0	1.85

---

* $\varepsilon Nd(0) = [{}^{143}Nd/{}^{144}Nd_{meas}/{}^{143}Nd/{}^{144}Nd_{CHUR}-1] \times 10^4$;
present day ${}^{143}Nd/{}^{144}Nd_{CHUR}$= 0.512638, normalized to ${}^{146}Nd/{}^{144}Nd = 0.7219$ (DePaolo & Wasserburg, 1976)

** $T_{DM}= 1/\lambda \times \ln[({}^{143}Nd/{}^{144}Nd_{meas}-{}^{143}Nd/{}^{144}Nd_{mantle}) / ({}^{147}Sm/{}^{144}Nd_{meas}-{}^{147}Sm/{}^{144}Nd_{mantle}) + 1]$ (DePaolo, 1981);
with Goldstein et al. (1984) values for ${}^{143}Nd/{}^{144}Nd_{mantle}$= 0.513163 and ${}^{147}Sm/{}^{144}Nd_{mantle}$= 0.2138.

yielded similar middle Early Proterozoic T_{DM} model ages ranging from 1.76 to 1.9 Ga. Sm-Nd data on the Muntele Mare granite (sample 4) intruded in the Someş assemblage yielded a less negative $\varepsilon Nd_{(295)}$ values of -4.7.

From the Codru assemblage two gneiss and three granitoid samples have been selected for Sm/Nd analysis. A chlorite-fibrolite bearing schist apparently derived from the adjacent granitoids yielded an εNd(0) value of -12.6 (sample 22) similar to the value yielded by the adjacent plagiogneiss from the Someş assemblage (-12.5, sample 3). The gneiss sample from the westernmost area (Codru Mountains) yielded a less negative εNd(0) value of -9.8, which is in the range obtained for the southern gneiss-carbonate assemblage. The three granitoids of the Codru assemblage yielded εNd(t) values of -4.9 to +2.6 and the youngest T_{DM} in the basement rocks of the Apuseni Mountains ranging from 1.38 to 0.96 Ga. The most positive εNd(t) value (+2.64, sample 24) was found in one of the most characteristic rock types of the Codru assemblage, the granodiorite that yielded an emplacement age of c. 372 Ma.

From the southern gneiss-carbonate assemblage one sample from each of the main three 'islands' have been analysed as well as the granitic intrusions dated by U-Pb. The gneisses yielded a relatively narrow range of εNd(0) values from -7.2 to -11.7 and T_{DM} model ages of 1.7-1.8 Ga. The Mădrigeşti gneiss (sample 5) shows the least depleted εNd(0) value of -7.2, whilst the Vidolm gneiss (sample 10) yielded a value of -9.9, in the range obtained for the gneisses (samples 7, 8) in the main Baia de Arieş island (-9.5 and 11.7, respectively). Sm-Nd data indicate that all basement 'islands' incorporate similar ancient crustal material with addition of more juvenile material at Mădrigeşti. Meanwhile, they reveal a distinct evolution of the gneiss-carbonate crust from the southern Apuseni compared to the gneiss-granitic crust in the central-northern Apuseni Mountains.

The Mădrigeşti granite (sample 6) with the emplacement age of c. 392 Ma yielded less negative εNd values but the same T_{DM} model age as the adjacent gneisses. The stock-like Vinţa granite which intrudes the gneisses with more depleted εNd(0) in the Baia de Arieş 'island', yielded even less depleted εNd values and younger T_{DM} model age indicating that the mixing process was dominated by the juvenile material.

Within the Highiş-Biharia shear zone, the quartz-clasts bearing mylonite or metaconglomerate (sample 14) shows εNd and T_{DM} model age values of -12.2 and 1.68 Ga which are comparable to those of the gneisses. This rock-type may be interpreted either as a Paleozoic conglomerate derived from a gneiss-granitic (Someş type) protolith, or as tectonic enclaves of highly deformed gneissic basement underlying the igneous complex which were tectonically intercalated within the phyllonitic belt. Sm-Nd and isotopic ratios from variably deformed pods of granitoid rocks (samples 11,12,13,15, 16,17,18,19) yielded εNd(i) values ranging from +1 to -4 and T_{DM} model ages ranging from 1.35 Ga to 3.4 Ga. These ranges

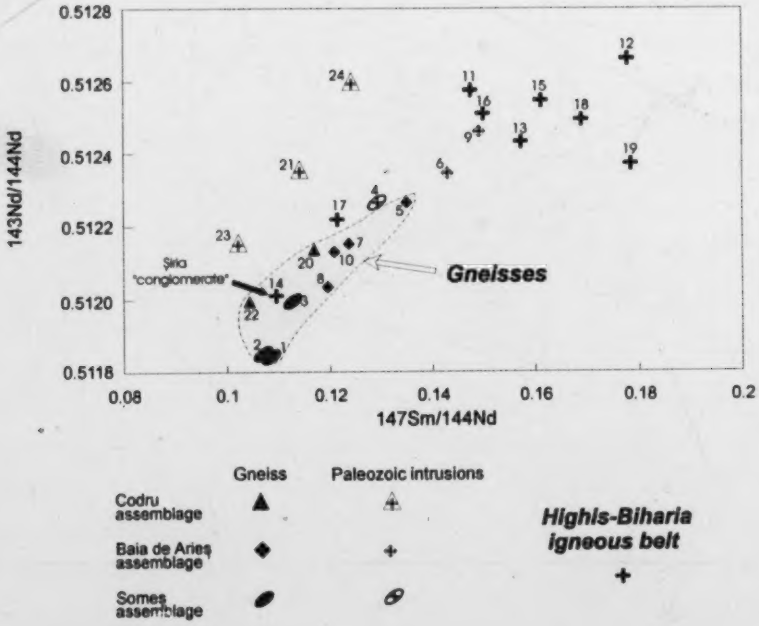

Fig. 3-6. Nd isotopic characteristics of the gneissic assemblages and associated Paleozoic intrusions from the basement units of the Apuseni Mountains. Symbols correspond to the main lithotectonic assemblages and numbers indicate the sample numbers in Table 3-2.

contrast significantly with those yielded by the adjacent gneissic assemblages. The extremely old T_{DM} model ages do not have a direct geologic significance since they correspond to samples with 147Sm/144Nd ratios close to, or higher than 0.17. Samples with 147Sm/144Nd < 1.5 yielded Middle Proterozoic T_{DM} model ages ranging from 1.35 to 1.56 Ga. The wide range of εNd(t) from -4 to +1 (even when recalculated for the same age of 300 Ma) indicate isotopically heterogeneous sources and/or very diverse petrogenetic processes. Similar variability was reported from the anorogenic granite from Corsica (e.g., Poitrasson et al., 1995)

Fig. 3-6 shows the spread in the Sm-Nd isotopic composition of the Highiş-Biharia igneous samples with no clear isotope mixing pattern with older crustal material. Two sets of εNd(t) values recalculated for each of the adjacent gneissic assemblages at the time *t* corresponding to the two dated magmatic events within HBSZ show no clear correlation with the Paleozoic intrusions (except for the sheared phaneritic Mihoieşti granite, sample 17) (Appendix II). In contrast, a mixing line can be traced between the southern gneiss-carbonate crust (samples 10, 7, 5) and the Mădrigeşti (sample 6) and Vinţa (sample 9) granites intruding the former rock units. Similarly, the Muntele Mare granite (sample 4) plots in the continuation of the Someş (samples 1, 2, 3) and eventually Codru gneisses samples (20, 22) suggesting mixing of the old crust with Late Carboniferous juvenile material. These data suggest a "hybrid" crust-mantle (Barbarin, 1990) origin for the Muntele Mare granite. The Codru intrusions do not seem to be isotopically related to the Codru gneisses. They plot along a distinct line whose *y* intercept is 0.51 corresponding to a 3 Ga poorly constrained isochrone age of uncertain geologic significance.

The samples from the Romanian Carpathians (Fig. 3-7 and Table 3-3) have been selected from lithologic assemblages similar to those separated in the Apuseni Mountains: the Sebeş kyanite-garnet bearing gneisses (samples 25, 26) in the South Carpathians and the Bretila garnet plagiogneiss (sample 29) are part of a gneiss-granitic assemblage without significant carbonate lenses, similar to the Someş assemblage in the Apuseni Mountains. The Suru (sample 27) retrogressed plagiogneiss in the South Carpathians and the Rebra (sample 31) andalusite-garnet bearing gneiss in the East Carpathians belong to a plagiogneiss-micaschist carbonate lenses assemblage similar to the Baia de Arieş assemblage of the Apuseni Mountains. Samples 28 and 30 from low-grade mylonites on igneous rocks of the controversial Tulgheş assemblage yielded εNd(0) values of ca. -4.8 and T_{DM} model ages around 1.6 Ga similar to those of the Highiş-Biharia igneous phyllonite rocks.

Fig. 3-8 comparatively presents the Sm-Nd evolution of similar lithologic assemblages from the Apuseni and Carpathians mountains. The gneiss-granite assemblage plots bellow all the other assemblages; an irregular pattern characterises the carbonate lense dominated assemblage A very consistent evolution is suggested by the Mândra and Pângăraţi sheared

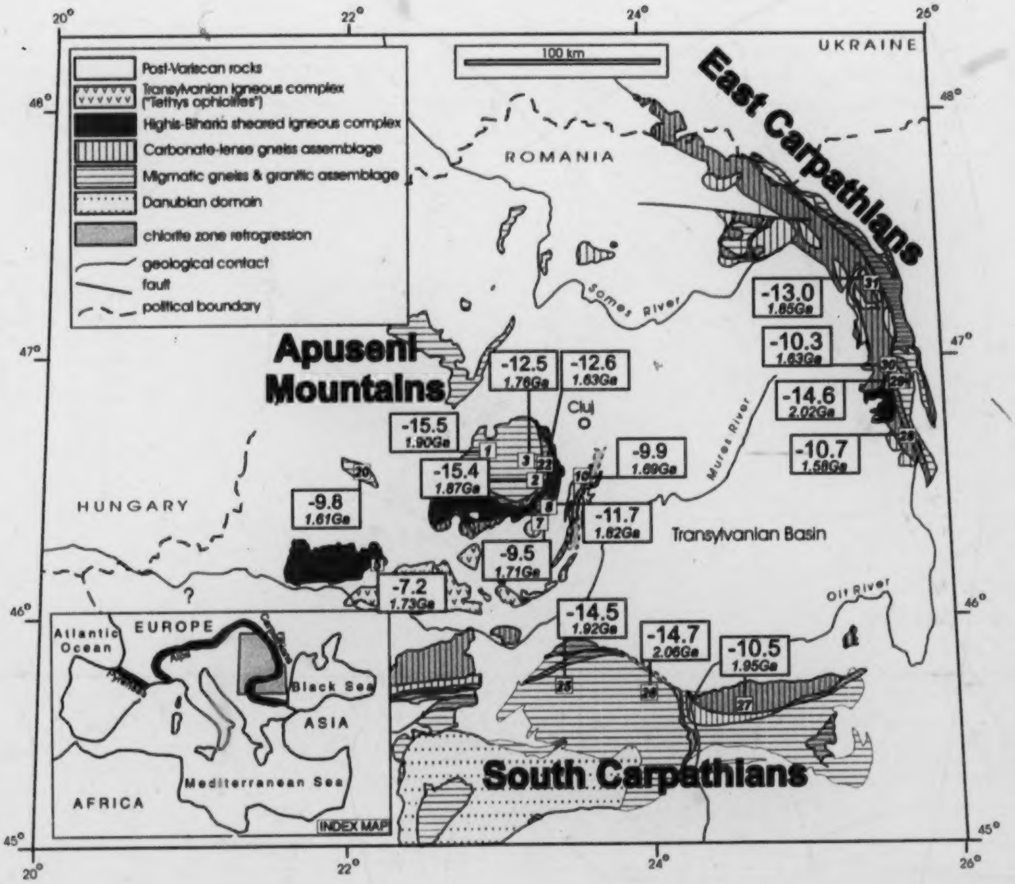
Post-Variscan rocks
Transylvanian igneous complex ("Tethys ophiolites")
Highis-Biharia sheared igneous complex
Carbonate-lense gneiss assemblage
Migmatic gneiss & granitic assemblage
Danubian domain
chlorite zone retrogression
geological contact
fault
political boundary
100 km
UKRAINE
ROMANIA
HUNGARY
East Carpathians
Apuseni Mountains
South Carpathians
Transylvanian Basin
Somes River
Mures River
Olt River
Cluj
-13.0 1.65Ga
-10.3 1.63Ga
-14.6 2.02Ga
-10.7 1.58Ga
-12.5 1.76Ga
-12.6 1.63Ga
-15.5 1.90Ga
-15.4 1.87Ga
-9.9 1.69Ga
-9.8 1.61Ga
-11.7 1.82Ga
-9.5 1.71Ga
-7.2 1.73Ga
-14.5 1.92Ga
-14.7 2.06Ga
-10.5 1.95Ga
1
2
3
7
8
19
20
22
25
26
27
28
29
30
31
20°
22°
24°
26°
45°
46°
47°
48°
Atlantic Ocean
EUROPE
Black Sea
ASIA
AFRICA
Mediterranean Sea
INDEX MAP

Fig. 3-7. Sketch map of the distribution of the metamorphic assemblages in the Apuseni and Romanian Carpathians mountains with the location of Sm-Nd samples; $\varepsilon Nd_{(0)}$, T_{DM} and sample number as in Tables 3-2 and 3-3.

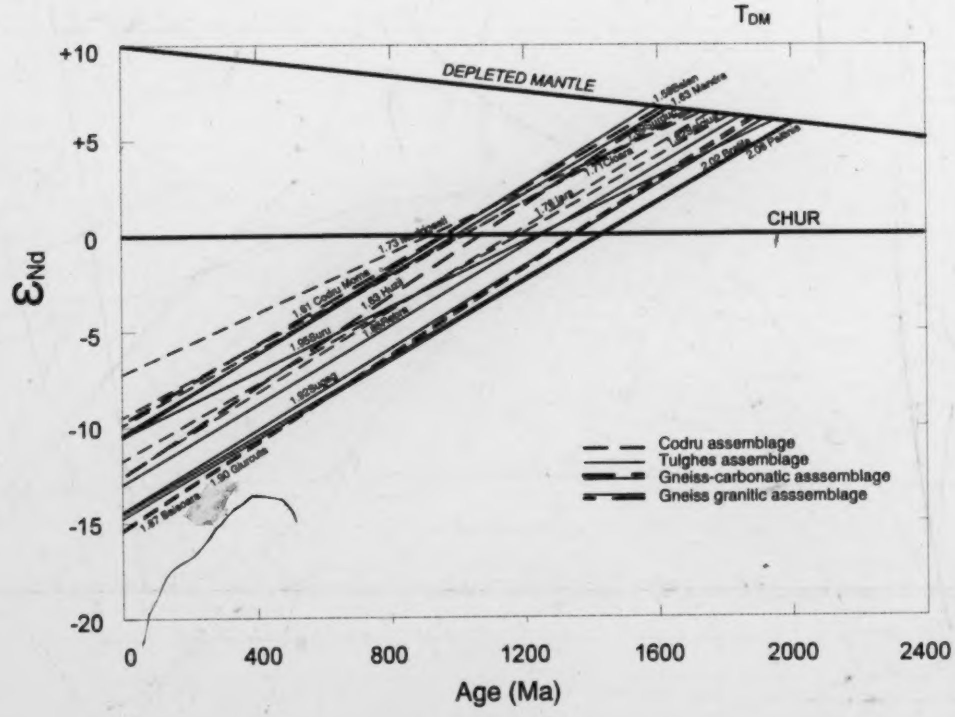

Fig. 3-8. Evolution of εNd through time for analysed samples from the Apuseni Mountains and Romanian Carpathians. The depleted mantle model after Goldstein et al., (1984). Continuous line - assemblages from the Carpathians; broken line - assemblages from the Apuseni Mountains; note that the gneiss-granitic assemblage plots below all the other assemblages; a very irregular pattern characterises the gneiss-carbonatic assemblage while a very consistent evolution is typical for gneisses in the Tulghes assemblage.

granitoids in the Tulgheş shear zone. A tentative isochron age for the sheared granitoids, although poorly constrained (Appendix II) suggests a Lower Paleozoic magmatic event which can be correlated to the 500 Ma intrusions in the Biharia Mountains and may be related to the Latest Proterozoic-Early Paleozoic crust-forming event documented in the central and western Europe (e.g., Pin, 1991).

3.5. SUMMARY AND COMPARISON WITH CENTRAL-WESTERN EUROPE

Variscan collision is interpreted to have welded pieces of the northern passive margin of Gondwana to the active Laurasian margin between 500 and 330 Ma (e.g., Gebauer et al., 1989) or during the Early Carboniferous (e.g., von Raumer and Neubauer, 1994). Age estimates of 2-3 Ga, in different western and central European sectors of the Variscan orogen although model dependent, allow the intriguing possibility that Variscan Europe comprise recycled Archean crust (Liew and Hofmann, 1988).

Early Alpine rifting resulted in the development of new oceanic troughs and separation of several crustal fragments. The same Alpine crustal fragment may contain distinct Variscan terranes and distinct Alpine panels may be constituted by the same Variscan basement. In the Western Alps, the Valais trough partly separates Europe from its foreland, the Penninic basement and its continuation in the external Alpine units, the Helvetic basement. The major Ligurian / Piemontais ophiolitic suture separates the European Helvetic/Penninic basement from the African Austro-Alpine basement. In the Carpathian sector of the Alpine belt, the basement units are separated from Europe by the Vahicum-Sinaia-Severin trough. Between the Dinarides and Carpathians branches of the Alpine orogen, several associations of Mesozoic deep-water strata and mafic rocks interpreted as suture zones (Vardar, Transylvanian, Bükk-Meliata) apparently define a coherent Early Alpine continental fragment ("Tisia" -Kovács et al., 1987) which includes the basement units exposed in the Apuseni Mountains. Subsequent Alpine compression resulted in the consumption of the supposed wide oceanic troughs accompanying large translation/rotation and strain in the continental fragment.

Sm-Nd and U-Pb data that constrain the pre-Alpine evolution of individual crustal fragments provide a basis for regional correlation of basement units across the supposed Alpine sutures.

Various pre-Permian-Mesozoic medium-grade assemblages from the Apuseni and Carpathians basement units yielded a range of Early Proterozoic T_{DM} model ages which suggest a similar crustal evolution. The very narrow ranges of $\varepsilon Nd(0)$ values (-15.4; -15.5 in the Apuseni Mountains; -14.5; -14.7 in the South Carpathians; -14.6 in the East Carpathians) and T_{DM} model ages (1.87 and 1.90 in the Apuseni Mountains; 1.92 and 2.06 Ga in the South Carpathians; 2.02 Ga in the East Carpathians) for the granite gneiss assemblages indicate a relatively uniform protolith. A uniform protolith of sedimentary origin for all regionally extensive gneiss-granitic assemblages appears unlikely because it would involve a unique and constant provenance in a huge sedimentary basin for a long time interval. Instead, the uniform Sm/Nd ratios may indicate a uniform Early Proterozoic mantle-derived protolith multiply recycled during subsequent tectonism. A trondjemite-tonalite-granite (TTG) association is a good candidate for the likely precursor of the gneiss granitic crust of the Carpathians and Apuseni mountains. Its evolution included: a) Precambrian TTG and granulite stages, b) Paleozoic granitization and incorporation of upper mantle materials followed by evolution through mid-crustal levels and c) localized, intense Alpine shearing and retrogression.

The carbonate lense and micaschist dominated assemblage yielded wider ranges for both εNd(0) (-9.2 to -4.2 in the Apuseni Mountains; -13 in the South Carpathians and -10.5 in the East Carpathians) and T_{DM} (1.82 to 1.69 in the Apuseni Mountains; 1.95 Ga in the South Carpathians and 1.85 Ga in the East Carpathians) and suggest various additions of more juvenile material. The carbonate lense dominated assemblage appears to be located at the interior of the Carpathian Arc and Eastern Alps and to occupy a structurally higher position in respect with the gneiss-granitic crust.

Paleozoic granitoids yielded consistently younger Nd model ages ranging from 1.96 Ga to 0.9 Ga with a cluster between c. 1.5 to 1.6 Ga and a relatively wide range of ε Nd(t) values (-4.9 to +2.6) providing compelling evidence for broad mixing processes involving adjacent mature crust and Paleozoic juvenile end-members. These data are consistent with data reported in the central and western Europe where the almost complete lack of unequivocal evidence for magmatic events in the 1.8-0.7 Ga range contrasts markedly with the abundance of Nd model ages falling in this time interval. A "middle Proterozoic hiatus" in the crust-forming processes similar to other parts of Europe (Pin, 1991) may be interpreted in the crustal fragments exposed in the Romanian segments of the Alpine orogen.

Low-grade assemblages yielded ε Nd(0) and T_{DM} model ages similar to either the gneissic assemblages or to the Paleozoic granitoids. In the South Carpathians, a retrogressive schist (sample 27) yielded a T_{DM} in the range of the gneisses (sample 25 and 26) and in the East Carpathians granitic phyllonites (samples 28 and 30) yielded T_{DM} model ages in the same range as the Paleozoic intrusions dated in the Apuseni Mountains. Corroborated with field and petrographical data, Sm-Nd data may be interpreted to indicate direct derivation of the low-grade assemblages by shearing and retrogression of distinct units of the pre-existing crust.

Lithologically similar assemblages across the local expression of the Tethys ocean have similar ε Nd(0) and T_{DM} model ages. The Someş assemblage from the Apuseni Mountains shows the same isotopic signature as the Sebeş-Lotru and Bretila gneiss-granite assemblages of the Carpathians. The Baia de Arieş carbonate lense dominated assemblage yielded similar isotope concentrations and ratios as the Suru and Rebra assemblages of the Carpathians. Since the Carpathians crustal fragment is of European origin we propose the same origin for the basement units of the Apuseni crustal fragment. Similarly to the Alpine stratigraphy, isotope data on pre-Alpine basement suggest that tectonic models that assume consumption of wide oceans and amalgamation of far travelled crustal fragments of African origin in the Carpathian-Pannonian region are suspicious.

Four groups of Paleozoic emplacement ages have been determined in the basement rocks of the Apuseni Mountains: Late Cambrian-Early Ordovician (c. 516 - 495 Ma), Early Devonian (c. 392 and 372 Ma), Late Carboniferous (c. 295 Ma) and late Early Permian (c. 267-261 Ma) magmatic events (Table 3-4).

Table 3-4. Summary of the isotope data on granitoid samples from the Apuseni Mountains

SAMPLE #	LOCATION	ROCK TYPE	U-Pb AGE	ε Nd(t)	T_{DM}
9	Vinţa	granite	c. 261	-1.9	1.65
12	Jernova	пmicrogranite	264+/-2	+1.1	-
11	Cladova	alkali-diorite	267+/-4	+0.4	1.35
4	Muntele Mare	granite	295 +/- 1	-4.7	1.62
24	Codru	granodiorite	372+/-1	+2.6	0.96
6	Mădrigeşti	granite	392+/-6	-3.0	1.75
16	Leucii	granite	516+/-8	+0.6	1.56
S	Săvârşin	granite	c. 55		

1. The c. 516 Ma old Leucii plagiogranite (sample 16) is the oldest age determined so far in the Apuseni Mountains. The discordant fraction from the Mădrigeşti granite that yielded a 207Pb/206Pb age of c. 495 Ma may indicate inheritance from the same tectonomagmatic event. In central and western Europe the Early Paleozoic igneous activity suggests ensialic rifting processes (Weber, 1984) that may have evolved to a seafloor spreading stage (Pin, 1991). Bimodal suites of similar age ("leptino-amphibolitic" assemblages) received controversial geodynamic interpretation as back-arc (e.g., Giraoud et al., 1985; Briand et al., 1988) or ensialic rifting unrelated to subduction (Pin and Vielzeuf, 1988). In the West Carpathians the "leptino amphibolite complex" of Tatricum is interpreted to represent a slice of 500(?) to 430 Ma old oceanic crust (Putiš, 1994). In the Alps, ultra-basic, basic and acidic rocks of different ages from various basement units of the Penninic, Helvetic (Gotthard), Ultrahelvetic (Aar) and Austro-Alpine domains are interpreted to represent a cryptic Variscan suture zone with remnants of the Proterozoic-Early Ordovician "Penninic-Austro-Alpine mobile belt" (von Raumer and Neubauer,

1994). A Late Proterozoic oceanic crust interpreted in the Danubian units of South Carpathians, based on Nd and Sr isotope data on amphibolites from the Drăgşani assemblage followed by copious Late Proterozoic and Cambrian crustal melting indicated by abundant granitoids (Liégeois et al., 1995, Dallmeyer et al., 1996) corresponds to a period of significant continental growth. It appears that the "Pan-African" crustal evolution documented along the northern margin of the Gondwana supercontinent extended over most of the mid-European domain (Pin, 1991; Liégeois et al., 1995). A direct tectonic relationship of the Danubian units to the Pan-African evolution recorded along the northern margin of Africa is uncertain since no such record was reported so far from the intervening Carpathian-Rodopian crust.

No record of a Middle-Late Ordovician tectonothermal event was found so far in the Apuseni crust in contrast with the intense tectonomagmatic activity documented in the Alps. The presence of eclogite and granulite facies rocks of uncertain age in various Helvetic units (Silurian-Early Devonian-Paquette et al., 1989; Ordovician-Gebauer, 1993) and of granitic rocks with chemical characteristics similar to modern subduction-related igneous rocks in most units of the Central, Western and Southern Alps has been interpreted to document Ordovician subduction (von Raumer and Neubauer, 1993). The Ordovician granitoids were also interpreted as the result of a "thermal event" caused by Early Paleozoic under-plating (Schmid, 1993).

2) The Mădrigeşti granite (sample 6) intruded the southern gneiss-carbonate assemblage at c. 392 Ma (Middle Devonian). On the Alpine crustal fragment that includes the Apuseni Mountains, Rb-Sr data on granodiorite from the Mecsek Mountains, suggest an Early Silurian (c. 430 Ma) magmatic event (Svingor and Kovach, 1981). Devonian high-pressure metamorphism in the Austro-Alpine units of the Eastern Alps (Neubauer, 1993) and the external massifs of the Helvetic domain (Paquette et al., 1989) is currently interpreted to document a Silurian-Devonian phase of collision at the level of the lower and middle crust (von Raumer and Neubauer, 1994). In the West Carpathians, the Gemericum leucogranite that yielded an emplacement age of 403+/-5 Ma (U-Pb zircon Shcherbak et al., 1988) the Rb-Sr isochron data in the Tatricum (380+/-20 Ma) and Veporicum (391+/-6 Ma) (Cambel and Kral, 1989) would be related to compression during the Early Devonian.

The 372+/-1 Ma old Codru granodiorite with no microscopically visible zircon inheritance and the most juvenile +2.6 $\varepsilon Nd_{(372)}$ belongs to the Codru assemblage, a discontinuous belt mainly consisting of igneous rocks along the southern and eastern margin of the Someş assemblage. Strike-parallel tectonic flow lines and $^{40}Ar/^{39}Ar$ dates on amphibolite (405-366 Ma) suggest Devonian transcurrent tectonism accompanied by magma intrusion and uplift of the crust. The positive $\varepsilon Nd(t)$ may be interpreted as the least contaminated, juvenile material possibly related to a zone of Late Devonian crustal thinning. Devonian continental thinning and rifting accompanied by intrusion of trondhjemitic melts is recorded by the Riouperoux-Livet igneous complex in the external massifs (Ménot and Paquette, 1993). The tectonic significance of other isotopic ages in this range is unclear. In the Mecsek Mountains, Late Devonian migmatization processes are documented by the U-Pb zircon age of 365+/-8 Ma (Balogh et al., 1983). An isolated $^{40}Ar/^{39}Ar$ plateau age of 375 Ma on a hornblende concentrate has been reported from the East Carpathians (Dallmeyer et al., 1997).

General Early Carboniferous collision in the Alps (360-320 Ma) is inferred to be the main Variscan tectonic event. Dextral transpression is interpreted to have resulted in south verging nappe-tectonics accompanied by migmatitic and magmatic events in the Helvetic domain (324+/-12 Ma K-Ar on amphiboles, Ménot et al., 1987; 317 Ma U-Pb monazite, Bussy and von Raumer, 1993).

In the Apuseni Mountains, the main Paleozoic tectonic event documented in the Alps was only recorded by $^{40}Ar/^{39}Ar$ ages of c. 340-335 Ma on muscovite in minor gneissic units from the Codru assemblage (Dallmeyer et al., 1998). A transcurrent plate margin can be inferred along the Codru assemblage that evolved from transtensive during the Late Devonian intrusion of Codru granodiorite to transpressive in the Carboniferous (?). In the Mecsek Mountains an Early Carboniferous (c. 335 Ma) tectonothermal event accompanied by metasomatism is suggested by Rb-Sr (Svingor and Kovach, 1981) and K-Ar (Balogh et al., 1983) data. In the West Carpathians, Early Carboniferous tectonothermal event is documented by $^{40}Ar/^{39}Ar$ plateaus on muscovite and hornblende in the Tatricum (Malusky et al., 1993; Dallmeyer et al., 1996). The interpreted compressive tectonic regime (Putis, 1994) corresponds to the stepwise decrease in K-Ar ages from hornblende, to muscovite and biotite which suggest progressive uplift of Tatricum during the Devonian-Carboniferous and of Veporicum during the Late Carboniferous.

3) A Late Carboniferous tectonothermal event in the Apuseni Mountains is recorded by the intrusion of Muntele Mare batholith (c. 295 Ma) and $^{40}Ar/^{39}Ar$ ages on hornblende (317-306 Ma) and muscovite (314-303 Ma) in the adjacent Someş assemblage (Dallmeyer et al., 1998). However, the tectonic setting of the Apuseni basement units is uncertain. The Someş assemblage evolved above the ~500° C and ~400° C isotherms corresponding to hornblende and muscovite argon retention, respectively and exhumed following the intrusion of the Muntele Mare granite. Widespread Carboniferous (?)- Permian conglomerates in the western Apuseni Mountains suggest rapid uplift and erosion of the Someş-Muntele Mare crustal fragment.

Late Carboniferous I-type granites accompanied by high-temperature metamorphism in the middle Austro-Alpine units would record a phase of "Late" Variscan collision/subduction (von Raumer and Neubauer, 1994). In the East Carpathians $^{40}Ar/^{39}Ar$ plateau ages (Dallmeyer et al., 1996) on muscovite and hornblende indicate Late Carboniferous strike-slip tectonism along the Tulgheş shear zone (c. 307-304 Ma) followed by Early Permian uplift of core complexes (c. 283 -

267 Ma). In the South Carpathians $^{40}Ar/^{39}Ar$ plateaus ages on hornblende ranging from c. 323 to 317 Ma and from c. 310 to 286 Ma on muscovite (Dallmeyer et al., 1996) indicate the general Late Carboniferous uplift of the medium-grade metamorphic basement. The tectonic significance of other isotope ages reported in regions adjacent to the Apuseni Mountains are uncertain. In the Velence Mountains K-Ar data indicate a Late Carboniferous-Early Permian tectonothermal event (c. 290-270 Ma, Balogh et al., 1983) and in the Mecsek Mountains, Rb-Sr isochrone ages and K-Ar ages indicate tectonism and metasomatism between c. 284 and 270 Ma (Svingor and Kovach, 1981; Balogh et al., 1983) probably related to shearing and retrogression of the Mecsek granodiorite into the Ofalu carbonate shear zone.

4) Late Early Permian igneous activity in the Highiş Mountains took place in a relatively short time interval during the (c. 267 to c. 264 Ma). Although equivocal, the geochemical data suggest an extensional tectonic setting at least during the initial mafic intrusions. Since the metamorphism recorded by the surrounding low-grade rocks is Jurassic and Cretaceous, the evolution of the Highiş-Biharia igneous belt should be related to the Alpine (development of Paleotethys ?) rather than to the Variscan "cycle". No record of the Variscan orogeny could be recognized so far in the Highiş Mountains, previously a classical example of the Variscan tectonism.

Available data from other segments of the Alpine orogen suggest that Late Carboniferous/ Permian evolution was dominated by strike-slip tectonics accompanied by uplift and erosion as a precursor to the Alpine cycle. In the Alps, major extensional lineaments of igneous activity developed in the Helvetic and Penninic basement (Bonin et al., 1993). Clastic sedimentation in elongate troughs and volcanic activity related to pull-apart basins are interpreted in the Western and Ligurian Alps. In the West Carpathians, Rb-Sr whole rock and mineral isochrons indicate magmatic activity during the Late Carboniferous in the Tatricum (300 Ma, High Tatra) and Early Permian in the Veporicum (285+/-5 Ma) and Gemericum (282+/-2 Ma)(Cambel et al., 1989). The 264+/-18 Ma K-Ar isochrone age on hornblende from the Gemericum (Burchart et al., 1987), from rocks which have provided pebbles to the non-metamorphosed Carboniferous cover strata may be related to cooling during uplift and erosion following the Early Permian granitic intrusions. In this general framework, the Highiş igneous complex (c. 267-264 Ma) and eventually the emplacement of Vinţa granite (c. 261 Ma) in the southern gneiss-carbonate assemblage may record Early Permian rifting of the continental fragment.

In current models for the Alpine evolution of the region (e.g., Rădulescu and Săndulescu, 1973; Bleahu et al., 1981; Săndulescu, 1984; Savu, 1983; Nicolae et al., 1992; Rădulescu et al., 1993; Lupu et al., 1993), intra-oceanic subduction is suggested to have resulted in Cretaceous emplacement of the Săvârşin granite within Callovian tholeiitic rocks of the Tethyan crust. Late Cretaceous nappe stacking and obduction would have brought the composite igneous crust onto the Apuseni continental crust. Our U-Pb zircon data indicate that the emplacement age is in fact Early Eocene. Consequently, no evidence of Cretaceous subduction at the now southern margin of the Apuseni exists. The only contaminant during the Eocene emplacement of the Săvârşin granite appears to be the tholeiitic crust. The proposed major Late Cretaceous obduction onto the Apuseni continental fragment is questionable because subsequent intrusions did not sample continental crust.

REFERENCES

Autran, A., and Cogné, J., 1980, La zone interne de l'orogène varisque dans l'Ouest de la France et sa place dans le développment de la chaine hercynienne. 26th Int Geol Congr, Colloq. C6 Geol. Eur., Mém. Bur. Rech. Géol. Min., 108, p. 90-111.

Balla, Z., 1982, Development of the Pannonian Basin Basement through the Cretaceous-Cenozoic collision: a new synthesis. Tectonophysics, 88, p.61-102.

Balintoni, I., 1985, Corrélation des unités litostratigraphiques et tectoniques longeant le ruisseau d'Aries entre la vallée de Iara et le Mont Găina (Monts Apuseni), D. S. Inst. Geol. Geofiz., v. LXIX/5, p. 5-15.

Balintoni, I., 1986, Petrologic and Tectonic Features of the Highiş-Drocea Crystalline Massif (Apuseni Mountains), D. S. Inst. Geol. Geofiz., v. 70-71/5, p. 5-21.

Balintoni, I. 1994, Structure of the Apuseni Mountains, *in* 'Geological evolution of the Alpine-Carpathian-Pannonian system' Conference, Covasna, Field Guidebook, J. of Tect. & Reg. Geol., v. 75/2, p. 51-57.

Balogh, K., Árva-Soós, E., and Buda G., 1983, Chronology of granitoid and metamorphic rocks of Transdanubia (Hungary), Anuarul Institutului de Geologie şi Geofizică, 61, p. 359-364.

Barbarin, B., 1990, Granitoids: main petrogenetic classifications in relation to origin and tectonic setting. Geological Journal, vol. 25, p.227-238.

Bleahu, M. 1976, Structural position of the Apuseni Mountains in the Alpine System, Rev. Roum. Géol., Géophys. Géogr., ser. Géol., v. 20, p. 7-19, Bucureşti.

Bonin, et al., 1993, Late Variscan Magmatic Evolution of the Alpine Basement. In Pre-Mesozoic Geology in the Alps. J. von Raumer and F. Neubauer (eds). Springer, Heidelberg, New York, p.171-201.

Briand, B., Piboule, M., and Bouchardon, J. L., 1988, Diversité des métabasites des groupes leptyno-amphibolitiques du Rouergue et de Marvejols (Massif Central). Origine et implications, Bull. Soc. Géol. France, 8, IV, p. 489-498.

Burchart, J., Cambel, B., and Kral, J., 1987, Isochron reassessment of K-Ar dating from the west Carpathian crystalline complex. Geologica Carpatica, 38, 2, p.131-170.

Burchfiel, B.C., 1980, Eastern Alpine system and the Carpathian orocline as an example of collision tectonics, Tectonophysics, 63, p. 31-62.

Bussy, F., and von Raumer, F.J., 1993, U-Pb dating of Palaeozoic events in the Mont-Blanc crystalline massif, Western Alps. Terra Nova, v.5, suppl.1, 56-57.

Cambel, B., and Kral, J., 1989, Isotope geochronology of the western Carpathian crystalline complex; the present state. Geologica Carpathia, 40, p. 387-420.

Cambel , B., Bagbasaryan, G., Gukasyan, R., and Veselsky, J., Rb-Sr Geochronology of leucocratic granitoid rocks from the Spissko-Gemerske Rudohorie Mts. and Veporicum. Geologica Carpatica, 40, 3, p.323-332.

Csontos, L., Nagymarosy, A., Horváth, F., and Kovác, M., 1992, Tertiary evolution of the Intra-Carpathian area: a model, Tectonophysics, 208, p.221-241

Dallmeyer, R.D., Neubauer, F., Handler, R., Fritz, H., Müller, W., Pană, D., and Putis, M., 1996,Tectonothermal evolution of the internal Alps and Carpathians: Evidence from ^{40}Ar/^{39}Ar mineral and whole-rock data. Eclogae geol. Helv. 89/1 p.203-227.

Dallmeyer, R.D., Pană, D., Neubauer, F., and Erdmer, P., 1997, Tectonothermal evolution of the Apuseni Mountains, Romania: Resolution of Variscan vs. Alpine Events with ^{40}Ar/^{39}Ar ages, Tectonophysics, submitted.

Davis, D.W., 1982, Optimum linear regression and error estimation applied to U-Pb data. Can. J. Earth Sci., 19, p.2141-2149.

Dimitrescu, R. 1985, Early Caledonian event in the pre-Alpine metamorphic sequences of the Romanian Carpathian, Acta Mineralogica-Petrographica, Szeged, XXVII, p. 59-70.

Dimitrescu, R. 1988, Observations sur la structure du cristallin des monts Bihor et Gilău meridional. D.S. Inst. Geol. Geofiz., v.72-73/5, p.

Gebauer, D., Williams, I. S., Compston, W., Grünenfelder, M., 1989, The development of the Central European continental crust since the early Archaean based on conventional and ion-microprobe dating of up to 3.84 b.y. old detrital zircons, Tectonophysics, 157, 81-96.

Gebauer, D., 1993, The Pre-Alpine Evolution of the continental crust of the central Alps - an Overview, in J. von Raumer and Neubauer, F. (eds). Pre-Mesozoic Geology in the Alps. Springer, Heidelberg, New York 1993, p.93-117.

Giraud, A., Marchand, J., Dupuy, C., and Dostal, J., 1985, Geochemistry of leptininoamphibolite complex from Haut-Allier (French Massif Central), Lithos, 17, p. 203-214.

Giuşcă, D. Savu, H., and Borcoş, M., 1968, La stratigraphie des schistes cristallins des Monts Apuseni, Rev. Roum. Géol., v. 12/2, p. 143-159.

Giuşcă, D.,1979, Masivul cristalin al Highişului, St. Cern. Geol., Geofiz., Geogr., Geol., v. 24, p. 15-43.

Guerrot, C., Peucat, J. J., Capdevilla, R., 1987, The oldest granulitic crust involved in the Hercynian belt: preliminary U-Pb and Sm-Nd isotopic data. Terra Cognita, Abstract, 7/159.

Haas, J., Kovács, S., Krystyn, L., and Lein, R., 1995, Significance of Late Permian-Triassic facies zones in terrane reconstructions in the Alpine-North Pannonian domain. Tectonophysics, 242, p. 19-40.

Hârtopanu, I., and Hârtopanu, P., 1986, Intersecting isograds - a possible way to find out the polymetamorphism. An example: the Someş series, D.S. Inst.Geol. Geofiz., v. 70-71/1, p. 291-299.

Heaman, L. M., and N. Machado, 1992, Timing and origin of midcontinent rift alkaline magmatism, North America: evidence from the Coldwell Complex, Contributions to Mineralogy and Petrology, 110, p. 289-303.

Ianovici, V., Borcoş, M., Bleahu, M., Patrulius, D., Lupu, M., Dimitrescu, R., and Savu, H., 1976, Geologia Munţilor Apuseni, Ed. Acad. Rom. 631 p., Bucuresti.

Jaffey, A.H., Flynn, K.F., Glendenin, L.E., Bentley, W.C, and Essling, A.M., 1971, Precision measurements of half-lives and specific activities of ^{235}U and ^{238}U. Phys. Rev., C4, p. 1889-1906.

Kovács, S., Császár, G., Galácz, A., Haas, J., Nagy, E. and Vörös, A., 1989, The Tisza Superunit was originally part of the North Tethyan (European) margin. Mem.Soc. Geol. France 154 (II) p.81-100.

Kräutner, H., 1980, Lithostratigraphic correlations of Precambrian in the Romanian Carpathians, An. Inst. Geol. Geog., v. LVII, p. 229-296.

Krogh, T.E., 1973, A low-contamination method for hydrothermal decomposition of zircon and extraction of U and Pb for isotopic age determinations. Ceochim. Cosmochim. Acta, 37, p. 485-494.

Krogh, T.E., 1982, Improved accuracy of U-Pb zircon ages by the creation of more concordant systems using an air abrasion technique. Ceochim. Cosmochim. Acta, 46, p.637-649.

Krogh, T.E., and Davis, G.L., 1975, The production and preparation of ^{205}Pb for use as a tracer for isotope dilution analyses. Carnegie Inst. Washington Yearb. 74, p. 416-417.

Liew, T. C., and Hofmann, A. W., 1988, Precambrian crustal components, plutonic associations, plate environment of the Hercynian Fold Belt of Central Europe: Indications from a Nd and Sr isotopic study. Contrib. Mineral., Petrol., 98, p. 129-138.

Indications from a Nd and Sr isotopic study. Contrib. Mineral., Petrol., 98, p. 129-138.

Liégeois, J.P., Berza, T., Tatu, M., and Duchesne, 1996, The Neoproterozoic Pan-African basement from the Alpine lower Danubian nappe system (South Carpathians,Romania). Precambrian Research, 80, 3-4, p. 281-301.

Maluski, H., Rajlich, P., and Matte, P., ^{40}Ar/^{39}Ar dating of the Inner Carpathians Variscan basement and Alpine mylonitic overprinting. Tectonophysics, 223, p. 313-337.

Márton, E., and Mauritsch, H.J., 1990, Structural applications and discussion of a paleomagnetic post-Paleozoic data base for the Central Mediterranean, Physics of the Earth and Planetarey Intyeriors, 62, p.46-59.

Ménot, R.P., and Paquette, J.L., 1993, Geodynamic significance of basic and bimodal magmatic events in the external domain. In J. von Raumer and F. Neubauer (esd). Pre-Mesozoic Geology in the Alps. Springer, Heidelberg, New York, p.241-254.

Ménot, R.P., Bonhomme, M.G., and Vivier, G., 1987, Structuration tectono-métamorphique carbonifère dans le massif de Belledonne (Alpes occidentales françaises) Apport de la géochronologie K/Ar des amphiboles. Schwiez. Mineral. Petrogt. Mitt. 67, p.273-284.

Neubauer, F. 1988, Bau und Entwicklungsgeschichte des Rennfeld-Mugel- und des Gleinalmkristallings (Ostalpen). Abh. Geol. B. - A., 42, p. 1-137.

Neubauer, F., and von Raumer, J.F., 1993, The Alpine basement - linkage between Variscides and east-Mediterranean mountain belts. In J. von Raumer and F. Neubauer (eds). Pre-Mesozoic Geology in the Alps. Springer, Heidelberg, New York, p. 641-663.

Pană, D., and Ricman, C., 1988, The lower complex of the Păiuşeni series - a blastomylonitic shear belt. Rev. Roum. Géol., Géophys. et Géogr., ser. Géol., tome 32, p. 21-35.

Pană, D., Erdmer, P., Dallmeyer, R.D., and Neubauer, F., 1998 (submitted), Tectonothermal evolution of the Apuseni Mountains, Romania: Implications of strain partitioning, Tectonics.

Paquette, J.L., Ménot., R.P., Peucat J.J., 1989, Sm-Nd and U-Pb zircon study of eclogites from the Alpine External Massifs (Western Apls): evidence for crustal contamination. Earth and Planetary Science Letters, 96, 1/2, p. 181-198.

Pavelescu, L., Pop, G., Ailenei, G., Ene, I., Soroiu, M., and Popescu, G., 1975, K-Ar age determinations from the Apuseni and Banat Mountains, Rev. Roum. Géophys., v. 19, p. 67-69.

Peucat, J. J., Jegouzo, P., Vidal, P., and Bernard-Griffiths, J., 1988, Continental crust formation seen through the Sr and Nd isotope systematics of S-type granites in the Hercynian belt of Western Europe, Earth. Planet. Sci. Lett., 88, p. 60-68.

Pin, C., 1991, Central-Western Europe: Major Stages of Development During Precambrian and Paleozoic Times, d'une subduction éo-hercynienne. Implications sur l'origine des groupes leptyno-amphibolitiques, Bull. Soc. Géol. France, 8, IV, p. 13-20.

Putis, M., 1994, South Tatric-Veporic Basement Geology: Variscan Nappe Structures; Alpine Thick-Skinned and Extensional Tectonics in the West Carpathians (Eastern Low Tatra Mountains, Northwester Slovak Ore Mountains), Mitt.Osterr. Geol.Ges. 86, p. 83-99

Săndulescu, M., 1994, Overview on Romanian geology. Rom. J. of Tect. & Regional Geology, v. 75/2, p. 3-15, ALCAPA II, Covasna conference, Field Guidebook.

Shcherbak, N.P., Bartinsky, E.N., Mitskievich, N.Y., Stepanyuk, L.M., Cambel, B., and Grecula, P., 1988, U-Pb radiometric determination of the age of zircons from Modra granodiorite (Malé Karpaty) and porphyroid from Spissko-gemerske rudohorie Lower Paleozoic (Western Carpathians), Geologica Carpatica, 39, 4, p. 427-436.

Soroiu, M., Popescu, G., Kasper, U., and Dimitrescu, R., 1969, Contributions préliminaires à la géologie des massifs cristallins des Monts Apuseni, An. St. Univ. "Al.I.Cuza", Sect.IIb (Geol), v. 15, p. 25-33.

Schmid, S.M., 1993, Ivrea-zone and adjacent Southern Alpine basement. In: J. von Raumer and F. Neubauer (eds). The Pre-Mesozoic Geology in the Alps. Springer, Heidelberg, New York, p.567-583.

Stacey, J.S., and Kramers, J.D., 1975, Approximation of terrestrial lead isotope evolution by a two-stage model. Eatrh. Plan. Sci. Lett., 26, p. 207-221.

Steiger, R.H., and Jäger, E., 1977, Subcommission on geochronology: Convention on the use of decay constants in geo- and cosmochronology. Earth. Plan. Sci. Lett., 36, p. 359-362.

Svingor, É., and Kovách, Á., 1981, Rb-Sr isotopic studies on granodioritic rocks from the Mecsek Mountains, Hungary. Acta Geologica Hungaricae, 24, 2-4, p. 295-307.

von Raumer, J., and Neubauer, F., 1994, The Paleozoic evolution of the Alps, Schweiz. Mineral. Petrogr. Mitt. 74, p. 459-467.

Wasserburg, G. J., Jacobsen, S. B., DePaolo, D. J., McCulloch, M. T. and Wen, T., 1981, Precise determination of Sm/Nd ratios, Sm and Nd isotopic abundances in standard solutions. Geochim. Cosmochim. Acta, 45, p. 2311-2323.

Weber, K., 1984, Variscan events: early Paleozoic continental rift metamorphism and late Paleozoic crustal shortening, *in* Hutton, D. H. W., and Sanderson, D. J., (Eds.): Variscan tectonics of the North Atlantic region, Geol. Soc. Spec. Publ., 14, p. 3-22.

York, D., 1969, Least squares fitting of a straight line with correlated errors. Earth Planet. Sci. Let., 5, p. 320-324.

CHAPTER 4*

TECTONOTHERMAL EVOLUTION OF THE APUSENI MOUNTAINS, ROMANIA: RESOLUTION OF VARISCAN VS. ALPINE EVENTS WITH $^{40}Ar/^{39}Ar$ AGES

This chapter contains an article submitted to Geologische Rundschau by R.D. Dallmeyer[1], D.I. Panǎ[2], F. Neubauer[3] and P. Erdmer[2]

[1] Department of Geology, University of Georgia, Athens, GA 30602 USA
[2] Department of Earth & Atmospheric Sciences, University of Alberta, Edmonton, Canada T6G 2E3
[3] Geology and Paleontology Institute, Paris-London University, A-5020 Salzburg, Austria

4.1. INTRODUCTION

The Alpine-Carpathian orogen originated during the Mesozoic-Cenozoic collision of Europe with continental crustal fragments derived from Gondwana. These continental plates were initially separated by oceanic crust of the Penninic and at least part of the Tethyan oceans. Stratigraphic constraints and previously published geochronologic data suggest that initial phases of oceanic subduction and localized high-pressure metamorphism occurred during the Late Jurassic-Cretaceous (e.g., "Early" Alpine tectonothermal events: Frank et al., 1976, 1983, 1987; Krist et al., 1992; Cambel and Kral, 1989; Maluski et al., 1993; Thoni and Jaquoz, 1992; Dallmeyer et al., 1996). As a result, nappe assembly and associated imbrication of internal units occurred within the Alpine-Carpathian orogen. However, the exact chronology of thrusting and the sequence of internal deformation from hanging wall to footwall has not been clearly resolved. Final collision of Europe and Gondwana occurred in the Paleogene ("Late" Alpine orogenesis: e.g., Burchfiel, 1980; Tollmann, 1987; Trümpy, 1988), and resulted in the emplacement of previously assembled nappe complexes onto external tectonic elements of the Alpine-Carpathian orogen. The Paleogene collisional suture separates internal tectonic units which experienced both Cretaceous and Paleogene penetrative Alpine deformation from external tectonic units which record only "Late" Alpine events. Resolution of the chronology of Alpine events and distinction from pre-Alpine evolution has been difficult within internal structural units which include basement tectonic elements. Among these, the Apuseni Mountains have particular tectonic significance because they are separated from other basement units in the Alpine-Carpathian orogen by an ophiolitic suture.

Back-arc extension and/or strike-slip translation associated with the Neogene development of the Pannonian Basin system variably overprinted older compressional structures of the Carpathian arc. Basement and Mesozoic cover sequences in the Apuseni Mountains represent critical exposures regionally situated between the Pannonian and Transylvanian basins (Fig. 4-1). Previous workers considered metamorphic basement rocks exposed in the Apuseni Mountains to have evolved in three distinct tectonothermal cycles, with highest grade sequences being considered the oldest (see reviews in Giuşcă et al., 1968; Ianovici et al.,1976; Kräutner, 1980; Dimitrescu, 1985, 1988a). The location of boundaries between the contrasting metamorphic sequences has been controversial, and there have been conflicting interpretations of the nature of unit boundaries and the age and origin of protoliths. The effects of Alpine orogenesis have generally been interpreted as translations of rigid thrust sheets with relatively insignificant internal ductile strain (e.g., Ianovici et al., 1976; Săndulescu, 1984; Balintoni, 1985, 1986, 1994; Dimitrescu, 1988b). Recent field work and structural analysis in the Apuseni Mountains (Pană and Ricman, 1988; Pană and Erdmer, 1994; and Pană et al., 1996) have uncovered an extensive record of non-coaxial strain in basement areas affected by retrogressive

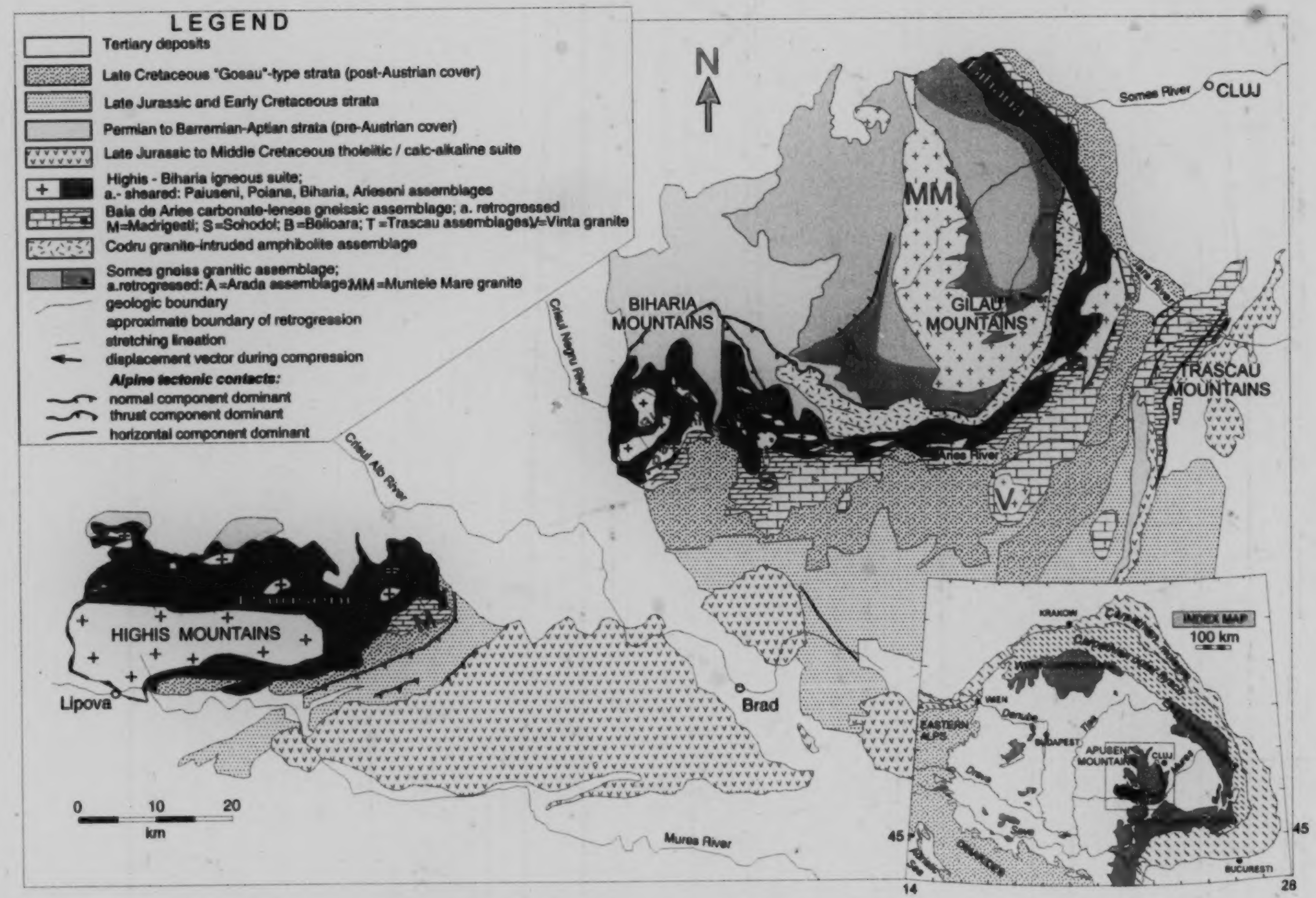
LEGEND
Tertiary deposits
Late Cretaceous "Gosau"-type strata (post-Austrian cover)
Late Jurassic and Early Cretaceous strata
Permian to Barremian-Aptian strata (pre-Austrian cover)
Late Jurassic to Middle Cretaceous tholeiitic / calc-alkaline suite
Highis - Biharia igneous suite;
a.- sheared: Paiuseni, Poiana, Biharia, Arieseni assemblages
Baia de Aries carbonate-lenses gneissic assemblage; a. retrogressed
M=Madrigesti; S=Sohodol; B=Belioara; T=Trascau assemblages V=Vinta granite
Codru granite-intruded amphibolite assemblage
Somes gneiss granitic assemblage;
a.retrogressed: A=Arada assemblage MM=Muntele Mare granite
geologic boundary
approximate boundary of retrogression
stretching lineation
displacement vector during compression
Alpine tectonic contacts:
normal component dominant
thrust component dominant
horizontal component dominant
N
Somes River
CLUJ
MM
GILAU MOUNTAINS
BIHARIA MOUNTAINS
Crisul Negru River
Crisul Alb River
Aries River
TRASCAU MOUNTAINS
V
S
M
HIGHIS MOUNTAINS
Lipova
Brad
Mures River
0
10
20
km
INDEX MAP
100 km
KRAKOW
WIEN
Danube
BUDAPEST
Tisa
EASTERN ALPS
APUSENI MOUNTAINS
CLUJ
Drava
Sava
BUCURESTI
45
45
14
28

Fig. 4-1. Structural map of the Apuseni Mountains

metamorphism (Fig. 4-1). The data suggest regional Alpine reactivation of basement units within the Apuseni Mountains. A systematic $^{40}Ar/^{39}Ar$ dating program has been carried out to help resolve the extent, intensity, and detailed chronology of Alpine vs. earlier tectonothermal events within the Apuseni Mountains.

These results are presented here. They suggest a complex tectonothermal evolution that involved "Early" and "Late" Variscan and polyphase Alpine events. These new data necessitate a revision of the traditional interpretation of the geological history of the region and its role within the overall Alpine-Carpathian orogen.

4.2. GEOLOGIC SETTING, PREVIOUS GEOCHRONOLOGY

The Apuseni Mountains expose various structural elements consisting of contrasting metamorphic and igneous basement rocks and Permian-Tertiary cover sequences with "Western Carpathian" - "Austroalpine" affinities (Fig. 4-1).

Basement units of the Apuseni Mountains were previously interpreted to represent volcanic-sedimentary sequences which originated and were metamorphosed during three successively superposed geosynclinal cycles (e.g., Giuşcă et al., 1968; Ianovici et al., 1976, Kräutner, 1980; Dimitrescu, 1985; 1988b). The age of tectonothermal events was established on the basis of relative metamorphic grade and lithostratigraphic correlations. The highest-grade and most complexly deformed units were considered the oldest. Garnet-bearing gneiss / micaschist / amphibolite associations were assigned to a Middle Proterozoic cycle (e.g., the Someş, Codru, Baia de Arieş and Mădrigeşti "series"), transitional upper greenschist-lower amphibolite grade units were considered Upper Proterozoic-Early Paleozoic (e.g., the Biharia, Arada and/or Bistra "series" and/or "formations") and chlorite-dominated rocks were assigned a Late Paleozoic age (e.g., the Păiuşeni, Arieşeni, Sohodol, Muncelu, Belioara, Vidolm and Trascău "series" and/or "formations"). Regional orogenic unconformities were inferred between assemblages of different matamorphic grade and were interpreted to record a succession of superposed Precambrian, Early Paleozoic ("Caledonian") and Late Paleozoic ("Variscan") events. As a result, a formal stratigraphic classification of the metamorphic assemblages was developed (e.g., Kräutner, 1980; Dimitrescu, 1985, 1988b)

Previous geochronology consisted of a relatively large number of K-Ar data for most of the representative basement units of the Apuseni Mountains (Soroiu et al., 1969; Pavelescu et al., 1975). In contrast to the proposed classification, all isotopic ages reported so far for low-grade (greenschist) samples are Alpine whereas all gneissic and granitic samples have yielded Middle Paleozoic or younger ages (Table 4-1). Mesozoic and Tertiary K-Ar mineral ages reported from several areas of medium- and low-grade metamorphic rocks were interpreted to record local fault reactivation (e.g., Dimitrescu, *in* Soroiu et al., 1969).

Table 4-1. Previous radiogenic data in the Apuseni Mountains (K-Ar neutron activation)

Assemblage	Locality	Rock type	Analysed sample	K-Ar age (Ma)	
				Soroiu et al., 1969	*Pavelescu et al., 1975*
LOW-GRADE ROCKS					
Arada	Valea Mare Valley, Bistra	sericite-feldspar schist	WR	49	
Arada	Albacului Valley	sericite schist	WR	111	
Arada	Bistra Valley	sericite-feldspar schist	WR	164	
Arada	Bistra Valley	sheared hornfels	WR	204	
Biharia	Ariesul Mare Valley,Vadul Motilor	sericite schist	WR	115	
Biharia	Bistra Valley	Chl-Mu-Ab schist	WR	181	
Biharia	Valea Mare Valley, Bistra	sericite schist	WR	106	
Paiuseni	Highis Valley, Casoaia	sericite schist	WR	113	
Paiuseni	Highis Valley, Casoaia	Chl-Mu-Ab schist	WR	115	
Paiuseni	Siria Fortress	"metaconglomerate"	WR	123	
MEDIUM-GRADE ROCKS					
Somes	Cosului Valley	micaschist	WR		227+/-8
Somes	Iara Valley	amphibolite	Ho		209+/-6
Somes	Iara Valley	quartz-feldspar schist	Bi		79+/-5
Somes	Cosului Valley	garnet micaschist	WR	268	
Somes	Bulzului Valley	garnet micaschist	WR	381	
IGNEOUS ROCKS					
Somes	Preluca Mountains, Copalnic	pegmatoid granite	Mu	90	
Somes	Preluca Mountains, Copalnic	pegmatoid granite	Mu	107	
Somes	Valea Mare Valley, Bistra	Muntele Mare pegmatite	Mu		237+/-6
Somes	Valea Mare Valley, Bistra	Muntele Mare pegmatite	Mu		199+/-6
Somes	Valea Mare Valley, Bistra	Muntele Mare granite	Bi		119+/-3
Somes	Calatele	Muntele Mare granite	Bi		85+/-3
Somes	Somesul Rece Valley	Muntele Mare granite	Bi	90	
Somes	Somesul Rece Valley	Muntele Mare granite	K-F	89	
Somes	Valea Mare Valley, Bistra	Muntele Mare granite	Bi	115	
Somes	Valea Mare Valley, Bistra	Bi-enclave in the MM granite	Bi	160	
Somes	Somesul Rece Valley	Muntele Mare pegmatite	Mu	156	
Somes	Valea Mare Valley, Bistra	Muntele Mare pegmatite	Mu	194	
Somes	Valea Mare Valley, Bistra	Muntele Mare pegmatite	Mu	232	
Codru	Dosul Neagului	pegmatoid granite	Mu	296	
Codru	Dosul Neagului	pegmatoid granite	Mu	305	
Codru	Valea Mare Valley, Bistra	pegmatoid granite	Mu	326	
Codru	Bistra Valley	pegmatoid granite	Mu	343	
Codru	Ariesul Mare Valley, Pojorata	trondhjemite	Bi	303	
Codru	Bistra Valley	pegmatoid diorite	Ho	288	
Codru	Valea Mare Valley, Bistra	pegmatoid diorite	Ho	300	
Codru	Valea Mare Valley, Bistra	hornblendite	Ho		357+/-10
Codru	Valea Mare Valley, Bistra	pegmatite	Mu		356+/-9
Codru	Ariesul Mare Valley, Pojorata	biotitite	Bi		340+/-9
Codru	Ariesul Mare Valley, Pojorata	pegmatoid granite	Bi		281+/-10
Codru	Ariesul Mare Valley, Pojorata	trondhjemite	Bi		230+/-9

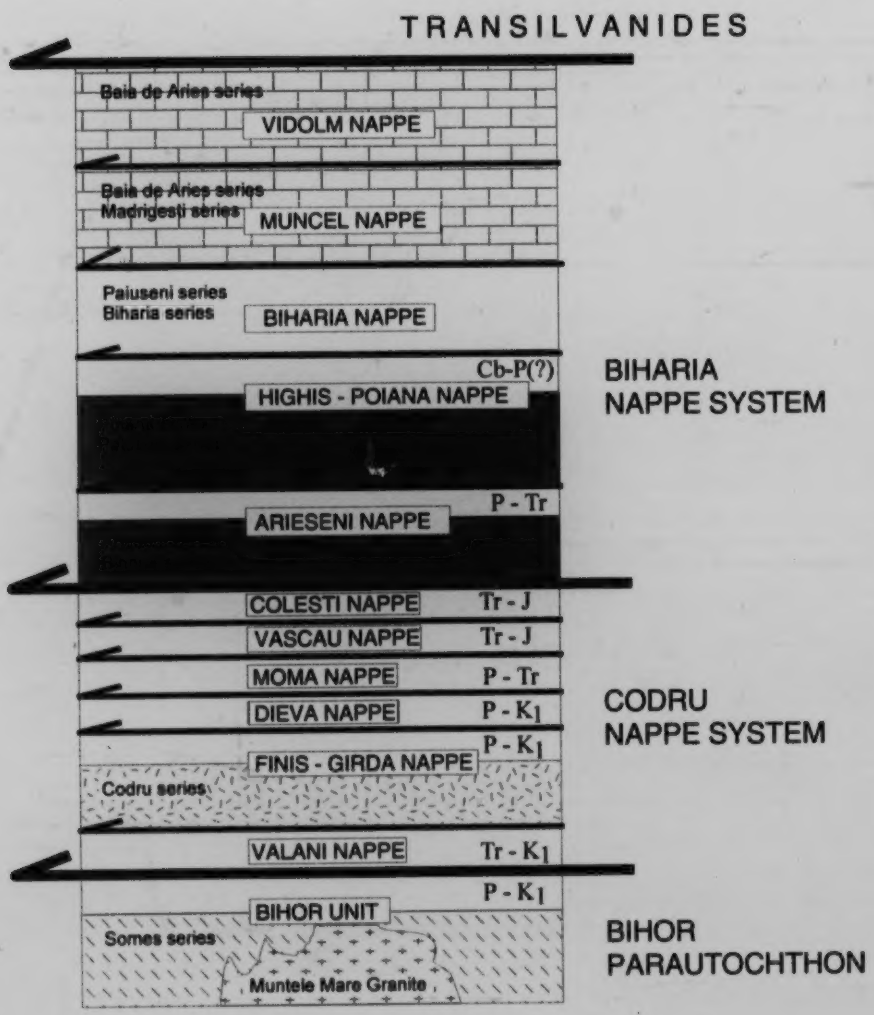
TRANSILVANIDES
Baia de Aries series
VIDOLM NAPPE
Baia de Aries series
Madrigesti series
MUNCEL NAPPE
Paiuseni series
Biharia series
BIHARIA NAPPE
Cb-P(?)
HIGHIS - POIANA NAPPE
P - Tr
ARIESENI NAPPE
BIHARIA NAPPE SYSTEM
COLESTI NAPPE
Tr - J
VASCAU NAPPE
Tr - J
MOMA NAPPE
P - Tr
DIEVA NAPPE
$P - K_1$
$P - K_1$
FINIS - GIRDA NAPPE
Codru series
CODRU NAPPE SYSTEM
VALANI NAPPE
$Tr - K_1$
$P - K_1$
BIHOR UNIT
Somes series
Muntele Mare Granite
BIHOR PARAUTOCHTHON

Fig. 4-2. Nappe stacking model for the Apuseni Mountains (compiled from Bleahu, 1981; Săndulescu, 1984; Balintoni, 1994).

Alpine tectonism was largely considered to be the Cretaceous (pre-Gosau) assembly of several nappe complexes associated with rigid translation of basement and cover units. An idealized thrust stack derived from existing compilations (Bleahu et al., 1981, Săndulescu, 1984, Balintoni, 1994) is presented in Fig. 4-2. Resolution of the timing of individual Alpine events was based on stratigraphic controls. In northern sectors of the Apuseni Mountains, a climactic "Mediterranean", intra-Turonian deformation was reported to have followed initial Middle Cretaceous tectonism and to have resulted in emplacement of the contrasting Codru and Biharia nappe complexes onto the Bihor "autochthon" (e.g., Bleahu et al., 1981; Săndulescu, 1984). The Codru nappe complex was inferred to consist of six or seven distinct thrust units dominated by cover sequences. Only one nappe near the base of the Codru nappe complex was considered to include basement rocks (the Codru assemblage). In contrast, the Biharia nappe complex was described as comprising only basement units (Bleahu et al., 1981; Săndulescu, 1984). Balintoni (1986, 1994) considered that each Alpine thrust sheet comprised several Variscan nappes. The Codru nappe complex was considered to have been assembled and thrust over the Bihor para-autochthon in the Turonian. The Biharia nappe complex structurally overlies different Permian to Barremian-Aptian cover sequences within various Codru nappe units. Senonian, Gosau-type sequences stratigraphically overlie the Biharia nappe complex (Bleahu et al., 1981; Săndulescu, 1984). Alpine nappe assembly in southern sectors of the Apuseni Mountains has been considered to be of Middle Cretaceous age in the Trascău Mountains (Lupu, in Bleahu et al., 1981) and of Early Laramian age (Maastrichtian) in other areas. However, no unambiguous stratigraphic constraints are available, and rocks ranging up to Paleogene are locally involved in Alpine thrusting (Bordea, 1992).

4.3. GEOLOGICAL UNITS

Pană and Erdmer (1994) and Pană et al. (1996) described continuous zones of concentrated ductile strain within the Apuseni Mountains. They interpreted these to record regionally significant horizontal displacements between distinct lithologic assemblages, and questioned the extent of rigid Alpine thrusting within most sectors of the Apuseni Mountains. They recognized several regionally mappable "lithotectonic assemblages" which record marked along-strike variations in Alpine tectonism. These include the Someş, Codru, and Baia de Arieş medium-grade assemblages and the Păiuşeni, Biharia, Arieşeni and Poiana low-grade assemblages (Fig. 4-1).

Pană and Erdmer (1994) and Pană et al. (1996) described the Bihor structural unit ("autochthon") as plagiogneiss, amphibolite, micaschist, and variably deformed granite which together comprise the Someş assemblage. The last medium-grade tectonothermal event recorded in this assemblage predated emplacement of the large Muntele Mare granite. Pană et al. (1996) described the Codru assemblage to include gabbro-diorite, dolerite, microdiorite, and amphibolite, which together are cut by veins and stocks of granite and granodiorite. The distinct Highiş, Biharia and Arieşeni assemblages comprise a penetratively sheared, upper crustal igneous complex composed of variably transformed mafic-felsic subvolcanic units and local gabbro-diorite-granite tectonic enclaves. An early, low-grade contact metamorphism is locally preserved in mafic rocks adjacent to large granitic units. The Highiş-Biharia composite magmatic crust was affected by polyphase ductile-brittle shearing. Heterogeneous strain partitioning resulted in localized preservation of early fabric elements. The medium-grade Baia de Arieş assemblage is composed of plagiogneiss, micaschist, amphibolite, quartzite, granite pegmatite, and discontinuous lenses of variably dolomitic marble. It is characterized by less significant low-temperature retrogressive alteration than the Highiş-Biharia assemblage.

4.4. TECTONOTHERMAL EVOLUTION

The Someş assemblage records a complex metamorphic history. The oldest recognizable fabrics reflect medium-pressure, medium-grade metamorphic conditions up to the garnet- staurolite zone. The Barrovian zonation initially proposed by Dimitrescu et al. (1974) has been questioned in later work (Balintoni, 1985; Pană et al., 1996). Sillimanite and cordierite (Dimitrescu, 1988a) and sillimanite and magnetite-biotite (Pană et al., 1996) occur along the periphery of the Muntele Mare granite. A distinct sillimanite zone was mapped by Hârtopanu and Hârtopanu (1986) within garnet and staurolite-bearing gneiss, which may relate to an unexposed stock of the Muntele Mare granite. Field relationships suggest that initial phases of the last post-metamorphic uplift of the Someş assemblage from middle crustal levels resulted in development of sillimanite - or biotite/magnetite- bearing mylonitic gneiss with gently dipping fabrics. These were variably overprinted by generally lower grade, more steeply dipping mylonitic-brittle fabric elements also developed under greenschist facies metamorphic conditions. Erdmer and Pană (1995) suggested that these fabrics record the development of a late chlorite-grade detachment zone during extensional exhumation of the Someş assemblage. This contrasts with previous interpretations of the low-grade rocks ("Arada series") as a Late Proterozoic volcanic-sedimentary succession affected by Early Paleozoic ("Caledonian") tectonic activity (e.g., Dimitrescu, 1985) or by retrogression of the Someş assemblage during Cretaceous thrusting (Balintoni, 1985).

The Codru assemblage comprises igneous rocks deformed under medium- to low-grade metamorphic conditions. Layered mylonitic amphibolite is commonly spatially associated with massive dolerite (e.g., Bistra Mare Valley) or pegmatitic gabbro/diorite (e.g. Bistra Valley). Quartzofeldspatic gneiss generally contains either biotite or muscovite, or chlorite and muscovite and appear to have been derived from a Codru granodiorite protolith. Fibrolite occurs in sheared

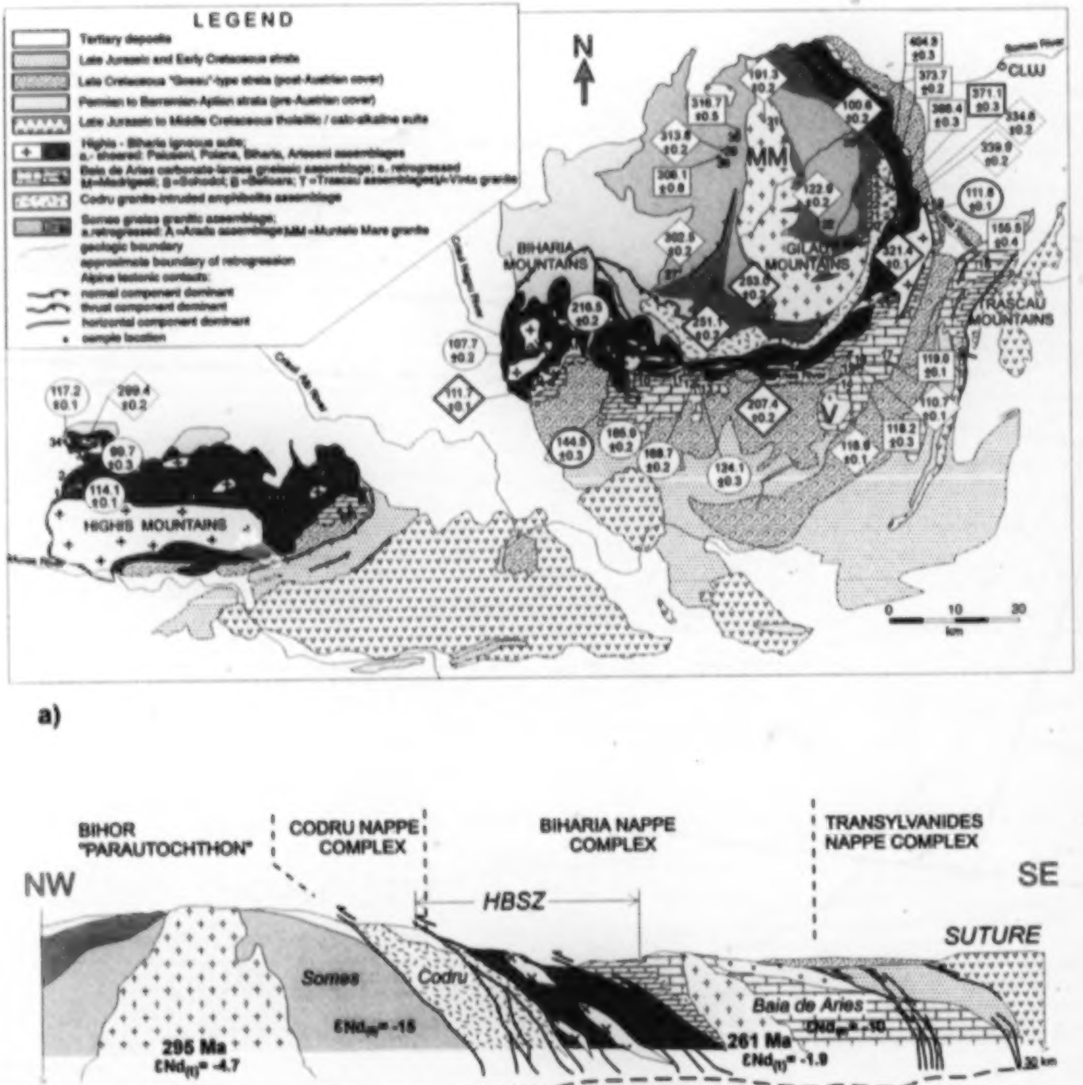
LEGEND
Tertiary deposits
Late Jurassic and Early Cretaceous strata
Late Cretaceous "Gosau"-type strata (post-Austrian cover)
Permian to Barremian-Aptian strata (pre-Austrian cover)
Late Jurassic to Middle Cretaceous tholeiitic / calc-alkaline suite
Highis - Biharia igneous suite;
a.- sheared: Paiuseni, Poiana, Biharia, Arieseni assemblages
Baia de Aries carbonate-laness gneissic assemblage; a. retrogressed
Codru granite-intruded amphibolite assemblage
Somes gneiss granitic assemblage;
a.retrogressed: A =Arada assemblage; MM =Muntele Mare granite
geologic boundary
approximate boundary of retrogression
Alpine tectonic contacts:
normal component dominant
thrust component dominant
horizontal component dominant
sample location
N
CLUJ
MM
BIHARIA MOUNTAINS
GILAU MOUNTAINS
TRASCAU MOUNTAINS
HIGHIS MOUNTAINS
0
10
20
km
a)
BIHOR "PARAUTOCHTHON"
CODRU NAPPE COMPLEX
BIHARIA NAPPE COMPLEX
TRANSYLVANIDES NAPPE COMPLEX
NW
SE
HBSZ
SUTURE
Somes
Codru
Baia de Aries
295 Ma
εNd(t)= -4.7
261 Ma
εNd(t)= -1.9
35 km
30 km
MOHO
b)

Fig. 4-3. a) Generalized geologic-tectonic map of the Apuseni Mountains. Localities for which $^{40}Ar/^{39}Ar$ ages have been determined are indicated by: open-circle = whole-rock; square = hornblende; diamond = muscovite. For hornblende and muscovite: thin frame = plateau age; thick frame = total-gas age;
b) Interpretative NW-SE cross-section in the central Apuseni Mountains ("nappe complexes" compiled from Bleahu et al., 1981, and Sandulescu, 1984).

chlorite-bearing rocks, indicating that peak metamorphic conditions locally reached the "sillimanite-in" isograd. Textural characteristics suggest local relative aluminum enrichment together with fibrolite blastesis during shearing and retrogression. However, the rocks rarely display medium-grade textures. Most frequently, massive or non-penetratively deformed diorite/dolerite/granite are enveloped by phyllonite. Shallow-dipping mullions and fold hinges in the amphibolite mylonite everywhere trend parallel to strike, and surround the Bihor autochthon. Kinematic indicators in phyllonite suggest concurrent or successive strike-parallel and normal dip-slip translations. The tectonic boundaries of the Codru assemblage are difficult to trace between the Someş and Biharia assemblages. Continuous thrust surfaces cannot be mapped and there is no evidence for the extensive Alpine thrusting which was previously proposed (e.g., Săndulescu, 1984; Balintoni, 1985). Pană et al. (1996) suggested that an amphibolite/ granodiorite mid-crustal domain was structurally emplaced over the Someş assemblage during early Variscan tectonism. This allochthon was structurally disrupted during Alpine strike-slip and normal detachment, resulting in development of a tectonically composite Codru assemblage. The dominant low-grade structures record this evolution at relatively shallow crustal depths.

Coniacian strata unconformably overlie a thrust contact between a Codru structural unit and underlying Turonian cover of the Bihor autochthon (Bleahu et al., 1981). In western parts of the Apuseni Mountains, both the Someş and Codru assemblages are unconformably overlain by a Permian clastic sequence which can be traced stratigraphically upward into Lower Cretaceous units. The Permian-Lower Cretaceous sequence records locally penetrative Alpine strain.

Lithotectonic assemblages within the Highiş-Biharia shear zone record evolution under low- to very low-grade metamorphic conditions. In the Highiş Mountains, the Păiuşeni assemblage consists of a composite igneous crust surrounded by polyphase, variably mylonitic units that have been thrust over Permian-Mesozoic cover in lowermost Codru structural units. Kinematic indicators suggest top-to-the-northwest thrusting followed by normal dip-slip motion. Protoliths of the foliated rocks are controversial. The rocks were interpreted initially to represent a Middle Paleozoic clastic sequence affected by Variscan metamorphism and magmatism (Ianovici et al., 1976; Giuşcă, 1979; Dimitrescu, 1985). Assuming different protoliths for parts of the Păiuşeni assemblage, Balintoni (1986) assigned them to Variscan and Cretaceous nappes. Pană and Ricman (1988) proposed that the foliated rocks are low-grade mylonites formed within a Middle Cretaceous thrust zone affecting composite igneous crust. Thrust kinematics are supported by structural data (Pană et al., 1996), but there is no evidence for distinct tectonic boundaries within the Păiuşeni assemblage (Balintoni, 1986; 1994). The Arieşeni, Biharia, and Păiuşeni assemblages exposed in the Biharia Mountains consist of low-grade, polyphase mylonites derived from different protoliths. These structurally overlie imbricated Permian to Barremian-Aptian cover within Codru structural units. Internal strain in all assemblages is similar, and records northwest thrusting followed by extension (similar to the Highiş Mountains). In the southern and eastern Gilău Mountains, the Biharia assemblage records evidence of strike-slip and local reverse-slip motion, followed by extensive down-dip slip motion. Pană et al. (1996) suggested that oblique Alpine compression between the Someş and Baia de Arieş continental fragments was accommodated mainly within the Highiş-Biharia igneous belt by west-directed tectonic extrusion and thrusting. Subsequent extension overprinted previous zones of crustal weakness.

The Baia de Arieş assemblage occupies upper structural positions south and east of the Highiş-Biharia shear zone. It underwent sillimanite-grade metamorphism. Fine-grained biotite +/-garnet +/- kyanite mylonite bands are spatially associated with two-mica garnet +/- aluminosilicate protoliths, indicating a tectonic evolution from lower- to mid-crustal levels. Chlorite-bearing mylonite zones overprint this assemblage in places: one in the southern Gilău Mountains along the Highiş-Biharia shear zone and the second one in the Trascău Mountains along the TSZ. In both zones, kinematic indicators record movement parallel to strike. Senonian, Gosau-type sedimentary sequences unconformable overlie both low-grade assemblages within the Highiş-Biharia shear zone and medium-grade rocks of the Baia de Arieş assemblage.

4.5. ANALYTICAL METHODS

The Apuseni mineral concentrates and whole-rock samples were analyzed using incremental - release, ^{40}Ar/^{39}Ar analysis. The techniques used generally followed those described by Dallmeyer and Gil Ibarguchi (1990). Variations in flux of neutrons along the length of the irradiation assembly were monitored with several mineral standards, including MMhb-1 (Sampson and Alexander, 1987). Intra-laboratory uncertainties have been calculated by statistical propagation of uncertainties associated with measurements of each isotopic ratio (at two standard deviations of the mean) through the age equation. Inter laboratory uncertainties are c. ±1.25-1.5% of the quoted age (Dallmeyer and Gil Ibarguchi, 1990). A "plateau" is considered defined if the ages recorded by four or more contiguous gas fractions (with similar apparent K/Ca ratios) each representing > 4% of the total ^{39}Ar evolved (and together constituting > 50% of the total ^{39}Ar evolved) are mutually similar within + 1% Intra laboratory uncertainty. Analyses of the MMhb-1 monitor show that apparent K/Ca ratios may be calculated through the relationship 0.518 (+0.005) x ^{39}Ar/^{40}Ar vs. ^{39}Ar/^{40}Ar isotope correlation diagrams. Regression techniques followed methods described by York (1969). A mean square of the weighted deviated (MSWD) has been used to evaluate the isotopic correlations.

4.6. RESULTS

^{40}Ar/^{39}Ar incremental-release heating techniques were used to date 34 representative samples collected within various structural units comprising the Apuseni Mountains. These included 24 multigrain mineral concentrates (9 hornblende and 15 muscovite) and 10 whole-rock samples of slate/phyllite or phyllonite (Fig. 4-3). Sample locations and descriptions of the petrographic characteristics of the dated samples are listed in Table 4-2. The ^{40}Ar/^{39}Ar analytical data are listed in Tables III-1 to III-4 (Appendix III) and are portrayed as apparent age spectra in figures 4-4 to 4-13.

4.6.1. HORNBLENDE

Nine hornblende concentrates from the Someş, Codru and Baia de Arieş assemblages display internally discordant ^{40}Ar/^{39}Ar age spectra of variable complexity (Figs. 4-4 to 4-6). Apparent K/Ca ratios are relatively small and display little intra sample variation. All spectra are marked by considerable variations in apparent ages recorded by gas fractions evolved at low experimental temperatures. These are matched by fluctuations in apparent K/Ca ratios that suggest experimental evolution occurred from compositionally distinct, relatively non-retentive phases. These could be represented by: 1) very minor, optically undetectable contaminant minerals in the hornblende concentrates; 2) petrographically unresolved exsolution or compositional zonation within constituent hornblende grains; 3) minor chloritic replacement of hornblende; and/or 4) intra crystalline inclusions. Most intermediate- and high-temperature gas fractions evolved from the hornblende concentrates display little intra sample variation in apparent K/Ca ratios, suggesting that experimental evolution of gas occurred from populations of compositionally uniform intra crystalline sites. These fractions generally display little intra sample variations in apparent ages and correspond to well-defined plateaus.

Someş Assemblage

Two samples of amphibolite were collected within the non-retrogressed (pre-Permian / Mesozoic) crystalline basement of the Bihor "autochthon" (Someş assemblage) at locations 28 and 30. Hornblende concentrates from these samples yielded well-defined intermediate- and high-temperature plateaus (Fig. 4-4) which correspond to ages of 306.1 ± 0.8 Ma (28) and 316.7 ± 0.5 Ma (30). The plateau data yield well-defined ^{36}Ar/^{40}Ar vs. ^{39}Ar/^{40}Ar isotope correlations (MSWD < 2.0: Table III-1, in Appendix III) with inverse ordinate intercepts (^{40}Ar/^{36}Ar ratio) are slightly larger than the ^{40}Ar/^{36}Ar ratio in the present-day atmosphere. This suggests that there is no significant intra crystalline contamination with extraneous ("excess") argon components. Using the inverse abscissa intercepts (^{40}Ar/^{39}Ar ratio) in the age equation yields plateau isotope-correlation ages of 300.4 ± 1.0 Ma (28) and 313.6 ± 1.0 Ma (30). Because calculation of

Table 4-2. Ar / Ar sample localities and petrography

	Lithotectonic assemblage	Locality	Rock type	Sample	Plateau Age	Isotope Correlation age	Total Gas Age
HIGHIS - BIHARIA SHEAR ZONE							
1	*Black Series*	*Cuvin quarry*	*phyllonite*	WR	114.1		114.4
2	*Paiuseni*	*Covasint Hill*	*phyllonite*	WR	99.7		106.1
3	*Paiuseni*	*Siria Fortess*	*"metaconglomerate"*	Mu	299.4		288.6
4	*Poiana*	*Criscior Village*	*phyllonitic granite*	WR	107.7		110.5
5	*Paiuseni*	*Baresti Valley*	*"metaconglomerate"*	Mu			111.7
6	*Arieseni*	*Arieseni Village*	*green phyllonite*	Wr	216.5		192.2
7	*Biharia*	*Vadul Motilor Villag*	*curly schist*	Mu			251.1
8	*Biharia*	*Bistra Village*	*sheared granite*	Mu			207.4
9	*Biharia*	*Fiti Mount*	*sheared granite*	Mu			321.4
BAIA DE ARIES ASSEMBLAGE							
10	*Sohodol*	*Avram Iancu Villag*	*phyllonite*	WR			144.5
11	*Biharia*	*Dragoiesti Village*	*mylonitic quartzite*	WR	185.9		217.3
12	*Sohodol*	*Doli Valley*	*u-mylonite orthogneiss*	WR	168.7		177.5
13	*Sohodol*	*Doli Valley*	*u-mylonite orthogneiss*	WR	124.1		128.6
14	*Baia de Aries*	*Cioara Valley*	*micaschist*	Mu	116.9		116.9
15	*Baia de Aries*	*Sartas Village*	*amphibolite*	Hb	118.2		124.2
16	*Baia de Aries*	*Sartas Village*	*gneiss*	Mu	110.7		111.9
17	*Baia de Aries*	*Salciua de Sus Ville*	*amphibolite*	Hb	119.0	115.0	133.4
18	*Baia de Aries*	*Surduc Village*	*amphibolite*	Hb	155.5	151.0	167.2
19	*Baia de Aries*	*Baisoara Village*	*phyllonite*	WR			111.8
CODRU ASSEMBLAGE							
20	*Codru*	*Husi Valley*	*chl-muscovite schist*	Mu	339.9		336.3
21	*Codru*	*Husi Valley*	*chl-muscovite schist*	Hb	334.6		326.4
22	*Codru*	*Selasele Valley*	*amphibolite*	Hb			371.1
23	*Codru*	*Iara Valley*	*amphibolite*	Hb	366.4	364.0	367.1
24	*Codru*	*Iara Valley*	*amphibolite*	Hb	373.7		380.8
25	*Codru*	*Iara Valley*	*amphibolite*	Hb	404.9	400.8	405.0
SOMES ASSEMBLAGE							
26	*Arada*	*Bistra Valley*	*retrogressed plagiognei*	Mu			253.0
27	*Bihor*	*Rusesti Village*	*sericite quartzite*	Mu	302.5		295.1
28	*Bihor*	*Ciurtuci Village*	*amphibolite*	Hb	306.1	300.0	298.8
29	*Bihor*	*Ciurtuci Village*	*retrogressed plagiognei*	Mu	313.8		311.4
30	*Bihor*	*Beliu Village*	*amphibolite*	Hb	316.7	313.0	319.6
31		*Marisele Village*	*M.M. Granite*	Mu	191.3		189.8
32	*Arada*	*Iara Valley*	*plagiogneiss*	Mu	122.9		116.0
33	*Arada*	*Tarnita Lake*	*mylonitic orthogneiss*	Mu	100.6		99.6
TRIASSIC							
34		*Siria quarry*	*sheared siltstone*	WR	117.2		111.1

isotope-correlation ages does not require assumption of a present-day $^{40}Ar/^{36}Ar$ ratio, they are more reliable than ages calculated directly from the analytical data and, therefore, are considered geologically significant. They are interpreted to date the last cooling through temperatures required for intra crystalline retention of radiogenic argon in the constituent hornblende grains. Harrison (1981) suggested that temperatures of c. 500 ± 25°C are appropriate for argon retention within most hornblende compositions in the range of cooling rates likely to characterize most geologic settings.

Codru Assemblage

Hornblende concentrates were prepared from four samples of amphibolite collected within non-retrogressed (pre-Permian/Mesozoic) crystalline structural units of the Codru assemblage (locations 22-25). Concentrates from samples 23-25 yielded well-defined intermediate- and high-temperature plateaus (Fig. 4-5) corresponding to ages ranging between 366.4 ± 0.3 Ma (23) and 404.9 ± 0.3 Ma (25). Isotope-correlations of the plateau analytical data yield slightly younger ages which range between 364.4 ± 0.3 (23) and 400.8 ± 1.2 Ma (25). The isotope-correlation ages are considered geologically significant and are interpreted to date the last post-metamorphic cooling through appropriate argon retention temperatures. The analysis of sample 22 was poorly resolved (Fig. 4-5), and corresponded to a total-gas age of 371.1 ± 0.3 Ma. Insufficient spectrum resolution precludes definition of a meaningful isotope-correlation.

Baia de Arieş Assemblage

Amphibolite samples were collected at three locations within pre-Permian / Mesozoic crystalline structural units of the Baia de Arieş assemblage (15, 17 and 18). Hornblende concentrates from these samples record well-defined intermediate- and high- temperature plateaus (Fig. 4-6). Samples 17 and 15 yielded similar results (119.0 ± 0.1 Ma and 118.2 ± 0.3 Ma), which are markedly younger than the 155.5 ± 0.4 Ma plateau recorded by sample 18. Similar contrasts are seen in the plateau isotope-correlation ages which range between 151.6 ± 1.2 Ma (18) and 115.8 ± 0.3 Ma (17). The plateau isotope-correlation ages are interpreted to date contrasting times of post-metamorphic cooling through appropriate argon retention temperatures.

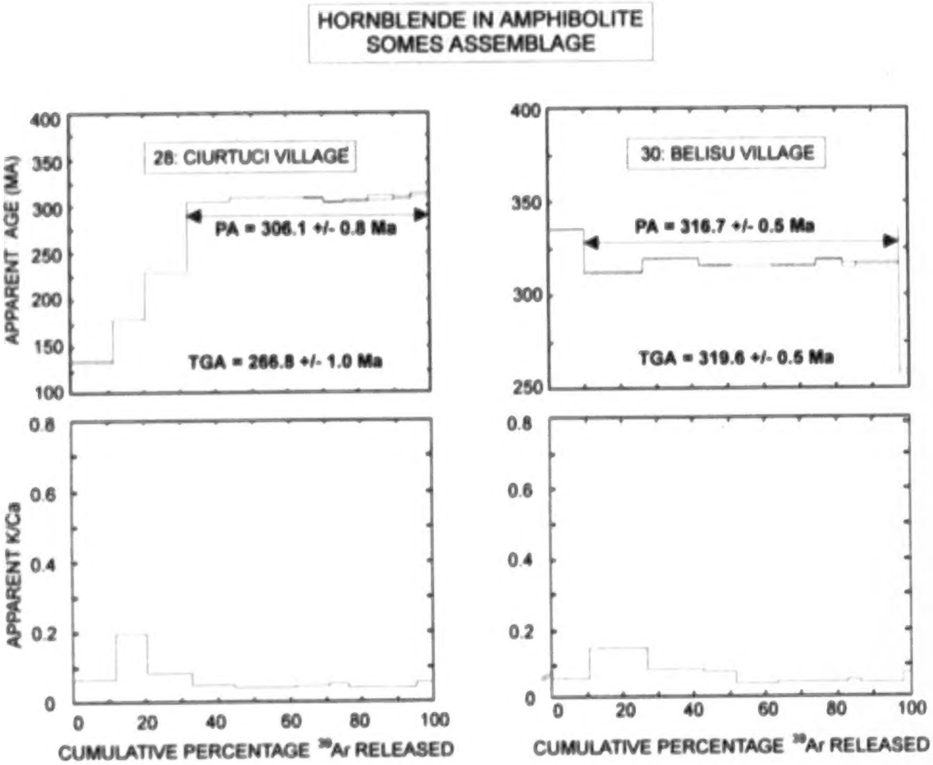

Fig. 4-4. $^{40}Ar/^{39}Ar$ age and apparent K/Ca spectra for multigrain hornblende concentrates from amphibolite collected within the Somes assemblage. Analytical uncertainties (two sigma, intra laboratory) are represented by vertical width of bars. Experimental temperatures increase from left to right. Plateau (PA) and/or total-gas (TGA) ages are listed on each spectrum. Sample number as in Fig. 4-3a.

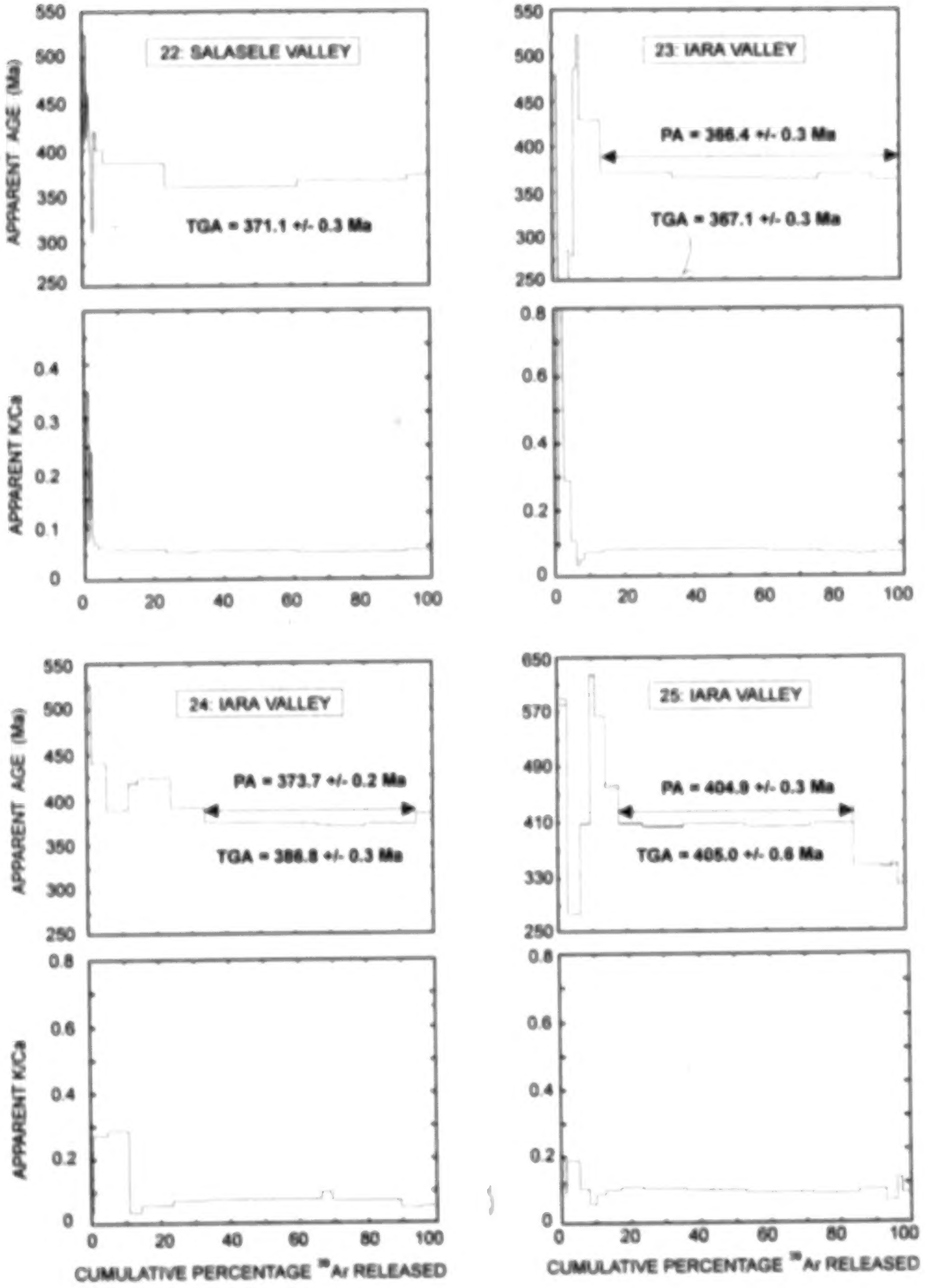

Fig. 4-5. ^{40}Ar/^{39}Ar age and apparent K/Ca spectra for multigrain hornblende concentrates from amphibolite collected within the Codru assemblage. Data plotted as in Figure 4-4.

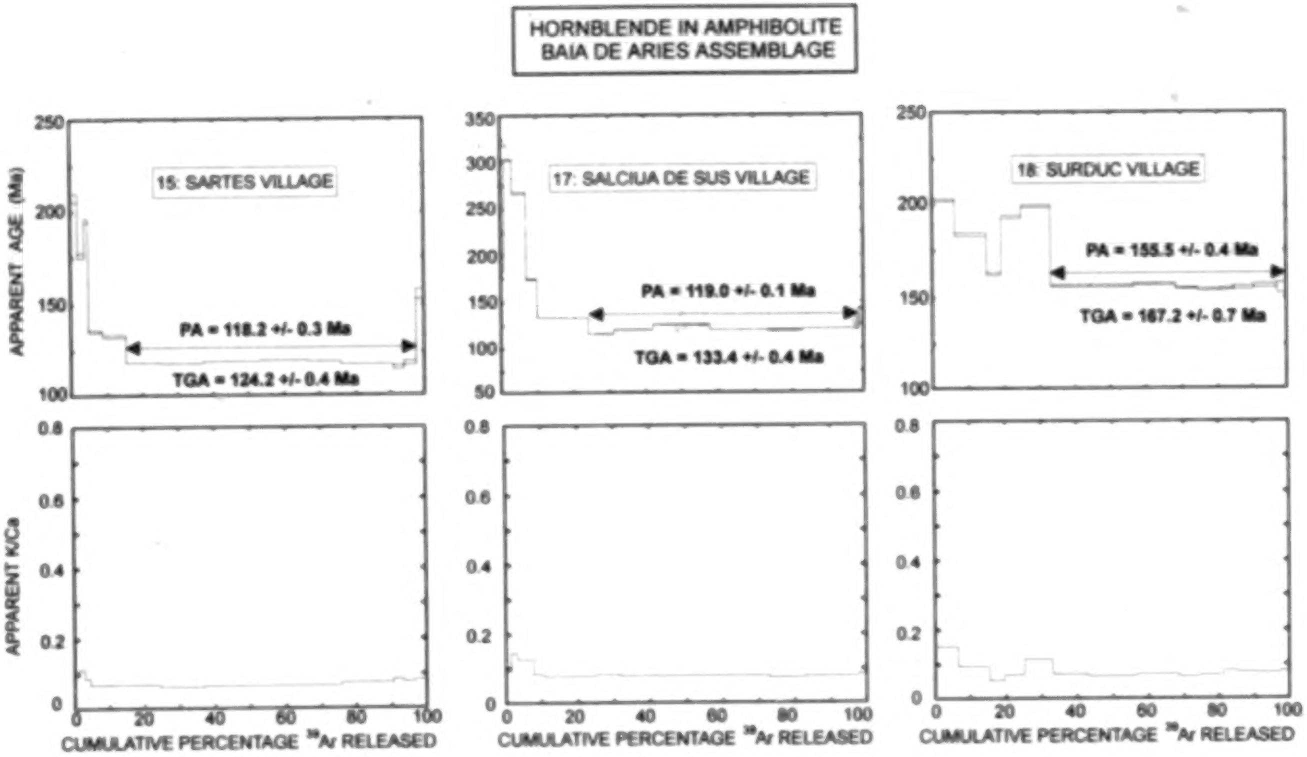

Fig. 4-6. $^{40}Ar/^{39}Ar$ age and apparent K/Ca spectra for multigrain hornblende concentrates from amphibolite collected within the Baia de Aries assemblage. Data plotted as in Figure 4-4.

4.6.2. MUSCOVITE

The 15 muscovite concentrates yielded variably discordant $^{40}Ar/^{39}Ar$ age spectra (Figs. 4-7 to 4-10). Apparent K/Ca ratios are very large, with considerable uncertainties. Consequently, they are not shown with the age spectra. The K/Ca ratios display minor and non-systematic intra sample variations, suggesting that experimental evolution of gas occurred from compositionally uniform populations of intra crystalline sites.

Someş Assemblage

Muscovite concentrates were prepared from samples of variably retrogressed gneiss and schist collected within variably retrogressed pre-Permian/Mesozoic crystalline rocks (Someş assemblage) of the Bihor "autochthon" at locations 27 and 29. A sample of sericite quartzite was also collected within lower grade crystalline sectors ("Arada series") of the Bihor "autochthon" at location 26. The muscovite concentrates yielded variably discordant $^{40}Ar/^{39}Ar$ spectra with generally similar characteristics (Fig. 4-7). Apparent ages systematically increase throughout the low- and initial intermediate-temperature increments evolved from the three concentrates. Little intra sample variation in apparent ages is observed in the higher temperatures portions of the analysis of samples 27 and 29. These define plateaus corresponding to 302.5 ± 0.2 Ma (27) and 313.8 ± 0.2 Ma (29). Apparent ages systematically increase throughout the analysis of sample 26. Characteristics of the three internally discordant apparent age spectra are similar to those described for muscovite from partially rejuvenated intra crystalline systems in other poly-metamorphic terranes (e.g., Dallmeyer and Takasu, 1992) and suggest that initial post-metamorphic cooling through appropriate argon retention temperatures (c. 400 ± 25°C: Cliff, 1985; Blankenburg et al., 1989) likely occurred between c. 300 and 315 Ma (plateau ages defined by samples 27 and 29). This appears to have been followed by a variable thermal rejuvenation at c.150-125 Ma (low-temperature ages recorded by sample 26). Rejuvenation was most extensive in sample 26.

A muscovite concentrate was prepared from a sample of penetratively retrogressed, mylonitic orthogneiss collected within a ductile shear zone developed in the Someş assemblage exposed in easternmost sectors of the Bihor "autochthon" (location 33). The concentrate displays an internally concordant $^{40}Ar/^{39}Ar$ spectrum corresponding to a plateau age of 100.6 ± 0.2 Ma (Fig. 4-7). This is interpreted to date cooling through argon retention temperatures following synkinematic growth of muscovite during the mylonitic overprint. The relatively low-grade character of the associated mylonitic mineral assemblage suggests that synkinnematic muscovite growth likely occurred at approximately the same temperatures required for intra crystalline argon retention. Therefore, the c. 100 Ma plateau age likely closely dates the ductile strain event.

Muscovite concentrates were prepared from a sample of retrogressed orthogneiss

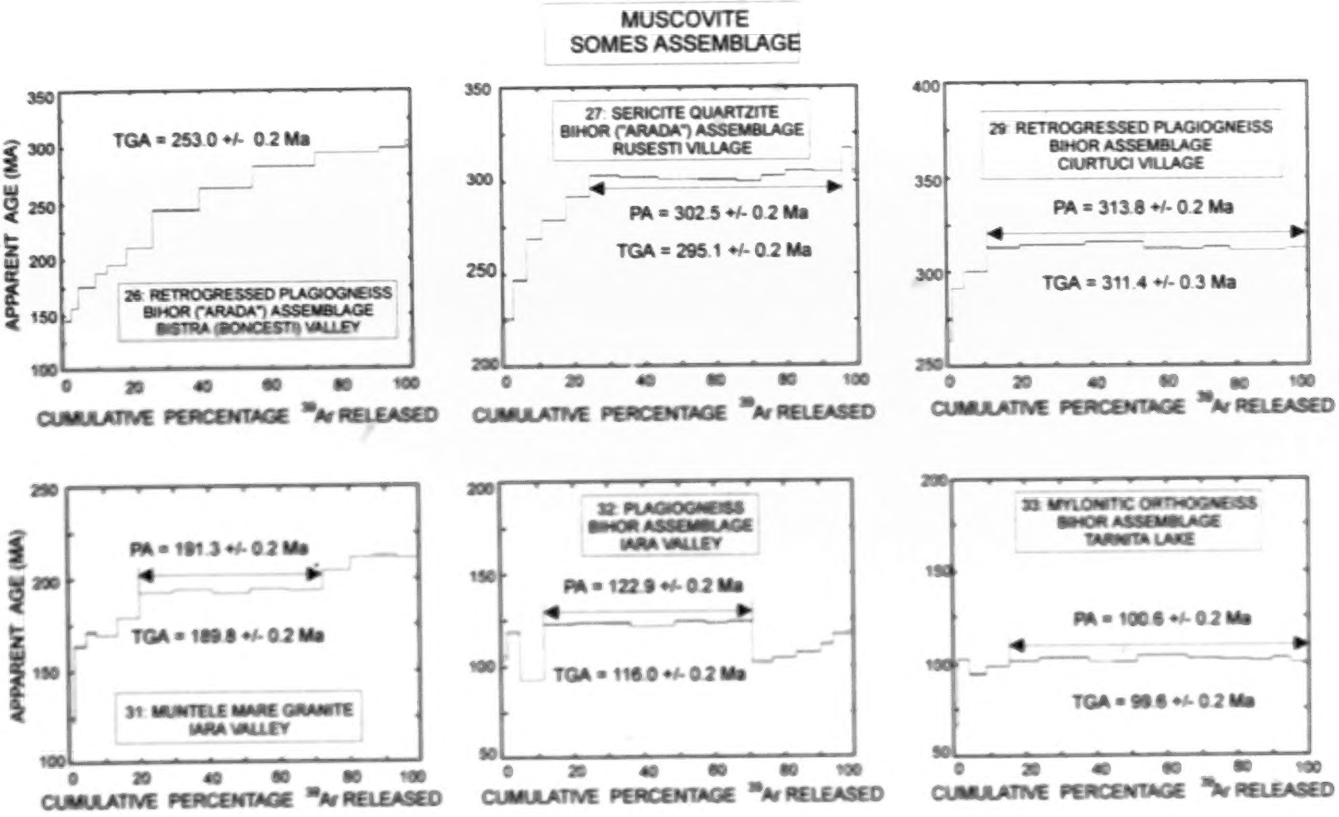

Fig. 4-7. ^{40}Ar/^{39}Ar age for multigrain muscovite concentrates from the Somes assemblage. Data plotted as in Figure 4-4.

collected within the Someş assemblage (location 32) and from a sample of massive granite collected within the Muntele Mare batholith (location 31). Both concentrates are characterized by internally discordant $^{40}Ar/^{39}Ar$ apparent age spectra (Fig. 4-7). Although intermediate - temperature plateaus are defined (191.3 ± 0.2 Ma, 31; 122.9 ± 0.2 Ma, 32), the complexity of the two analyses does not permit a reliable interpretation of their geologic significance.

Codru Assemblage

Muscovite concentrates were prepared from two samples of slightly retrogressed schist collected within pre-Permian/Mesozoic crystalline structural units of the Codru assemblage (locations 20 and 21). Both are characterized by internally discordant $^{40}Ar/^{39}Ar$ spectra (Fig. 4-8) in which apparent ages systematically increase through low-temperature portions of the analyses. The intermediate- and high-temperature increments display little intra sample variations in apparent age and define plateaus of 339.9 ± 0.2 Ma (20) and 334.6 ± 0.2 Ma (21). These are interpreted to date initial post-metamorphic cooling through appropriate argon retention temperatures. The character of the low-temperature age discordance is interpreted to reflect the effects of a minor, subsequent thermal rejuvenation.

Baia de Arieş Assemblage

Muscovite concentrates were prepared from samples of pre-Permian/Mesozoic crystalline structural units of the Baia de Arieş assemblage. These included penetratively retrogressed mylonitic granite (location 16) and progressively metamorphosed pelitic schist (location 14). Both concentrates are characterized by internally concordant $^{40}Ar/^{39}Ar$ spectra (Fig. 4-9) which correspond to plateau ages of 110.7 ± 0.1 Ma (16) and 116.9 ± 0.1 Ma (14). These are interpreted to date the last cooling through appropriate argon retention temperatures.

Highiş-Biharia Shear Zone

Muscovite concentrates were prepared from samples of variably mylonitic granite collected at three locations within pre-Permian/Mesozoic crystalline rocks exposed within the Highiş-Biharia shear zone (3, 5, 7, 8 and 9). These are characterized by internally discordant apparent age spectra (Fig. 4-10) of contrasting character. The concentrate from sample 9 displays a marked and systematic increase in apparent age throughout low-temperature portions of the analysis. Intermediate and high-temperature portions of the analysis record apparent ages which vary between c. 340 Ma and 330 Ma; although this portion of the analysis was poorly resolved, the results suggest an initial cooling at c. 340-330 Ma. The concentrate from sample 8 displays an internally complex age spectra with an intermediate-temperature age maximum. The geologic significance of the two analyses is uncertain. However, the low portion of both spectra indicate Alpine rejuvenation.

A concentrate of metamorphic muscovite was prepared from a sample of pre-Permian/ Mesozoic mylonitic schist collected at location 7 within the Highiş-Biharia shear zone. The

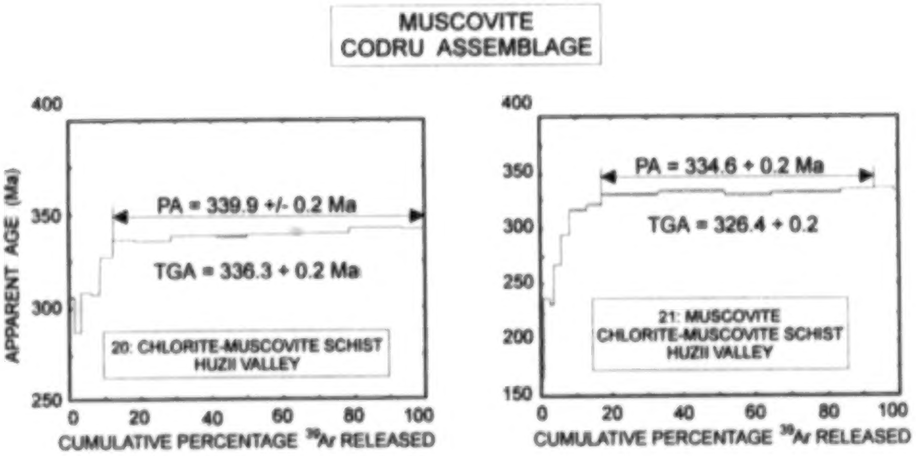

Fig. 4-8. ^{40}Ar/^{39}Ar age spectra for multigrain muscovite concentrates from the Codru assemblage. Data plotted as in Figure 4-4.

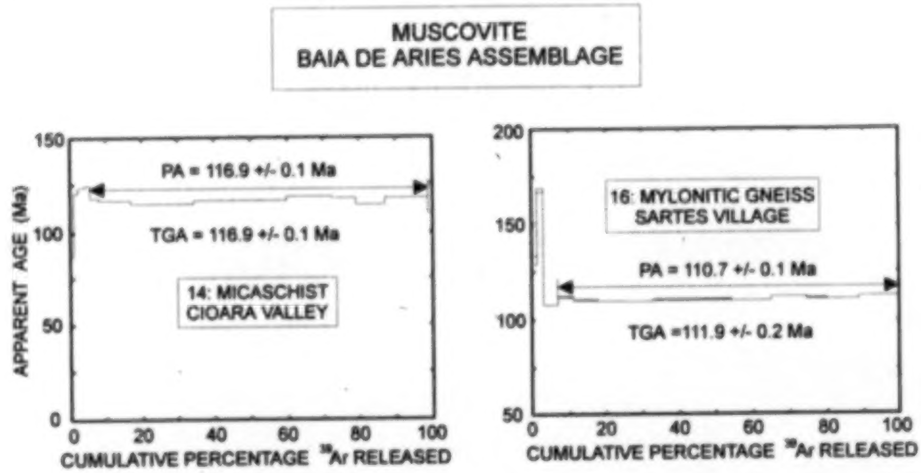

Fig. 4-9. ^{40}Ar/^{39}Ar age spectra for multigrain muscovite concentrates from the Baia de Aries assemblage. Data plotted as in Figure 4-4.

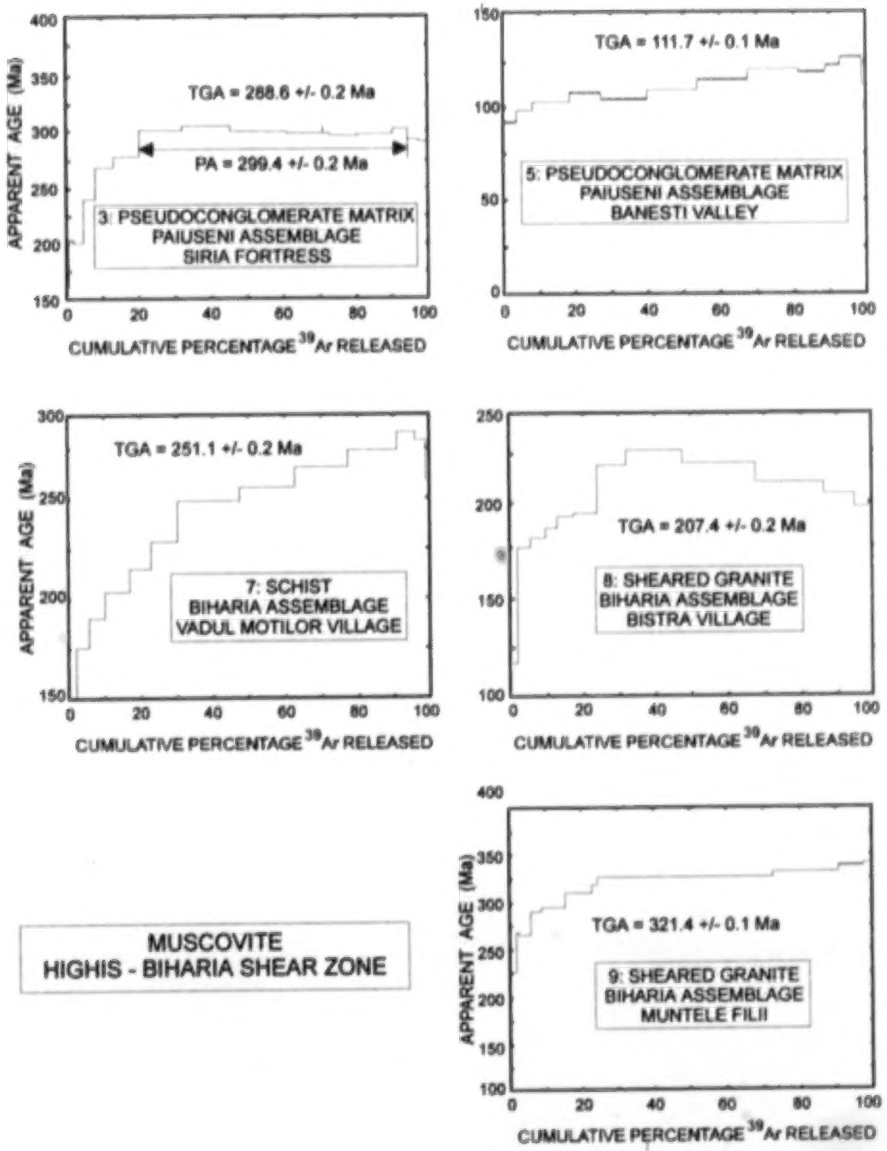

Fig. 4-10. ^{40}Ar/^{39}Ar age spectra for multigrain muscovite concentrates from the Highis - Biharia shear zone. Data plotted as in Figure 4-4.

concentrate displays an internally discordant apparent age spectrum (Fig. 4-10) in which apparent ages systematically increase from c. 125 Ma at low temperatures to c. 275 Ma at highest temperatures. These characteristics suggest that initial post-metamorphic cooling occurred sometime prior to c. 275 Ma and was followed by extensive Alpine rejuvenation.

Two concentrates of muscovite were prepared from samples of pre-Permian/Mesozoic mylonitic "metaconglomerate" collected at locations 3 and 5. The concentrate from sample 3 displays an internally discordant age spectrum (Fig. 4-10) in which apparent ages systematically increase throughout low-temperature portions of the analysis to define an intermediate- and high- temperature plateau of 299.4 ± 0.2 Ma. The internally discordant spectrum suggests that the muscovite originated within a protolith that experienced cooling through argon retention temperatures at c. 300 Ma. The muscovite experienced slight thermal rejuvenation, probably during the low-grade metamorphism which accompanied development of mylonitic fabrics. The muscovite concentrate from sample 5 is characterized by a slight but systematic increase in apparent age from c. 90 Ma in low-temperature increments to c. 127 Ma in high-temperature portions of the analysis.

4.6.3. WHOLE-ROCK

The 10 low-grade whole-rock samples display variably discordant apparent age spectra (Figs. 4-11 to 4-13). Variable and relatively young apparent ages are typically recorded in the small- volume increments evolved at low experimental temperatures, accompanied by relatively small and fluctuating apparent K/Ca ratios. Gas fractions liberated during intermediate- and high-temperature portions of the analysis generally display large and only slightly fluctuating apparent K/Ca ratios. Although the samples consist primarily of very fine-grained white mica, systematic intra sample variations in apparent K/Ca ratios suggest that several other phases likely contributed gas at various stages in the whole-rock analyses. Relative to white mica, these appear to have included 1) a non-retentive phase present in variable modal abundance, with relatively low apparent K/Ca ratio, and 2) a more refractory phase with relatively low apparent K/Ca ratio, also present in minor modal abundance. Mineralogical characteristics and observed modal variations suggest that these phases may be chlorite and plagioclase feldspar, respectively. Apparent ages recorded throughout intermediate- and initial high-temperature portions of the analyses are attributed to gas largely evolved from constituent, very fine-grained white mica.

Triassic Cover Of The Codru Assemblage

A sample of phyllonite derived from a pelitic protolith was collected within ductilely sheared Triassic cover of the Codru assemblage near the lower thrust contact with the Highiş-Biharia assemblage (location 34). Intermediate- and high-temperature portions of the whole-rock

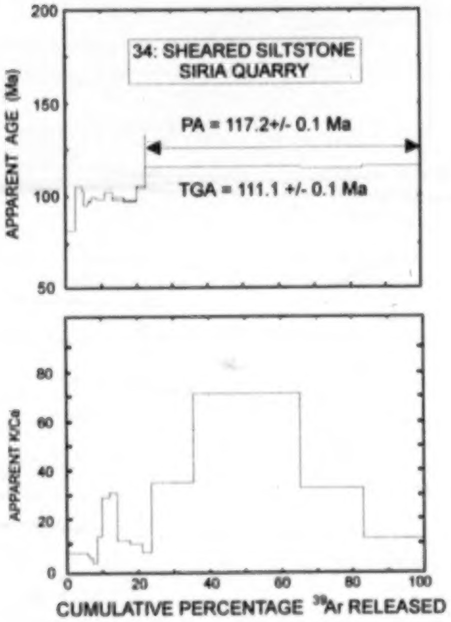

Fig. 4-11. ^{40}Ar/^{39}Ar age and apparent K/Ca spectra for a whole rock sample of phyllonite collected within Triassic cover of the Codru assemblage. Data plotted as in Figure 4-4.

analysis record similar apparent ages corresponding to a plateau age of 117.2 ± 0.1 Ma (Fig. 4-11). This is considered geologically significant and interpreted to date the synkinematic grown near or below the closure temperature of constituent fine-grained white mica during thrusting.

Baia de Arieş Assemblage

Five samples of phyllonite derived from pre-Permian/Mesozoic crystalline protoliths were collected for $^{40}Ar/^{39}Ar$ analysis within the Baia de Arieş assemblage. These included mylonitic quartzite (11), ultramylonitic orthogneiss (12 and 13) and phyllonite (10 and 19). The five whole-rock analyses are characterized by variably discordant $^{40}Ar/^{39}Ar$ apparent age spectra (Fig. 4-12). The mylonitic quartzite (sample 11) yielded an internally complex spectrum with considerable variation in apparent ages at low and intermediate experimental temperatures. In contrast, the high- temperature increments record similar apparent ages corresponding to a plateau of 185.9 ± 0.2 Ma. The ultramylonitic orthogneiss samples (12 and 13) record intermediate- and high- temperature plateaus which yield contrasting ages of 168.7 ± 0.2 Ma (12) and 124.1 ± 0.3 Ma (13). These three plateaus are considered geologically significant and interpreted to closely date the diachronous growth of synkinnematic white mica during formation of the mylonitic fabrics. The two phyllonite samples (10 and 19) are characterized by complex, internally discordant age spectra with uncertain geologic significance.

Highiş-Biharia Shear Zone

A dark-gray phyllonite was collected within the "Black Series" exposed within the Highiş-Biharia shear zone (location 1). The whole-rock sample yielded a well-defined intermediate temperature plateau corresponding to an age of 114.1 ± 0.1 Ma (Fig. 4-13). This is interpreted to closely date the synkinematic growth of constituent, fine-grained white mica during mylonitization.

Three phyllonite samples were collected within pre-Permian/Mesozoic structural units exposed within the Highiş-Biharia shear zone. These included two samples of mylonitic schist (locations 2 and 6) and a sample of ultramylonitic granite (location 4). The whole-rock phyllonitic granite yielded a well-defined intermediate-temperature age of 107.7 ± 0.2 Ma (sample 4 in Fig. 4-13) which is considered geologically significant and interpreted to closely date development of the mylonitic fabric. The two samples of mylonitic schist yielded markedly contrasting results (Fig. 4-13). Intermediate- temperature increments experimentally evolved from sample 2 recorded a plateau of 99.7 ± 0.3 Ma (Fig. 4-13) which is considered to date development of the mylonitic fabric. The analysis of sample 6 was characterized by apparent ages which generally increase from c. 100-75 Ma at low temperatures to define an intermediate- and high-temperature plateau age of 216.5 ± 0.2 Ma. These characteristics may reflect partial rejuvenation of older intra crystalline argon systems during the mylonitic overprint.

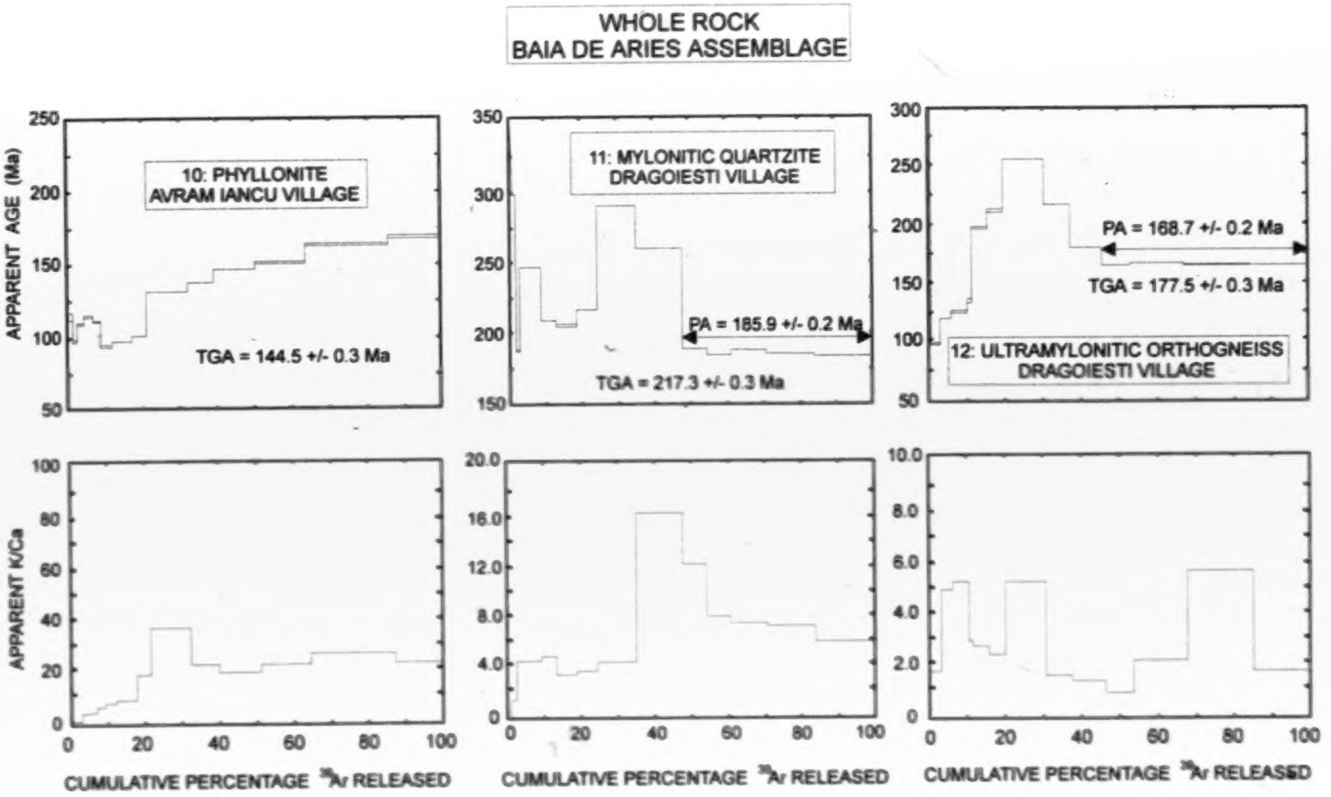

Fig. 4-12. ^{40}Ar/^{39}Ar age and apparent K/Ca spectra for a whole-rock sample of phyllonite collected within the Baia de Aries assemblage. Data plotted as in Figure 4-4.

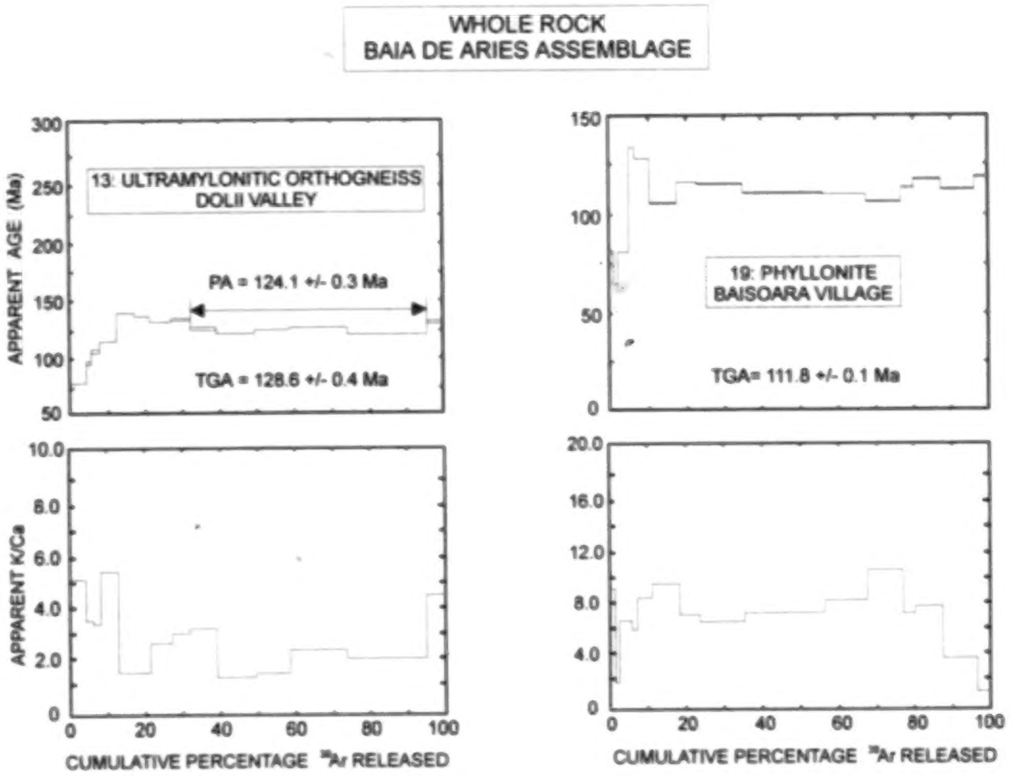

Fig. 4-12 (continued). ^{40}Ar/^{39}Ar age and apparent K/Ca spectra for whole-rock samples of phyllonite collected within the Baia de Aries assemblage. Data plotted as in Figure 4-4.

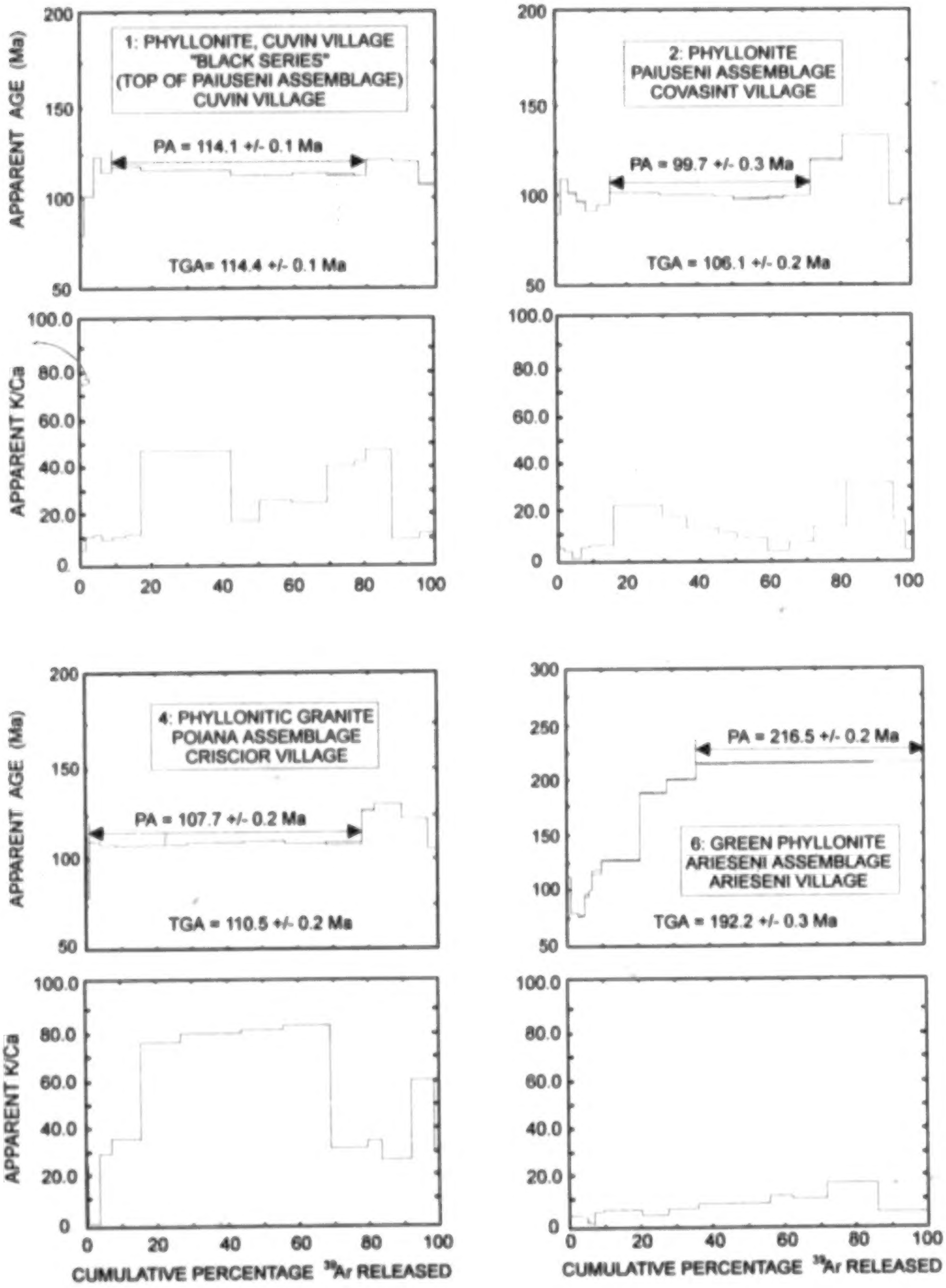

Fig. 4-13. ^{40}Ar/^{39}Ar age and apparent K/Ca spectra for whole-rock samples of phyllonite collected within the Highis-Biharia shear zone. Data plotted as in Figure 4-4.

4.7. SIGNIFICANCE

The $^{40}Ar/^{39}Ar$ results record a complex tectonothermal evolution of basement units in the Apuseni Mountains. Plateau ages can be grouped into distinct Paleozoic and Mesozoic intervals (Table 4-3). Interpretation and integration of the new data relies upon calibrations of the geologic time-scale by Palmer (1983) and Gradstein et al. (1994).

Table 4-3. Summary of the $^{40}Ar/^{39}Ar$ plateau ages on rocks from the Apuseni Mountains

Assemblage	Hornblende	Muscovite	Whole Rock	Tectonism
Triassic cover			117	middle Cretaceous imbrication
Baia de Arieş	156; 119; 118	117; 111		Jurassic to middle Cretaceous diachroneous tectonism and resetting
zone of low grade retrogression			186; 169; 124	
HBSZ		321; 299	216; 114; 108; 100	mid-Cretaceous tectonism on Variscan protoliths
zone of low grade retrogression		123; 101		middle Cretaceous tectonism
Someş	317; 306	314; 303		"Late Variscan" tectonism
Codru		340; 335		main phase of Variscan transpression
Codru	405; 374; 366			"Early Variscan" tectonism (?)

The spread in $^{40}Ar/^{39}Ar$ hornblende ages recorded by amphibolite of the Codru assemblage could indicate delayed post-metamorphic Devonian cooling similar to the "early" Variscan tectonothermal events recorded in parts of northwest Iberia (e.g., Dallmeyer et al., 1991) and the Bohemian Massif (Tepla Barrandian Zone; Dallmeyer and Urban, 1994).

Muscovite in gneiss of the Codru assemblage records cooling ages of c. 340 and c. 335 Ma. Structures in the mylonitic gneisses indicate dominant strike-slip tectonism with a northward thrust component. Contemporaneous tectonism in the Alps has been interpreted to represent Variscan collision accommodated by dextral transpression and south verging nappe emplacement (e.g., von Raumer and Neubauer, 1994). Because the Apuseni crustal element underwent c. 90° Tertiary clockwise rotation (Pătraşcu et al. 1990), the $^{40}Ar/^{39}Ar$ ages from the Codru gneisses may record the same tectonothermal event.

Hornblende and muscovite within non-retrogressed sectors of the Someş assemblage record post-metamorphic cooling ages which range between c. 315 and c. 300 Ma. The concordance of the hornblende and muscovite ages suggests relatively rapid post-metamorphic cooling in the middle Late Carboniferous. This implies that the cooling followed a regionally penetrative "Late Variscan" tectonothermal overprint of similar age to that of pre-Permian/ Mesozoic sequences exposed throughout much of Iberia and central Europe (e.g. Dallmeyer and Martinez-Garcia, 1990; Dallmeyer et al., 1995), in the West Carpathians (Malusky et al., 1993 and Dallmeyer et al., 1996) and East and South Carpathians (Dallmeyer et al., 1996). In the Alps, Late Carboniferous tectonism accompanied by granite intrusion and high temperature metamorphism. This has been interpreted to record a final phase of Variscan subduction / collision (von Raumer and Neubauer, 1994). Although the Muntele Mare batholith intruded the Someş assemblage at c. 295 Ma (Pană et al., 1996), no evidence of a Variscan subduction setting exists in the Apuseni Mountains.

A record of Variscan tectonothermal activity in the Apuseni Mountains is also provided by muscovite from pre-Permian/Mesozoic lithologic elements exposed within the Highiş-Biharia shear zone. Although the rocks were variably rejuvenated during Mesozoic orogenesis, initial cooling between c. 320 Ma and c. 300 Ma is recorded by muscovite from variably mylonitized granite and schist.

Mesozoic effects are recorded within most structural elements of the Apuseni Mountains. Post-Variscan resetting is relatively weak within central and northwestern sectors of the Someş assemblage. It was limited to localized and relatively minor rejuvenation of muscovite intra crystalline argon systems (manifested in the low-temperature age discordance observed in muscovite). There is no evidence of post-Variscan rejuvenation of hornblende. The intensity of Mesozoic thermal and structural effects increases eastward and southward across the central Apuseni Mountains. The c. 100 Ma plateau age of synkinnematic muscovite within a ductile shear zone in the eastern part of the Bihor "autochthon" suggests that a low-grade event occurred in the late Albian.

The effects of Early-Middle Cretaceous tectonism are also evident throughout the Highiş-Biharia shear zone, where variable rejuvenation of Variscan muscovite occurred at c. 100-90 Ma. Whole-rock samples of phyllonite within the shear zone yield ages between c. 114 Ma and c. 100 Ma. Aptian internal imbrication at a relatively high crustal level within the Codru assemblage is dated by a c. 117 Ma whole-rock phyllonite age. These ages can be interpreted to date phases of Austrian compression if the subsequent extension recorded by kinematic indicators throughout HBSZ (Pană et al., 1996) occurred at temperatures too low to effect partial rejuvenation.

Aptian to early Albian tectonism is also recorded in the Baia de Arieş assemblage, where hornblende within foliated amphibolite yielded plateau isotope-correlation ages of c. 117 Ma and c. 116 Ma, and muscovite from gneiss and schist yielded plateau ages of c. 117 Ma and c. 111 Ma. The general concordance of hornblende and muscovite ages suggests relatively rapid cooling following higher grade penetrative Early-Middle Cretaceous tectonothermal activity in the Baia de Arieş assemblage. However, both amphibolite and gneiss units of the Baia de Arieş assemblage at different locations yielded older $^{40}Ar/^{39}Ar$ dates which indicate local Mesozoic activity that pre-dated the middle Cretaceous. The regional extent and tectonic significance of the pre-middle Cretaceous tectonic phase is uncertain. Whole-rock samples of ultramylonitic granite yielded plateau ages of c. 124 Ma, 169 Ma and 186 Ma, which have been interpreted to date diachronous growth of synkinematic white mica during formation of mylonitic fabrics at the elusive contact with the HBSZ. Hornblende from an amphibolite in the easternmost basement unit of the Apuseni Mountains yielded c. 150 Ma. Consequently, the ages locally recorded on amphibolite and gneiss units within the Baia de Arieş assemblage date different times of cooling following several distinct phases of structural imbrication associated with Alpine oblique convergence. As a result, medium- and high-grade Baia de Arieş rocks were transported to relatively shallower crustal levels at several different times.

4.8 CONCLUSIONS

^{40}Ar/^{39}Ar results suggest that pre-Permian-Mesozoic lithologic units of the northern Apuseni record three distinct phases of Variscan tectonism at mid-crustal levels. Amphibolite of the Codru assemblage records stepwise Devonian uplift, and the associated gneiss, Early Carboniferous transpression within a relatively narrow belt along the southern margin of the Someş assemblage. The Codru assemblage may represent a segment of the Variscan suture subsequently disrupted by Alpine tectonism. The Someş assemblage records Late Carboniferous uplift, interpreted to follow a regional medium-grade tectonometamorphic event.

^{40}Ar/^{39}Ar data for basement units to the south record only Alpine tectonothermal events. The phyllonitic belt that marks the HBSZ developed during polyphase Alpine tectonism with a climactic Aptian-Albian phase of compression. South of the HBSZ, slices of medium-grade rocks experienced thermal resetting during tectonic transport at shallower crustal levels during multiple phases of Jurassic-Cretaceous tectonism. This suggests that Alpine compression in the interior of the Carpathian arc was gradually accommodated within wide shear zones with complex strain patterns that include transpression and thrusting followed by normal detachment. No regionally significant rigid basement nappe with distinct Alpine kinematics and tectonothermal imprint can be inferred in the Apuseni Mountains.

REFERENCES

Balintoni, I., 1985, Corrélation des unités litostratigraphiques et tectoniques longeant le ruisseau d'Aries entre la vallée de Iara et le Mont Găina (Monts Apuseni), D. S. Inst. Geol. Geofiz., LXIX/5, p. 5-15.

Balintoni, I., 1986, Petrologic and Tectonic Features of the Highiş-Drocea Crystalline Massif (Apuseni Mountains), D. S. Inst. Geol. Geofiz., 70-71/5, p. 5-21.

Balintoni, I. 1994, Structure of the Apuseni Mountains, *in* Geological evolution of the Alpine-Carpathian-Pannonian system' Conference, Covasna, Field Guidebook, J. of Tect. & Reg. Geol., 75/2, p. 51-57.

Bleahu, M., Lupu, M., Patrulius, D., Bordea, S., Ştefan, A., and Panin, S. 1981, The structure of the Apuseni Mountains, Carpatho-Balkan Geological Association, XII Congress, Bucharest, Romania, Guide to Excursion-B3, 103 p.

Bordea, S., 1992, Stratigrafia depozitelor neojurasice si cretacice din partea vestic a Munţilor Metaliferi, (Stratigraphy of the Late Jurassic and Cretaceous deposits from the western part of the Metaliferi Mountains), Abstract of PhD Thesis, Univ. Al.I.Cuza"-Iaşi, 27 p.

Burchfiel, B.C., 1980, Eastern Alpine system and the Carpathian orocline as an example of collision tectonics, Tectonophysics, 63, p. 31-62.

Cambel, B. & Kral, J., 1989, Isotope geochronology of the western Carpathian crystalline complex; the present state. Geologica Carpathia, 40, p. 387-420.

Cliff, R.A.,1985, Isotopic dating in metamorphic belts, J. Geol. Soc. London, 142, p. 97-110.

Dallmeyer, R.D. and Martinez-Garcia, I., 1990, Pre-Mesozoic Geology of Iberia: Springer-Verlag, Heidelberg, 416 p.

Dallmeyer, R.D. and Gil Ibarguchi, J. I., 1990, Age of amphibolitic metamorphism in the ophiolitic unit of the Morais allochthon (Portugal): implications for early Hercynian orogenesis in the Iberian Massif. J. Geol. Soc. London, 147, p. 873-878.

Dallmeyer, R.D., Ribeiro, A. and Marques, F., 1991, Polyphase Variscan emplacement of exotic terranes (Morais and Braganca Massifs) onto Iberian successions: evidence from ^{40}Ar/^{39}Ar mineral ages: Lithos, 27, p. 133-144.

Dallmeyer, R.D. and A. Takasu, 1992, ^{40}Ar/^{39}Ar of detrital muscovite and whole rock slate/phyllite, Narragansett Basin, RI-MA, USA: implications for rejuvenation during very low-grade metamorphism, Contrib. Mineral, Petrol., 110, p. 515-527.

Dallmeyer, R. D. and Urban, M., 1994, Variscan vs. Cadomian tectonothermal evolution within the Tepla-Barrandian Zone, Bohemian Massif, Czech Republic: evidence from ^{40}Ar/^{39}Ar mineral and whole-rock slate ages: Abstract, Journ. Czech Geol. Soc., 39/I, p. 2.

Dallmeyer, R. D., Franke, W. and Weber, K., 1995, Pre-Permian Geology of Central and Eastern Europe: Springer-Verlag, Heidelberg, 604 p.

Dallmeyer, R.D., Neubauer, F., Handler, R., Fritz, H., Müller, W., Pană, D., and Putis, M., 1996, Tectonothermal evolution of the internal Alps and Carpathians: Evidence from ^{40}Ar/^{39}Ar mineral and whole-rock data. Eclogae geol. Helv., 89/1, p.203-227.

Dimitrescu, R. 1985, Early Caledonian event in the pre-Alpine metamorphic sequences of the Romanian Carpathian, Acta Mineralogica-Petrographica, Szeged, XXVII, p. 59-70.

Dimitrescu, R. 1988 a, Observations sur la structure du cristallin des monts Bihor et Gilău meridional. D.S. Inst. Geol. Geofiz., 72-73/5, p. 85-91.

Dimitrescu, R. 1988 b, Apuseni Mountains *in* Precambrian in Younger Fold Belts, Zoubek,V., Cogné, J., Kozhoukharov, D., and Kräutner, H., (Eds.), p. 665-674.

Dimitrescu, R., Bordea, J. and Bordea, S., 1974, Geologic Map of Romania: 1:50,000 Câmpeni Sheet, Romanian Geological Institute, Bucharest.

Erdmer, P., and Pană, D., 1995, Lithotectonic Assemblages and Kinematic Indicators in the Basement Rocks of the Apuseni Mountains. European Union of Geosciences, Abstract Volume, p. 272, Strasbourg.

Frank, W., Klein, P., Nowy, W. and Scharbert, S. 1976: Die Datierung geologisher Ereignisse im Altkristallin der Gleinalpe (Steiermark) mit der Rb/Sr-Methode. Tscherm. Min. Petr. Mitt., 23, p. 191-203.

Frank, W., Esterlus, M., Frey, I., Jung, G., Krohe, A. and Weber, J., 1983: Die Entwicklungs geschichte von Stub- und Koralpenkristallin und die Beziehumg zum Grazer Paläosoklum. Jber. Hochschulschwerpkt. s 15: Die frühalpine Geschichte der Ostalpen, 3, p. 263-292.

Frank, W., Kralik, M., Scharbert, S. and Thoni, M., 1987, Geochronologial data from the Eastern Alps: in, Geodynamics of the Eastern Alps: H.W. Flugel and P. Faupl, Eds.: Deutike, Vienna, p. 272-281.

Giuscă, D. Savu, H., and Borcoş, M., 1968, La stratigraphie des schistes cristallins des Monts Apuseni, Rev. Roum. Géol., 12/2, p. 143-159.

Giuşcă, D.,1979, Masivul cristalin al Highişului, St. Cerc. Geol., Geofiz., Geogr., Geol., 24, p.15-43

Gradstein, F.M., Agterberg, F.P., Ogg, J.G., Hardenbol, J., van Veen, P., Thierry, J. and Huang, Z., 1994, A Mesozoic time-scale: Journal of Geophysical Research, 99, p. 24051-24074.

Harrison, T.M., 1981, Diffusion of ^{40}Ar in Hornblende. Contrib. Mineral. Petrol., 78, p. 324-331.

Hârtopanu, I., and Hârtopanu, P., 1986, Intersecting isograds - a possible way to find out the polymetamorphism. An example: the Someş series, D.S. Inst.Geol. Geofiz., 70-71/1, p. 291-299.

Ianovici, V., Borcoş, M., Bleahu, M., Patrulius, D., Lupu, M., Dimitrescu, R., and Savu, H., 1976, Geologia Munţilor Apuseni, Ed. Acad. Rom., 631 p., Bucureşti.

Krist, E., Korikovsij, S.P., Putis,M., Janak, M. & Faryad, S.W., 1992: Geology and petrology of metamorphic rocks of the Western Carpathian crystalline complexes. Comenius University Press/Bratislava, 324 p.

Kräutner, H., 1980, Lithostratigraphic correlations of Precambrian in the Romanian Carpathians, An. Inst. Geol. Geog., LVII, p. 229-296.

Maluski, H., Rajlich, P., and Matte, P., ^{40}Ar/^{39}Ar dating of the Inner Carpathians Variscan basement and Alpine mylonitic overprinting. Tectonophysics, 223, p. 313-337.

Palmer, A.R., 1983, The 1983 DNAG time-scale: Geology, 11, p. 503-504.

Pană, D., and Ricman, C., 1988, The lower complex of the Păiuşeni series - a blastomylonitic belt. Rev. Roum. Géol., Géophys. et Géogr., ser. Géol., 32, p. 21-35.

Pană, D. and Erdmer, P., 1994, Alpine Crustal Shear zones and pre-Alpine basement terranes of the Romanian Carpathians and Apuseni Mountains, Geology, 22, p. 807-810.

Pană, D., Erdmer, P., and Dallmeyer, R.D., 1996, Lithotectonic assemblages of the Apuseni Mountains: strain partitioning and timing of tectonism, Anuarul Institutului de Geologie al Romaniei, v. 69, Supplement 1, p. 168-172.

Pătraşcu, S., Bleahu, N., and Panaiotu, C., 1990, Tectonic implications of the paleomagnetic research into Upper Cretaceous magmatic rocks in the Apuseni Mountains, Romania, Tectonophysics, 180, p. 309-322.

Pavelescu, L., Pop, G., Ailenei, G., Ene, I., Soroiu, M., and Popescu, G., 1975, K-Ar age determinations from the Apuseni and Banat Mountains, Rev. Roum. Géophys., 19, p. 67-69.

Sampson, D.S. & Alexander, E.C., 1987, Calibration of the Inter laboratory ^{40}Ar/^{39}Ar dating standard, MMhb-1. Chem. Geol. (Isot. Geosci, Sect.), 66, p. 27-34.

Săndulescu, M., 1975, Essai de synthèse structurale des Carpathes: Bull. Geol. Soc. Fr., 17(3): p. 299-358.

Săndulescu, M., 1984, Geotectonica Romaniei, 336 p., Editura Technică, Bucharest.

Săndulescu, M., 1988, Cenozoic tectonic history of the Carpathians, *in* The Pannonian Basin: A Study in Basin Evolution, by Royden, L., and Horvath, F., (Eds.), Mem. Am. Assoc. Petr. Geol., 45, p. 17-25.

Săndulescu, M., 1994, Overview on Romanian geology. Rom. J. of Tect. & Regional Geology, v. 75/2, p. 3-15, ALCAPA II, Covasna conference, Field Guidebook.

Soroiu, M., Popescu, G., Kapser, U., and Dimitrescu, R., 1969, Contributions préliminaires à la géologie des massifs cristallins des Monts Apuseni, An. St. Univ. "Al.I.Cuza", Sect. II b (Geol), v. 15, p. 25-33.

Thoni, M., and Jagoutz, E., 1993, Isotopic constrains for eo-Alpine high-P metamorphism in the Austroalpine nappes of the Eastern Alps: bearing on Alpine orogenesis. Schweiz. mineral. petrogr. Mitt., 73, p. 177-189.

Tollmann, A., 1987, The Alpidic evolution of the Eastern Alps *in*: Geodynamics of the Eastern

(Ed. by Flügel, H.W. & Faupl, P.). Deuticke/Vienna, p. 361-378.

Trümpy, R., 1988, A possible Jurassic-Cretaceous transform system in the Alps and Carpathians. *in*: Processes in Continental Lithospheric Deformation (Ed. by Clark, S.P., Burchfiel, B.C. & Suppe, J.), Geol. Soc. Amer. Spec. Pap., 218, p. 93-109.

York, D., 1969, Least squares fitting of a straight line with correlated errors. Earth Planet. Sci. Let., 5, p. 320-324.

CHAPTER 5*

TECTONOTHERMAL EVOLUTION OF THE APUSENI MOUNTAINS, ROMANIA: IMPLICATIONS OF STRAIN PARTITIONING

---

* *A shorter version of this chapter is prepared for submission to Tectonics by Dinu Pană[1], Philippe Erdmer[1], David Dallmeyer[2] and Franz Neubauer[3]*

[1] Department of Earth and Atmospheric Sciences, University of Alberta, Edmonton, AB, T6G 2E3, Canada
[2] Department of Geology, University of Georgia-Athens, GA 30602, USA
[3] Geology and Paleontology Institute, Paris-London University, A-5020 Salzburg, Austria

5.1. INTRODUCTION

The arcuate Carpathian orogen of eastern Europe (Fig. 5-1) is a response to the tectonic filling of a westward-facing oceanic embayment in early Tertiary time. The outer part of the Carpathians is a coherent thrust-fold belt. The inner part is a discontinuous belt of disrupted pre-Mesozoic continental basement and dismembered Mesozoic strata, a poorly understood aggregate of crustal fragments that record Mesozoic and Cenozoic rifting, drifting, and accretion and are largely covered by Neogene fill of the Pannonian Basin. The Apuseni Mountains of Romania are the main area of basement exposure in the Pannonian Basin, consisting of metamorphic and igneous rocks and Permian to Mesozoic strata. The rocks contrast greatly with basement exposures in the Transdanubian Central Range to the west and the Bükk Hills to the north, and are similar to basement exposures in the Villany and Mecsek hills to the southwest.

The heterogeneous character of the Pannonian basement has led to contrasting paleotectonic interpretations. Some reconstructions assigned the Apuseni crust during early Alpine extension to a coherent micro-continental fragment which included the West Carpathians and Eastern Alps (e.g. Săndulescu, 1975; 1994; Bleahu, 1976). Subduction of a hypothetical Mureş-Pienniny branch of the Tethys Ocean beneath this micro-plate was proposed (Rădulescu and Săndulescu, 1973; Rădulescu et al., 1993, Săndulescu, 1984, 1994). Other reconstructions interpreted the Apuseni crust as a small continental fragment surrounded by Mesozoic oceanic crust (e.g., Mišic et al., 1989; Hamilton, 1990; Dal Piaz et al., 1995;) consumed during complex Tertiary translations and rotations (e.g., Balla, 1982, 1985,1986; Csontos et al., 1992; Márton and Mauritsch, 1990).

Tectonic interpretations of the Apuseni Mountains have emphasized pre-Late Cretaceous ("pre-Gosau") and Laramide phases of nappe stacking with no metamorphic overprinting (Ianovici et al. 1976; Bleahu et al., 1981; Săndulescu, 1975; 1984; Balintoni, 1985; 1986). The nappe interpretation extends to the unexposed basement of the South Pannonian Basin (e.g., Szepesházy, 1979; Dimitrescu, 1981; Balázs et al., 1986) and has thus been proposed for most of the Alpine Orogen in eastern Europe.

The aim of this paper is to show that strain partitioning during Mesozoic tectonism in the Apuseni Mountains was more complex than simple nappe stacking. We show that crustal deformation was not confined to discrete thrust surfaces but was gradually accommodated within wide strain zones. A range of structural levels are now exposed as wide retrogressive ductile to brittle shear zones in the pre-Alpine basement rocks, and as "wildflysch" assemblages in cover sequences. We present data on the nature, distribution, penetrative structure, geothermometry, and kinematics of metamorphic rocks in the Apuseni Mountains. We discuss the regional implications of the data and propose a geodynamic model that contrasts significantly with existing interpretations for the region.

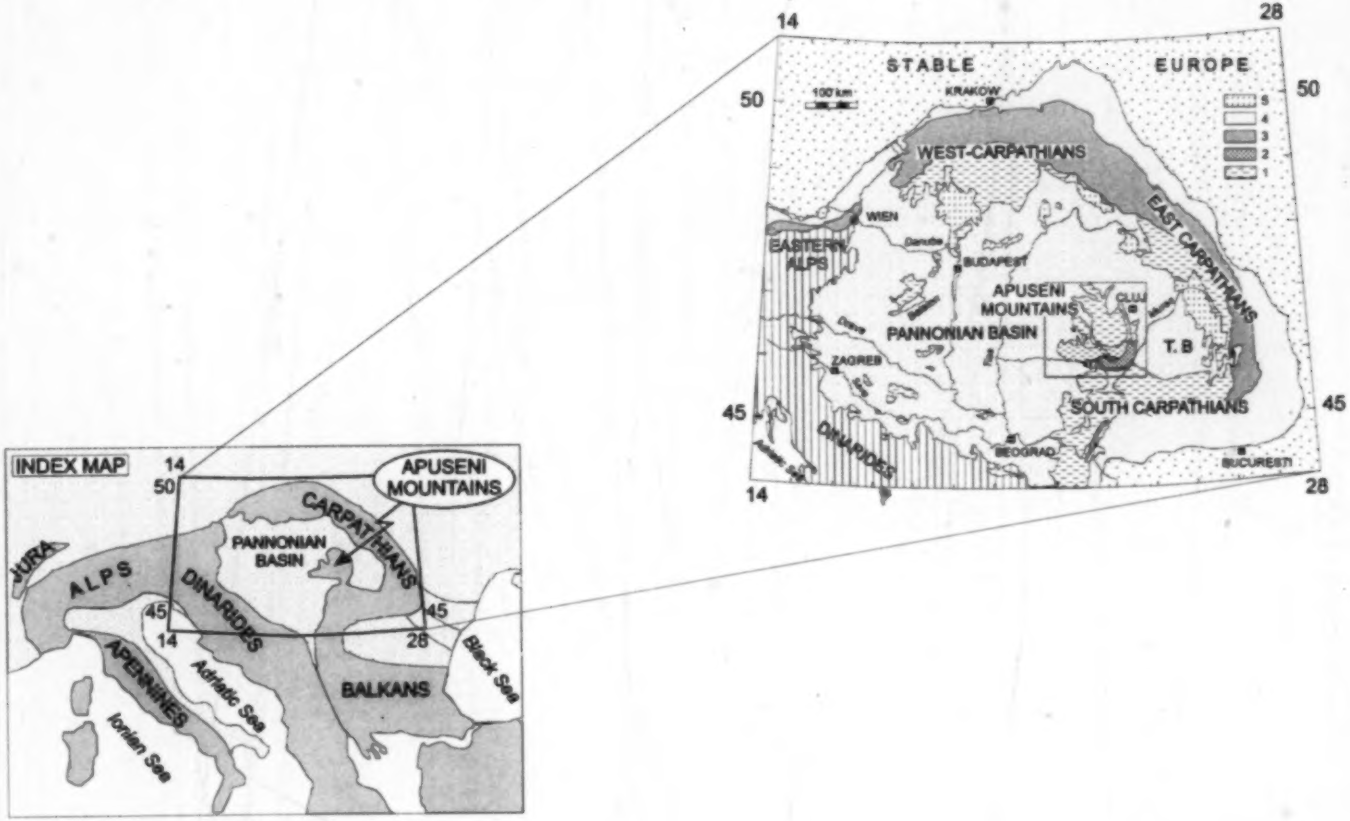
INDEX MAP
APUSENI MOUNTAINS
JURA
ALPS
PANNONIAN BASIN
CARPATHIANS
DINARIDES
APENNINES
Adriatic Sea
Ionian Sea
BALKANS
Black Sea
STABLE
EUROPE
100 km
KRAKOW
WEST-CARPATHIANS
EAST CARPATHIANS
WIEN
Danube
EASTERN ALPS
BUDAPEST
APUSENI MOUNTAINS
CLUJ
PANNONIAN BASIN
T.B
ZAGREB
SOUTH CARPATHIANS
DINARIDES
BEOGRAD
BUCURESTI
5
4
3
2
1
14
28
50
45

Fig. 5-1. Bottom: European segments of the Alpine chain mentioned in the text. Top: main tectonic units of the Carpathians and Apuseni Mountains reffered to in the text: 1- pre Permo-Mesozoic basement; 2 - Late Jurassic to Cretaceous Mureş Basin ("Tethys remnant"); 3 - Outer Carpathian flysch; 4 - Carpathian foredeep strata; 5 - Neogene igneous rocks. T.B. - Transylvanian Basin.

5.2. REGIONAL SETTING: PREVIOUS WORK

The metamorphic sequences of the Apuseni Mountains were initially classified as *meso-*, *epi-*, and *anchi*-metamorphic (Geologic Map of Romania, 1: 500 000 scale, 1958) and assigned to the Precambrian, Late Proterozoic, and Paleozoic, respectively (Geologic Map of Romania, 1: 200 000 scale, 1967). Scarce age data were used to propose a stratigraphy inferred to include the products of three pre-Alpine orogenies, the Grenvillian, Cadomian or Caledonian, and Variscan, respectively (Giuşcă et al., 1968; Ianovici et al., 1976; Dimitrescu, 1985; 1988 b). A formal lithostratigraphic nomenclature was established (Kräutner, 1980; Bleahu et al., 1981; Dimitrescu, 1988b) (Tab. 5-1). The Permian to Mesozoic sedimentary cover of the Apuseni Mountains has been assigned to two distinct sedimentary basins (Bleahu et al., 1981): a northern one, with a nearly complete Permian to Eo-Cretaceous platformal sequence of East-Alpine/Carpathian affinity with increasing southward "Mesogean" character (Patrulius, 1976), and a southern, tectonically active basin with Late Jurassic to Late Cretaceous flysch and wildflysch associated with tholeiitic to calc-alkaline igneous activity (Savu,1980; Cioflica and Nicolae, 1981; Lupu et al., 1993; Nicolae, 1994, 1995).

In the northern Apuseni Mountains, two nappe systems of presumed Cretaceous, pre-Gosau age were proposed (Ianovici et al., 1976; Bleahu et al., 1981). The Bihor "autochthon" (Fig. 5-2) was inferred to consist of Permian to Lower Turonian sedimentary cover and underlying metamorphic basement (the latter consisting of the Someş "series", of amphibolite grade, and the Arada "series", of upper greenschist grade). The Codru nappe system was inferred to consist of several cover nappes of Permian to Lower Cretaceous sequences and a lowermost nappe involving basement rocks (the Codru "series" of amphibolite grade). The Biharia nappe system was inferred to consist of either four (Ianovici et al., 1976) or three basement nappes (Balintoni, 1985). In the sedimentary basin of the southern Apuseni Mountains, eleven Laramide (Bleahu et al., 1981) or seven Austrian and eight Laramide nappes (Balintoni, 1994) have been proposed.

5.3. LITHOTECTONIC ASSEMBLAGES: DISTRIBUTION, NATURE OF PROTOLITHS AND METAMORPHIC CONDITIONS

5.3.1 *Low-grade rocks*

Low-grade metamorphic rocks are distributed along a belt that wraps around the Bihor autochthon; a second belt is less well exposed in the Trascău Mountains (Fig. 5-2). Fine-grained foliated rocks were previously considered to be prograde phyllite, and coarse ones to preserve sedimentary structures (Papiu, 1960; Savu, 1965; Dimitrescu, 1962; 1993; Giuşcă, 1979; Balintoni, 1986).

Our mapping (Figs. 5-2, 5-16 and 5-17) shows that lithologic assemblages previously

PREVIOUSLY PROPOSED STRATIGRAPHY

"SUPERGROUP"	"GROUP"	"SUBGROUP", "SERIES" or "FORMATION"	AGE DATA				
			PALYNOLOGIC DATA	K / Ar DATA (Ma)			
			a	b	c	d	e
286 Ma		"Izvoarele formation" # "Trascau series" ***,+					
		"Belioara-Vulturese series" ***					
"Variscan" *		"Paiuseni series" ***	*Stenozonotriletes s.* *Leiotriletes m.* *Zonotriletes cf. e.*	260	327	113-123	
		Highis granitoids			350		
505 Ma		"Arieseni Formation" **	*Zonotriletes a.* *Leiotriletes sp.* *Calamospora sp.*				
"Marisian" *	"Bihor" *	"Muncel Formation" *	*Protosphaeridium sp.* *Zonosphaeridium d.* *Kildinella cf. h.*			106-115	
		"Biharia Formation" *	*Protosphaeridium l.* *Kildinella sp.* *Laminarites sp.*			181	
		"Arada Formation" *	*Protosphaeridium sp.* *Leiosphaeridium sp.* *Laminarites sp.*			49-164	
		"Codru series"					
		Codru pegmatite-Gilau Mts			488-596	288-343	230-357
900 Ma		Gaisa pegmatite-Highis Mts.				243-246	
"Carpian" *	"Somes" *** ("Gilau" *)	"Upper micaschist Formation" *** "Giurcuta leptino-amphibolite Formation" *** "Valea Cosuri micaschist Formation" ***				268-381	79-227
		Muntele Mare granite			522	156-232	199-237
	"Aries" *	"Baia de Aries series" * "Vidolm series" * "Madrizesti series" *	*Fibularix sp.* *Cetinella p.* *Leiosphaeridium sp.*				
1600 Ma		Vinta granite					172

CORRESPONDING LITHOTECTONIC ASSEMBLAGES USED IN THE TEXT

ALPINE TECTONISM		PRE-ALPINE TECTONISM
Trascau assemblage	TSZ	*Baia de Aries assemblage*
Sohodol-Belioara assemblage	HBSZ	
Poiana assemblage		*Highis-Biharia upper crustal igneous complex*
Paiuseni assemblage		
Arieseni assemblage		
Biharia assemblage		
Arada assemblage		*Somes assemblage*
		Codru assemblage
		Somes assemblage
		Baia de Aries assemblage

Table. 5-1. ***Left:*** Summary of lithostratigraphic classification previously used for the metamorphic/magmatic basement of the Apuseni Mountains; note the inconsistency between the radiogenic data and postulated stratigraphic position. Compiled from: # - Ianovici et al., 1976; *- Krautner, 1980; **- Bleahu et al., 1981; *** - Dimitrescu, 1986, 1988; + - Balintoni and Iancu, 1986. Age data from: a - Visarion and Dimitrescu, 1971; Ianovici et al., 1976; b - Filipescu and Vincentiu, 1963, fide Soroiu et al., 1969; c - Giusca et al., 1967, 1968; d - Soroiu et al., 1969; e - Pavelescu et al., 1975. Only apparently reliable K/Ar data are shown; we did not consider a number of dates that are suspect because of incompatibility with field relations (e.g., granite host dated as younger than dykes cutting it) or because method limitations(dates reported for hornblende+biotite concentrate). ***Right:*** corresponding lithotectonic assemblages discussed in the text.

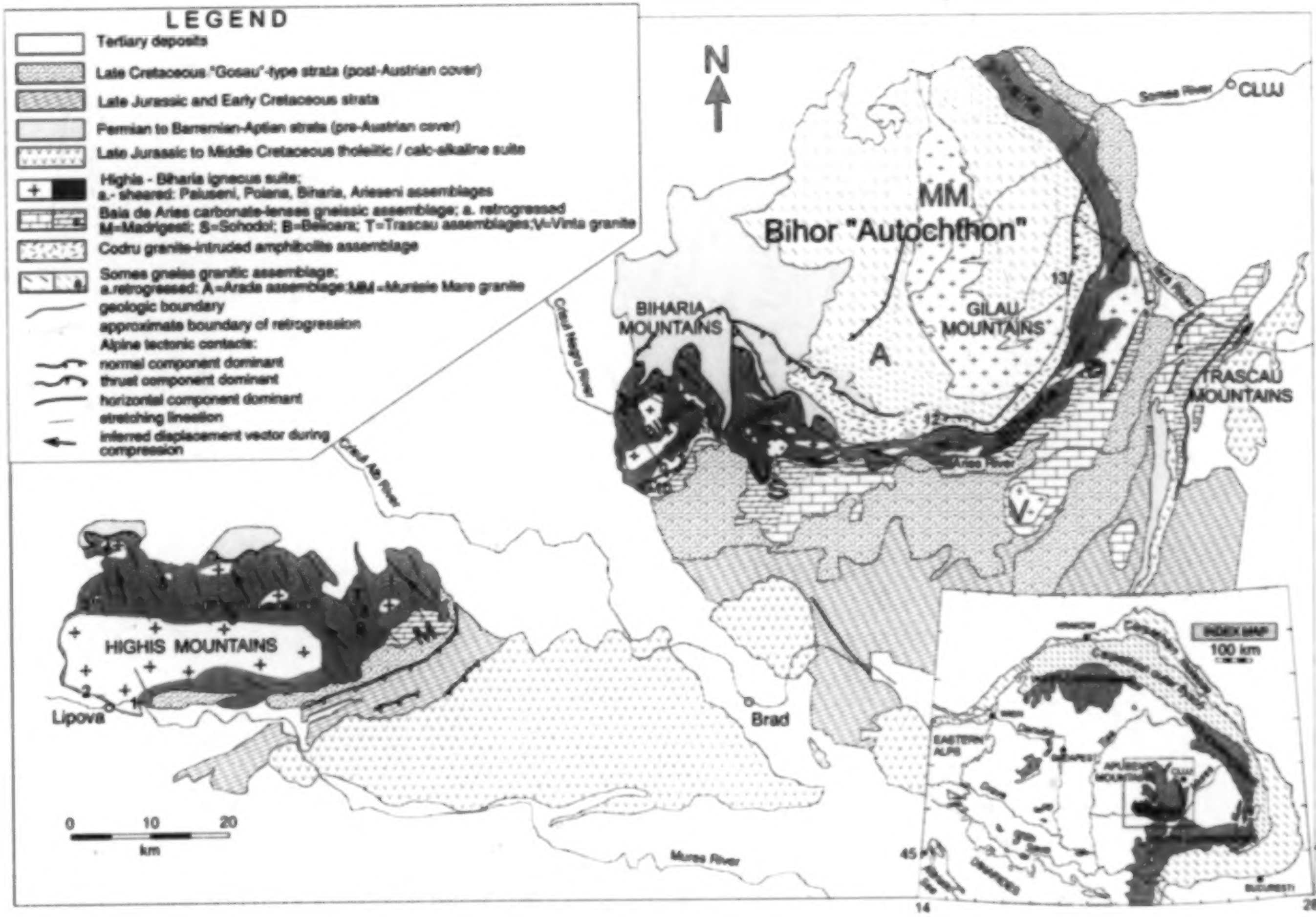
LEGEND
Tertiary deposits
Late Cretaceous "Gosau"-type strata (post-Austrian cover)
Late Jurassic and Early Cretaceous strata
Permian to Barremian-Aptian strata (pre-Austrian cover)
Late Jurassic to Middle Cretaceous tholeiitic / calc-alkaline suite
Highis - Biharia igneous suite;
a.- sheared: Paiuseni, Poiana, Biharia, Arieseni assemblages
Baia de Aries carbonate-lenses gneissic assemblage; a. retrogressed
M=Madrigesti; S=Sohodol; B=Belioara; T=Trascau assemblages;V=Vinta granite
Codru granite-intruded amphibolite assemblage
Somes gneiss granitic assemblage;
a.retrogressed: A=Arada assemblage;MM=Muntele Mare granite
geologic boundary
approximate boundary of retrogression
Alpine tectonic contacts:
normal component dominant
thrust component dominant
horizontal component dominant
stretching lineation
inferred displacement vector during compression
N
Bihor "Autochthon"
MM
A
GILAU MOUNTAINS
BIHARIA MOUNTAINS
TRASCAU MOUNTAINS
HIGHIS MOUNTAINS
CLUJ
Somes River
Crisul Negru River
Crisul Alb River
Aries River
Mures River
Brad
Lipova
S
V
M
12
13
1
2
0
10
20
km
INDEX MAP
100 km
EASTERN ALPS
APUSENI MOUNTAINS
45
14
28

Fig. 5-2. Structural map of the Apuseni Mountains; numbers are lacalities refered to in text.

assigned to the Late Proterozoic and Paleozoic (Tab. 5-1) contain rocks texturally and mineralogically equilibrated under low-grade metamorphic conditions, as well as rocks with disequilibrium textures. Within each assemblage, occur metre- to kilometre-sized lensoid bodies of incompletely reequilibrated or unaffected rocks. On the basis of mineralogic and lithologic relics, lithotectonic assemblages can be separated that contain petrographically similar tectonites and either igneous or medium-grade metamorphic relics. Sheared igneous rocks previously considered as intrusions into the pre-metamorphic sedimentary succession exhibit strong foliation and/or compositional layering and obvious stretching lineation (i.e., they are L-S or L tectonites). All stages of deformation and metamorphism of massive igneous rocks of various mineralogy and grain size into completely equilibrated greenschist facies tectonites are recorded. A continuous progression from granitoid to pseudo sedimentary textures was reported in the Highiş Mountains by Pană and Ricman (1988).

We assign to the *Păiuşeni assemblage* a lithologic succession dominated by quartz-sericite-albite schist and secondary-quartz-clast bearing tectonites, associated with numerous granitic, microgranitic, and rhyolitic bodies and rare metamorphic carbonate lenses in the northern Highiş Mountains and southern Biharia Mountains. Crosscutting quartz veins indicate multiple phases of silica release within the HBSZ. We interpret quartz-pebble-like clasts in the Păiuşeni assemblage to result from local shearing and stretching of quartz veins in a more competent mylonitic matrix (Figs. 5-3 and 5-4). In the Biharia Mountains, we observed a gradual transition from biotite- and/or hornblende-bearing diorite to chlorite-albite schist. Carbonate mineral reactions accompanied the process, as evidenced by widespread carbonate layers or carbonate-pebble-like structures (Fig. 5-7). We term this association the *Biharia assemblage*. On the western slope of the Biharia Mountains, it overlies the *Poiana assemblage* consisting of foliated tectonic breccia and conglomerate, largely overprinted by thermal metamorphism associated with Paleogene quartz diorite ("Banatite") intrusions. On the eastern slope, the Biharia assemblage overlies an association of mainly fine-grained silky schist and small aplite, hornfels, and diorite relic bodies that can be separated as the *Arieşeni assemblage*. At different locations (e.g., Arieşul Mic, Bucura, and Ghizghiţului valleys) a conglomerate-like fabric resulted from the dismembering of a porphyritic rock within a microgranitic host.

Fine-grained magnetite/epidote/sericite hornfels of aplite and basalt constitutes one of the protoliths of the Păiuşeni and Arieşeni assemblages. The hornfelsing likely resulted from the youngest bodies of the upper crustal igneous complex. In the Biharia Mountains, diopside hornfels overprints the foliation and is interpreted to result from Paleogene ("Banatite") magmatism.

Farther along strike to the east, these separate assemblages cannot be recognized and schist with large sheared granitoid pods defines the Biharia assemblage; in the Arieş Valley,

Figure 5-3. Quartz-filled tension gashes in a microgranite of the Păiuşeni assemblage, Cigher Creek, central Highiş Mountains.

a.

b.

Figure 5-4. Pseudo-metaconglomerate in the Păiuşeni assemblage; a) and b) Otcovac Peak, western Highiş Mountains; c) Hulumoş Creek, and d) Highiş Peak, central Highiş Mountains.

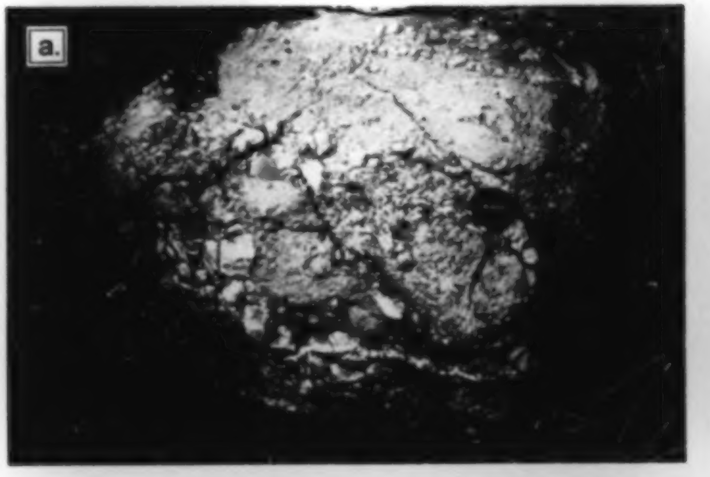
a.

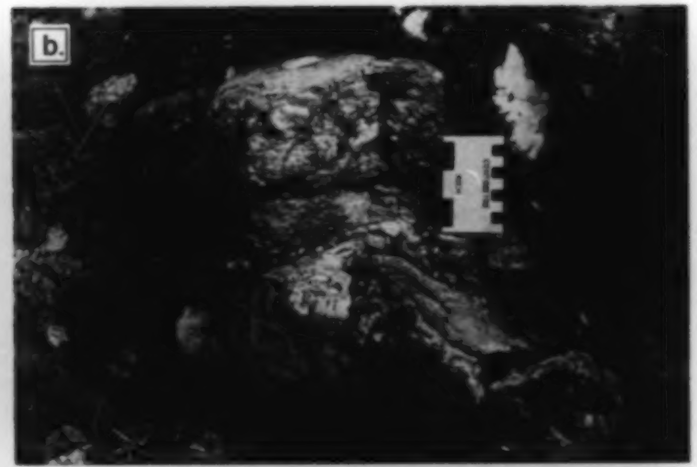
b.

c.

d.

Fig. 5-5. Late granite intrusions in diorite within the Highiş igneous complex of the Păiuşeni assemblage: a) Şoimoş quarry; b) Lipova-Arad highway.

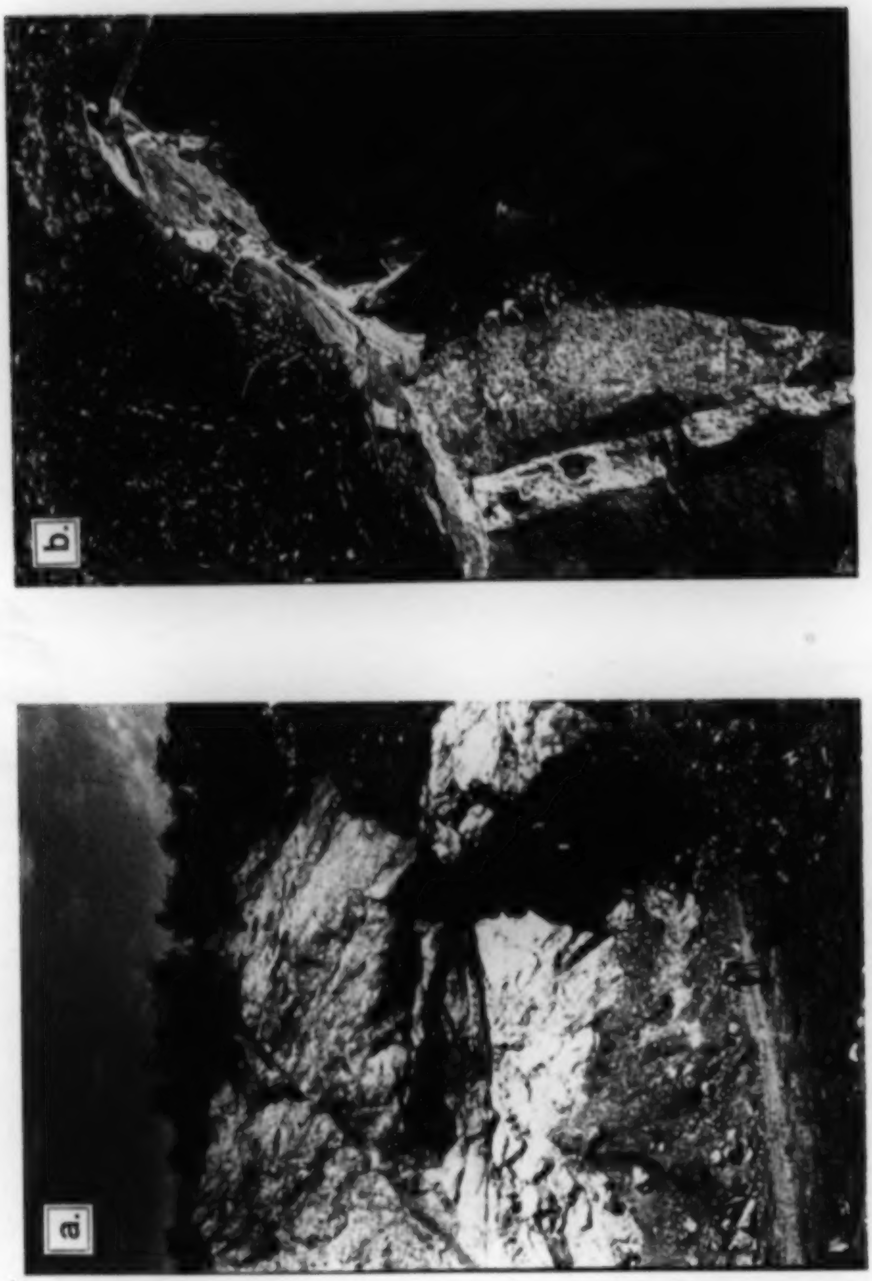
a.
b.

concordant quartzo-feldspathic rock bodies previously interpreted as sills (e.g. the Lunca Largă granites - Balintoni, 1985) or as sedimentary layers (e.g. the Mihoeşti metaconglomerate - Dimitrescu, 1973) are sheared intrusions which have gradational boundaries with the enveloping tectonites. Metre- to kilometre-sized bodies of incompletely metamorphosed granite to diorite are commonly hosted by chlorite schist. Unsheared domains several tens of square kilometres in area in the Highiş Mountains expose all igneous rock types found along the belt. Various granitoids intrude and partly assimilate older mafic intrusions (Fig. 5-5).

Stable isotope data from the low-grade assemblages

Carbonate and silicate rocks from the low-grade assemblages have been analysed for carbon and oxygen isotope ratio and oxygen isotope ratios, respectively.

Carbonate rocks. Lenses and nodules of calcite, dolomite and ankerite occur (usually as mixtures of end-members) throughout the low-grade assemblages and are traditionally interpreted as metamorphosed limestone strata. Their sedimentary origin is questionable because carbonate rocks were found at different structural levels as discontinuous metre-sized lenses which rarely can be followed for more than a few hundred metres. Augen (Fig. 5-7) and lens-shaped (Figs. 5-6 and 5-8) carbonate structures and microstructures indicate widespread carbonate reactions in all low-grade rocks. Carbonate rocks consist of a fine-grained, preferentially oriented carbonate +/- quartz matrix with micro-lenses of coarser carbonate grains, ribbon-like quartz grains and corroded relics or pseudomorphs of feldspar and mica. The matrix is commonly affected by discrete shear zones locally highlighted by white mica flakes and opaque minerals indicating polyphase deformation. A mylonitic layering is locally defined by carbonate versus ribbon-like quartz layers. Kinematic indicators are similar with those displayed by the surrounding quartzo-feldspathic rocks.

Analytical method. The carbonate samples were ground to < 200 mesh (<70 µm), and phase composition of each sample was verified by X-ray difractometry. The carbonates were reacted with 100 % phosphoric acid. In the case of calcite-dolomite mixtures, CO_2 was extracted separately from calcite and dolomite. To minimize potential cross-contamination CO_2 from calcite was removed after two hours reaction at 25°C, then the vessel was closed and the reaction was continued for a few days more at 25°C, or 24 hours at 50°C (Al-Aasm et al., 1990). Isotopic analysis of extracted carbon dioxide were carried out on VG 602 and Finnigan MAT 252 mass spectrometers at the University of Alberta. The δ-values are reported with respect to PDB (carbon) and SMOW (oxygen) and are precise to ~0.05 $^{0}/_{00}$. A correction factor of 0.72 was used for dolomite and ankerite $\delta^{18}O$ values determined at 25°C. Most of the samples have been analyzed twice under the same and/or different conditions in order to verify the validity of data and possible kinetic effects due to grain size, time and temperature of reaction. Analysis that yielded unusually low $\delta^{13}C$ values have been repeated two or three times. The kinetic effect of

Fig. 5-6. Centimetre-size veins of carbonate within igneous rocks affected by strain under low-grade metamorphic conditions; a) sheared microgranite, Păiuşeni assemblage, Căsoaia resort, Arăneag Creek, Highiş Mountains; b) granodiorite, Codru assemblage, Neagu Creek, southern Gilău Mountains.

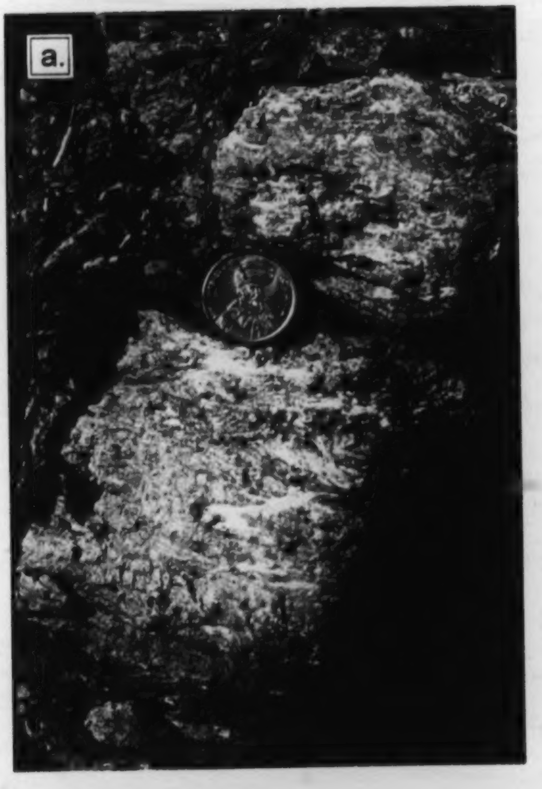
a.

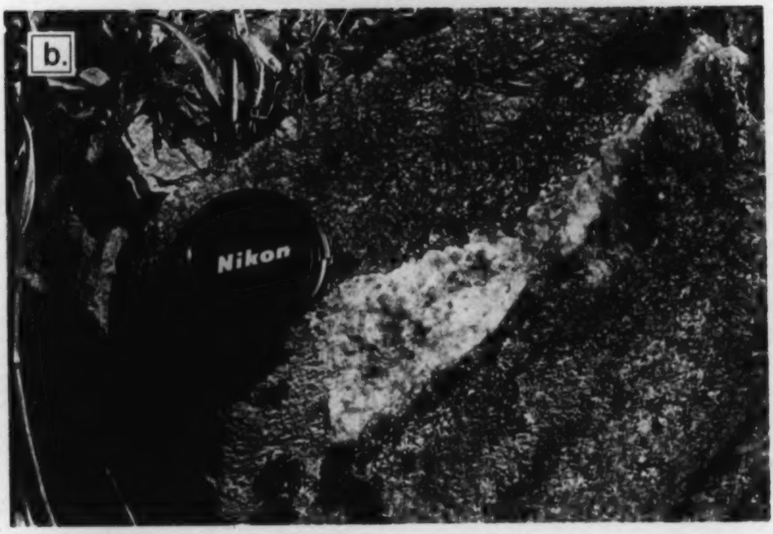
b.
Nikon

Fig. 5-7. Carbonate nodules within quartz-muscovite-carbonate-epidote±albite± chlorite schist ("metaconglomerate"); a) Băneşti Creek, southern Biharia Mountains, b) Arieşul Mic River, Biharia Mountains.

a.

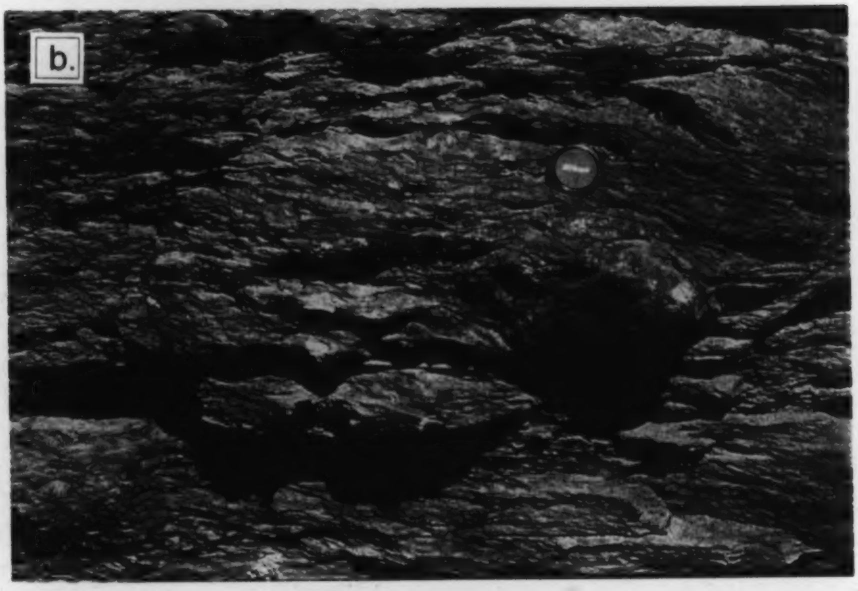
b.

Fig. 5-8. a) Massive replacement of a diorite by carbonate, Neagu Creek, southern Gilău Mountains; b) carbonate layer developed within the chlorite schist matrix; incomplete substitution at the top of the carbonate layer.

b.

a.

grain size was found to be insignificant for calcite reacted more than two hours (sample 11 106). No fractionation occurred after the completion of the reaction; similar isotopic values have been obtained for ankerite (sample 11 162) analyzed after one hour at 25°C, after one week at 25°C, and after one week at 50°C, and for calcite (sample 11 083) analyzed at 25°C after 2 hours and 2 months. Differently colored carbonate bands within the same layer have slightly different isotopic compositions. The same observation is valid for calcite vs. dolomite from mixtures. This suggests that perfect homogenization did not occur.

Results and Discussion. Analytical data are summarized in Table 5-2 and Fig. 5-9.

Stable isotope ratios record information about the origin of samples (source information) and their subsequent reaction history. The source sets an isotopic baseline that can subsequently be shifted by isotopic fractionation.

The $\delta^{13}C$ values of carbonate rocks of marine origin of Cambrian to Tertiary age are virtually constant and have values close to zero on PDB scale. Marine carbonate rocks of Precambrian age are enriched in $\delta^{13}C$ by about 3 $^{o}/_{oo}$ (Veizer and Hoefs, 1976). Although much wider ranges of variation have been also reported from different areas (+6 to +11 by Schidlowski et al., 1976, -5 to +6 by Veizer and Hoefs, 1976), a field of most common isotopic values is defined by carbon (-2 to +4) and oxygen (20 to 26) for unmetamorphosed marine limestones (Fig. 5-9) based on data compiled by Valley (1986). Sedimentary whole rock isotopic values (including marble and calcareous quartzite) are preserved through greenschist and amphibolite facies metamorphism (Schwarcz et al., 1970). Isotopic values of greenschist facies limestone range from -0.3 to +5.6 (mean of +3) and 18.1 to 28.1 (mean of 21.4) for carbon and oxygen, respectively (Dunn and Valley, 1985). The low $\delta^{18}O$ and $\delta^{13}C$ values yielded by the carbonate lenses from the low-grade assemblages of the Apuseni Mountains are outside the reported range for marine limestone affected by prograde metamorphism (Valley, 1986).

The "batch" volatilization model implies a "calc-silicate limit" of 0.6 which limits the $\delta^{18}O$ depletion at less 2 $^{o}/_{oo}$. Larger depletions in ^{18}O require decarbonation reactions with F-oxygen vs. F-carbon trends that cross the calc-silicate limit i.e., a "silicate absent decarbonation" trend. Since the carbonate lenses in the Apuseni Mountains are interfingered with silicate rocks, carbonates must have volatilized without maintaining isotopic equilibrium with coexisting silicates ("decarbonation-silicate disequilibrium", Lattanzi et al., 1980). Disequilibrium conditions suggest large amounts of reaction involving massive rock-volume loss and are consistent with the "open system" metamorphic conditions of a shear zone overprinting marine limestone. Alternatively, the plot of isotopic data along the skarn trend (Bowman et al., 1985) is the combined effect of infiltration of chemically evolved superficial waters and volatilization of "juvenile" low-$\delta^{13}C$ carbonates. The depleted isotopic ratios of mantle-origin CO_2 (eg. Wyman and Kerrich, 1988) incorporated in the igneous protolith or released along the shear zone

Table 5-2. Carbon and oxygen isotope data from carbonate lenses within the HBSZ.

SAMPLE	LOCATION	PHASE	ANALYSED FRACTION	REACTION TIME							
				a few hours		*2 days*		*7 days*		*10 days*	
				$^{13}C_{PDB}$	$^{18}O_{PDB}$	$^{13}C_{PDB}$	$^{18}O_{PDB}$	$^{13}C_{PDB}$	$^{18}O_{PDB}$	$^{13}C_{PDB}$	$^{18}O_{PDB}$
CODRU ASSEMBLAGE											
11115	Aries Valley S	D		0.34	-14.33	-4.20	-12.25				
13211	Bistrisoara Valley	C+ minor D	bulk	-3.90	-18.58						
13230	Neagului Spring	C				-5.60	-21.23				
13232	Neagului Spring	C		-4.46	-17.55						
11162	Lupsei Valley N	A		-1.64	-17.08	-0.55	-15.44	-1.78	-17.67	-1.70	-17.67
11241	Aries Valley N	A	*							-1.10	-15.27
PAIUSENI ASSEMBLAGE											
11077	Covasint Hill	C		-8.78	-15.76	-7.56	-15.96	-7.56	-14.79		
			*	-7.61	-14.79						
11083	Otcovac Hill	C	bulk	0.29	-17.34	-2.22	-17.42	0.95	-17.09		
		C	white layer	0.84	-15.45						
		C	brown layer	0.74	-16.99						
13673	Agrisul Mare Valley	C+25%D						-0.14	-14.75		
13686	Highis Valley (casoaia)	C+25%D									
			C	-1.23							
			D					-1.6	-20.09		
11091	Highis Valley	C+22.5%D	bulk	-1.45	-15.93					0.31	-14.19
			*	-1.56	-16.14					-0.45	-15.04
		C		-1.50	16.00						
		D						-0.50	-15.72		
11106	Radesti Valley	C	bulk	-3.99	-13.96	-4.02	-13.91	-5.21	-17.08		
		C	coarse fraction	-4.17	-14.27						
		C	pinkish layer	-3.38	-13.84						
		C	grey layer	-2.64	-13.70						
11057	Cladovita Valley N	C	bulk			-0.29	-18.58				
		C	yellow layer	-4.86	-12.30						
		C	black layer	-1.62	-18.40						
11058	Cladovita Valley S	C	bulk								
		C	greenish layer	-2.59	-14.75						
		C	grey layer	-2.22	-17.56						
BIHARIA ASSEMBLAGE											
11110	Dolii Valley	D+3%C	bulk	0.84	-19.34	1.53	-18.47	0.84	-17.28	0.75	-17.35
		D						0.80	-18.02		
		C		0.80	-19.30						
13727	Trib. Banesti Valley	C		-0.56	-17.74						
13773	Ariesul Mic Spring	C		-4.84	-21.25						
13776	Ariesul Mic Valley	D+v. minorC	bulk					-3.14	-16.94		
13789	Avram Iancu Village	D						-1.09	-18.67		
13324/1	Caselor Valley (Cimpe	D						1.51	-14.03		
13324	Caselor Valley (Cimpe	D						1.58	-13.39		
13111	Bistra Valley	D+v. minorC	bulk					-1.29	-15.38		
11203	Lupsei Valley S	D		-6.42	-16.44	-4.39	-15.10	-6.33	-16.06		
13892	Sagacea Valley	C+D	bulk	0.96	-16.05						
		C		0.57	-14.57						
13904	Ocolis Valley	D						0.59	-17.00		
13933	Baisorii Valley	C+D	bulk								
		C		-3.44	-14.39						
		D						-5.68	-15.80		
13936	Baisorii Valley	D+v. minorC	bulk					0.02	-14.93		
BAIA DE ARIES ASSEMBLAGE											
11020	Ungurului Valley	D+3%C	bulk	-1.86	-8.39	-2.10	-9.10	-0.85	-6.42		
		D						-2.00	-9.22		
		C		-1.90	-8.40						
13720	Madrigesti Valley	C				-7.90	-15.64				
11116	Sohodol	C		1.96	-7.40	2.46	-7.09	2.43	-6.79		
11119	Vinta	C		1.96	-7.36	2.32	-6.97				
13812	Cioara Valley	C		0.52	-10.56						
13860	Belioara Valley	C		2.33	-4.75						
13863	Posaga Valley(Belioar	D+v. minorC	bulk					2.20	-4.06		
13864	Posaga Valley(Belioar	C		2.44	-1.33						
13914	Ocolis Valley (Belioara	D						2.09	-3.90		
13980	Iara Valley (Surduc)	C		2.63	-10.19						
9947	Iara Valley (Surduc)	D+22.2%C	bulk	2.07	-9.74	2.31	-8.77			0.45	-6.25
			*	1.68	-11.08					2.70	-7.24
			*	1.23	-8.67						
		D						2.7	-7.92		
		C		1.7	-11						

* Repeat analysis

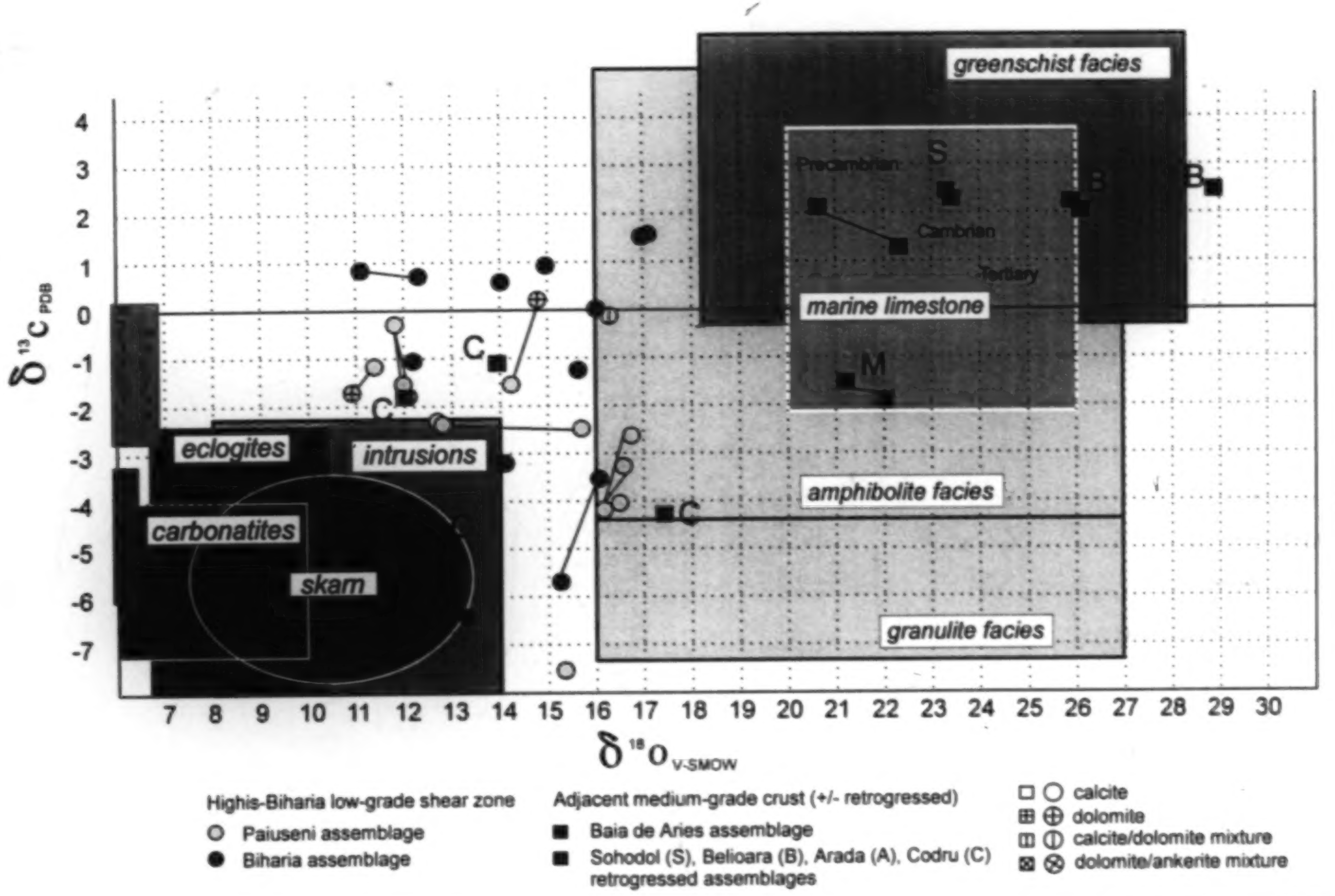

Fig. 5-9. Stable isotope composition of the carbonate layers within the metamorphic assemblages of the Apuseni Mountains

(eg. Taylor and Green, 1986) may have been altered by the overwhelming influx of surficial water in the shear zone. Local massive replacement of preexisting country rocks by metasomatic carbonates as inferred elsewhere (e.g., Baratov et al., 1984; Bohlke and Kistler, 1986; Lapin et al., 1987; Cameron, 1988; Groves et al 1988; Goldfarb et al., 1988) may have resulted in the carbonate layers and nodules from the low-grade assemblages of the Apuseni Mountains.

Silicate Rocks. Oxygen isotope ratios of quartzo-feldspathic schist and interlayered igneous pods of the Păiuşeni assemblage are presented in Table 5-3. Traditionally, the low-grade sequence is interpreted to represent a volcano-clastic sequence metamorphosed under low-grade conditions. The analyzed samples from the HBSZ show considerably lower $\delta^{18}O$ values than greenschist facies metasediments (Valley, 1986). SMOW $\delta^{18}O$ values of 7.18 for the diorite and 10.03 for the granite samples (11 060 and 11 063, respectively) collected from the Highiş igneous complex are in the expected range for igneous rocks (Taylor and Sheppard, 1986). $\delta^{18}O$ value of 6.32 for the "albite porphyroblast schist" (11 109) is lower than the $\delta^{18}O$ value of the diorite (11 060) and indicates its direct derivation from an igneous protolith. $\delta^{18}O$ values of 14.37 and 12.67 for the rhyolite samples (11 107 and 11 100, respectively) and of 15.67 for the granite sample (11 090) from metric size pods within the schist matrix are considerably higher and indicate enrichment by exchange with the metamorphic fluid. There is a clear overlap between the $\delta^{18}O$ values of some rhyolite pods (11 100 and 11 107) and the matrix of the "metaconglomerate" (11 087) and "phyllite" samples (11 103 and 11104), respectively (Tab. 5-3). These data indicate that the schist matrix and small igneous pods have locally reached isotopic equilibrium with a pervasive metamorphic fluid. An igneous protolith appears obvious for at least some of the schists. The source of fluid cannot be inferred in the absence of δD values.

Temperature estimates

Mineral assemblages in the low-grade rocks indicate metamorphic conditions below the biotite isograd. Chloritoid, fine-grained biotite, and an isolated occurrence of kyanite along the southern margin of the Păiuşeni assemblage show that at least parts of the shear zone experienced higher metamorphic conditions. However, no regular distribution of index minerals can be mapped and the low- to very low-grade silicate rocks are not amenable to thermobarometric analysis. The calcite-dolomite solvus thermometer (Anovitz and Essene, 1987) shows that temperatures in carbonate mixtures in lenses throughout the schistose matrix (Fig. 5-7) are in agreement with general metamorphic conditions in surrounding quartzo-feldspathic and mafic schists (i.e., below biotite stability). However, peak temperatures retained by some lenses (Fig. 5-10) are above the biotite isograd, suggesting that biotite in the surrounding matrix was altered during subsequent shearing. Trapping temperatures of fluid

Table 5-3. Oxygen isotope composition of silicate-rocks within the Paiuseni assemblage

SAMPLE	LOCATION	ROCK TYPE	MINERAL PHASES	$^{18}O_{ref}$	Yield	$^{18}O_{SMOW}$
Mylonitic schist						
11 087	Siria Hill	secondary qz-clasts schist	Qz + Mu	-11.870	13.20	12.58
11 098	Paiuseni Valley	white silky schist	Qz + Mu +c-chlor	12.880	15.46	11.57
11 103	Paiuseni Valley	greenisch silky schist	Qz + Mu +c-chlor	-10.408	14.18	14.04
11 092	Paiuseni Valley	massive qz-feldspathic rock		-11.430	14.38	13.02
11 104	Paiuseni Valley	gray silky schist	Ab + Mu + c-chlor + Hm	-9.741	12.90	14.71
11 077	Covasna Hill	layered silky schist	Qz + Mu + c-chlor + Hm	-11.110	14.16	13.34
11 109	Leucii Valley	Ab-clasts schist	Qz + Ab + c-chlor + Mu	-18.127	13.93	6.32
Massive igneous rocks						
11 063	Jernova Valley	granite	Qz + Ab + Mi + Mu	-14.424	14.03	10.03
11 090	Highis Valley-Casoaia	granite	Qz + Ab + Mi + Mu	-8.783	10.77	15.67
11 100	Paiuseni Spring	dark-grey rhyolite	Qz + Ab + Mi + Mu + c-chlor	-11.778	15.15	12.67
11 107	Radesti Valley	white-grey rhyolite	Qz + Ab + Mu + c-chlor + Cc +	-10.080	12.34	14.37
11 060	Cladovita Valley	alkali-diorite	Qz + Ab + Mi + Ph + mg-Hb	-17.828	13.00	7.18

$^{18}O_{SMOW} = {}^{18}O_{ref} + 24.45$

Theoretical yelds for the involved minerals (oxygen as CO_2):

Qz:	16.64	Ch:	14.92
Ab:	15.25	Ph:	14.38; $Ph_{66}An_{33}$: 13.37; $Ph_{50}An_{50}$: 12.91
Kf:	14.37	Hb:	13.76
Ko:	17.43	Cc:	9.99
Hm:	9.34	Do:	10.84

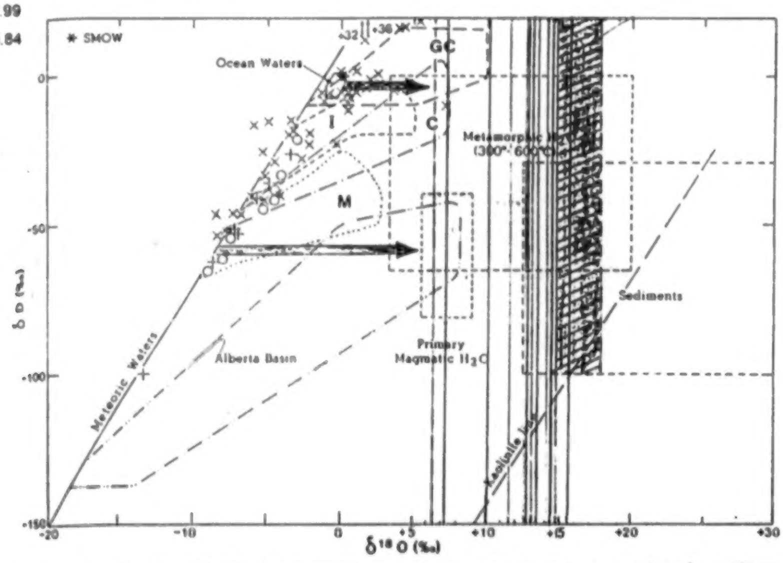

Fig. 5. Isotopic composition and fields for formation waters, ocean waters, meteoric waters, metamorphic waters, magmatic waters, and common sedimentary rocks (after Sheppard, 1984). Hatched - field of common greenschist grade metasediments. Vertical lines - samples from the Paiuseni assemblage. The Kaolinite weathering line from Savin and Epstein (1970).

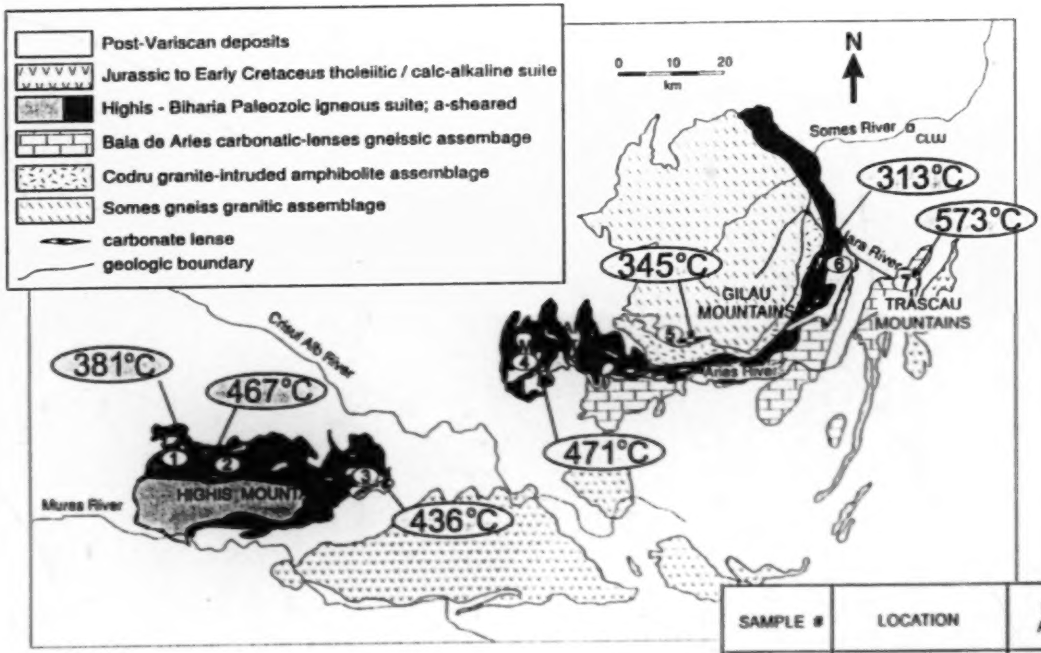
Post-Variscan deposits
Jurassic to Early Cretaceus tholeiitic / calc-alkaline suite
Highis - Biharia Paleozoic igneous suite; a-sheared
Baia de Aries carbonatic-lenses gneissic assembage
Codru granite-intruded amphibolite assemblage
Somes gneiss granitic assemblage
carbonate lense
geologic boundary
0
10
20
km
N
Somes River
CLUJ
313°C
573°C
345°C
GILAU MOUNTAINS
Iara River
TRASCAU MOUNTAINS
Crisul Alb River
381°C
467°C
Aries River
471°C
436°C
Mures River
HIGHIS MOUNT.
1
2
3
4
5
6
7

Fig. 5-10. Peak reequilibration temperatures recorded by carbonate rocks in the Apuseni Mountains; size of carbonate lenses along the belt of low-grade rocks is highly exagerated. Numbers in white circles on the map correspond to sample numbers in the teble.

SAMPLE #	LOCATION	LITHOLOGIC ASSEMBLAGE	CALCITE	
			X-MgCO$_3$	T (°C)
1	Agrisu Mare Valley	Paiuseni (Highis-Biharia)	0.0234 0.0168	382 313
2	Highis Valley	Paiuseni (Highis-Biharia)	0.0367 0.0236	468 383
3	Ungurului Valley	Madrigesti (Baia de Aries)	0.0311 0.0154	436 292
4	Leuicii Valley	Biharia (Highis-Biharia)	0.0374 0.0130	471 268
5	Bistrisoara Valley	Arada (Somes)	0.0195 0.0078	345
6	Baisoara Valley	Biharia (Highis-Biharia)	0.0168 0.0073	312
7	Iara Valley	Baia de Aries	0.0627 0.0147	573 282

inclusions in secondary quartz clasts range from 320 to 285°C (Savu et al., 1967). Our preliminary data on fluid inclusions from quartz grains in carbonate lenses indicate wide ranges of homogenization temperatures of 275° to 135°C and 180° to 90°C. All fluid inclusions are pseudo secondary- to secondary two-phase hydrous, low-salinity mixtures (4-5 weight % NaCl) and we interpret them to be surficial water trapped late in the tectonic evolution.

We propose that a wide shear zone, the Highiş-Biharia shear zone (HBSZ), overprinted a composite igneous crust of diorite to basalt and aplite intruded by granite to rhyolite, and gave rise to the Păiuşeni, Arieşeni, Poiana and Biharia lithotectonic assemblages. Although sedimentary cover strata may have been incorporated into the Păiuşeni, Poiana, or Arieşeni assemblages, the presently exposed structural levels of the HBSZ consist essentially of highly strained igneous rocks. The carbonate lenses developed by metamorphic differentiation and grew by metasomatism. Temperature ranges from c. 470°C to less than 300°C recorded within the same lens indicate gradual cooling and continued growth during shearing and progressive exhumation of the shear zone.

At its margins, the greenschist-grade belt contains relics from the adjacent medium-grade metamorphic rocks.

5.3.2 *Medium-grade rocks*

To the north, in the Gilău Mountains, a lithologic association of amphibolite, mafic igneous rocks similar to those in the HBSZ axial zone, and a distinctive muscovite-bearing granite-granodiorite can be separated as the *Codru assemblage*. Although discontinuous and with elusive boundaries, this assemblage rims the southern and eastern margins of the Bihor autochthon. Fibrolite within sheared granodiorite in the Huzii Valley indicates a metamorphic peak at sillimanite grade. Farther north, retrograde garnet- and (or) biotite-bearing rocks occur in the greenschist-grade matrix of the *Arada assemblage*, and an association of plagiogneiss, micaschist, and amphibolite in the central and northern Gilău Mountains, the *Someş assemblage*, records peak metamorphism at sillimanite grade and is intruded by the post-kinematic two-mica and garnet-bearing Muntele Mare granite. The batholith is bounded by a discontinuous aureole of sheared sillimanite- and/or magnetite-biotite hornfels that grades outward into a diffuse zone of chlorite retrogression.

To the south, the apparently low-grade sequence also contains relics of medium-grade rocks. Along the Arieş Valley, a marker of graphitic mylonite can be followed nearly continuously for several tens of kilometres. A chloritized garnet-bearing schist forms a belt a few hundred metres thick north of the graphitic marker. On either side of the marker, sheared, stretched, and dismembered granite bodies show that granitic intrusions were not confined to Highiş-Biharia crust before shearing but also invaded medium-grade crust to the south. The metamorphic rocks here are dominated by large lenses of marble and crystalline dolomite and can be separated as the *Sohodol-Belioara assemblage*. This is in gradational contact to the south and east with aluminosilicate-bearing rocks hosting abundant carbonate lenses, the *Baia de Arieş assemblage*, which is intruded by the two-mica and garnet-bearing Vinţa granite. Local names previously used for this lithologic association are, to the west in the Drocea Mountains, the "Mădrigeşti series" (Papiu, 1960), and to the east in the Trascău Mountains, the "Vidolm series" (Kräutner, 1980). In the Trascău Mountains, the Baia de Arieş carbonate lense-gneissic assemblage is overlain by Tithonian-Oxfordian carbonate cover strata and is retrograded and brecciated along a north-striking sinistral shear zone (the Trascău shear zone, TSZ) associated with Paleogene granodiorite, andesite, and explosion breccia. At the confluence of the Arieş and Iara rivers, amphibolite lenses commonly show symplectitic rims (mainly epidote-quartz) around garnet that may record earlier eclogitic facies conditions for at least parts of the Baia de Arieş assemblage.

Stable Isotope Data On Medium-Grade Rocks

Several samples from the large, variably dolomite marble lenses of the Baia de Arieş assemblage have been analysed for carbon and oxygen isotope ratios. Analytical data are grouped in a narrow range +1.5 to +2.7 for carbon and 19.5 to 23.7 for oxygen (Table 5-2) and plot in the field defined for metamorphosed limestone under medim- and high-grade metamorphic conditions (Fig. 5-9). Sample 11 120 represents a carbonate lens from the southern terrane affected by the shear zone. It is depleted 4 $^{0}/_{00}$ in ^{13}C but only 1-2 $^{0}/_{00}$ in ^{18}O in respect with the marbles from the unretrogressed domain of the southern gneissic terrane.

Geothermobarometry

Metamorphic conditions for the medium-grade assemblages have been previously estimated based on petrographical observations and existing petrogenetic grids. The originally proposed prograde metamorphic zonation (e.g., Dimitrescu et al., 1974), was shown to be apparent, and to have resulted by retrogression (Balintoni, 1985). The distribution of index minerals in the eastern part of the Someş assemblage was interpreted to be the result of two medium-grade metamorphic events overprinted by a chlorite-zone aureole around the Muntele Mare granite-granodiorite batholith (Hârtopanu and Hârtopanu, 1986). Similarly, the Baia de Arieş assemblage is interpreted to record two medium-grade metamorphic events and local retrogression to the chorite zone (Balintoni and Iancu, 1986). Alumosilicate minerals have been reported from all medium-grade assemblages but their distribution is random.

P-T estimates for the Someş and Baia de Arieş assemblages are based on the garnet-biotite thermometer and GASP barometer (first formulated by Thompson, 1976 and Ghent, 1976, respectively) for gneiss samples and calcite-dolomite thermometer (Anovitz and Essene, 1987) for a marble sample from the Baia de Arieş assemblage (Fig. 5-10). Chemical analysis of minerals have been determined with a JEOL JXA-8900R electron microprobe at the University

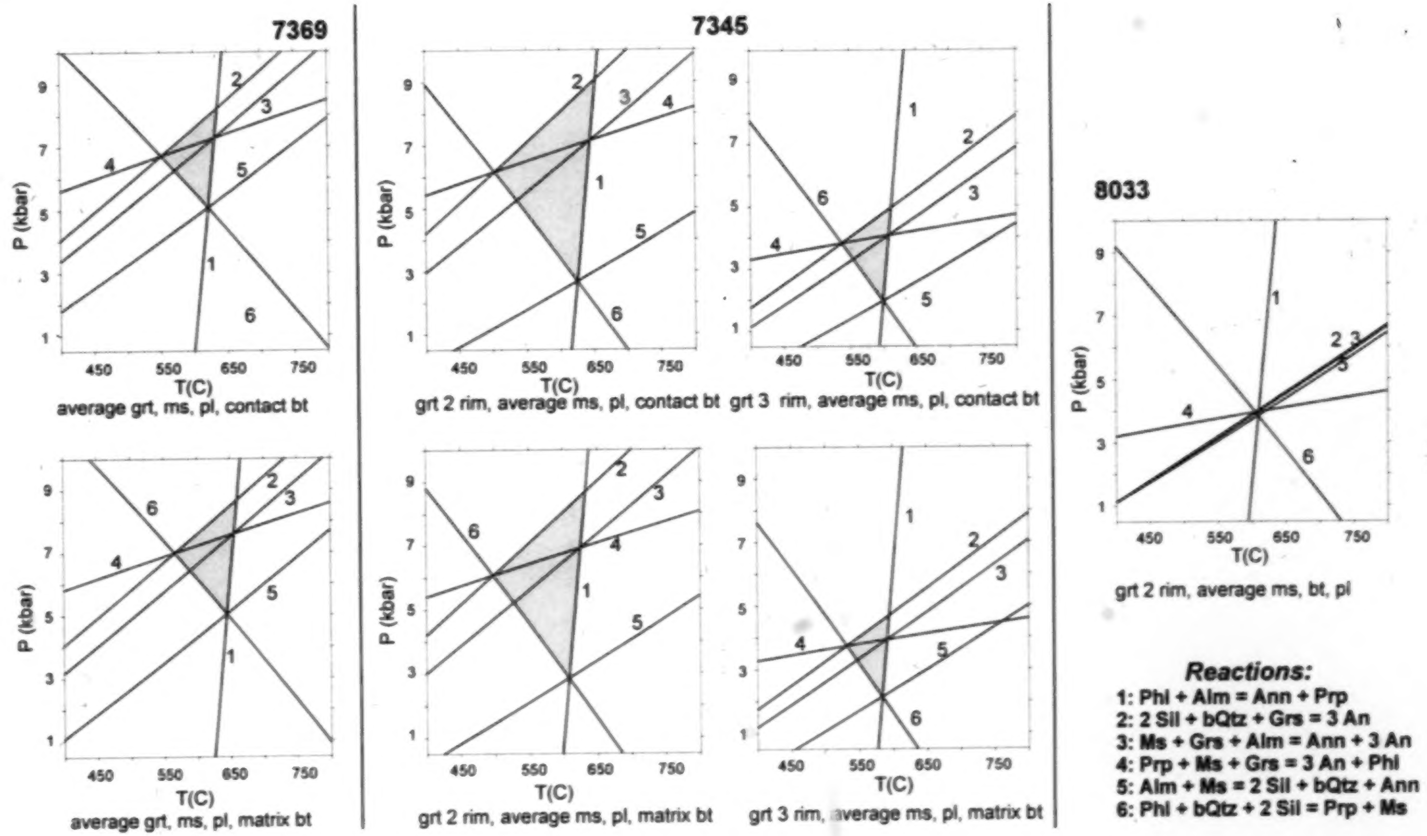

average grt, ms, pl, contact bt

grt 2 rim, average ms, pl, contact bt

grt 3 rim, average ms, pl, contact bt

average grt, ms, pl, matrix bt

grt 2 rim, average ms, pl, matrix bt

grt 3 rim, average ms, pl, matrix bt

grt 2 rim, average ms, bt, pl

Reactions:

1: Phl + Alm = Ann + Prp
2: 2 Sil + bQtz + Grs = 3 An
3: Ms + Grs + Alm = Ann + 3 An
4: Prp + Ms + Grs = 3 An + Phl
5: Alm + Ms = 2 Sil + bQtz + Ann
6: Phl + bQtz + 2 Sil = Prp + Ms

Fig. 5-11. Pressure-temperature estimates for the eastern part of the Baia de Aries assemblage, Iara Valley.

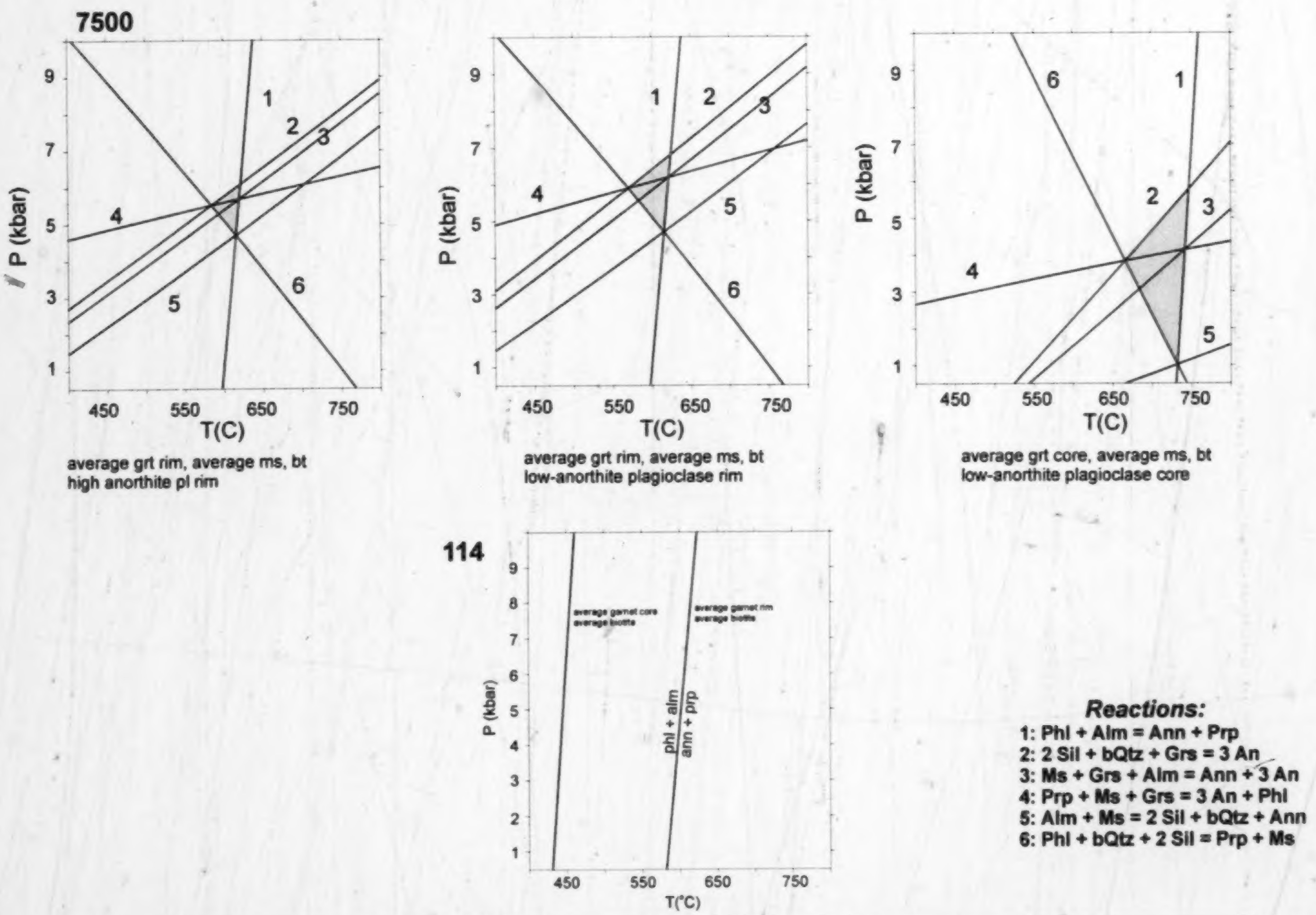

Fig. 5-12. Pressure-temperature estimates for the central part of the Baia de Aries assemblage, Aries Valley.

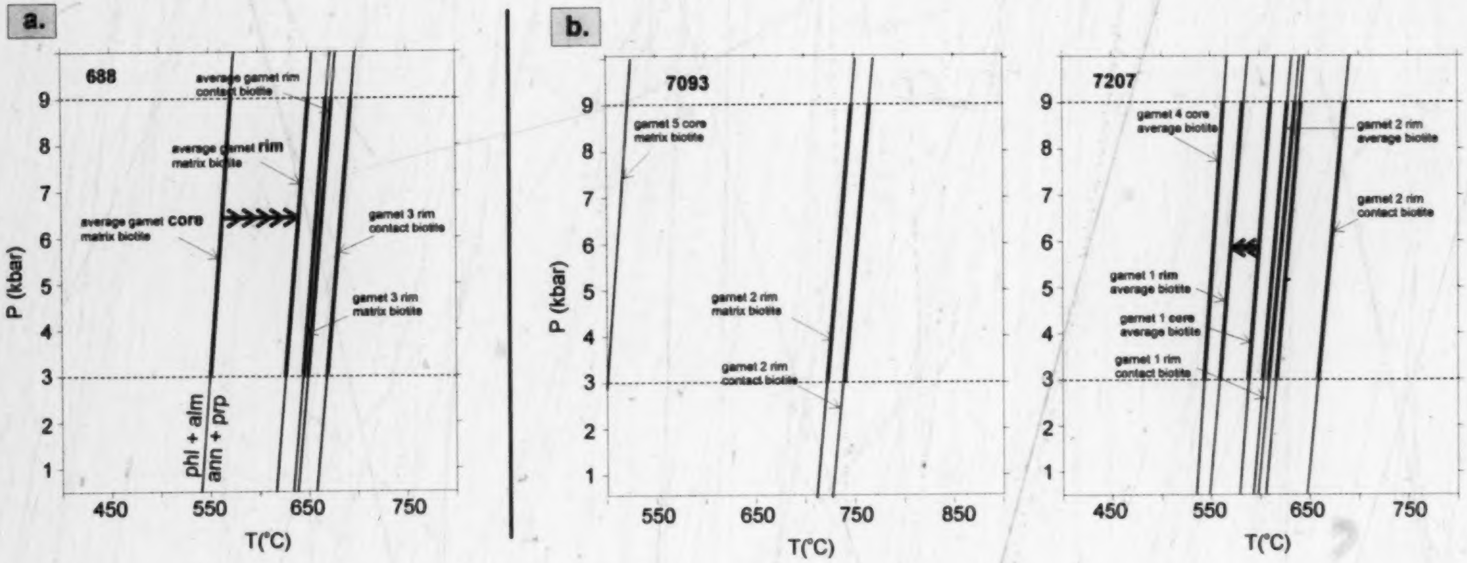

Reaction: **Phl + Alm = Ann + Prp**

Fig. 5-13. Temperature estimates for the easternmost exposures of the Somes (a) and Baia de Aries (b) assemblages using the garnet-biotite exchange thermometer.

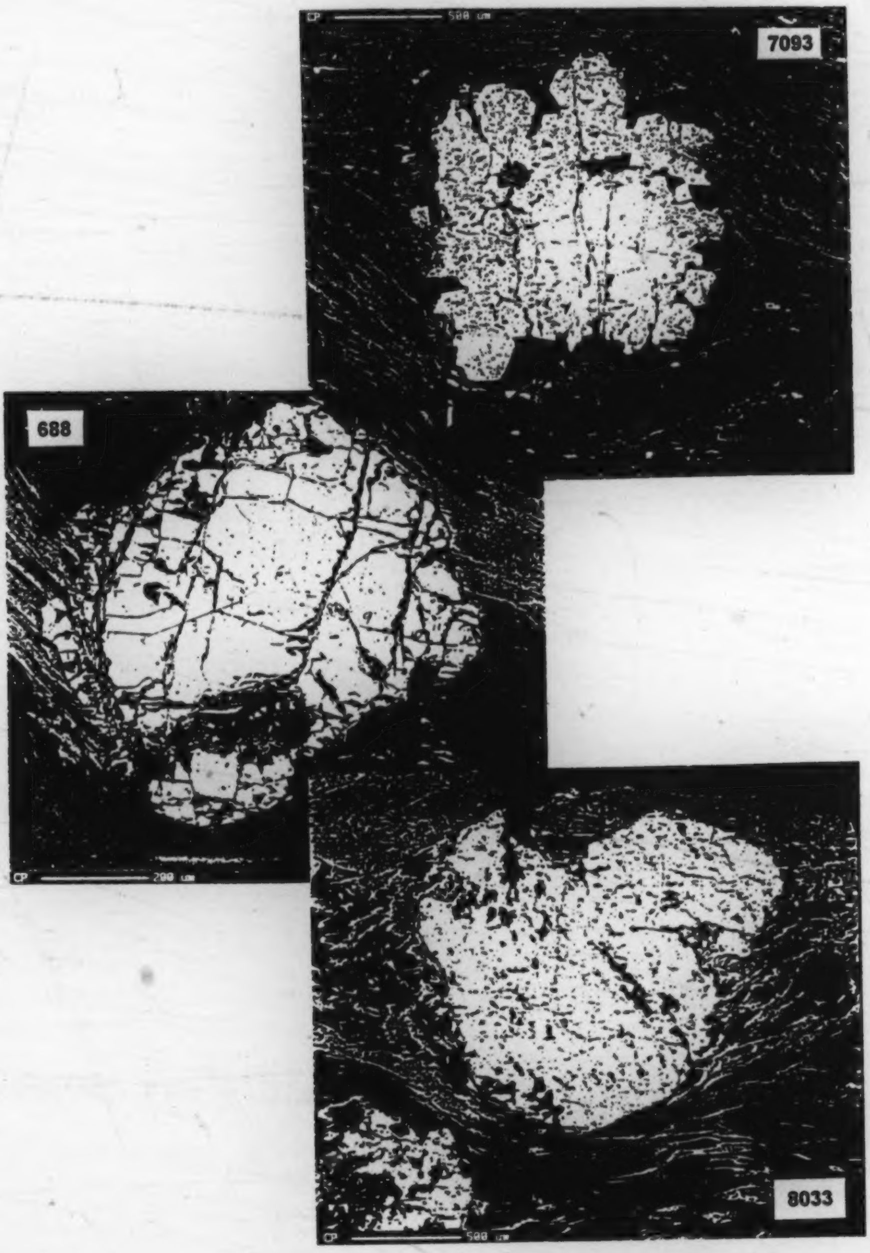
CP
500 um
7093
688
CP
200 um
8033
CP
500 um

Fig. 5-14. Microphotographs of probed garnet grains

of Alberta; uncertainties in the microprobe analysis likely contributed less than 10 % to the total PT uncertainty (Kohn and Spear, 1991). P-T calculations for the gneiss samples have been performed using the internally consistent thermodynamic data base incorporated in the computer software TWQ 2.02 (Berman, 1996). The relevant reactions and the estimated PT conditions are presented in Figs. 5-11; 5-12 and 5-13. Tentative interpretations follow, although more data are needed (e.g., on chemical equilibrium between matrix biotite and garnet core).

In the eastern part of the Baia de Arieş assemblage ("Vidolm island") a staurolite- and andalusite (?)-bearing plagiogneiss (sample 8033, Fig. 5-11) yielded a very good intersection at 3.8 kb and 610°C which roughly corresponds to the center of the triangle error defined in a nearby gneiss (garnet 3 - sample 7345, Fig. 5-11) by a population of small garnets. Data on a distinct population of larger broken garnets (garnet 2 - sample 7345) suggest higher pressures, but the PT values are poorly constrained. PT estimates of 6-7 kb on an adjacent mylonitic gneiss with very fine grained biotite garnet and kyanite (7369, Fig. 5-11) and symplectitic coronas on garnet in nearby amphibolite lenses suggest a complex PTt path for the Baia de Arieş assemblage that included isothermal decompression from deep- to mid-crustal conditions. Temperature estimates using garnet rim and contact biotite range between 550 and 750°C, but the preservation of zoning in garnets (Fig. 5-14) constrain temperatures to less than c. 600-650°C. A sample from a large marble layer hosted by the analyzed gneiss retained a peak temperature of 573°C (Fig. 5-10). The eastern part of the Baia de Arieş assemblage ("Vidolm island") was uplifted above the 500°C isotherm during the Middle/Late Jurassic (Dallmeyer et al., 1998).

In the central part of the Baia de Arieş assemblage, PT estimates using garnet core and rim data (sample 7500, Fig. 5-12) suggest an evolution from approximately 3 kb/675°C to 5kb/575°C on a counterclockwise PTt loop. The Baia de Arieş assemblage was intruded by the spessartin-bearing Vinţa granitoid during the Permian (c. 261 Ma, Pană et al., 1998) and was uplifted above the c. 400°C isotherm during the Early Cretaceous (Dallmeyer et al., 1998).

Temperatures recorded by the two-mica garnet-bearing gneiss exposed in the eastern part of the Someş assemblage (samples 688) range from c. 550 to c. 650°C. This region was uplifted above the c. 400°C isotherm during the Early Cretaceous (Dallmeyer et al., 1998).

The lithologic units defined here have no stratigraphic connotation. We interpret the medium-grade assemblages and the igneous rocks to represent pre-Alpine crust, and the low-grade metamorphic rocks to represent wide Alpine retrogressive shear zones overprinting this crust.

5.4. PROTOLITH AGES AND TIMING OF TECTONISM

Fossil microflora have been reported from both low- and medium- to high-grade metamorphic rocks (see Tab. 5-1); their relation to the host rock is unclear and their significance is therefore uncertain (e.g., infiltration after metamorphism cannot be ruled out). Early K-Ar data for both medium- and low-grade rocks indicate a range of Variscan to Alpine ages (Soroiu et al., 1969; Pavelescu et al., 1975), but these may have no geologic significance because the dates are randomly distributed throughout the lithologic assemblages and recently obtained $^{40}Ar/^{39}Ar$ spectra indicate strong disturbance (Dallmeyer et al., 1996). Tectonothermal evolution is directly constrained by $^{40}Ar/^{39}Ar$ results (Dallmeyer et al., 1996) and by U-Pb zircon data from granites in several of the lithologic assemblages outlined above (Fig. 5-15).

The non- or only slightly retrograded medium-grade Someş assemblage records late Variscan ages (c. 315 to c. 300 Ma). A zircon U-Pb crystallization age of c. 295 Ma was obtained for the Muntele Mare granite that intrudes the Someş assemblage (Pană et al., 1998). An $^{40}Ar/^{39}Ar$ plateau age of c. 191 Ma for muscovite from the same granite suggests Early Jurassic uplift and erosion. In the retrograded Arada assemblage, $^{40}Ar/^{39}Ar$ spectra indicate Alpine disturbance of the Variscan ages, or Austrian plateau ages. In the Codru assemblage, an U-Pb zircon age of c. 372 Ma was obtained from a granodiorite and the amphibolites record Early Variscan ages (405 to 335 Ma). In the Highiş-Biharia shear zone, U-Pb ages of the igneous protolith vary from c. 267 Ma in the Highiş Mountains to c. 500 Ma in the Biharia Mountains (Pană et al., 1998). The re-equilibrated greenschist rocks of the HBSZ record Austrian tectonism (plateau ages of c. 114 to 110 Ma), and the relic-bearing rock types have yielded disturbed spectra with various Paleozoic and Mesozoic ages.

The southern medium-grade Baia de Arieş assemblage yielded a Jurassic plateau age (156 Ma) near Surduc, and Austrian ages (c. 119 to 111 Ma) closer to the HBSZ. The retrograded Sohodol assemblage yielded three plateau ages: c. 186 Ma, 169 Ma and 124 Ma and a disturbed Variscan spectrum. However, because the c. 260 Ma Vinţa granitoid and the c. 390 Ma Mădrigeşti granite intrude the Baia de Arieş assemblage we infer that the medium-grade fabric in the Baia de Arieş assemblage is pre-Variscan and that the Middle Cretaceous dates record uplift and cooling. The retrogressive Trascău shear zone is the locus of Paleogene intrusions ("Banatite"), suggesting Early Tertiary tectonism and surficial-water enhanced melting.

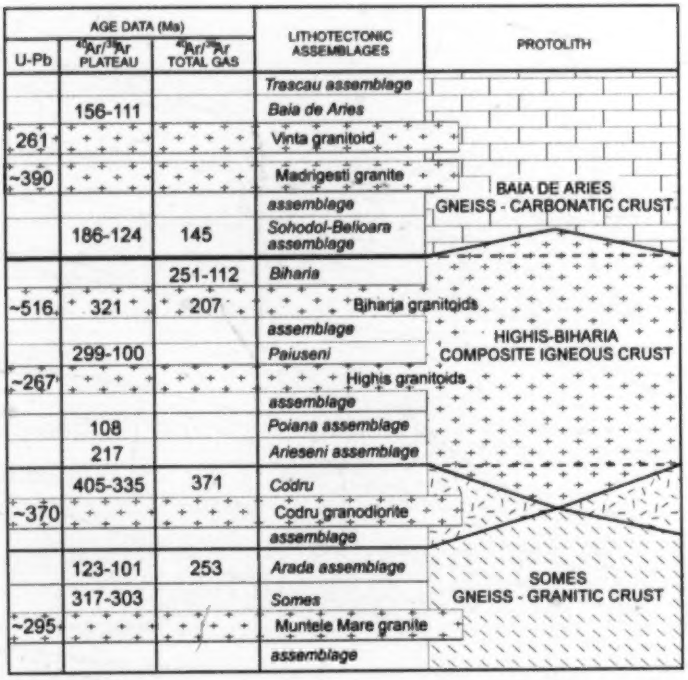
AGE DATA (Ma)
U-Pb
^{40}Ar/^{39}Ar PLATEAU
^{40}Ar/^{39}Ar TOTAL GAS
LITHOTECTONIC ASSEMBLAGES
PROTOLITH
Trascau assemblage
156-111
Baia de Aries
261
Vinta granitoid
~390
Madrigesti granite
assemblage
186-124
145
Sohodol-Belioara assemblage
BAIA DE ARIES
GNEISS - CARBONATIC CRUST
251-112
Biharia
~516
321
207
Biharia granitoids
assemblage
299-100
Paiuseni
HIGHIS-BIHARIA
COMPOSITE IGNEOUS CRUST
~267
Highis granitoids
assemblage
108
Poiana assemblage
217
Arieseni assemblage
405-335
371
Codru
~370
Codru granodiorite
assemblage
123-101
253
Arada assemblage
317-303
Somes
~295
Muntele Mare granite
assemblage
SOMES
GNEISS - GRANITIC CRUST

Figure 5-15. Proposed informal classification of the metamorphic-magmatic basement rocks in the Apuseni Mountains. U-Pb zircon dates indicate the approximate emplacement age of the granitoid plutons; ^{40}Ar/^{39}Ar data from Dallmeyer et al., 1998.

5.5. REGIONAL ORIENTATION DATA AND EVIDENCE OF STRAIN PARTITIONING ALONG THE BELT OF LOW-GRADE ROCKS

A complex pattern of strain distribution is recorded by both planar (Fig. 5-16) and linear (Fig. 5-17) structural elements in the greenschist belts.

Outcrop-Scale Structures. As seen in road cut exposures at least several hundred square metres in area, rock bodies of contrasting lithology are tabular or linear. Centimetric to decametric mullions and mineral stretching lineations are strike-parallel along the Iara and Arieş rivers and gradually change to oblique or dip-parallel in the Biharia and Highiş mountains. Isoclinal minor folds are mostly subparallel to mullions. Around the Bihor autochthon, low-grade rocks display a later set of normal-slip striations.

Microscopic Fabrics. Most rock types along the greenschist belt show non-equilibrium textures with strained aggregates and clasts of quartz, feldspar, amphibole, and pyroxene set in a matrix of sub-granulated quartz, sericite and/or chlorite. On the basis of detailed sampling of massive pods, from the core outward to the highly sheared matrix, all protoliths of the HBSZ are of igneous origin. Shear-sense indicators including S-C fabric, shear bands, rotated remnants of fractured minerals, and strain shadows show a dominant component of non coaxial strain (Fig. 5-18).

Equilibrium textures are characterized by compositional layering and a simple mineralogy of albite + quartz + sericite + chlorite +/- carbonate +/- magnetite +/- epidote. Differences exist only in the relative proportion of particular minerals, grain size, and internal structure. Calcite, quartz, phyllosilicate, quartz-feldspar, and quartz-feldspar-phyllosilicate lithons can be recognized in a continuum of microstructures stretched in the foliation plane. Microstructures indicate a change in flow pattern from dominantly continuous, steady-state deformation at high temperature to more localized discontinuous deformation at lower temperature. This flow partitioning allowed the preservation of earlier-formed microstructures at a range of stages of development. Higher-temperature microstructures are common at the periphery of the HBSZ in fine-grained amphibolite derived from diorite along the northern boundary of the Codru assemblage and in fine-grained biotite-bearing mylonitic orthogneiss along the southern boundary of the Sohodol and Belioara assemblages. Within the same low- or very low grade of metamorphism, a range of stages of transformation can be seen for each protolith. We consider that metamorphic textures within the Păiuşeni, Arieşeni, and Biharia assemblages of the HBSZ were derived from igneous textures by shearing and hydration.

Tectonic fabric elements vary in orientation along the HBSZ but show identical orientation across lithotectonic assemblages within a segment. There is no structural discordance between successions previously assigned to different nappes. Stretching lineations and mullions are parallel, and mesoscopic fold axes are slightly discordant to subparallel with

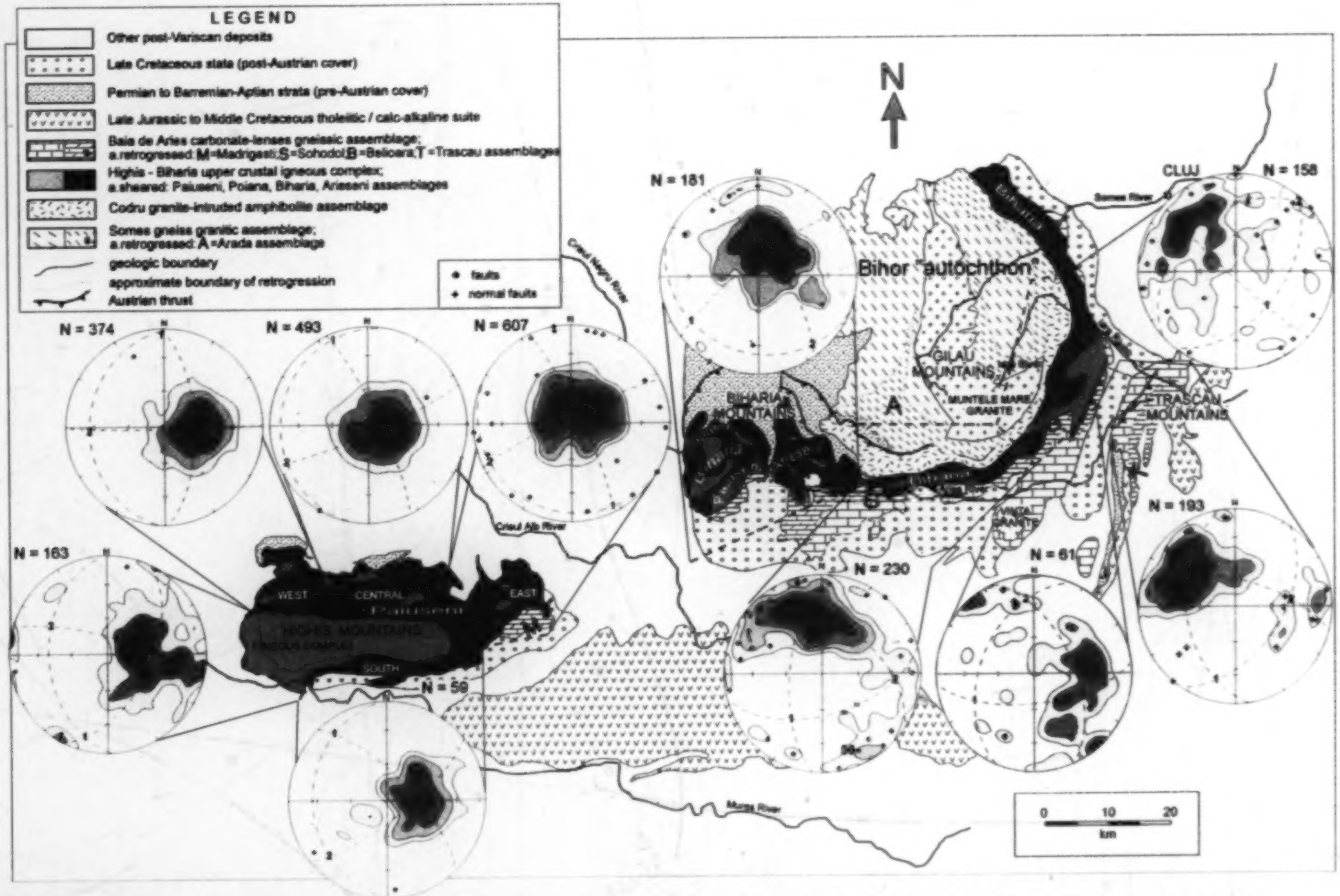
LEGEND
Other post-Variscan deposits
Late Cretaceous stata (post-Austrian cover)
Permian to Barremian-Aptian strata (pre-Austrian cover)
Late Jurassic to Middle Cretaceous tholeiitic / calc-alkaline suite
Baia de Aries carbonate-lenses gneissic assemblage; a.retrogressed: M=Madrigesti; S=Sohodol; B=Belioara; T=Trascau assemblages
Highis - Biharia upper crustal igneous complex; a.sheared: Paiuseni, Poiana, Biharia, Arieseni assemblages
Codru granite-intruded amphibolite assemblage
Somes gneiss granitic assemblage; a.retrogressed: Å=Arada assemblage
geologic boundary
approximate boundary of retrogression
Austrian thrust
faults
normal faults
N
N = 374
N = 493
N = 607
N = 163
N = 59
N = 181
N = 230
N = 61
N = 193
N = 158
CLUJ
Somes River
Crisul Negru River
Crisul Alb River
Mures River
Bihor "autochthon"
A
GILAU MOUNTAINS
MUNTELE MARE GRANITE
BIHARIA MOUNTAINS
TRASCAU MOUNTAINS
VINTA GRANITE
WEST
CENTRAL
EAST
SOUTH
Paiuseni
HIGHIS MOUNTAINS
IGNEOUS COMPLEX
0
10
20
km

Fig. 5-16. Planar structures along the belt of low-grade rocks in the Apuseni Mountains: lines from each stereogram define the domain boundaries of data displayed; contour lines are for poles to metamorphic foliation; numbers and brocken lines in each stereogram are calculated eigenvectors and the corresponding principal planes.

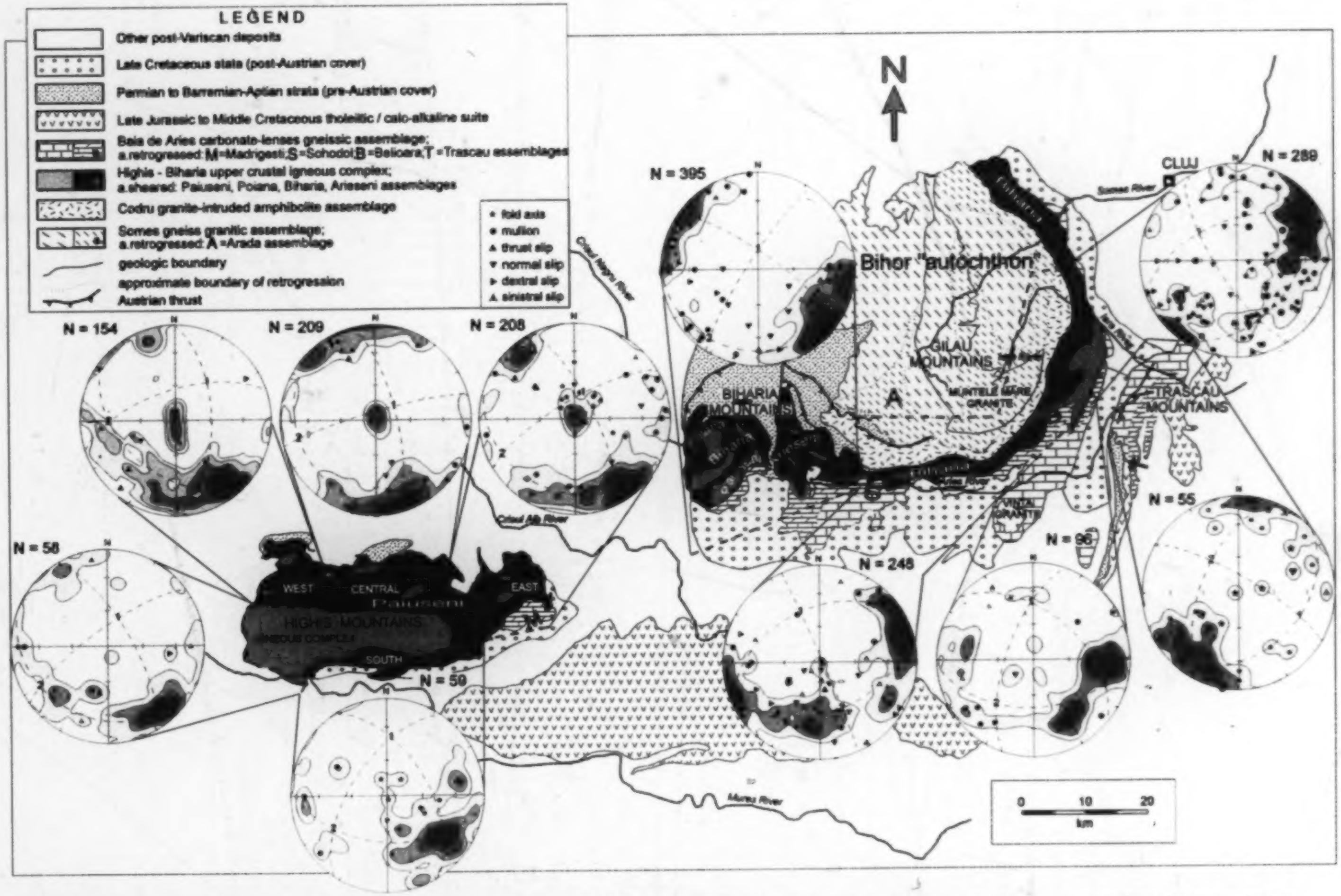
LEGEND
Other post-Variscan deposits
Late Cretaceous stata (post-Austrian cover)
Permian to Barremian-Aptian strata (pre-Austrian cover)
Late Jurassic to Middle Cretaceous tholeiitic / calc-alkaline suite
Baia de Aries carbonate-lenses gneissic assemblage;
a.retrogressed: M=Madrigesti; S=Sohodol; B=Belioara; T=Trascau assemblages
Highis - Biharia upper crustal igneous complex;
a.sheared: Paiuseni, Poiana, Biharia, Arieseni assemblages
Codru granite-intruded amphibolite assemblage
Somes gneiss granitic assemblage;
a.retrogressed: A=Arada assemblage
geologic boundary
approximate boundary of retrogression
Austrian thrust
fold axis
mullion
thrust slip
normal slip
dextral slip
sinistral slip
N
N = 154
N = 209
N = 208
N = 58
N = 59
N = 395
N = 245
N = 96
N = 55
N = 289
CLUJ
Somes River
Crisul Negru River
Crisul Alb River
Mures River
Bihor "autochthon"
GILAU MOUNTAINS
MUNTELE MARE GRANITE
TRASCAU MOUNTAINS
BIHARIA MOUNTAINS
VINTA GRANITE
A
WEST
CENTRAL
EAST
SOUTH
Paiuseni
HIGHIS MOUNTAINS
0
10
20
km

Fig. 5-17. Linear structures along the belt of low-grade rocks in the Apuseni Mountains: lines from each stereogram define the boundaries of data displayed; contour lines are for all linear structures; stretching lineations of uncertain sense of displacement are not shown; numbers and brocken lines in each stereogram are calculated eigenvectors and the corresponding principal planes.

the stretching structures, suggesting incomplete realignment of early structures along tectonic flow lines during later strain. Distinct tectonic regimes are apparent from a gradational change of strain axes between domains of uniform orientation and a change of tectonic regime in time is obvious in some domains.

In the northern Highiş Mountains, the structurally lowest Păiuşeni assemblage is thrust over Permian and Triassic strata of the Codru assemblage and displays subhorizontal shear planes and mainly SE plunging ductile (mullions, stretching lineation) and brittle (slickenside striae and striated dip-parallel cleavage) linear fabrics. Shear-sense criteria in thin section indicate mainly normal dip-slip, suggesting a "deck-of-cards" style of deformation within the thrust sheet, and/or post-thrust isostatic reequilibration accommodated by normal slip on the original thrust-related foliation (Fig. 5-18). At several locations, strong E-W along-strike stretching lineation is developed.

Timing remains ambiguous. The independent maxima in the centre of the stereograms indicate late vertical displacement on young E-W faults, which likely caused the observed northward tilting of some foliation and lineation. The structurally overlying igneous complex to the south shows similar albeit more scattered orientations with a greater proportion of subvertical N-S fault planes, suggesting a similar deformation history. No structural evidence of an older event is apparent, which is at variance with the proposal of an early metamorphic record by Balintoni (1986). The southern, upper part of the Păiuşeni assemblage shows foliation and stretching orientations similar to the northern one and a secondary, poorly preserved E-W stretching fabric. The NW-SE trending faults in the eastern Highiş Mountains are likely related to the development of the adjacent Neogene Brad-Gurahonţ Basin (Fig. 5-20).

In the Biharia Mountains, the average orientations of foliation and stretching lineation within the Păiuşeni, Biharia, Poiana, and Arieşeni assemblages indicate oblique to dip-slip displacement. Shear-sense indicators in outcrop and thin section are compatible with thrusting to the NW and subsequent inversion (Fig. 5-19). Striated dip-parallel vertical fractures are commonly invaded by Tertiary rhyolite dykes, suggesting that thrust-related anisotropy was a control during subsequent extension.

Farther east, along the Arieş Valley, most foliations are steeply south-dipping and most lineations gradually change to an ENE trend; a second-order, dispersed maximum defined by normal dip-slip slickenside striations on south-dipping foliation planes mainly in the retrograde Arada and Codru assemblages suggests normal-sense detachment (Fig. 5-18) related to the uplift and erosion of the Muntele Mare granite in the core of the Bihor autochthon. To the north, in the Iara Valley, foliation gradually changes to southeast-dipping and stretching lineations form a girdle as the belt wraps around the eastern boundary of the Bihor autochthon. Within the adjacent Someş assemblage, similarly-oriented mullions in plagiogneiss and stretching

---

Fig. 5-18. Microscopic shear-sense indicators:

a) Pressure-solution enhanced σ structure showing sinistral sense of shear within highly sheared, serpentinized gabbro/diorite of the Păiuşeni assemblage, Highiş Creek, Highiş Mountains; foliation 200/45; stretching lineation 130/27. Data indicate oblique thrust to NW (crossed polars, scale bar = 0.6 mm).

b) Domino structures show dextral slip on shear planes affecting previous foliation within sheared granite of the Păiuşeni assemblage, on a right tributary of Arăneag creek, Highiş Mountain; foliation 240/35; stretching lineation 190/20. Data indicate post-thrust extension to the south (crossed polars, scale bar = 0.6 mm).

c) Tail of rotated quartz-clast in "metaconglomerate" indicates dextral shear, foliation 160/25, stretching lineation 125/15; Păiuşeni assemblage, Băneşti Creek, southern Biharia Mountains. Data indicate normal-slip detachment to the southeast (crossed polars, scale bar = 0.6 mm)

d) S_i structure in albite shows dextral sense of slip in sheared granodiorite of the Codru assemblage, Neagu Creek, southern Gilău Mountains; foliation 180/45, stretching lineation 190/30. Data indicate extension under greenschist facies conditions within the Codru assemblage (crossed polars, scale bar = 0.24 mm).

e) δ structure of garnet shows dextral slip in slightly retrogressed gneiss of Someş assemblage; Iertii Creek, upstream of the Muntele Băişorii village; foliation 160/35; lineation 50/20; Data indicate northeastward extension along the eastern margin of the Bihor autochthon (parallel polars, scale bar = 0.6 mm).

f) Sinistral sense of shear from asymetric "δ" feldspar porphyroclast within sheared granite of the retrogressed Someş assemblage, Bistra Creek, southern Gilău Mountains; foliation 182/67; stretching lineation 170/65; Data indicate local thrusting to the north along the southern margin of the Bihor "authochthon"; (crossed polars, scale bar = 2.4 mm).

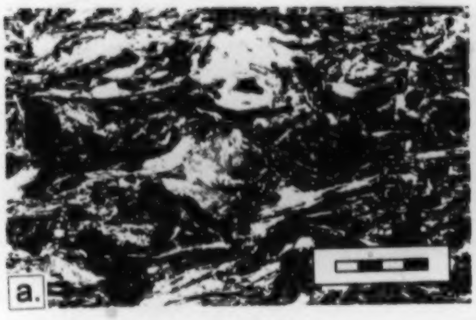
a.

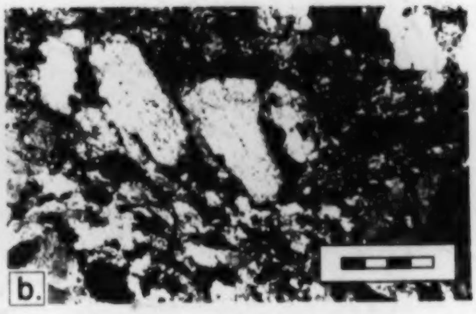
b.

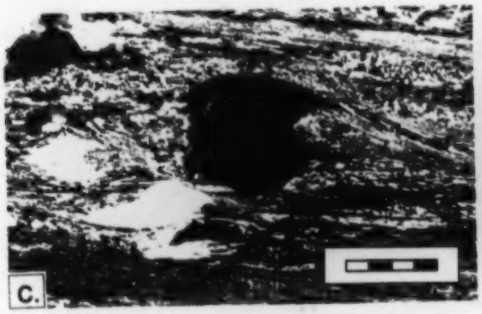
c.

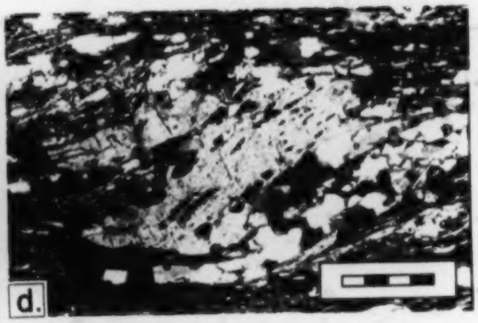
d.

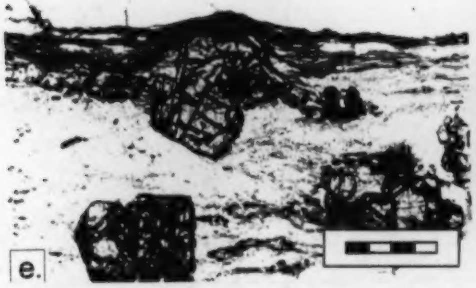
e.

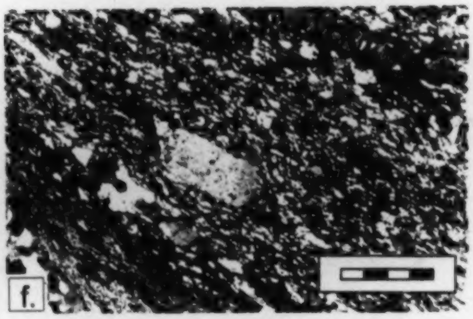
f.

Fig. 5-19. Outcrop scale kinematic indicators:

a) Prismatic "cleavage mullions" (~25/7) at the intersection of closely spaced, subhorizontal thrust related shear planes (S_1=80/18, L_1=160/5) with subsequent widely spaced, steeper normal-slip shear planes (S_2=110/55, L_2=140/50); Păiuşeni assemblage, Gubului Creek, central Highiş Mountains.

b) Sheared microgranite, stretching lineation in all shear planes is subhorizontal, oriented perpendicular to the outcrop: L = 140/5; Păiuşeni assemblage, Cornului Creek, eastern Highiş Mountains.

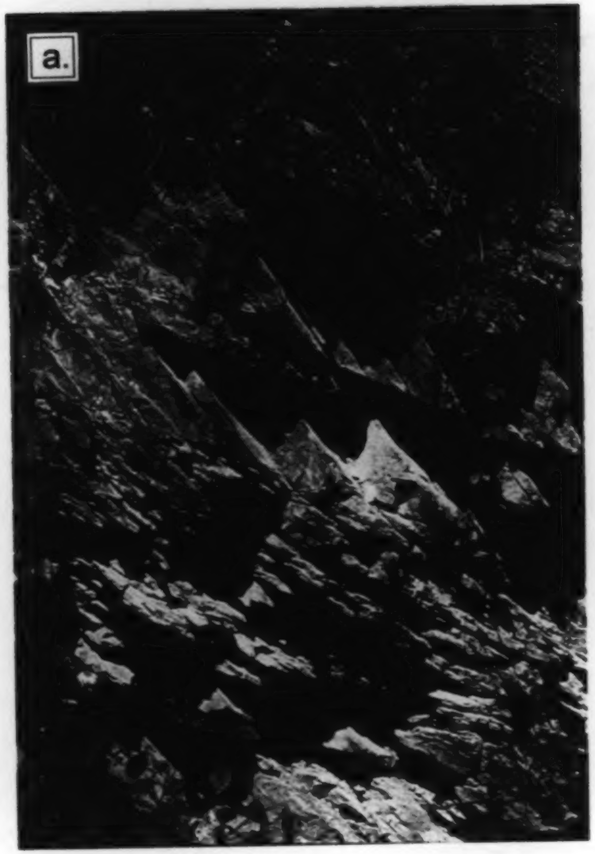
a.

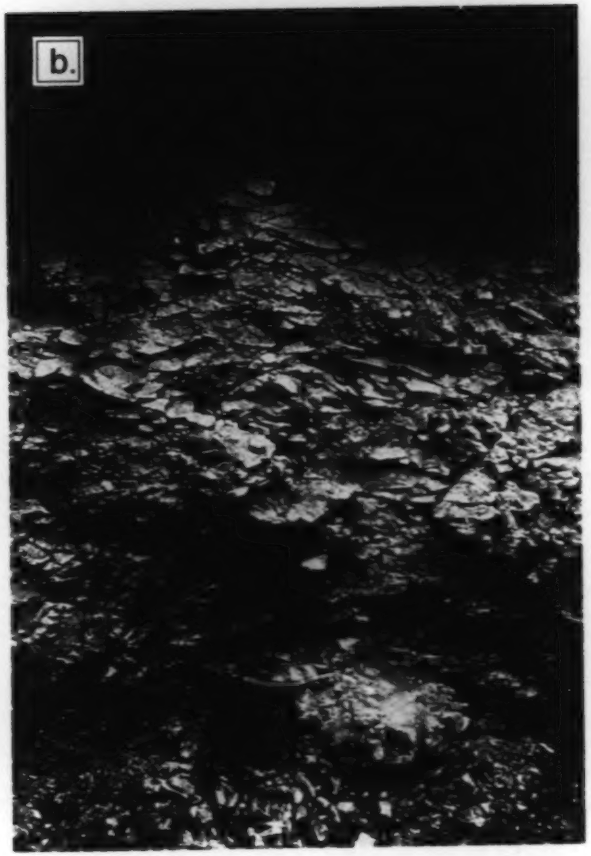
b.

Fig. 5-19 (continued). Outcrop scale kinematic indicators:

a) Mylonitic layering developed within granite of the Biharia assemblage, road cut along the Arieşul Mare River, 1km upstream from its confluence with the Arieşul Mic River, Biharia Mountains;

b) Detail of the same outcrop: duplex-type structure in sheared granite; foliation 160/10, stretching lineation 130/7. Data indicate initial top to the NW thrusting within the Biharia assemblage;

c) Detail of the same outcrop: granitic pods within the mylonitic layering.

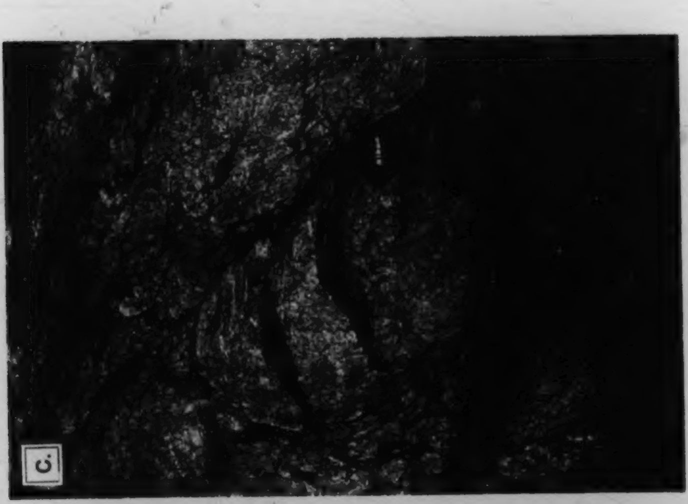
c.

a.

b.

lineations in the gneissose tail of the Muntele Mare granite suggest formation by clockwise rotation of the Bihor autochthon followed by extension (Fig. 5-18). Although thrust-sense shear indicators occur locally along the southern (Fig. 5-18) and eastern boundaries of the Bihor autochthon, a thrust fault cannot be mapped unequivocally.

5.6. TECTONIC EVOLUTION OF THE NORTHERN APUSENI SEDIMENTARY BASIN

Permian and Mesozoic cover strata record the isostatic and tectonic evolution of the Variscan Someş and Codru medium-grade assemblages in the western part of the Apuseni Mountains. A red-bed sequence with interbedded basalt flows and ignimbrite is assumed to be Permian in age. Ladinian to Early Norian sedimentation took place on subsiding carbonate platforms, with basinal accumulation. This was followed by mainly clastic continental sedimentation in the Hettangian, shallow and slightly subsident shelf conditions in the Sinemurian, phosphate and glauconite deposition in the Pliensbachian to Aalenian, and intense biochemical activity probably controlled by upwelling currents in the Pliensbachian to Oxfordian. Beginning in the Tithonian, sedimentation records existing topographic contrast: a carbonate platform developed in the north and a rapidly subsiding trough in the south, with flysch of Tithonian-Berriasian age (Patrulius, 1976). The distribution of rock units suggests a long-lived strain zone between the Gilău-Bihor and Codru mountains which evolved as an arm of the Tithonian-Neocomian Mureş Basin (Fig. 5-20). Subsequent compression resulted in high strain in clastic sequences and northwestward thrusting, consistent with kinematic indicators in the tectonically overlying metamorphic assemblages of the Biharia Mountains. Timing of thrusting is uncertain. In one locality east of Beiuş, a local thrust is stratigraphically constrained as intra-Turonian in age. However, there is no evidence for the existence of large, coherent, and far-travelled thrust sheets. Nappe correlation across the Neogene Beiuş Basin into the Codru Mountains is contradicted by facies correlations of the Mesozoic sequences (Bleahu et al., 1981). The medium-grade basement exposed in the Codru Mountains is similar to the Someş assemblage of the Bihor autochthon (Fig. 5-20). The similarity of Permian to Jurassic extensional structures and of mafic rocks in adjacent carbonate-dominated successions currently assigned to separate nappes suggest to us only modest relative displacement.

5.7. TECTONIC EVOLUTION OF THE SOUTHERN APUSENI SEDIMENTARY BASIN

A tectonically active Middle Jurassic to Cretaceous basin overlying the gneiss-carbonate assemblage is presently exposed in the southern Apuseni Mountains and in the South Carpathians. Characterized by a suite of tholeiitic to calc-alkaline rocks extruded within a complex sedimentary environment, its remnants are known as the "Mureş Basin".

Middle Jurassic tholeiitic rocks crop out over a limited area in the westernmost

Figure 5-20. Tectonic sketch of the Apuseni Mountains; large letters refer to mountain segments mentioned in the text: H - Highiş Mountains, D - Drocea Mountains, C - Codru Mountains, B - Biharia Mountains, G - Gilău Mountains,T - Trascău Mountains, P - Plopiş Mountains, M -Mezeş Mountains, R - Poiana Ruscă Mountains; capital letters indicate the age of the platformal deposits: J_3 = Upper Jurassic limestone; small letters indicate the age of flysch and molasse deposits: *th-ne* = Thitonic to Neocomian, *br-ap*= Barremian to Aptian, *ap-al* = Aptian to Albian, *al_2-cm* = Late Albian to Cenomanian, *cm_2-ma* = Late Cenomanian to Maastrichtian, *tu-ma* = Turonian to Maastrichtian, *co-ma* = Coniacian to Maastrichtian, *st-ma* = Santonian to Maastrichtian, *ma* = Maastrichtian. White numbers in black circles refer to the "wildflysch" sequences, interpreted here as shallow structural levels of major shear zones: 1- parts of the Ponor formation (Albian); 2- part of the Râmeţi Formation (Vraconian to Maastrichtian); 3 - "Mateş Formation" (Upper Aptian to Albian); 4 - southern part of the Suharu formation (Upper Aptian to Albian); 5 - the "Ciuruleasa Formation" (Barremian to Aptian); 6 - the "Valea Morgaşului Formation" (Aptian to Albian); 7 - part of the Groşi Formation (Barremian-Aptian to Paleogene (?); 8 - the "Bejani Formation" (Barremian to Aptian).

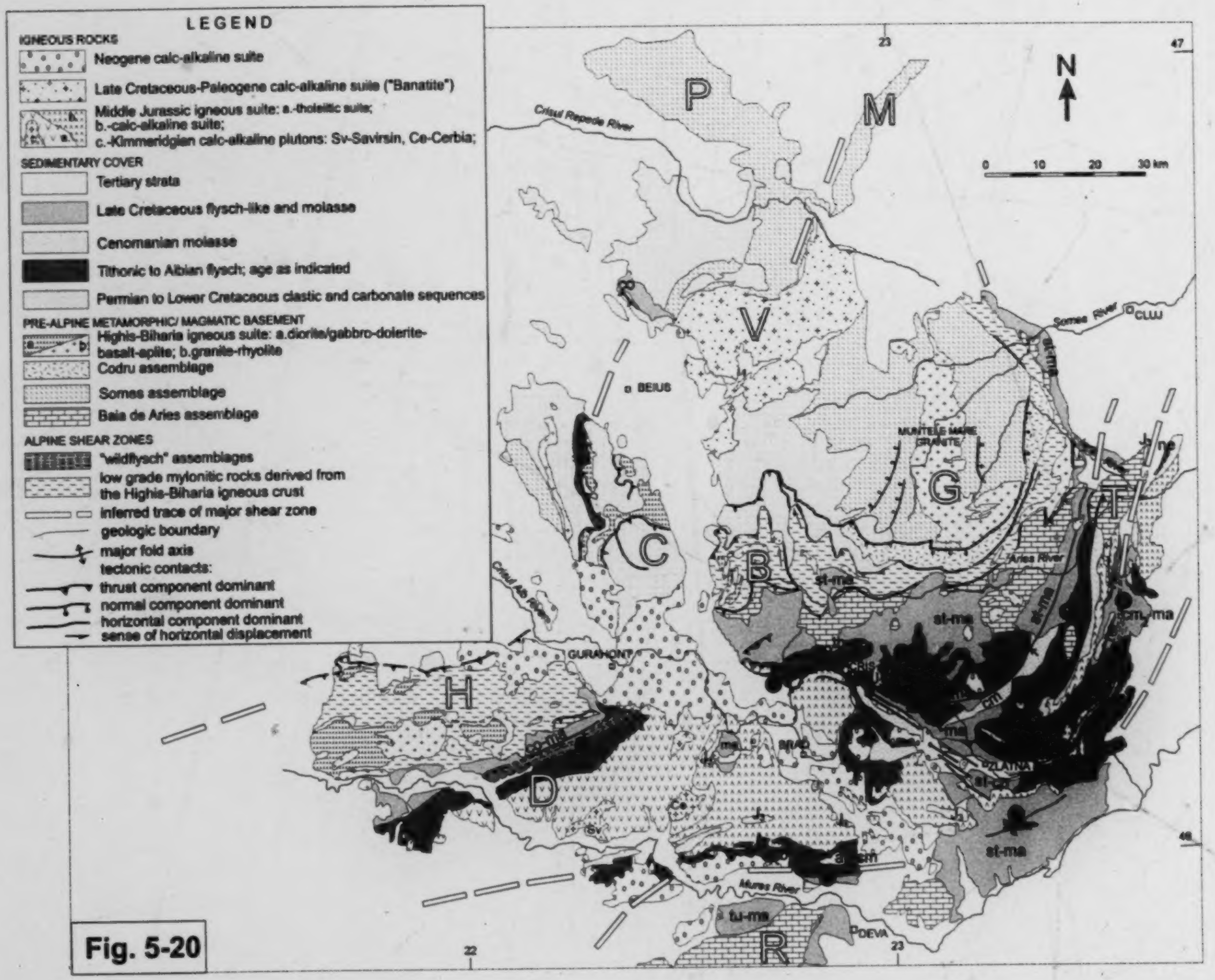
LEGEND
IGNEOUS ROCKS
Neogene calc-alkaline suite
Late Cretaceous-Paleogene calc-alkaline suite ("Banatite")
Middle Jurassic igneous suite: a.-tholeitic suite;
b.-calc-alkaline suite;
c.-Kimmeridgian calc-alkaline plutons: Sv-Savirsin, Ce-Cerbia;
SEDIMENTARY COVER
Tertiary strata
Late Cretaceous flysch-like and molasse
Cenomanian molasse
Tithonic to Albian flysch; age as indicated
Permian to Lower Cretaceous clastic and carbonate sequences
PRE-ALPINE METAMORPHIC/ MAGMATIC BASEMENT
Highis-Biharia igneous suite: a.diorite/gabbro-dolerite-basalt-aplite; b.granite-rhyolite
Codru assemblage
Somes assemblage
Baia de Aries assemblage
ALPINE SHEAR ZONES
"wildflysch" assemblages
low grade mylonitic rocks derived from the Highis-Biharia igneous crust
inferred trace of major shear zone
geologic boundary
major fold axis
tectonic contacts:
thrust component dominant
normal component dominant
horizontal component dominant
sense of horizontal displacement
N
0
10
20
30 km
23
47
46
22
23
P
M
V
C
B
G
T
H
D
R
Crisul Repede River
Crisul Alb River
Somes River
CLUJ
BEIUS
MUNTELE MARE GRANITE
Aries River
st-ma
cm-ma
GURAHONT
BRAD
CRIS
ZLATNA
cm
Mures River
tu-ma
DEVA
Sv
Ce
al-cm

Fig. 5-20

part of the Mureş Basin (Savu, 1980; Nicolae, 1994). They are intruded by granite stocks (e.g., at Săvârşin and Cerbia) and grade eastward into calc-alkaline rocks. An Oxfordian to Berriasian carbonate platform was established both on the southern Apuseni continental crust, the Baia de Arieş assemblage (e.g. in the Trascău Mountains), and on rocks of the Mureş igneous suite (Fig. 5-20). Stretching along the poorly defined northern contact of the Mureş igneous suite and the Apuseni continental fragment was accompanied by the deposition of Tithonian to Albian flysch-like sequences interlayered with mafic detritus and intruded by calc-alkaline dykes and sills. The retrogressive Trascău shear zone projects into the northeastern extremity of the flysch basin. A wide belt of slices and tectonic enclaves of the underlying carbonate and igneous rocks in a highly sheared flysch matrix can be followed along the northern boundary of the Mureş igneous arc. It correlates with the wildflysch formations (horizons) of the Tithonic to Albian flysch (see Fig. 5-20) previously assigned to different nappes. Its continuity along the northern boundary of the Mureş igneous arc (Fig. 5-20) is inconsistent with a nappe interpretation. Moreover, the Maastrichtian cover (Bordea, Constantinescu, 1975; Bordea et al., 1979) of the HBSZ can be traced across some of the "nappes" postulated in the southern Apuseni Mountains (Săndulescu, 1984). The southern side of the Mureş magmatic arc is also bounded by an Early Cretaceous flysch sequence and a wildfysch belt that projects into the Tisa shear zone (Dinică et al., 1996) (Fig. 5-20). We suggest that the flysch basins that bound the Mureş igneous arc record Middle Jurassic to Early Cretaceous tangential stretching of the Carpathian crust and that wildflysch assemblages are linear domains of high strain accumulation that accommodated Middle Cretaceous compression through folding and local thrusting. Post-Middle Cretaceous tectonic relaxation is recorded by Cenomanian molasse (Fig. 5-20). Segments of these crustal strain zones were reactivated during subsequent tectonism. Late Cretaceous strain is recorded in the northeastern part of the basin by wildflysch horizons in the Cenomanian-Senonian Râmeţi Formation in the Trascău Mountains, by Campanian wildflysch along the southern bank of the Arieş Valley, and by sandstone flysch of the Bozeş Formation (Santonian to Maastrichtian) in the southeast. Tertiary reactivation of the Trascău shear zone is recorded by a discontinuous belt of Paleogene dioritic to andesitic rocks and by folding of Maastrichtian strata. West of Zlatna, the Mureş Basin is cut by NW-trending dextral transtensional faults plugged by the Miocene to Pliocene Brad-Gurahonţ andesite belt, transversely oriented to the postulated subduction zone in the southern Apuseni.

5.8. REGIONAL CORRELATIONS

The Permian-Mesozoic cover of the Someş and Codru assemblages of the Apuseni Mountains is lithologically similar to rocks in the Villany and Mecsek hills of southern Hungary (Patrulius, 1976). Drill-core data indicate the presence of Permian-Mesozoic strata beneath the south Pannonian Basin (Bérczi-Makk, 1986). Correlative Triassic cover of Eastern Alps-Carpathian affinity has been recognized to the southwest in the Slavonian Mountains (Šikić, 1981 *fide* Pamić, 1993). The metamorphic sequences of the Apuseni Mountains are also recognizable beneath the Pannonian Basin and in the Slavonian Mountains. The pre-Alpine polymetamorphic evolution proposed for the basement of the southern Pannonian Basin (Árkai et al., 1985) is similar to the record in the Someş assemblage (Hârtopanu and Hârtopanu, 1986).

Low-grade metamorphic rocks and associated granitic bodies similar to the Highiş-Biharia lithotectonic assemblages occur in drill cores from the Vojvodine region of Serbia (Kamenci and Čanovic, 1975)(Fig. 5-21) and farther west in the central Slavonian Mountains.

North of the HBSZ, between the Slavonian and Apuseni mountains, drill holes have intersected a wide zone of retrogressed medium/high grade crust. Intense sodium and/or carbonate metasomatism associated with shearing and retrograding resulted in locally complete pseudomorphing of mica and feldspar by carbonate (Nusszer, 1986). The retrograde overprint diminishes northward, and SW- striking "metamorphic regional units" have been recognized in several hundred drill-core samples from the southern Pannonian basement (Szili-Gyémánt, 1986; Nusszer, 1986; Cserepes-Meszéna, 1986). These match rock types in the westernmost outcrops of the Apuseni Mountains. An association similar to the Codru assemblage can be recognized in drill core from the Körös-Berettyó and Szank areas and in outcrops in the Mecsek, northern Papuk and Moslavacka Gora mountains (Szili-Gyémánt, 1986; Nusszer, 1986; Cserepes-Meszéna, 1986; Pamic, 1986); some variability is seen along strike. The northernmost outcrop of the Bihor assemblage in the Plopiş Mountains correlates with the "Álmosd Unit" (Szili-Gyémánt, 1986) of the Pannonian basement (Fig. 5-21).

In the central Slavonian Mountains a belt of low-grade rocks similar those described in the HBSZ separate two medium-grade "complexes", the Papuk-Jankovak complex, to the north, and the Psunj-Kutjevo complex (Pamić, 1986; 1993). The Papuk-Jankovak complex correlates with the Codru assemblage in the Apuseni Mountains, and the Psunj-Kutjevo complex, with the Baia de Arieş assemblage. As in the Apuseni Mountains, shearing and retrogression of medium/high grade rocks resulted in the development of a phyllonitic belt across the Papuk-Jenkovac complex, the Ravna Gora sequence, and of mappable bands of graphite- or chloritoid-blastomylonite and gneissic or phyllonitized granite across the Psunj-Kutjevo complex (Pamić, 1986). Along the Sava shear zone, the Prosara-Motajica complex (Pamić, 1986) represents the westernmost exposure of the Baia de Arieş assemblage.

Facies similarities and basement/cover thrust relations recognized in drill holes at two localities led to the application of the nappe model to the southeastern part of the Pannonian basement, with the proposal of a central Hungarian autochthon and a south Hungarian nappe system (Dimitrescu, 1981; Szederkényi, 1982; Balázs et al., 1986, Grow et al., 1989). On the

Figure 5-21. Proposed correlation of the metamorphic assemblages from the Apuseni Mountains along the unexposed basement of the southern Pannonian Basin, to the Mecsek and Slavonian mountains; 1 - exposed metamorphic/igneous basement of the Carpathian-Pannonian area; 2 - amphibolite-lense dominated assemblage; 3 -carbonate -lense dominated assemblage; 4 -migmatite; 5 - granite-phyllonite assemblage; 6 - Pieniny-Dămuc belt of arc parallel shear at the transpressional contact between the inner and outer Carpathian units; 7 - flysch sequences; 8 - Neogene igneous rocks; 9 - diffuse chlorite zone retrogression; 10 - mylonitic zones in the unexposed basement of the southern Pannonian basement; 11 - Early Alpine boundary of the "Tisia" crustal fragment; 12 - major faults related to its Tertiary 90-100° clockwise rotation; 13 - Pleistocene alkaline igneous rocks (mostly basalts); *Pi* - Pieniny; *D* - Dămuc; *P-J* - Papuk-Jankovak; *P-K* - Psunj-Kutjevo; *Ra* - Ravna Gora; *P-Mj* - Prosara-Motajica; *Vo* - Vojevodina; *K* - Kecsemét; *Sz* - Szank; *K-B* - Körös-Berettyö; *A* - Álmosd; *Hi-Bi* - Highiş-Biharia upper crustal igneous complex; *S* - Someş; *C* - Codru assemblage; *BA* - Baia de Arieş; Mo - Moslavacka Gora; S - Slavonian Mountains; M - Mecsek Hills, V - Villany Hills; TDR - Transdanudian Range; B - Bükk Hills; Z - Zemplin Hills; P - Plopiş Mountains; Ps - Perşani Mountains; Rmcc - Rodna metamorphic core complex; Bmcc - Banat system of metamorphic core complexes (eg., Godeanu, Porţile de Fier, Bahna); DVFZ - Dragoş Vodă sinistral fault zone; STFZ - South Transylvanian dextral fault zone. SFZ - Sava fault zone.

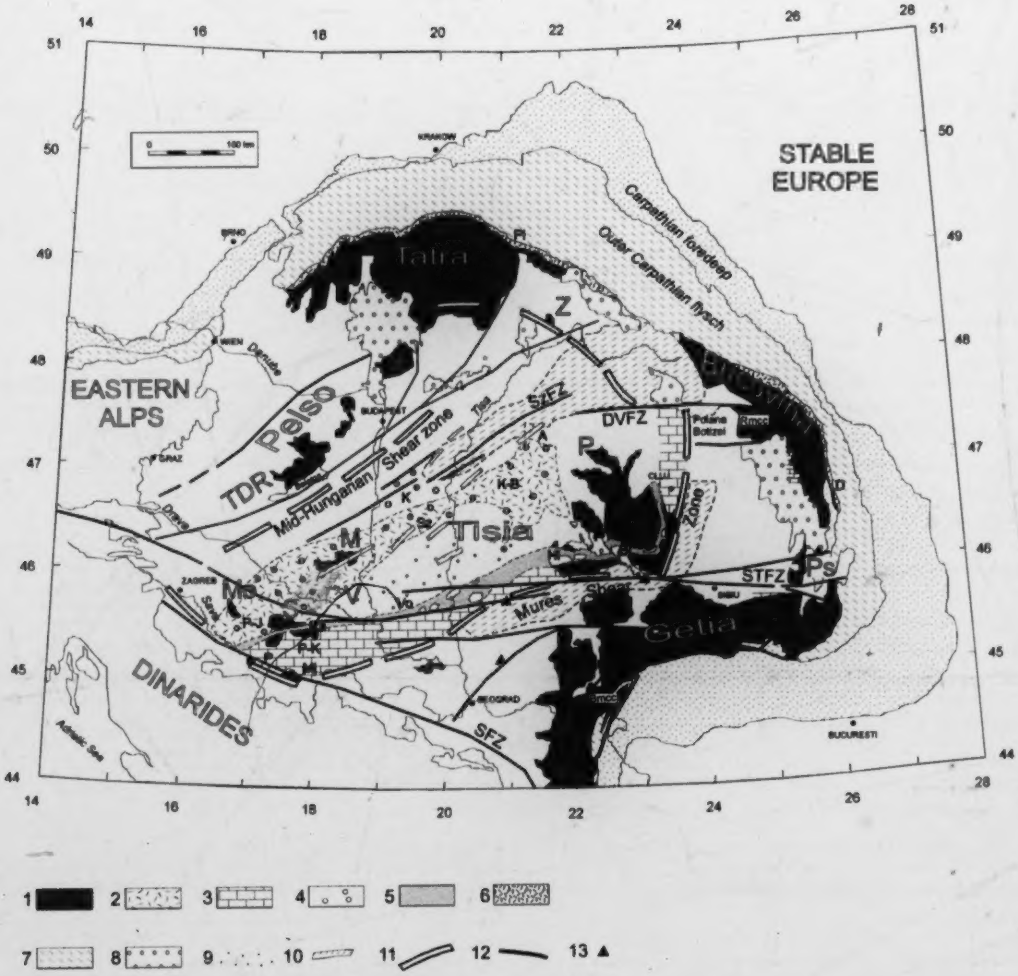
14
16
18
20
22
24
26
28
51
50
49
48
47
46
45
44
0
100 km
KRAKOW
BRNO
WIEN
Danube
GRAZ
Drava
ZAGREB
Sava
BUDAPEST
BEOGRAD
BUCURESTI
SIBIU
CLUJ
Adriatic Sea
STABLE EUROPE
EASTERN ALPS
DINARIDES
Carpathian foredeep
Outer Carpathian flysch
Tatra
Pi
Z
Pelso
TDR
Mid-Hunganan Shear zone
Tisa
SzFZ
DVFZ
Poiana Botizei
Rmcc
Bucovina
D
P
A
K-B
K
Sz
M
Tisia
Zone
STFZ
Ps
Mures Shear
Getia
Ma
V
Vo
P-J
P-K
M
SFZ
1
2
3
4
5
6
7
8
9
10
11
12
13

Fig. 5-21.

basis of the parallelism of mylonite zones in drill holes and the Szolnok transcurrent fault zone (Fig. 5-21), we infer a genetic relationship, which casts doubt on a nappe interpretation.

5.9. PROPOSED GEODYNAMIC MODEL

In a paleotectonic reconstruction of Early Alpine evolution, the Apuseni Mountains, Villany Hills, and Slavonian Mountains belong on the European margin as the south(west)ernmost expression of the Carpathian crust. Facies correlations and similarities of the Apuseni-south Pannonian continental fragment with the present East- and South Carpathians fragments have been noted both for the Paleozoic to Mesozoic sedimentary cover (Mišik et al., 1989) and for the metamorphic assemblages (Pană and Erdmer, 1994). The Sava Fault Zone defines the southwestern boundary with the South Alpine-Dinaric facies zones (Pamić, 1986; 1993), and the enigmatic "mid-Hungarian line" to the northwest separates the Apuseni-south Pannonian facies zones (Tisia) from the allochthonous Pelso unit (Haas et al., 1995) (Fig. 5-21). These major long-lived transcurrent discontinuities may have obliterated the vestiges of the Vardar-Bükk-Meliata branch of the Triassic Tethys Ocean. To the east, the Middle Jurassic to Early Cretaceous Mureş transcurrent shear zone separated the Apuseni from the Carpathian crust. Beyond the present exposure of the Mureş basin, its trajectory is difficult to infer but there is no unequivocal evidence for the proposed continuation of a Triassic branch of Tethys from Vardar along the Mureş Basin into the Pieninny Basin(s) (e.g. Săndulescu, 1984, 1994). In addition, significant facies differences between the Permian to Mesozoic sequences of the Apuseni Mountains and the West Carpathians exist (Patrulius, 1976; Mišic et al., 1989). The vergence and style of deformation in the Apuseni Mountains preclude structural correlation with the thrust sheets interpreted in the West Carpathians. In contrast, the granite/orthogneiss-dominated Tatra (Jaraba) assemblage of the West Carpathians (Kamenicky and Kamenicky, 1988) is similar to the Pietrosu-Hăghimaş-Bretila granite/orthogneiss assemblage of the East Carpathians and occupies the same tectonic position as the first basement unit in transpressional contact with the Carpathian outer flysch (Fig. 5-21). In both regions, medium- to high-grade assemblages are cut by retrogressive, orogen-parallel shear zones, suggesting a common Alpine evolution.

Early attempts to integrate the Apuseni Mountains into Alpine plate tectonics (e.g. Rădulescu and Săndulescu, 1973; Bleahu et al, 1973, Bleahu, 1976) inferred the Mureş Basin to represent the main branch of the Tethys Ocean. Models of a single arc (Cioflica and Nicolae, 1981), dual converging arcs (Savu, 1983), or changing subduction polarity (Săndulescu, 1984) were proposed to accommodate the juxtaposition of tholeiitic and calc-alkaline rocks. The igneous petrochemistry and sedimentologic characteristics of the western part of the Mureş Basin have also been interpreted as those of a marginal basin developed on continental crust

(Lupu et al., 1993). Remnants of the Tethys Ocean were postulated to be obscured by Tertiary cover of the Transylvanian Basin (e.g., Săndulescu, 1994; Rădulescu et al. 1993) but core samples from the Transylvanian basement are gneiss or calc-alkaline igneous rocks (I. Nicolae, personal communication, 1995).

Westward subduction beneath the Apuseni crustal fragment was considered to have resulted in subduction magmatism and the thrusting of a large number of antithetic nappes but the number, composition, age, and boundaries of the proposed nappes varied between authors (e.g. Ianovici et al., 1976; Bleahu et al., 1981; Săndulescu, 1984; Balintoni, 1994). The present spatial distribution of rock assemblages and their temporal relationships are incompatible with ocean opening and subduction.

We propose that general crustal extension of the European margin is recorded by igneous activity (commonly alkali basalt) in Permian to Triassic platformal sequences in the West, East, and South Carpathians, as well as in the Codru Mountains and Poiana Botizei klippen. Middle Jurassic to Early Cretaceous tangential stretching of the European continental margin resulted in a network of anastomosing crustal-scale faults and local adiabatic upwelling of material from a mantle of constant potential temperature. In this model (*cf.* McKenzie and Bickle, 1988), a hot rising sheet is not required to induce crustal spreading, and mid-ocean ridge magmatism is not required. A releasing bend of a transcrustal strike-slip shear zone overprinting the gneiss-carbonate assemblage in Carpathian crust allowed the emplacement of most igneous rocks of the Mureş Basin in the Kimmeridgian. During early extension, cold, mature, and highly strained crust was intruded by mantle magma dissipating heat over a large depth range. Following a model of progressive extension of continental lithosphere (at $\beta > 2$ and $T_p > 1380^\circ$C, McKenzie and Bickle, 1988), we interpret that a gradual increase in the amount of melting was accompanied by a change in melt composition: the initial alkali basalts were replaced during the Middle to Late Jurassic by tholeiitic to calc-alkaline rocks. The presence of tholeiite records a specific rate and amount of crustal stretching in a particular region and does not require the existence of a major ocean. Tholeiites crop out only in the westernmost part of the Mureş tectonic zone, where Rb/Sr dates of 180-140 Ma were estimated (Hertz et al., 1974) and K/Ar ages of 168-143 Ma have been obtained (Nicolae et al., 1992). An inherited population of zircon in the Săvârşin granite that intruded the tholeiitic suit yielded a U-Pb age of c. 155 Ma which corresponds to the Callovian age of the oldest sediments interlayered with the tholeiitic rocks (Lupu et al., 1995). Strongly layered crust below the brittle-ductile transition provided favourable conditions for sill intrusion. Intracrustal mixing and hybridization resulted in the emplacement of the Tithonian to Albian calc-alkaline suite in the adjacent subsiding flysch basins and in the Eocene emplacement of the Săvârşin (c. 55 Ma, Pană et al., 1998) and Cerbia granites within the tholeiitic complex. The Callovian-Kimmeridgian age of mafic igneous activity in the Mureş

Basin correlates with the c. 156 Ma ^{40}Ar/^{39}Ar cooling age of hornblende within the most external Baia de Arieş assemblage. Similar ages yielded by high-pressure rocks of the Meliata assemblage in the southern West Carpathians (Dallmeyer et al., 1996) suggest a link along a Jurassic tectonic lineament.

Continued crustal thinning and rifting led to the development of Late Jurassic to Early Cretaceous elongate flysch basins separating the Apuseni-south Pannonian (Tisia) and East (Bucovina) and South (Getia) Carpathians crustal fragments from the European continent. Kinematic indicators in the Bucovinian and Getic crust record Late Paleozoic to Alpine orogen-parallel stretching (Pană and Erdmer, 1994). Similarly to earlier models (e.g., Le Pichon et al., 1988) we assume Jurassic to Early Cretaceous sinistral displacement along the Mureş transtensional zone. Oblique compression of the Bihor autochthon against the Highiş-Biharia igneous complex and the Baia de Arieş gneissic crust resulted in strain concentration within the igneous complex and uplift and thrusting of the Baia de Arieş gneissic crust. West of the Bihor block, lateral extrusion of the sheared igneous crust resulted in a wide northwestward verging thrust zone and high strain throughout the cover sequences in the footwall. Compression ceased at about 100 Ma. Subsequent extensional structures throughout the HBSZ were followed by deposition of Santonian-Campanian "Gosau"-type strata that overlap the metamorphic assemblages in the central Apuseni Mountains. Campanian wildflysch exposed in the Arieş Valley along the EW segment of the HBSZ indicate a long-lived zone of crustal weakness. The Late Cretaceous to Early Tertiary Vlădeasa taphrolite (Ştefan, 1980) records breakup of the Bihor block (Fig. 5-20) and independent trajectories for the resulting crustal fragments.

Middle Cretaceous compression was also accommodated by the wildflysch belts along the Mureş igneous arc. The overlapping Cenomanian molasse record post-Austrian tectonic relaxation and flysch- and wildflysch-type sequences indicate active Late Cretaceous tectonism in the southeastern part of the Mureş Basin. Tertiary tectonism reactivated the Trascău shear zone and resulted in Paleogene igneous activity and in a SSE-trending fold system involving strata as young as Maastrichtian. The bend of the sinistral Trascău shear zone and of the associated fold system in the southern Apuseni Mountains (Fig. 5-20) suggests a clockwise rotation of the northern structural units during compression between the Apuseni and the Carpathian/Moesian promontory. More data are needed to link the major structures described here with the paleomagnetic data which suggest that the Apuseni-South Pannonian crustal fragment ("Tisia") travelled more than 1000 km northward and rotated about 90-100° clockwise during the Late Cretaceous to Miocene (Márton, 1986; Pătraşcu, et al., 1990; Márton and Mauritsch, 1990).

Neogene isostatic reequilibration resulted in post-orogenic collapse accommodated by major fault zones with associated igneous activity along the margins of the Apuseni-

Transylvanian block: to the east, a NNW striking, southward-propagating fault zone was progressively plugged by the Miocene to Pleistocene Călimani-Harghita volcanic belt; to the south-west, a wide dextral NW striking fault zone is plugged by the Miocene to Pliocene Brad-Gurahonţ volcanic belt. Post-Miocene eastward translation of the Apuseni-Transylvanian fragment was accommodated to the south by the dextral South Transylvanian fault zone which is overlapped by Pleistocene alkaline intrusives, and to the north by the sinistral Dragoş Vodă fault zone.

5.10. CONCLUSIONS

The previous stratigraphic interpretation of metamorphic rocks in the Apuseni Mountains was internally inconsistent. We propose that they can be grouped into the Someş gneissic assemblage to the north and the Baia de Arieş carbonate-lense dominated gneissic assemblage to the south, separated by the Highiş-Biharia upper crustal igneous complex and the Codru amphibolite-dioritic assemblage. Shearing and hydration of igneous and gneissic protoliths during Alpine tectonism resulted in the development of several low-grade lithotectonic assemblages. Two belts of high strain concentration have been mapped: the Highiş Biharia shear zone, overprinting mainly igneous rocks across the central Apuseni Mountains, and the Trascău shear zone, overprinting the Baia de Arieş crust along the eastern margin of the Apuseni Mountains.

The widespread internal strain in Cretaceous metamorphic assemblages indicates that revision of the previous model of coherent nappes is required. In the western Apuseni Mountains, thrust-related structures within the low-grade assemblages are consistent with the imbrication and NW-thrusting of underlying Permian-Mesozoic cover. In the eastern Apuseni Mountains, contemporaneous transpressional structures are dominant throughout the low-grade assemblages and regionally significant thrust faults cannot be mapped. Widespread late extensional structures obliterate variably the Early to Middle Cretaceous compressional structures.

Tectonosedimentary and igneous activity in the Mureş Basin is consistent with the evolution of a transtensional shear zone during the Middle Jurassic to Early Cretaceous. We propose a model in which extension of the European crust by tangential stretching was accompanied by local mantle intrusion. Middle Cretaceous compression and Tertiary compression and rotation were accommodated in wide shear zones that record deformation during complex plate interaction. We explain the intrusion of calc-alkaline plutons within the tholeiitic rocks of the Mureş Basin by intracrustal hybridization within a transcurrent setting. The Neogene volcanism likely resulted from mantle processes unrelated to subduction.

REFERENCES

Al-Aasm, I. S., Taylor, B. E., and South, B., 1990, Stable isotope analysis of multiple carbonate samples using selective acid extraction, Chemical Geology, Isotope Geoscience Section, 80, p. 119-125.

Anovitz, L. M., and Essene, E. J., 1987, Phase equilibria in the system $CaCO_3$-$MgCO_3$-$FeCO_3$, Journal of Petrology, 28, p. 389-414.

Árkai, P., Nagy, G., Dobosi, G., 1985, Polymetamorphic evolution of the south-Hungarian crystalline basement, Pannonian Basin: geothermometric and geobarometric data, Acta Geologica Hungarica, 28, (3-4), p. 165-190.

Balla, Z., 1982, Development of the Pannonian basin basement through the Cretaceous-Cenozoic collision: a new synthesis, Tectonophysics, 88, p. 61-102.

Balla, Z., 1985, The Carpathian loop and the Pannonian basin: A kinematic analysis, Geophysical Transactions, 30, p. 313-353.

Balla, Z., 1986, Palaeotectonic reconstruction of the central Alpine-Mediterranean belt for the Neogene, Tectonophysics, 127, p. 213-243

Balázs, B., Meszéna, B. C., Nusszer, A., and Gyémánt, S.P., 1986, An attempt to correlate the metamorphic formations of the Great Hungarian Plain and the Transylvanian central mountains (Munţii Apuseni), Acta Geologica Hungarica, 29, (3-4), p. 317-320.

Balintoni, I., 1985, Corrélation des unités litostratigraphiques et tectoniques longeant le ruisseau d'Arieş entre la vallée de Iara et le Mont Găina (Monts Apuseni), Dări de Seamă ale Institutului de Geologie şi Geofizică, LXIX/5, p. 5-15.

Balintoni, I., 1986, Petrologic and tectonic features of the Highiş-Drocea Crystalline Massif (Apuseni Mountains), Dări de Seamă ale Institutului de Geologie şi Geofizică, 70-71/5, p. 5-21.

Balintoni, I., 1994, Structure of the Apuseni Mountains, *in* Berza T. (Ed.): "Geological evolution of the Alpine-Carpathian-Pannonian system", ALCAPA II Conference, Covasna, Field Guidebook, Romanian Journal of Tectonics and Regional Geology, 75, suppl. 2, p. 51-57.

Balintoni, I., Iancu, V., 1986, Lithostratigraphic and tectonic units in the Trascău Mountains north of Mănăstirea Valley, Dări de Seamă ale Institutului de Geologie şi Geofizică, 70-71/5, p. 45-56.

Baratov, R. B., Gnutenko, N. A., and Kuzemko, V. N., 1984, Regional carbonization conected with the epi-Hercynian tectogenesis in the southern Tien Shan, Dokl. Akad. Nauk SSSR, 274, p. 124-126.

Berman, R.G., 1996, TWQ (vesion 2.02)

Bérczi-Makk, 1986, Mesozoic formation types of the Great Hungarian Plain, Acta Geologica

Hungarica, 29 (3-4), p.261-282.

Bleahu, M.D., 1976, Structural position of the Apuseni Mountains in the Alpine System, Revue Roumaine de Géologie, Géophysique, Géographie, ser. Géologie, 20, p. 7-19.

Bleahu, M.D., Boccaletti, M., Manetti, P., and Peltz, S., 1973, Neogene Carpathian arc: A continental arc displaying the features of an "island arc", Journal of Geophysical Research, 78, p. 5025-5032.

Bleahu, M.D., Lupu, M., Patrulius, D., Bordea, S., Ştefan, A., and Panin, S., 1981, The structure of the Apuseni Mountains, Carpatho-Balkan Geological Association, XII Congress, Bucharest, Romania, Guide to Excursion-B3, 103 p.

Bombiţă, G, and Savu, H., 1986, Sur les roches volcaniques associées aux Klippes Pienines de Poiana Botizii (Maramouresh Roumain), Annales Societatis Geologorum Poloniae, 56, p. 337-348.

Bordea, S., 1992, Stratigrafia depozitelor neojurasice si cretacice din partea vestică a Munţilor Metaliferi, (Stratigraphy of the Upper Jurassic and Cretaceous deposits from the western part of the Metaliferi Mountains), Abstract of the PhD Thesis, Univ.'Al.I.Cuza'-Iaşi, 27 p.

Bordea, S., Constantinescu, R., 1975, Geologic Map of Romania, 1:50 000 scale, Blăjeni Sheet

Bordea, S., Ştefan, A., and Borcoş, M., 1979, Geologic Map of Romania, 1:50 000 scale, Abrud sheet.

Bowman, J. R., O'Neil, J. R., and Essene, E. J., 1985, Contact skarn formation at Elkhorn, Montana II: Origin and evolution of C-O-H skarn fluids. Am. J. Sci., 285, p. 621-660.

Böhlke, J. K., and Kistler, R. W., 1986, Rb-Sr, K-Ar, and stable isotope evidence for the ages and sources of fluid components of gold-bearing quartz veins in the northern Sierra Nevada foothills metamorphic belt, California, Econ. Geol., 81, p. 296-322.

Cameron, E. M., 1988, Archean gold: relation to granulite formation and redox zoning in the crust, Geology, 16, p. 109-112.

Cioflica, G., and Nicolae, I., 1981, The Origin, Evolution and Tectonic Setting of the Alpine Ophiolites from the Southern Apuseni Mountains, Revue Roumaine de Géologie,Géophysique, Géographie, ser. Géologie, 25, p. 19-29.

Cserepes-Meszéna, B., 1986, Petrography of the crystalline basement of the Danube-Tisza interfluve (Hungary), Acta Geologica Hungarica, 29, (3-4), p. 321-339.

Csontos, L., Nagymarosy, A., Horváth, F., and Kovác, M., 1992, Tertiary evolution of the intra-Carpathian area: A model, Tectonophysics, 208, p. 221-241.

Dal Piaz, V.G., Martin, S., Villa, M.I., Gosso, G., and Marschalko, R., 1995, Late Jurassic blueschist facies pebbles from the Western carpathian orogenic wedge and paleostructural implications for Western Tethys evolution, Tectonics, 14, 4, p. 874-885.

Dallmeyer, R.D., Neubauer, F., Pană, D., and Erdmer, P., 1997, Tectonothermal evolution of the Apuseni Mountains, Romania, Part II: Tectonophysics, (submitted)

Dimitrescu, R., 1962, Cercetari geologice in regiunea Şiria, Dări de Seamă ale Institutului de Geologie şi Geofizică, XLV, p. 75-87.

Dimitrescu, R., 1973, Notă asupra unor gneise oculare din seria de Muncel (Munţii Bihorului), Studii şi Cercetări, Geologie, Geofizică, Geografie, Seria Geologie, 18, 1, p. 29-32.

Dimitrescu, R., 1981, Hypothèses sur la structure du soubassement du secteur sud-oriental de la dépression Pannonique, Revue Roumaine de Géologie, Géophysique, Géographie, ser.Géologie, 25, p. 31-35.

Dimitrescu, R., 1985, Early Caledonian event in the pre-Alpine metamorphic sequences of the Romanian Carpathian, Acta Mineralogica-Petrographica, Szeged, XXVII, p. 59-70.

Dimitrescu, R., 1988a, Observations sur la structure du cristallin des monts Bihor et Gilău méridional, Dări de Seamă ale Institutului de Geologie şi Geofizică, 72-73/5, p. 85-91.

Dimitrescu, R., 1988b, Apuseni Mountains, *in* Zoubek, V., Cogné, J., Kozhoukharov, D., and Kräutner, H., (Eds.): Precambrian in Younger Fold Belts,, p. 665-674.

Dimitrescu, R., 1993, Asupra unor concepţii despre structura părţii de nord-vest a munţilor Highiş, Romanian Journal of Tectonics and Regional Geology, 75, p. 39-43.

Dinică, I., Pană, D., Conovici, M., and Roşu, E., 1997, Dynamometamorphism at the southern transform boundary of the Mureş igneous suite (Tisa-Coşteiu-Groşi, Apuseni Mountains), Romanian Journal of Tectonics and Regional Geology, *submitted.*

Dunn, S.R., and Valley, J. W., 1985, Fluid infiltration of the Tudor gabbro during regional metamorphism, Geol. Soc. Am. Abstr. Prog., 17, p. 570.

Ghent, E. D., 1976, Plagioclase-gernet-Al_2SiO_5-quartz: a potential geobarometer-geothermometer, Am. Mineral., 61, p. 710-714.

Geological Map of Romania, 1958, Scale 1:500 000, sheet 1b, published by the Romanian Academy and the Geological Committee.

Geological Map of Romania, 1967, Scale 1:200 000, sheets: Şimleul Silvaniei, Cluj, Turda, Brad, published by the Geological Institute of Romania.

Giuşcă, D., Savu, H., and Borcoş, M., 1968, La stratigraphie des schistes cristallins des Monts Apuseni, Revue Roumain de Géologie, Géophysique, Géographie, ser. Géologie, 12/2, p. 143-159.

Goldfarb, R. J., Leach, D. L., Pickthorn, J., and Paterson G. J., 1988, Origin of lode-gold deposits of the Juneau gold belt, southeastern Alaska, Geology, 16, p. 440-443.

Groves, D. I., Golding, S. D., Rock, N. M. S., Barley, M. E., and McNaughton, N. J., 1988, Archean carbon reservoirs and their relevance to the fluid source for gold deposits, Nature, 331, p. 254-257.

Grow, J. A., Pogácsás, Gy., Bérczi-Makk, A., Várnai, P., Hajdú, D., Varga, E., and Péró, Cs., 1989, Tectonic and structural conditions of the Bekes basin, Magy. Geofiz., 30 (2-3), p. 63-97

Ianovici, V., Borcoş, M., Bleahu, M., Patrulius, D., Lupu, M., Dimitrescu, R., and Savu, H., 1976, Geologia Munţilor Apuseni, Editura Academiei Române, 631 p., Bucureşti.

Hamilton, W.B., 1990, On terrane analysis, *in* Dewey, J.F., Gass, I.G., Curry, G.B., Harris, N.B.W., and Sengör, A.M.C., (Eds.): Allochthonous Terranes, p.55-66, Cambridge, U.K.

Haas, J., Kovács, S., Krystyn, L., and Lein, R., 1995, Significance of Late Permian-Triassic facies zones in terrane reconstructions in the Alpine-North Pannonian domain, Tectonophysics, 242, p. 19-40.

Hârtopanu, I., and Hârtopanu, P., 1986, Intersecting isograds - a possible way to find out the polymetamorphism. An example: the Someş series, Dări de Seamă ale Institutului de Geologie şi Geofizică, 70-71/1, p. 291-299.

Herz, N., Jones, L. M., Savu, H., and Walker, R.L., 1974, Strontium Isotope Composition of Ophiolitic and Related Rocks, Drocea Mountains, Romania, Bulletin Volcanologique, XXXVIII, 4, p. 1110-1124.

Kamenci, R., and Čanovic, M., 1975, Pre-Neogene basement in the Pannonian Basin of Vojvodina, Radovi Znanst Sovjeta za naftu Jazu, A 5, p. 248-256.

Kamenicky, L., and Kamenicky, J., 1988, Precambrian of the West Carpathians, *in* Zoubek V., Cogné, J., Kozhoukharov, D., and Kräutner, H., (Ed.): Precambrian in Younger Fold Belts, p. 675-685.

Kohn, J. M., and Spear, F. S., 1991, Error propagation for barometers, 1. Accuracy and precision of experimentally located end-member reactions, Am. Mineral., 76, p. 128-137.

Kovács, S., 1989, Triassic and Jurassic oceanic/paraoceanic belts in the Carpathian-Pannonian region and its surroundings, *in* Sengör, A.M.C., (Ed.): Tectonic of the Tethyan Region, p. 77-92.

Kräutner, H., 1980, Lithostratigraphic correlation of Precambrian in the Romanian Carpathians, Anuarul Institutului de Geologie şi Geofizică, LVII, p. 229-296.

Lapin, A. V., Ploshko, V. V., and Malyshev, A. A., 1987, Carbonatites of the Tatar deep-seated fault zone, Siberia, Int. Geol. Rev., 29, p. 551-567.

Lattanzi, P., Rye, D. M., and Rice, J.M., 1980, Behavior of ^{13}C and ^{18}O in carbonates during contact metamorphism at Marysville Montana: Implications for isotope systematics in impure dolomitic limestone, Am. J. Sci., 280, p. 890-906.

Lupu, M., Avram, E., Antonescu, E., Dumitrică, P., Lupu, D., and Nicolae, I., 1993, The

Neojurassic and the Cretaceous of the Drocea Mountains: the stratigraphy and the structure of an ensialic marginal basin, Romanian Journal of Tectonics and Regional Geology, 75, p. 53-66.

Lupu, M., Antonescu, E., Avram, E., Dumitrică, P., and Nicolae, I., 1995, Comment on the age of some ophiolites from the North Drocea Mountains, Romanian Journal of Tectonics and Regional Geology, 76, p. 21-25.

Le Pichon, X., Bergerat, F., and Roulet, M.J., 1988, Plate kinematics and tectonics leading to the Alpine belt formation; a new analysis, Geological Society of America Special Paper, 218, p. 111-131.

McKenzie, D., and Bickle, M. J., 1988, The Volume and Composition of Melt Generated by Extension of the Lithosphere, Journal of Petrology, 29, 3, p. 625-679.

Márton, E., 1986, Paleomagnetism of igneous rocks from the Velence Hills and Mecsek Mountains, Geophysical Transaction, 32, p. 83-145.

Márton, E., and Mauritsch, H.J., 1990, Structural applications and discussion of a paleomagnetic post-Paleozoic data base for the Central Mediterranean, Physics of the Earth and Planetary Interiors, 62, p. 46-59.

Mišik, M., Mock, R., Rakús, M., and Biely, A., 1989, The Area of Mesozoic Sedimentation of the Mecsek and Northern Apuseni Mountains was not situated in the West Carpathians, IGCP Project 198, Memoire Societé Géologique, France, 154(II), p. 69-79.

Nicolae, I., 1994, The ophiolitic rocks from the Mures valley, *in* Berza T. (Ed.): "Geological evolution of the Alpine-Carpathian-Pannonian system", ALCAPA II Conference, Covasna, Field Guidebook, Romanian Journal of Tectonics and Regional Geology, 75, suppl. 2, p. 136-140.

Nicolae, I., 1995, Tectonic setting of the ophiolites of the South Apuseni Mountains: magmatic arc and marginal Basin, Romanian Journal of Tectonics and Regional Geology, 76, p. 27-39.

Nicolae, I., Soroiu, M., and Bonhomme, G.M., 1992, Ages K-Ar de quelques ophiolites des Monts Apuseni du Sud (Roumanie) et leur signification géologique, Géologie Alpine, 68, p. 77-83.

Nusszer, A., 1986, Formations of the Pusztaföldvár metamorphite regional unit, Acta Geologica Hungarica, 29, (3-4), p. 283-304.

Pamić, J.J., 1986, Magmatic and metamorphic complexes of the adjoining area of the northernmost Dinarides and Pannonian mass, Acta Geologica Hungarica, 29, (3-4), p. 203-220.

Pamić, J.J., 1993, Eoalpine to Neoalpine magmatic and metamorphic processes in the northwestern Vardar Zone, the easternmost Periadriatic Zone and the southwestern Pannonian Basin, Tectonophysics, 22, p. 503-518.

Pană, D., and Ricman, C., 1988, The lower complex of the Paiuseni series - a blastomylonitic shear belt. Revue Roumain de Géologie, Géophysique, Géographie, ser.Géologie, 32, p. 21-35.

Pană, D., and Erdmer, P., 1994, Alpine Crustal Shear zones and pre-Alpine basement terranes in the Romanian Carpathians and Apuseni Mountains, Geology, 22, p. 807-810.

Pană, D., Erdmer, P., Heaman, L., and Creaser, R., 1996, Stable and radiogenic isotope study of lithotectonic assemblages from the Apuseni Mountains, Romania, GSA Annual Meeting, Denver, Abstract Volume, p. A 369.

Papiu, C.V., 1960, Recherches Géologiques dans le Massif de Drocea, Annuaire du Comité Géologique, XXVI-XXVIII, p. 317-346.

Patrulius, D., 1976, Les formations mésozoïques des Monts Apuseni septentrionaux: corrélations chronostratigraphique et faciale, Revue Roumain de Géologie, Géophysique, Géographie, ser. Géologie, 20, p. 49-57.

Pavelescu, L., Pop, G., Ailenei, G., Ene, I., Soroiu, M., and Popescu, G., 1975, K-Ar age determinations from the Apuseni and Banat Mountains, Revue Roumain de Géologie, Géophysique, Géographie, ser.Géophysique, 19, p. 67-79.

Pătraşcu, S., Bleahu, M., and Panaiotu, C., 1990, Tectonic implications of the paleomagnetic research into Upper Cretaceous magmatic rocks in the Apuseni Mountains, Romania, Tectonophysics, 180, p.309-322.

Rădulescu, D., and Săndulescu, M., 1973, The plate-tectonics concept and the geological structure of the Carpathians, Tectonophysics, 16, p. 155-161.

Rădulescu, D., Săndulescu, M., and Borcoş, M., 1993, Alpine magmatogenetic map of Romania: an approach to the systematization of the igneous activity, Revue Roumain de Géologie, Géophysique, Géographie, ser. Géologie, 37, p. 3-8.

Savu, H., 1965, Masivul eruptiv de la Bârzava (Munţii Drocea), Memorii, Comitetul Geologic Român, VIII, 148 p., Bucureşti.

Savu, H., Borcoş, M., Hanumolo, I., Hanumolo, A., Trifulescu, M., and Ianidu C., 1967, Date noi asupra stratigrafiei şi petrologiei şisturilor cristaline din partea centrală a munţilor Drocea, Dări de Seamă ale Institutului de Geologie şi Geofizică LIII, 1, p. 187-214.

Savu, H., 1980, Genesis of the Alpine ophiolites from Romania and their associated calco-alkaline volcanics, Anuarul Institutului de Geologie şi Geofizică, 56, p. 55-78.

Savu, H, 1983, Geotectonic and magmatic evolution of the Mureş Zone (Apuseni Mountains)-Romania, Anuarul Institutului de Geologie şi Geofizică, LVI, p. 55-77.

Săndulescu M., 1984, Geotectonica Romaniei, 336 p., Editura Tehnică, Bucureşti.

Săndulescu M., 1994, Overview on Romanian geology, *in* Berza T. (Ed.): "Geological evolution of the Alpine-Carpathian-Pannonian system", ALCAPA II Conference, Covasna, Field

Guidebook, Romanian Journal of Tectonics and Regional Geology, 75, suppl. 2, p. 3-15.

Schwarcz, H. P., Clayton, R. N., and Mayeda, T. 1970, Oxygen isotopic studies of calcareous and pelitic metamorphic rocks, New England, Geol. Soc. Am. Bull., 81, p. 2299-2316.

Soroiu, M., Popescu, G., Kasper, U., and Dimitrescu, R., 1969, Contributions préliminaires à la géologie des massifs cristallins des Monts Apuseni, Analele Ştiintifice ale Universităţii Al. I. Cuza, Sect. IIb (Geol.), 15, p. 25-33.

Szederkényi, T., 1982, Lithostratigraphic division of the Crystalline Mass in South Transdanubia and the Great Hungarian Plain, Newsletter of IGCP Project No. 5, Bratislava, 4, p.100-106.

Szepesházy, K., 1979, A Tiszántúl és az Erdélyi Kozéphegység (Munţii Apuseni) nagyszerkezeti és rétegtani kapcsolatai (megatectonic and stratigraphic relationships of the Tiszántúl and the Apuseni Mountains), Ált. Földt. Szemle, 12, p. 121-198.

Szili-Gyémnt, P., 1986, Metamorphic formations in Tiszantul: the Körös-Berettyó and the Álmosd units, Acta Geologica Hungarica, 29, (3-4), p. 305-316.

Ştefan, A., 1980, Petrographic Study of the eastern Part of the Vlădeasa Eruptive Massif, Anuarul Institutului de Geologie şi Geofizică, LV, p. 207-325.

Taylor, H. P. Jr., and Sheppard, S. M. F., 1986, Igneous Rocks: I. Processes of Isotopic fractionation and Isotope systematics, *in* Valley J.W., Taylor, H.P.Jr., and O'Neil, J.R. (Eds.): Stable isotopes in high temperature geological processes, Reviews in Mineralogy, 16, p. 227-271.

Thompson, A. B., 1976, Mineral reactions in pelitic rocks II: Calculations of some P-T-X (Fe-Mg) phase relations, Am. J. Sci., 276, p. 425-454.

Valley, J. W., 1986, Stable isotope geochemistry of metamorphic rocks, *in* Valley J.W., Taylor, H.P.Jr., and O'Neil, J.R. (Eds.): Stable sotopes in high temperature geological processes, Reviews in Mineralogy, 16, p. 445-489.

Veizer, J., and Hoefs, J., 1976, The nature of $^{18}O/^{16}O$ and $^{13}C/^{12}C$ secular trends in sedimentary carbonate rocks, Geochm. Cosmochim. Acta, 40, p. 1387-1395.

Visarion, A., and Dimitrescu, R., 1971, Contribuţii la determinarea vârstei unor şisturi cristaline din Munţii Apuseni (Contributions à la détermination de l'age de certains schistes cristallins des Monts Apuseni), Analele Ştiinţifice ale Universităţii 'Al. I. Cuza', Sect. II b (Geol.), 17, p.1-13.

CHAPTER 6

ALPINE STRAIN DISTRIBUTION AND LITHOLOGICAL CORRELATION OF BASEMENT ASSEMBLAGES IN THE CARPATHIAN-PANNONIAN REGION

6.1. INTRODUCTION

The current tectonic model for the Romanian Carpathians and Apuseni Mountains has been derived from the facies distribution of sedimentary cover strata and inferred suture zones (e.g., Codarcea, 1940; Rădulescu and Săndulescu, 1973; Săndulescu, 1984). Basement units have been regarded as rigid slices, and passive carriers of the sedimentary record. The paradoxical interpretation of Carpathian metamorphic tectonites as tectonically irrelevant entities was enhanced by the stratigraphic approach to the metamorphic lithology. Lithologic units have been regarded as metamorphosed Precambrian and Paleozoic strata in original stratigraphic succession (e.g., Kräutner 1980,1988; Dimitrescu, 1988; Gheuca, 1988). The metamorphic record and lithologic content of the basement units were considered of little or no relevance for the Alpine paleogeographic reconstructions. The kinematic indicators were overlooked (e.g., Săndulescu, 1984; Balintoni et al., 1983; 1989; Berza et al., 1994). At the scale of the Carpathian-Pannonian region, paleotectonic reconstructions based essentially on Alpine facies distribution and interpreted suture zones resulted in conflicting evolutionary models (Săndulescu, 1975; 1988; Bala, 1985; Birkenmayer, 1986; Debelmas and Săndulescu, 1987; Haas et al., 1995; Del Piaz et al., 1995).

It is now clear that the fragments of continental crust involved in Alpine tectonics record polyphase tectonothermal evolution. $^{40}Ar/^{39}Ar$ dating indicates that most low-grade lithotectonic assemblages record Alpine growth of syn-kinematic muscovite (e.g., Malusky, 1993; Dallmeyer et al., 1996). Metamorphic petrogenesis of low-grade assemblages is likely related to syn-kinematic hydration/carbonation of older crust within crustal scale shear zones (e.g., Pană and Erdmer, 1994).

This chapter emphasises the Alpine strain and accompanying metamorphic reactions within basement units adjacent to the Apuseni Mountains and discusses their implications for the tectonic evolution of the Carpathian-Pannonian region.

6.2. BASEMENT UNITS OF THE APUSENI MOUNTAINS

Lithotectonic assemblages of the Apuseni Mountains can be grouped into the Someş gneiss-granite assemblage to the north and the Baia de Arieş carbonate-lense dominated gneissic assemblage to the south, separated by the Highiş-Biharia upper crustal igneous complex and the Codru amphibolite-diorite assemblage. Shearing and hydration of igneous and gneissic protoliths resulted in the development of several low-grade lithotectonic assemblages. Two belts of high strain and retrograde metamorphism define the Highiş-Biharia shear zone (HBSZ) and the Trascău shear zone (TSZ), overprinting mainly igneous rocks across the central Apuseni Mountains, and the Baia de Arieş crust along the eastern margin of the Apuseni Mountains, respectively.

In the western Apuseni Mountains, compressional structures within the low-grade assemblages are consistent with local imbrication and NW-thrusting of underlying Permian-Mesozoic cover (Fig. 6-1). In the eastern Apuseni Mountains, contemporaneous transpressional structures are dominant throughout the low- and adjacent medium-grade assemblages (Fig. 6-2), and regionally significant thrust faults cannot be mapped. Penetrative extensional structures variably obliterate compressional structures.

The two principal medium-grade assemblages yielded Early Proterozoic T_{DM} model ages and the most negative $\varepsilon Nd_{(0)}$ values, but show relatively distinct isotopic signatures (see chapter 3). The Someş gneiss-granite assemblage yielded the oldest T_{DM} of c. 1.8-1.9 Ga and most depleted $\varepsilon Nd_{(0)}$ values that reach -15.5. Various Paleozoic granitoids yielded Early to Middle Proterozoic T_{DM} model ages between 1.9-1.4 Ga and less depleted $\varepsilon Nd_{(t)}$ values, indicating different degrees of crustal contamination. Positive $\varepsilon Nd_{(t)}$ values of the Codru diorite and Highiş-Biharia alkali diorite appear to correspond to Paleozoic rift-like settings, whilst the most negative $\varepsilon Nd_{(t)}$ values are similar to those of intrusions in the Someş-Codru crust.

δO^{18} -δC^{13} values of carbonate layers within the low-grade assemblages plot outside the field of limestone strata metamorphosed under low-grade conditions and suggest a mixing pattern between igneous values and chemically evolved surficial fluids (see chapter 5). Although, the data may be interpreted as the result of uncommon non-equilibrium metamorphic reactions, widespread carbonate reactions within igneous protoliths favour a metasomatic origin for the thin carbonate layers within the Highis-Biharia shear zone.

$^{40}Ar/^{39}Ar$ dating of medium- and low-grade assemblages from the Apuseni Mountains indicates a complex tectonothermal evolution that included "Early" and "Late" Variscan events as well as polyphase Alpine tectonism. Hornblende and muscovite within non-retrogressed northern sectors of the Someş gneissic assemblage yielded ages between c. 317 Ma and c. 300 Ma. The development of medium-grade textures during Variscan tectonism (Dallmeyer et al., 1998) is speculative and the cooling ages may simply record Carboniferous uplift accompanied by the emplacement of the Muntele Mare batholith at c. 295 Ma. Similarly, the Codru assemblage yielded $^{40}Ar/^{39}Ar$ dates that range from c. 405 to c. 335 Ma and may be interpreted as stepped Devonian to Carboniferous uplift.

Retrogressed domains within the Someş assemblage record Mesozoic thermal and structural effects. Shallow-dipping phyllonites overprinting various Paleozoic granitoids throughout western sectors of the HBSZ record effects of Aptian to Albian (114-100 Ma) north-vergent thrusting and concomitant low-grade metamorphism. A penetratively sheared Triassic siltstone in the footwall yielded a similar whole-rock plateau date of c. 117 Ma. Southern sectors of the Baia de Arieş carbonate-lense gneissic assemblage record both Jurassic (186 Ma; 156 Ma) and Early-Middle Cretaceous (124-111 Ma) plateau dates in different structural units.

Fig. 6-1. Stretching lineation within the Highiş-Biharia shear zone; highly variable orientation of planar structures contrasts with constant subhorizontal orientation of linear structures: a), b) and d) sheared leucogranite in the upper crustal igneous complex exposed in the northern Highiş Mountains, Arăneag Creek (L = 150-160 / 5-10); c) sheared granodiorite in the Biharia Mountains, Dedului Creek, L = 115/10. L - linear structure; S - foliation.

a.

b.

c.

d.

Fig. 6-2. Stretching lineation within the Baia de Aries assemblage metre-size mullions and mineral lineations are everywhere consistent and subhorizontal in the garnet-bearing plagiogneiss of the Baia de Arieş assemblage along the contact with the Highiş-Biharia shear zone: a) L = 70/3; b) 80/20; c) polyphase deformation in the Baia de Arieş assemblage: the main foliation S = 175/45 contains two lineations L1 = 90/10 (hammer) and L2 = 160/25 (marker pen); axis of isoclinal folds are subparallel to L1 stretching: B = 250/10.

a.

b.

c.

The Trascău shear zone has not been dated yet; it is cut by Late Cretaceous -Paleogene "Banatite" calc-alkaline intrusions. It projects southward into highly strained Late Jurassic-Cretaceous flysch-like sequences of the Mureş Basin.

Basement units of the Apuseni Mountains indicate that Alpine strain in interior sectors of the Carpathian arc was gradually accommodated within major shear zones. Transcurrent faulting and local thrusting are variably obliterated by widespread extensional structures around the central Someş-Muntele Mare basement unit and resulted in juxtaposition of contrasting structural units which include both metamorphic assemblages and Permian-Mesozoic cover.

No unequivocal data constrain the development of medium-grade textures to the time of Variscan tectonism. Internal strain in low-grade metamorphic assemblages indicates that revision of the previous model of coherent basement nappes is required. Synkinematic hydration and carbonation reactions within wide Alpine shear zones overprinting older crust resulted in the development of a low-grade lithology dominated by phyllonite and thin carbonate and quartzite layers.

Sedimentary record. In the northwestern Apuseni Mountains, Carboniferous (?) - Permian conglomerate records post-Variscan exhumation of the Someş assemblage following the emplacement of the Muntele Mare batholith at c. 295 Ma. Triassic to Middle Jurassic strata record a passive continental shelf and Tithonian to Neocomian flysch-like strata indicate a subsiding trough between the central Gilău Mountains and the western Codru Mountains. Flysch-like strata along the southern and eastern margin of the Apuseni Mountains, in the Mureş Basin, indicate active Middle Jurassic-Cretaceous tectonism. Around 90-100° clockwise rotation since Late Cretaceous documented by paleomagnetic data (Pătraşcu et al., 1990), indicates that the northern basin was facing the Mesozoic Vardar Ocean to the southwest, and that the Mureş Basin separated the Apuseni and Carpathian basement units to the northwest. Mafic intrusions in Albian flysch strata indicate extension during flysch deposition. "Wildflysch" belts within flysch sequences are spatially and most likely genetically related to zones of Alpine strain overprinting basement rocks.

6.3. BASEMENT UNITS OF THE NEOGENE PANNONIAN BASIN

Low-grade metamorphic rocks and associated granitic bodies similar to those exposed in the HBSZ have been reported in drill cores from the Vojvodine region of Serbia (Kamenci and Čanovic, 1975). North of the HBSZ, intense carbonate and/or sodium metasomatism associated with shearing and retrogression of medium- to high-grade crust resulted in locally complete pseudomorphing of mica and feldspar by carbonate and/or albite (Nusszer, 1986). The retrograde overprint diminishes northward, and southwest-trending "metamorphic regional units" recognized in core samples from the southern Pannonian basement (Szili-Gyémánt, 1986;

Nusszer, 1986; Cserepes-Meszéna, 1986), roughly match lithotectonic assemblages exposed in the westernmost part of the Apuseni Mountains (Fig. 5-21). An association similar to the Codru assemblage can be recognized in drill core from the Körös-Berettyó and Szank areas and in outcrops in the Mecsek, northern Papuk, and Moslavacka Gora mountains (Szili-Gyémánt, 1986; Nusszer, 1986; Cserepes-Meszéna, 1986; Pamič, 1986). The northernmost outcrop of the Someş assemblage in the Plopiş Mountains correlates with the basement rocks drilled in the Álmosd region of the Pannonian Basin (Szili-Gyémánt, 1986). Some variability is seen along strike. Several northwest trending mylonite zones in drill holes are parallel with the Szolnok transcurrent fault zone (Fig. 5-21), suggesting a genetic relationship which casts doubt on the current nappe interpretation extrapolated from the Apuseni Mountains (Dimitrescu, 1981; Szederkényi, 1982; Balázs et al., 1986, Grow et al., 1989).

Farther west, in the central Slavonian Mountains, low-grade rocks similar to those of the HBSZ assemblage separate the northern Papuk-Jankovak and the southern Psunj-Kutjevo medium-grade complexes (Pamić, 1986; 1993) each with strata correlative with the Codru and Baia de Arieş assemblages, respectively. As in the Apuseni Mountains, shearing and retrogression of medium/high grade rocks resulted in the development of the Ravna Gora phyllonitic belt across the Papuk-Jenkovac complex and of mappable bands of graphite- or chloritoid-blastomylonite and gneissic or phyllonitized granite across the Psunj-Kutjevo complex (Pamić, 1986). Along the dextral Sava shear zone, cut by Tertiary calc-alkaline intrusions, the Prosara-Motajica complex (Pamić, 1986) represents the westernmost, slightly retrogressed exposure of the Baia de Arieş assemblage.

In the Mecsek Mountains, the Mecsek migmatitic gneiss is separated from the Moragy-Gorcsony staurolite and kyanite-bearing gneiss, with eclogite and pyroxenite pods, by the retrogressive Ófalu assemblage. Retrogressed gneiss, granites, amphibolite, pyroxenite with calc-silicate schist and marble define a 1-2 km wide NNE trending lineament of high strain and retrogression sealed to the south by Upper Carboniferous coal bearing strata (Fig. 5-21). Rb-Sr isochron dates and K-Ar dates indicate tectonism and metasomatism between c. 284 - 270 Ma (Svingor and Kovach, 1981; Balogh et al., 1983). In the western Mecsek, a 200 m-wide zone of retrogression overprints migmatitic gneiss, micaschist and mafic protoliths, and west of the Mecsek Mountains, phyllonite that overprints granulite rocks drilled at Gorgeteg-Babocsa (Jantsky et al., 1988) can be traced southwestward into the Molve area of the Slavonian Mountains.

Post-kinematic Variscan granitoids exposed in the Transdanubian Mountains yielded Rb-Sr and K-Ar dates of 310-330 Ma along Lake Balaton and K-Ar dates of 270-290 Ma at Velence (Balogh et al. 1983). Southeast of Lake Balaton, drillholes reached a partly retrogressed marble-bearing assemblage that records medium-grade, medium-pressure metamorphism (garnet and staurolite) followed by low-pressure overprint (up to andalusite) related to Variscan granitoid intrusions (Árkay, 1987). The rock-type described as "porphyroid" in the Bakony Mountains is located along a wide lineament of Alpine tectonism defined by retrogression of the gneissic basement at Lake Balaton and prograde metamorphism of Paleozoic-Mesozoic strata in the Bükk-Uppony Mountains.

"Porphyroids" described in a limited area close to Zemplin, at the Hungarian-Slovakian border, appear to be the result of shearing and retrogression of the adjacent gneiss-granitic crust. Kyanite-staurolite-sillimanite bearing gneiss from Zemplin yielded K-Ar dates for amphibole and muscovite of 307+/-14 Ma and 222+/- 9 Ma, respectively. The overprinting strain accompanied by retrogression is likely related to Alpine tectonism.

6.4. BASEMENT UNITS OF THE SOUTH CARPATHIANS

In the northern part of the South Carpathians, the Suru and Padeş micaschist plagiogneiss and amphibolite assemblages include kilometre-sized lenses of variably dolomitic marble. To the south, the Cumpăna, Sebeş-Lotru, Leaota, and Danubian assemblages define a granite-plagiogneiss crust with scattered ultramafic and eclogite lenses and insignificant marble layers. Sebeş-Lotru, the largest exposure of medium-grade rocks shows flat-lying lithological units draped around granite domes (e.g., Stelea, 1994). The Sebeş-Lotru succession is regarded as a composite Precambrian assembly of crustal slices with distinct M1 evolution, stacked during M2 collision at intermediate crustal levels; this was followed by diapiric addition of lower crust during M3 (Săbău, 1994).

Several zones of retrogression throughout the South Carpathians show progression from intact medium-grade assemblages through rocks variably overprinted by chlorite, sericite, carbonate, sulfide and oxide, to a zone of complete mineral and textural reequilibration (see chapter 2). Ultimately, gneissic rocks are replaced by various phyllonites with discontinuous layers or lenses of carbonate and white and black quartzite with graphite and sulfides which can be followed tens of kilometres along strike (e.g., Piatra Dracului crystalline limestone and Boldanu Quartzite along the southern periphery of the Sâmbăta shear zone, Pană, 1990). Kinematic indicators are consistent with strike-parallel and/or normal detachment.

The best- expressed asymmetric normal shear zones are the Moldele, Ursu, and Vidra chlorite ± chloritoid phyllonite assemblages overprinting the Suru, Sebeş-Lotru and Danubian assemblages, respectively.

The most prominent transcurrent low-grade shear zones are the Leşcoviţa shear zone mainly in a composite igneous protolith and in the adjacent Sebeş-Lotru assemblage and its Carboniferous cover strata (Fig. 6-3a), the Sibişel shear zone in Sebeş-Lotru assemblage (Fig. 6-3b and 6-4), the Sâmbăta shear zone in Suru assemblage (Fig. 6-5), the Corbu, Vodna and

Lainici shear zones in Danubian assemblages (Fig. 6-6 and 6-7).

Sm-Nd data for two samples of kyanite-bearing plagiogneiss from the Sebeş-Lotru assemblage yielded very similar T_{DM} model ages of c. 2 Ga and εNd values of c. -14.5, suggesting similar protoliths with Early Proterozoic inheritance. One sample of a retrogressed plagiogneiss from the Suru carbonate assemblage yielded the same T_{DM} but a less negative $\varepsilon Nd_{(0)}$ value of -10.5. These data are in good agreement with data on the gneiss-granite and carbonate lense-bearing assemblages from the Apuseni Mountains. Scattered Carboniferous $^{40}Ar/^{39}Ar$ dates from muscovite and hornblende concentrates have been interpreted to record a penetrative, relatively high-grade Variscan tectonothermal event (Dallmeyer et al., 1996). The interpretation is questionable because contemporaneous cover strata in the western part of the Getic assemblage do not record metamorphism and c. 10 My younger dates from muscovite (286-309 Ma) compared to hornblende (322-319 Ma) suggest cooling during uplift. Lithotectonic assemblages originally interpreted as Proterozoic stratigraphic units appear to be slices of the lower and middle crust assembled sometime prior to Late Carboniferous. Consistency with interpretations in the Alps would require Early Carboniferous collision (M2) and Late Carboniferous doming (M3). Consequently, $^{40}Ar/^{39}Ar$ data record only the Late Carboniferous passage of the Sebeş-Lotru assemblage across the c. 500°C and c. 400°C isotherms. Similarly, fossiliferous Ordovician-Silurian strata (Stanoiu, 1982) constrain $^{40}Ar/^{39}Ar$ dates of c. 296 Ma from medium-grade rocks of the Danubian units to represent Late Paleozoic cooling during isostatic uplift. K-Ar dates of c. 99 Ma and c. 86 Ma along the Getic-Danubian contact at Petroşani from muscovite concentrate from quartzo-feldspathic and carbonate mylonite, respectively (Ratschbacher et al., 1993) may record development of mylonitic fabric during Cenomanian-Santonian dextral transpression. The same tectonic phase is recorded by a $^{40}Ar/^{39}Ar$ date of c. 99 Ma for a muscovite concentrate (Dallmeyer et al., 1996) along the dextral transpression contact between the Danubian Drăgşani and Lainici-Păiuş assemblages. K-Ar dates of c. 70 Ma (Grünenfelder et al., 1983) for phyllonite from the chloritoid-bearing Schela shear zone suggest Late Cretaceous tectonism along the contact of the southern Danubian Lainici and Schela units, contemporaneous with the shearing of the northern Danubian units suggested by a Rb-Sr data of c. 76 Ma (Ratschbacher et al., 1993). $^{39}Ar/^{40}Ar$ whole-rock dates of c.118 and c. 118.6 Ma within the phyllonite of the Leşcoviţa shear zone record Aptian dextral transpression.

Similarly to the Apuseni Mountains, there are no unequivocal constrains for the development of medium-grade textures during the Variscan tectonism. Fossiliferous early Paleozoic strata overlain medium-grade/granite units of the Danubian basement (Stanoiu, 1982). Kinematic indicators along tectonic contacts are in conflict with the previously inferred major thrusts.

Fig. 6-3. Kinematic indicators along different segments of the shear zone through the Getic crust ("Supra Getic / Getic thrust contact", see Appendix I). a) Kinematic indicators along the Leşcoviţa shear zone in the western part of the South Carpathians; outcrop along Reşiţa-Bocşa highway at Moniom: variably sheared granite pebbles and matrix of the assumed Carboniferous conglomerate underlaying the Getic crust are stretched (L = 37/15) along a subvertical contact roughly oriented 320/70; b) Kinematic indicators along the Sibişel shear zone in the northern part of South Carpathians, south of Pianu village, Strugari Valley; carbonate-mica layer within the Sibişel shear zone display E-W stretching lineation (L = 95/20) in shallowly dipping shear planes (S = 140/25); a few tens of metres to the north, augen gneiss in the "Supra-Getic nappe" display similar stretching lineation (L = 270/22) in steeply dipping shear planes (S = 350/80); S - foliation; L - lineation.

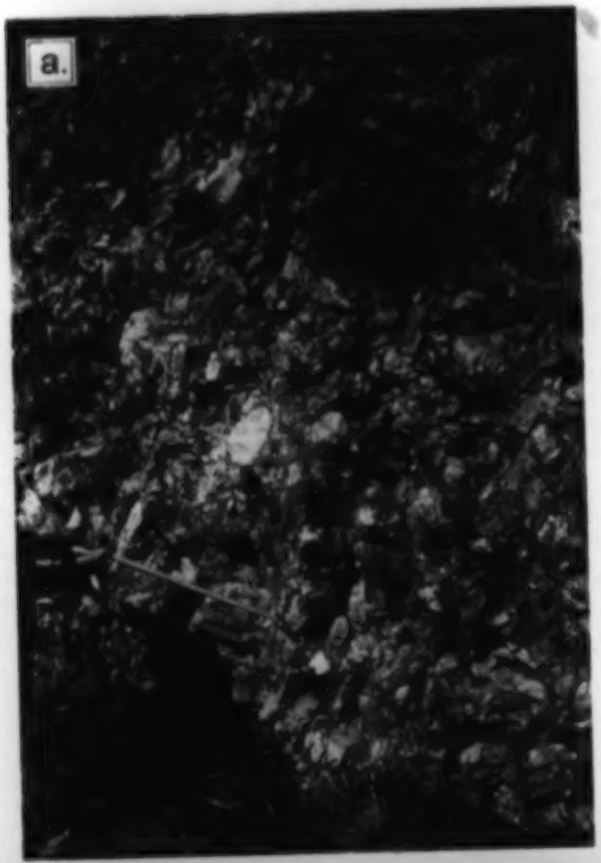
a.

b.

Fig. 6-4. Kinematic indicators along the Sibişel shear zone overprinting the Getic crust in the northern part of South Carpathians, Sebeş Valley ("Supra Getic / Getic thrust contact", see Appendix I); a) progressively sheared and retrogressed augen gneiss of the Sebeş-Lotru assemblage, looking towards the low-grade Sibişel assemblage. S = 185/75; L1 = 270/3; L2 = 255/65. Sinistral shear along L1 (c) is locally overprinted by steeply dipping normal detachment along L2 (b). S - foliation; L - lineation.

a.

b.

c.

Fig. 6-5. Kinematic indicators in the northern Făgăraş Mountains, eastern part of the South Carpathians, Bâlea Valley; linear structures have variable plunges but very consistent trend throughout the retrogressed garnet-bearing plagiogneiss; a) Bâlea Falls, L = 290/35; b) Bâlea Lake, L = 80/15. In both cases L is the orientation of fold axis which is consistent with the mineral stretching and with the local trend of the orogen. L - lineation.

a.

b.

Fig. 6-6. Kinematic indicators along the Corbu shear zone overprinting the Danubian crust in the southwestern part of the South Carpathians ("the Upper Danubian Duplex", see Appendix I); Ponicova Creek 7 km upstream from the confluence with the Danube River, locality 8 in Fig. I-4. The sheared eastern periphery of the Iuţi gabbro, S = 237/85, L = 155/2. S - foliation; L - lineation.

a.

b.

Fig. 6-7. Kinematic indicators in the southwestern part of the South Carpathians along the contact between the Getic and Danubian units ("the Getic / Danubian thrust contact", see Appendix I); a) Armeniş village; biotite plagiogneiss interlayered with marble, S = 30/75, L = 305/5. b) along the Danube River at Portile de Fier; the foliation wraps around steeply plunging linear structures developed in two mica garnet plagiogneiss, L = 200/47; c) Urgonian limestone of the Danubian cover at Obârşia Cloşani; S = 130/30, L = 190/20. S - foliation; L - lineation.

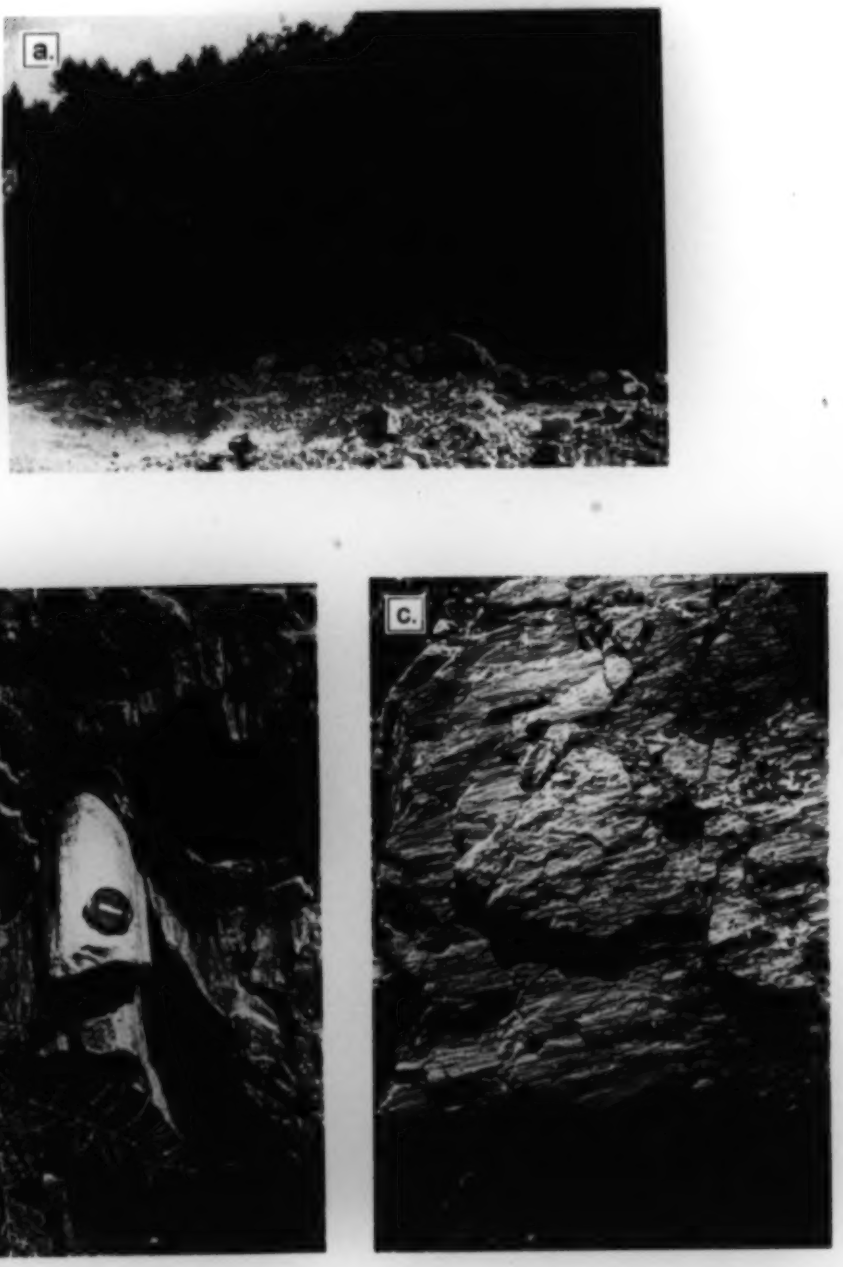
a.
b.
c.

Stratigraphic Record. Several faults and fault zones are overlain by Cenomanian or Upper Senonian strata deposits. Barremian-Aptian reef deposits of the Reşiţa-Moldova Nouă Basin on Getic crust extend as isolated outliers on the adjacent "Supra-Getic" basement indicating the same Early Cretaceous facies zone and modest relative displacement between the two units. Along the Mureş River, a succession of Vraconian to Coniacian strata overlie Supra-Getic and Transylvanide units, in total conflict with their previous interpretation as Late Cretaceous nappes verging south and north, respectively.

6.5. BASEMENT UNITS OF THE EAST CARPATHIANS

In the eastern part of the East Carpathians, the Bretila assemblage includes the Hăghimaş-Pietrosu-Rarău granitoids and gneiss; the Rebra assemblage dominated by the presence of crystalline dolo/limestone and amphibolite within mica-plagiogneiss crops out mainly in the western part of the East Carpathians (Fig. 6-8).

The original relationships between the two medium-grade assemblages are obliterated by a mesh of north-south trending, steeply dipping retrograde shear zones. Lens-shape domains of granitic crust are preserved at Rarău and Hăghimaş (former "nappe outliers") and of Rebra-type crust at Iacobeni (former "tectonic window"). Various stages of shearing and retrogression are recorded from the Hăghimaş intact granitic crust to augen gneiss on the Rarău granite or to low-grade mylonites ("porphyroides") on the Pietrosu granodiorite. The axial zone of the phyllonite belts are dominated by graphite and mineralized quartzite and schist, thin and discontinuous layers of calc-silicate rocks and marble. The Bălan shear zone separates the western carbonate and the eastern granitic crust. The Tulgheş shear zone overprints the non-carbonate assemblage separating the eastern Rarău-Bretila gneiss unit and the western Hăghimaş-Pietrosu granitoid unit. Zones of incomplete retrogression along the low-grade shear zones previously mapped as distinct stratigraphic units (e.g., Chiril and Ţibău "Series" -Nedelcu, 1984, Negrişoara "Series"-Balintoni et al., 1983; Balaj "Formation"-Bindea et al., 1990), include metasomatic quartzite layers previously interpreted to mark stratigraphic unconformities (e.g., Gliganu Quartzite between the Vaser [Tulgheş equivalent] and Rebra groups in the Maramureş Mountains).

Along strike, the subvertical transcurrent shear zones dip east or west. Thus, the northern segment of the Bălan shear zone dips steeply mainly eastward (at Iacobeni) whilst the southern segment dips steeply mainly westward (at Bălan); the Tulgheş shear zone dips generally westward in the northern segment (at Pojorita), eastward in the central segment and is subvertical in the southern segment (at Dămuc) (Fig. 6-9). Everywhere, stretching lineation is subhorizontal and orogen-parallel (Figs. 6-9 and 6-10).

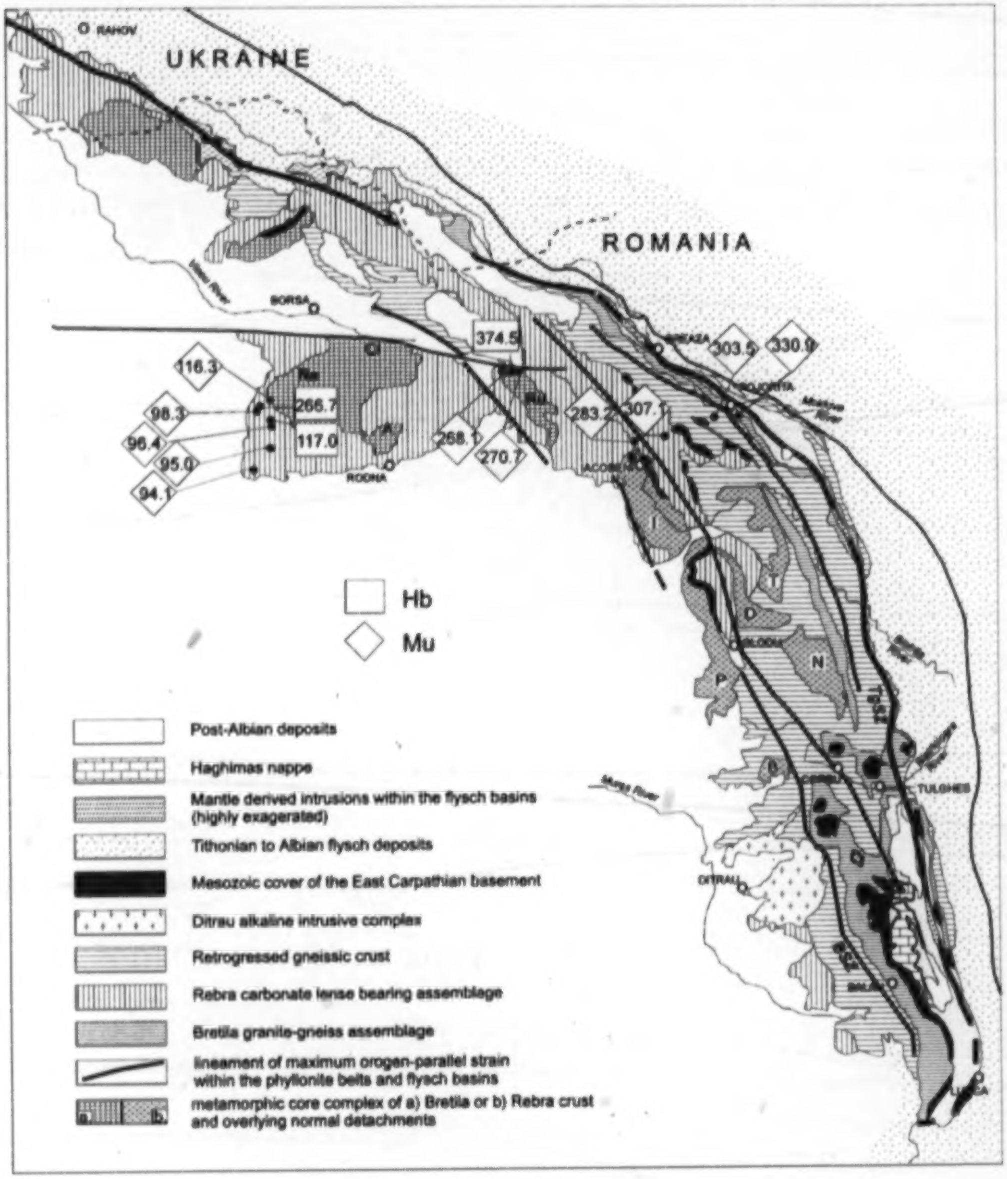
RAHOV
UKRAINE
ROMANIA
BORSA
374.5
116.3
Re
98.3
266.7
96.4
117.0
95.0
94.1
Ci
Ru
A
RODNA
268.1
270.7
283.2
307.1
303.5
330.9
ACOBENI
I
T
D
N
P
B
TgSZ
BSZ
TULGHES
DITRAU
Mures River
Hb
Mu
Post-Albian deposits
Haghimas nappe
Mantle derived intrusions within the flysch basins (highly exagerated)
Tithonian to Albian flysch deposits
Mesozoic cover of the East Carpathian basement
Ditrau alkaline intrusive complex
Retrogressed gneissic crust
Rebra carbonate lense bearing assemblage
Bretila granite-gneiss assemblage
lineament of maximum orogen-parallel strain within the phyllonite belts and flysch basins
a
b.
metamorphic core complex of a) Bretila or b) Rebra crust and overlying normal detachments

Fig. 6-8. Tectonic sketch with the major low-grade shear zones exposed in the East Carpathians; transcurrent shear zones: TgSZ - Tulghes shear zone, BSZ - Balan shear zone. Normal detachment shear zones overprinting the Bretila and the overlying Rebra assemblages: Re - Repedea SZ; Ru - Rusaia SZ; A - Anies SZ. Normal detachment within the Bretila assemblage: Ci - Cimpoiasa SZ. Gneissic dome structure in the Rebra assemblage: I-P - Iacobeni-Panaci; D - Darmoxa; T - Tomnatec. Normal detachment overprinting the Rebra assemblage: N - Neagra SZ; B - Borsec SZ. $^{40}Ar/^{39}Ar$ dates from Dallmeyer et al., 1998.

Fig. 6-9. Kinematic indicators along the contact of the East Carpathian basement with the internal flysch unit are consistent with kinematic indicators within the low-grade shear zones: a) S = 270/80 and L = 0/10; Glodu Creek, a right tributary of the Dămuc Creek (less than 10 metres from the unexposed contact of the "Bucovinic nappe" with the most internal flysch unit in the Central East Carpathians); b) detail of the same outcrop; c) linear structures in a mylonitized leucogranite of the Tulgheş shear zone few hundred metres from the contact, Dămuc valley 1.3 km upstream from the confluence with the Glodu Creek. S - foliation; L - lineation.

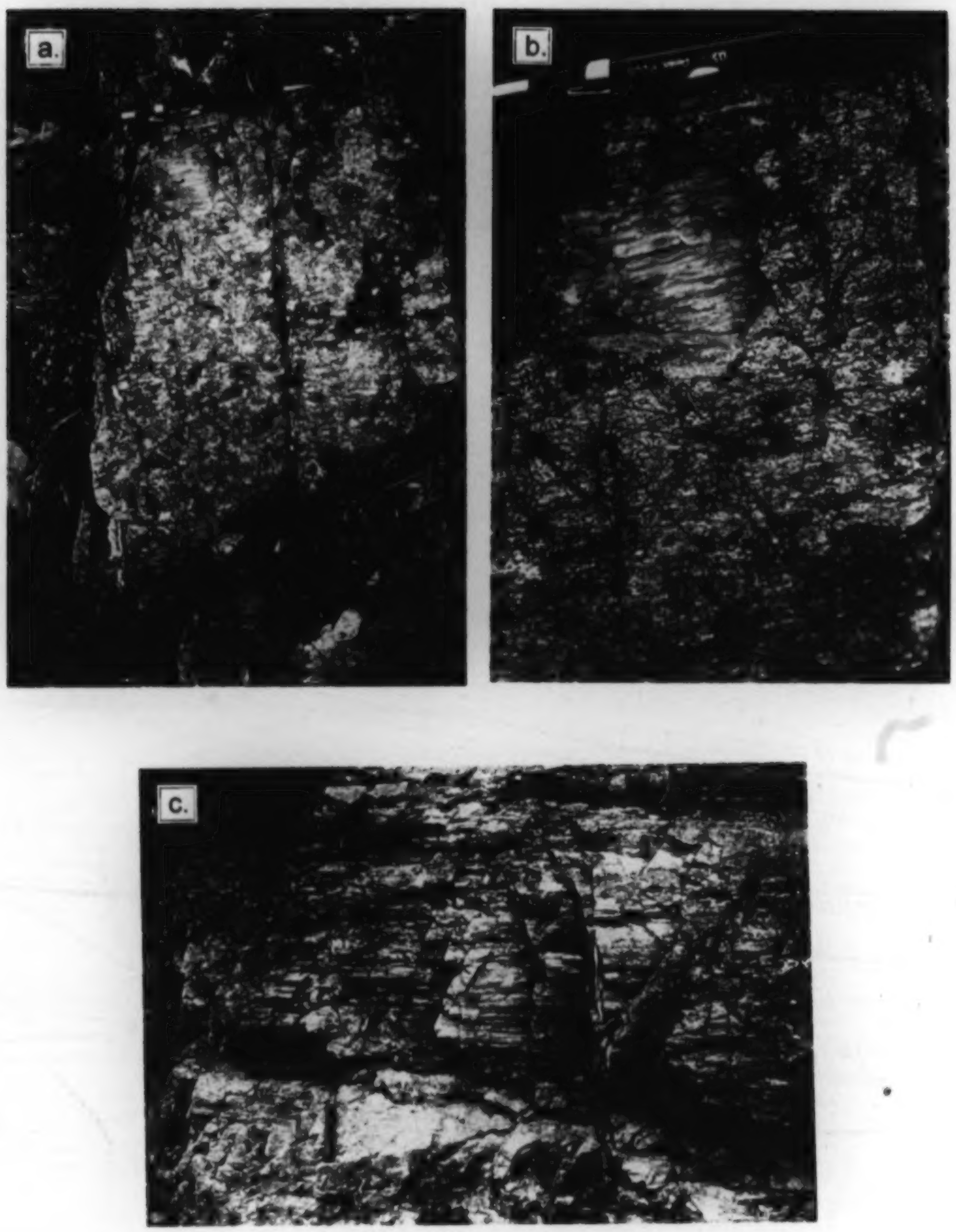
a.
b.
c.

Fig. 6-10. Stretching lineation within the Tulgheş shear zone is everywhere parallel to the local trend of the orogen; a) mylonitic layering in a biotite granodiorite; b) detail: S = 72/40; L = 145/25; the confluence of Bistriţa Valley with the Chiril Valley, central East Carpathians; c) strain in the Bucovinian cover appears consistent with the stretching in the basement: L = 165/5 to 330/25, in variably oriented shear surfaces; Middle Jurassic limestone along the Gheorghieni-Bicaz highway. S - foliation; L - lineation.

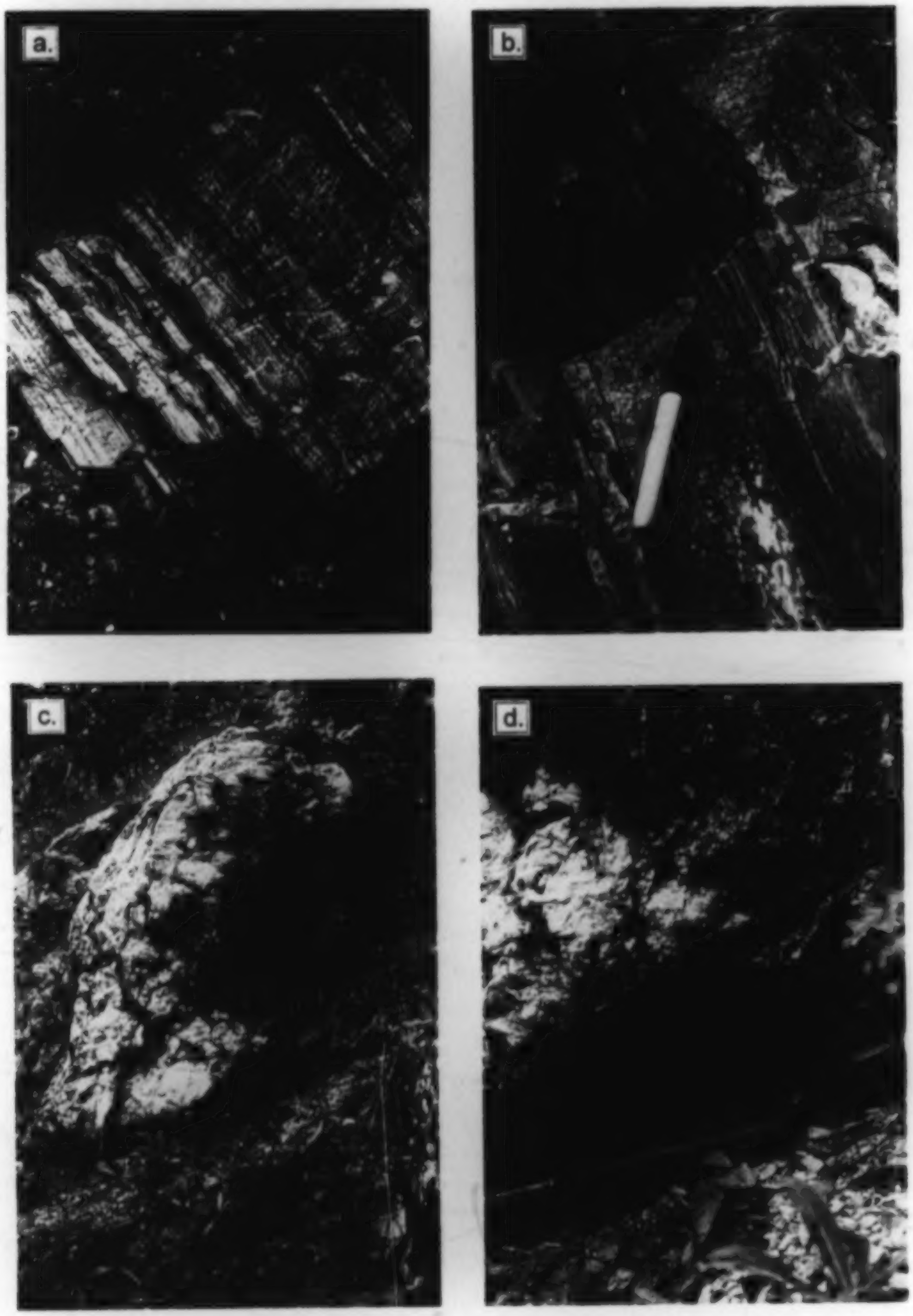
a.
b.
c.
d.

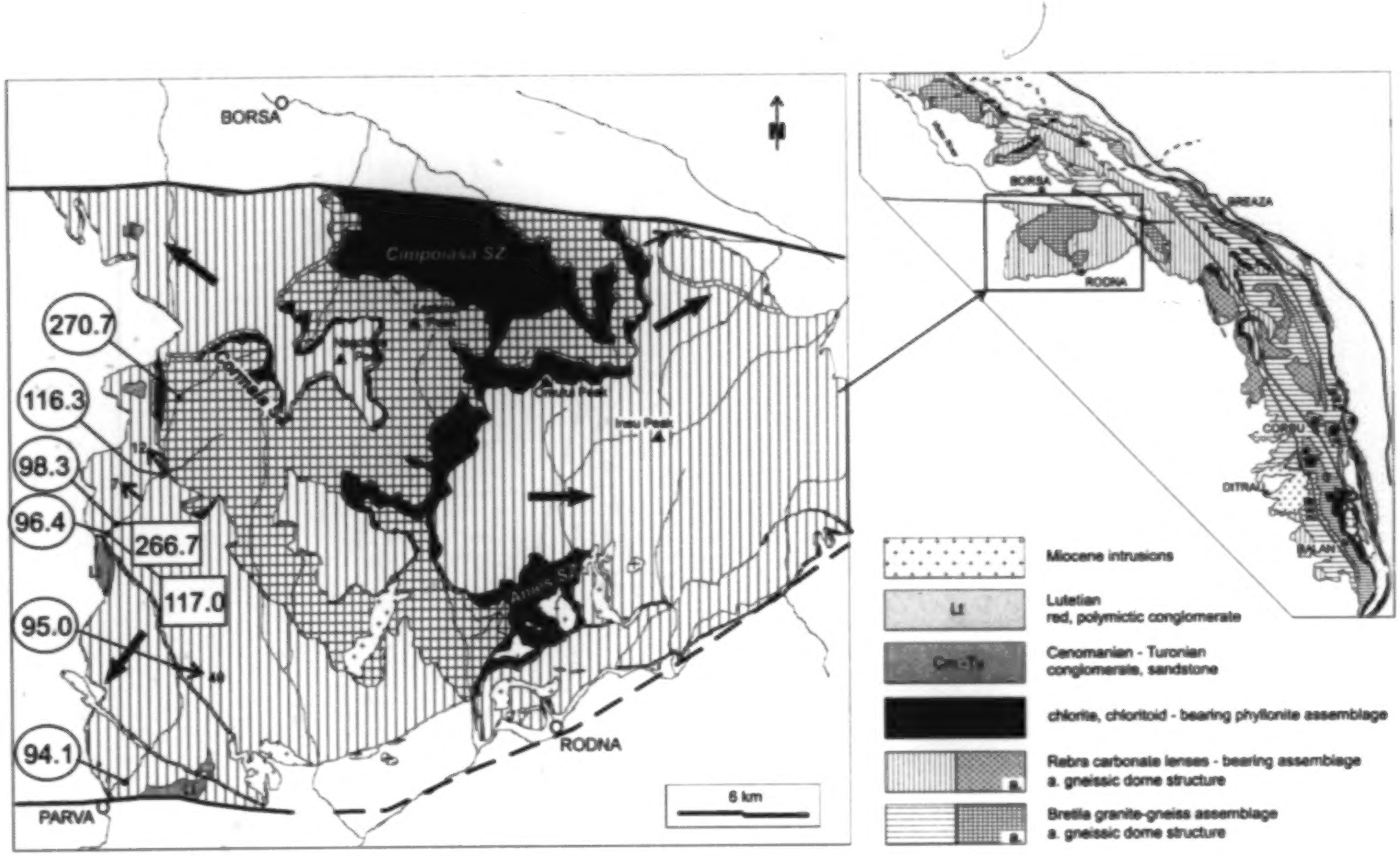
BORSA
Cimpoiasa SZ
Cormaia SZ
Anies SZ
Gargalau Peak
Ineu Peak
RODNA
PARVA
270.7
116.3
98.3
96.4
266.7
117.0
95.0
94.1
N
6 km
BORSA
BREAZA
RODNA
CORBU
DITRAU
BALAN
Miocene intrusions
Lt
Lutetian
red, polymictic conglomerate
Cm - Tu
Cenomanian - Turonian
conglomerate, sandstone
chlorite, chloritoid - bearing phyllonite assemblage
Rebra carbonate lenses - bearing assemblage
a. gneissic dome structure
Bretila granite-gneiss assemblage
a. gneissic dome structure

Fig. 6-11. Tectonic sketch of the Rodna metamorphic core complex (reinterpreted after Krautner et al., 1978; 1982; 1983; 1989). The Anies and Cormaia normal detachment shear zones overprint both the lower Bretila and the upper Rebra assemblages; the Cimpoiasa normal SZ overprints mainly Bretila assemblage and merges with the Anies SZ; ^{40}Ar/^{39}Ar ages from Dallmeyer et al.,1998.

In the Rodna Mountains, spectacular phyllonite belts separate the Bretila augen gneiss core from the mantle of Rebra micaschist-pagiogneiss-marble assemblage defining the easward Anieş and the westward Cormaia normal detachments (Fig. 6-11). The Cimpoiasa normal shear zone cuts through gneissic crust in the northern Rodna Mountains and marks the contact with the overlaying Rebra assemblage in the central part of the Rodna Mountains. The dome structure was likely achieved during several phases of Alpine tectonism related to the Cretaceous evolution of the Bǎlan and Tulgheş shear zones and to the Miocene evolution of the North Transylvanian sinistral fault zone.

A garnet plagiogneiss from the Bretila assemblage yielded a T_{DM} model age of 2 Ga and $\varepsilon Nd_{(0)}$ of -14.6, almost identical to those obtained from the gneiss-granite assemblages of the East Carpathians and Apuseni Mountains. An andalusite-bearing gneiss from the Rebra assemblage (N - in Fig. 6-8) yielded a T_{DM} model age of 1.85 Ga and $\varepsilon Nd_{(0)}$ values of -13, in the range obtained from carbonate-lense bearing assemblages in the other analysed segments of the orogen. Granite phyllonite in the Bǎlan shear zone yielded a very similar T_{DM} model age around 1.6 Ga and $\varepsilon Nd_{(0)}$ values around -10.5, in the same range as the Paleozoic granitoids from the Apuseni Mountains.

$^{40}Ar/^{39}Ar$ data from a few muscovite concentrates from the Tulgheş phyllonitic granite indicate Late Carboniferous syn-kinematic development of mica. However, Mesozoic strata, especially Triassic dolomite, incorporated in the low-grade shear zone in the Bistriţa and Maramureş mountains indicate its Alpine exhumation and reactivation.

In the Bistriţa Mountains $^{40}Ar/^{39}Ar$ analyses of medium-grade rocks yielded c. 375 Ma from a hornblende concentrate and dates between c. 283 to 271 Ma from muscovite concentrates, suggesting Devonian and Permian uplift above the 500°C and 400°C isotherms, respectively. In the Rodna Mountains, medium-grade rocks yielded a range from c. 117 to c. 94 Ma, indicating an evolution from intermediate to shallow structural levels during the middle Cretaceous.

Stratigraphic record. The main remnant of the Mesozoic cover sequence preserved in the Hǎghimaş syncline includes two lineaments of megabreccias and mafic rocks previously mapped as wildflysch horizons within the Albian flysch (Sǎndulescu et al, 1975). Mafic rocks interpreted as remnants of a far-travelled Transylvanian Nappe are located exclusively along these lineaments and are spatially associated with *in situ* vesicular and spilitic basaltic flows (Panǎ and Bindea, 1982, unpublished data). The main lineament is 1 to 1.5 km wide and stretches NNW-SSE on the eastern side of the syncline. It projects northward into the Tulgheş shear zone and farther north it follows the centre of the Rarǎu syncline marked by the middle Triassic limestone at Botuş cut by a mafic dyke and by the large serpentinized dunite-gabbro at Breaza. The second lineament is less well expressed, runs through the centre of the Hǎghimaş

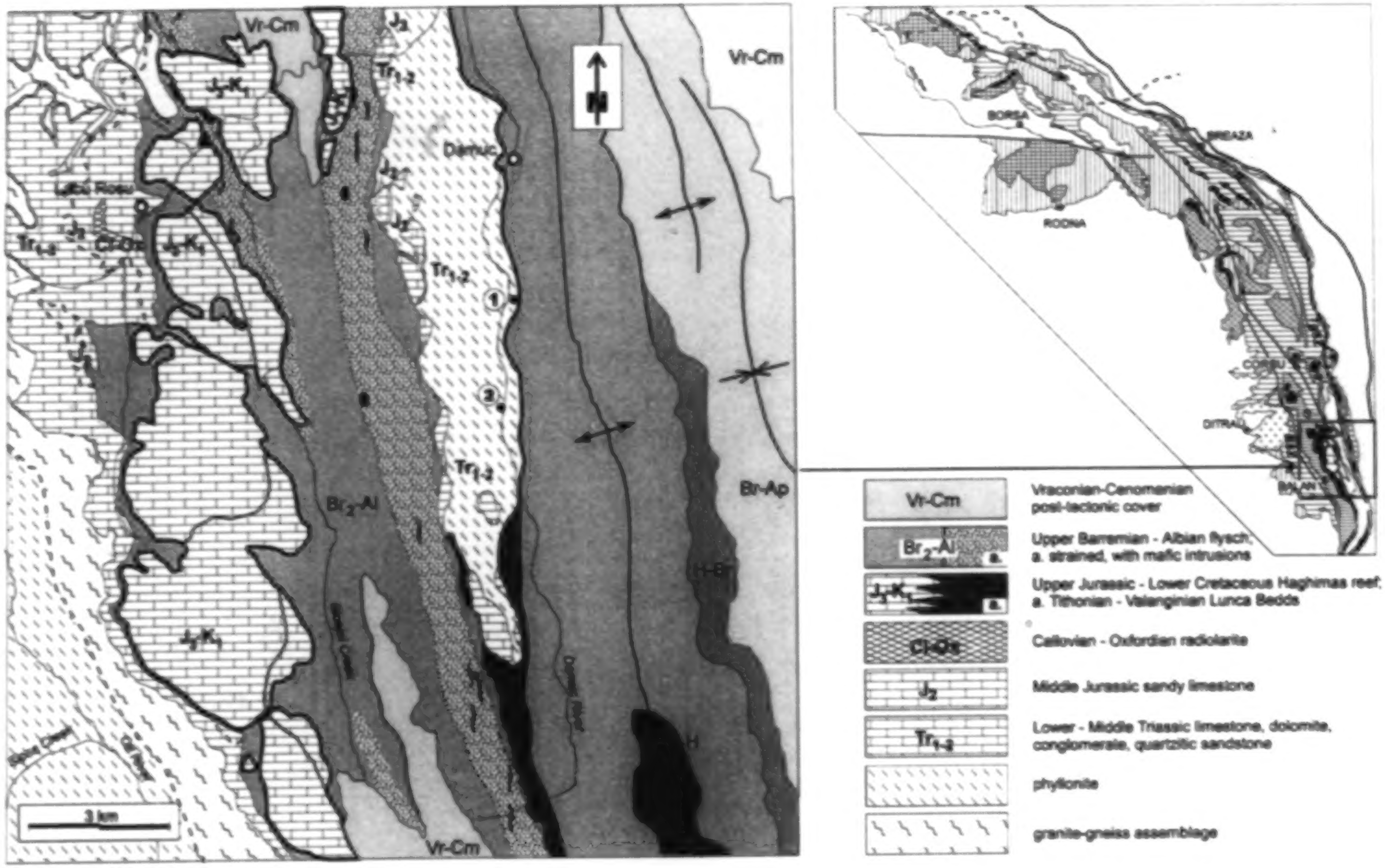
Vr-Cm
J2
Tr1-2
J3-K1
Damuc
Lacu Rosu
J2
Cl-Ox
J3-K1
Tr1-2
1
2
Br2-Al
Br-Ap
H-Br
H
J3-K1
Vr-Cm
3 km
N
BORSA
BREAZA
RODNA
CORBU
DITRAU
BALAN
Vr-Cm
Vraconian-Cenomanian post-tectonic cover
Br2-Al
a.
Upper Barremian - Albian flysch; a. strained, with mafic intrusions
J3-K1
a.
Upper Jurassic - Lower Cretaceous Haghimas reef; a. Tithonian - Valanginian Lunca Bedds
Cl-Ox
Callovian - Oxfordian radiolarite
J2
Middle Jurassic sandy limestone
Tr1-2
Lower - Middle Triassic limestone, dolomite, conglomerate, quartzitic sandstone
phyllonite
granite-gneiss assemblage

Fig. 6-12. Tectonic sketch of the Haghimas sincline on the eastern margin of the East Carpathians basement; reinterpreted after Sandulescu et al., 1975. Numbers are locations discussed in text. Location 1 is shown in Figs. 6-9 a and b, and location 2 in Fig. 6-9 c.

syncline and projects into the spectacular northwest trending graphite-mylonite at Capu Corbului (Fig. 6-8)

The rock distribution along the eastern lineament suggests a transcrustal discontinuity along the eastern margin of the East Carpathian crustal fragment which provided a conduit for mantle derived materials.

The main body of the Hăghimaş nappe consists in fact of the missing members of the Bucovinian sequence in the western limb of the syncline (Fig. 6-12). A normal detachment formed approximately at the level of the Kimmeridgian jasper appears to have allowed about 10 kilometres of eastward gravitational gliding of the Late Jurasic-Early Cretaceous reef into the Albian flysch basin.

The compiled stratigraphy of the Transylvanian nappe (Săndulescu, 1984) is misleading, as the paleogeography of the Mesozoic Bucovinian shelf towards the eastern flysch basins can be reconstructed. The only reasonably constrained nappe structure is a typical gravitational nappe with a horizontal displacement of a few kilometres. Similarly to the Fatric nappes of the West Carpathians and to the Bajuvaric, Tirolic, and Juvavic nappes of the Eastern Alps (Northern Calcareous Alps), the Hăghimaş nappe is a cover sequence that glided from the uplifted basement towards the external Cretaceous flysch basin. The derived generalization of huge and far-travelled basement nappes appears completely unsupported.

Relics of the most "internal" flysch trough on the Carpathian crust are represented by the Rarău and Hăghimaş synclines. Similarly to the southern Apuseni Mountains, extensional tectonism during Albian flysch deposition was accompanied by mantle intrusions into the flysch basins. The extensional tectonic regime up to the Albian is in conflict with the interpreted phase of major Aptian-Albian ("Austrian") thrusting.

Rock assemblages previously interpreted as wildflysch successions in the East Carpathians are strictly confined to a linear zone of orogen-parallel strain concentration within flysch strata with slices of the underlying Triassic and Jurassic cover ("klippe"). Deeper levels of the high-strain zone expose the graphite-phyllonite Tulgheş shear zone developed on the Bucovinian basement.

6.6. BASEMENT UNITS OF THE WEST CARPATHIANS

Gneiss-granitic crust is represented by the Hron - Cierny Balog assemblage of plagiogneiss-micaschist-amphibolite-serpentinized peridotite intruded by the Carboniferous Dumbier and other Tatric granitoids in the northern part, and by the Veporic and Hrancok granitoids in the southern part of the West Carpathians. To the interior of the West Carpathians arc, the Kohut assemblage of micaschist, micaceous quartzite, graphite quartzite, amphibolite, crystalline dolo-limestone and metasomatic magnesite serpentinite and talc is the local

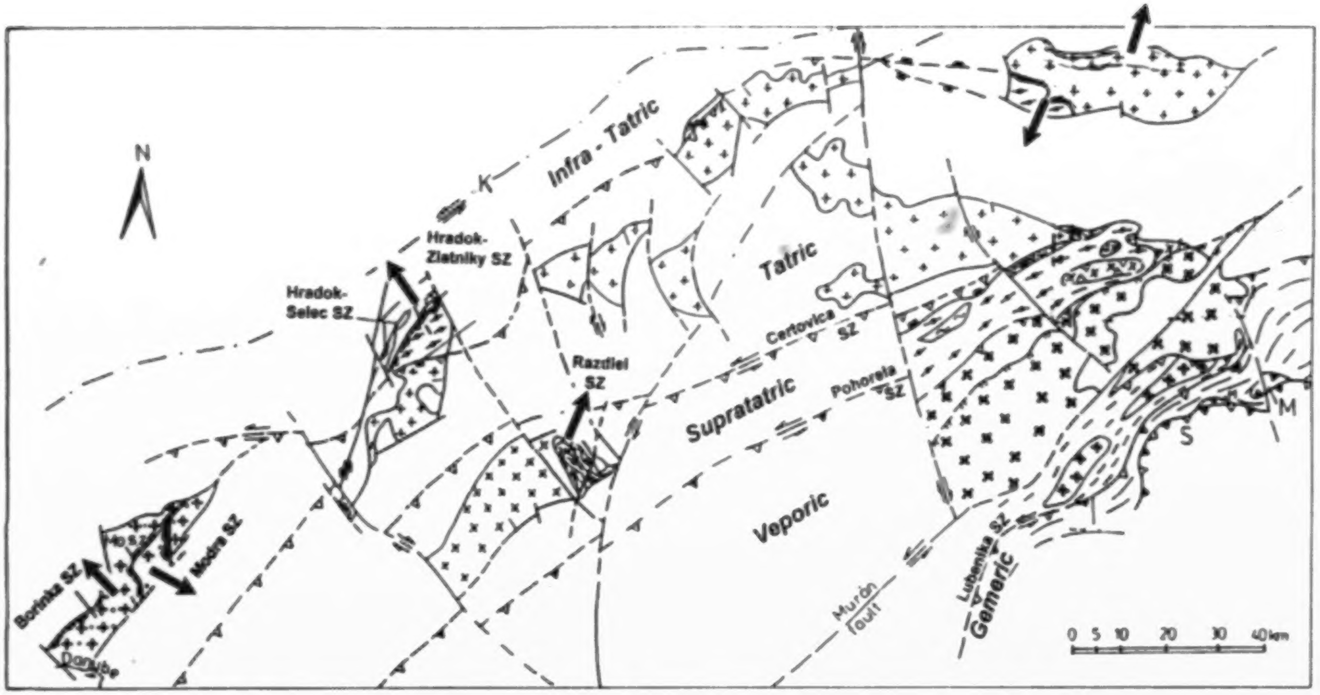
N
Infra - Tatric
K
Hradok-Zlatniky SZ
Hradok-Selec SZ
Tatric
Certovica SZ
Razdiel SZ
Supratatric
Pohorela SZ
Veporic
Muráň fault
Lubenika SZ
Gemeric
S
M
Borinka SZ
Modra SZ
Danube
0 5 10 20 30 40km

Fig. 6-13. Tectonic sketch of the basement units in the West Carpathians with the inferred transcurrent and normal shear zones (Modified after Biely et al., 1966 and Putis, 1994)

expression of the micaschist-carbonate crust.

Flat-lying medium-grade successions are overprinted by moderately to steeply dipping sinistral strike-slip and low-angle normal shear zones. Intermediate and shallow structural levels of transcurrent shear zones are now exposed in the central West Carpathians (Fig. 6-13). The Certovica and north Pohorela low-grade shear zones overprint gneiss-granitic crust. The elusive contact between granite-gneiss and carbonate assemblages is overprinted by the sinistral Muran shear zone. Quartz and feldspar microstructures in the foliated granite indicate ductile deformation, and the breakdown of the granitic and/or medium-grade paragenesis indicates mylonitization temperatures at and below 450° C and abundant hydration. Wide zones of ductile deformation developed under mid-crustal conditions were gradually exhumed and are obliterated by brittle faults with similar kinematics. Variably dipping gneissic foliation shows stretching lineation consistent with the adjacent strike-slip brittle faults.

The inferred Veporic sole thrust, the "Certovica line", is a major strike-slip fault recently interpreted to cut Tatric basement (Putiš, 1994). Shearing under low-grade conditions of the Tatric granitoids along the Certovica line resulted in mylonitic granite assemblages: to the north, the Boca Formation is derived from the Dumbier granodiorite, and to the south the Lubietova zone of mylonite and retrogression is derived from Tatric granitoids. Steeply dipping foliation (Zoubek, 1960) and subhorizontal stretching lineation with sinistral shear sense (Putiš, 1994) is indicative of transcurrent kinematics. Lower Triassic quartzitic conglomerate/quartzite and Middle Triassic dolo-limestone (Zoubek, 1960) of the Tatric cover sequence is locally strained and slightly metamorphosed (Plašienka et al., 1989) within the Certovica shear zone, suggesting post-Middle Triassic transpression.

South of the Certovica tectonic lineaments, the Tatric granite-gneiss assemblage is overlain by the Hron micaschist, plagiogneiss, quartzite, and amphibolite assemblage locally associated with orthogneiss and small size lenses of serpentinized peridotite. Shearing and retrogression led to the development of the Janov Grun complex of phyllonitized micaschist and various low-grade mylonitic granites.

The gneiss and granite assemblage to the south is assigned to the "Austrian" Veporic nappe. The tectonic contact is represented by the Pohorela sinistral shear zone which dips more than 50° south. Associated thrust shear zones in the footwall dipping from 10° to 60° and gently plunging E stretching lineation in the hanging wall suggest transpression along the Pohorela shear zone (Putiš, 1994).

Shearing and retrogression of the Kohut assemblage resulted in the Hladnomorna Dolina assemblage being overprinted by contact metamorphism (Vozarova and Kristin, 1986) around the Variscan Rimavica leucogranites (Bibikova et al., 1988). The sinistral Lubenik fault zone is the Cenozoic expression of long lasting intense tectonism within the Gemeride and Meliata

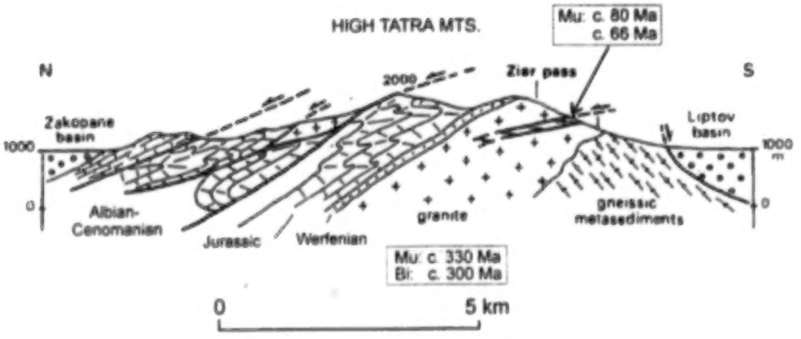

Fig. 6-14. Late-Cretaceous and Paleogene low-grade normal shear zone developed within the gneiss-granite core of the High Tatra metamorphic core complex (*adapted from* Malusky et al., 1993).

lithotectonic assemblages.

To the north, in the High Tatra Mountains, the basement core is a medium-grained, locally porphyritic Variscan granodiorite (324-330 Ma, Malusky et al., 1993) tectonically overlain by Carboniferous to Cretaceous strata of the Veporic (Middle Austroalpine units). Synkinematic sericite on gently northward dipping normal shear zones overprinting the basement records several phases of Alpine rejuvenation at c. 190, 80 and 67 Ma (Fig. 6-14). The best expressed event is the one at the Cretaceous-Tertiary boundary (c. 67 Ma), which corresponds to the initiation of the adjacent Paleogene Podhale Basin.

To the west, the gneiss-granite assemblage is exposed in isolated massifs consisting of a Taric core and Veporic cover of Paleozoic-Mesozoic strata. In the Povazsky Inovec Mountains, a northwest-dipping normal detachment developed across the Tatric gneiss-granite core and resulted in the phyllonitic Hradok-Selec assemblage. In the Little Carpathians, the Borinka and Modra phyllonitic assemblages mark westward and eastward normal detachments respectively, flanking the 347 Ma old (Rb-Sr data) Bratislava granodiorite pluton (Biely et al, 1966; Putiš, 1994). In the Tribec Mountains, the Razdiel phyllonitic assemblage marks a normal detachment northeast of the Tribec granitoid pluton. The "melaphire series" in the northeastern Lower Tatra Mountains defines a north-dipping shear zone of uncertain sense between High and Low Tatra.

The traditional model (e.g., Machel, 1981; Săndulescu, 1988) postulates that the Vahicum branch of Tethys was subducted underneath the Tatric-Veporic continental fragment (Apulian) of African origin which developed Cretaceous nappe stacking. There is no evidence of large-scale Alpine thrusting within the Tatric basement. The only regionally significant record of Alpine tectonism is represented by sinistral transcurrent shear zones accompanied by normal detachment of the Fatric cover.

Striking similarities between the rock types and metamorphic evolution of the basement of the West and East Carpathians casts doubt on their interpretation as distinct African and European crustal fragments, respectively. The granite/orthogneiss-dominated Tatra (Jaraba) assemblage of the West Carpathians (Kamenický and Kamenický, 1988) is similar to the Pietrosu-Hăghimaş-Bretila granite/orthogneiss assemblage of the East Carpathians and occupies the same tectonic position as the first basement unit in transpressional contact with the Carpathian outer flysch. In both regions, medium- to high-grade assemblages are cut by retrogressive, orogen-parallel shear zones, suggesting a common Alpine evolution.

Stratigraphic record. Seismic data show that the Pieniny Klippen Belt is not overthrust by the Tatric crust. The vertical orientation of the Pieniny Klippen belt is proven by deep boreholes and seismic profiles down to 10 km in its central-eastern area (Birkenmayer, 1986) and its extension down to c. 20 km depth is well constrained by deep seismic transects in the central and western parts (Tomek, 1993; Tomek and Hall, 1993) (see Appendix I). The tectonism recorded by the Pieniny Klippen Belt is strike-parallel and affects Mesozoic to Tertiary strata (Birkenmayer, 1986). The Fatric units characterized by the uniform upper Triassic continental sediments (Carpathian Keuper) are gravitational cover nappes of limited extent and displacement around the Tatric granite-gneiss dome structures.

6.7. BASEMENT UNITS AT THE JUNCTION OF THE WEST CARPATHIANS WITH THE EASTERN ALPS

The Leitha Mountains (Fig. 6-15) expose plagiogneiss and staurolite-bearing micaschist intruded by two mica granodiorite-granite-leucogranite. This assemblage is partly retrogressed to quartz-biotite-phyllonite and greenschist with carbonate layers. It is very similar to rocks exposed in the Little Carpathians and to the Grobgneis complex of the Eastern Alps. Granitoid intrusion is coeval: Rb-Sr data from the Bratislava granodiorite pluton of the Little Carpahtians yielded 347 Ma, and the granitoids of the Grobgneis complex, c. 343 Ma. Permian(?) and Triassic cover strata and the underlying retrogressed assemblage in the Leitha Mountains are similar to the "Lamac formation" of the Little Carpathians (Tollmann and Spendlingwimmer, 1978).

To the south in the Sopron Hills, strong shearing/retrogression resulted in a mylonitic assemblage dominated by hornblende-bearing, chlorite-carbonate phyllonite overlain by a distinct assemblage, the Sopron granite-gneiss and the Obrennberg andalusite-sillimanite-microcline gneiss/micaschist, that can be correlated to the Grobgneis of the Eastern Alps. Strong shearing / retrogression and intense metasomatism led to the development of the chloritoid bearing

Vöröshidi phyllonite with kyanite and garnet relics, which defines a subhorizontal shear zone of unknown sense of displacement.

The Rechnitz quartz-phyllite and greenschist-serpentinite assemblages may represent a zone of intense shearing and retrogression overprinting a gneissic protolith and mafic pods, respectively. Most prominent kinematic indicators consist of shallow to moderately SE dipping shear planes with south-west trending subhorizontal stretching lineation and fold axes (Ratschbacher et al., 1990) (see Appendix I). Therefore, strain at the sole of the Austro-Alpine basement nappes interpreted to have accommodated 270 km of northwestward or westward thrust is in fact orogen-parallel. It is likely related to the evolution of the Raba transcurrent shear zone.

6.8. BASEMENT UNITS OF THE EASTERN ALPS

Assemblages dominated by plagiogneiss and various Paleozoic granitoids are known as the Grobgneiss Complex in the easternmost part, as the Core Complex in the north-central part and as the Koriden Complex in the south-central Eastern Alps (Fig. 6-15). Assemblages dominated by micaschist and marble are known as the Micaschist-Marble Complex in the central Eastern Alps (Muriden), and as the Plankogel Complex in the south-central Eastern Alps.

"Quartz phyllite series" appear to define normal shear zones developed asymmetrically around granitic-gneiss domes. Several examples follow:

1. The easternmost part of the Eastern Alps is dominated by the Grobgneiss Complex which consists of plagiogneiss and micaschist with minor intercalations of amphibolitised gabbro and diorit, intruded by various Carboniferous to Permian granites.

    a. The structurally lower Wechsel plagiogranite is sheared and retrogressed to albite porphyroblast plagiogneiss towards its top; mylonitization progressed to a phyllonite (the "Wechsel phyllite") that defines a low-angle normal shear zone to the north and west; to the south, incipient retrogression progressed upwards from an assemblage of albite plagiogneiss interlayered with epidote amphibolite (the "Variegated Wechsel gneiss unit"), to greenschist, white or black quartzite and then decreases through phyllonitized micaschist to the overlying garnet-micaschist, amphibolite, sulphide-bearing black micaschist and quartzite, hornblende diorite-gneiss.

    b. The Wiesmath leucogranite ("Waldbach Complex") grades structurally up into the "Hangenden schiefer", a southeastward low-grade normal shear zone that includes the "Semmering quartzite" at the bottom of the plagioclase micaschist of the Grobgneis Complex.

2. The central part of the Eastern Alps, the Muriden complex shows a dome-like shape, with the more massive plagiogneiss of the structurally lowermost Core assemblage, mantled by plagiogneiss, amphibolite, garnet micaschist, and rare intercalations of thin calc-silicate rocks. A spessartine-bearing mylonitic quartzite within the micaschist suggests a mid-crustal tectonic discontinuity within the Core assemblage similar to the one interpreted in the Sebeş-Lotru assemblage of the South Carpathians (Săbău, 1994). The overlying Speik assemblage is a few hundred meters thick, and dominated by garnet amphibolite with discontinuous layers of augen gneiss, mixed siliceous and dolomitic marble, and serpentinite that contains relics of olivine-gabbro and eclogite. This assemblage grades through a zone of high strain with sulfide-rich quartzite and retrogressed micaschist, into a structurally higher assemblage of garnet micaschist, biotite amphibolite, quartite, black schist, and variably dolomitic marble with abundant pegmatitic bodies.

3. Within the Tauern Window, the Penninic Zentralgneis assemblage consists of various dome-shaped Carboniferous and Permian granitoids generally deformed under low-grade conditions. The Habach-Storz Group consists of biotite plagiogneiss, amphibolite, micaschist and quartzite, and subordinate cummulate pyroxenite. Both micaschist and quartzite are locally graphitic and associated with phyllonite. The overlying Stubach Group consists of amphibolite and gneiss, micaschist, and quartzite with variably serpentinized layered cumulate (Neubauer et al., 1989).

The subdivisions and structure of the Penninic and Austro-Alpine basement are strikingly similar. Their adjacent location at about the same latitude within the orogen suggest their appurtenance to the same continental fragment.

Interpretations of crustal evolution in the Eastern Alps benefit from the greatest number of isotopic data in the orogen. U-Pb data from a hornblende gneiss of the Frauenberg assemblage involved in the Kaintaleck tectonic slices, record emplacement ages of 2.53 Ga for the igneous protolith and contamination with 2.8 Ma old crustal material. U-Pb zircon dates from the tonalitic rocks of the Core Complex yielded upper intercept dates near 3 Ga and 2.25 Ga (Neubauer and Frisch, 1993). These data indicate that Precambrian granitoids are part of the plagiogneiss-granite dominated assemblage, which is widespread in the Alpine-Carpathians orogen.

U-Pb lower intercepts at c. 516 Ma and 356 Ma in orthogneisses from the Frauenberg and Core, respectively (Neubauer and Frisch, 1993;Haiss, 1991) and Rb-Sr dating (c. 518 Ma - Frank et al., 1976) suggest an Early Paleozoic (Caledonian) tectonomagmatic event. Several dates from igneous rocks ranging between 460-425 Ma suggest Late Ordovician-Early Devonian igneous activity.

U-Pb and Rb-Sr dates from granites, granite gneiss and migmatite of the lowermost assemblage of the Eastern Alps range from Ordovician to Carboniferous and are interpreted as

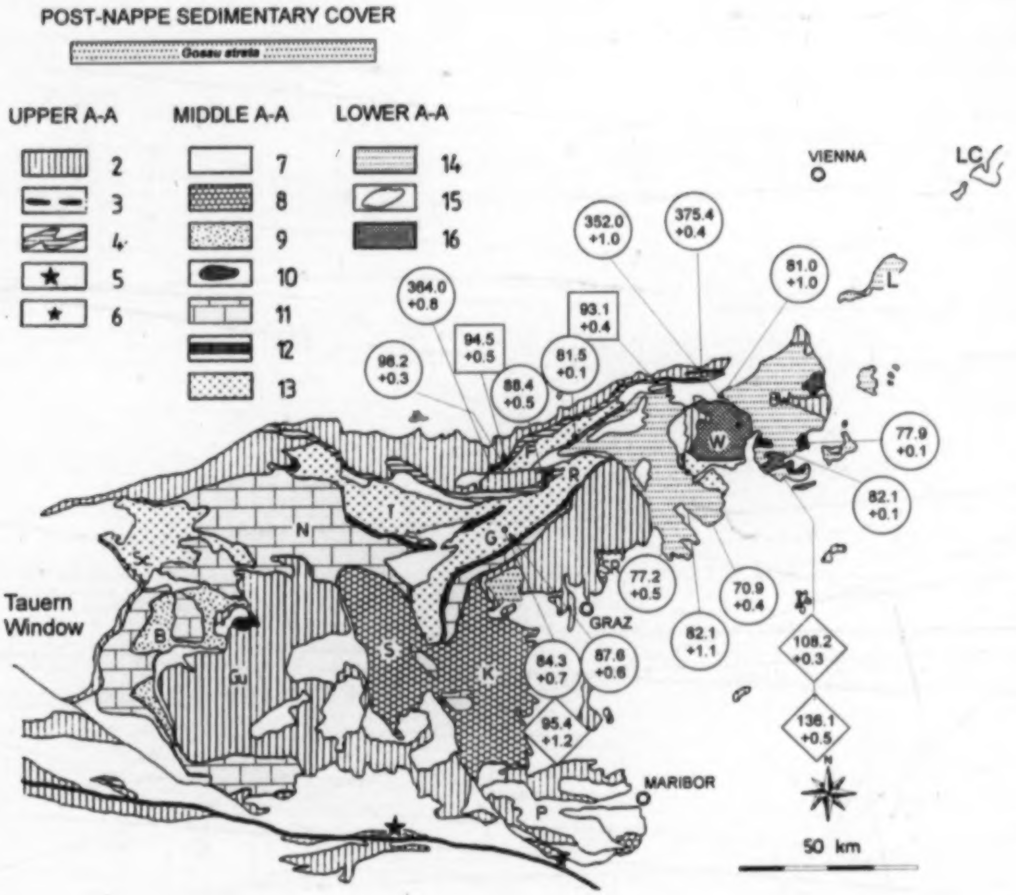
POST-NAPPE SEDIMENTARY COVER
Gosau strata
UPPER A-A
MIDDLE A-A
LOWER A-A
2
3
4
5
6
7
8
9
10
11
12
13
14
15
16
VIENNA
LC
L
352.0 ±1.0
375.4 ±0.4
81.0 ±1.0
384.0 ±0.8
94.5 ±0.5
93.1 ±0.4
98.2 ±0.3
88.4 ±0.5
81.5 ±0.1
77.9 ±0.1
82.1 ±0.1
W
N
T
F
R
G
77.2 ±0.5
70.9 ±0.4
82.1 ±1.1
Tauern Window
B
Gu
S
K
GRAZ
84.3 ±0.7
87.6 ±0.6
95.4 ±1.2
108.2 ±0.3
136.1 ±0.5
MARIBOR
P
N
50 km

Fig. 6-15. Simplified map of the Austro-Alpine basement units east of the Tauern Window (*compiled after* Neubauer and Frisch, 1993 and Dallmeyer et al., 1996); non-metamorphosed strata omitted, except for the tectonically significant Gosau strata. 1 - Late Cretaceous Gosau strata; 2 - Quartz-phyllite and fossiliferous Paleozoic formations; 3 - Kaintaleck slices and Ackerl Complex; 4 - Carboniferous and Permian of the Veitsch Nappe; 5 - Eisenkappel Complex; 6 - Pohorje garnet-peridotite-granulite Complex; 7 - Plankogel Complex and similar micaschist complexes;8 - Koriden Gneiss Complex; 9 - Bundschuh Complex; 10 - Sieggrabener Complex; 11 - Micaschist-Marble Complex; 12 - Speik Complex; 13 - Core Complex; 14 - Grobgneis Complex; 15 - Tatric unit; 16 - Wechsel Gneiss Complex; Gu - Gurktaler Alpen; K - Koralpen; L - Leitha Mountain; LC - Little Carpathians; N - Niedere Tauern; P - Pohorje Mountains; W - Wechsel.

assemblage of the Eastern Alps range from Ordovician to Carboniferous and are interpreted as Variscan tectonomagmatic events. Rb-Sr data from coarse-grained porphyritic granite-gneiss of the Grobgneis Complex are interpreted as Carboniferous emplacement ages (326+/-11Ma; 338+/-12 to 343+/-20 Ma; 353 Ma), similar to the granitoid intrusions in the basement of the West Carpathians (Neubauer et al., 1993; Sharbert, 1981).

^{40}Ar/^{39}Ar dates from basement rocks in the north-central Eastern Alps range from c. 98 to c. 84 Ma. To the east, ^{40}Ar/^{39}Ar data on muscovite throughout the Grobgneis Complex range between c. 82 Ma and c. 71 Ma, and two dates from hornblende concentrates from amphibolitised eclogite yielded c. 108 and 136 Ma (Dallmeyer et al., 1996). The Santonian clastic sequences of the "Gosau" basins clearly overstep shear zones interpreted to be related to Alpine nappe assembly. Intra- and post "Gosauian" ^{40}Ar/^{39}Ar dates reported from ductile shear zones in the Eastern Alps record extension which led to Gosau basin development (c. 86 Ma, Gradstein et al., 1994). Overlapping pre-, syn- and post-Gosau date ranges obtained from muscovite in medium-grade rocks and syn-kinematic muscovite within phyllonite belts record uplift and cooling of intermediate structural levels and diachronous normal shear zones respectively, as required by local isostatic re-equilibration of the crust.

No Tertiary overprint has been detected in the Austro-Alpine units, in contrast with the currently interpreted major phase of Eocene thrusting.

Stratigraphic record. Paleo-geographic reconstructions based on Permo-Mesozoic isopic zones (e.g., Bechstädt, 1978; Schmidt et al., 1991; Haas et al., 1995) indicate 300-400 km of eastward lateral dislocation of the Drauzug, and Transdanubian Mountains. Malm to Early Neocomian compression resulted in the uplift of the basement and gravity nappes gliding northward toward the Neocomian Rossfeld flysch. E-W trending facies zones are stacked in the Alpine nappe pile, with the southernmost zone in the northernmost and structurally uppermost position. Deposition of the Senonian Gosau facies is regarded as a post-tectonic succession with the Santonian (86 Ma, Gradstein et al., 1994) clastic sequences commonly overlying Eoalpine thrust contacts. Late Tertiary strike-slip and normal faulting suggest a pattern of eastward extrusion tectonics.

6.9. CONCLUDING REMARKS

6.9.1. LITHOTECTONIC ASSEMBLAGES WITHIN THE OROGENIC BASEMENT

Medium-grade rocks discontinuously exposed along the Carpathian orogen can be roughly assigned to two distinct lithotectonic assemblages: one dominated by various gneisses subordinate micaschist, and amphibolite, intruded by Paleozoic granitoids, and another dominated by kilometre-size marble lenses within a matrix of micaschist, amphibolite, graphite-ore schist and/or quartzite and subordinate granitoids. Mafic-ultramafic and eclogite lenses are scattered throughout both lithotectonic assemblages and were variably overprinted during their evolution under intermediate and shallow crustal conditions.

Unless obliterated by Alpine strain, medium- to high-grade assemblages display flat-lying fabrics with a record of coaxial strain and two, locally three, superposed parageneses. Although the timing and tectonic significance of metamorphic events is still controversial, recent petrologic and petrostructural studies agree upon the tectonic assembly of medium- to high-grade rock units (e.g., Hârtopanu, 1978; Iancu et al., 1987; Săbău, 1994, Putiš, 1994). Several generations of granitoids were incorporated into the medium-grade metamorphic assemblages as orthogneiss, and several phases of anatexis are documented mainly in the non-carbonate assemblage.

Medium-grade assemblages record a complex polyphase pre-Alpine tectono-metamorphic evolution and variable Alpine rejuvenation. No classical Barrovian metamorphic zonation on a sedimentary protolith can be mapped. Instead various decompression PTt paths through the high- and medium-grade fields have been modelled (e.g., Árkai, 1985; Şeclăman et al., 1987; Săbău, 1994).

Attempting to recover original stratigraphy in the medium- to high-grade rocks of the Carpathian-Pannonian system (e.g., Kräutner in Zoubeck et al., 1988) is unrealistic. Detailed paleogeographic reconstructions of the pre-metamorphic environment based on sedimentary facies zones inferred from the lithology of metamorphic assemblages (Neubauer and Frisch, 1993) are suspect. No plausible evidence exists for interpretation of mafic-ultramafic assemblages as oceanic assemblages obducted during Variscan tectonism. Routinely applied in the Eastern Alps, and exclusively based on geochemical data, this interpretation has resulted in a confusing tectonic model that includes west-directed obduction of the "Plankogel ophiolitic mélange" and south-directed obduction of the "Speik ophiolitic complex" in a relatively limited area of the central Eastern Alps (e.g., Frisch et al., 1984, 1993; Neubauer and Frisch, 1993). Various models for the incorporation of upper mantle rocks within the crust (e.g., Mărunţiu, 1987; Săbău, 1994) challenge the simplistic Variscan obduction model. The common association of ultramafic and eclogitic relics with granulite and granites (e.g., Sebeş-Lotru and Leaota in the South Carpathians, Speik in the central Eastern Alps, Pohorje in the southern Eastern Alps) suggests that most of them reached mid-crustal levels during gneissic doming and/or granite emplacement.

Sm-Nd data from gneiss samples from two lithologically distinct assemblages in the Apuseni Mountains and Romanian Carpathians yielded Early Proterozoic T_{DM} model ages. Corroborated with the U-Pb data from lithologically similar assemblages in the central Eastern Alps, these data suggest that basement units involved in the Alpine tectonism are fragments of ancient crust multiply and variously rejuvenated through tectonism, magmatism, and anatexis. There is no unequivocal evidence of Paleozoic addition of sedimentary protoliths. $^{40}Ar/^{39}Ar$ dates record various Middle to Late Paleozoic and Cretaceous events. U-Pb zircon data and field relationships constrain the Paleozoic ages to represent cooling during uplift associated with granitoid emplacement. There is no unambiguous evidence of Variscan development of the medium-grade textures. Cretaceous ages are commonly recorded within medium-grade rocks involved in the development of Alpine gneissic dome structures.

Most low-grade assemblages in the Carpathian-Pannonian region show retrograde metamorphic reactions (e.g., Balintoni, 1969; Giuşcă et al., 1977; Hann and Szász, 1986; Pană, 1990; Stelea, 1994). Mineral and lithologic relics are consistent with their derivation from the adjacent rocks. A large component of non-coaxial strain associated with retrogression indicate that most low-grade rocks formed within hydrated shear zones (Pană and Erdmer, 1994). Anastomosing low-grade mylonite belts throughout the Carpathians and Apuseni Mountains define an irregular mesh of transcurrent and normal shear zones overprinting continental crust. Sm-Nd analyses from low-grade rocks yielded a wide range of εNd values that overlap with the medium-grade rocks and the Paleozoic granitoids. $^{40}Ar/^{39}Ar$ data from whole rock phyllonite and synkinematic muscovite indicate that fabric developed in different segments of the low-grade shear zones at different times, from Late Carboniferous to Late Cretaceous.

Low-grade rock units resulted from strain concentration and hydration metamorphic reactions in formerly higher grade and igneous rocks. Synkinematic metasomatic reactions commonly contributed to the development of carbonate, quartzite and metallic oxide and/or sulphide layers. Lithologic associations previously viewed as slightly re-crystallised sedimentary sequences are here interpreted as lithotectonic assemblages derived from preexisting crust, without any stratigraphic connotation. Field relations and stable isotope data suggest that carbonate layers traditionally interpreted as evidence of a sedimentary protolith may be metasomatic. Progressive deformation and exhumation of shear zones with continuous textural reequilibration resulted in the evolution of microstructures from ductile to brittle accompanied by mineral reactions. The shallowest structural levels may have incorporated cover sequences (e.g., Triassic sequences within the Certovica shear zone in the West Carpathians and within the Tulgheş and Bălan shear zones in the East Carpathians). Followed along strike, the zones of strain concentration may expose different structural levels. Consequently, a variety of rock assemblages may trace the same tectonic lineament (e.g., the Trascău and Tulgheş transcurrent shear zones are marked by subvertical phyllonite belts that project into highly strained flysch strata previously interpreted as "wildflysch").

The stratigraphy of metamorphic rocks is an unacceptable oversimplification. Interpretations of Alpine nappes derived from omission in the stratigraphy of metamorphic assemblages (e.g., Bucovinic/Subbucovinic nappe contact in the East Carpathians, Kräutner, 1988) are unrealistic and inconsistent with observable kinematic indicators.

No structural evidence of major overthrusts is preserved at the contact of the basement units with the peri-Carpathian flysch previously interpreted as upper plate and "subducting wedge" respectively. Where exposed, the contact of the Carpathian basement with strata from the peri-Carpathian basin invariably shows orogen-parallel stretching (Pieniny Klippen Belt in the West Carpathians, Black Flysch-Dămuc in the East Carpathians, Severin in the South Carpathians) in shear planes dipping steeply towards the interior or towards the exterior of the arc. The current interpretation of such relationships as nappe contacts obliterated by late faulting is unsatisfactory.

6.9.2 OCEANIC REMNANTS IN THE CARPATHIAN-PANNONIAN REGION

Combining classical Alpine overthrusting explanations with actualistic plate tectonics, the existing evolutionary models postulate several subduction zones in the Carpathian-Pannonian region. The Early Alpine evolution is inferred from traditional nappe interpretations modified to accommodate Alpine facies zonation with respect to one or several hypothetical basins floored by oceanic crust. The complex Tertiary evolution, relatively well constrained by kinematic analyses, paleomagnetic and geochemical data, is regarded as the final plate interaction in a region of long lasting subduction. Quantitative evaluations of continental collision based on these interpretations arrive at the paradoxical conclusion that about half of the total amount of continental crust involved must have disappeared into the mantle (e.g., Le Pichon et al., 1988).

A) Mesozoic oceanic crust between the European and the Carpathian continental crust ?

Danubian and Stara Planina basement and cover units indicate direct continuation of the European Moesian platform into the Carpathian and Balkan segments of the orogen. The projection of lithotectonic assemblages and structures from the East Carpathians into the West Carpathians and similarities between the Tatric crust of the West Carpathians and the adjacent Moldanubicum crust of the European Bohemian Massif may be regarded as additional evidence of little travel of the Carpathian crust away from stable Europe. The direct continuation of the West Carpathian lithotectonic assemblages into the Eastern Alps makes the interpretation of the

Austro-Alpine nappes as African crust, untenable.

Major tectonostratigraphic assemblages defining a subduction zone are not present.

a) The boundary between the "subduction wedge" and the "overriding plate" is elusive: Cretaceous flysch sequences of the peri-Carpathian basin are in contact with contemporaneous flysch troughs located on the external margin of the Carpathian crust. Moreover, the Balkanic Trojan and Kotel flysch strata are located in a zone of gradational structural transition from the Moesian platform to the Balkan segment of the Alpine orogen.

b) The evolution of flysch troughs associated with mantle intrusions on the West and East Carpathians continental crust, the intracontinental basalts in the internal flysch (Russo-Săndulescu and Bratosin, 1985) and the continental floor of the external flysch troughs (eg. Băncilă, 1965; Ştefănescu, 1983; Săndulescu, 1984; Birkenmayer, 1986) do not support the current interpretation of an oceanic crust (Sinaia - Măgura = Vahicum) in front of the Carpathian arc. Continuously, rapidly evolving morphology of the flysch basins indicated by the change of transport directions, isochronous heteropic facies development (e.g., Şotrile vs. Tarcău) and intervals of inward migration of the furrow axis (Ştefănescu, 1983), indicate complex translation with local compression or extension kinematics, rather than steady cratonward migration of a classical subduction wedge.

The reconstruction of an Early Alpine Severin suture between the Danubian and Getic units in the interior of the South Carpathians is at variance with several lines of evidence. In particular, the location of the Late Jurassic-Early Cretaceous Severin sequence (Sinaia flysch associated with peridotite pods and pillow-basalt) exclusively on the external Danubian units suggests that the Sinaia flysch trough rimmed the East and South Carpathians segments of the orogen in a similar tectonic position to the Trojan and Kotel flysch of the Balkans. Slices of mafic and ultramafic rocks in the East Carpathians are located along an orogen-parallel zone of high strain accompanied by basalt flows and various intrusions. Because tholeiitic- to calc-alkaline rocks are located along a transcurrent shear zone, the oceanic and island arc Cretaceous paleogeography inferred exclusively from rock chemistry is unrealistic.

There is no evidence that a significant Mesozoic ocean opened between the Carpathians and the European continental crust.

B) Mesozoic oceanic crust between the Carpathian and Apuseni-South Pannonian continental crustal fragments ?

East of the presently exposed Mureş belt of flysch and calk-alkaline igneous rocks, the basement of the Transylvanian Basin consists of continental crust underlain by a slightly elevated Moho (e.g., Visarion et al., 1973, Rădulescu, 1981; Horvath, 1993). Mafic rocks were only sampled in drill holes near Ocna Mureş and Zoreni along steeply dipping mantle penetrating fractures (Visarion et al, 1973, Rădulescu, 1981) and show a calc-alkaline chemical character (Nicolae, personal communication, 1996). A vertical conduct to the upper mantle is suggested by magnetotelluric data in the southern Apuseni Mountains (Stănică and Stănică, unpublished report).

The postulated subduction/obduction in the southern Apuseni Mountains is at variance with rock unit distribution and their space-time relationships (see chapter 5). The interpretation of an eastward-obducted slab of oceanic crust (Rădulescu et al., 1976; Săndulescu and Visarion, 1978) is contradicted by mathematical modelling of a magnetic anomaly in the western part of the Transylvanian Basin which suggests a deep crustal magnetic source (Botezatu et al., 1971), and by gneiss core samples at Pogăceaua, in the centre of the anomaly (Săndulescu and Visarion, 1978). The proposed Transylvanian (Tethys) origin of sparse mafic and ultramafic rocks on the external margin of the East Carpathian basement (Rarău and Hăghimaş synclines) is contradicted by their association with *in situ* basalts and by the lack of correlative rocks in the basement of the Transylvanian basin.

Geophysical data and core samples from the unexposed basement of the Tertiary Transylvanian basin constrain the local expression of Tethys to a narrow vertical zone at the southern and eastern periphery of the Apuseni Mountains (Figs. 6-16 and 6-18).

There is no unequivocal evidence for the proposed continuation the Mureş Basin across the Carpathian arc into the Pieniny Basin(s). None of the facies zones reconstructed from the Pieniny Klippen Belt can be correlated with the Poiana Botizei klippen in northwestern Transylvania (Birkenmayer, 1986). Moreover, the proposed direct correlation of facies zones and structures from the Apuseni Mountains into the West Carpathians (e.g., Săndulescu, 1975) is contradicted by significant facies differences in the Permian to Mesozoic sequences (Patrulius, 1976; Misič et al., 1989) and by opposite vergence of the interpreted Cretaceous nappes.

6.10. TOWARDS A NEW TECTONIC MODEL FOR THE CARPATHIAN-PANNONIAN REGION: BLOCK ROTATION AND OROGEN-PARALLEL TECTONICS

Time and space relationships between major lithotectonic assemblages and tectonic events discussed in previous chapters suggest that the inferred allochthoneity of adjacent crustal fragments is less significant, and thrusting less dramatic than currently interpreted. Pre-Mesozoic basement everywhere in the Carpathians and Eastern Alps records strong Late Paleozoic to Cretaceous orogen-parallel strain. Direct dating of deformational fabrics and kinematic analysis along individual zones of strain cannot yet constrain a consistent kinematic picture. Nevertheless, the poor evidence of subduction and the overwhelming evidence of transcurrent motions point to an alternative tectonic model (Fig. 6-16).

Mantle intrusions (commonly alkali basalt) in Permian to Triassic platformal sequences

Fig. 6-16. Proposed kinematic model for the Alpine evolution of the Carpathian-Pannonian region. 1 -continental crust; a. Paleozoic granitoids: MM -Muntele Mare granite, T - Tatra granitoids, H -Hăghimaş granitoids; 2 - thinned continental crust; 3 - oceanic crust and loci of mantle leaking along Jurassic sinistral transcurrent shear zones; 4 -Paleozoic composite igneous arc; 5 -active flysch basins; 6 -wedged flysch strata; 7 -calc-alkaline rocks along the Mureş transcurrent; 8 -regional sense of displacement; 9 -sense of displacement for individual crustal panels; 10 -fault; 11 -Miocene to Pleistocene volcanics along faults related to the orogenic collapse; 12 -Pleistocene shoshonite and mantel xenolites bearing alkali basalts along late transcurrent fault zones.

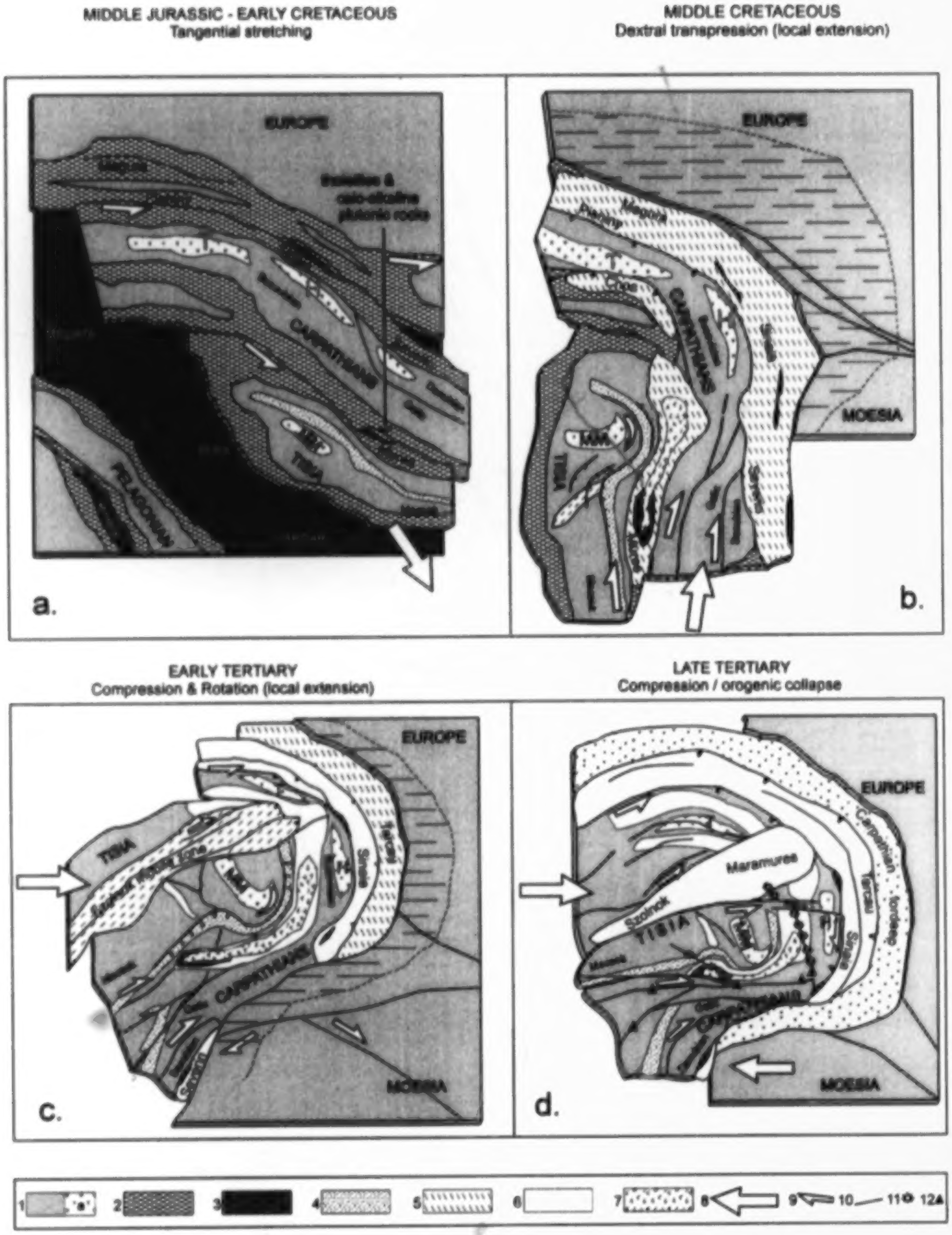
MIDDLE JURASSIC - EARLY CRETACEOUS
Tangential stretching
MIDDLE CRETACEOUS
Dextral transpression (local extension)
EUROPE
Magura
calc-alkaline
plutonic rocks
CARPATHIANS
TISIA
MM
PELAGONIAN
a.
EUROPE
Pieniny
Magura
CARPATHIANS
MM
TISIA
MOESIA
b.
EARLY TERTIARY
Compression & Rotation (local extension)
LATE TERTIARY
Compression / orogenic collapse
EUROPE
TISIA
MM
CARPATHIANS
Tarcau
MOESIA
c.
EUROPE
Maramures
Szolnok
TISIA
Tarcau
Carpathian foreland
CARPATHIANS
MOESIA
d.
1
2
3
4
5
6
7
8
9
10
11
12

in the West, East, and South Carpathians, as well as in the Codru Mountains and Poiana Botizei klippen record local extension and cannot be directly correlated with each other. Global-scale geodynamic analysis (e.g., Le Pichon et al., 1988) indicate that Jurassic opening of the southern Atlantic basin resulted in a large-scale sinistral transcurrent system marking the southern margin of Europe. Middle Jurassic to Early Cretaceous tangential stretching of the European continental margin resulted in a network of anastomosing crustal-scale shear zones and southeast migration of crustal panels. Narrow flysch troughs developed on thinned continental crust and releasing bends of the transcurrent shear zones allowed the emplacement of various mantle-derived materials within the flysch basins. Regional Late Jurassic to middle Cretaceous flysch troughs locally intruded by mantle materials define the Carpathian-Eastern Alps and the Apuseni-South Pannonian terranes. Extension probably never reached the spreading stage and the two fragments were never completely separated from each other and from stable Europe by intervening oceanic crust (Fig. 6-16 a). Various degrees of extension along the peri-Carpathian flysch troughs are suggested by variably serpentinized peridotite intrusions at Severin (within Danubian / Moesian crust) and Breaza (Bucovinian crust) and by intracontinental basalts of the Sinaia and Black Flysch sequences. Similarly, the Mureş basin is intruded by tholeiitic rocks in the Drocea Mountains and calc-alkaline rocks elsewhere. Extension within the Mureş basin and rejuvenation of the basement in the eastern Apuseni Mountains (c. 155 Ma) synchronous with high-pressure metamorphism in the southern West Carpathians (Meliata sequence) indicate complex Jurassic strain partitioning at the interior of the Carpathian Orogen.

The early Late Jurassic age of the oldest mafic rocks preserved in flysch troughs of the southern Apuseni and the East Carpathians indicates initiation of extension at about the same time and does not support the notion of a Triassic Tethys ocean along the southern Apuseni Mountains.

Cretaceous spreading at higher rates documented in the southern Atlantic requires northward migration of the African plate and reversal in the displacement of crustal fragments located between Africa and Europe (Fig 6-16 b). Early Cretaceous oblique compression is recorded in the western part of the South Carpathians. Thickening and uplift of the Carpathian basement and gravitational gliding of cover sequences is locally recorded along the orogen. However, the Albian age of the youngest basaltic rocks associated with flysch deposition (e.g., the Zliechov trough on Tatric basement in the West Carpathians, the Rarău-Hăghimaş trough on the Bucovinian basement in the East Carpathians, the Feneş trough in the southern Apuseni Mountains) casts doubts on the middle Cretaceous, "Austrian" phase of general thrusting interpreted in the entire orogen. The extrapolation from reasonably-defined gravitational cover nappes (e.g., nappes of the Northern Calcareous Alps, the Fatric nappes, the Haghimaş Nappe) to a wilde involvement of the basement in thrusting is unrealistic. Consequently, Early and

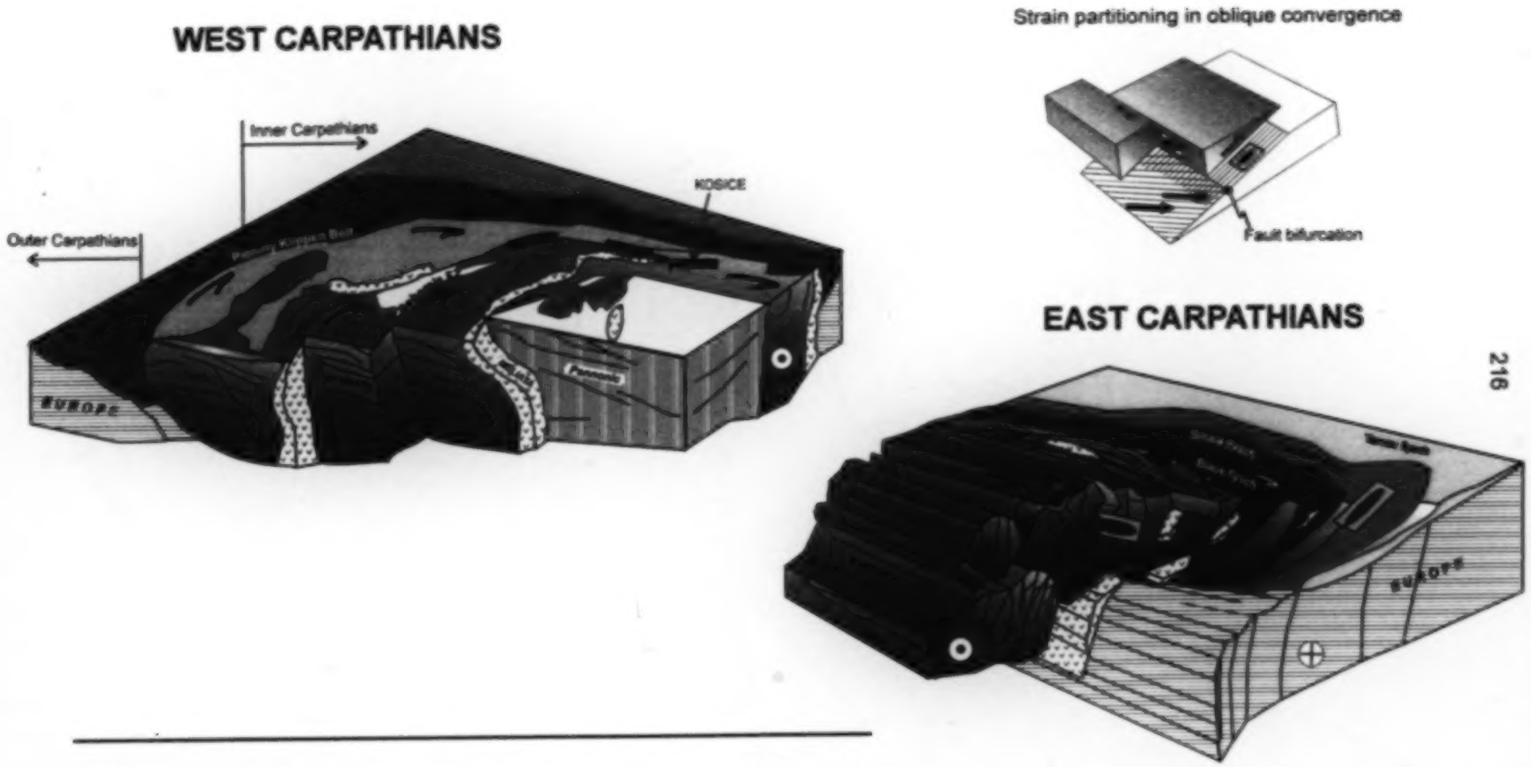
WEST CARPATHIANS
Inner Carpathians
Outer Carpathians
Pieniny Klippen Belt
KOSICE
EUROPE
Strain partitioning in oblique convergence
Fault bifurcation
EAST CARPATHIANS
EUROPE

Fig. 6-17. Proposed model of strain partitioning during oblique compession between the Carpathians and stable Europe: orogen-parallel strain in the basement and imbrication in the peri-Carpathians basin.

middle Cretaceous ^{40}Ar/^{39}Ar dates routinely interpreted to record the major "Austrian" phase of nappe stacking require revision.

Widespread Cenomanian molasse overlapping internal units of the Carpathian Orogen records post-middle Cretaceous tectonic relaxation.

Local stratigraphic unconformities indicate Late Cretaceous tectonism. The development of Gosau basins, and Vraconian to Paleogene basin development along the contact of the Apuseni Mountains and South Carpathians, indicate widespread Late Cretaceous extension. Contemporaneous ^{40}Ar/^{39}Ar dates and the kinematic indicators from phyllonite belts in the Eastern Alps and West Carpathians are consistent with transcurrent motion accompanied by the development of gneissic dome structures and normal detachment shear zones. However, Late Cretaceous oblique compression in internal units of the South Carpathians prevents regional generalizations.

Jurassic and Cretaceous tectonism was accommodated in wide shear zones that record deformation during complex plate interaction with phases of compression and stress release alternated with phases of tectonic relaxation. Neither the sedimentary record nor the kinematic indicators in the basement rocks are consistent with the interpretation of two distinct phases of Cretaceous general thrusting. The boundaries of the initially detached terranes migrated over time, defining new domains with independent kinematics.

During the Early Tertiary compression, the Apuseni-South Pannonian crustal fragment travelled more than 1000 km across latitude, probably on an oblique trajectory, to its present position (Pătraşcu, et al., 1990; Márton and Mauritsch, 1990) (Fig. 6-16 c). About 100° clockwise rotation of the Apuseni-South Pannonian crustal fragment (Márton, 1986; Pătraşcu et al., 1990) during Tertiary compression and eastward translation of the fragment south of the Szolnok sinistral transcurrent system may have been driven by Eocene eastward crustal extrusion from the Alps. The Carpathian crustal fragment(s) advanced progressively from west to east, accompanied by front lengthening and curving through internal stretching of the arc to fill a bay sketched on the European continental crust. Lateral ramps developed along the West and South Carpathians, while in front of the advancing continental arc strain was partitioned: a coherent thrust-and-fold belt developed in the peri-Carpathians flysch strata and rode up obliquely on the surrounding thinned continental crust, whilst orogen-parallel shear zones accommodated strain in the internal units (Fig. 6-17). The most stretched and thinned portions of the arc were transgressed by the Pannonian sea (e.g., Vienna, Trans-Carpathian basins).

The fault pattern in the basement units in Romania (Fig. 6-18) suggests that oblique compression against the northern part of the Transylvanian basement was mostly accommodated in southward escape towards the Carpathians bend. The diverging fan of transcrustal vertical faults documented in the Moesian basement, in front of the Carpathian

Fig. 6-18. Major fractures significant for the Tertiary kinematics of the Apuseni and Carpathian crustal fragments. Data compiled from Airinei et al., 1963; Socolescu et al., 1964; Visarion et al., 1973; Rădulescu et al., 1976; Airinei, 1977. Capital and small letters are first and second order basement fractures respectively, as defined by Socolescu et al., 1964. 1 - Apuseni-South Pannonian crustal fragment ("Tisia"); 2 - Carpathian - Rodopian crustal fragment; 3 - The southern margin of Europe; 4 - Late Jurassic - Cretaceous flysch sequences of the Mureş Basin; 5 - Calc-alkaline and subordinate tholeiitic rocks of the Mureş Basin; 6 - Peri-Carpathian Cretaceous - Paleogene flysch sequences; 7 - Neogene to Pleistocene weakly deformed mainly clastic sequences; 8 - Neogene to Pleistocene volcanic centres; 9 - inferred sense of displacement of the crustal fragments during the early Tertiary tectonism; 10 - relative sense of movement along major fault zones.

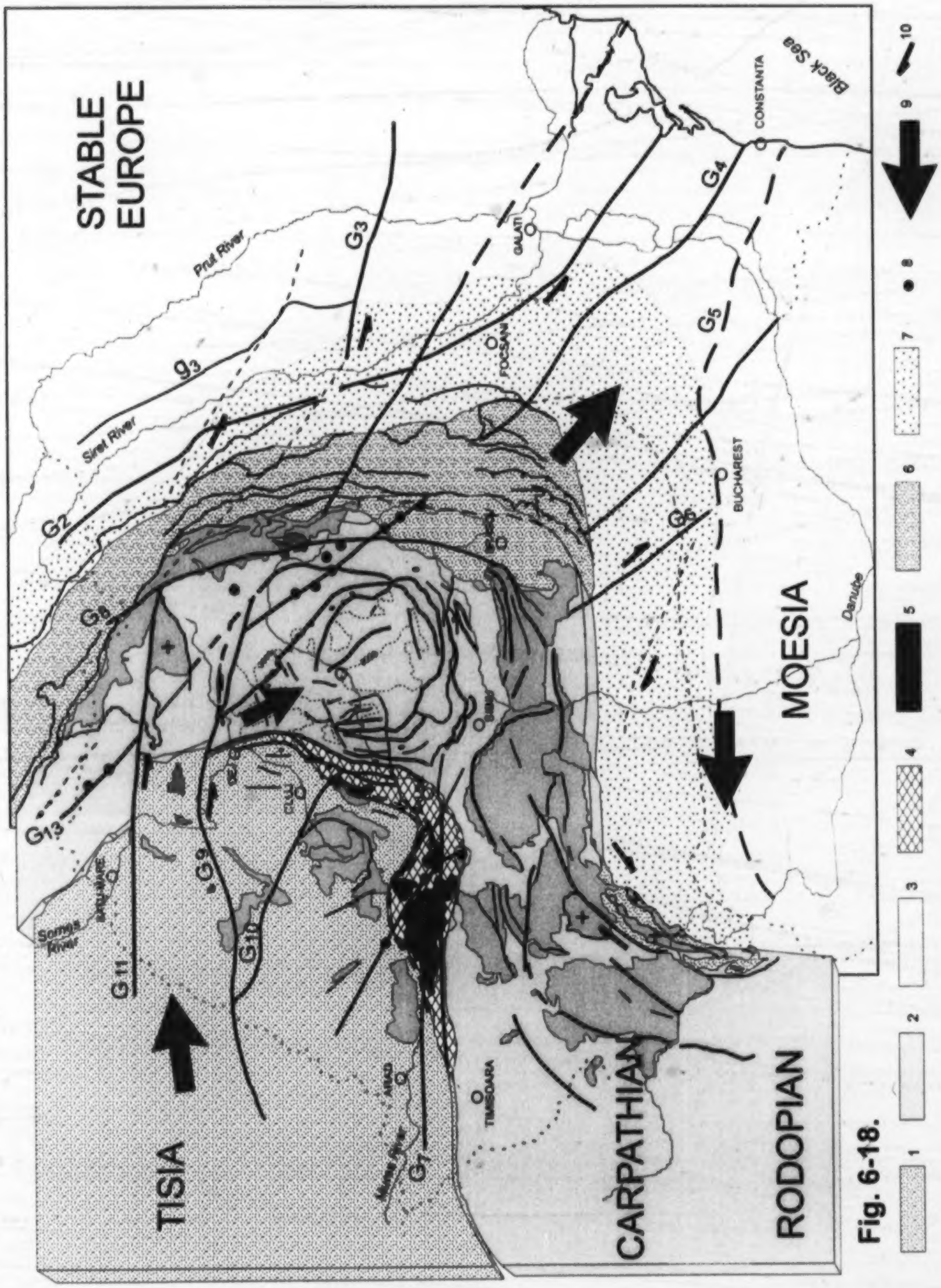

STABLE EUROPE
TISIA
CARPATHIAN
RODOPIAN
MOESIA
Black Sea
CONSTANTA
GALATI
FOCSANI
BUCHAREST
Danube
Prut River
Siret River
Somes River
Mures River
BAIA MARE
CLUJ
Sibiu
ARAD
TIMISOARA
G2
G3
g3
G4
G5
G6
G7
G8
G9
G10
G11
G13
1
2
3
4
5
6
7
8
9
10

Fig. 6-18.

bend, suggests the propagation of Tertiary strain in the foreland and independent westward migration of the western part of Moesia. Therefore, Miocene dextral shearing at the western tip of Moesia is the combined result of north and eastward Tertiary translations of microplates as required to fill a sketched Carpathian recess and the westward indentation of Moesia. The recess north of Moesia was likely smaller than assumed in previous models that regard Moesia as a stable promontory.

Miocene to Quaternary igneous activity has a diffuse and discontinuous character, with weakly expressed trends of propagation outward from the Pannonian Basin and southeastward. The volcanos pinpoint loci of extension cutting previous structures (Figs. 6-16 d and 6.18), which precludes any relationship with inferred former plate boundaries.

Igneous activity appears to have initiated through crustal melting and the development of magma-chambers at mid-crustal levels. Geochemical data suggest that a basalt derived from depleted mantle sampled a markedly different lower crust and mixed with crustal melts; storage, mixing, assimilation, and homogenization processes within the crust resulted in an "enriched" chemical character.

Spatial and temporal distribution of Neogene volcanos suggest Miocene orogenic collapse and decompression melting of the overthickened crust or alternatively, the advection of a thermal anomaly by mantle up-welling. The Miocene development of the Pannonian Basin accommodated by contemporaneous divergent thrusting in the Outer Carpathians suggests that unloading of the dome apex resulted in a general mass-transfer towards the circular periphery of the dome and loading of the surrounding European foreland.

REFERENCES

Árkai, P., 1987, New data on the petrogenesis of metamorphic rocks along the Balaton Lineament, Transdanubia, W-Hungary, Acta Geologica Hungarica, 30, 3-4, p. 319-338.

Árkai, P., Nagy, G., Dobosi, G., 1985, Polymetamorphic evolution of the south-Hungarian crystalline basement, Pannonian Basin: geothermometric and geobarometric data, Acta Geologica Hungarica, 28, 3-4, p.165-190.

Árkai, P., Horváth, Z.A., and Tóth, M. N., 1987, Regional metamorphism of the East Alpine type Paleozoic basement, Little Plain, W-Hungary: Mineral assemblages, illite crystallinity, -b_0 and coal rank data, Acta Geologica Hungarica, 30. 1-2, p. 153-175.

Bagdasaryan, G. P., Gukasyan, R. Kh., Cambel, B., and Veselsky, J., 1986, Rb-Sr isochron age of the Vepor pluton granitoids, Geol. Zbor, 37, 3, p. 365-374.

Balázs, B., Meszéna, B. C., Nusszer, A., and Gyémánt, S.P., 1986, An attempt to correlate the metamorphic formations of the Great Hungarian Plain and the Transylvanian central mountains (Munţii Apuseni), Acta Geologica Hungarica, 29, 3-4, p. 317-320.

Balintoni, I., 1969, Asupra caracterului retromorf al paragneiselor biotitice cu clorit de pe Bâsca Groşetului (Făgăraş), Buletinul Societăţii Ştiintifice de Geologie, XI, p. 275-281.

Balintoni, I., 1994, Structure of the Apuseni Mountains, *in* Berza T. (Ed.) "Geological evolution of the Alpine-Carpathian-Pannonian system", ALCAPA II Conference, Covasna, Field Guidebook, *Romanian Journal of Tectonics and Regional Geology*, 75, suppl. 2, p. 51-57.

Balintoni, I., Gheuca, I., and Vodă, Al., 1983, Alpine and Hercynian overthrust nappes from central and southern areas of the East Carpathian Crystalline-Mesozoic Zone: Anuarul Institutului de Geologie şi Geofizică, LX, p. 15-22.

Balintoni, I., Berza, T., Hann, H.P., Iancu, V., Kräutner, H.G., and Udubaşa, G., 1989, Precambrian Metamorphics in the South Carpathians, Multilateral Cooperation of the Academies of Sciences of the Socialist Countries, Earth Crust Structure Evolution and Metallogeny, Guide to Excursions, 89 p., Bucureşti.

Balla, Z., 1982, Development of the Pannonian Basin Basement through the Cretaceous-Cenozoic Collision: A New Synthesis, Tectonophysics, 88, 2, p. 61-102.

Balla, Z., 1985, The Carpathian Loop and the Pannonian Basin: a Kinematic Analysis, Geophys. Transactions, 30, 4, p. 313-353.

Balla, Z., 1986, Paleotectonic Reconstruction of the Central Alpine-Mediterranean Belt for the Neogene, Tectonophysics, 127, p. 213-243.

Balla, Z., 1988, Clockwise paleomagnetic rotations in the Alps in the light of the structural pattern of the Transdanubian Range (Hungary), Tectonophysics, 145, p. 277-292.

Balogh, K., Árva-Soós E., and Buda G., 1983, Chronology of granitoid and metamorphic rocks of Transdanubia (Hungary), Anuarul Institutului de Geologie şi Geofizică, 61, p. 359-364.

Baldi-Beke, M., and Nagymarosy, A., 1992, On the age of the Szolnok flysch and its possible correlation with the Carpathian flysch units, Knihovnicka ZPN, 2, p. 37-48.

Băncilă, I., 1958, Geologia Carpaţilor Orientali, 368 p., Editura Stiintifică, Bucureşti.

Băncilă, I., 1965, Sur la tectonique des Carpates Orientales, Carpatho-Balkan Geological Association, VII Congress, Sofia, Reports, Part 1, p. 257-266.

Bechstädt, T., 1978, Faziesanalyse permischer und triasicher Sedimente des Drauzuges als Hinweis auf eine grossraumige Lateralverschiebung Innerhalb des Ostalpins. Jb. Geol. B.-A., 121, p. 1-122.

Bercia, I., Kräutner, H.G., and Mureşan, M., 1976, Pre-Mesozoic Metamorphites of the East Carpathians: Anuarul Institutului de Geologie şi Geofizică, L, p. 37-70.

Berza, T., Balintoni, I., Iancu, V., Seghedi, A., and Hann, P. H., 1994, South Carpathians, *in* Berza T. (Ed.): Geological evolution of the Alpine-Carpathian-Pannonian system, Rom. J. Tect. Reg. Geol., 75, 2, p. 37-49.

Berza, T., Seghedi, A., and Stănoiu, I., 1988, Unităţile Danubiene din partea estică a Munţilor Retezat (Carpaţii Meridionali), Dări de Seamă ale Institutului de Geologie şi Geofizică, 72-72. 5, p. 5-22.

Bibikova, E. V., Cambel, B., Korikowsky, S. P., Broska, I., Gracheva, T. V., and Arakeliants, M. M., 1988, U-Pb and K-Ar isotopic dating of Sinec (Rimavica) granites (Kohut zone of Veporides), Geol. Zb., 39, 2, p. 147-157.

Biely, A., 1989, The geological structure of the West Carpathians, Mém. Soc. Géol. France, 154, II, p. 51-57.

Biely, A., and 17 co-authors, 1966, Geological Map of Czechoslovakia, Praha.

Birkenmayer, K., 1986, Stages of structural evolution of the Pieniny Klippen Belt, Carpathians, Stud. Geol. Pol., 90 p. 7-37.

Birkenmayer, K., 1988, Exotic Andrusov Ridge: its role in the plate-tectonic evolution of the West Carpathians foldbelt, Stud. Geol. Pol., 90, p. 7-37.

Bleahu, M.D., Lupu, M., Patrulius, D., Bordea, S., Ştefan, A., and Panin, S., 1981, The structure of the Apuseni Mountains, Carpatho-Balkan Geological Association, XII Congress, Bucharest, Romania, Guide to Excursion-B3, 103 p., Bucureşti.

Botezatu, R., Cornea, I., Visarion, M., and Costantinescu, P., 1981, Some possibilities of deep structures delineation by geophysical methods, Revue Roumaine de Géologie, Géophysique, Géographie, sér. Géophysique, 15, 1, p. 79-87.

Cioflica, G., and Nicolae, I., 1981, The Origin, Evolution and Tectonic Setting of the Alpine

Opholites from the Southern Apuseni Mountains, Revue Roumaine de Géologie, Géophysique, Géographie, sér. Géologie, 25, p. 19-29.

Codarcea, A., 1940, Vues nouvelles sur la tectonique du Banat méridional et du Plateau de Mehedinţi, Anuarul Institutului de Geologie şi Geofizică, XX, p. 1-74.

Cserepes-Meszéna, B., 1986, Petrography of the crystalline basement of the Danube-Tisza interfluve (Hungary), Acta Geologica Hungarica, 29, (3-4), p.321-339.

Csontos, L., Nagymarosy, A., Horváth, F., and Kovác, M., 1992, Tertiary Evolution of the Intra-Carpathian Area: A Model, Tectonophysics, 208, p. 221-241.

Dal Piaz, G. V., Martin, S., Villa, I. M., Gosso, G., and Marschalko, R., 1995, Late Jurassic blueschist facies pebbles from the Western Carpathian orogenic wedge and paleostructural implications for Western Tethys evolution, Tectonics, 14, 4, p. 874-885.

Dallmeyer, R.D., Neubauer, F., Fritz, H., Handler, R., and Müller, W., Diachronous Early Alpine Thrusting within the Austro-Alpine Unit, Eastern Alps: Reinterpretation of a Classical Thrust Complex Based on New Mineral Age Data, Terra Abstracts, Supl2, to Terra Nova, 4, p.14-15.

Dallmeyer, R.D., Neubauer, F., Handler, R., Fritz, H., Müller, W., Pană, D., and Putiš, M., 1996, Tectonothermal evolution of the internal Alps and Carpathians: Evidence from ^{40}Ar/^{39}Ar mineral and whole-rock data. Eclogae geol. Helv. 89/1 p.203-227.

Dallmeyer, R.D., Pană, D., Neubauer, F., Erdmer, P., 1998, Tectonothermal evolution of the Apuseni Mountains, Romania: Resolution of Variscan vs. Alpine events with ^{40}Ar/^{39}Ar ages, Journal of Geology, in press.

Dimitrescu, R., 1981, Hypothèses sur la structure du soubassement du secteur sud-oriental de la dépression Pannonique, Revue Roumaine de Géologie, Géophysique, Géographie, ser. Géologie, 25, p. 31-35.

Doglioni, C., 1987, Tectonics of the Dolomites, J. Struct. Geol., 9, p. 181-193.

Dumitrescu, I., Săndulescu, M., Lăzărescu, V., Mirăuţă, O., Pauliuc, S., and Georgescu, C., 1962, Mémoire pour la carte tectonique de la Roumanie, Annu. Com Geol., XXXII, p. 5-96.

Frisch, W., Neubauer, F., and Satir, M., 1984, Concepts of the evolution of the Austroalpine basement complex (Eastern Alps) during the Caledonian Variscan cycle, Geol. Rundsch., 73, p. 47-68.

Frisch, W., Vavra, G., and Winkler, M., 1993, Evolution of the Panninic Basement of the Eastern Alps, *in* von Raumer, J. and Neubauer, F., (Eds.): Pre-Mesozoic geology of the Alps, p. 349-360, Springer Verlag, Heidelberg.

Fritz, H., Neubauer, F., Janak, M., and Putis, M., 1992, Variscan mid-crustal thrusting in the

Carpathians. Part II: Kinematics and Fabric evolution of the Western Tatra basement, Terra Abstracts, Suppl. 2 to Terra Nova, 4, p. 24.

Fuchs, K., Bonjer, K.-P., Bock, G., Cornea, I., Radu, C., Enescu, D., Jianu, D., Nourescu, A., Merkler, G., Moldoveanu, T., and Tudorache, G., 1979, The Romanian earthquake of March 4, 1977; II. Aftershocks and migrations of seismic activity, Tectonophysics, 53, p. 225-247.

Fülöp, J., Brezsnyánszky, K and Haas, J., 1987, The new map of basin basement of Hungary, Acta Geol. Hung., 30, p. 3-20.

Gheuca, I., 1988, Versantul sudic al Munţilor Făgăraş, litostratigrafie si tectonică, Dări de Seamă ale Institutului de Geologie şi Geofizică, 72-73, 5, p. 93-117.

Giuşcă, D., Anastasiu, N., Popescu, Gh., and Şeclăman, M., 1977, Observaţii asupra şisturilor cristaline din zona centrală a masivului Făgăraş (Cumpăna-Valea Cîrţişoara): Analele Universităţii Bucureşti, Geologie, v. XXVI, p. 3-17.

Gradstein, F. M., Agterberg, F. P., Ogg, J. G., Hardenbol, J., van Veen, P., Thierry, J., and Huang, Z., 1994, A Mesozoic time scale, J. Geophys. Res., 99, p. 24051-24074.

Grow, J. A., Pogácsás, G., Bérczi-Makk, A., Várnai, P., Hajdú, D., Varge, E., and Péró, Cs., 1989, Tectonic and structural conditions of the Békés Basin, Magyar GeofiziKa, 30, p. 63-97

Grünenfelder M., Popescu, Gh., Soroiu, M., Arsenescu, V., Berza, T., 1983, K-Ar and U-Pb Dating of the metamorphic formations and the associated igneous bodies of the Central South Carpathians, Anuarul Institutului de Geologie şi Geofizică, XLI, p. 37-46.

Frank, W., Klein, P., Nowy, W., Scharbert, S., 1976, Die Datierung geologischer Ereignisse im Altkristallin der Gleinalpe (Steiermark) mit der Rb/Sr Methode, Tschermaks Mineral Petrogr. Mitt, 23, p. 191-203.

Haas, J., Kovács, S., Krysteyn, L., and Lein, R., 1995, Significance of Late Permian-Triassic facies zones in terrane reconstructions in the Alpine-North Pannonian domain: Tectonophysics, 242, p. 19-40.

Haiss, N., 1991, Untersuchungen zur Genese von Plagioklasgneisen im Basiskristallin der Ostalpen (Gleinalm-, Ötztal- und Silvrettakristallin, Ph. D. Thesis, Univ. Tübingen, 142 p.

Hamilton, W., B., 1990, On Terrane analysis, *in* Dewey, J. F., Gass, I., G., Şengor, A, M., C., (Eds.): Allochtonous Terranes, p. 55-66.

Handy, M. R., Herwegh, M., and Regli, R., 1993, Tektonische Entwicklung der westlichen Zone von Samedan (Oberhalbstein, Graubünden, Schweiz). Eclogae geol. Helv. 86, p. 785-817.

Hann, H. P., and Szász, L., 1984, Geological structure of the Olt Valley between Câineni and Brezoi (South Carpathians). Dări de Seamă ale Institutului de Geologie şi Geofizică, LXVIII, 5, p. 23-39.

Hârtopanu, I., 1978, Cristalinul Getic: Metamorphism polifazic sau polimetamorphism ? Studii şi Cercetări de Geologie, Geofizică şi Geografie, ser. Geologie, 23, 2, p. 185-193.

Horváth, F., 1993, Towards a mechanical model for the formation of the Pannonian basin, Tectonophysics, 226, p. 333-357.

Horváth, F., and Rumpler, J., 1984, The Pannonian basement: extension and subsidence of an Alpine orogene, Acta Geologica Hungarica, 27, p. 229-235.

Hovorka, D., and Meres, S., 1993, Leptino-amphibolite complex of the Western Carpathians: occurences and lithology, Mineralia Slov., 25, p. 1-9.

Iancu, V., Conovici, M., and Gridan, T., 1987, Eclogite-granulite-peridotite assemblage - an argument for a Proterozoic cryptic paleosuture in the supracrustal rocks of the Sebes-Lotru Group (South Carpathians), Dări de Seamă ale Institutului de Geologie şi Geofizică, 72-73, 1, p. 203-223.

Iancu, V., Balintoni, I., Săbău, G 1988, Variscan Tectonic units from the Getic domain, Bozovici zone, Dări de Seamă ale Institutului de Geologie şi Geofizică, 72-73, 5, p. 153-161.

Ianovici, V., Borcoş, M., Bleahu, M., Patrulius, D., Lupu, M., Dimitrescu, R., and Savu, H., 1976, Geologia Munţilor Apuseni, Editura Academiei Române, 631 p., Bucureşti.

Janak, M., 1992, Variscan mid-crustal thrusting in the Carpathians, I: Metamorphic conditions and P-T paths of the Tatry Mountains, Terra Abstracts, Suppl. 2 to Terra Nova, 4, p. 35.

Jantsky, B., Balázs, E., and Cserepes-Meszéna, B., 1988, Precambrian in the Basement of the Pannonian Basin, *in* Zoubek V., Cogné, J., Kozhoukharov, D., Kräutner, H. (Eds.): Precambrian in Younger Fold Belts, p. 687-711.

Kamenci, R., and Canovič, M., 1975, Preneogena podloga Vojvodanskog dela Pannonskog Basena, Radovi Znanstvenog Saveta Za Naftu Pri Jug. Akad. Znan. I Umetn. 5, Zagreb.

Kamenický, L., and Kamenický, J., 1988, Precambrian of the West Carpathians, *in* Zoubek V., Cogné, J., Kozhoukharov, D., Kräutner, H. (Eds.): Precambrian in Younger Fold Belts, p. 675-685.

Kázmér, M., and Kovács, S., 1985, Permian-Paleogene paleogeography along the eastern part of the Insubric-Periadriatic lineament system: evidence for the continental escape of the Bakony-Drauzug unit, Acta Geologica Hungarica, 28, p. 71-84.

Kázmér, M., and Kovács, S., 1989, Triassic and Jurassic oceanic and paraoceanic belts in the Carpatho-Pannonian region and its surroundings, *in* Sengör, A.M.C. (Ed.): Tectonic evolution of the Tethyan region. NATO ASI Series C, 259, p. 77-93.

Kober, L., 1931, Das alpine Europa und sein Rahmen. Ein geologisches Gestaltungsbild, Borntraeger, 500 p., Berlin.

Kovács, S., 1982, Problems of the "Pannonian Median Massif" and the plate tectonic concept, Contribution based on the distribution of Late Paleozoic-Early Mesozoic isopic zones, Geol. Rundschau, 71, p. 617-640.

Kovács, S., 1992, Tethys "western ends" during the Late Paleozoic and Triassic and their possible genetic relationships, Acta Geologica Hungarica, 35, p. 329-369.

Kräutner, H.G., 1980, Lithostratigraphic Correlation of Precambrian in the Romanian Carpathians: Anuarul Institutului de Geologie şi Geofizică, v. LVII, p. 229-296.

Kräutner, H.G., Năstaseanu, S., Berza, T., Stănoiu, I., and Iancu, V., 1981, Metamorphosed Paleozoic in the South Carpathians and Its Relations with the Pre-Paleozoic Basement, Carpatho-Balkan Geological Association XII Congress, Bucharest, Guide to Excursion A1, 116 p., Bucureşti.

Kräutner, H.G., 1988, Interregional Correlations, *in* Zoubek V., Cogné, J., Kozhoukharov, D., (Eds.): Precambrian in Younger Fold Belts, p. 853-862.

Kröll, A., Flügel, H. W., Seiberl, W., Weber, F., Walach, G., and Zych, D., 1988, Erläuterungen zu den Karten uber den steirischen Beckens und der südburgenlandischen Schwelle, Gelogische Bundesanstalt, 47 p., Vienna.

Laubscher, H.P., 1986, The late Alpine (Periadriatic) intrusions and the Insubric Line, Mem. Soc. Geol. Ital., 26, p. 21-30.

Le Pichon, X., Bergerat, F., and Roulet, M-J., 1988, Plate kinematics and tectonics leading to the Alpine belt formation; A new analysis, Geological Society of America, Special Paper, 218, p. 111-131.

Lexa, J., Konečný, V., Kaličiak, M. and Hojstičová, V., 1993, Distribution of Neogene volcanism in Carpatho-Pannonian region in space and time, *in* Rakús, M., and Vozar, J., (Eds.): Geodynamický vývoj a hlbinná stavba Záppadných Karpát, p. 57-69.

Liégeois, J.P., Berza, T., Tatu, M., and Duchesne, 1996, The Neoproterozoic Pan-African basement from the Alpine lower Danubian nappe system (South Carpathians, Romania) Precambrian Research, 80, 3-4, p. 281-301.

Linzer, H. G., 1996, Kinematics of retreating subduction along the Carpathian arc, Romania, Geology, 24, p. 167-171.

Lupu, M., Avram, E., Antonescu, E., Dumitrică, P., Lupu, D., and Nicolae, I., 1993, The Neo-Jurassic and the Cretaceous of the Drocea Mts: the stratigraphy and the structure of an ensialic marginal basin, Romanian Journal of Tectonics and Regional Geology, 75, p. 53-66.

Lupu, M., Antonescu, E., Avram, E., Dumitrică, P., and Nicolae, I., 1995, Comment on the age of some ophiolites from the North Drocea Mountains, Romanian Journal of

Tectonics and Regional Geology, 76, p. 21-25.

Mahel, M. (Ed.) , 1974, Tectonics of the Carpathian Balkan Region, GUDS, Bratislava, 455 p.

Mahel, M., 1981, Island character of Klippen Belt; Vahicum, Geol. Zb., Geologica Carpatica, 32, 3, p. 293-305.

Maluski, H., Rajlich, P., and Matte, P., 1993, ^{40}Ar/^{39}Ar dating of the Inner Carpathians Variscan basement and Alpine mylonitic overprinting. Tectonophysics, 223, p. 313-337.

Massari, F., 1990, The foredeeps of the northern Adriatic margin: evidence of diachroneity in deformation of the Southern Alps, Riv. It. Geol. Mineral. Univ. Padova, 28, p. 1-63.

Masson, P. R. D., Downes, H., Seghedi, I., Szakacs, A., and Thirlwall, M. F., 1995, Low-pressure evolution of magmas from the Calimani, Gurghiu and Harghita Mountains, East Carpathians, Acta Vulcanologica, 7, 2, p. 43-52.

Márton, E., 1986, Paleomagnetism of igneous rocks from the Velence Hills and Mecsek Mountains, Geophysical Transaction, 32, p. 83-145.

Márton, E., and Mauritsch, H.J., 1990, Structural applications and discussion of a paleomagnetic post-Paleozoic data base for the Central Mediterranean, Physics of the Earth and Planetary Interiors, 62, p. 46-59.

Misík, M. and Marschalko, R., 1988, Exotic conglomerates in flysch sequences: Examples from the West Carpathians, Mém. Soc. Géol. France, 154, I, p. 95-113.

Mišik, M., Mock, R., Rakús, M., and Biely, A., 1989, The Area of Mesozoic Sedimentation of the Mecsek and Northern Apuseni Mountains was not situated in the West Carpathians, IGCP Project 198, Memoire Societé Géologique, France, 154(II), p. 69-79.

Moeller, St., 1989, Deep-reaching geodynamic processes in the Alps, in Coward, M.P., Dietrich, D., and Park, R.G., (Eds.): Alpine Tectonics, p. 303-328.

Murgeanu, G., 1933, Sur une cordillère ante-sénonienne dans le géosynclinal du flysch carpatique, Dări de Seamă ale Institutului Geologic Român, XXXI.

Mutihac, V., 1990, Structura Geologică a Teritoriului României, 423 p. Editura Tehnică, Bucureşti.

Nagymarosy, A., 1990, Paleogeographicaland paleotectonical outlines of some intra-Carpathian Paleogene basins, Geol. Zbor., Geol. Carp., 41, p. 259-274.

Năstaseanu, S., Bercia, I., Iancu, V., Vlad, Ş., and Hârtopanu, I., 1981, The Structure of the South Carpathians, Carpatho-Balkan Geological Association XII Congress, Bucharest, Guide to Excursion B2, 100 p., Bucureşti.

Nedelcu, L., 1984, Prezenţa granatului în metamorfitele seriei de Ţibău din regiunea Cârlibaba (Carpaţii Orientali), Dări de Seamă ale Institutului de Geologie şi Geofizică,

Neubauer, F., 1992, The Gurktal nappe complex, *in* Neubauer, F., (ed.): The Eastern Central Alps of Austria, ALCAPA-meeting field guidebook, p. 71-82.

Neubauer, F., and Frisch, W., 1993, The Austro-Alpine Metamorphic Basement East of the Tauern Window, *in* von Raumer, J. and Neubauer, F., (Eds.): Pre-Mesozoic geology of the Alps, p. 515-536, Springer Verlag, Heidelberg.

Neubauer, F., Frisch, W., and Hansen, B. T., 1989, A Late Archean rock in the Eartern Alps ? Terra Abstr. 1, 1 p. 5.

Neubauer, F., Frisch, W., and Hansen, B. T., 1993, The pre-Alpine tectonothermal evolution of the Rennfeld region, Eastern Alps: a U-Pb zircon study, Lithos,

Neubauer, F., Müller, W., Peindl, P., Moyschewitz, Wallbrecher, E., and Thöni, M., 1992, Evolution of Lower Austroalpine units along the eastern margins of the Alps: a review, in Neubauer, F., (Ed.): The Eastern Central Alps of Austria, ALCAPA-meeting field guidebook, p. 97-114.

Nievergelt, P., Liniger, M., Froitzheim, N., and Ferreiro-Maehlmann R., 1991, The Turba mylonitè zone: An Oligocene extensional fault at the Pennine-Austroalpine boundary in eastern Switzerland, Terra abstracts, 3, p. 248.

Nusszer, A., 1986, Formations of the Pusztaföldvár metamorphite regional unit, Acta Geologica Hungarica, 29, (3-4), p. 283-304.

Oncescu, M. C., Burlacu, V., Anghel, M., and Smalbergher, V., 1984, Three-dimentional P-wave velocity image under the Carpathian arc, Tectonophysics, 106, p. 305-319.

Pamić, J., 1986, Magmatic and metamorphic complexes of the Adjoining area of the northernmost Dinarides and Pannonian mass, Acta Geologica Hungarica, 29, 3-4, p. 203-220.

Pamić, J., 1993, Eoalpine to Neogene magmatic and metamorphic processes in the northwestern Vardar Zone, the easternmost Periadriatic Zone and the southwestern Pannonian Basin, Tectonophysics, 226, p. 503-518.

Pană, D.,, 1990, Central and northern Fagaras - Lithological sequences and structure, Dări de Seamă ale Institutului de Geologie şi Geofizică, 74, 5, p. 81-99.

Pană, D., and Erdmer, P., 1994, Alpine crustal shear zones and pre-Alpine basement terranes in the Romanian Carpathians and Apuseni Mountains, Geology, 22, p. 807-810.

Pană, D., and Erdmer, P., 1996, Comment on: Linzer, H. G., 1996, Kinematic of retreating subduction along the Carpathian arc, Romania, Geology, 24, p. 862-863.

Patrulius, D., 1976, Les formations mésozoïques des Monts Apuseni septentrionaux: corrélations chronostratigraphique et faciale, Revue Roumain de Géologie, Géophysique, Géographie, ser. Géologie, 20, p. 49-57.

Patrulius, D., Popa, E., Popescu, I., 1966, Anuarul Comitetului Geologic, 35, p. 397-444.

Pătraşcu, S., Bleahu, M., and Panaiotu, C., 1990, Tectonic implications of the paleomagnetic research into Upper Cretaceous magmatic rocks in the Apuseni Mountains, Romania, Tectonophysics, 180, p. 309-322.

Peccerillo, A., and Taylor, S. R., 1976, Rare earth elements in East Carpathians volcanic rocks, Earth Planet, Sci. Letters, 32, p. 121-126.

Pécskay, Z., Edelstein, O., Seghedi, I., Szakács, A., Kovacs, M., Crihan, M., and Bernad, A., 1995, K-Ar datings of Neogene-Quaternary calc-alkaline volcanic rocks in Romania, Acta Vulcanologica, 7, 2, p. 53-61.

Pécskay, Z., and 14 Co-authors, 1995, Space and time distribution of Neogene-Quaternary volcanism in the Carpatho-Pannonian Region, Acta Vulcanologica, 7, 2, p. 15-28.

Plašienka, D., 1990, Regional shear and transpression zones in the Tatric unit of the Little Carpathians, Mineralia Slovaca, 22, p. 55-62.

Plašienka, D., Janak, M., Hacura, A., and Vrbatovic, P., 1989, First illite-crystalinity data from Alpine metamorphic rocks of the Veporicum, Mineralia Slovaca, 21, 1, p. 43-51.

Pospíšil, L., Bezák, V., Nemčok, M., Feranec, J., Vass, D., and Obernauer, D., 1989, The Muran tectonic system as example of horizontal displacement in the West Carpathians, Mineralia Slovaca, 21, p. 305-322.

Putis, M., 1994, South Tatric-Veporic Basement Geology: Variscan Nappe Structures; Alpine Thick-Skinned and Extensional Tectonics in the Western Carpathians (Eastern Low Tatra Mountains, Northwestern Slovak Ore Mountains), Mitt. Osterr. Geol. Ges., 86, p. 83-99.

Rakus, M., Misik, M., Michalik, J., Mock, R., Durkovic, T., Koráb, T., Marschalko, R., Mello, J., Polák, M., and Jablonsky, J., 1990, Paleogeographic development of the West Carpathians, Mem. Soc. Géol. France, 154, III, p. 39-62.

Ratschbacher, L., 1986, Kinematics of Austro-Alpine cover nappes: changing translation path due to transpression, Tectonophysics, 125, p. 335-356.

Ratschbacher, L., and Frisch, W., 1993, Palinspastic Reconstruction of the Pre-Triassic Bassement Units in the Alps: The Eastern Alps, *in* von Raumer, J. and Neubauer, F., (Eds.): Pre-Mesozoic geology of the Alps, p. 41-51, Springer Verlag, Heidelberg.

Ratschbacher, L., Behrmann, J. H., and Pahr, A., 1990, Penninic windows at the eastern end of the Alps and their relation to the intra-Carpathian basins. Tectonophysics, 172, p. 91-105.

Ratschbacher, L., Linzer, H. G., Moser, F., Strusievicz, R. O., Bedelean, H., Har, N., and Mogoş, P. A., 1993, Cretaceous to Miocene thrusting and wrenching along the central South Carpathians due to a corner effect during collision and orocline formation: Tectonics, v. 12, no. 4, p. 855-873.

Rădulescu, D., and Săndulescu, M., 1973, The Plate-Tectonics Concept and the Geological Structure of the Carpathians: Tectonophysics, v. 16, p. 155-161.

Rădulescu, D., Peltz, S., and Stanciu, C., 1973, Neogene volcanism in the East Carpathians (Călimani-Gurghiu-Harghita Mts.), Guide to excursion 2AB, Symposium Volcanism and Metallogenesis, Bucharest.

Rădulescu, D., Cornea, I., Săndulescu, M., Constantinescu, P., Rădulescu, F., and Pompilian, A., 1976, Structure de la croûte terrestre en Roumanie, essai d'interpretation des études sismiques profondes, Anuarul Institutului de Geologie şi Geofizică, 50, p. 5-36.

Rădulescu, D., Săndulescu, M., and Borcoş, M., 1993, Alpine magmatogenetic map of Romania: an approach to the systematization of the igneous activity, Revue Roumain de Géologie, Géophysique, Géographie, ser. Géologie, 37, p. 3-8.

Rădulescu, F., 1981, Crustal seismic studies in Romania, Revue Roumaine de Géologie, Géophysique, Géographie, ser. Géphisyque, 25, p. 57-74.

Roman, C., 1970, Seismicity in Romania-Evidence for the Sinking Lithosphere, Nature, 228, p. 1176-1178.

Rothpletz, A., 1905, Geologische Alpenforschungen II, Ausdehnung und Herkunft der Rhaetischen Schubmasse. Lindauer, München.

Royden, L., 1988, Late Cenozoic Tectonics of the Pannonian Basin System, *in* Royden L., and Horváth (Eds.): The Pannonian Basin - A Study in Basin Evolution, AAPG Memoir, 45, p. 27-48.

Royden, L., and Báldi, T., 1988, Early Cenozoic Tectonics and Paleogeography of the Pannonian and Surrounding Regions, *in* Royden L., and Horváth (Eds.): The Pannonian Basin - A Study in Basin Evolution, AAPG Memoir, 45, p. 1-16.

Russo-Săndulescu, D., and Bratosin, T., 1985, Caracteres et signification du complexe basique de la nappe du Flysch Noir (Monts du Maramures, Carpates Orientales): Carpatho-Balkan Geological Association, XIII, Congress, Krakow, Proceedings Reports, p. 112-115.

Sackáci, A., and Seghedi, I., 1995, The Călimani-Gurghiu-Harghita volcanic chain, East Carpathians, Romania: volcanologic features, Acta Vulcanologica, 7, 2, p. 145-153.

Savu, H, 1983, Geotectonic and magmatic evolution of the Mureş Zone (Apuseni Mountains)-Romania, Anuarul Institutului de Geologie şi Geofizică, LVI, p. 253-262.

Săbău, G., 1994, Lithostratigraphic and metamorphic correlations: a tentative way of exploring the early history of the Getic crystalline, Romanian Journal of Tectonics and Regional Geology, 76, p. 119-128.

Săndulescu, M., 1975, Essai de synthèse structurale des Carpathes, Bull. Soc. Géol. France, 7, XVII, 3, p. 299-358.

Săndulescu, M., 1984, Geotectonica României, Editura Tehnică, 323 p.

Săndulescu, M., 1988, Cenozoic Tectonic History of the Carpathians, *in* Royden L., and Horváth (Eds.): The Pannonian Basin - A Study in Basin Evolution, AAPG Memoir, 45, p. 17-25.

Săndulescu M., 1994, Overview on Romanian geology, *in* Berza T. (Ed.): "Geological evolution of the Alpine-Carpathian-Pannonian system", ALCAPA II Conference, Covasna, Field Guidebook, Romanian Journal of Tectonics and Regional Geology, 75, suppl. 2, p. 3-15.

Săndulescu M., and Visarion, M., 1978, Considérations sur la structure tectonique du soubassement de la dépression de Transylvanie, Dări de Seamă ale Institutului de Geologie şi Geofizică, 64, 5, 153-173.

Săndulescu M., Mureşan, M., and Mureşan, G., 1975, Geological Map of Romania, scale 1: 50 000, Dămuc sheet, Geological Institute of Romania.

Săndulescu, M., Neagu, T., and Antonescu, E., 1982, Contributions à la connaissance des klippes de type pienin de Poiana Botizii, Maramures, Dări de Seamă ale Institutului de Geologie şi Geofizică, 67, 4, p. 79-96.

Scharbert, S., 1981, Untersuchungen zum Alter des Seckauer Kristallins, Mitt. Ges. Geol. Bergbaustud. Osterr., 27, p. 173-188.

Schmid, S. M., and Haas, R., 1989, Transition from near-surface thrusting to intrabasement decollement, Schlinig thrust, Eastern Alps, Tectonics, 8, 4, p. 697-718.

Schmidt, T., Blau, J., and Kázmér, M., 1991, Large-scale strike-slip displacement of the Drauzug and the Transdanudian Mountains in early Alpine history: evidence from Permo-Mesozoic facies belts, Tectonophysics, 200, p. 213-232.

Schönborn, G., 1992, Alpine Tectonics and kinematic models of the Central Southern Alps, Mem. Sci. Geol. Padova, 44, p. 229-393.

Schönlaub, H.P., 1979, Das Paläozoikum in Österreich. Abh. Geol. Bundesanstalt, 33, 1-124.

Seghedi, I., Szakács, A., and Mason, P. R. D., 1995, Petrogenesis and magmatic evolution in the East Carpathian Neogene volcanic arc (Romania), Acta Vulcanologica, 7, 2, p. 135-143.

Sollogub, V. B., Prosen, D., and Co-Workers, 1973, Crustal Structure of Central and Southeastern Europe by Data of Explosion Seismology, Tectonophysics, 20, p. 1-33.

Spakman, W., 1990, Tomographic images of the upper mantle below central Europe and the Mediterranean, Terra Nova, 2, p. 542-553.

Stanoiu, I., 1982, Notă preliminară asupra prezenţei unei asociaţii macrofloristice în formaţiunea cristalină de Tusu (autohtonul danubian), Dări de Seamă ale Institutului de Geologie şi Geofizică, 67, 3, p. 167-172.

Stelea, I., 1994, Pre-Alpine and Alpine shear zones in the central South Carpathians, Romanian

Journal of Tectonics and Regional Geology, 75, Suppl. 1, p. 58-59.

Svingor, É., and Kovách, Á., 1981, Rb-Sr isotopic studies on granodioritic rocks from the Mecsek Mountains, Hungary. Acta Geologica Hungaricae, 24, 2-4, p

Szaderchy-Kardoss, E., 1975, The belts of subduction in the Carpathian-Pannonian-Dinaric area, *in* Machel, M., (Ed.): Tectonic problems of the Alpine system, Bratislava, p. 69-85.

Sztanó, O., 1990, Submarine fan-channel conglomerate of Lower Cretaceous, Gerecse Mts., Hungary, N. Jb. Geol. Paläont. Mh., p. 431-446.

Szederkenyi, T., 1977, Geological evolution of South Transdanubia (Hungary) in Paleozoic time, Acta Miner. Petrol., Szeged, 13, 1, p. 3-14.

Szederkényi, T., 1982, Lithostratigraphic division of the Crystalline Mass in South Transdanubia and the Great Hungarian Plain, Newsletter of IGCP Project No. 5, Bratislava, 4, p. 100-106.

Szili-Gyémnt, P., 1986, Metamorphic formations in Tiszantul: the Körös-Berettyó and the Álmosd units, Acta Geologica Hungarica, 29, (3-4), p. 305-316.

Ştefănescu, M., 1983, General Remarks on the Eastern Carpathians Flysch and its Depositional Environment, Révue Roumaine de Géologie Géophysique Géographie, Serie Géologie, 27, p. 59-64.

Tollmann, A., 1986, Geologie von Österreich, Band III. Gesamtübersicht. Deuticke, 718 p, Wien

Tollmann, A., 1987, The Alpidic evolution of the Eastern Alps, *in* Flugel, W. H., and Faupl, P. (Eds.): Geodynamics of the Eastern Alps, p. 361-378.

Tollmann, A., 1989, The Eastern Alpine sector, northern margin of the Tethys, Mem. Géol. Soc. France, 154, p. 23-49.

Tollmann, A., and Spendlingwimmer, 1978, Crinoiden im Anis (Mitteltrias) der Tatriden der Hainburger Berge (Niederösterreich), Mitt. Österr. Geol. Ges., 68, p. 59-77.

Tomek, Č., 1993, Deep crustal structure beneath the central and inner West Carpathians, Tectonophysics, 226, p. 417-431.

Tomek, Č and Hall, J., 1993, Subducted continental margin imaged in the Carpathians of Czechoslovakia, Geology, 21, p. 535-538.

Vazarova, A., and Kristin, J., 1986, Thermodynamic conditions at the contact of Alpine granitoids with metasediments of Slatvina Formation in Krokava surroundings (southern Veporicum) Rep. Geol. Invest. Dioni Stur Inst. Bratislava, 21, p. 33-38.

Visarion, M., Ali-Mehmed E., and Polonic P., 1973, Studiul integrat al datelor geofizice privind morfologia şi structura fundamentului cristalin in depresiunea Transilvaniei, Studii şi Cercetări de Geologie, Geofizică şi Geografie, ser. Gofizică, 11, 2, p. 193-201.

Zoubek, V., Cogné, J., Kozhoukharov, D., and Kräutner, H. G., (Eds.) 1988, Precambrian in Younger Fold Belts, John Willis, 665 p.

APPENDIX I

OUTLINE OF THE MAJOR TECTONOSTRATIGRAPHIC UNITS OF THE CARPATHIANS-PANNONIAN BASIN SYSTEM AND OUTSTANDING PROBLEMS IN THE INTERPRETATION OF THE ALPINE EVOLUTION OF BASEMENT ASSEMBLAGES

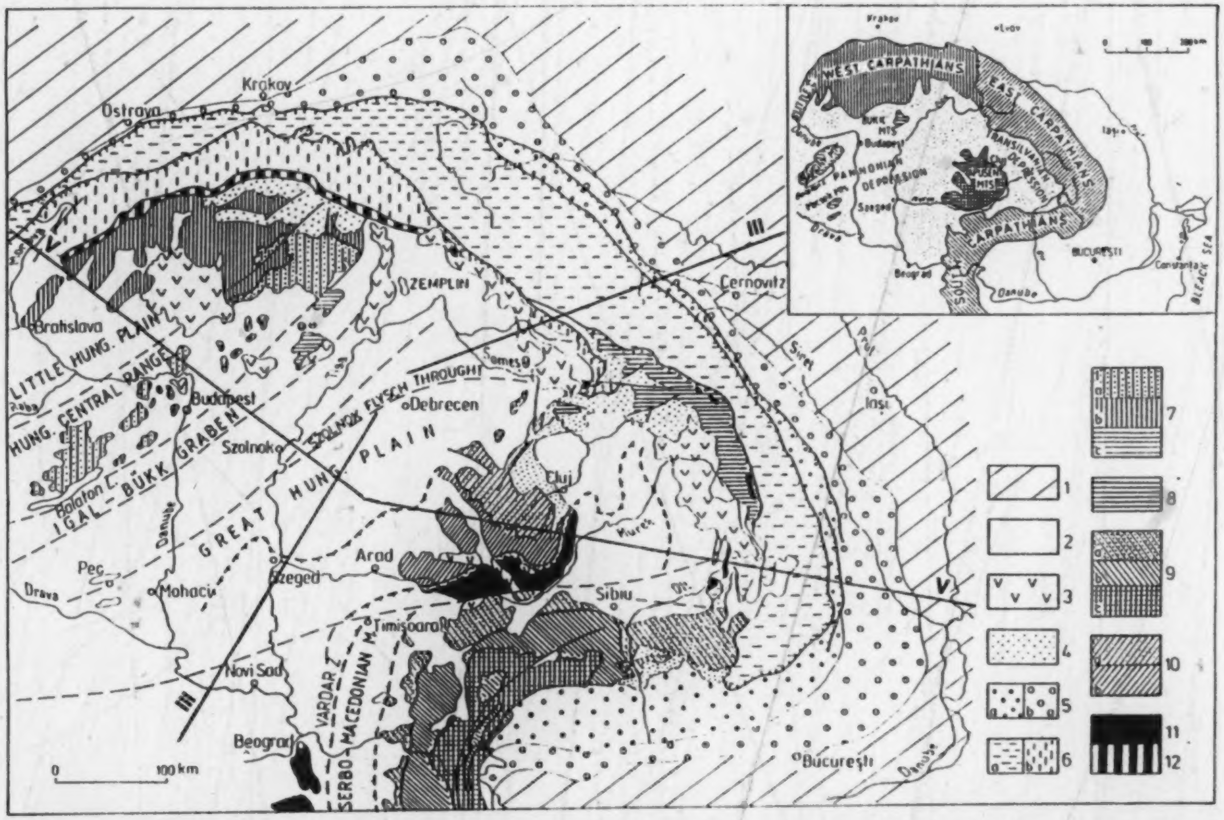
Ostrava
Krakov
Cernovitz
ZEMPLIN
Bratislava
LITTLE HUNG. PLAIN
HUNG. CENTRAL RANGE
Budapest
Balaton L.
IGAL - BÜKK GRABEN
Szolnok
SZOLNOK FLYSCH THROUGH
Debrecen
GREAT HUNG. PLAIN
Somes
Cluj
Mures
Siret
Prut
Iasi
Arad
Szeged
Pec
Drava
Mohacu
Danube
Timisoara
Sibiu
Novi Sad
Beograd
VARDAR Z.
SERBO-MACEDONIAN M.
Bucureşti
Danube
III
V
0
100 km
1
2
3
4
5
6
7
8
9
10
11
12
WEST CARPATHIANS
EAST CARPATHIANS
SOUTH CARPATHIANS
TRANSILVANIAN DEPRESSION
PANNONIAN DEPRESSION
BUKK MTS
APUSENI MTS
Budapest
Szeged
Drava
Beograd
Danube
BUCUREŞTI
Constanta
BLACK SEA
Lvov
Praha

Fig. I-1. Simplified tectonic sketch of the Carpathian-Pannonian system (compiled after Sandulescu, 1975, 1980; Dimitrescu, 1981; Iansky, 1988; Krautner, 1988). 1 - Foreland of the Carpathians; 2 - Internal molasse depressions; 3 - Neogene andesitic volcanics; 4 - Post nappe sedimentary cover; 5 - Foredeep units: a - on epiorogenic basement (internal foredeep); b - on platform basement (external foredeep); 6- Flysch nappes: a - External Dacides and Moldavides (East Carpathians), b - Internal Moldavides (Magura and DragovoPetrova Nappes). Units with pre-Permian metamorphic rocks: 7 - Occidental Dacides: a - Gemerides, b - Tetroveporides, c - Bukkides; 8 - Oriental Dacides (Central East Carpathian Nappes); 9 - Meridional Dacides: a - Supragetic units, b - Getic units, c - Danubian units; 10 - Inner Dacides; a - Bihor Unit,b - Codru and Biharia Nappes; 11 - Units with Mesozoic ophiolotes (Vardar, Mures, Transylvanides); 12 - Pieniny Klippen Belt. Stright lines are geophysical traverses discussed in text (Sollogub et al., 1973)

I.1. INTRODUCTION

The following review of the main tectonostratigraphic units in different segments of the Carpathian-Pannonian system introduces the tectonic setting for the study area. The traditional Alpine nappe concepts in the central part of the Alps were extrapolated to different segments of the Carpathians at different times. Heterogeneous approaches and levels of detail and the proliferation of local names along the orogen, as well as the complexity of the geological processes have prevented a straightforward interpretation of the geologic evolution of the region. The least controversial and most explicit tectonic and stratigraphic representation of the Alpine geology appears on the geological map of Austria. The model was extrapolated in recent compilations to the scale of the entire Carpathian-Pannonian region (Fig. I-1) for pre-Alpine stratigraphy (Zoubek et al., 1988) and for Alpine stratigraphy (Tari, 1994). Figures adapted from these and other published papers are used here to present the distribution and currently inferred evolution of the major tectonostratigraphic units in the Carpathian-Pannonian system. The legend for lithostratigraphic columns is in Fig. I-2.

Inconsistencies in the current evolutionary models relevant to the alternative interpretations proposed in this study are pointed out. Recent contributions which depart from the traditional stratigraphic approach to metamorphic terranes and from their currently interpreted Alpine kinematics are discussed in the final chapter - a first step towards a new tectonic model for the Carpathian-Pannonian region.

I.2 EASTERN ALPS

An arbitrary boundary between the Eastern and Western Alps corresponds to the N-S trending outline of the Austroalpine overthrust on the Penninic units. The major Neogene Insubric (Periadriatic) transcurrent fault marks the sharp southern boundary of the Eastern Alps, while the molasse basin can be regarded as the northern geological border. To the east, the Vienna and Danube Tertiary basins cover the link with the Western Carpathians segment of the orogen(Fig. I-3).

The following brief summary of the geology of the Eastern Alps is based on synthesis work by Oberhauser (1974, 1980), Tollmann (1977; 1986; 1989), Janoschek and Matura (1980), Flügel and Faupl (1987), Neubauer (1992) and Schmidt et al. (1994).

Major tectonostratigraphic units

From north to south, and structurally upward, the main Alpine tectonic units emplaced on the European foreland during the Alpine tectonism are the Helvetic-Ultrahelvetic foreland thrust-and-fold-belt that involves shallow-water carbonates, marly facies or coal-bearing Lower Jurassic "Gresten" facies, followed ocean-ward by the Cretaceous-Eeocene Rhenodanudian flysch. The Mesozoic Hochstegen and Schieferhülle cover sequence in the central Eastern Alps and the Jurassic succession from Rechnitz at the eastern extremity are assigned to the South

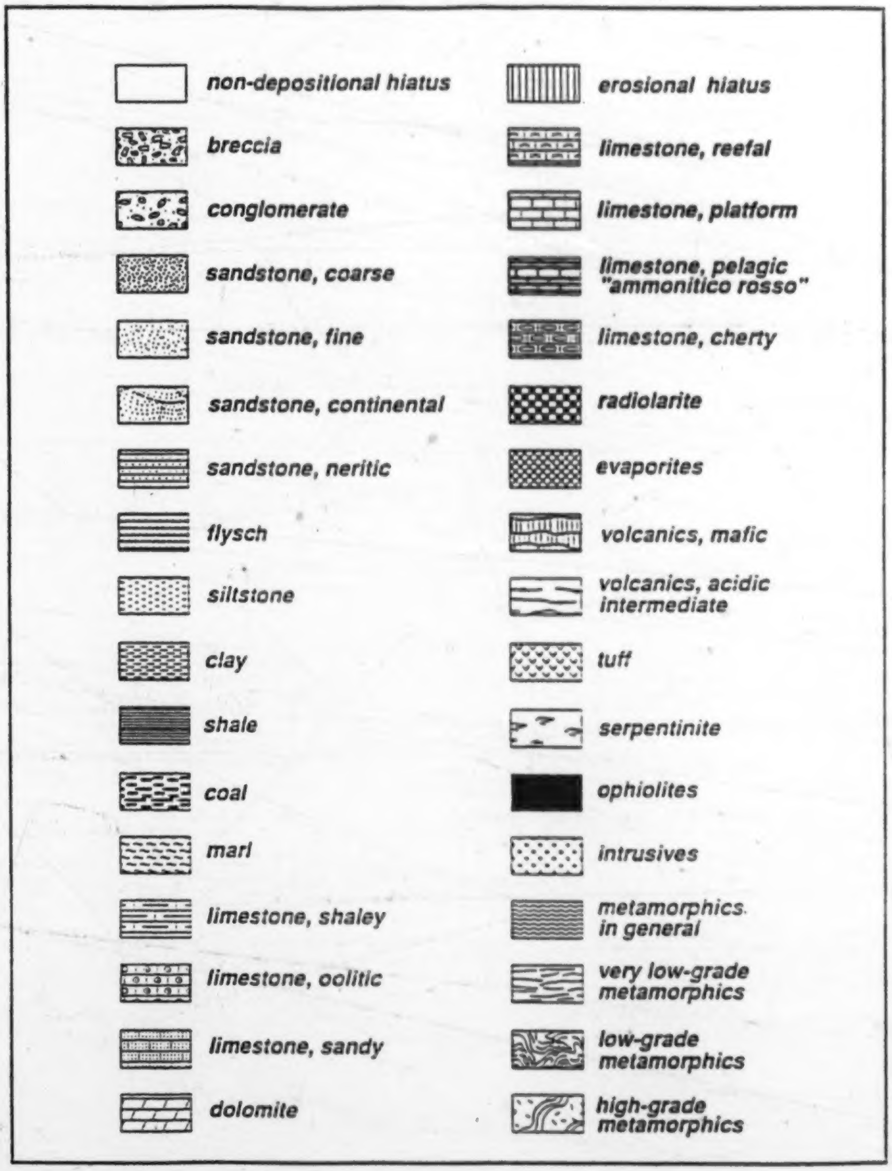
non-depositional hiatus
erosional hiatus
breccia
limestone, reefal
conglomerate
limestone, platform
sandstone, coarse
limestone, pelagic "ammonitico rosso"
sandstone, fine
limestone, cherty
sandstone, continental
radiolarite
sandstone, neritic
evaporites
flysch
volcanics, mafic
siltstone
volcanics, acidic intermediate
clay
tuff
shale
serpentinite
coal
ophiolites
marl
intrusives
limestone, shaley
metamorphics in general
limestone, oolitic
very low-grade metamorphics
limestone, sandy
low-grade metamorphics
dolomite
high-grade metamorphics

Fig. I-2. Legend of the lithostratigraphic columns compiled for the segments of the Alpine-Carpathian orogen discussed in text (*after* Tari, 1994).

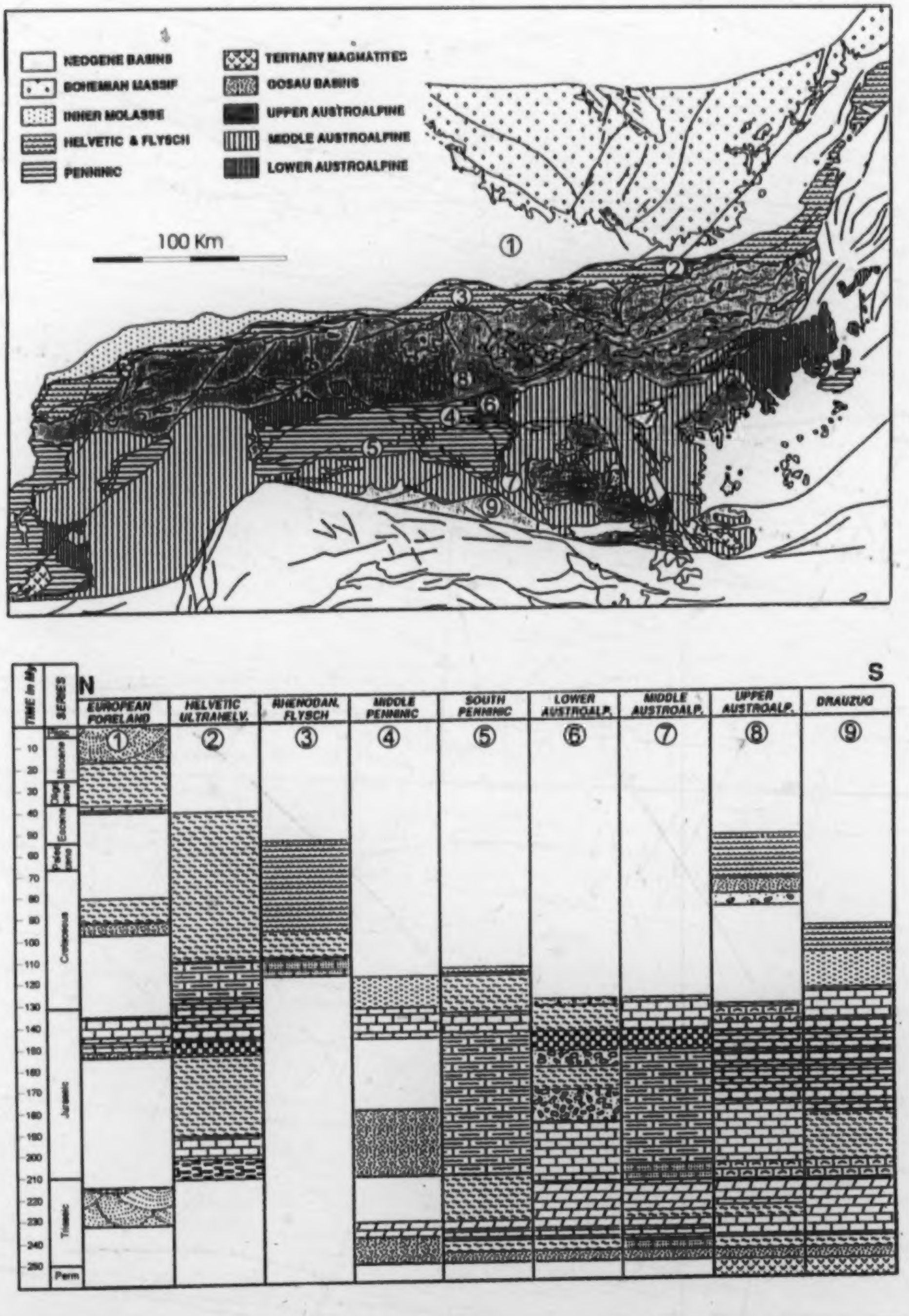
NEOGENE BASINS
BOHEMIAN MASSIF
INNER MOLASSE
HELVETIC & FLYSCH
PENNINIC
TERTIARY MAGMATITES
GOSAU BASINS
UPPER AUSTROALPINE
MIDDLE AUSTROALPINE
LOWER AUSTROALPINE
100 Km
①
②
③
④
⑤
⑥
⑦
⑧
⑨
TIME in My
SERIES
N
S
EUROPEAN FORELAND
HELVETIC ULTRAHELV.
RHENODAN. FLYSCH
MIDDLE PENNINIC
SOUTH PENNINIC
LOWER AUSTROALP.
MIDDLE AUSTROALP.
UPPER AUSTROALP.
DRAUZUG
Plioc.
Miocene
Oligocene
Eocene
Paleocene
Cretaceous
Jurassic
Triassic
Perm
10
20
30
40
50
60
70
80
90
100
110
120
130
140
150
160
170
180
190
200
210
220
230
240
250

Fig. I-3. a) Simplified tectonic sketch of the Eastern Alps; b) Alpine stratigraphy; (*adapted from* Tari, 1994).

Penninic oceanic basin. The African-derived Austro-Alpine nappe complex dominates the structure of the Eastern Alps. In the south, adjacent to the Periadriatic lineament, basement units and isolated Permo-Mesozoic cover are interpreted as structurally lower units. Permo-Mesozoic sequences exposed in the northern Calcareous Alps are high-level gravitational nappes.

Basement assemblages

The metamorphic basement of the Central and Eastern Alps belongs to the Austro-Alpine nappes and the Penninic Tauern window (Fig. I-4).

The Penninic basement exposed in the Tauern Window consists of the Paleozoic Venediger nappe system that includes from top to bottom: the Stubach Group, the Habach-Storz Group, and Variscan granitoids of the Zentralgneis (Frisch et al., 1993).The Zentralgneis Group consists of sheared I-type and subordinate S-type granitoids ranging in age from Carboniferous to Permian. Tonalite, granodiorite, granite batholites are exposed in dome-like or antiformal structures ("kerne" = core). The Habach-Storz Group consists of biotite plagiogneiss, amphibolite, micaschist and quartzite, and subordinate cummulate pyroxenite interpreted to represent a volcanic island arc association. Both micaschist and quartzite are locally graphitic and associated with phyllonite. A Late Proterozoic to Early Paleozoic age is assigned based on microfossils and U-Pb zircon ages and Sm-Nd whole rock ages ranging from 640-490 Ma. The Stubach Group consists of amphibolite and gneiss, micaschist, and quartzite with variably serpentinized layered cumulate (Neubauer et al., 1989). From the chemical characteristics of the ultramafic lenses which are similar to MORB and island arc tholeiite, the Stubach Group is interpreted as an ophiolitic association obducted during Variscan tectonism (Frisch et al., 1993). The ophiolitic assemblage is defined by the Stubachtal and Ochsner ultramafic/mafic rocks and several splinters of serpentinite within a matrix of plagiogneiss, micaschist and amphibolite. U-Pb and Sm-Nd mineral isochron ages in the range of 660-640 Ma on a gabbro-amphibolite are interpreted as formation ages (von Quadt, 1989).

The Austro-Alpine basement is relatively homogeneous west, and highly diverse east of the Tauern Window. It is commonly separated into fossil free medium to high-grade lithotectonic assemblages ("Altkristallin"), low-grade "quartzphyllite units", and nearly un-metamorphosed fossiliferous Paleozoic sequences. Geochemical data are considered to document all stages of the Variscan Orogeny (Neubauer and Frisch, 1993).

In different parts of the Eastern Alps, similar lithotectonic assemblages are separated as distinct "complexes" and assigned to a multitude of Variscan and Alpine nappes (e.g., Neubauer and Frisch, 1993; Ratschbacher et al., 1990; Dallmeyer et al., 1996) (Table I-1). The age of the protolith is unknown and the age of the medium-grade textures is uncertain.

The easternmost part of the Eastern Alps is dominated by the Grobgneis Complex which consists of plagiogneiss and micaschist with minor intercalations of amphibolitised gabbro and diorite (e.g., at Birkfeld and Kulm), intruded by various Carboniferous to Permian granites. Low-grade retrogression resulted in various phyllonite assemblages (Murztal and Birkfeld) with quartzite and talc schist.

Table I-1. Lithostratigraphic and tectonic units of the basement in Central and Eastern Alps (*compiled from* Tollmann, 1977; Neubauer and Frisch, 1993; Frisch et al., 1993)

Upper Austro-Alpine	Kaintaleck slices, Ackerl complex
Middle Austro-Alpine	Muriden complexes: Core, Speik, Micaschist-Marble complexes Koriden gneiss complexes, Plankogel micaschist complex
Lower Austro-Alpine	Semmering system: Grobgneis Raabalpen(=Tatric) Wechsel system: Waldbach and Wechsel gneiss complexes
Tauern Window	Venediger system: Stubach group, Habach-Storz group, Zentralgneis Group

In the central Eastern Alps up to the Tauern Window, the Grobgneis assemblage can be correlated with the "Core assemblage" of the Muriden Complex. Structurally upwards, the Muriden Complex is subdivided into a plagiogneiss-amphibolite ("Core"), a metaophiolite ("Speik"), and a micaschist - marble assemblage. Gneissic layers of the lowermost assemblage include relics of tonalitic rocks: porphyritic biotite granite and assorted amphibolite gneiss or amphibolite with pyroxenite, wehrlite, hornblendite, and gabbro. The more massive plagiogneiss of the Core assemblage shows a dome-like shape, mantled by plagiogneiss, amphibolite, garnet micaschist, and rare intercalations of thin calc-silicate rocks. A spessartine-bearing mylonitic quartzite within the micaschist suggests a mid-crustal tectonic discontinuity within the Core assemblage similar to the one interpreted in the Sebeş-Lotru assemblage of the South Carpathians (Săbău, 1994). The overlying assemblage (the Speik Complex) is a few hundred meters thick, and dominated by garnet amphibolite with discontinuous layers of augen gneiss, mixed siliceous and dolomitic marble, and serpentinite that contains relics of olivine-gabbro and eclogite. This assemblage grades through sulfide-rich quartzite and micaschist, into a structurally higher assemblage of garnet micaschist, biotite amphibolite, quartite, black schist, and variably dolomitic marble with abundant pegmatitic bodies.

To the south in the central Eastern Alps, the Koriden Complex consists of plagiogneiss enclosing up to kilometer-sized lenses of amphibolitized eclogite, gabbro, calc-silicate rocks marble, and manganese-rich mylonitic quartzite; typically, the plagiogneiss shows kyanite pseudomorphs after andalusite. The nature of the protolith and the age of eclogitization are uncertain. Kyanite-bearing low-Ti eclogite and kyanite-free high-Ti eclogite are interpreted to be

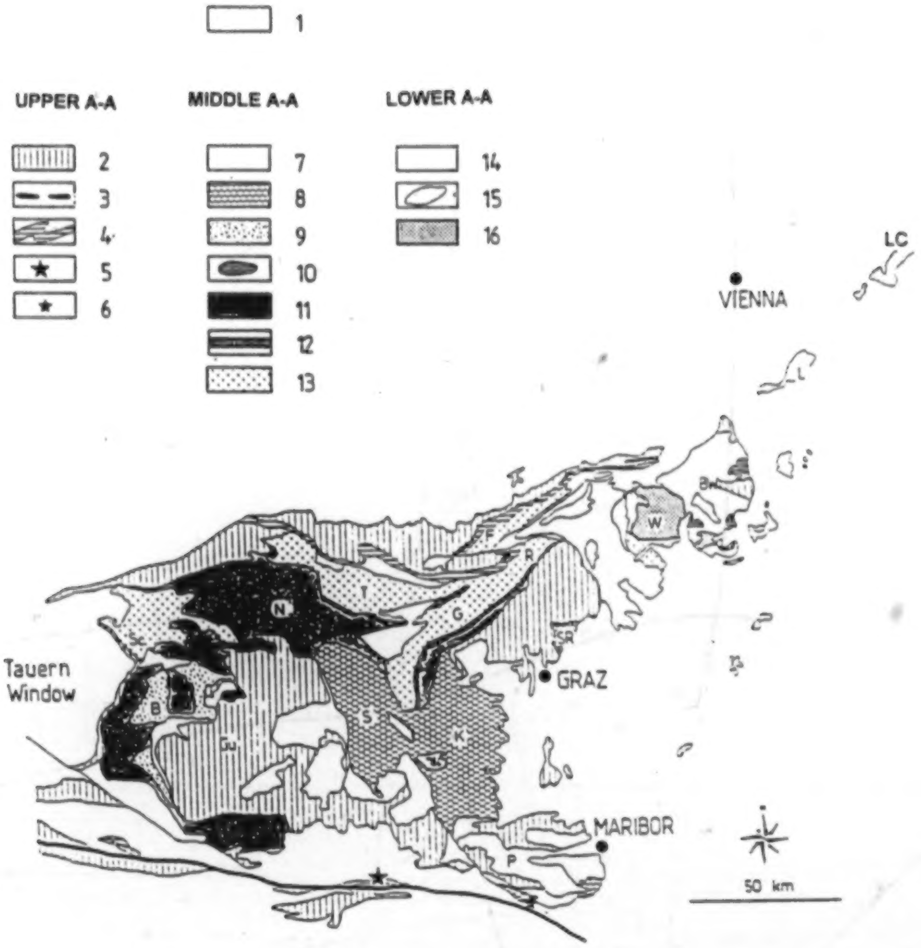
1
UPPER A-A
MIDDLE A-A
LOWER A-A
2
3
4
5
6
7
8
9
10
11
12
13
14
15
16
LC
VIENNA
L
W
F
R
T
N
G
SR
GRAZ
Tauern Window
B
Gu
S
K
MARIBOR
P
50 km

Fig. I-4. Simplified map of the Austro-Alpine basement units east of the Tauern window (*modified after* Neubauer and Frisch, 1993). 1 - Permian to Cenozoic formations; **Upper A-A nappes**: 2 - fossiliferous Paleozoic formations and "Qquartzphyllites" 3 - Kaintaleck slices and Ackerl complex; 4 - Carboniferous and Permian of the Veitsch nappe; 5 - Eisenkappel crystalline complex; 6 - Pohorje garnet-peridotite-granulite complex; **Middle A-A nappes**: 7 - Plankogel complex and related micaschist complexes; 8 - Koriden gneiss complex; 9 - Bundschuh complex; 10 - Sieggrabener complex; 11 - Micaschist-Marble complex; 12 - Speik complex; 13 Core complex; **Lower A-A nappes** 14 - "Grobgneis" complex. 15 - Tatric unit; Wechsel gneiss complex. *Geographic markers:* Gu - Gurktaler Alpen; K - Koralpe; L - Leitha Mountain; LC - Little Carpathians; N - Niedere Tauern; P - Pohorje Mountains; W - Wechsel.

derived from gabbro and MORB basalt, respectively. To the south, the Koriden plagiogneiss assemblage is overlain by the Plankogel complex of staurolite-garnet micaschist matrix with up to kilometer-size lenses of silicate-marble, amphibolite, variably serpentinised ultramafic lenses, manganese quartzite overlain by the Kräuping micaschist, and quartzite with thick amphibolite lenses.

Lithotectonic assemblages similar to the Koriden Complex are known east of the Tauern Window as the Bundschuh-Einach and Ackerl complexes, and further east as the Sieggrabener Complex. The Bundschuh-Einach Complex consists of plagiogneiss and granite gneiss. The Ackerl Complex consists of staurolite-bearing plagiogneiss, rare orthogneiss, micaschist, quartzite and amphibolite and concordant phyllonitic shear zones. The Sieggrabener Complex consists of garnet ± kyanite plagiogneiss, serpentinized peridotite, amphibolitised eclogite, calc-silicate rocks, and marble.

The northern basement exposures are represented by the Kaintaleck tectonic slices with diverse rock types (Ritting, Frauenberg and Prieselbauer assemblages) and are bounded to the north by the highly strained Kalwang trondhjemite and covered by Carboniferous fossiliferous greywacke.

All mafic assemblages of the Eastern Alps are routinely interpreted as pre-Alpine ophiolitic sequences. In the Austro-Alpine nappes, the Speik assemblage of the Muriden Complex is considered an ophiolite sequence obducted southward (Neubauer and Frisch, 1993). Similarly, the Plankogel Complex is interpreted as a pre-Alpine east-vergent ophiolitic melange (e.g., Frisch et al., 1984). In the basement of the Tauern Window, the Stubach assemblage is also interpreted as an obducted ophiolite complex (Frisch et al., 1993).

Interpretations of crustal evolution in the Eastern Alps benefit from the greatest number of isotopic data in the orogen. Within the Frauenberg assemblage involved in the Kaintaleck tectonic slices a population of rounded zircons from a hornblende garnet gneiss yielded a U-Pb upper intercept of c. 2.53 Ga with a lower intercept of c. 516 Ma. A population of brown, metamictic zircons yielded an upper intercept of c. 2.8 Ga. The lower intercept is interpreted to date the Caledonian metamorphism, the 2.53 Ga date to be the crystallization age of the protolith, and the 2.8 Ma date to indicate crustal contamination of the igneous source (Neubauer and Frisch, 1993). The age of metamorphism is suspicious because it corresponds to the c. 500 Ma age of emplacement of the Kalwang trondjemite of the Kaintaleck slices suggested by the U-Pb zircon upper intercept. However, these U-Pb zircon data indicate that Precambrian granitoids are part of the plagiogneiss-granite dominated assemblage, which is widespread in the Alpine-Carpathians orogen.

U-Pb zircon dates from the tonalitic rocks of the Core Complex yielded upper intercept dates near 3 Ga and 2.25 Ga and a lower intercept of c. 356 Ma. U-Pb zircon (c. 500 Ma -Haiss, 1991). Rb-Sr dating (c. 518 Ma - Frank et al., 1976) in the plagiogneiss matrix (tonalite gneiss) also suggests an Early Paleozoic tectonomagmatic event. Several dates from igneous rocks ranging between 460-425 Ma suggest Late Ordovician-Early Devonian igneous activity. Other othogneisses yielded Carboniferous ages (Sharbert, 1981). The assemblage is invaded by trondjemitic migmatite at c. 353 Ma (Neubauer et al., 1993), indicating an Early Carboniferous magmatic event. U-Pb and Rb-Sr dates from granites and granite gneiss of the lowermost assemblage range from Ordovician to Carboniferous. Rb-Sr data from coarse-grained porphyritic granite-gneiss of the Grobgneis Complex are interpreted as Carboniferous emplacement ages (326+/-11Ma; 338+/-12 to 343+/-20 Ma), similar to the granitoid intrusions in the basement of the West Carpathians.

In the Muriden Complex, evidence of Early Carboniferous Variscan tectonism consists of U-Pb zircon lower intercepts of c. 425 Ma and c. 365 Ma from an augen gneiss and a metatonalite lense, respectively (Neubauer and Frisch, 1993). These ages correspond to the main phases of plutonism documented within the Lower Muriden succession between 460-425 Ma and 360-350 Ma. ^{40}Ar/^{39}Ar plateau dates of c. 364 and c. 375 Ma are in the Keintaleck nappes are interpreted to record Early Variscan orogenesis.

^{40}Ar/^{39}Ar data from hornblende concentrate of the Sieggrabener eclogite yielded c. 136 Ma and c. 108 Ma whilst a muscovite concentrate yielded c. 82 Ma, in the range of all Ar/Ar ages obtained on the subjacent Grobgneis Complex. The Sieggrabener is interpreted as a klippe of the Koriden Complex emplaced during Cretaceous thrusting. The interpretation is suspect because rock types of the Grobgneis and Koriden complexes are similar and the eclogite pods may have been incorporated in the gneissic crust prior to the Alpine tectonism.

^{40}Ar/^{39}Ar dates from basement rocks in the north-central Eastern Alps (Dallmeyer et al., 1996) range from c. 98 to c. 84 Ma. To the east, ^{40}Ar/^{39}Ar data on muscovite throughout the Grobgneis Complex range between c. 82 Ma and c. 71 Ma, and two dates from hornblende concentrates from amphibolitised eclogite yielded c. 108 and 136 Ma. Intra-Gosau (c. 86-65 Ma) dates on non-mylonitic basement are interpreted to date exhumation and cooling following nappe assembly (e.g., Ratschbacher et al. 1989; Neubauer et al., 1995). Dates within ductile shear zones of the Lower Austro-Alpine units range between c. 78 and c. 71 Ma and are interpreted as thrusting in deep crustal levels (Dallmeyer et al., 1992).

Paleogeographic and tectonic evolution

After the Hercynian orogeny, during the Late Permian, the area of the original Eastern Alps was invaded by sea. The Lower Triassic neritic sandy shales and sandstones were replaced by Anisian carbonate platforms, followed in the Ladinian, mainly to the south, by the deep-water Hallstatt facies strata probably related to deep fault-controlled troughs. A broad Late Triassic carbonate platform suggests a phase of regional thermal subsidence most active in the south. In the Early Jurassic, the centres of subsidence shifted to the northernmost part of the North Alpine shelf as a result of the initial extension of the South Penninic ocean, and by the end of the Jurassic, deep-water environments with radiolarite deposition prevailed in the whole region. The Malm to Early Neocomian initial phase of compression resulted in the uplift of the basement and gravity nappes gliding towards the north. E-W trending facies zones are stacked in the Alpine nappe pile, with the southernmost zone in the northernmost and structurally uppermost position. The whole edifice was pushed northward toward the Neocomian Rossfeld flysch trough interpreted as a trench in front of a N-vergent accretionary complex. The Austro-Alpine nappe pile overthrust the Penninic facies zones during the Albian-Turonian. The Engandine, Tauern, and Rechnitz tectonic windows expose the Penninic foreland of Europe.

Deposition of the Senonian Gosau facies began in the Coniacian. It is regarded as a post-tectonic succession commonly overlying Eoalpine thrust contacts. The Gosau strata are commonly involved in Tertiary thrusting and folding. Late Tertiary strike-slip and normal faulting suggest a pattern of eastward extrusion tectonics.

Geophysical data

Most data indicate subhorizontal seismic reflectors dipping north or south toward an inflexion zone outlining a low-velocity crustal root along the southern boundary of the Central Alps (Moeller, 1989)(Fig. I-5) and major upper mantle heterogeneities interpreted to record subduction (Spakman, 1990) (Fig. I-6).

Inconsistencies

Recent structural data and paleogeographic reconstructions have largely improved knowledge of the tectonic evolution of the Austroalpine domain, but their accommodation in the traditional nappe stacking interpretation appears speculative:

- Austro-Alpine lithotectonic assemblages on the northern and southern side of the Tauern Window are different.

- the subdivisions and structure of the Penninic basement and of the Muriden Complex of the Austro-Alpine nappe system (A-A) are almost identical: the Zentralgneis unit correlates with the Grobgneis and the Holbach-Storz correlates with the assemblage of plagiogneiss, micaschist, amphibolite, phyllonite and quartzite forming the matrix of the Grobgneis in the Eastern Alps. The Stubach ophiolitic association comprises few lenses of more or less serpentinized layered gabbro-cumulate, common in all basement units of the Alps. Their location at about the same latitude within the orogen casts doubts on the current tectonic interpretation that places Penninic basement on the lower European plate and A-A on the upper African plate following subduction of the South Penninic ocean and complex collision.

- the interpretation of the Sieggrabener eclogite-bearing complex as a klippe of the Koriden Complex emplaced during Cretaceous thrusting is suspect because rock types of the

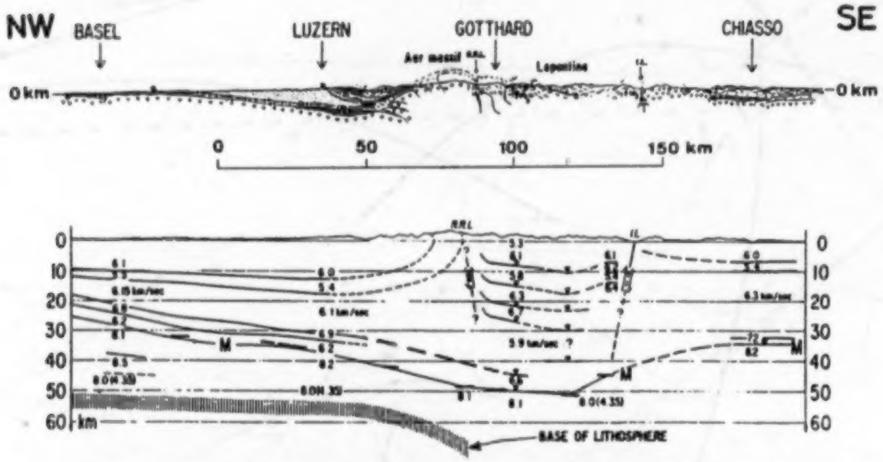
NW
BASEL
LUZERN
GOTTHARD
CHIASSO
SE
Aar massif
RRL
Lepontine
IL
0 km
0
50
100
150 km
M
km
BASE OF LITHOSPHERE

Representative lithospheric cross section along the 'Swiss Geotraverse' from Basel to Chiasso/Como (cf. Mueller 1982a). P-wave velocities in km/s. RRL = Rhine–Rhône Line; IL = Insubric Line; M = Crust–mantle boundary (Mohorovičić Discontinuity). The base of the lithosphere ('fence' hachures, cf. Fig. 11) has been determined from a regional analysis of seismic surface-wave dispersion (S-wave velocities given in brackets).

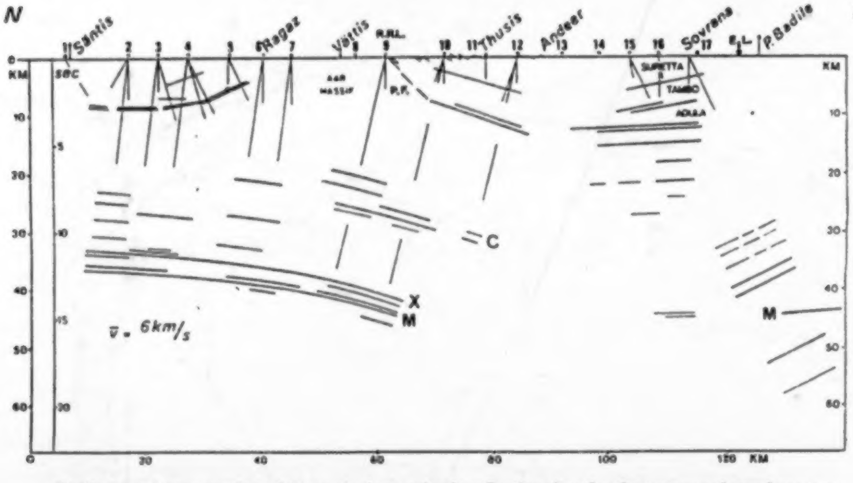
N
S
Säntis
Ragaz
Vättis
R.R.L.
Thusis
Andeer
Sovrana
EL
P. Badile
KM
AAR MASSIF
P.F.
SURETTA
TAMBO
ADULA
C
X
M
v̄ = 6km/s
0
20
40
60
80
100
120 KM

Preliminary interpretation of the explosion–seismic reflection data for the traverse through eastern Switzerland (cf. Fig. 3b). The most conspicuous reflection 'bands' are represented by hand-migrated line drawings (after Finckh *et al.* 1987). In the north the lower and middle crust with the C, X and M reflectors appear to be 'decoupled' from the upper crust and seem to move intact down into the steeply southward dipping subduction zone (cf. Figs 11, 13b and 14a). In the upper crust the Aar Massif which is exposed in a 'window' near Vättis separates the Helvetic domain with its distinct Triassic marker (cf. Fig. 5) from the Penninic domain with the Suretta, Tambo and Adula nappes (cf. Fig. 3a). The 'Penninic Front' (PF) outcrops at the Rhine–Rhône Line (RRL) near Tamins (shotpoint 9). The steeply northward dipping reflectors in the southernmost part of the section have not been properly migrated. There is a distinct gap in the reflection bands (C, X and M) delineating the lower crust between shotpoints 10 and 12 in the north and shotpoints 16 and 17 in the south which has not yet been explained. When approaching the Engadine Line (EL) the M-discontinuity seems to rise gently towards the south. It should be noted that the crust-mantle boundary (M) as derived from seismic refraction measurements appears to be continuous.

Fig. I-5. Deep structure of the Alps (*from* Moeller, 1989).

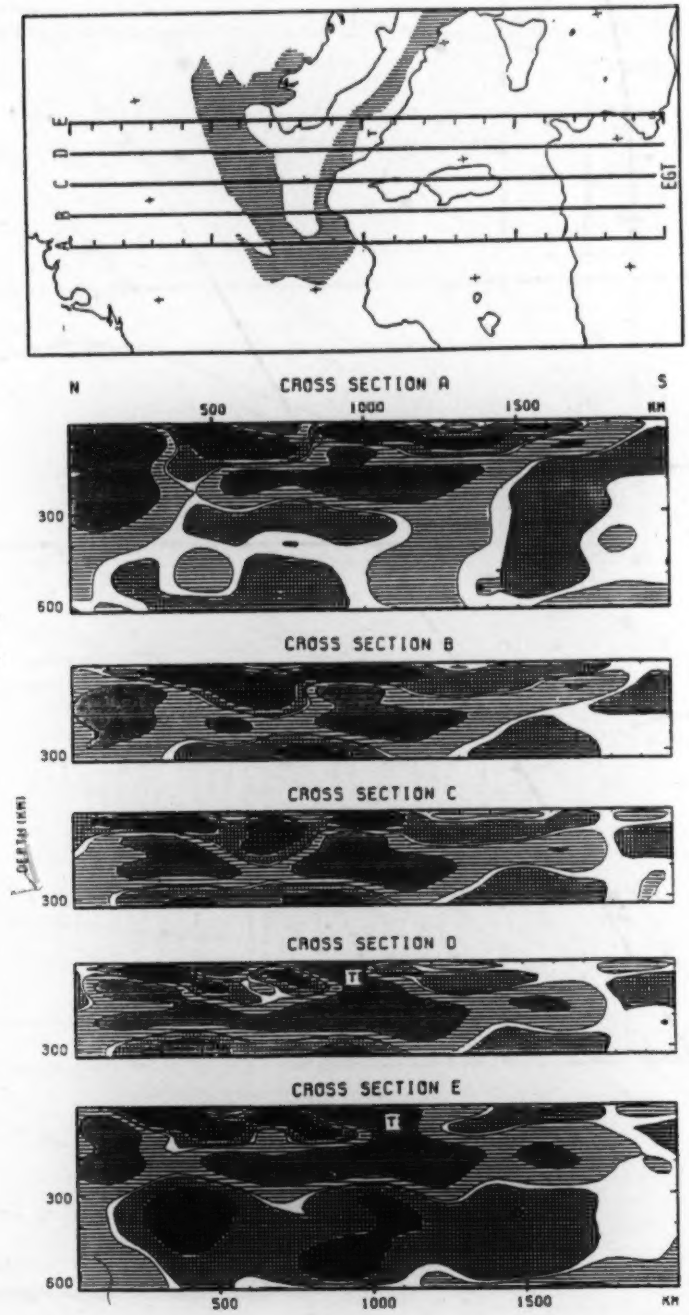
A
B
C
D
E
EGT
N
CROSS SECTION A
S
500
1000
1500
KM
300
600
CROSS SECTION B
300
CROSS SECTION C
DEPTH (KM)
300
CROSS SECTION D
T
300
CROSS SECTION E
T
300
600
500
1000
1500
KM

Fig. I-6. Tomographic images of the upper mantle under the Alps (*from* Spakman, 1990). See caption on next page.

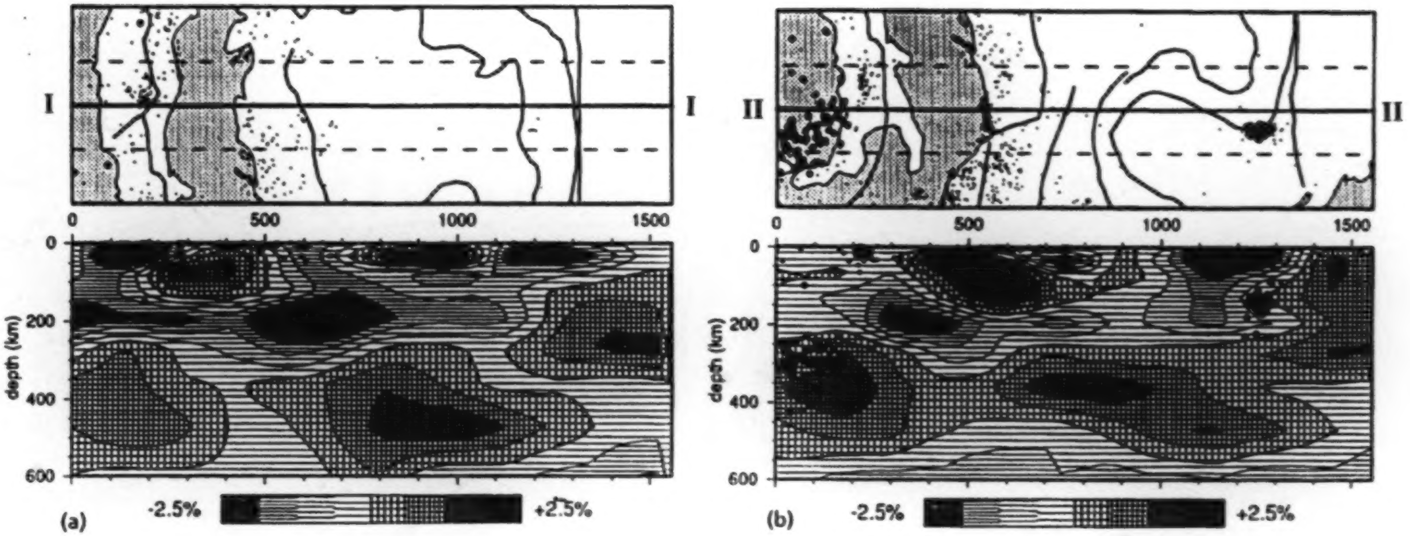

Fig. I-6 (continued). Tomographic images of the upper mantle under the Dinarides and the Carpathians (*from* Spakman, 1990). *Top*: regional map for reference. The map is centered around the upper mantle profile (heavy line). Dots represent epicentres of earthquakes with magnitudes larger than 3.5. Events enclosed in the area indicated by the straight dashed lines are also shown in the upper mantle section as projected hypocentres on the plane of intersection. The distance from the dashed lines to the profile is 110 km. Other dashed lines represent the tectonic lines, also displayed in Fig. 1a. *Bottom*: upper mantle section to a depth of 605 km. This depth corresponds to the central depth of the last layer of cells. The contouring displays the tomographically inferred seismic velocity heterogeneity of P wave.The results are displayed as percentages of the ambient Jeffreys-Bullen mantle velocity. Cross-hatched are positive (or high) velocity regions, horizontally hatched -negative (or low) velocity regions. Dots denote the projection of hypocentres on the cross sectional plane (from Spakman, 1990).

adjacent Grobgneis are similar and the eclogite pods may have been incorporated in the gneissic crust prior to the Alpine tectonism.

- the Helvetic/Penninic facies zone exposed in tectonic windows is only present west of the windows and not north or in front of the originally interpreted Austro-Alpine front.

- the thicker Triassic and the low-grade Radstatt (Jurassic?) succession of the lower Austroalpine units, are similar to contemporaneous Penninic successions; existing differences can be explained by lateral facies variations of cover strata similar to those documented in the Austro-Alpine units (e.g., the facies of the Upper Triassic changes from peritidal carbonate (Hauptdolomite) in the west to continental variegated clays (Carpathian Keuper) to the east.

- there are significant facies differences between the Upper Triassic carbonate facies of the upper Austroalpine nappes (lagoonal-Hauptdolomite, reefal platform-Dachstein limestone, to basinal carbonate-Hallstatt limestone) and contemporaneous sequences in the supposed root zone, in the Drauzug area (Upper Triassic and Lower to Middle Jurassic sequence of Licicum).

- the Triassic Hauptdolomit facies of Drauzug and the Transdanubian mountains (Fig. I-23) is also exposed on the Austro-Alpine basement, in the "Gurktal Nappe". Clasts of South Alpine origin within the Gosau strata from Graz suggest a relatively uniform cover of South Alpine affinity for the southern Austro-Alpine basement.

- no structural evidence exists for the involvement of Drauzug and Transdanubian (Figs. I-3 and I-23) mountains in a gigantic pre-Gosau "Ultrastyrian nappe"as postulated by Tollmann (1987), to explain the Triassic facies distribution and Gosau clasts. Instead paleo-geographic reconstructions based on Permo-Mesozoic isopic zones (e.g., Bechstädt, 1978; Schmidt et al., 1991; Haas et al., 1995) indicate 300-400 km of eastward lateral dislocation of the Drauzug, Transdanubian mountains, and implicitly the "Gurktal Nappe".

- the northwest-trending displacement vectors in the lower basement "nappes" are parallel to dextral strike slip faults in the upper cover nappes of the Northern Calcareous Alps (Ratschbacher and Frisch, 1993) and suggest widespread dextral internal strain in the Austro-Alpine units.

- there is no kinematic evidence for the popular interpretation of all mafic assemblages of the Eastern Alps as pre-Alpine ophiolitic sequences obducted during the Variscan tectonism; consequently, the confusing kinematic picture includes Variscan obductions in different directions: eastward for the Plankogel "ophiolitic mélange" (Frisch et al., 1984), southward for the Skeik "ophiolitic assemblage" (Neubauer and Frisch, 1993).

- the vergence of Austro-Alpine nappes is highly controversial (Oberhauser, 1991); the vergence of cover nappes was originally inferred to be northwest or west (e.g., Termier, 1903; Rothpletz, 1905), then north (e.g., Tollmann, 1963). Recent models argue for Cretaceous west-directed thrusting and Tertiary piggyback transport of the whole nappe pile to the north (e.g., Schmid and Haas, 1989). A paradoxical orogen-parallel nappe stacking model resulted from the combination of modern kinematic analysis (e.g., Ratschbacher, 1986) with the originally interpreted outlines of the "Penninic windows": a narrow (less than 100 km) wedge of African crustal slices would have travelled from east to west over 260 km of the narrow Penninic continental fragment. Moreover, no Tertiary overprint has been detected in the Lower Austro-Alpine Nappes, in contrast with the currently interpreted major phase of Eocene thrusting.

- micro-structural work showed that many faults and shear zones previously interpreted as thrusts are in fact low-angle extensional faults (e.g., Nievergelt et al., 1991, Werling, 1992; Handy et al., 1993). Even some spectacular recumbent folds (e.g., the Ela "frontal fold") are not related to thrusting and crustal shortening, but to crustal extension (Froitzheim, 1992).
- sinkinematic muscovite in ductile shear zones are contemporaneous with the development of Gosau basins; 'intra-Gosauian" mineral ages cannot be interpreted as thrust related.

It appears that previous models have largely overestimated the thrust tectonics and overlooked tangential strain and displacement.

I.3. THE JUNCTION BETWEEN THE EASTERN ALPS AND THE WEST CARPATHIANS

The Neogene fill of the Vienna Basin prevents direct correlation of major tectono-stratigraphic units of the Eastern Alps and Carpathians. However, the Leitha Mountain exposes the same plagiogneiss-micaschist association intruded by granitoids as the eastern extremity of the Alps and the Little Carpathians (Fig., I-4). South of the Leitha ridge to the Raba fracture zone, metamorphic assemblages in the southeasternmost spurs of the Eastern Alps can be recognized in isolated exposures in the Rechnitz-Koszeg and Sopron regions and in drill holes in the Little Hungarian Plain (Fig. I-7).

The Rechnitz-Koszeg series (Schönlaub, 1979) consists of three low-grade lithotectonic assemblages; from north to south, these are quartz phyllite, phyllite, and greenschist with pods of metadiabase and serpentinite. The protolith is considered to be a Jurassic to Lower Cretaceous sedimentary sequence that correlates with the Penninicum sequence. Glaucophane relics suggested affinities to the Meliata lithotectonic assemblages of the West Carpathians. Zircon fission track data ranging from 19 to 13 Ma (Dunkl, 1992) indicate a Miocene metamorphic core-complex evolution, interpreted to have partly obliterated structures related to major Cretaceous thrusts (e.g., Tari, 1996). To the north, it is tectonically overlain by Lower Austro-Alpine units (the Wechsel Series and the Grobgneis unit), and to the south, by Paleozoic to Mesozoic rocks assigned to the Upper Austroalpine units (essentially the Graz Paleozoic). The model implies that the Lower and Middle Austro-Alpine units are missing on the southern

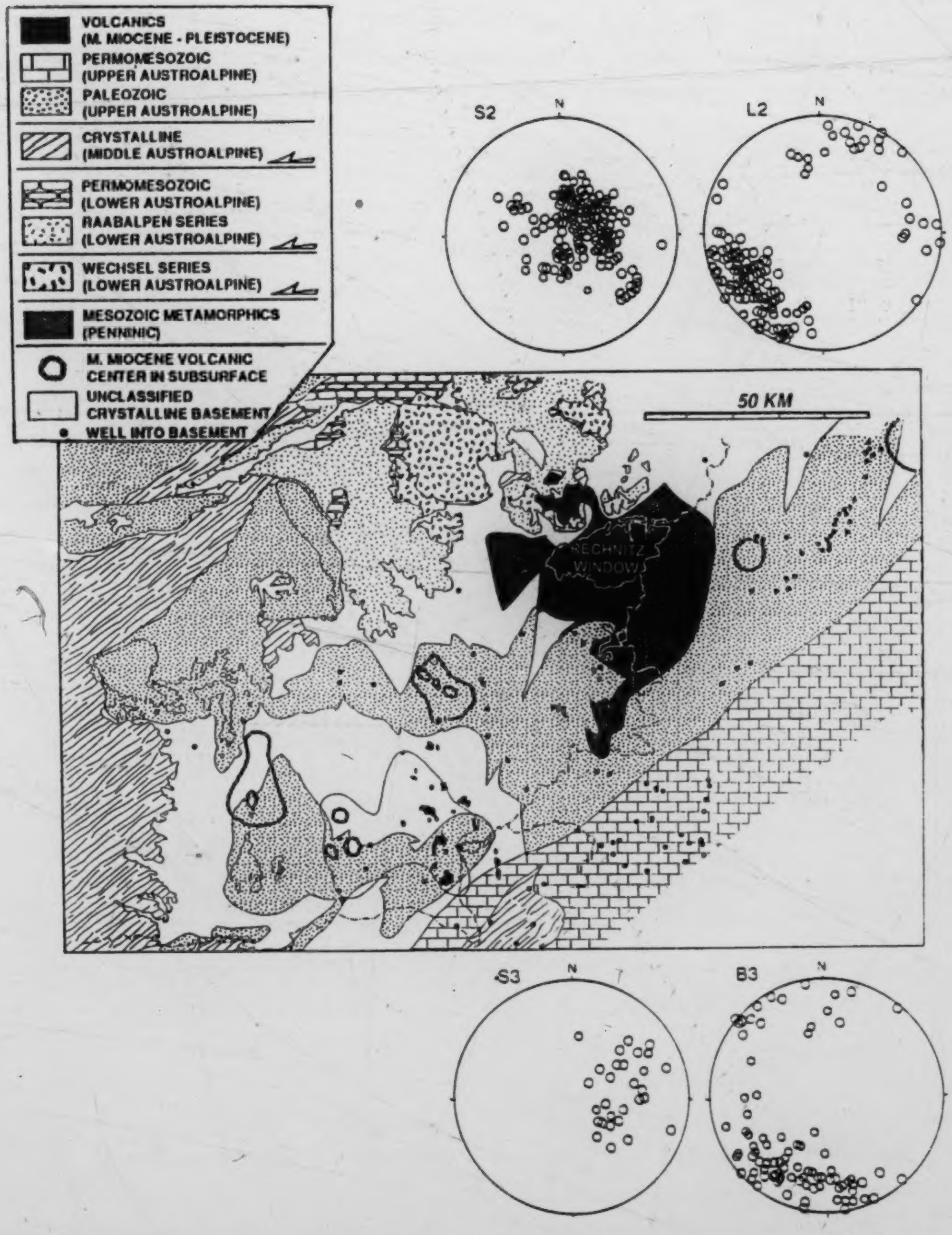
VOLCANICS (M. MIOCENE - PLEISTOCENE)
PERMOMESOZOIC (UPPER AUSTROALPINE)
PALEOZOIC (UPPER AUSTROALPINE)
CRYSTALLINE (MIDDLE AUSTROALPINE)
PERMOMESOZOIC (LOWER AUSTROALPINE)
RAABALPEN SERIES (LOWER AUSTROALPINE)
WECHSEL SERIES (LOWER AUSTROALPINE)
MESOZOIC METAMORPHICS (PENNINIC)
M. MIOCENE VOLCANIC CENTER IN SUBSURFACE
UNCLASSIFIED CRYSTALLINE BASEMENT
WELL INTO BASEMENT
S2
N
L2
N
50 KM
RECHNITZ WINDOW
S3
N
B3
N

Fig. I-7. Subsurface geology around the Rechnitz window compiled *after* Flugel and Neubauer (1984); Kröll et al. (1988); Neubauer et al. (1992); Stereographic projections of mesoscopic planar and linear fabrics in outcrops, *after* Ratschbacher et al. (1990): S2-main foliation; L2 - main stretching lineation; S3 - subsequent foliation; B3 - minor fold axis.

gneiss is tentatively correlated with the Wechsel series of the Eastern Alps (Jantsky et al., 1988). limb of the nappe antiform and that Paleozoic strata in northern Hungary represent a thrust sheet.

In the Sopron region, the Fertörákos-Csapod assemblage of amphibolites and two-mica It is overlain by the Sopron granite-gneiss and the Obrennberg andalusite-sillimanite-microcline gneiss/micaschist that can be correlated with the Grobgneis unit of the Eastern Alps. Strong shearing/retrogression resulted in a mylonitic assemblage dominated by chloritoid-bearing phyllonite with kyanite, garnet relics . In contrast to the Eastern Alps where the Grobgneis and Wechsel series are interpreted as distinct Lower Austro-Alpine nappes, no sharp contact can be traced between the Fertörákos and Sopron-Orennberg assemblages.

Table I-2. Correlation of the main tectonic units in the Alpine-Carpathian transition zone (*modified after* Horváth, 1993)

Alpine Units	**HW Hungary**	**Carpathian - Pannonian Units**
Alpine molasse foredeep		Carpathian molasse foredeep
Alpine flysch zone		Carpathian flysch zone
St. Veit klippen		Pieniny klippen
Upper and Middle Austroalpine		Hronic, Gemeric
Lower Austroalpine Grobgneiss Wechsel	Sopron Fertorakos, Leitha	Tatric
South Penninic	Rechnitz	
		Veporic
Drauzug		Transdanubian Central Range
South Alpine		Igal-Bükk-Meliata zone

Inconsistencies

Stretching lineations and axes of minor folds, within the Rechnitz window, although assigned to distinct events (Ratschbacher et al., 1990), are roughly parallel (Fig. I-4). Their subhorizontal plunge and NE-SW trend in a subhorizontal foliation are inconsistent with the NW- or W-ward thrusting of the Austro-Alpine nappe complex.

The Graz Paleozoic strata cover Middle Austroalpine units in the Eastern Alps and Penninic units at Rechnitz. No unequivocal data exist to support a thrust contact between the Paleozoic strata and the Rechnitz sequence. The continuity of the Graz Paleozoic succession overlying different Austro-Alpine nappes makes the thrust interpretation suspect.

In contrast to the Alps, the lowermost nappe of the West Carpathians occupies the northernmost position, which implies that the horizontal transport of the upper nappes in the

West Carpathians is considerably less significant than in the Alps. The South Penninic oceanic trough closes eastward. The Meliata sequence is geometrically above equivalents of the Austro-Alpine nappes and shows south Alpine (?) Dinaric facies affinities (e.g., Balla, 1987). Penninic oceanic remnants from Rechnitz project along the orogenic trend into the remnants of the Meliata assemblage of the West Carpathians Vardar-Bukk- oceanic trough.

I.4. WEST CARPATHIANS

The West Carpathians segment of the orocline is exposed between the Neogene depressions of the Vienna basin to the west and the Transcarpathian basin to the east. The northern boundary is located between the molasse and the European foreland. The southern boundary with the north Pannonian unit is marked by the Meliata oceanic sequence (Fig. I-8).

Major Tectonostratigraphic units

The following geologic summary is based on work of Andrusov (1968) Mahel (1974), Birkenmayer (1985;1986), Kamenický and Kamenický (1988), Rakus et al. (1990) and Putis (1994).

The West Carpathian are traditionally subdivided into the Outer Tertiary and Inner pre-Tertiary units, separated by the Pienniny Klippen Belt. The Mesozoic cover and Miocene molasse of the European foreland is tectonically overlain by Malm to Oligocene age deep-water clastic strata involved in the Neogene Sub-Silesian and Silesian foreland thrust-and-fold belt, and in the Paleogene Magura thrust-and-fold belt which includes Early Cretaceous flysch. The Pieniny Klippen Belt is a 1-20 km wide belt of highly deformed, chaotically disrupted, and jumbled Triassic to middle Tertiary rocks, which extends along the inner side of the thrust belt. The Upper Cretaceous and Paleogene component of this mélange is mostly deep-water clastic sediment, whereas older sedimentary rocks include both abyssal carbonate rocks, pelagic radiolarites, and shallow-water carbonates; correlative rocks now juxtaposed record widely contrasting facies with quite different faunas. The Klippen belt is subdivided into four north-vergent units (Csorsztyn, Pieniny, Klape and Manin) based on facies differences of generally deep-water Jurassic to Cretaceous strata (Birkenmajer, 1986, 1988; Misik and Marschalko, 1988). Chrome spinel, serpentine, and glaucophane grains are interpreted to be clasts derived from a composite nappe stack including multiple subduction-derived metamorphic units (Dal Piaz et al., 1995).

Along the Ukrainian Carpathians, the polymict mélange loses its identity and its southward continuation in front or behind the East Carpathian basement is a matter of debate.

Basement assemblages

Metamorphic and igneous rocks of the West Carpathians crop out in the central part of the Inner West Carpathians and in several isolated exposures (Fig. I-9) along the arc. Based on isotope and palynological data, they were interpreted as products of the Dalslandian, Cadomian,

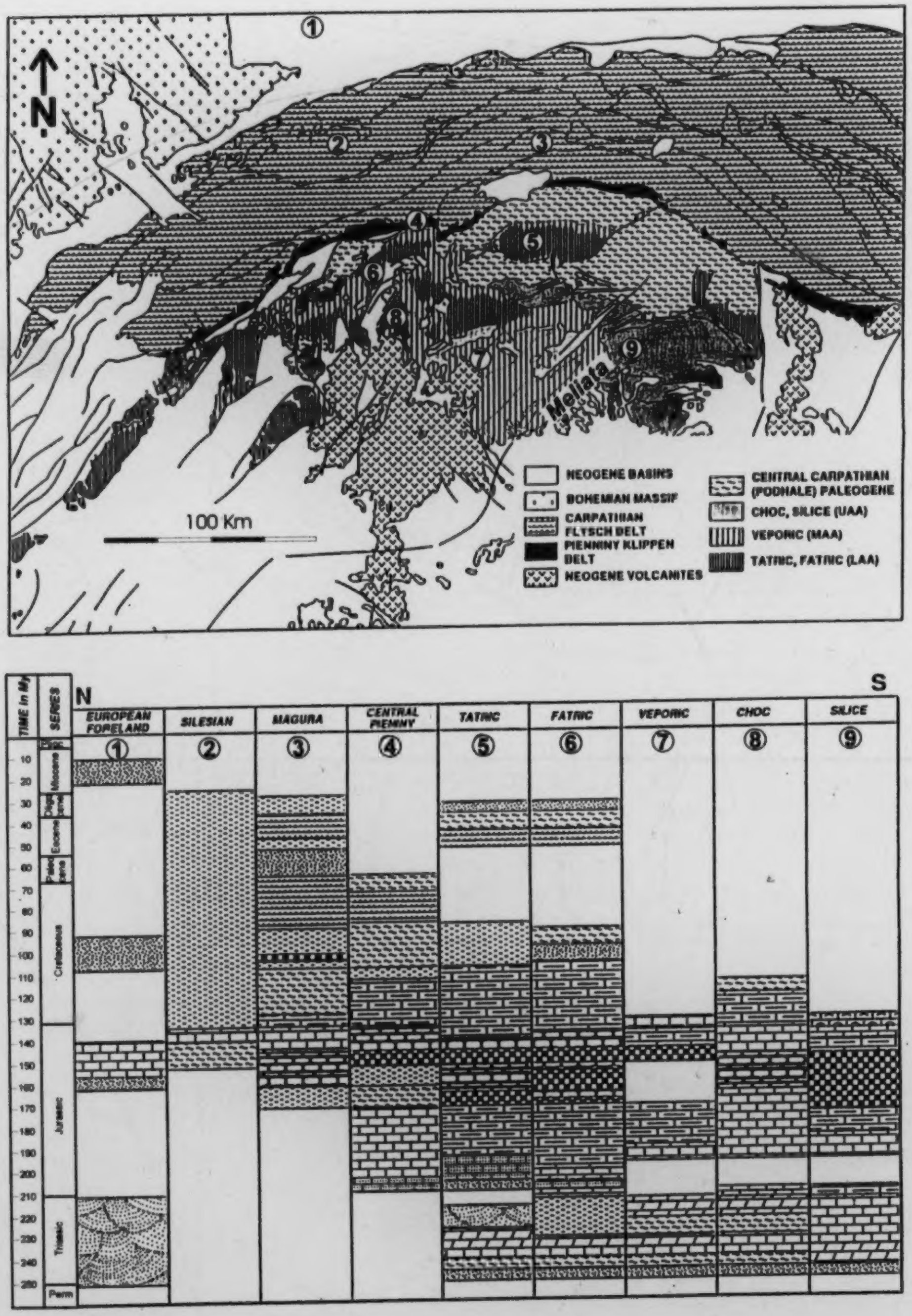
①
②
③
④
⑤
⑥
⑦
⑧
⑨
N
Meliata
100 Km
NEOGENE BASINS
BOHEMIAN MASSIF
CARPATHIAN FLYSCH BELT
PIENNINY KLIPPEN BELT
NEOGENE VOLCANITES
CENTRAL CARPATHIAN (PODHALE) PALEOGENE
CHOC, SILICE (UAA)
VEPORIC (MAA)
TATRIC, FATRIC (LAA)
N
S
TIME in My
SERIES
EUROPEAN FORELAND
SILESIAN
MAGURA
CENTRAL PIENINY
TATRIC
FATRIC
VEPORIC
CHOC
SILICE
Plioc.
Miocene
Oligocene
Eocene
Paleocene
Cretaceous
Jurassic
Triassic
Perm
10
20
30
40
50
60
70
80
90
100
110
120
130
140
150
160
170
180
190
200
210
220
230
240
250

Fig. I-8. a) Simplified tectonic sketch of the West Carpathians; b) Alpine stratigraphy; (*adapted from* Tari, 1994)

Caledonian, and Variscan cycles (Table I-3) and partly affected by Alpine tectonism.

An association of granite-gneiss and migmatite with subordinate kyanite and/or sillimanite plagiogneiss and amphibolite is assigned to the Proterozoic Jarabá (Tatra) and Kazimir (Zemplin) groups. The association of micaschist, graphite quartzite, carbonaceous rocks, and amphibolite is assigned to the Early Paleozoic Kohút (Kokava) Group. Several low-grade assemblages are dominated by metarhyolite, phyllite, metasandstone and graphite schist are assigned to the Middle-Late Paleozoic. The southernmost metamorphic assemblage is a discontinuous lineament (Fig. I-9) of deep-water Mesozoic strata associated with basic and ultrabasic rocks, the Meliata sequence, overprinted by late Middle Jurassic (Dallmeyer et al., 1996) low-temperature high pressure metamorphism (glaucophane schist).

Correlation between individual exposures along the arc is uncertain due to isolated exposures and multiple phases of tectonism. Various names are in use and the contacts between most lithologic associations are controversial. The stratigraphic classification appears obsolete, since most basement assemblages incorporated in Alpine nappes were recently reinterpreted as south-vergent Variscan nappes (e.g., Janak, 1992; Fritz et al., 1992;). For example, the Tatra and Cierny Balog gneiss-granitoid association were considered as Variscan thrust sheets overlaying the micaceous/amphybolitic Hron association (Putiš, 1994). Serpentinite-amphibolite-gneiss associations found at isolated locations were interpreted as a

Table I-3. Lithostratigraphic units of the West Carpathians basement (*after* Kamenický and Kamenický, 1988)

Age	Group	Subgroup	Formation		
			Tatride	*Veporide*	*Gemeride*
	W-Carpathian (Variscan)	Raztoky			Rakovec
LatePz			Harmonia(Little		
				Hron	
MiddPz			Klinisko (Low Tatra)		
				Upper Hladomorna	
EarlyPz	(Caledonian)	Gelnica			X
		Cierny Balog		X	
		Kohút		Lower Hladomorna	
LatePtz	Jaraba (Cadomian)	Bystra (Low Tatra)	X		
		Muranska Lehota		X	
		Podbrezova	Boca		
				Lũbietová	
Mid-Ptz	Kazimir (Dalslandian)				

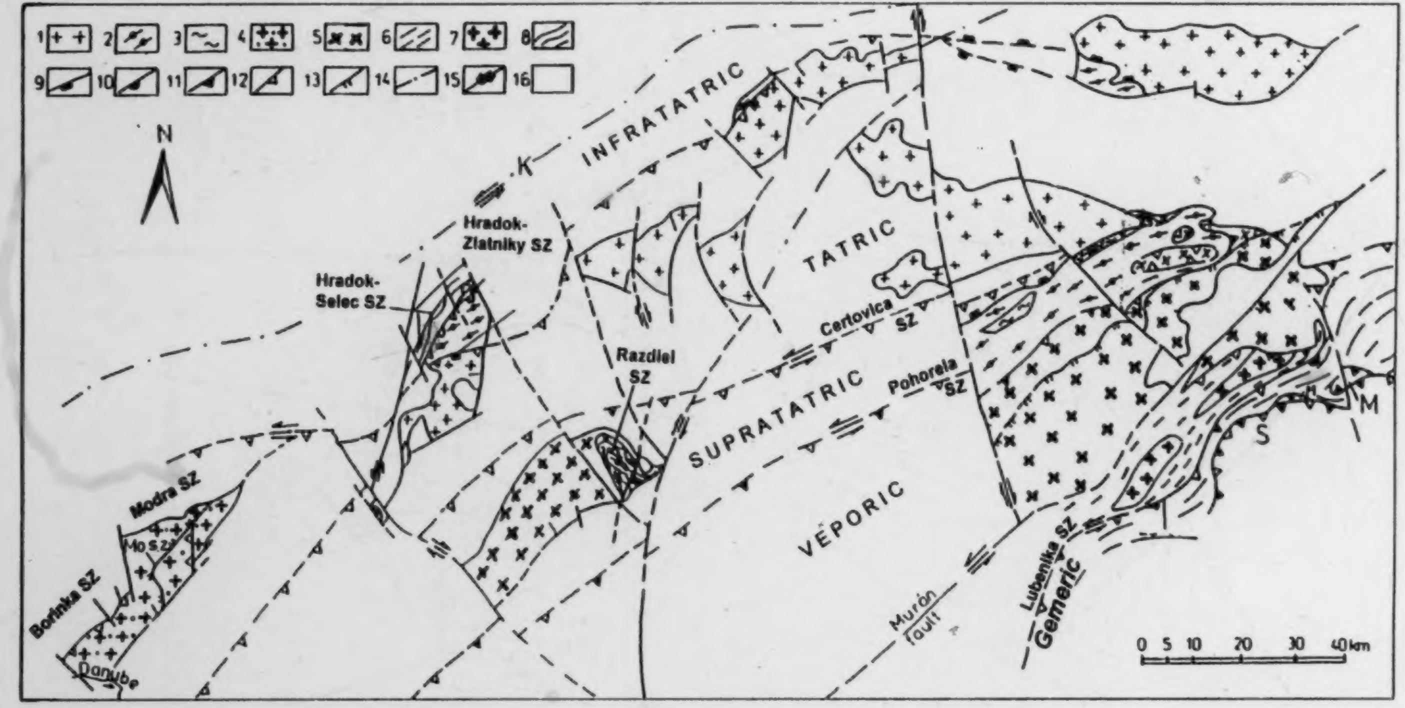
1
2
3
4
5
6
7
8
9
10
11
12
13
14
15
16
N
INFRATATRIC
K
TATRIC
SUPRATATRIC
VÉPORIC
Gemeric
Hradok-Zlatniky SZ
Hradok-Selec SZ
Razdiel SZ
Certovica SZ
Pohorela SZ
Lubenika SZ
Murán fault
Modra SZ
Mo SZ
Borinka SZ
Danube
S
M
0 5 10 20 30 40km

Fig. I-9. Tectonic sketch of the main basement units in the West Carpathians (*modified after* Putis, 1994). Tatric basement: 1 - Tatra complex; 2 - Hron complex; 3 - Lubietova sequence as part of the Tatra complex; 4 - Little Carpathians complexex. Veporic basement: 5 - Cierny Balog complex; 6 & 7 - South Veporic complexex: 8 - Gemeric basement; 9 - Early Devonian thrust; 10 - Early Carboniferous thrust; 11 - Late Jurassic-Early Cretaceous thrust; 12 - Middle Cretaceous thrust; 13 - reverse fault; 14 - Pieniny Klippen belt axix; 15 - strike-slip fault; 16 - post Early Carboniferous deposits; M - Meliata assemblage; S - Silice nappe.

dismembered leptino-amphibolite complex, evidence of a Paleozoic suture (Hovorka and Meres,1993). The Jaraba Group is intruded by Late Variscan Vepor, Hroncok, and (I-type) Sihla granites (c. 303 - 280 Ma, U-Pb zircon dates by Bibikova et al., 1988; c. 284 Ma, Rb-Sr isochron age by Bagdasaryan et al., 1986).

Basement rocks are assigned to three north-vergent Middle Cretaceous nappe complexes the Tatride, Veporide, and Gemeride (e.g., Andrusov, 1968). The North Veporicum region was recently assigned to Supratatricum nappe based on similarities of the Permian-Middle Cretaceous Velky Bok cover succession to the Tatricum cover, and the Veporide nappe complex was restricted to the basement units to the south covered by the Foederata succession (Putiš, 1994; Fig. I-9). Other interpretation considered the basement of the West Carpathians as a rigid tectonic lid with minor Alpine internal thrusts (Grecula and Roth, 1978).

Paleogeographic and tectonic evolution

The Foederata cover succession records Triassic extension on the South Veporic basement. Extension progressed to the Middle Triassic opening of the Meliata oceanic basin south of the Gemeric basement. Middle Jurassic subduction of the Meliata ocean is contemporaneous with extension of the European shelf to the north recorded by the Velky Bok cover succession of the North Veporic (Supratatric), Tatric and infra-Tatric basement (Putiš, 1993). Jurassic to Middle Cretaceous extension of the Tatric basement resulted in deep-water basins. The Vahic furrow is regarded as the eastern continuation of the Penninic ocean (Plasienka, 1990). Extension culminated with the Barremian-Early Albian emplacement of basanitic rocks in the Tatric and Fatric units. It coincided with the development of a flysch sequence in the Zliechov trough on the Tatric basement. Flysch deposition apparently ceased first in the southern and then in the northern Inner West Carpathians: in Cenomanian time in the Krizna unit in the Cenomanian-Turonian of the southern Tatric and in the Turonian-Coniacian of the northern Tatric unit. During the Turonian, units of the Krizna zone gravitationally spread north over the Tatric units. South-vergent thrusts are also reported in the Inner West Carpathians (e.g., Biely, 1989).

The Pieniny Klippen Belt marks the elusive boundary between the Inner and Outer West Carpathians. It consists of tectonically juxtaposed rock types originating in separate deep-water basins and is currently interpreted to represent a subduction mélange (e.g., Birkenmajer, 1988; Hamilton, 1990). Tectonism within this narrow belt is post-Paleogene, and vertical tectonic boundaries and recorded strain are consistent with sinistral strike-slip (Birkenmajer, 1986; Csontos et al. 1992). In the Outer West Carpathians, the Magura nappes formed between the Early Oligocene and Middle Miocene, and were backthrust along the Pieniny Klippen Belt onto the Inner West Carpathians.

Geophysical data

The crust/mantle interface under the Outer West Carpathians is horizontal and no relic of subducted slab has been depicted by any geophysical method (Sologub et al., 1973; Chekunov and Sollogub, 1989; Tomek and Hall, 1993) (Fig. I-10). Several subhorizontal reflectors in the Inner West Carpathian crust were interpreted to define shear zones and Cretaceous thrust sheets (Tomek, 1993) (Fig. I-11).

In the western extremity of the West Carpathians, an almost symetrical lithospheric root reaches c. 180 km in the axial zone under the Little Carpathians and is cut by steeply dipping to vertical, deep-reaching tectonic discontinuities (Chekunov and Sollogub, 1989). Similarly, at the eastern extremity, several subhorizontal reflectors define a crustal root under the West Carpathians-East Carpathians junction region reaching 60 km depth. Deep tectonic discontinuities dip steeply towards the European foreland. The tomographic image of the uppermost portion of the mantle under the central West Carpathians indicates a high velocity domain dipping northward under the European crust (Spakman, 1990; Fig I-6,continued).

Inconsistencies

The far travelled Eoalpine nappe complexes of the West Carpathians are inferred exclusively from the interpretation of the Permian Mesozoic cover sequences. The proposed basement thrust sheets are separated by steep south-dipping tectonic discontinuities that coincide with major sinistral Cenozoic strike-slip faults: Certovica, Pohorela, Muran, Lubenik (e.g., Pospíšil et al., 1989, Putiš, 1994). A mesh of splays with various kinematics related to the main Cenozoic tectonic lineaments overprint the whole region. The tectonic juxtaposition of cover sequences previously interpreted as major Eoalpine thrusts may be the result of Cenozoic faulting.

The interpretation of subhorizontal seismic reflectors in the West Carpathians basement as a nappe stack (Tomek, 1993) is speculative because basement assemblages originating at middle and lower crustal levels are inherently sub-horizontal. The projection of the inferred nappes and thrusts into the shear zones at surface (Tomek, 1993) is contradicted by the subhorizontal stretching in outcrop.

The main exposures of calc-alkaline volcanic rocks from Central Slovakia and Tokaj-Presov are clearly related to the Tertiary Muran-Hurbanovo and Hernad strike-slip faults, respectively. Moreover, the Tokaj-Presov volcanic lineament is perpendicular to the proposed subduction zone and the Vihorlat volcanic lineament in the eastern extremity of the West Carpathians segment overlaps the postulated suture, the Pieniny Klippen Belt.

Geologic map

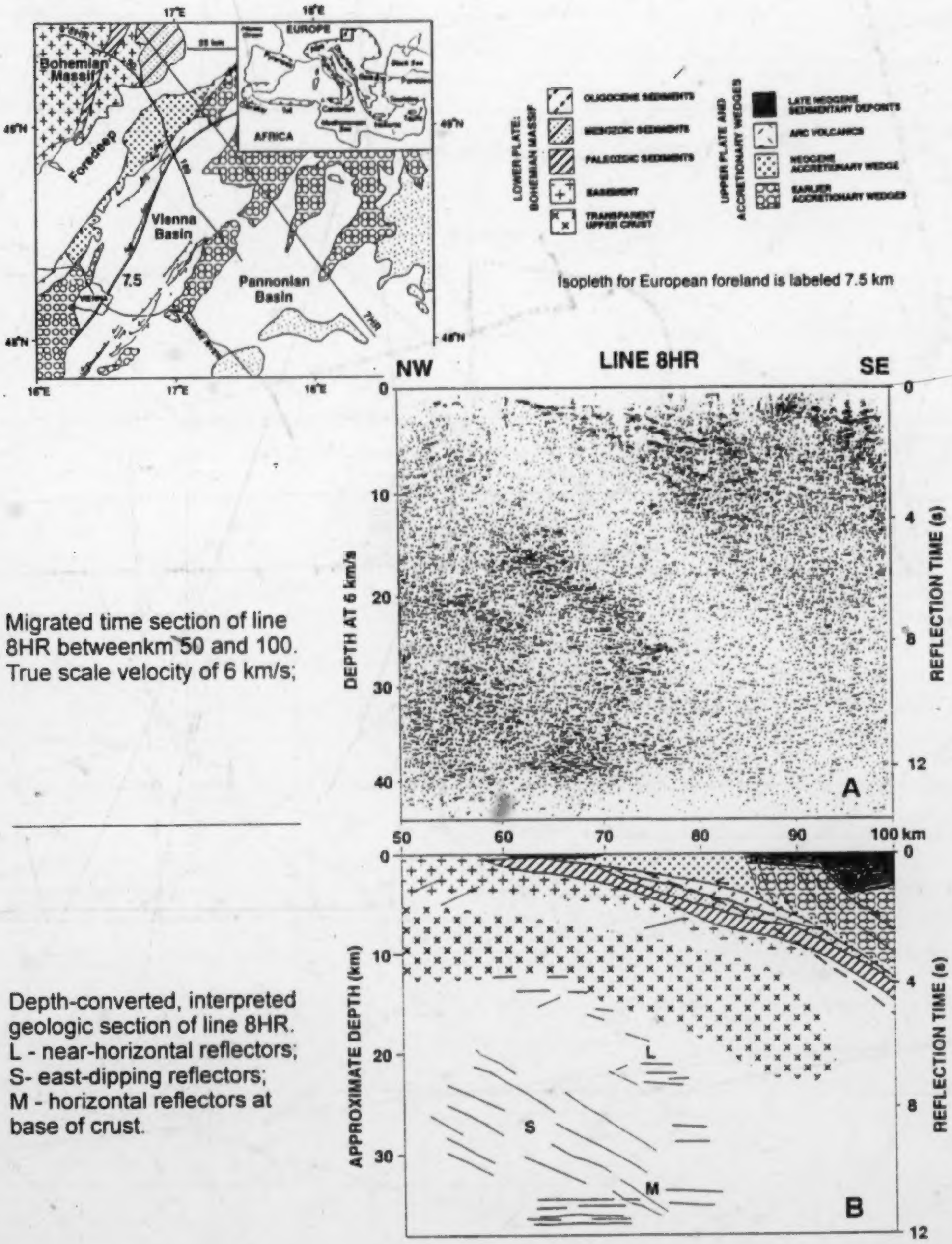
17°E
18°E
25 km
EUROPE
AFRICA
Bohemian Massif
Foredeep
Vienna Basin
7.5
Pannonian Basin
49°N
48°N
16°E
LOWER PLATE: BOHEMIAN MASSIF
OLIGOCENE SEDIMENTS
MESOZOIC SEDIMENTS
PALEOZOIC SEDIMENTS
BASEMENT
TRANSPARENT UPPER CRUST
UPPER PLATE AND ACCRETIONARY WEDGES
LATE NEOGENE SEDIMENTARY DEPOSITS
ARC VOLCANICS
NEOGENE ACCRETIONARY WEDGE
EARLIER ACCRETIONARY WEDGES
NW
LINE 8HR
SE
DEPTH AT 6 km/s
REFLECTION TIME (s)
A
50
60
70
80
90
100 km
APPROXIMATE DEPTH (km)
L
S
M
B

Isopleth for European foreland is labeled 7.5 km

Migrated time section of line 8HR betweenkm 50 and 100. True scale velocity of 6 km/s;

Depth-converted, interpreted geologic section of line 8HR.
L - near-horizontal reflectors;
S- east-dipping reflectors;
M - horizontal reflectors at base of crust.

Fig. I-10. Deep structure of the westernmost West Carpathians imaged by deep seismic reflection (from Tomek and Hall, 1993)

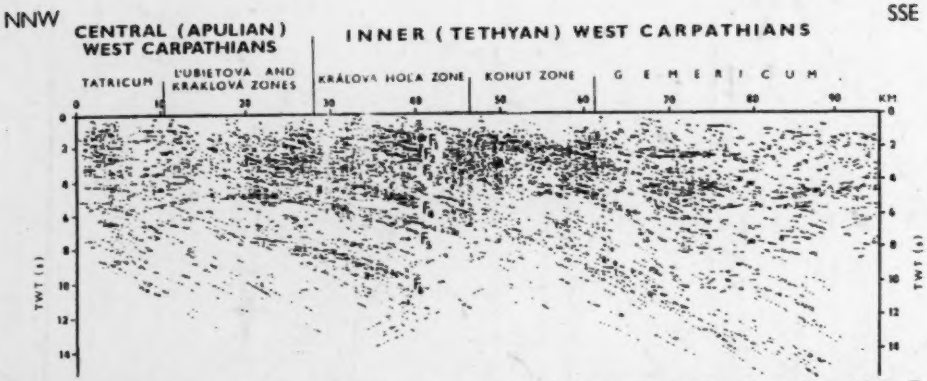
NNW
SSE
CENTRAL (APULIAN) WEST CARPATHIANS
INNER (TETHYAN) WEST CARPATHIANS
TATRICUM
ĽUBIETOVÁ AND KRAKLOVÁ ZONES
KRÁLOVA HOĽA ZONE
KOHUT ZONE
G E M E R I C U M
KM
TWT (s)
F_1
F_2
F_3
F_4
F_5
F_6

Unmigrated time section, detailed line drawing of the line 2T beneath the Vepor–Gemer block of the Central and Inner West Carpathians. F_1–F_6 are interpreted as reflections due to the fault zones of the Apulian–Briançonnais continental collision zone. The F_1 event represents the Pohorelá thrust zone between the Northern and Southern Veporicum, F_2 is the intra-North Veporic thrust, the F_3 event is interpreted as the Čertovica thrust zone where the Krížna nappe is rooted, F_4 might be interpreted as the Ligurian Ocean suture, and F_5 together with F_6 can represent the Briançonnais crystalline thrust zones. Vertical scale is two-way travel time in seconds, horizontal scale is in kilometres. Section has a vertical : horizontal ration of 1 assuming on unrealistic crustal velocity of 4.0 km/s.

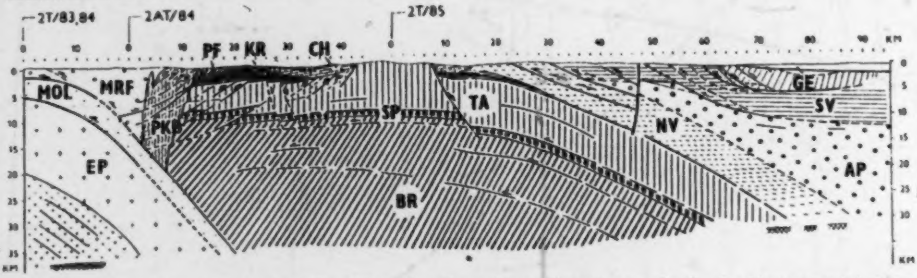
2T/83,84
2AT/84
2T/85
KM
MOL
MRF
PKB
PF
KR
CH
SP
TA
NV
GE
SV
AP
EP
BR

Schematic geologic section summarizing the structural framework of the Slovakian West Carpathians. Note the steeply dipping Neogene subduction of the European (*EP*) passive margin beneath the West Carpathian plate which is composed of three orogenic systems: Cenozoic MRF + PKB, Late Cretaceous central (Apulian) West Carpathians (CH + NV + KR + TA + SP + BR) orogen and the inner (Tethyan) West Carpathians (GE + SV + AP). Explanations: *EP* = European passive margin; *MOL* = Moldavian acretionary wedge; *MRF* = Magura–Rhenodanubian flysch; *PF* = Podhale flysch; *TA* = Tatricum; *KR* = Krížna overthrust sheet; *NV* = Northern Veporicum; *CH* = Choč overthrust sheet; *GE* = Gemeric thrust sheet containing Paleozoic and Mesozoic (subduction melange?) sequences as well as early Mesozoic ophiolites; *SV* = Southern Veporicum, crystalline nappes, sheared and tectonized beneath the Gemeric overthrust; *AP* = Apulian (?) hypothetical autochthon beneath the GE and SV.

Fig. I-11. Deep structure of the central West Carpathians imaged by deep seismic reflection (*from* Tomek and Hall, 1993)

I.5. EAST CARPATHIANS

The East Carpathians are the only segment of the orogen with a subduction zone anatomy: accretionary wedge, continental island arc, and volcanic arc (Fig. I-12).

The following presentation is based on syntheses by Băncilă (1958), Săndulescu (1975; 1984; 1988), Bercia et al. (1976), Kräutner (1980, 1988), and Balintoni at al. (1983).

Major tectonostratigraphic units

The outer part of the Carpathian arc consists of a coherent thrust-and-fold belt generally interpreted as an accretionary wedge related to westward subduction. Concentrically inward away from the European platform, Mesozoic and Cenozoic strata define the following facies zones: foreland-basin syn-thrust Neogene strata; mostly Upper Cretaceous and Tertiary outer-shelf strata; Jurassic to middle Tertiary inner-shelf strata; deep-water strata of Jurassic to Late Cretaceous age. Tectonic units derived from the innermost strata, interpreted as Cretaceous nappes from an internal trough floored by oceanic or thinned continental crust are assigned to the "External Dacides". Tectonic units to the east are interpreted as Miocene syn-collision nappes and assigned to the "Moldavides" (Dumitrescu et al., 1962; Săndulescu, 1984; 1988).

The upper plate represented by the East Carpathians continental crust (ECC) is currently interpreted as a stack of four Alpine nappe complexes (Fig. I-14). From bottom to top, these are: the Infrabucovinian nappes, the Subbucovinian nappe, the Bucovinian nappe, and the Transylvanian nappes. The Infra-Bucovinian, Sub-Bucovinian, and Bucovinian nappes are crystalline basement nappes with distinct Mesozoic cover strata (Fig I-13) postulated to originate in different facies zone facing the Tethys ocean. The uppermost nappes would carry deep-water strata from the most internal facies zone and slices of the Transylvanides oceanic crust.

The lowermost Infra-Bucovinian nappes are exposed in small tectonic windows or as slivers pushed in front of the overlaying nappes (Figs. I-13 and I-14). The thin Mesozoic sedimentary cover typically starts with the Lower Jurassic sandstones and coal seams (Gresten facies) and is characterized by several stratigraphic gaps attributed to erosion. The Sub-Bucovinian nappe is exposed mainly in the northern part of the ECC fragment and has reduced Mesozoic cover. The most widespread Bucovinian nappe is characterized by a Lower Cretaceous flysch and an Upper Barremian to Lower Albian wildflysch. The Transylvanian nappes would carry rocks from different oceanic environments. The Triassic to Jurassic of the Persani Mountains showing a typical Austroalpine development with mafic rocks and Hallstatt limestone is interpreted as an oceanic slice, the Olt succession suggests a shelf margin, and the stratigraphy of the Hăghimaş reconstructed in part from olistoliths found in the Bucovinian wildflysch, suggests an island arc succession. The nappes are supposed to have been emplaced between Aptian (Infrabucovinian) and Late Albian (Bucovinian).

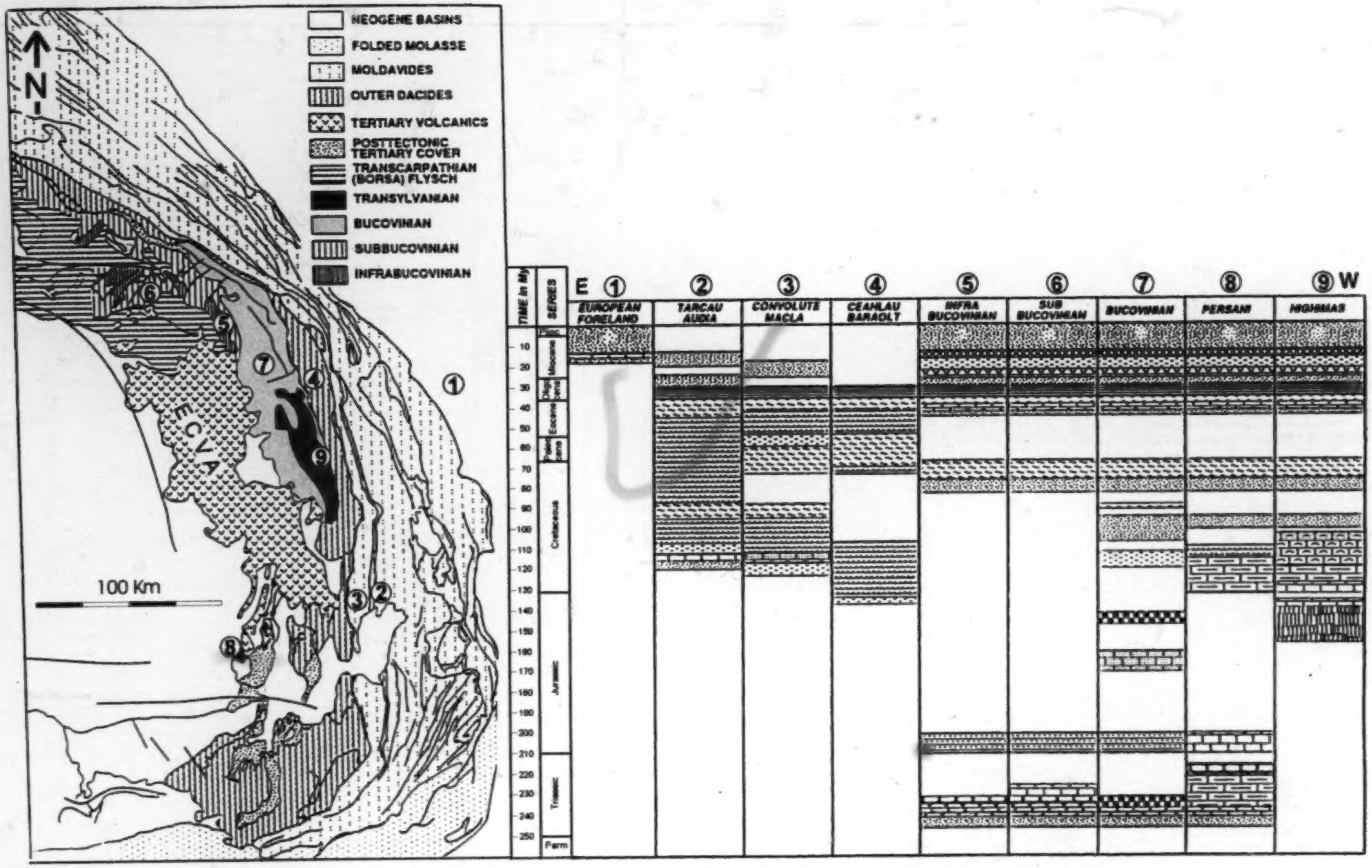
NEOGENE BASINS
FOLDED MOLASSE
MOLDAVIDES
OUTER DACIDES
TERTIARY VOLCANICS
POSTTECTONIC TERTIARY COVER
TRANSCARPATHIAN (BORSA) FLYSCH
TRANSYLVANIAN
BUCOVINIAN
SUBBUCOVINIAN
INFRABUCOVINIAN
N
ECVA
100 Km
TIME in My
SERIES
E
①
EUROPEAN FORELAND
②
TARCAU AUDIA
③
CONVOLUTE MACLA
④
CEAHLAU BARAOLT
⑤
INFRA BUCOVINIAN
⑥
SUB BUCOVINIAN
⑦
BUCOVINIAN
⑧
PERSANI
⑨
HIGHMAS
W
Plioc.
Miocene
Oligocene
Eocene
Paleocene
Cretaceous
Jurassic
Triassic
Perm
10
20
30
40
50
60
70
80
90
100
110
120
130
140
150
160
170
180
190
200
210
220
230
240
250

Fig. I-12. a) Simplified tectonic sketch of the East Carpathians; b) Alpine stratigraphy (*adapted from* Tari, 1994). ECVA - East Carpathians Volcanic Arc.

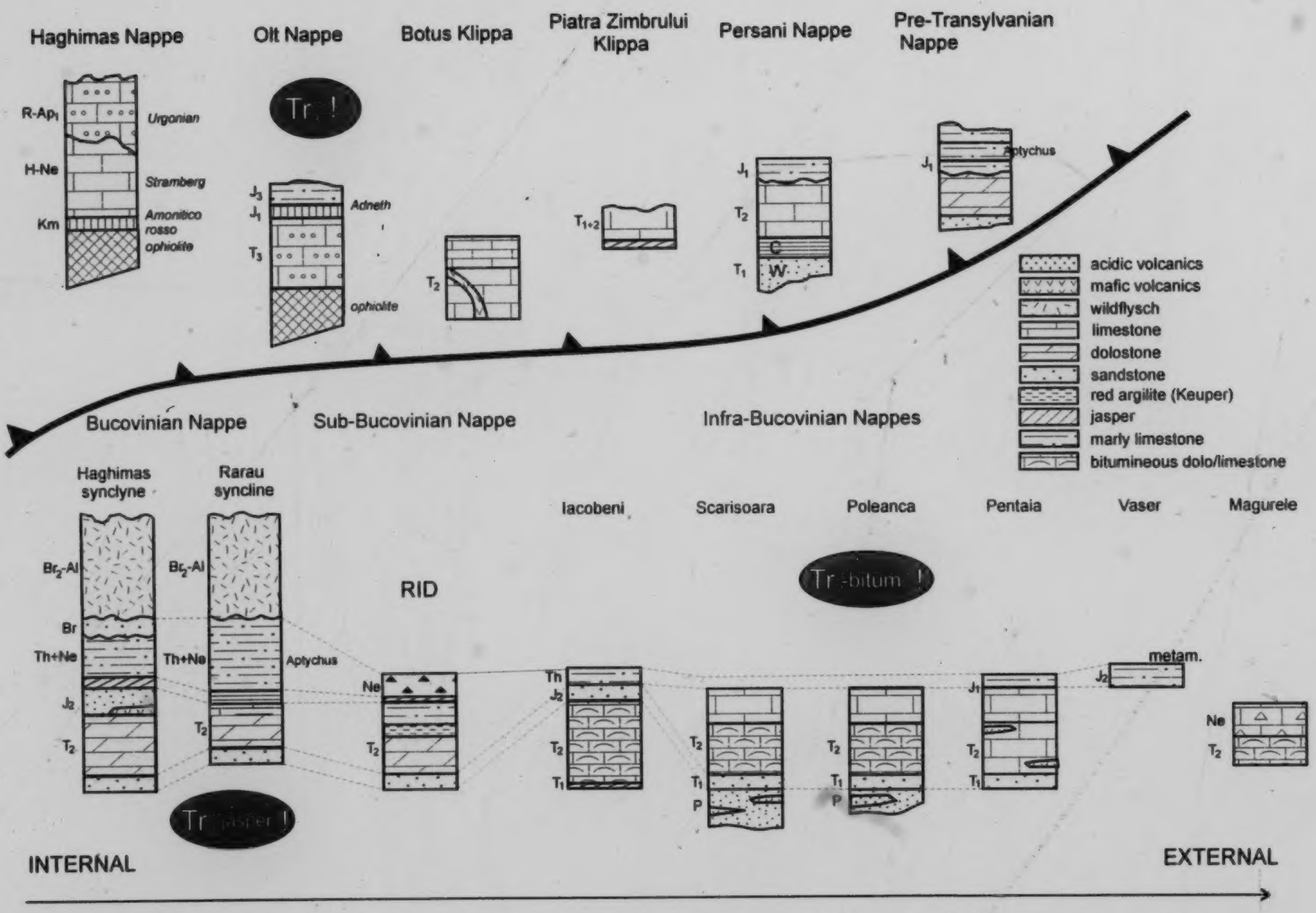
Haghimas Nappe
Olt Nappe
Botus Klippa
Piatra Zimbrului Klippa
Persani Nappe
Pre-Transylvanian Nappe
R-Ap1
H-Ne
Km
Urgonian
Stramberg
Amonitico rosso
ophiolite
Tr !
J3
J1
T3
Adneth
ophiolite
T2
T1+2
J1
T2
T1
C
W
J1
Aptychus
acidic volcanics
mafic volcanics
wildflysch
limestone
dolostone
sandstone
red argilite (Keuper)
jasper
marly limestone
bitumineous dolo/limestone
Bucovinian Nappe
Sub-Bucovinian Nappe
Infra-Bucovinian Nappes
Haghimas synclyne
Rarau syncline
Iacobeni
Scarisoara
Poleanca
Pentaia
Vaser
Magurele
RID
Tr-bitum !
Br2-Al
Br
Th+Ne
J2
T2
Br2-Al
Th+Ne
Aptychus
T2
Ne
T2
Th
J2
T2
T1
T2
T1
P
T2
T1
P
J1
T2
T1
J2
metam.
Ne
T2
Tr jasper !
INTERNAL
EXTERNAL

Fig. I-13. Stratigraphic columns for the cover sequences which differenciate the postulated East Carpathians basement nappes (*modified after* Sandulescu, 1984)

Basement rocks

West of the flysch basin, the inner part of the Carpathian arc is an irregular and poorly defined tract of widely varied and highly stretched crystalline rocks and stratigraphically overlying and tectonically interspersed upper Paleozoic, Mesozoic sedimentary rocks (the "Crystallino-Mesozoic Zone").

The medium-grade rocks are assigned to the Middle Proterozoic Bretila and Rebra groups, of the Carpian Supergroup (Kräutner, 1988) (Table I-4). Most of the low-grade rocks are assigned to the Cambrian Tulgheş Group and to several Middle Paleozoic formations. K-Ar dates from the Bretila and Tulgheş groups are generally spread between c. 500 and c. 100 Ma, with a maximum at c. 300 Ma which may suggest a Variscan record. K-Ar dates from the Rebra Group are widely spread (Kräutner, 1988). All basement assemblages are currently separated in distinct Variscan nappes (e.g., Bercia et al., 1976; Balintoni et al., 1983). The assumed nappe contacts show various dips and have led to conflicting interpretations regarding the vergence of the thrusts.

Table I-4. Principal lithostratigraphic groups of Precambrian metamorphic rocks and their position in the main structural units of the East Carpathians (*after* Kräutner, 1980).

Supergroup	***Group***	***Series (Formations)***	
		Bistriţa nappes	***Maramureş nappes***
Marisian	Bucovinian	Tulgheş (U.Delovetsk)	
Carpian	Aluta	Rebra (Negrişoara, L.Delovetsk)	
		Bretila (Rarău, Cernii Div)	Bretila (Belipotok)

The East Carpathians Volcanic Arc

From north to south along the inner part of the Romanian East Carpathians (Fig. I-12), large occurrences of calc-alkaline rocks are clustered in three principal segments: 1) Oaş-Gutâi (OG); 2) Tibleş-Toroioaga-Rodna-Bârgău (TTRB); 3) Călimani-Gurghiu-Harghita(CGH), the longest (160 km) continuous volcanic range in the Carpatho-Pannonian region. The general location behind the East Carpathians accretionary prism and calc-alkaline geochemical signatures led Rădulescu and Săndulescu (1973), Boccaletti et al. (1973) and Bleahu et al. (1973) to interpret these successions as a subduction-related volcanic arc. The model has been extrapolated to accommodate Neogene to Quaternary volcanism at the scale of the entire Carpathians-Pannonian Basin system (e.g., Bala, 1982; Royden, 1988).

Based on extensive published and unpublished petrographic, geochemical and isotopic data for the East Carpathians volcanic arc (ECVA) (e.g., Rădulescu et al., 1973; Peltz et al.,

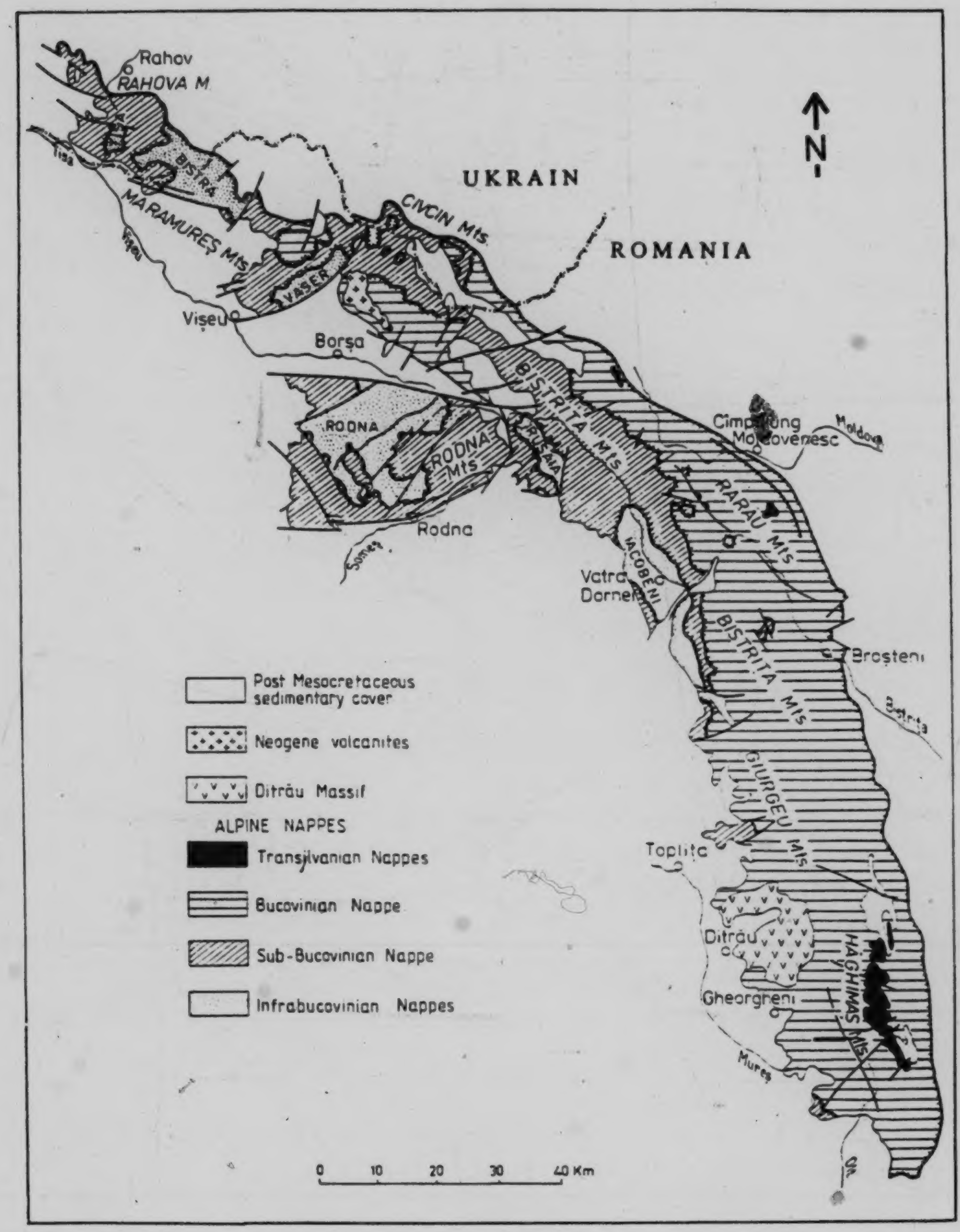
Rahov
RAHOVA M.
BISTRA
MARAMUREȘ Mts
VASER
CIVCIN Mts
UKRAIN
ROMANIA
N
Tisa
Vișeu
Vișeu
Borșa
RODNA
RODNA Mts
BISTRITA Mts
Cimpulung Moldovenesc
Moldova
RARĂU Mts
Rodna
Someș
IACOBENI
Vatra Dornei
Broșteni
BISTRITA Mts
Bistrita
GIURGEU Mts
Toplița
Ditrău
Gheorgheni
HAGHIMAȘ Mts
Mureș
Olt
Post Mesocretaceous sedimentary cover
Neogene volcanites
Ditrău Massif
ALPINE NAPPES
Transilvanian Nappes
Bucovinian Nappe
Sub-Bucovinian Nappe
Infrabucovinian Nappes
0 10 20 30 40 Km

Fig. I-14. The main Alpine nappes involving basement rocks in the East Carpathians (*simplified after* Bercia et al., 1976; Săndulescu et al., 1981).

1974; Peccerillo and Taylor 1976; Udubaşa et al., 1983; Seghedi et al., 1987, 1995; Masson et al., 1995), the complex petrogenetic evolution can be summarized as follows:

1) magma shows a "subduction-related" chemical signature; most of the volcanic rocks belong to the calc-alkaline suite, ranging from basalts to dacites and rhyolites, but andesites are most abundant; weak tholeiitic trends are shown by some of the earliest rocks in the Călimani Mountains.

2) the rocks in South Harghita have a different mantle source and resulted from a gradually decreasing degree of partial melting;

3) in areas of large volumes of erupted magmas (Călimani, Gutâi), the dominant petrogenetic processes are fractional crystallization combined with crustal assimilation; in areas of smaller volumes of erupted products (Oaş, Tibleş, Toroioaga, Rodna), the petrogenesis is the result of extensive mixing between magmas derived in deep-seated intracrustal magma chambers; in the South Harghita, fractional crystallization was combined with crustal assimilation and magma mixing. None of the ECVA rocks, even the most basic ones, are representative of parental or close to parental mantle-source partial melts (Fig. I-15).

Paleogeography and tectonic evolution

The Early Alpine development of the Inner Eastern Carpathians includes the opening of a Triassic to Late Jurassic Transylvanian-Pienniny branch of the Tethys ocean west of the ECC. Isolated exposures of Permo(?)-Mesozoic cover strata on the ECC have been interpreted as relics of facies zones stretching parallel to the postulated ocean (Săndulescu 1975, 1984). The original location of the deep water (internal) facies zone and mafic rocks would be to the west, on the Transylvanide oceanic crust. Cratonward, thin and lacunar successions have been assigned to successive facies zones facing the ocean: the Bucovinian, Sub-Bucovinian, and Infra-Bucovinian. The present reversed order would have resulted from nappe stacking with hinterland nappes (originating in the Tethys domain) overthrusting underlying nappes (originating in the ECC fragment). Transylvanian nappe(s) would have been transported piggy-back fashion on the Bucovinian nappe.

Cover strata of the ECC show an evolution typical of the European margin, characterized by the absence of Upper Triassic and of Lower Jurassic Gresten facies. Two sedimentary cycles have been separated, a Permo-Triassic-Liassic one and a Aalenian-Neocomian one (e.g., Băncilă, 1958; Săndulescu, 1984).

A relatively large intracontinental basin resulted from Jurassic rifting and separation of the Carpathian crustal fragment from the edge of stable Europe. A complicated morphology was characterized by elongated ditches and furrows filled with flysch deposits separated by swells (with condensed successions) or even transient "cordilleras". An ensimatic basin was assumed for the Black flysch and for the outer (Rădulescu and Săndulescu, 1973) or inner part

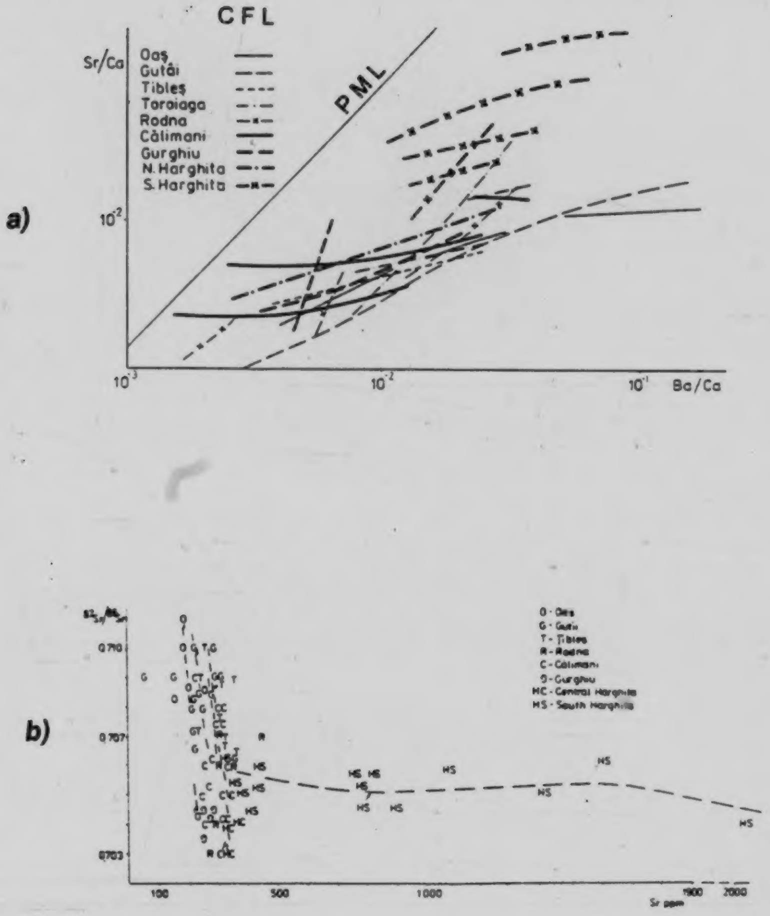

Fig. I-15. a) Sr/Ca - Ba/Ca systematics of magmatic rocks from the Eastern Carpathians Volcanic Arc; PML - Partial Melting Line; CFL - Crustal Fractionation Line; numbers represent phases of volcanic activity; b) $^{87}Sr/^{86}Sr$ vs. Sr diagram for volcanics from the East Carpathians Volcanic Arc (*from* Seghedi et al., 1995).

(Ştefănescu, 1983) of the Sinaia flysch, but its existence and extent remain speculative.

In the inner part of the flysch belt (External Dacides), folding and thrusting started in the Middle Cretaceous but the main thrust phase is intra-Turonian. Deep-water materials were pushed up onto the outer continental shelf and shelf strata were pushed further cratonward. Meanwhile, during the initial phases of collision the inner deep-water facies and strips of associated oceanic crust were scraped under the Bucovinic tract (eg. Maramureş Mountains). They were uplifted and were subject to tectonic erosion as accretionary-wedge materials were stuffed beneath them.

The oldest strata in the first (most internal) flysch trough to the east are Kimmeridgian, but subsidence and sedimentation of the Sinaia flysch took place in Late Tithonian to Late Albian, and consists of a 2200 m thick sequence of schist, sandstone, argilite, and black limestone. The Lower Cretaceous Black Schist series is similar to the Silesian lithofacies of the West Carpathians. To the north, the Black Flysch is defined by a Pienniny-type facies with graphite-bearing schist, sandstone, tuff, basalt, and Aptychus- and Calpionella- bearing limestone. Albian - Vraconian (locally up to Cenomanian) Curbicortical flysch strata were involved in the Ceahlău, Baraolt, Teleajen, and Macla nappes during the Early Miocene, followed by the Late Cretaceous Bistra Comarnic, and Ceahlău-Zaganu flysch.

To the east, a furrow with non-flysch sedimentation contains Lower Cretaceous to Vraconian black argillaceus schist and siltstone with subordinate bituminous strata (Băncilă, 1958). The upper strata that include banded mudstone and quartz or glauconite sandstone correlate with the Silesian facies of the Western Carpathians and Eastern Alps. Vraconian-Turonian banded argillaceous strata with tuffite and cherty intercalations record volcanism. Similar successions known both in more external units (the Tarcău nappe) and internal units (the Pienniny Klippen-Birkenmajer, 1977) would indicate andesite volcanism related to an island arc within the basin in front of the East Carpathian crustal fragment related to Middle Cretaceous subduction (Rădulescu and Dimitrescu, 1982). Breccia and coarse sandstone beds with red granodiorite fragments are interpreted to originate in a string of Vraconian-Turonian islands between the Audia and Tarcău furrows, the "Cuman Cordillera" (Murgeanu, 1933). This sequence is involved in highly imbricated Late Cretaceous folds and interpreted to define the intra-Burdigalian Audia nappe.

The third trough was located east of the Audia sedimentation zone and consists of Barremian-Late Badenian poly-facial deposits. Flysch deposition started in Early Senonian. This sequence is assigned to the Medio-Marginal Unit.

Four distinct areas (Putna-Suceava, Bistriţa, Oituz-Caşin, Vrancea) with correlative sequences are interpreted to represent tectonic half-windows under the Medio-Marginal Unit. The first thin flysch-like sequence is of Paleogene age. During the Eocene, flysch strata were deposited only in parts of the Vrancea region. The Oligocene-Miocene sequence is characterized by bituminous lithofacies (Kliwa sandstone) with coarse clastic strata, and by both longitudinal and transversal facies variations that define the External Unit (Dumitrescu, 1952).

Oligocene cherty and bituminous facies including the Kliwa sandstone is overlain by Burdigalian - Lower Badenian molasse strata interpreted to define the Peri-Carpathian Nappe (or sub-Carpathian Nappe) (Băncilă, 1958).

Geophysical data

Roman (1970) defined a vertical lithospheric slab oriented NE-SW located in the Vrancea region in front of the East Carpathians bent. Constantinescu et al. (1973) interpreted the same data as "subduction streams" in the upper mantle. Fochs et al. (1979) and Oncescu (1986) interpreted seismic data in the Vrancea region to indicate to westward subduction. Magnetotelluric data in the central East Carpathians depict two subvertical discontinuities; the western discontinuity corresponds to the Neogene volcanic lineament, and the weaker eastern one is located under the most external Carpathian units (Stănică and Stănică, 1993)(Fig. I-16). A lithospheric root and subvertical mantle reaching fractures are depicted by a combination of geophysical methods (Sollogub et al., 1986) (Fig. I-17).

Inconsistencies

The presence of Transylvanian deep-water strata and mafic rocks only on the eastern edge of the ECC fragment in contact with the deep-water sediments of the eastern basin is inconsistent with the interpretation of far travelled basement nappes.

Relationships between tectonic processes and magmatism in the East Carpathians show that a subduction model cannot be applied (Sackáci and Seghedi, 1995). Recent attempts to integrate new data in the subduction model (Linzer, 1995) have major shortcomings (Pană and Erdmer, 1996). A detailed discussion is offered in the last chapter.

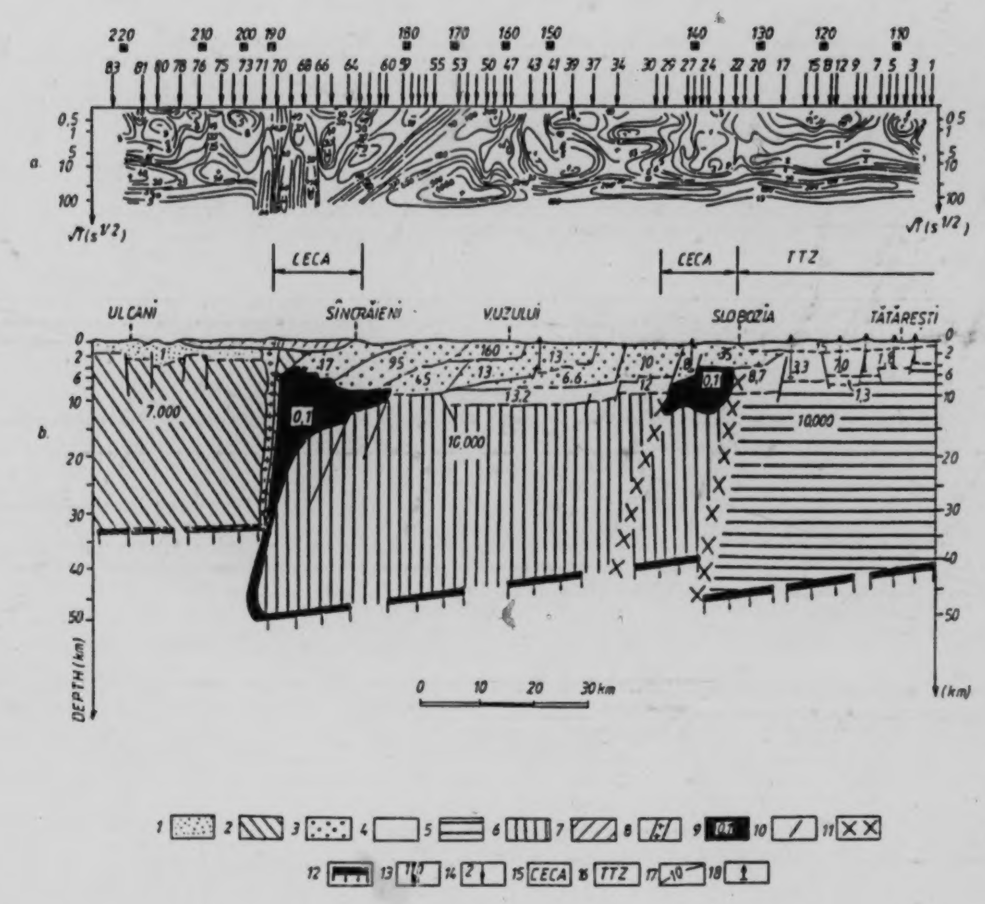
a
b
CECA
TTZ
ULCANI
SÎNCRĂIENI
VUZULUI
SLOBOZIA
TĂTĂREŞTI
0.1
7.000
10.000
10.000
DEPTH (km)
0 10 20 30 km
$\sqrt{T}(s^{1/2})$
1
2
3
4
5
6
7
8
9
10
11
12
13
14
15 CECA
16 TTZ
17
18

A resistivity pseudo-section (a) and a pseudo-2D model created by compiling the 1D results of the ρ_{det} responses at each location (b). 1, Post-nappe sedimentary cover; 2, folded socle of the Transylvanian Depression; 3, Flysch Nappes system; 4, sedimentary cover of platform; 5 and 6, folded basement of the Scythian and Moesian Platforms; 7, volcanic sedimentary formation; 8, subvolcanic formation; 9, high-conducting zone; 10, fault; 11, crustal fault; 12, Moho discontinuity; 13, deep MT location; 14, MT location; 15, Carpathian electrical conductivity anomaly (CECA); 16, Tornquist–Teisseyre zone (TTZ); 17, isoresistivity curves; 18, borehole.

Fig. I-16. Deep structure of the East Carpathians as depicted by magnetotelluric data (*from* Stănică and Stănică, 1993).

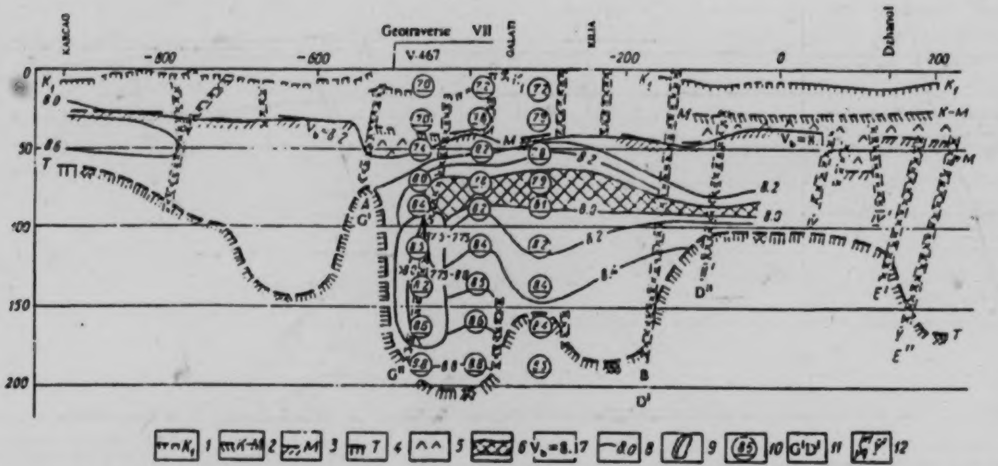

Velocity structure in the lithosphere beneath the Apuseni Mounatins and Romanian Carpathians along Geotraverse V: 1-top of the metamorphic/magmatic basement; 2-crust-mantle layer; 3-Moho discontinuity, V_b= 8.1-8.2 km/s; 4-top of the asthenosphere from heat flow data; 5-crust-mantle layer, V=7.4-7.5 km/s; 6-low-velocity layer in upper mantle, V=7.9-8.0 km/s; 7-boundary velocity; 8-isovelocity line; 9-Vrancea body of anomalous velocity from earthquake data; 10-velocity from earthquake data; 11-mantle faults; 12-transcrustal faults

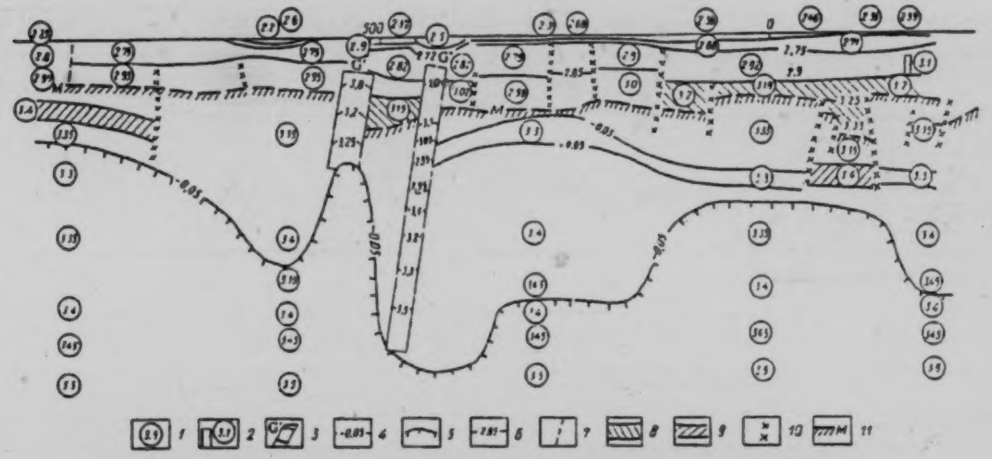

Density distribution in the lithosphere beneath the Apuseni Mountains and Romanian Carpathians along Geotraverse V: 1-mean density in crust and upper mantle; 2-intrusions of basic and ultrabasic rocks in crust; 3-fault zones and calculated densities; 4-upper mantle boundaries and density contrasts; 5-top of astenosphere; 6-isodensity line; 7-boundaries between blocks of different density; 8-crust-mantle layer; 9-mass-excess body in upper mantle; 10-faults from seismic data; 11-Moho discontinuity from seismic data

Fig. I-17. Deep structure of the East Carpathians along Geotraverse V (for location see Fig. I-1) as depicted by seismic and gravimetric data (*from* Sollogub et al., 1986)

2.6. SOUTH CARPATHIANS

The geographic boundaries of the South Carpathians may be arbitrarily placed along the Prahova and Timiş rivers towards the Eastern Carpathians and along the Danube River towards the Balkans. To the north, the South Carpathians are bounded by the Transylvanian Basin and to the south, by the Moesian platform.

The following summary is based on syntheses by Năstăseanu et al., (1981), Kräutner et al., (1981), Săndulescu (1975, 1984, 1988), Balintoni et al., (1989), and Berza et al., (1994).

Major tectonostratigraphic units

The Moesian platform is regarded as a promontory of the European foreland covered by the Neogene to Recent molasse basin. The molasse also covers the deep Getic depression with a 3 km-thick Middle Eocene to Lower Miocene sequence. The Senonian Mokranje flysch is located in a similar tectonic position as the internal flysch units of the Moldavides in the East Carpathians.

The Danubian units crop out only in the western half of the South Carpathians and are grouped into upper and lower nappes. In the South Carpathians, Late Proterozoic oceanic crust is interpreted from Nd and Sr isotope data from amphibolites of the Drăgşani assemblage (Liégeois et al., 1996). U-Pb zircon data from an orthogneiss in the Drăgşani assemblage suggested a 777+/-3 Ma emplacement age of the protolith. A Late Paleozoic-Early Cambrian tectonomagmatic event is represented by the Tismana granite (565-507 Ma K-Ar, Grünenfelder et al. 1983; 567 Ma, U-Pb zircon date, Liégeois et al., 1996) and the Novaci granite (588+/-5 Ma, U-Pb zircon date, Grünenfelder et al., 1983, recalculated by Liégeois et al., 1996). These granites intrude the medium-grade Lainici-Păiuş assemblage which has yielded several Cambrian K-Ar dates (Grünenfelder et al., 1983) and a 560 Ma ^{40}Ar/^{39}Ar plateau date for muscovite concentrate (Dallmeyer et al., 1996). These dates probably record uplift and cooling following the intrusion of the granitic batholiths.

The sedimentary cover of the Danubian units is slightly metamorphosed. The lowermost Schela nappe has a Liassic cover with metasandstone, metapelite, and anthracite suggesting a coal-bearing Gresten facies.

The Severin nappe overlies the Danubian unit and consists of the Lower Cretaceous Sinaia flysch and slices of basalts and ultramafics interpreted as Jurassic ophiolite.

The Getic nappe involves mainly crystalline basement rocks assigned to the Sebeş assemblage which includes (Săbău, 1994): the Armeniş complex of sillimanite-bearing biotite gneiss, quartz-feldspar and hornblende gneiss, subordinate calc-silicate and marble layers; the Vaideeni complex dominated by ultramafic and eclogite pods associated with anatectic granitoids in a matrix of amphibole, quartz-feldspar or mica gneisses; discontinuous layers of mylonite gneiss with microblastic biotite throughout this package; the Negovanu Mare complex

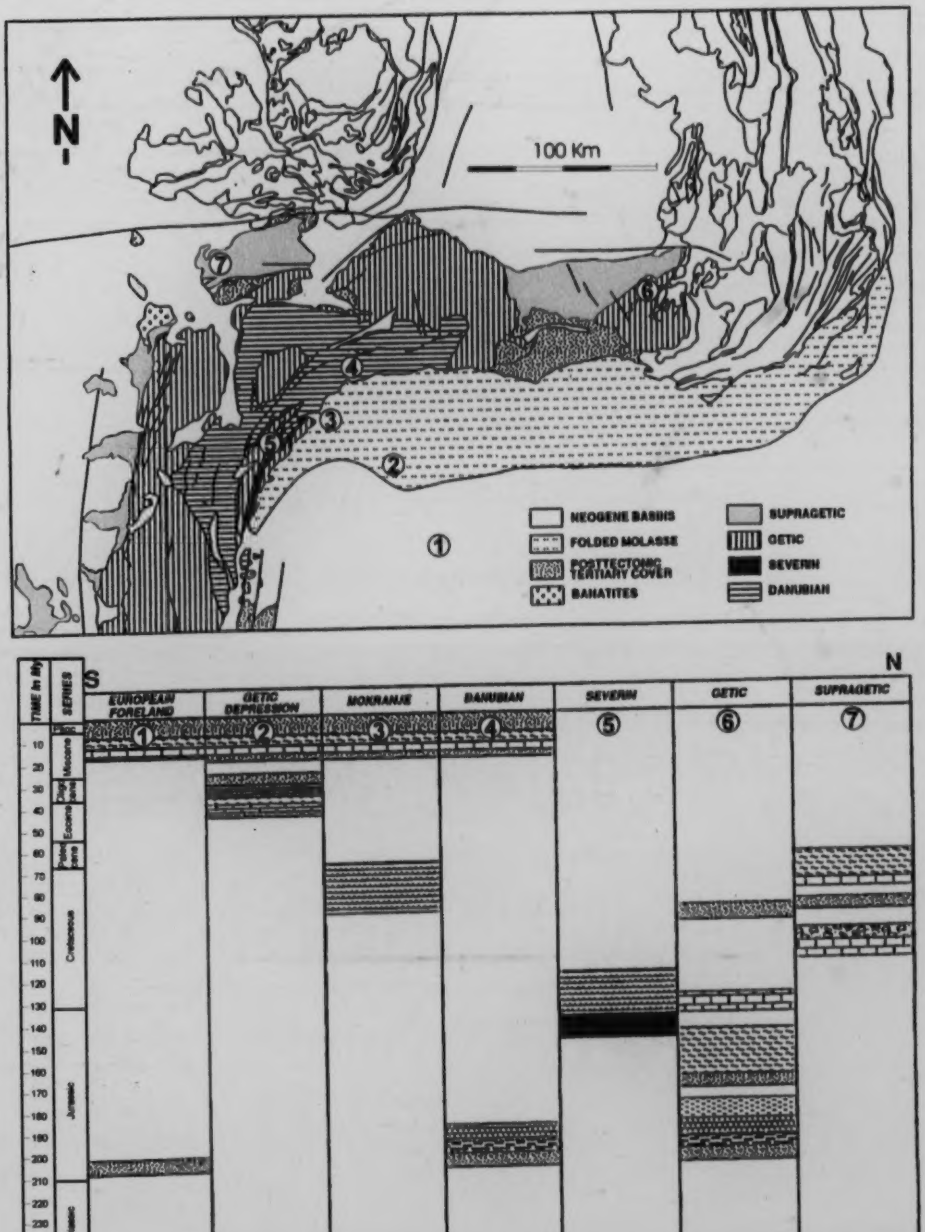
N
100 Km
NEOGENE BASINS
FOLDED MOLASSE
POSTTECTONIC TERTIARY COVER
BANATITES
SUPRAGETIC
GETIC
SEVERIN
DANUBIAN
①
②
③
④
⑤
⑥
⑦
S
N
TIME in My
SERIES
EUROPEAN FORELAND
GETIC DEPRESSION
MOKRANJE
DANUBIAN
SEVERIN
GETIC
SUPRAGETIC
Plioc.
Miocene
Oligocene
Eocene
Paleocene
Cretaceous
Jurassic
Triassic
Perm
10
20
30
40
50
60
70
80
90
100
110
120
130
140
150
160
170
180
190
200
210
220
230
240
250

Fig. I-18. a) Simplified tectonic sketch of the South Carpathians; b) Alpine stratigraphy; (*adapted from* Tari, 1994).

dominated by garnet-kyanite-staurolite-rutile-bearing micaschist; the interpreted tectonic boundary between the Vaideeni and the Negovanu assemblages is marked by a Mn-rich discontinuous package of spessartine quartzite and schist or by a thin discontinuous quartzite layer; the Ursu complex includes orthoclase-biotite-sillimanite-cordierite gneiss, amphibolite, quartz-feldspar gneiss and leptinite. The Sebeş-Lotru succession is regarded as a composite Precambrian assembly of crustal slices with distinct M1 evolution, stacked during M2 collision at intermediate crustal levels; this was followed by diapiric addition of lower crust during M3 (Săbău, 1994) (Fig. I-19).

Cover strata preserved in isolated exposures, span from the Upper Carboniferous to the Upper Cretaceous with several unconformities. Upper Paleozoic strata exposed in the western extremity (Reşiţa-Moldova Nouă) are considered as Variscan molasse. Lower and Middle Triassic strata are known at the eastern extremity (Braşov). At the base of the Lower Jurassic Gresten facies, an angular unconformity was recognised in the Postăvaru Massif. The Jurassic to Lower Cretaceous succession is generally complete. The first regional unconformity is pre-Albian. It was interpreted to date the first Getic phase (Codarcea, 1940) of nappe emplacement. The Upper Cretaceous shows local episodes of flysch (Haţeg, Rusca Montană, Şopot) and wildflysch (Rusca Montană) sedimentation.

Table 2-5. The principal lithostratigraphic groups of Precambrian metamorphic rocks and their position in the main structural units of the South Carpathians (*after* Kräutner, 1980).

	Supergroups	***Groups***	***Series (Formations)***
	Variscan		Cârtişoara
Făgăraş nappe	Marisian		
	Carpian		Făgăraş Cumpăna
Leaota nappe	Marisian	Leaota	Lereşti
	Carpian	Ezer	Călineşti
Getic nappe	Marisian	Cibin	Sibişel, Râuşorul, Răşinari, Dăbâca, Miniş, Buceava
	Carpian	Sebeş-Lotru	
Danubian nappes	Marisian		Riul Şes, Corbu
	Carpian	Paring, Petreanu, Bistra, Neamtu, Almaj	Lainici Păiuş, Drăgşani, Bodu, Petreanu Bistra-Bucovei, Ielova, Poiana Mraconia

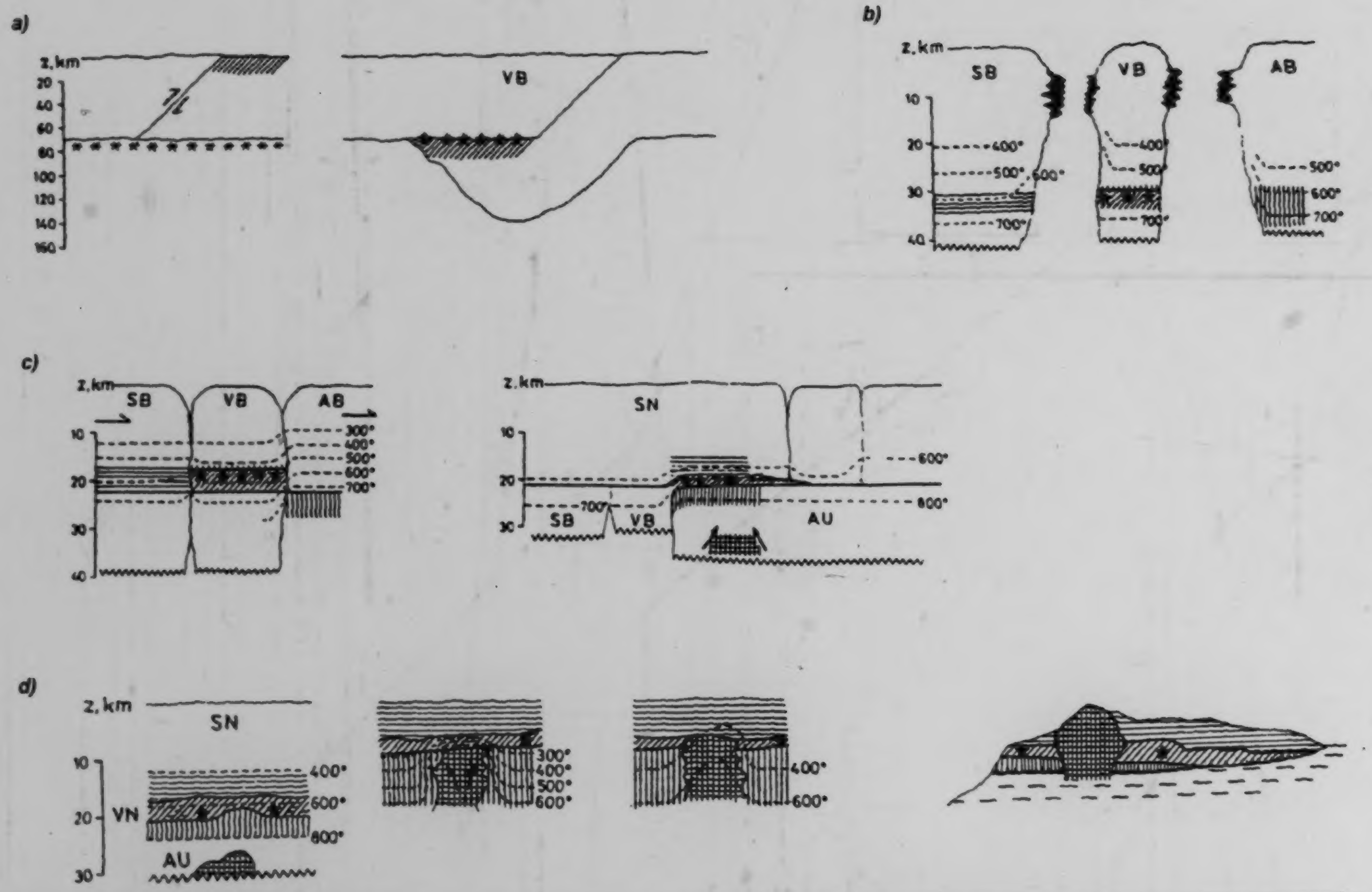
a)
z, km
20
40
60
80
100
120
140
160
VB
b)
z, km
SB
VB
AB
10
20
30
40
400°
500°
600°
700°
c)
z, km
SB
VB
AB
10
20
30
40
300°
400°
500°
600°
700°
SN
SB
VB
AU
600°
800°
700°
d)
z, km
SN
VN
AU
10
20
30
400°
600°
800°
300°
400°
500°
600°
400°
600°

Fig. I-19. Tectonometamorphic evolution of the medium to high-grade rocks in the best exposed basement unit of the Carpathians, the "Getic Nappe". a) eclogite incorporated in the crust by subfluence; b) crustal blocks at M1: SB - Semenic block ; AB - Armenis block; V B - Voineasa block; c) crustal blocks at M2, achievement of metamorphic nappe structure; AU -Armenis Unit; VN - Voineasa nappe; SN - Semenic Nappe; d) M3 piercing of the nappe stack by lower crust materials. (*after* Săbău, 1994)

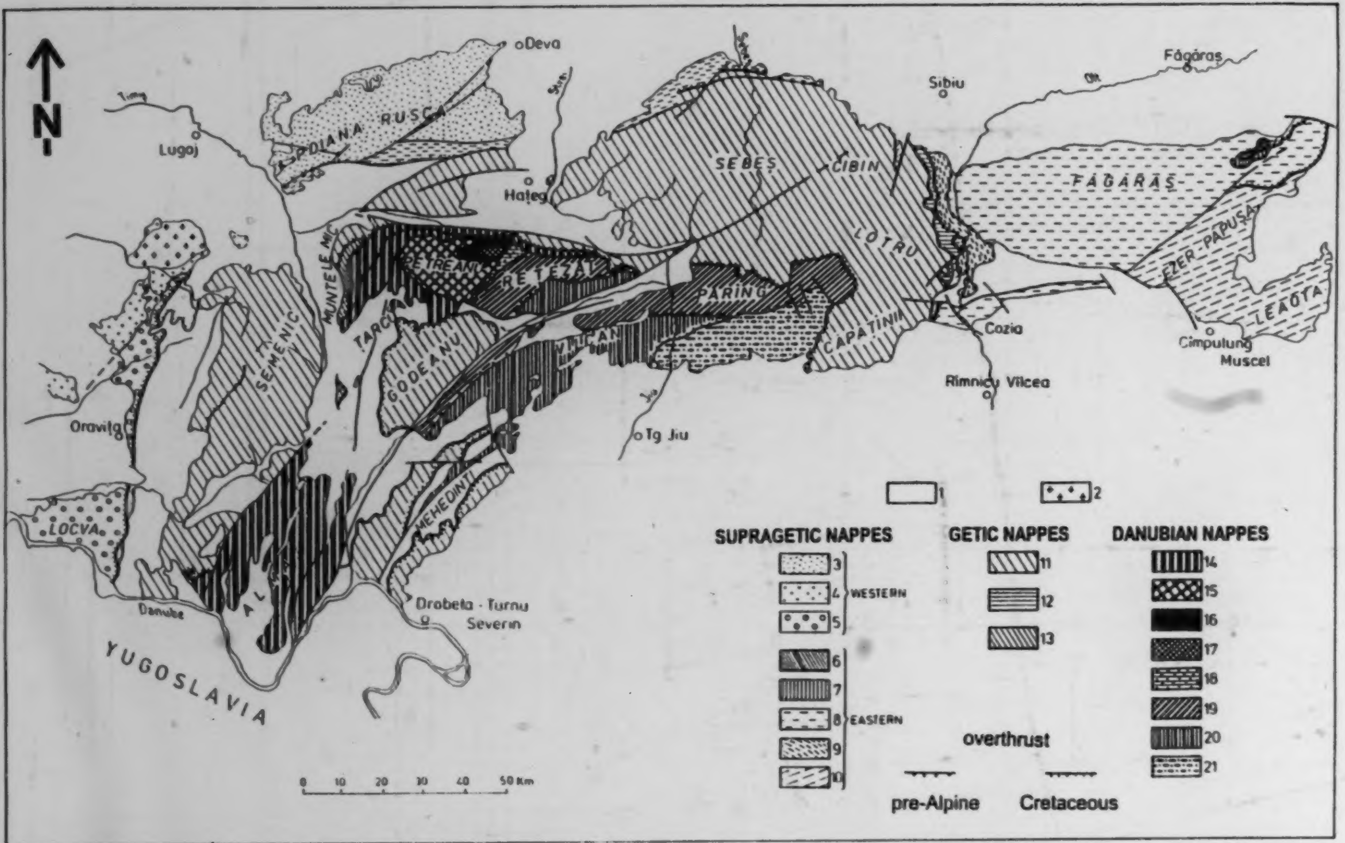
N
oDeva
Timiş
Lugoj
POIANA RUSCA
Strei
Haţeg
SEBEŞ
CIBIN
Sebeş
Sibiu
Olt
Făgăraş
FĂGĂRAŞ
IEZER-PĂPUŞA
LEAOTA
Cîmpulung Muscel
LOTRU
CĂPĂŢÎNII
Cozia
Rîmnicu Vîlcea
PARÎNG
VULCAN
RETEZAT
PETREANU
MUNTELE MIC
TARCU
SEMENIC
GODEANU
MEHEDINŢI
ALMAJ
Jiu
oTg. Jiu
Oraviţa
LOCVA
Danube
Drobeta - Turnu Severin
YUGOSLAVIA
0 10 20 30 40 50 Km
1
2
SUPRAGETIC NAPPES
3
4
5
WESTERN
6
7
8
9
10
EASTERN
GETIC NAPPES
11
12
13
DANUBIAN NAPPES
14
15
16
17
18
19
20
21
overthrust
pre-Alpine
Cretaceous

Fig. I-20. The main Alpine nappes involving basement rocks in the South Carpathians (simplified after compilations by Kräutner et al., 1988; Balintoni et al., 1989; Berza et al., 1994). 1 - Paleozoic to Recent sedimentary cover; 2 - Paleocene ("Banatitic") granodiorite intrusions; **Supragetic nappes**: 3 - Poiana Ruscă; 4 - Bocşa; 5 - Locva; 6 - Strâmba; 7 - Bârsa Fierului; 8 - Făgăraş; 9 - Câineni; 10 - Leaota; **Getic nappes**: 11 - Getic; 12 - Uria; 13 - Turnu Ruieni; **Danubian nappes**: 14 - Upper Danubian; 15 to 21 - Lower Danubian: 15 - Petreanu; 16 - Furcătura; 17 - Rof; 18 - Nucşoara; 19 - Retezat-Parâng; 20 - Vâlcan-Pilugu; 21 - Schela.

The Supra-Getic nappes described in the western Banat, Poiana Ruscă Mountains, and the Făgăraş Mountains involve mainly basement rocks. Paleozoic and Mesozoic strata known in few small exposures are thin and with many stratigraphic gaps. The Upper Triassic, Lower Jurassic, Tithonian, and Neocomian are absent. Middle Triassic strata similar to those in the Median Dacides of the East Carpathians crop out only in the eastern part (Stan Valley and Făgăraş Mountains). The Urgonian-Aptian strata of the eastern Făgăraş Mountains are similar to those of the Transylvanian nappe in the Perşani Mountains. This suggests that paleogeographic relations did not change by thrusting.

Palogeography and tectonic evolution

Similarly to the East Carpathians, the very condensed shallow-water Early Alpine successions suggest a proximal facies of European affinity. The Jurassic ophiolites of the Severin nappe are interpreted as remnants of an oceanic basin between the Getic and Danubian crustal fragments. The Danubian unit was initially regarded as an autochthonous basement (Murgoci, 1907; 1910) due to its southward projection into the Pre-Balkans which are a continuation of the Moesian platform. The reinterpretation of its internal structure as a stack of pre-Alpine and Alpine nappes, and of the Late Paleogene Getic depression as a foredeep setting, led to the reinterpretation of the Danubian as an allochthonous crustal fragment (e.g., Berza et al., 1994).

The Getic and Supra-Getic nappes involve two phases of thrusting with complex cross-cutting relationships between different thrust sheets. The intra-Aptian "first Getic phase" resulted in the closure of the Severin basin and partial overriding of the Severin flysch units by the Getic nappe. The intra-Senonian "second Getic phase" resulted in a main detachment in front of the Severin - Ceahlău flysch units. The Supra-Getic nappe system is also interpreted to have been emplaced during the Middle Cretaceous and Late Cretaceous (pre-Maastrichtian) phases of overthrusting.

Geophysical data

Megnetotelluric data in the western part of the South Carpathians revealed a crustal depression on the Getic foreland in front of the Danubian units. No transcrustal discontinuity has been recorded in the postulated suture zone between the Danubian and Getic units (Stănică, pers. communication, 1996).

Inconsistencies

The nappe structure of the South Carpathians was developed starting from the classification of the metamorphic basement in two groups (Mrazec, 1897). Murgoci (1905, 1910) assigned them to the Danubian Autochthon and the Getic nappe, imagined as a "suprafolding nappe". The original model invoked a mechanism of regional folding common for the basement and cover sequences. It was later realized that the Alpine cover is in fact more or less flat-laying

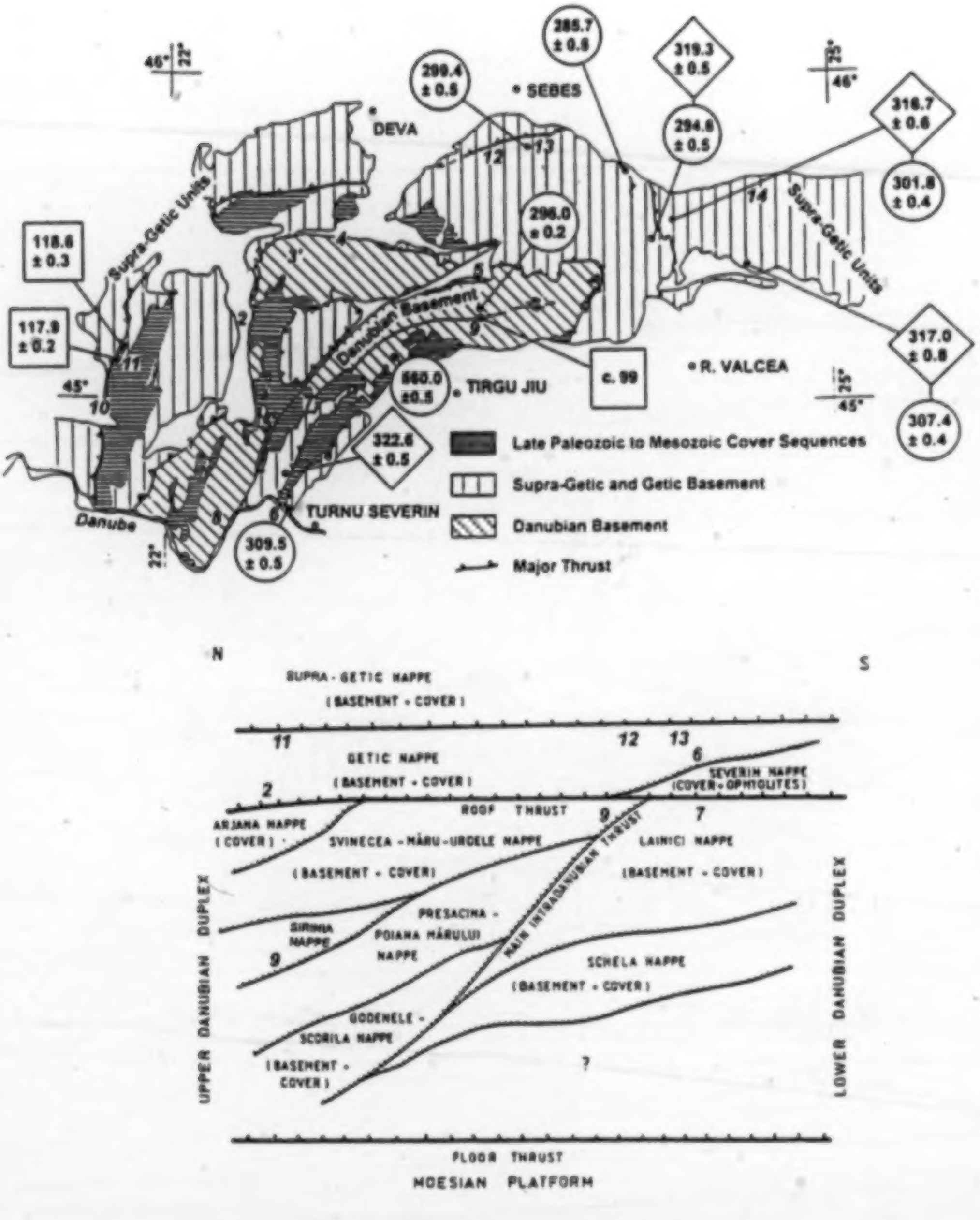
46°
22°
25°
46°
299.4
± 0.5
285.7
± 0.8
319.3
± 0.5
294.6
± 0.5
316.7
± 0.6
301.8
± 0.4
SEBES
DEVA
12
13
14
Supra-Getic Units
298.0
± 0.2
118.6
± 0.3
117.9
± 0.2
Danubian Basement
c. 99
R. VALCEA
317.0
± 0.8
307.4
± 0.4
45°
25°
45°
11
10
560.0
±0.5
TIRGU JIU
322.6
± 0.5
Late Paleozoic to Mesozoic Cover Sequences
Supra-Getic and Getic Basement
Danubian Basement
Major Thrust
TURNU SEVERIN
Danube
22°
309.5
± 0.5
N
S
SUPRA - GETIC NAPPE
(BASEMENT + COVER)
11
12
13
6
GETIC NAPPE
(BASEMENT + COVER)
SEVERIN NAPPE
(COVER + OPHIOLITES)
2
ROOF THRUST
9
7
ARJANA NAPPE
(COVER)
SVINECEA - MÂRU - URDELE NAPPE
(BASEMENT + COVER)
MAIN INTRADANUBIAN THRUST
LAINICI NAPPE
(BASEMENT + COVER)
UPPER DANUBIAN DUPLEX
LOWER DANUBIAN DUPLEX
SIRINIA NAPPE
9
PRESACINA -
POIANA MĂRULUI
NAPPE
SCHELA NAPPE
(BASEMENT + COVER)
GODENELE -
SCORILA NAPPE
(BASEMENT +
COVER)
?
FLOOR THRUST
MOESIAN PLATFORM

Fig. I-21. a) Simplified tectonic sketch of the South Carpathians with the existing $^{40}Ar/^{39}Ar$ data; circle - muscovite, square - whole rock phyllonite; diamond - amphibole concentrates (*from* Dallmeyer et al., 1996). b) Idealized scheme of the tectonostratigraphy of the South Carpathians (*compiled from* Berza et al., 1994; Dallmeyer et al., 1996). Numbers are locations refered in text.

and since the internal structure and stratigraphy of the metamorphic assemblages was considered synmetamorphic, i.e., Precambrian, the mechanism of nappe emplacement was reinterpreted as a huge thrust shear zone at the sole of the Getic basement. Thus, the premises of the original nappe interpretation have been disproved. Nevertheless, the nappe model was further enriched with the Supra-Getic nappes (Streckeisen, 1934) and the Severin nappe (Codarcea, 1934; 1940). In the last two decades an impressive number of local nappes have been added in different parts of the South Carpathians. The Danubian basement originally regarded as "autochthon" is currently interpreted as a stack of Alpine and pre-Alpine nappes (e.g., Berza et al, 1994) (Fig. I-21).

Kinematic indicators along the postulated thrust surfaces of the huge basement nappes interpreted in the South Carpathians record oblique compression or extension associated to major transcurrent shear zones (see Chapter 6).

Tectonic contacts along the shear zones have been consistently interpreted as major thrusts. A simplified scheme based on correlation of basement units as nappes along the South Carpathians includes some 22 Cretaceous nappes and several pre-Alpine nappes (Balintoni et al., 1989, Berza et al., 1994). The Getic nappe is now regarded as a large rigid nappe, thrust more than 100 km from the west or northwest during Cretaceous subduction of the Severin Ocean (e.g., Codarcea, 1940; Săndulescu, 1984) (Fig. I-21). The Danubian units are regarded as a complicated Alpine duplex that includes several Variscan nappes (e.g., Berza et al., 1994) exposed in a large tectonic window under the Getic structural cover (Fig. I-21). The kinematics of all basement overthrusts was never a mater of concern; similarly to the 'unquestionable' Getic Nappe, a vergence normal to the orogen was implicitly assumed.

The Getic thrust. The southwestern and northern outline of the Danubian nappe complex with the Getic Nappe is supposed to be the locus of the major suture along which the Severin Ocean was subducted and its remnants squeezed and dragged under the advancing Getic front. The southwestern contact is represented by the Miocene northeast-southwest trending Rudaria fault (locality 1 in Fig. I-21) which follows the lithological boundary between the Ielova gneiss amphibolite assemblage and the Sebeş-Lotru plagiogneiss-micaschist assemblage. The presence of calc-alkaline "Banatitic" intrusions within the Ielova assemblage conflicts with its interpretation as the lower plate.

To the north, at Armeniş (locality 2 in Fig. I-21), strain recorded within the Getic nappe a few hundred metres from the inferred thrust contact is represented by steeply dipping foliation with spectacular horizontal stretching lineation (Fig. 6-7 a). In the nothwestern, extremity a wide northwest trending fault zone with subhorizontal stretching partly obliterated by normal faults overprints both the Getic (Turnu Ruieni) and the Danubian (Măru) units (locality 3 in Fig. I-21). Most of the northern contact is represented by the Zeicani low-grade mylonitic assemblage

(Berza et al., 1988) with yet unknown kinematics.

Strain analysis along a segment of the inferred thrusts of the Getic and Severin nappes on the Danubian basement (locality 5 in Fig. I-21) showed that a penetrative foliation defined by low-grade mineral assemblages parallels the moderately northwest dipping contacts and contains a subhorizontal northeast trending stretching lineation. These data have been interpreted to record top-to-northeast shearing during Cretaceous nappe emplacement (Ratschbacher et al., 1993). Similarly to the Eastern Alps, strain analysis indicates material flow parallel to the local trend of the orogen in contrast to the originally inferred nappe vergence. However, the analysed region is located along the Cerna-Jiu fault zone; consequently, kinematic indicators interpreted as "top-to-northeast" (Ratschbacher et al., 1993) record in fact orogen parallel, dextral transpression as previously inferred from regional criteria (Berza and Drăgănescu, 1988). Strain within the Sebeş-Lotru assemblage at Porţile de Fier, interpreted as a Getic outlier on the eastern limb of the nappe antiform (locality 6 in Fig. I-21), is in fact consistent with orogen parallel shearing and associated normal detachment on transfer shear zones bounding a metamorphic core complex (Fig. 6-7 b). Strain under the sole thrust of the huge Getic nappe, within the Urgonian limestone cover of the Lower Danubian Lainici nappe (locality 7 in Fig. I-21) is orogen parallel (Fig. 6-7 c).

The Intra-Danubian thrusts. The eastern contact of the mafic-ultramafic Iuţi complex (locality 8 in Fig. I-21) interpreted as a pre-Alpine obduction-related thrust is in fact a vertical low-grade shear zone with spectacular horizontal stretching lineation consistent throughout the Corbu shear zone (Fig. 6-6). Similarly, the contact between the main Danubian Drăgşani and Lainici-Păiuş assemblages, (locality 9 in Fig. I-21) traditionally interpreted to be a major pre-Alpine thrust (e.g., Kräutner et al., 1981; Berza et al., 1994), is an Alpine orogen-parallel shear zone (Dallmeyer et al., 1996). The contact between the Căleanu and Petreanu "nappes" (Berza et al., 1994) is in fact a low-angle normal detachment shear zones defined by the Vidra chlorite-chloritoid-bearing phyllonitic assemblage (locality 3' in Fig. I-21).

The Supra-Getic Thrust. The western outline of the Supra-Getic Nappe corresponds to the Oraviţa N-S trending vertical fault which is cut by Late Cretaceous "banatite" intrusions. At Moniom (location 11 in Fig. I-21), stretching lineation records dextral transpression (Fig. 6-3a) consistent throughout the adjacent Leşcoviţa shear zone. In the northern Sebeş Mountains (localities 12 and 13 in Fig. I-21), the south-dipping contact was interpreted as a Laramian back-thrust (Balintoni et al., 1989). The recorded strain is consistent with sinistral shear followed by high-angle normal detachment (Fig. 6-4). Within one of the Supra-Getic "nappes" (locality 14 in Fig. I-21), retrogressed assemblages mapped throughout an area of c. 80 x 10 km in the northern Făgăraş Mountains (Pană, 1990) display orogen-parallel stretching lineation (Fig. 6-5).

Sm-Nd data for two samples of kyanite-bearing plagiogneiss from the Sebeş-Lotru assemblage yielded very similar T_{DM} model ages of c. 2 Ga and εNd values of c. -14.5, suggesting similar protoliths with Early Proterozoic inheritance. One sample of a retrogressed plagiogneiss from the Suŕu carbonate assemblage yielded the same T_{DM} but a less negative $\varepsilon Nd_{(0)}$ value of -10.5. These data are in good agreement with data on the gneiss-granite and carbonate lense-bearing assemblages from the Apuseni Mountains. Scattered Carboniferous $^{40}Ar/^{39}Ar$ dates from muscovite and hornblende concentrates have been interpreted to record a penetrative, relatively high-grade Variscan tectonothermal event (Dallmeyer et al., 1996). The interpretation is questionable because contemporaneous cover strata in the western part of the Getic assemblage do not record metamorphism and c. 10 My younger dates from on muscovite (286-309 Ma) compared to hornblende (322-319 Ma) suggest cooling during uplift. Lithotectonic assemblages originally interpreted as Proterozoic stratigraphic units appear to be slices of the lower and middle crust assembled sometime prior to Late Carboniferous. Consistency with interpretations in the Alps would require Early Carboniferous collision (M2) and Late Carboniferous doming (M3). Consequently, $^{40}Ar/^{39}Ar$ data record only the Late Carboniferous passage of the Sebeş-Lotru assemblage across the c. 500°C and c. 350°C isotherms. Similarly, fossiliferous Ordovician-Silurian strata (Stănoiu, 1982) constrain $^{40}Ar/^{39}Ar$ dates of c. 296 Ma from medium-grade rocks of the Danubian units to represent Late Paleozoic cooling during isostatic uplift. K-Ar dates of c. 99 Ma and c. 86 Ma along the Getic-Danubian contact at Petroşani from muscovite concentrate from quartzo-feldspathic and carbonate mylonite, respectively (Ratschbacher et al., 1993) may record development of mylonitic fabric during Cenomanian-Santonian dextral transpression. The same tectonic phase is recorded by a $^{40}Ar/^{39}Ar$ date of c. 99 Ma for a muscovite concentrate (Dallmeyer et al., 1996) along the dextral transpression contact between the Danubian Drăgşani and Lainici-Păiuş assemblages. K-Ar dates of c. 70 Ma (Grünenfelder et al., 1983) for phyllonite from the chloritoid-bearing Schela shear zone suggest Late Cretaceous tectonism along the contact of the southern Danubian Lainici and Schela units, contemporaneous with the shearing of the northern Danubian units suggested by a Rb-Sr data of c. 76 Ma (Ratschbacher et al., 1993). $^{39}Ar/^{40}Ar$ whole-rock dates of c.118 and c. 118.6 Ma within the hanging wall phyllonite close to the Getic / Supra-Getic contact record Aptian dextral transpression.

No unequivocal constraint exists for the timing of thrusting. The large number of nappes is currently assigned to the first two acts of the three-act drama of catastrophic thrusting events in the Carpathians: the Middle Cretaceous "first Getic phase", and the Late Cretaceous "second Getic phase"(e.g., Codarcea, 1940; Săndulescu, 1984, 1988; Balintoni et al., 1989).

"The first Getic phase" is interpreted to be Middle Cretaceous because the youngest strata in the underlaying Severin sequence are Lower Aptian. Tectonic contacts dip eastward and the oldest strata overlying both the Getic basement and the Severin sequence are Miocene, along the Danube River. Several hundred kilometres to the east near Braşov, at the junction of the South and East Carpathians, ambiguous contacts of Jurassic limestone assigned to the Getic nappe and Barremian-Aptian flysch strata assigned to the Ceahlău nappe are covered by the Albian Postăvaru conglomerates. This is considered as the evidence of Middle Cretaceous ("Austrian") thrusting of the Getic nappe onto the Ceahlău nappe (Săndulescu, 1984), although a thrust contact of the basement can not be mapped anywhere in that region.

"The second Getic phase" interpreted to have resulted in the final overthrust of the Severin and Getic nappes on the Danubian units is supposed to be intra-Senonian because the youngest strata on the underlying Danubian units are Lower Senonian. The first strata with pebbles of both Getic and Danubian rocks are Eocene strata at Bucova, on the other side of the orogen, in a region of polyphase Tertiary strike-slip displacement (Ratschbacher et al., 1993). There is no constraint on the Late Cretaceous ("Laramian") thrusting of the Severin-Getic nappes.

There is no stratigraphic constraint on the two Cretaceous phases of thrusting in the Danubian units. The angular unconformity underlying the Cenomanian-Turonian Nadanova Strata would record the "first Getic phase" of thrusting, and the Turonian-Senonian "wildflysch" is interpreted to correspond to the initiation of the "second Getic phase" (Săndulescu, 1984).

The main phase of Supra-Getic thrusting is interpreted to be Middle Cretaceous, contemporaneous with "the first Getic phase" because several tectonic contacts are overlain by Cenomanian deposits. Tectonic contacts overlain by Upper Senonian strata are believed to record "the second Getic phase". Barremian-Aptian reef deposits of the Reşiţa-Moldova Nouă Basin on Getic crust extend as isolated outliers on the adjacent Supra-Getic basement indicating the same Early Cretaceous facies zone and modest relative displacement between the two units. Along the Mureş River (locality 15 in Fig. I-21), a succession of Vraconian to Coniacian strata overlie Supra-Getic and Transylvanide units, in total conflict with their interpretation as Late Cretaceous nappes verging south and north, respectively.

The Tithonian-Neocomian Sinaia and Comarnic flysch sequences assigned to the Severin nappe and interpreted to represent the subducting wedge dragged eastward at the sole of the Getic nappe are only located on the eastern margin of the Danubian units, i.e., on the external margin of the orogen similarly to the East Carpathians; their local westward thrusts are likely related to Tertiary dextral transpression at the tip of the Moesian Platform.Calc-alkaline intrusions located on the Danubian units contradict the current tectonic model which postulates westward subduction and underthrusting of the Danubian. Barremian-Aptian reef deposits of the Reşiţa-Moldova Nouă Basin on Getic crust are also present as isolated outliers on the adjacent Supra-Getic basement.

I.7. DINARIDES

The Dinarides are located south of the Pannonian basin, between the Vardar suture and the median line of the Adriatic Sea. To the west, they merge into the Southern Alps of Italy, and to the south into the Hellenides.

The following summary of the geology of the Dinarides is based on Aubouin (1970), Channel and Horváth, 1976; Dimitrijevic, 1982, 1991; Dimitrijevic and Dimitrijevic (1973, 1987), Herak (1986), Pamic (1986, 1993), Kovács (1992) .

Major tectonostratigraphic units

From bottom to top, the following four southwest-verging major tectonostratigraphic units were differentiated: the Adriatic zone in an autochthonous position, overthrust by the Budva, Dinaric, and Internal (or Vardar s.l.) zones (Fig. I-22).

Along the Adriatic coast, in the Istrian Peninsula and on the islands south of Split, the Adriatic zone is an almost uninterrupted Ladinian-Middle Eocene carbonate platform succesion followed by Eocene flysch strata. In the southern Dinarides, it is overridden by the Mesozoic deep-water deposits and Paleogene flysch of the Budva zone which represent the northernmost continuation of the oceanic Pindos - Cukali - Kreasta zone of the Hellenides.

The Dinaric zone is involved in a nappe complex that consists of the vast Triassic - Cretaceous platform carbonate sequence interrupted by bauxite horizons mainly in the Cretaceous. It is geographically subdivided into the High Karst Zone to the southwest and the Pre-Karst Zone to the northeast. Mesozoic carbonates in the Pre-Karst Zone are overlain above a major unconformity by Upper Paleocene-Lower Miocene clastic strata. To the NE, the uppermost tectonostratigraphic unit is the complicated accretionary wedge of the Vardar zone s.l. comprising the Upper Cretaceous-Paleogene Bosnian flysch, overthrust by the Durmitor Upper Jurassic ophiolitic melange and flysch, the Drinja-Ivanjica units, and the Vardar zone s.s. Several strips of ophiolitic rocks in the internal zone are interpreted as obducted oceanic crust dismembered by subsequent tectonism. Rare Ladinian pillow lavas and radiolarites in the Dinarides suggest a Triassic opening of the Vardar Ocean. However, the bulk of the Vardar zone s.s. consists of Late Jurassic serpentinite and gabbro forming isolated blocks within the mélange. Locally, Lower Cretaceous intermediate and acidic calc-alkaline volcanics and granites are interpreted as island arc magmatism. To the north, the Vardar zone is covered by Neogene to Recent succession of the Pannonian Basin.

Paleogeographic and tectonic evolution

The Dinaric zone is interpreted as a thin-skinned thrust-fold belt overlying the carbonatic platform of the Adriatic promontory of Africa (Channel and Horváth, 1976). Thrusts in the Vardar Zone s.l. are assumed to have involved the crystalline basement and to be responsible for large-scale allochthony. The ophiolitic mélange and blueschist-facies rocks formed during the Late

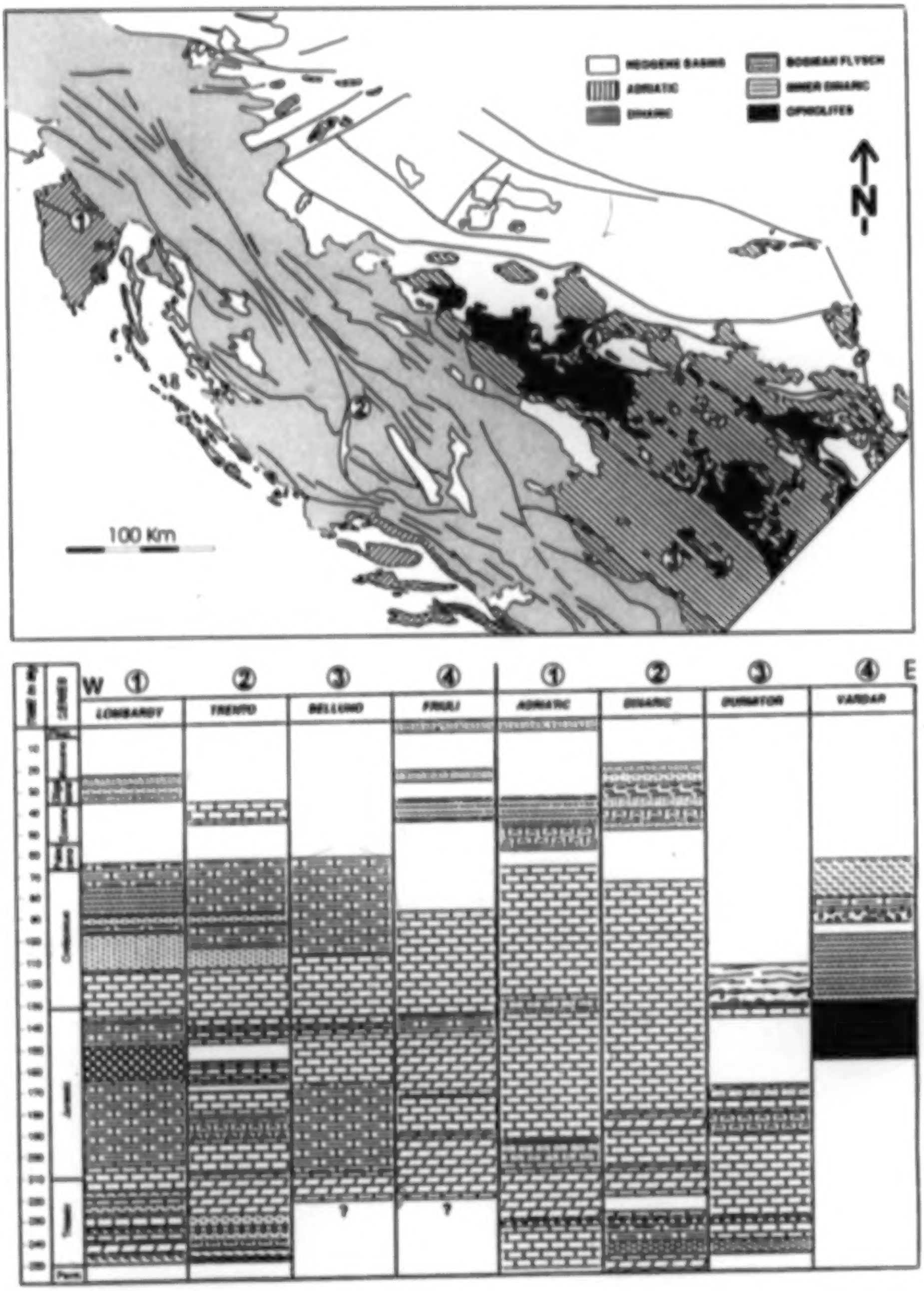
NEOGENE BASINS
ADRIATIC
DINARIC
BOSNIAN FLYSCH
INNER DINARIC
OPHIOLITES
N
100 Km
W
①
②
③
④
①
②
③
④
E
LOMBARDY
TRENTO
BELLUNO
FRIULI
ADRIATIC
DINARIC
DURMITOR
VARDAR

Fig. I-22. a) Simplified tectonic sketch of the Dinarides; b) Alpine stratigraphy for the Dinarides-right and Southern Alps-left (*adapted* from Tari, 1994).

Jurassic-Early Cretaceous closure/subduction of the Vardar ocean. The Maastrichtian - Paleogene Bosnian flysch is interpreted either as a flysch basin in front of the major thrusts of the Vardar s.l. imbricates or as a local subduction zone. In the Vardar zone, Miocene calc-alkaline igneous activity including andesite are spatially related to the Sava SE-trending dextral strike-slip fault zone.

I.8. SOUTHERN ALPS

The Southern Alps are bounded to the North by the Insubric (Periadriatic) Line. To the south, the Southern Alpine foreland is hidden below the Po Plain.

Major tectonostratigraphic units

The following summary is based on several synthesis papers including Winterer and Bosellini (1981), Doglioni and Bosellini (1987), Massari (1990), Bernoulli et al., (1990), Bigi et al., (1990). The subdivision of the Southern Alps is based on early Alpine facies zones. These roughly N-trending zones include from W to E the Lombard Basin, the Trento Plateau, the Belluno Trough, and the Friuli Platform (Fig. I-23).

The stratigraphic sequence of the Friuli Platform dominated by shallow-water carbonates is comparable to that of the Adriatic zone of the Dinarides. Similarly, the Eocene Friuli flysch correlates with the Late Eocene flysch of the Adriatic zone. It is unconformably overlain by an Upper Oligocene to Lower Miocene clastic sequence (Massari et al., 1986) which itself, above another major unconformity, is overlain by Late Neogene to Recent clastics. The Belluno Trough has a distinct deep-water Jurassic facies overlain by Cretaceous pelagic carbonates. The Trento Plateau represents a relatively elevated and undeformed carbonate platform from Early Mesozoic to Jurassic age, covered unconformably, by Upper Eocene carbonates. The Lombard basin has a distinct deep-water Jurassic sequence, characterized by deposition of radiolarites during the Bathonian - Oxfordian. Water depth remained considerable throughout the Cretaceous until the Turonian, when an E-W flysch trough developed perpendicular to the direction of the underlying Early Alpine zones, and submarine fans accumulated during the Middle Oligocene - Early Miocene.

Tectonic evolution of the Southern Alps

The Alpine evolution of the Southern Alps started with Middle Triassic magmatism. Although geochemical studies were inconclusive, the magmatic activity is related to rifting (e.g., Bechstädt et al., 1978) with a component of left-lateral strike-slip (Doglioni, 1987). Jurassic strata record the opening of the Penninic ocean to the west. Subsequent compression is indicated by the development of a south-vergent thrust and fold belt involving the Late Cretaceous Lombard flysch, (e.g., Bernoulli and Winkler, 1990) and thrusts within the Eocene Ternate Formation (e.g., Schönborn, 1992). The Adamello, Bergell, and Pohorje intrusions suggest an Oligocene

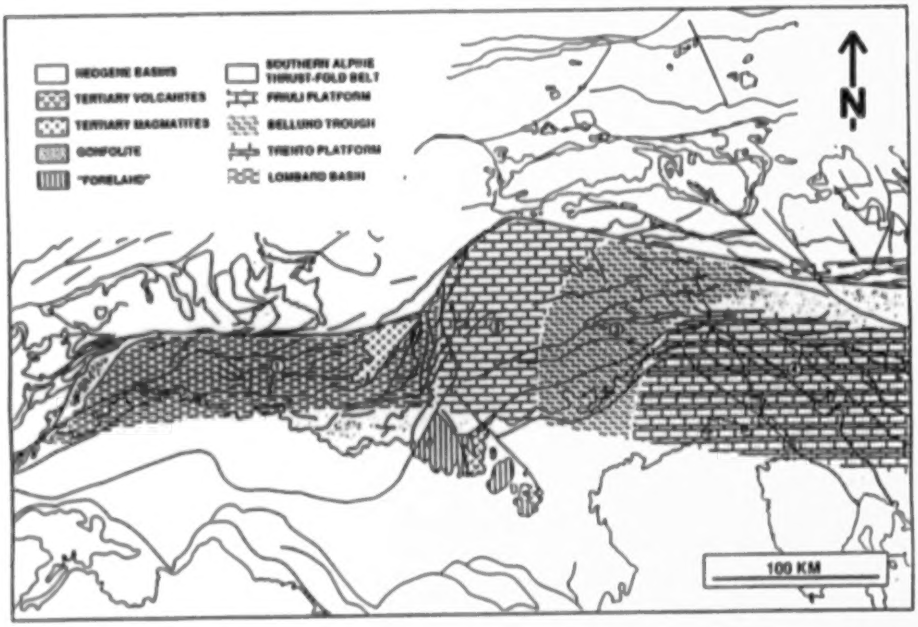
NEOGENE BASINS
TERTIARY VOLCANITES
TERTIARY MAGMATITES
GONFOLITE
"FORELAND"
SOUTHERN ALPINE THRUST-FOLD BELT
FRIULI PLATFORM
BELLUNO TROUGH
TRENTO PLATFORM
LOMBARD BASIN
N
100 KM

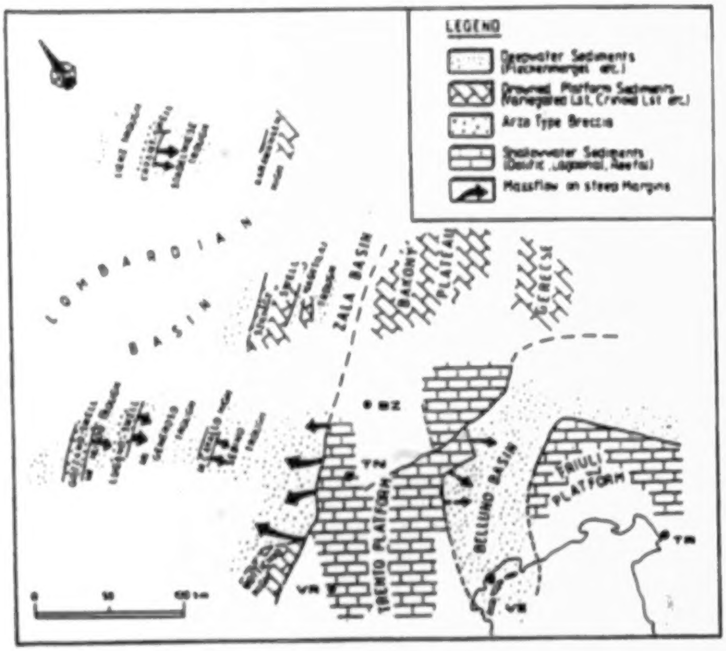
LEGEND
Deepwater Sediments (Fleckenmergel etc.)
Drowned Platform Sediments (Ammonitico Rosso, Crinoid Lst. etc.)
Arzo Type Breccia
Shallowwater Sediments (Oolitic, Lagoonal, Reefal)
Massflow on steep Margins
LOMBARDIAN BASIN
ZALA BASIN
BAKONY PLATEAU
GERECSE
TRENTO PLATFORM
BELLUNO BASIN
FRIULI PLATFORM
BZ
TN
VR
VE
TS
0
50
100 km

Fig. I-23. a) Simplified tectonic sketch of the Southern Alps; for Alpine stratigraphy see Fig. 2-13 b) Paleogeographic reconstruction of the South Alpine realm and its northern prolongation in the original position of the Drauzug and the Transdanubian Mountains (*modified after* Winterer and Bosellini, 1981).

extensional stage along the Periadriatic lineament (Laubscher, 1986). The Oligocene Venetian basin is considered the foredeep of the SW-vergent Eocene Dinaric thrust-and-fault belt that extends to the Southern Alps (Doglioni, 1987). A south-vergent Middle Miocene thrust and fold belt in the Southern Alps accommodated up to 100 km shortening and cuts the earlier Dinaric structures in the eastern part.

I.9. THE INTRA-CARPATHIAN REGION

Three major tectonostratigraphic levels suggest three main stages in the Alpine evolution of the 400 km wide intra-Carpathian region.

The upper, Neoalpine level comprises the Neogene Pannonian Basin s.s., consisting of a Miocene to Quaternary succession that covers almost the entire area and occurs in a number of small, irregular and diversely oriented subbasins (locally over 8 km thick). The upper strata represent largely passive filling, in general by deltas prograding from the northwest, followed by lacustrine and terrestrial sedimentation. Seismic-reflection profiles across many basins show no clear structure other than compaction of their fill. Positive Bouguer gravity anomalies whose amplitudes increase with the thickness of fill in the Bekes Basin of Hungary and Romania and in the southeastern-most Slovakian basin are interpreted to indicate syn-depositional shortening of open oceanic-lithosphere gaps (Hamilton, 1990). Abundant Neogene volcanic rocks are known in outcrops and subsurface.

The middle, Mesoalpine level consists of isolated Paleogene basins with either "flysch" (Szolnok-Maramureş and Podhale) or "epicontinental"(Krappfeld, Slovanian, Hungarian, and Transylvanian) sequences. The lower level is interpreted to consist of a collage of numerous Mesozoic-Paleozoic tectonostratigraphic units distinguished by their Early and Eoalpine lithofacies and/or structure. The basement of the Pannonian Basin s.s. was initially considered a median mass, "Tisia", situated between the Alps, the Carpathians and the Dinarides (eg. Kober, 1931). Its heterogeneities were interpreted as distinct Variscan complexes (Fig. I-24). As isotopic age determinations have yielded very dispersed data, the subdivision and age problems of the crystalline basement are very controversial.

Paleozoic to Mesozoic facies and sequences differ between neighbouring crustal blocks, which suggests that they were widely separated before aggregation. The widespread, mainly subsurface Cretaceous and Tertiary volcanic rocks are currently interpreted to be, byproducts of subduction between crustal blocks and island arcs now inside the Carpathian arc. Regional tectonic interpretations include:

-an aggregate of accreted terranes that record Mesozoic and Cenozoic rifting, drifting, and accretion; a number of small continental and island-arc fragments were squashed together

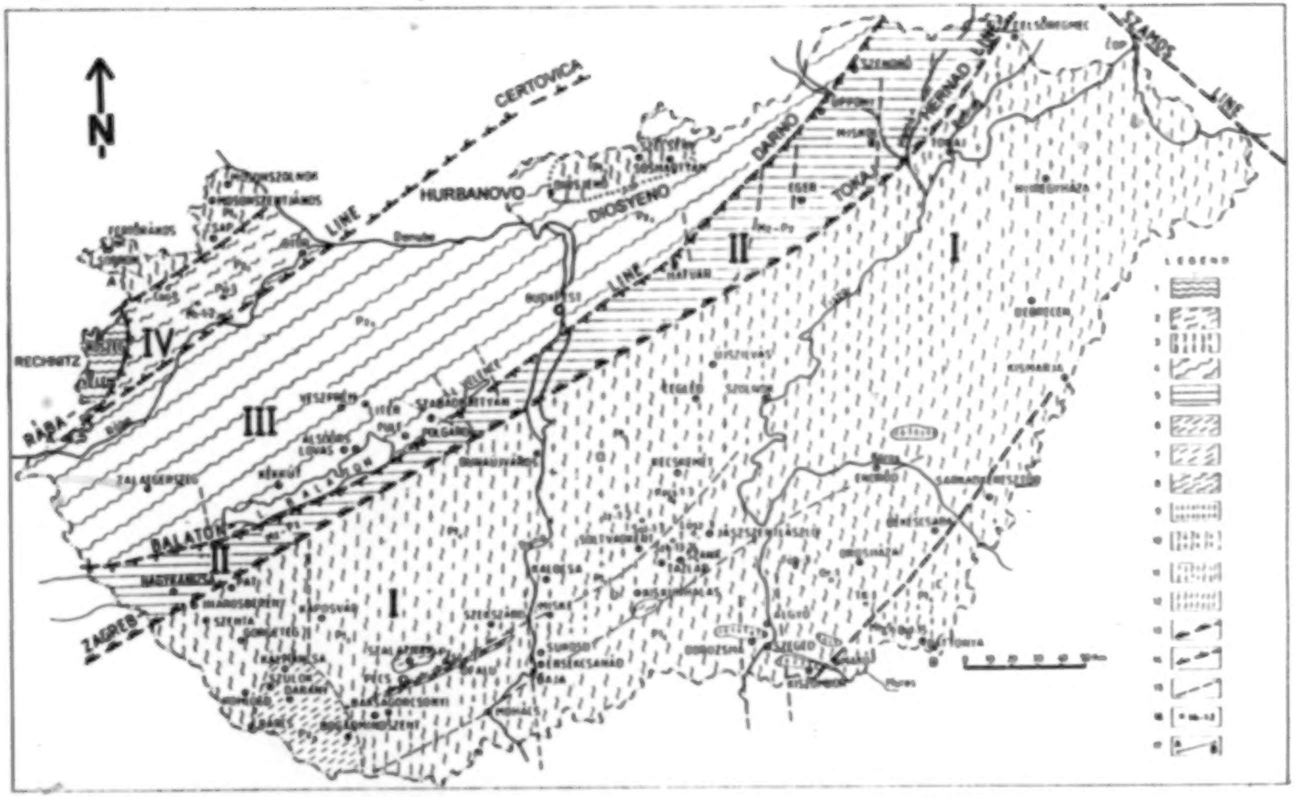
N
CERTOVICA
HURBANOVO
LINE
DIOSYENO
DARNO
TOKAJ
LINE
HERNAD
LINE
SZAMOS
LINE
RECHNITZ
RABA
IV
III
II
I
II
I
BALATON
ZAGREB
BUDAPEST
DEBRECEN
SZEGED
LEGEND

Fig. I-24. The main basement units of the Pannonian Basin (compiled from Jantsky et al., 1982; Balla, 1992). I. The continuation of the basement units from the Eastern Alps: 1 - Mesozoic (?) low grade rocks of the Rechnitz-Koszeg window; 2 - Unknown basement under the Gratz Paleozoic. 3 - Highly sheared and retrogresed medium grade rocks (Sopron-Fertorakos). II. Basement of the Transdanubian Central Range: 4 - Very low to low grade Paleozoic sequence on Balaton gneissic crust intruded by Variscan granites. III. Unknown basement of the Igal-Bukk Unit: Paleozoic and Mesozoic locally affected by Alpine low-grade metamorphism. IV. "Pannonian Median Mass": 6 - Upper Carboniferous, coal-bearing non-metamorphosed shales; 7 - Lower Paleozoic non-metamorphic slate complex; 8 - Upper Proterozoic greenschist facies rocks: phyllite, crystalline limestone, amphibolite and serpentinite; Lower Proterozoic, ultrametamorphic complex: 9 - microcline granite; 10 - rheomorphic migmatite; 11 - stromatitic migmatite; 12 - Lower Proterozoic sillimanite, staurolite and cordierite plagiogneiss. 13, 14, 15 - tectonic contacts; 16 - borehole.

during Tertiary time (Szadeczky-Kardoss, 1975; Balla, 1982; 1985; 1986; Hamilton, 1990).

-moderate Tertiary disruption of a previous coherent mass by linked strike-slip faults (Săndulescu, 1984; 1988; Royden, 1988).

Based on contrasting pre-Miocene stratigraphy and structure, the Panonnian Basin can be subdivided into the northern (Pelso) and southern (Tisia) units (see Fig. 5-21). Their paleogeographic positions have been reversed by complex plate motions: Jurassic fossils in limestone on the crustal fragments of the northern part of the inter-arc region are of southern Mediterranean types, whereas those in the southern part are much more like those of Europe to the north.

I.9.1 The North Pannonian Unit

The North Pannonian Unit (Fig. I-25) is bounded to the northwest and north by the Rába-Hurbanovo-Diósjenö Line and the northern tectonic boundary of the Meliata sequence; to the south and southeast, by the poorly understood Mid-Hungarian Line. To the northeast, the boundary is uncertain as the pre-Tertiary basement is covered by Miocene volcanics and the Neogene fill of the Transcarpatian Basin.

The following summary is based on Balla (1982; 1985; 1987), Árkai (1985; 1987a; 1987b), Jantsky et al. (1988), Kázmér and Kovács (1989), and Haas et al. (1995).

Pre-Tertiary rocks are exposed in the Transdanubian (TDM), Bükk, and southern West Carpathians (Meliata) mountains. While the early Alpine successions of the Transdanubian Mountains show a clear South Alpine affinity, the Bükk and Meliata sequences show a Dinaric-type evolution.

Based on the Liassic sedimentary record, the TDM can be divided into three paleogeographic units. According to Winterer and Bosellini (1981) and Kázmér and Kovács (1985) these units can be correlated with the South Alpine paleogeographic units in the following way: the Gerecse platform corresponds to the Belluno trough, the Bakony platform to the Trento platform, and the Zala basin to the Lombardian basin with deep-water black shales (Fig. I-23).

In the Zala Basin, continuous Mesozoic sedimentation was terminated in the Aptian; a Senonian carbonate succession was deposited above a major unconformity, in contrast to the coeval clastic Gosau facies of the Eastern Alps. The Senonian is unconformably overlain by a Middle to Upper Eocene carbonate and clastic sequence including Upper Eocene andesite and tuffs.

The Permo-Mesozoic succession of the Bakony unit unconformably overlies Hercynian low-grade metamorphic rocks. The Middle Triassic volcanoclastic sequence is similar to that of the Southern Alps. A thick (>3 km) Upper Triassic carbonate platform sequence is overlain without interruption by deep-water Jurassic radiolarites. By the Early Cretaceous, shallow-water carbonates were again being deposited. An unconformity-bounded Aptian to Cenomanian

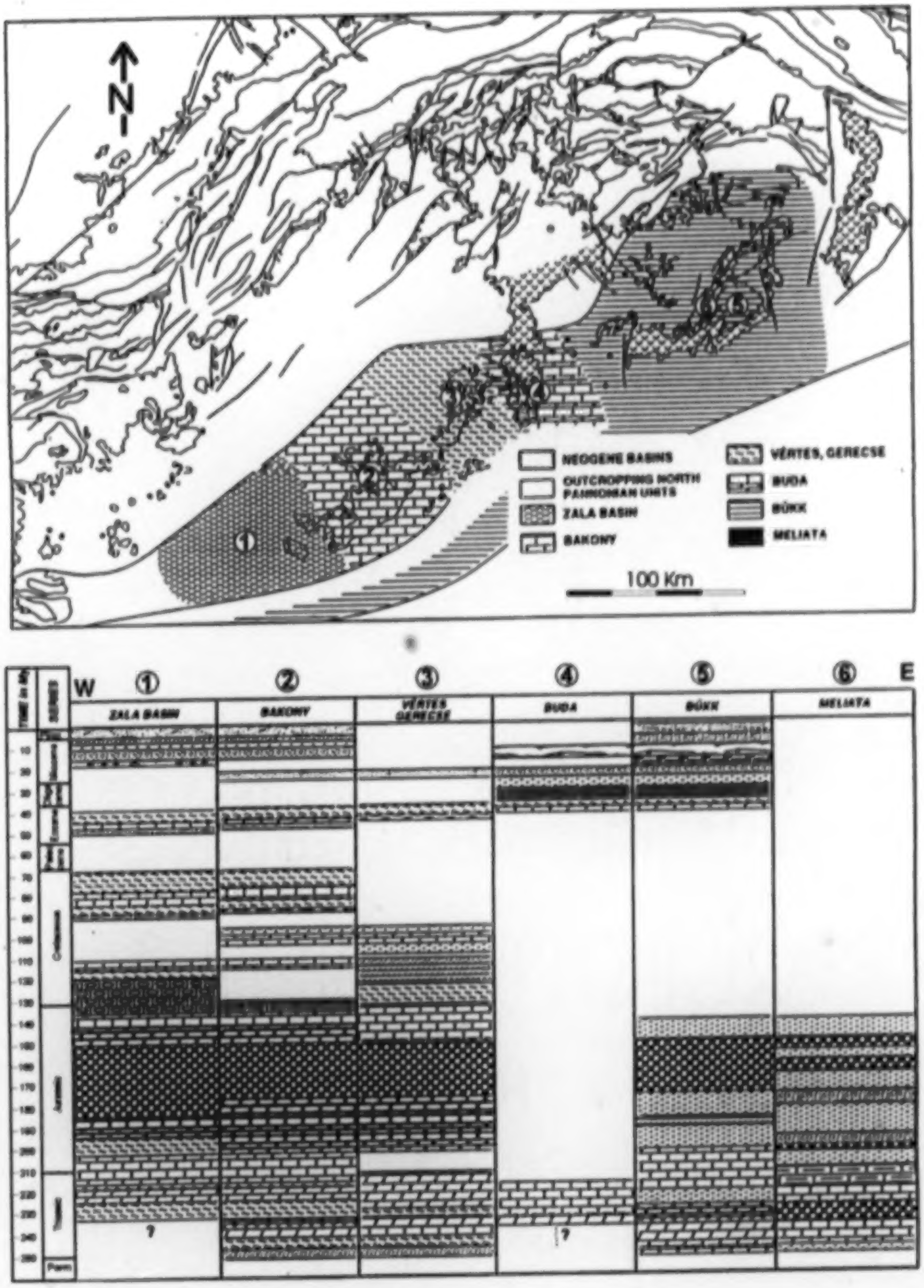
N
NEOGENE BASINS
OUTCROPPING NORTH PANNONIAN UNITS
ZALA BASIN
BAKONY
VÉRTES, GERECSE
BUDA
BÜKK
MELIATA
100 Km
W
E
①
②
③
④
⑤
⑥
ZALA BASIN
BAKONY
VÉRTES GERECSE
BUDA
BÜKK
MELIATA
?
?

Fig. I-25. a) Simplified tectonic sketch of the North Pannonian Unit; b) Alpine stratigraphy; (*adapted from* Tari, 1994).

sequence is followed by the Senonian carbonate succession in the Zala Basin. A Late Eocene transgressive sequence is overlain by Upper Oligocene to Lower Miocene continental clastics.

In the Gerecse unit, the early Mesozoic succession is similar to the units above but a significantly different Early Cretaceous evolution is suggested by Barremian flysch deposits. These are followed by deep-water Aptian - Lower Albian clastics.

Metamorphic/Magmatic basement

Basement rocks of the Northern Pannonian unit are very poorly exposed in the Transdanubian Mountains (Figs I-24 and I-25). Post-kinematic Variscan granitoids intruding along the Balaton fault zone yielded Rb-Sr and K-Ar dates of 310-330 Ma at Balaton and K-Ar dates of 280-290 Ma at Velence (Balogh et al. 1983). To the northwest, between the Balaton lineament and the Raba Fault zone, the basement is known from a few outcrops and numerous boreholes. Paleozoic strata of uncertain age include pelites, psammites, carbonate beds, marls with graptolites, conodonts, and acritarchs, and volcanics, metamorphosed under very-low to low-grade conditions during the Variscan orogeny (?). The distribution of the very-low grade rocks suggests over 20 km left lateral offset along the Raba Line. To the northeast, in the Uppony Mountains, Middle Devonian to Middle Carboniferous strata includes basaltic lavas and pyroclastics related to subsidence and are affected by very-low to low-grade Alpine metamorphism. Significantly, no Variscan metamorphism has affected the area (Árkai et al., 1987). In northern Hungary (Szecseny, Diosjeno, and Soshartyan), several boreholes encountered garnet micaschist and gneiss in a structural position that may correspond to the SW extension of the Veporic basement in the West Carpathians.

At the northern extremity, close to the Hungarian-Slovakian border, an area of 2 km^2 exposes basement rocks of uncertain affinity. The gneiss-granitic crust with kyanite-staurolite-sillimanite K-Ar data on amphibole and muscovite yielded 307+/-14 Ma and 222+/- 9 Ma, respectively. A Rb/Sr date of 962+39 Ma is suspect, as no other Middle Proterozoic ages are known in the region. Intense shearing and retrogression resulted in quartz- and feldspar-porphyroclast-bearing low-grade mylonite ("porphyroids").

Southeast of Lake Balaton, drillholles reached a partly retrogressed marble-bearing assemblage that records medium-grade, medium-pressure metamorphism (garnet, staurolite) followed by a low pressure overprint (up to andalusite) related to the Variscan granitoid intrusions (Árkay, 1987). The Kőszárhegy "metasiltstone", Alsóőrs "porphyroid", and "slate" from the Bakony Mountains are interpreted as Ordovician formations with a low-grade Variscan overprint. Petrographic descriptions suggest that the porphyroid-bearing sequence from Bakony and northeastern Hungary is an Alpine low-grade mylonitic assemblage contemporaneous with the retrogression of the Balaton gneissic basement and prograde metamorphism in the Bükk-Uppony Mountains.

Extreme alkali magmatism: monchiquite dyke 60 Ma. Andesite volcanism is dated by tuffs intercalated in the fossiliferous Late Eocene strata and K-Ar on lavas (30 Ma).

To the southeast, between the Balaton and Zagreb -Tokaj - Hernad tectonic lineaments is the Igal-Bükk region (Fig. I-24). No pre-Alpine crystalline basement is known. The stratigraphic column ranging from Devonian (?) / Carboniferous to Oligocene is poorly known. It includes marine Upper Carboniferous limestone, Lower and Middle Permian sandstone, slate, dolomite and limestone; Upper Permian fluviatile and lagoonal siltstone and dolomite, marine mainly carbonate Triassic with tuffitic intercalations, and Mesozoic ophiolite fragments with chert and shales. The Igal unit is generally interpreted as the connection between the Dinaride and Bükk-Meliata, i.e., the northern end of the Vardar oceanic realm. Formations of uncertain Paleozoic age are similar on either side of the Balaton tectonic lineament suggesting that this is not a sharp crustal discontinuity, but more likely a wide fault zone.

To the northeast, the Igal unit projects into the Bükk, Uppony, and Szendro Hills where a continuous sedimentary sequence from Devonian to Upper Triassic shows close relationship to the Southern Alps and Dinarides. The Lower Triassic is developed in a neritic carbonate facies with characteristic black dolomites. The Middle Triassic includes calc-alkaline intermediate to acidic volcanics. By the end of the Carnian, the carbonate shelf was drowned, and deep-water sedimentation with turbidites and olistostromes persisted during Late Triassic - Jurassic time. The whole early Alpine sequence is metamorphosed to zeolite to lower greenschist grade (Árkai et al., 1985). The Meliata sequence crops out in the southwestern part of the Bükk Mountains and in the southern West Carpathians. It consists of deep-water Triassic-Jurassic strata with ophiolites of Middle Jurassic (Darnó Hill) and Upper Jurassic (Szavaskő) age. The Meliata sequence is correlated with the Vardar zone of the Dinarides. It is involved in north-verging thrusts in the West Carpathians and in south verging thrusts in the Bükk Mountains, and records Middle Jurassic high pressure low temperature metamorphism (c. 155 Ma, ^{40}Ar/^{39}Ar data, Malusky et al., 1993; Dallmeyer et al., 1996).

The long lived sedimentary basin records no Variscan metamorphism.

Tectonic evolution of the North Pannonian unit

Widespread Middle Triassic volcanism in the Transdanubian region was regarded as an "aborted rift" (Bechstädt et al., 1978), and the contemporaneous calc-alkaline volcanics in the Bükk Mountains, as subduction magmatism (Kovács, 1992). The pelagic Jurassic sedimentation in the Transdanubian units suggest an oceanic realm to the NW in present-day coordinates (Galácz et al., 1985). In the Bükk Mountains, the Meliata branch of the Vardar Ocean opened in the Middle Triassic and expanded as an oceanic domain until the Jurassic. The Early Cretaceous flysch in the Gerecse Mountains is interpreted to be related to the closing of the

Vardar ocean (Sztanó, 1990). The emplacement of numerous south-verging Eoalpine nappes (including the Meliata-Szavaskő nappes) between 115 - 90 Ma (K-Ar dates, Árva-Sós et al., 1986), was accompanied by low-temperature and high-pressure metamorphism (Árkai, 1983). In contrast, only minor Middle Cretaceous thrusts have been recognized in the Transdanubian region (Balla, 1988), although large-scale allochthoneity was suggested based on subsurface data (Horváth and Rumpler, 1984).

The Senonian of the Zala and Bakony units and the whole Paleogene of the Northern Pannonian are considered to be post-tectonic, epicontinental or molasse-type sequences. (e.g., Haas et al., 1986; Nagymarosy, 1990) The Paleogene basin was also interpreted as a pull-apart feature related to regional dextral strike-slip (e.g. Royden and Báldi, 1988; Csontos et al., 1992).

Szolnock-Maramureş flysch belt

Approximately between the North and South Pannonian units, a belt of strained Middle Cretaceous basalt and abyssal pelagic sediments, and Upper Cretaceous through Upper Oligocene marls and turbidites (Dicea et al., 1980; Baldi-Beke and Nagymarosy, 1981; Fülöp et al., 1987) about 50 km wide trends northeast across Hungary (Fig. I-26). It is overlain by undeformed upper Miocene and younger strata. The west-southwest prolongation of the linear magnetic anomalies related primarily to Cretaceous basalts within the strained belt, and sparse well data (Fülöp et al., 1987) suggest its continuation in the subsurface across southwest Hungary. Along strike in the other direction, the belt swings north-eastward into northern Romania. Here, the "Maramureş Transcarpathian zone" consists of broken formation and scaly clay that includes abundant fragments of ophiolite and disrupted deep-water clastic strata at least as young as Oligocene (Dicea et al., 1980). Defined as a Tertiary mélange in an accretionary wedge, the belt is interpreted to record subduction of oceanic lithosphere. It merges with the polymictic mélange belt of the main Carpathian arc. Exposed and subsurface Miocene volcanics (andesite and allied) north of the belt are interpreted to define the paired volcanic arc trending west-southwestward from the southeast border of Slovakia across Hungary. The belt of strained strata and the volcanic rocks are considered the evidence of a long and complex history of rifting, convergence and subduction in the intra-Carpathian region (Szadeczky-Kardoss, 1975, Balla, 1982; Hamilton, 1990). An alternative interpretation suggests that the Szolnock - Maramureş complex is the Palaeogene fill of a narrow transtensional basin formed in a strike-slip system (Royden and Baldi, 1988).

I.9.2 THE SOUTH PANNONIAN UNIT AND THE APUSENI MOUNTAINS

The Early Pliocene subsidence of the Panonian Basin imposed a limitation on direct observation. Data are provided by lithological logs and isolated exposures from the Mecsek and Apuseni mountains (Fig. I-26).

The basement of the Great Hungarian Plain between the Apuseni Mountains to the east and the Zagreb -Tokaj fracture zone crops out only in the Mecsek Hills. In the divide between Danube and Tisa rivers and Trans-Tisa regions, Mecsek-type granite and migmatic gneiss are intensely retrogressed, suggesting Alpine reactivation. From Mohacs to Szeged and Debrecen, garnet-bearing plagiogneiss, micaschist and amphibolite are variably retrogressed. Granitic bodies are present around Szeged and North of Endrod. Intercalations of marble and dolomites are known only at Kiskundorozsma, west of Szeged.

In the south-eastern part close to the Hungarian-Romanian border the migmatic gneiss crust and the Battonya granite may represent the westward extension of the Cadru assemblage exposed in the Apuseni Mountains. Near Battonya, staurolite-bearing plagiogneiss was interpreted to represent the Baia de Arieş nappe of the Apuseni Mountains (Dimitrescu, 1981). At Backa, in Vojvodina (Yugoslavia) and in northern Banat (Romania) core samples indicate a mediun- to high-grade metamorphic basement that includes almandine, staurolite, sillimanite gneiss and migmatites, sheared and retrogressed to quartz-albite-epidote schist with interbedded marbles (Kamenci, 1975).

Early attempts to integrate the Apuseni Mountains into Alpine plate tectonics (e.g. Rădulescu and Săndulescu, 1973; Bleahu et al, 1973, Bleahu, 1976) inferred the Mureş Basin to represent the main branch of the Tethys Ocean. Models of a single arc (Cioflica and Nicolae, 1981), dual converging arcs (Savu, 1983), or changing subduction polarity (Săndulescu, 1984) were proposed to accommodate the juxtaposition of tholeiitic and calc-alkaline rocks. The igneous petrochemistry and sedimentologic characteristics of the western part of the Mureş Basin have also been interpreted as those of a marginal basin developed on continental crust (Lupu et al., 1993). Remnants of the Tethys Ocean were postulated to be obscured by Tertiary cover of the Transylvanian Basin (Fig. I-1) (Săndulescu, 1994; Rădulescu et al. 1993) but core samples from the Transylvanian basement are calc-alkaline igneous rocks (I. Nicolae, personal communication, 1995).

Westward subduction beneath the Apuseni region was considered to have resulted in subduction magmatism and the thrusting of a large number of antithetic nappes but the number, composition, age, and boundaries of the proposed nappes varied between authors (e.g. Ianovici et al., 1976; Bleahu et al., 1981; Săndulescu, 1984; Balintoni, 1994). The present spatial distribution of rock assemblages and their temporal relationships are incompatible with ocean opening and subduction.

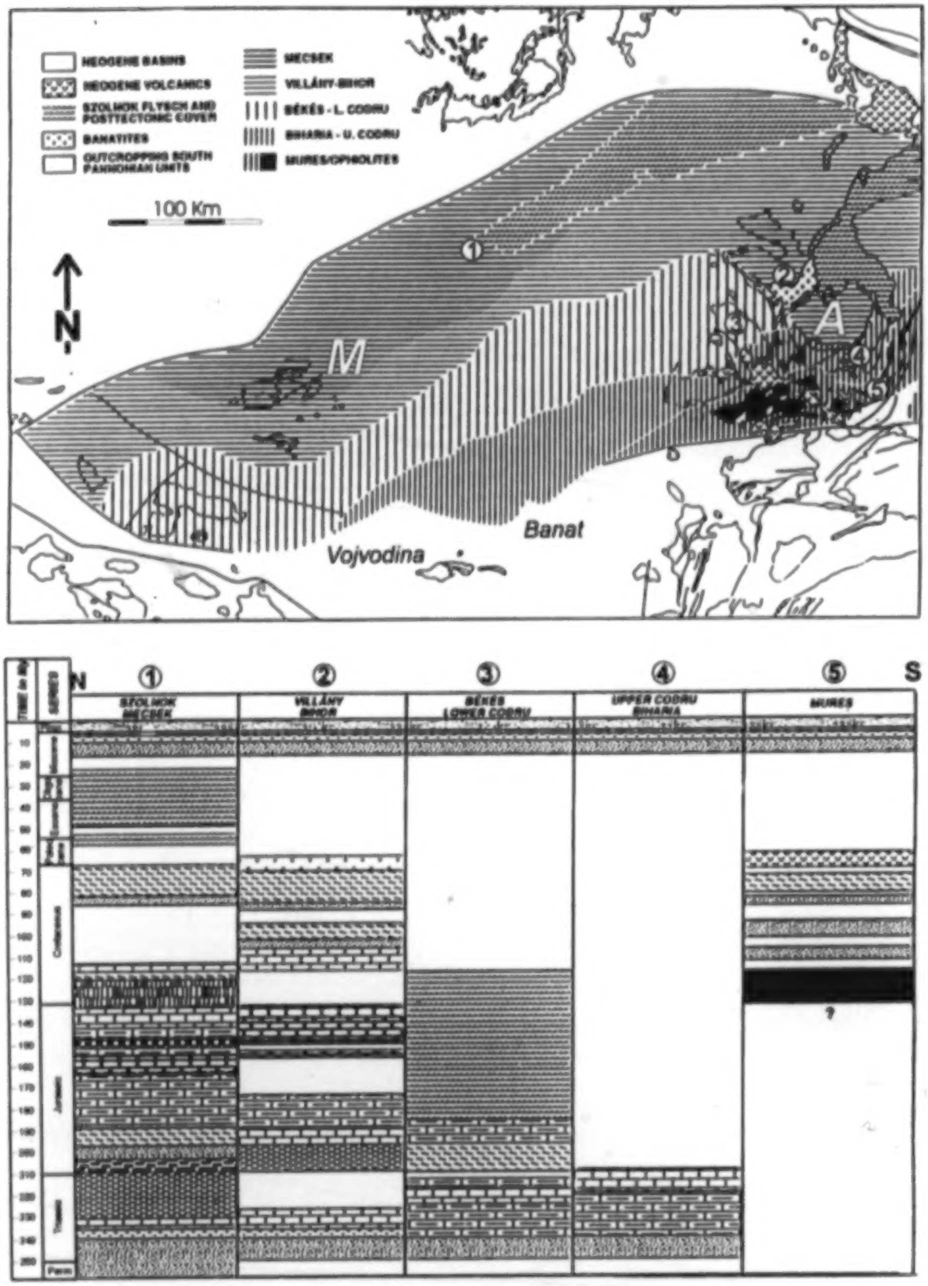
NEOGENE BASINS
NEOGENE VOLCANICS
SZOLNOK FLYSCH AND POSTTECTONIC COVER
BANATITES
OUTCROPPING SOUTH PANNONIAN UNITS
MECSEK
VILLÁNY-BIHOR
BÉKÉS - L. CODRU
BIHARIA - U. CODRU
MURES/OPHIOLITES
100 Km
N
①
②
③
④
⑤
M
A
Banat
Vojvodina
TIME (in Ma)
SERIES
N
S
SZOLNOK MECSEK
VILLÁNY BIHOR
BÉKÉS LOWER CODRU
UPPER CODRU BIHARIA
MURES
?

Fig. I-26. a) Simplified tectonic sketch of the South Pannonian Unit; b) Alpine stratigraphy; (*adapted from* Tari, 1994). *M* - Mecsek Mountains; *A* - Apuseni Mountains.

The Alpine nappes in the Apuseni Mountains (Fig. I-27) are inferred to have been emplaced during three tectonic events: middle Cretaceous, pre-Gosau and Laramian. Middle Cretaceous tectonism resulted in the emplacement of the Transylvanides, the pre-Gosau tectonism resulted in the emplacement of the Apusenide and the Laramian tectonism in the reactivation of the Transylvanides (Balintoni, 1994).

The Transylvanides of the southern Apuseni Mountains originate in an island arc and a marginal basin related to Middle Jurassic to Early Cretaceous subduction under the Apuseni continental crust (Nicolae, 1992). Middle Cretaceous ("Austrian") tectonism was originally inferred to have resulted the emplacement of a single nappe (Ilie, 1936). The interpretation of the Mureş igneous suite as an ophiolite complex led to ophiolite obduction models (Ianovici et al., 1976; Bleahu, 1981) involving at least seven "Austrian" nappes (Balintoni, 1994,and references therein).

The Apusenides are considered pre-Gosau nappes north of the Transylvanides. Nappes consisting mainly or only of basement are assigned to the upper Biharia Nappe System and nappes consisting of basement and cover sequences are assigned to the lower Codru Nappe System. The Biharia Nappe System consists of three major basement nappes. From top to bottom these are: a) the Baia de Arieş Nappe represented by the medium-grade Baia de Arieş assemblage, the Biharia, and Belioara low-grade assemblages; b) the Biharia Nappe consisting of the Biharia, Poiana, Păiuşeni, Cladova lithotectonic assemblages, the Upper Paleozoic Highiş granitoids and the Permian(?) Băişoara conglomerates; c) the Arieşeni Nappe of metabasites and Permian rhyolite-bearing clastic rocks overlain by Triassic carbonate cover strata. The Codru Nappe System includes from top to bottom: a) the Vaşcău-Coleşti Nappe consisting of Triassic to Lower Jurassic strata; b) the Moma Nappe consisting of Permian to Triassic cover strata; c) the Dieva-Bătrinescu-Vetre Nappe represented by three tectonic slices of Permian and/or Triassic cover strata; d) the Finiş Nappe consisting of the medium-grade Codru assemblage and associated granitoids and a Permian to Neocomian sedimentary cover; e) the Valani Nappe, a cover nappe of Permian to Albian strata. The Codru Nappe System overthrusts the Bihor "Autochthonous Unit" consisting of the medium-grade Someş assemblage intruded by the Muntele Mare granite. The sedimentary cover consists of Permian to Turonian strata.

The Laramian Transylvanides are nappes resulting from the Late Cretaceous reactivation of the Middle Cretaceous nappes interpreted in the southern Apuseni Mountains. The thirteen nappes originally defined by Bleahu et al. (1981) were redistributed by Balintoni (1994) to Middle and Late Cretaceous (Fig. I-27). The outline of the interpreted Laramian overthrusts in the southern Apuseni Mountains is roughly parallel to the Carpathian bend and interpreted to have resulted during clockwise rotation of the Apuseni and South Carpathians crustal fragments around the Moesian promontory of stable Europe (Ratschbacher et al., 1993).

Fig. I-27. Tectonic sketch of the Apuseni Mountains with the traditional Alpine nappe interpretation (*after* Balintoni, 1994): 1 - Neogene strata; 2 - Senonian; 3 - Turonian-Senonian; 4 - Vreconian - Coniacian; 5 - Neogene igneous rocks; 6 - Banatite igneous rocks; 7 - Eocretaceous granite. **Laramian Transylvanides**: 8 - Căpâlnaş-Techereu Nappe; 9 - Curechiu-Stănija Nappe; 10 - Feneş Nappe; 11 - Criş Nappe; 12 - Groşi Unit; 13 - Vulcan Nappe; 14 - Frasin Nappe; 15 - Bucium Unit. **Middle-Cretaceous Transylvanides**: 16 - Bedeleu Nappe; 17 - Colţul Trascăului Nappe; 18 - Valea Muntelui Nappe; 19 - Izvoarele Nappe; 20 - Ardeu Unit; 21 - Căbeşti Unit; 22 - Bejan Unit. **Apusenides-Biharia Nappe System**: 23 - Baia de Arieş Nappe; M - Muncelu Scale; V.B. - Vultureasa-Belioara Series; 24 - Biharia Nappe; Li - Lipova Nappe; H-P - Highiş-Poiana Nappe; P-G - Piatra Grăitoare Scale; 25 - Arieşeni Nappe; **Apusenides-Codru Nappe System**: 26 - Vaşcău-Coleşti Nappe; 27 - Moma Nappe; 28 - Dieva-Bătrânescu-Vetre Nappe; 29 - Finiş-Ferice-Gârda-Următ Nappe(s); 30 - Vâlcani Nappe; 31 - **Bihor Unit**; 32 - South Carpathian basement; 33 - fault; 34 - reverse fault; 35 - Laramian overthrust; 36 - Pre-Gosau overthrust; 37 - Middle Cretaceous overthrust; 38 - Variscan overthrust; 39 - transgression; 40 - outline of igneous rocks; 41 - transform fault, plate boundary; 42 - strike-slip displacement; 43 - dip-slip displacement; 44 - tectonic contact in general; 45 - Bozeş Beds.

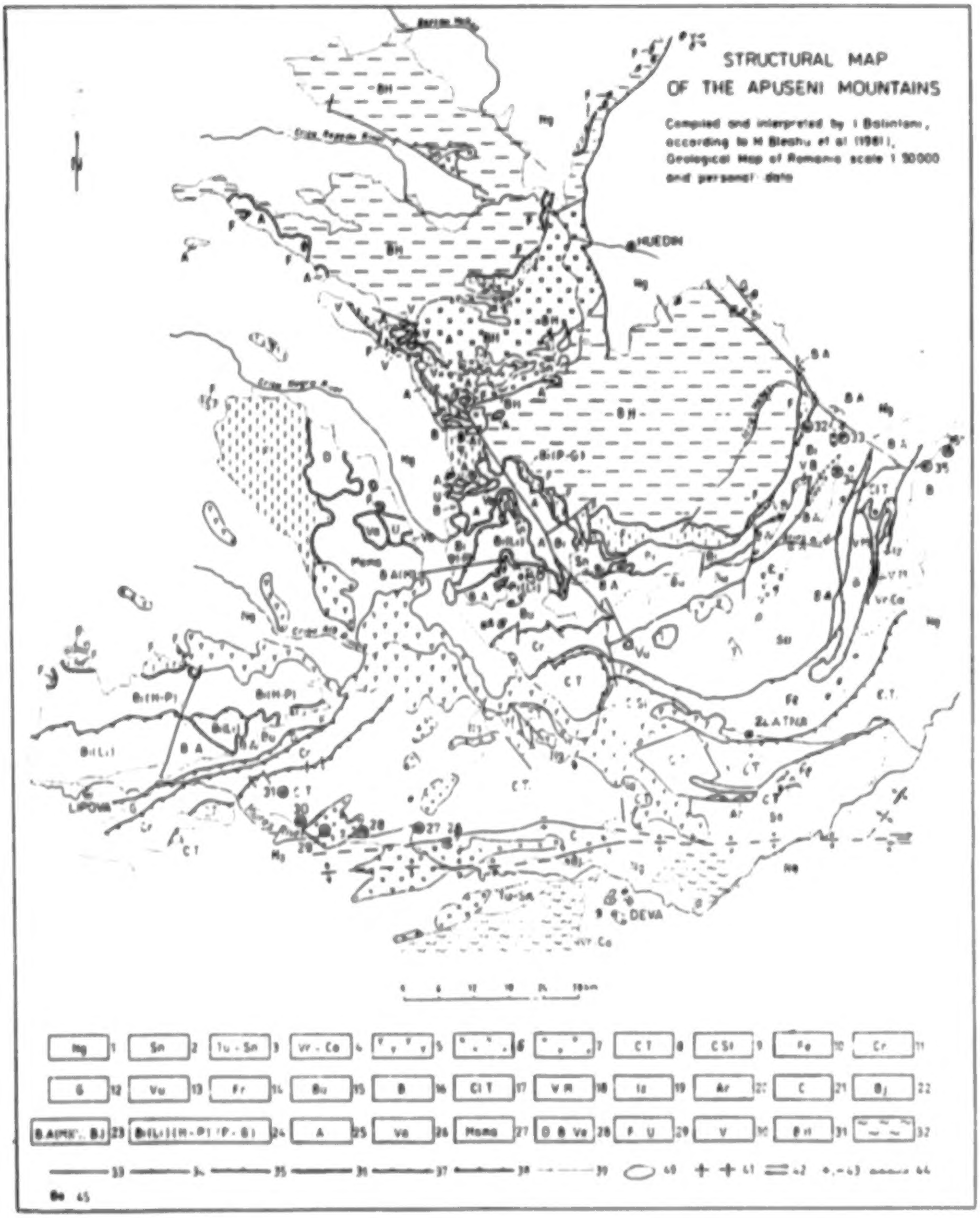
STRUCTURAL MAP
OF THE APUSENI MOUNTAINS
Compiled and interpreted by I Balintoni, according to M Bleahu et al (1981), Geological Map of Romania scale 1:50000 and personal data
N
HUEDIN
LIPOVA
ZLATNA
DEVA
Crisul Repede River
Crisul Negru River
Crisul Alb River
Mures River
BH
Bi(P-G)
Bi(H-P)
Bi(Li)
BA
Mg
CT
Sn
Tu-Sn
Vr-Co
Mg 1
Sn 2
Tu-Sn 3
Vr-Co 4
5
6
7
CT 8
CSt 9
Fe 10
Cr 11
G 12
Vu 13
Fr 14
Bu 15
B 16
CiT 17
VR 18
Iz 19
Ar 20
C 21
Bj 22
BA(MX, Bj) 23
Bi(Li)(H-P)(P-G) 24
A 25
Va 26
Mama 27
D B Va 28
F U 29
V 30
BH 31
32
33
34
35
36
37
38
39
40
41
42
43
44
Be 45

Fig. I-27.

I.10. Neogene to Quaternary volcanism in the Carpathians-Pannonian Region

The following summary is based on synthesis articles by Kovacs et al., 1992; Pécskay et al., (1995 a, 1995 b), Konečný et al., (1995); Kaličiak and Žec (1995), Lyashkevich (1995).

Similarly to the structures of the Carpathian arc, the Neogene volcanic rocks become younger eastward (Balla 1981; Poka 1988). They are of Early and Middle Miocene age in Slovakia, Middle to Late Miocene and Pliocene age in Ukraine, and of Late Miocene and Pliocene in Romania.

Recent K-Ar data indicate a more complex picture of volcanic events (Pécskay et al., 1995 a; 1995 b). The space and time distribution of the Neogene to Quaternary volcanism are interpreted to suggest three patterns: 1) Miocene acidic volcanism; 2) Miocene to Pleistocene mostly intermediate calc-alkaline arc-type magmatism related to contemporaneous subduction beneath the Carpathians arc; 3) alkaline (shoshonitic, alkali-basaltic, K-trachytic, and ultrapotassic) volcanism postdating convergence and related to back-arc extension.

Calc-alkaline subduction-related magmatism interpreted to have started at c. 20 Ma with acid calc-alkaline explosive high-volume eruptions in the Pannonian Basin and West Carpathians. From 17 to 0.2 Ma, calc-alkaline mainly intermediate stratovolcanic complexes were formed first in the West Carpathians and later in the East Carpathians. Rocks of this cycle (12.6 Ma), considered arc-type subduction-related, intrude the Pienniny belt generally interpreted to mark the main Tethys suture zone. In the Pannonian Basin, andesitic eruption centres are located on the intersection of major NE-SW tectonic lineaments with a set of perpendicular faults. In the Apuseni Mountains the intermediate calc-alkaline volcanic rocks occur mostly along a NW-SE alignment that cuts the supposed Tethys suture. The only region where a clear age progression was documented is in the East Carpathians but the progression is along the postulated subduction zone, and the volcanic arc consists of a lineament that intersects the local trend of the inferred subduction wedge.

The alkaline rocks interpreted to record back-arc extension following convergence have yielded two date groups: 17 to 7 Ma and 6 to 0.5 Ma. Back-arc extension would thus be contemporaneous with subduction and collision along the Carpathians arc.

Where both are present, the alkali volcanism is younger and follows calc-alkaline volcanism usually after a gap. However, in central Slovakia and the south Harghita and Perşani mountains, calc-alkaline, shoshonitic, and alkali basalt volcanism overlap in time and space. Their assignment to two distinct tectonic phases does not seem justified.

Inconsistencies

Magmatic rocks cannot be confidently matched with correlative sutures. The Neogene-Quaternary magmatic event does not show interpretable age progressions and chemical zoning, No age and/or geochemical distinction can be made between the Neogene volcanic rocks from the Carpathian volcanic arc and the Pannonian Basin. Their assignment to contrasting tectonic environments (arc vs. back-arc, e.g., Lexa et al., 1993) does not seem justified.

The East Carpathians Neogene to Pleistocene volcanoes (ECVA) define a 160 km long chain that cuts the strongly divergent inner flysch units. This is in conflict with the supposed curved subduction wedge which would imply a bent subducting slab and a curved isobath corresponding to the depth of magma generation.

Sr/Ca vs. Ba/Ca, and Sr-Nd systematics indicate that none of the ECVA rocks, even the most basic, are representative of parental or close to parental mantle source partial melts (Seghedi and Szakács, 1995; Masson et al., 1995). The evolution trends on fractionation plots start at a certain distance from the partial melting line and are parallel to the crustal fractionation line. Except for the southernmost segment, volcanism started with acid rocks which precludes their genesis through magmatic differentiation from basaltic magma. It can be explained either by partial melting of the lower crust that has facilitated the intrusion of mantle derived materials and accompanying magma mixing and assimilation processes, or by fractional crystallization within a crustal chamber of a mantle-derived andesitic magma.

High initial Sr isotopic ratios (0.710-0.711) and low ^{143}Nd/^{144}Nd (0.51245) in the oldest erupted rhyolite and dacite indicate a crustal source. K-enrichment, resulting in small-volume shoshonitic bodies, is evident at the southern end of the range.

Multi-system isotope studies concluded that there is no unequivocal evidence of enriched isotopic characteristics of parental magmas by addition of sediments to the mantle source via subduction (Mason et al., 1996). Coupled variations between radiogenic and oxygen isotopes indicate that crustal assimilation and fractional crystallization were the most likely processes to produce the enriched radiogenic isotopic signatures in most magmas (^{143}Nd/^{144}Nd <0.5127, δ^{18}O> 7‰). Differences in the isotopic characteristics of parental magmas in different parts of the Carpathian-Pannonian region may have resulted from mixing, assimilation, storage, and homogenization processes in a deep crustal zone. Trace elements and Sr, Nd, and Pb isotopes in most of the East Carpathians chain are more consistent with a depleted MORB-source mantle (the European Asthenospheric Reservoir) than with enriched mantle.

The Neogene-Pleistocene igneous activity in the Carpathian-Pannonian region appears to have initiated through crustal melting and the development of magma-chambers at mid-crustal levels; in the following stages, a mantle-derived basalt sampled a markedly different lower crust and mixed with crustal melts. The arc-like geochemical patterns could result from mantle geochemical processes unrelated to subduction. Alternative tectonic models for Neogene to Quaternary magmatism can incorporate plausible heating or decompression mechanisms for regional magma generation.

The Neogene-Pleistocene igneous activity in the Carpathian-Pannonian region appears to have initiated through crustal melting and the development of magma-chambers at mid-crustal levels; in the following stages, a mantle-derived basalt sampled a markedly different lower crust and mixed with crustal melts. The arc-like geochemical patterns could result from mantle geochemical processes unrelated to subduction. Alternative tectonic models for Neogene to Quaternary magmatism can incorporate plausible heating or decompression mechanisms for regional magma generation.

REFERENCES

Andrusov, D., 1968, Grundriss der Tektonik der Nordlichen Karpaten, Slovak Academy of Sciences, 189 p., Bratislava.

Árkai, P., 1983, Very low- and low-grade Alpine regional metamorphism of the Paleozoic and Mesozoic formations of the Bükkium, NE-Hungary, Acta Geologica Hungarica, 26, p. 83-101.

Árkai, P., 1987, New data on the petrogenesis of metamorphic rocks along the Balaton Lineament, Transdanubia, W-Hungary, Acta Geologica Hungarica, 30, 3-4, p. 319-338.

Árkai, P., Nagy, G., Dobosi, G., 1985, Polymetamorphic evolution of the south-Hungarian crystalline basement, Pannonian Basin: geothermometric and geobarometric data, Acta Geologica Hungarica, 28, 3-4, p.165-190.

Árkai, P., Horváth, Z.A., and Tóth, M. N., 1987, Regional metamorphism of the East Alpine type Paleozoic basement, Little Plain, W-Hungary: Mineral assemblages, illite crystallinity, -b_0 and coal rank data, Acta Geologica Hungarica, 30. 1-2, p. 153-175.

Árváné Soós, E., and Ravasz, Cs., 1978, K-Ar dating of the andesite of Komlo, SE Transdanubia), Annu. Rep. Hung. Geol. Inst., p. 201-208.

Aubouin, J., (Ed.) 1970, La Géologie des Dinarides, Bull. Soc. Geol de France, 7, XII, 6, p.941-

Bagdasaryan, G. P., Gukasyan, R. Kh., Cambel, B., and Veselsky, J., 1986, Rb-Sr isochron age of the Vepor pluton granitoids, Geol. Zbor, 37, 3, p. 365-374.

Balintoni, I., Gheuca, I., and Vodă, Al., 1983, Alpine and Hercynian overthrust nappes from central and southern areas of the East Carpathian Crystalline-Mesozoic Zone: Anuarul Institutului de Geologie şi Geofizică, LX, p. 15-22.

Balintoni, I., Berza, T., Hann, H.P., Iancu, V., Kräutner, H.G., and Udubaşa, G., 1989, Precambrian Metamorphics in the South Carpathians, Multilateral Cooperation of the Academies of Sciences of the Socialist Countries, Earth Crust Structure Evolution and Metallogeny, Guide to Excursions, 89 p. Bucureşti.

Balintoni, I., 1994, Structure of the Apuseni Mountains, *in* Berza T. (Ed.) "Geological evolution of the Alpine-Carpathian-Pannonian system", ALCAPA II Conference, Covasna, Field Guidebook, Romanian Journal of Tectonics and Regional Geology, 75, suppl. 2, p. 51-57.

Balla, Z., 1981, Neogene volcanites in the geodynamic reconstruction of the Carpathian region, Geophysical Transactions, 26, p. 5-33.

Balla, Z., 1982, Development of the Pannonian Basin Basement through the Cretaceous-Cenozoic Collision: A New Synthesis, Tectonophysics, 88, 2, p. 61-102.

Balla, Z., 1985, The Carpathian Loop and the Pannonian Basin: a Kinematic Analysis, Geophys.

Transactions, 30, 4, p. 313-353.

Balla, Z., 1986, Paleotectonic Reconstruction of the Central Alpine-Mediterranean Belt for the Neogene, Tectonophysics, 127, p. 213-243.

Balla, Z., 1987, Tectonics of the Bükkian (North Hungary) Mesozoic and relations to the West Carpathians and Dinarides, Acta Geologica Hungarica, 30, p. 257-287.

Balla, Z., 1988, Clockwise paleomagnetic rotations in the Alps in the light of the structural pattern of the Transdanubian Range (Hungary), Tectonophysics, 145, p. 277-292.

Balogh, K., Árva-Soós E., and Buda G., 1983, Chronology of granitoid and metamorphic rocks of Transdanubia (Hungary), Anuarul Institutului de Geologie şi Geofizică, 61, p. 359-364.

Baldi-Beke, M., and Nagymarosy, A., 1992, On the age of the Szolnok flysch and its possible correlation with the Carpathian flysch units, Knihovnicka ZPN, 2, p. 37-48.

Băncilă, I., 1958, Geologia Carpaţilor Orientali, 368 p., Editura Stiintifică, Bucureşti.

Bechstädt, T., 1978, Faziesanalyse permischer und triasicher Sedimente des Drauzuges als Hinweis auf eine grossraumige Lateralverschiebung Innerhalb des Ostalpins. Jb. Geol. B.-A., 121, p. 1-122.

Bercia, I., Kräutner, H.G., and Mureşan, M., 1976, Pre-Mesozoic Metamorphites of the East Carpathians: Anuarul Institutului de Geologie şi Geofizică, L, p. 37-70.

Bernoulli, D., and Winkler, W., 1990, Heavy mineral assemblages from the Upper Cretaceous South- and Austroalpine flysch sequences (Northern Italy and Southern Switzerland): source terranes and paleotectonic implications, Eclogae Geol. Helv., 83, p. 287-310.

Bernoulli, D., Heitzmann, P., and Zingg, A., 1990, Central and southern Alps in southern Switzerland: tectonic evolution and first results of reflection seismics, Mém. Soc. Géol., Suisse, 1, p. 289-302.

Bibikova, E. V., Cambel, B., Korikowsky, S. P., Broska, I., Gracheva, T. V., and Arakeliants, M. M., 1988, U-Pb and K-Ar isotopic dating of Sinec (Rimavica) granites (Kohut zone of Veporides), Geol. Zb., 39, 2, p. 147-157.

Biely, A., 1989, The geological structure of the West Carpathians, Mém. Soc. Géol. France, 154, II, p. 51-57.

Birkenmayer, K., 1986, Stages of structural evolution of the Pieniny Klippen Belt, Carpathians, Stud. Geol. Pol., 90 p. 7-37.

Birkenmayer, K., 1988, Exotic Andrusov Ridge: its role in the plate-tectonic evolution of the West Carpathians foldbelt, Stud. Geol. Pol., 90, p. 7-37.

Bleahu, M, D., Boccaletti, M., Manetti, P., and Peltz, S., 1973, Neogene Carpathian Arc: A Continental Arc Displaying the Features of an 'Island Arc', Journal of Geophysical Research, 78, 23, p. 5025-5031.

Bleahu, M.D., 1976, Structural position of the Apuseni Mountains in the Alpine System, Revue Roumaine de Géologie, Géophysique, Géographie, ser. Géologie., 20, p.7-19.

Bleahu, M.D., Lupu, M., Patrulius, D., Bordea, S., Ştefan, A., and Panin, S., 1981, The structure of the Apuseni Mountains, Carpatho-Balkan Geological Association, XII Congress, Bucharest, Romania, Guide to Excursion-B3, 103 p., Bucureşti.

Boccaletti, M., Manetti, P., Peccerillo, A., and Peltz, S., 1973, Young volcanism in the Călimani-Harghita Mountains (East Carpathians): evidence of paleoseismic zone, Tectonophysics, 19, p. 299-313.

Channel, J. E. T., and Horváth, F., 1976, The African / Adria promontory as a paleogeographycal premise for Alpine orogeny and plate movements in the Carpatho-Balkan region, Tectonophysics, 35, p. 71-101.

Chekunov, A. V., and Sollogub, V. B., 1989, The tectonosphere beneath South-Eastern Europe, Gerlands Beitr. Geophys., 98, p. 212-222.

Cioflica, G., and Nicolae, I., 1981, The Origin, Evolution and Tectonic Setting of the Alpine Ophiolites from the Southern Apuseni Mountains, *Revue Roumaine de Géologie, Géophysique, Géographie, ser. Géologie*, 25, p. 19-29.

Codarcea, A., 1940, Vues nouvelles sur la tectonique du Banat méridional et du Plateau de Mehedinţi, Anuarul Institutului de Geologie şi Geofizică, XX, p. 1-74.

Constantinescu, L., Cornea, I., and Lăzărescu, V., 1973, An appraoch to the seismotectonics of the Romanian Eastern Carpathians, Révue Roumaine de Géologie Géophysique Géographie, Serie Géophysique, 12, p. 133-143.

Csontos, L., Nagymarosy, A., Horváth, F., and Kovác, M., 1992, Tertiary Evolution of the Intra-Carpathian Area: A Model, Tectonophysics, 208, p. 221-241.

Dal Piaz, G. V., Martin, S., Villa, I. M., Gosso, G., and Marschalko, R., 1995, Late Jurassic blueschist facies pebbles from the Western Carpathian orogenic wedge and paleostructural implications for Western Tethys evolution, Tectonics, 14, 4, p. 874-885.

Dallmeyer, R.D., Neubauer, F., Handler, R., Fritz, H., Müller, W., Pană, D., and Putiš, M., 1996, Tectonothermal evolution of the internal Alps and Carpathians: Evidence from ^{40}Ar/^{39}Ar mineral and whole-rock data. Eclogae geol. Helv. 89/1 p.203-227.

Dicea, O., Duţescu, P., Antonescu, F., Mitrea, G., Botez, R., Donos, I., Lungu, V., Moroşanu, I., 1980, Contribuţii la cunoaşterea tectonicii zonei Transcarpatice din Maramureş, Dări de Seamă ale Institutului de Geologie şi Geofizică, 65, 4, p. 35-53.

Dimitrescu, R., 1981, Hypothèses sur la structure du soubassement du secteur sud-oriental de la dépression Pannonique, *Revue Roumaine de Géologie, Géophysique, Géographie, ser. Géologie*, 25, p. 31-35.

Dimitrijevic, M. D., 1982, Dinarides: An outline of the tectonics, Earth Evol. Sci., 2, p. 4-23.

Dimitrijevic, M. D., (Ed.), 1991, Geodynamic evolution of the Pannonian basin, Serbian Academy of Sciences and Arts, LXII, 4, 305 p.

Dimitrijevic, M. N., and Dimitrijevic, M. D., 1973, Olistostrome mélange in the Yugoslavian Dinarides and late Mesozoic plate tectonics, J. Geol., 81, p. 328-340.

Doglioni, C., 1987, Tectonics of the Dolomites, J. Struct. Geol., 9, p. 181-193.

Doglioni, C., and Bosellini, A., 1987, Eoalpine and mesoalpine tectonics in the Southern Alps, Geologische Rundschau, 76, p. 735-754.

Dumitrescu, I., Săndulescu, M., Lăzărescu, V., Mirăuţă, O., Pauliuc, S., and Georgescu, C., 1962, Mémoire pour la carte tectonique de la Roumanie, Annu. Com Geol., XXXII, p. 5-96

Dunkl, I., 1992, Latest milestones of the uplift history of the eastern margin of the Eastern Alps: compilation of fission track results, Terra Abstracts, Suppl., 2, 4, p.18.

Flügel, H. W., and Neubauer, F., 1984, Steiermark (Bundesländserie), Geol. B.-A., Wien, 127 p

Flügel, H. W., and Faupl, P., 1987, Geodynamics of the Eastern Alps, Deuticke, Wien,

Frisch, W., Vavra, G., and Winkler, M., 1993, Evolution of the Panninic Basement of the Eastern Alps, *in* von Raumer, J. and Neubauer, F., (Eds.): Pre-Mesozoic geology of the Alps, p. 349-360, Springer Verlag, Heidelberg.

Fritz, H., Neubauer, F., Janak, M., and Putis, M., 1992, Variscan mid-crustal thrusting in the Carpathians. Part II: Kinematics and Fabric evolution of the Western Tatra basement, Terra Abstracts, Suppl. 2 to Terra Nova, 4, p. 24.

Froitzheim, N., 1992, Formation of recumbent folds during synorogenic crustal extension (Austroalpine nappes, Switzerland), Geology, 20, p. 923-926.

Fuchs, K., Bonjer, K.-P., Bock, G., Cornea, I., Radu, C., Enescu, D., Jianu, D., Nourescu, A., Merkler, G., Moldoveanu, T., and Tudorache, G., 1979, The Romanian earthquake of March 4, 1977; II. Aftershocks and migrations of seismic activity, Tectonophysics, 53, p. 225-247.

Fülöp, J., Brezsnyánszky, K and Haas, J., 1987, The new map of basin basement of Hungary, Acta Geol. Hung., 30, p. 3-20.

Galácz, A., Horváth, F., and Vörös, A., 1985, Sedimentary and structural evolution of the Bakony Mountains (Transdanubian Central Range, Hungary): Paleogeographical implications, Acta Geologica Hungarica, 28, p. 85-100.

Ghoneim, M. F., and Szederkenyi, T., 1979 Petrological review of the Ófalu serpentinite, Mecsek Mts., Hungary, Acta Min. Petr, Szeged, 14, 1, p. 5-18.

Grecula, P., and Roth, Z., 1978, Kinematic model of the West Carpathians, Sb. Geol. Věd, Geologie, 32, p. 49-73.

Grünenfelder M., Popescu, Gh., Soroiu, M., Arsenescu, V., Berza, T., 1983, K-Ar and U-Pb Dating of the metamorphic formations and the associated igneous bodies of the Central South Carpathians, Anuarul Institutului de Geologie şi Geofizică, XLI, p. 37-46.

Haas, J. , Jocha-Edelenyi, E., and Partenyi, Z., 1986, Genetic circumstances of the Senonian coal measures of the Bakony, Annu. Rep., Hung. Geol. Survey-1984, p. 343-354.

Haas, J., Kovács, S., Krysteyn, L., and Lein, R., 1995, Significance of Late Permian-Triassic facies zones in terrane reconstructions in the Alpine-North Pannonian domain: Tectonophysics, 242, p. 19-40.

Hamilton, W., B., 1990, On Terrane analysis, *in* Dewey, J. F., Gass, I., G., Şengor, A, M., C., (Eds.): Allochtonous Terranes, p. 55-66.

Handy, M. R., Herwegh, M., and Regli, R., 1993, Tektonische Entwicklung der westlichen Zone von Samedan (Oberhalbstein, Graubünden, Schweiz). Eclogae geol. Helv. 86, p. 785-817.

Herak, M., 1986, A new concept of the geotectonics of the Dinarides, Acta Geol. Jug. Acad., Znan. I Umjetn. Zagreb, 20, p. 5-27.

Horváth, F., 1993, Towards a mechanical model for the formation of the Pannonian basin, Tectonophysics, 226, p. 333-357.

Horváth, F., and Rumpler, J., 1984, The Pannonian basement: extension and subsidence of an Alpine orogene, Acta Geologica Hungarica, 27, p. 229-235.

Hovorka, D., and Meres, S., 1993, Leptino-amphibolite complex of the Western Carpathians: occurences and lithology, Mineralia Slov., 25, p. 1-9.

Ianovici, V., Borcoş, M., Bleahu, M., Patrulius, D., Lupu, M., Dimitrescu, R., and Savu, H., 1976, Geologia Munţilor Apuseni, Editura Academiei Române, 631 p., Bucureşti.

Janak, M., 1992, Variscan mid-crustal thrusting in the Carpathians, I: Metamorphic conditions and P-T paths of the Tatry Mountains, Terra Abstracts, Suppl. 2 to Terra Nova, 4, p. 35.

Janoschek, W. R., and Matura, A., 1980, Otline of the geology of Austria. Abh. Geol. B.-A., 34, p. 7-98.

Jantsky, B., Balázs, E., and Cserepes-Meszéna, B., 1988, Precambrian in the Basement of the Pannonian Basin, *in* Zoubek V., Cogné, J., Kozhoukharov, D., Kräutner, H. (Eds.): Precambrian in Younger Fold Belts, p. 687-711.

Kaličiac, M. I., and Žec, B., 1995, Review of Neogene volcanism of Eastern Slovakia, Acta Vulcanologica, 7, 2, p. 87-95.

Kamenci, R., and Canovič, M., 1975, Preneogena podloga Vojvodanskog dela Pannonskog Basena, Radovi Znanstvenog Saveta Za Naftu Pri Jug. Akad. Znan. I Umetn. 5, Zagreb.

Kamenický, L., and Kamenický, J., 1988, Precambrian of the West Carpathians, *in* Zoubek V., Cogné, J., Kozhoukharov, D., Kräutner, H. (Eds.): Precambrian in Younger Fold Belts, p. 675-685.

Kázmér, M., and Kovács, S., 1985, Permian-Paleogene paleogeography along the eastern part of the Insubric-Periadriatic lineament system: evidence for the continental escape of the Bakony-Drauzug unit, Acta Geologica Hungarica, 28, p. 71-84.

Kázmér, M., and Kovács, S., 1989, Triassic and Jurassic oceanic and paraoceanic belts in the Carpatho-Pannonian region and its surroundings, *in* Sengör, A.M.C. (Ed.): Tectonic evolution of the Tethyan region. NATO ASI Series C, 259, p. 77-93.

Kober, L., 1931, Das alpine Europa und sein Rahmen. Ein geologisches Gestaltungsbild, Borntraeger, 500 p., Berlin.

Kovacs, M., Edelstein, O., Istvan, D., Grabari, G., Stoian, M., and Popescu, Gh., 1992, Distribution of REE, K, Rb, Sr, and of the ^{87}Sr/^{86}Sr ratios in the Neogene andesites of the Igniş Văratec (Gutâi) Mts., Romania, Rom. J. Petrol., 75, p. 45-156.

Kovács, S., 1982, Problems of the "Pannonian Median Massif" and the plate tectonic concept, Contribution based on the distribution of Late Paleozoic-Early Mesozoic isopic zones, Geol. Rundschau, 71, p. 617-640.

Kovács, S., 1992, Tethys "western ends" during the Late Paleozoic and Triassic and their possible genetic relationships, Acta Geologica Hungarica, 35, p. 329-369.

Kräutner, H.G., 1980, Lithostratigraphic Correlation of Precambrian in the Romanian Carpathians: Anuarul Institutului de Geologie şi Geofizică, v. LVII, p. 229-296.

Kräutner, H.G., Năstaseanu, S., Berza, T., Stănoiu, I., and Iancu, V., 1981, Metamorphosed Paleozoic in the South Carpathians and Its Relations with the Pre-Paleozoic Basement, Carpatho-Balkan Geological Association XII Congress, Bucharest, Guide to Excursion A1, 116 p., Bucureşti.

Kräutner, H.G., 1988, Interregional Correlations, *in* Zoubek V., Cogné, J., Kozhoukharov, D., (Eds.): Precambrian in Younger Fold Belts, p. 853-862.

Kröll, A., Flügel, H. W., Seiberl, W., Weber, F., Walach, G., and Zych, D., 1988, Erläuterungen zu den Karten uber den steirischen Beckens und der südburgenlandischen Schwelle, Gelogische Bundesanstalt, 47 p., Vienna.

Laubscher, H.P., 1986, The late Alpine (Periadriatic) intrusions and the Insubric Line, Mem. Soc. Geol. Ital., 26, p. 21-30.

Lexa, J., Konečný, V., Kaličiak, M. and Hojstičová, V., 1993, Distribution of Neogene volcanism in Carpatho-Pannonian region in space and time, *in* Rakús, M., and Vozar, J., (Eds.): Geodynamický vývoj a hlbinná stavba Záppadných Karpát, p. 57-69.

Liégeois, J.P., Berza, T., Tatu, M., and Duchesne, 1996, The Neoproterozoic Pan-African basement from the Alpine lower Danubian nappe system (South Carpathians, Romania) Precambrian Research, 80, 3-4, p. 281-301.

Linzer, H. G., 1996, Kinematics of retreating subduction along the Carpathian arc, Romania, Geology, 24, p. 167-171.

Lupu, M., Avram, E., Antonescu, E., Dumitrică, P., Lupu, D., and Nicolae, I., 1993, The Neo-Jurassic and the Cretaceous of the Drocea Mts: the stratigraphy and the structure of an ensialic marginal basin, Romanian Journal of Tectonics and Regional Geology, 75, p. 53-66.

Lupu, M., Antonescu, E., Avram, E., Dumitrică, P., and Nicolae, I., 1995, Comment on the age of some ophiolites from the North Drocea Mountains, Romanian Journal of Tectonics and Regional Geology, 76, p. 21-25.

Lyashkevich, Z. M., 1995, Neogene volcanic rocks of the Ukrainian Carpathians: a brief review, Acta Vulcanologica, 7, 2, p. 79-85.

Mahel, M. (Ed.) , 1974, Tectonics of the Carpathian Balkan Region, GUDS, Bratislava, 455 p.

Maluski, H., Rajlich, P., and Matte, P., 1993, ^{40}Ar/^{39}Ar dating of the Inner Carpathians Variscan basement and Alpine mylonitic overprinting. Tectonophysics, 223, p. 313-337.

Massari, F., 1990, The foredeeps of the northern Adriatic margin: evidence of diachroneity in deformation of the Southern Alps, Riv. It. Geol. Mineral. Univ. Padova, 28, p. 1-63.

Masson, P. R. D., Downes, H., Seghedi, I., Szakács, A., and Thirlwall, M. F., 1995, Low-pressure evolution of magmas from the Calimani, Gurghiu and Harghita Mountains, East Carpathians, Acta Vulcanologica, 7, 2, p. 43-52.

Misík, M. and Marschalko, R., 1988, Exotic conglomerates in flysch sequences: Examples from the West Carpathians, Mém. Soc. Géol. France, 154, I, p. 95-113.

Moeller, St., 1989, Deep-reaching geodynamic processes in the Alps, in Coward, M.P., Dietrich, D., and Park, R.G., (Eds.): Alpine Tectonics, p. 303-328.

Murgeanu, G., 1933, Sur une cordillère ante-sénonienne dans le géosynclinal du flysch carpatique, Dări de Seamă ale Institutului Geologic Român, XXXI.

Nagymarosy, A., 1990, Paleogeographicaland paleotectonical outlines of some intra-Carpathian Paleogene basins, Geol. Zbor., Geol. Carp., 41, p. 259-274.

Năstaseanu, S., Bercia, I., Iancu, V., Vlad, Ş., and Hârtopanu, I., 1981, The Structure of the South Carpathians, Carpatho-Balkan Geological Association XII Congress, Bucharest, Guide to Excursion B2, 100 p., Bucureşti.

Neubauer, F., 1992, The Gurktal nappe complex, *in* Neubauer, F., (ed.): The Eastern Central Alps of Austria, ALCAPA-meeting field guidebook, p. 71-82.

Neubauer, F., Müller, W., Peindl, P., Moyschewitz, Wallbrecher, E., and Thöni, M., 1992,

Evolution of Lower Austroalpine units along the eastern margins of the Alps: a review, in Neubauer, F., (Ed.): The Eastern Central Alps of Austria, ALCAPA-meeting field guidebook, p. 97-114.

Neubauer, F., and Frisch, W., 1993, The Austro-Alpine Metamorphic Basement East of the Tauern Window, *in* von Raumer, J. and Neubauer, F., (Eds.): Pre-Mesozoic geology of the Alps, p. 515-536, Springer Verlag, Heidelberg.

Nievergelt, P., Liniger, M., Froitzheim, N., and Ferreiro-Maehlmann R., 1991, The Turba mylonite zone: An Oligocene extensional fault at the Pennine-Austroalpine boundary in eastern Switzerland; Terra abstracts, 3, p. 248.

Oberhauser, R., (Ed.) 1980, Der geologische Aufbau Osterreichs, Springer, 701 p., Vienna,

Oberhauser, R., 1991, Westvergente versus nordvergente Tektonik - Ein Beitrag zur Geschichte und zum Stand geologischer Forschung, gesehen von der Ost-Westalpengrenze, Jb. Geol. Bundesanst, 134, p. 773-782, Wien.

Oncescu, M. C., Burlacu, V., Anghel, M., and Smalbergher, V., 1984, Three-dimentional P-wave velocity image under the Carpathian arc, Tectonophysics, 106, p. 305-319.

Pamić, J., 1986, Magmatic and metamorphic complexes of the Adjoining area of the northernmost Dinarides and Pannonian mass, Acta Geologica Hungarica, 29, 3-4, p. 203-220.

Pamić, J., 1993, Eoalpine to Neogene magmatic and metamorphic processes in the northwestern Vardar Zone, the easternmost Periadriatic Zone and the southwestern Pannonian Basin, Tectonophysics, 226, p. 503-518.

Pană, D., and Erdmer, P., 1996, Comment on: Linzer, H. G., 1996, Kinematic of retreating subduction along the Carpathian arc, Romania, Geology, 24, p. 862-863.

Peccerillo, A., and Taylor, S. R., 1976, Rare earth elements in East Carpathians volcanic rocks, Earth Planet, Sci. Letters, 32, p. 121-126.

Pécskay, Z., Edelstein, O., Seghedi, I., Szakács, A., Kovacs, M., Crihan, M., and Bernad, A., 1995, K-Ar datings of Neogene-Quaternary calc-alkaline volcanic rocks in Romania, Acta Vulcanologica, 7, 2, p. 53-61.

Pécskay, Z., and 14 Co-authors, 1995, Space and time distribution of Neogene-Quaternary volcanism in the Carpatho-Pannonian Region, Acta Vulcanologica, 7, 2, p. 15-28.

Peltz, S., Vasiliu, C., Udrescu, C., and Vasilescu, A., 1974, Geochemistry of volcanic rocks from the Călimani, Gurghiu and Harghita Mountains (major and trace elements), Ann. Inst. Geol., 42, p. 339-393.

Plasienka, D., 1990, Regional shear and transpression zones in the Tatric unit of the Little Carpathians, Mineralia Slovaca, 22, p. 55-62.

Pospíšil, L., Bezák, V., Nemčok, M., Feranec, J., Vass, D., and Obernauer, D., 1989, The Muran tectonic system as example of horizontal displacement in the West Carpathians, Mineralia Slovaca, 21, p. 305-322.

Póka, T., 1988, Neogene and Quaternary volcanism of the Carpathian-Pannonian region: changes in chemical composition and its relationship to basin formation, *in* Royden L., and Horváth (Eds.): The Pannonian Basin - A Study in Basin Evolution, AAPG Memoir, 45, p. 257-276.

Putis, M., 1994, South Tatric-Veporic Basement Geology: Variscan Nappe Structures; Alpine Thick-Skinned and Extensional Tectonics in the Western Carpathians (Eastern Low Tatra Mountains, Northwestern Slovak Ore Mountains), Mitt. Osterr. Geol. Ges., 86, p. 83-99.

Rakus, M., Misik, M., Michalik, J., Mock, R., Durkovic, T., Koráb, T., Marschalko, R., Mello, J., Polák, M., and Jablonsky, J., 1990, Paleogeographic development of the West Carpathians, Mem. Soc. Géol. France, 154, III, p. 39-62.

Ratschbacher, L., 1986, Kinematics of Austro-Alpine cover nappes: changing translation path due to transpression, Tectonophysics, 125, p. 335-356.

Ratschbacher, L., Behrmann, J. H., and Pahr, A., 1990, Penninic windows at the eastern end of the Alps and their relation to the intra-Carpathian basins. Tectonophysics, 172, p. 91-105.

Ratschbacher, L., and Frisch, W., 1993, Palinspastic Reconstruction of the Pre-Triassic Bassement Units in the Alps: The Eastern Alps, *in* von Raumer, J. and Neubauer, F., (Eds.): Pre-Mesozoic geology of the Alps, p. 41-51, Springer Verlag, Heidelberg.

Roman, C., 1970, Seismicity in Romania-Evidence for the Sinking Lithosphere, Nature, 228, p. 1176-1178.

Rothpletz, A., 1905, Geologische Alpenforschungen II, Ausdehnung und Herkunft der Rhaetischen Schubmasse. Lindauer, München.

Royden, L., 1988, Late Cenozoic Tectonics of the Pannonian Basin System, *in* Royden L., and Horváth (Eds.): The Pannonian Basin - A Study in Basin Evolution, AAPG Memoir, 45, p. 27-48.

Royden, L., and Báldi, T., 1988, Early Cenozoic Tectonics and Paleogeography of the Pannonian and Surrounding Regions, *in* Royden L., and Horváth (Eds.): The Pannonian Basin - A Study in Basin Evolution, AAPG Memoir, 45, p. 1-16.

Rădulescu, D., and Săndulescu, M., 1973, The Plate-Tectonics Concept and the Geological Structure of the Carpathians: Tectonophysics, v. 16, p. 155-161.

Rădulescu, D., Peltz, S., and Stanciu, C., 1973, Neogene volcanism in the East Carpathians

(Călimani-Gurghiu-Harghita Mts.), Guide to excursion 2AB, Symposium Volcanism and Metallogenesis, Bucharest.

Rădulescu, D., Săndulescu, M., and Borcoş, M., 1993, Alpine magmatogenetic map of Romania: an approach to the systematization of the igneous activity, Revue Roumain de Géologie, Géophysique, Géographie, ser. Géologie, 37, p. 3-8.

Sackáci, A., and Seghedi, I., 1995, The Călimani-Gurghiu-Harghita volcanic chain, East Carpathians, Romania: volcanologic features, Acta Vulcanologica, 7, 2, p. 145-153.

Savu, H, 1983, Geotectonic and magmatic evolution of the Mureş Zone (Apuseni Mountains)-Romania, Anuarul Institutului de Geologie şi Geofizică, LVI, p. 253-262.

Săbău, G., 1994, Lithostratigraphic and metamorphic correlations: a tentative way of exploring the early history of the Getic crystalline, Romanian Journal of Tectonics and Regional Geology, 76, p. 119-128.

Săndulescu, M., 1975, Essai de synthèse structurale des Carpathes, Bull. Soc. Géol. France, 7, XVII, 3, p. 299-358.

Săndulescu, M., 1984, Geotectonica României, Editura Tehnică, 323 p.

Săndulescu, M., 1988, Cenozoic Tectonic History of the Carpathians, *in* Royden L., and Horváth (Eds.): The Pannonian Basin - A Study in Basin Evolution, AAPG Memoir, 45, p. 17-25.

Săndulescu M., 1994, Overview on Romanian geology, *in* Berza T. (Ed.): "Geological evolution of the Alpine-Carpathian-Pannonian system", ALCAPA II Conference, Covasna, Field Guidebook, Romanian Journal of Tectonics and Regional Geology, 75, suppl. 2, p. 3-15

Săndulescu, M., Neagu, T., and Antonescu, E., 1982, Contributions à la connaissance des klippes de type pienin de Poiana Botizii, Maramures, Dări de Seamă ale Institutului de Geologie şi Geofizică, 67, 4, p. 79-96.

Seghedi, I., Szakács, A., and Masson, P. R. D., 1995, Petrogenesis and magmatic evolution in the East Carpathian Neogene volcanic arc (Romania), Acta Vulcanologica, 7, 2, p. 135-143.

Schmid, S. M., and Haas, R., 1989, Transition from near-surface thrusting to intrabasement decollement, Schlinig thrust, Eastern Alps, Tectonics, 8, 4, p. 697-718.

Schmidt, T., Blau, J., and Kázmér, M., 1991, Large-scale strike-slip displacement of the Drauzug and the Transdanudian Mountains in early Alpine history: evidence from Permo-Mesozoic facies belts, Tectonophysics, 200, p. 213-232.

Schönborn, G., 1992, Alpine Tectonics and kinematic models of the Central Southern Alps, Mem. Sci. Geol. Padova, 44, p. 229-393.

Schönlaub, H.P., 1979, Das Paläozoikum in Österreich. Abh. Geol. Bundesanstalt, 33, 1-124.

Sollogub, V. B., Prosen, D., and Co-Workers, 1973, Crustal Structure of Central and Southeastern Europe by Data of Explosion Seismology, Tectonophysics, 20, p. 1-33.

Spakman, W., 1990, Tomographic images of the upper mantle below central Europe and the Mediterranean, Terra Nova, 2, p. 542-553.

Szaderchy-Kardoss, E., 1975, The belts of subduction in the Carpathian-Pannonian-Dinaric area, *in* Machel, M., (Ed.): Tectonic problems of the Alpine system, Bratislava, p. 69-85.

Sztanó, O., 1990, Submarine fan-channel conglomerate of Lower Cretaceous, Gerecse Mts., Hungary, N. Jb. Geol. Paläont. Mh., p. 431-446.

Szederkenyi, T., 1977, Geological evolution of South Transdanubia (Hungary) in Paleozoic time, Acta Miner. Petrol., Szeged, 13, 1, p. 3-14.

Ştefănescu, M., 1983, General Remarks on the Eastern Carpathians Flysch and its Depositional Environment, Révue Roumaine de Géologie Géophysique Géographie, Serie Géologie, 27, p. 59-64.

Tari, G., 1994, Alpine Tectonics of the Pannonian Basin, Ph.D. Thesis, 501 p., Rice University.

Tari, G., 1996, Extreme crustal extension in the Rába River extensional corridor (Austria / Hungaria), Mitt. Ges. Geol. Bergbaustud. Österr. 41, p. 1-17.

Termier, P. 1903, Les nappes des Alpes orientales et la synthèse des Alpes. Bull. Soc. Géol. France, 4, 3, p.711-765.

Tollmann, A., 1963, Ostalpensynthese, Deuticke, Vienna, 256 p.

Tollmann, A., 1977, Geologie von Österreich, Band I. Die Zentralalpen. Deuticke, 766 p., Wien.

Tollmann, A., 1986, Geologie von Österreich, Band III. Gesamtübersicht. Deuticke, 718 p, Wien

Tollmann, A., 1987, The Alpidic evolution of the Eastern Alps, *in* Flugel, W. H., and Faupl, P. (Eds.): Geodynamics of the Eastern Alps, p. 361-378.

Tollmann, A., 1989, The Eastern Alpine sector, northern margin of the Tethys, Mem. Géol. Soc. France, 154, p. 23-49.

Tomek, Č., 1993, Deep crustal structure beneath the central and inner West Carpathians, Tectonophysics, 226, p. 417-431.

Tomek, Č and Hall, J., 1993, Subducted continental margin imaged in the Carpathians of Czechoslovakia, Geology, 21, p. 535-538.

Udubaşa, G., Edelstein, O., Răduţ, M., Pop, N., Istvan, D., Kovács, M., Pop, V., Stan, D., Bernad, A., and Gotz, A., 1983, The Ţibles Neogene igneous complex of North Romania: some petrologic and metallogenetic aspects, Anuarul Institutului de Geologie şi Geofizică, 61, p. 285-295.

Werling, E., 1992, Tonale-, Pejo- und Judikarien-Linie: Kinematic, Mikrostrukturen und Metamorphose von Tektoniten aus räumlich interferierenden aber verschiedenaltrigen

Verwerfungszonen. Diss. ETH Zürich, Nr. 9923.

Winterer, E.L., and Boselini, A., 1981, Subsidence and sedimentation on Jurassic passive continental margin, Bull. Amer. Assoc. Petr. Geol., 65, p. 394-421.

Zoubek, V., Cogné, J., Kozhoukharov, D., and Kräutner, H. G., (Eds.) 1988, Precambrian in Younger Fold Belts, John Willis, 665 p.

APPENDIX II

GEOCHEMICAL DATA FROM ROCKS OF THE HIGHIS-BIHARIA SHEAR ZONE APUSENI MOUNTAINS

Table II-1. Average compositions within the unsheared igneous complex, Highis Mountains (%)

	SiO2	Al2O3	Fe2O3	FeO	MnO	MgO	CaO	Na2O	K2O	TiO2	P2O5	CO2	S	H2O+	H2O-	Total
RHYOLIT	75.11	12.05	1.27	0.30	0.03	0.58	0.84	4.30	5.14	0.13	0.07	0.06	0.01	0.69	0.08	100.64
GRANOPHIRE	72.66	12.16	3.17	0.64	0.03	1.67	0.94	5.61	1.75	0.22	0.07	0.00	0.01	0.75	0.10	99.78
ALBITITE	68.72	14.93	4.09	1.39	0.05	0.56	1.40	6.35	0.89	0.30	0.06	0.00	0.04	0.27	0.06	99.11
SYENOGRANITE	71.10	14.30	2.68	0.51	0.02	0.15	1.04	4.87	4.51	0.24	0.05	0.00	0.10	0.25	0.13	100.05
MONZOGRANITE	73.48	12.13	2.03	0.69	0.03	0.73	1.23	4.46	4.21	0.29	0.09	0.02	0.04	0.41	0.10	99.93
GRANITE	73.21	12.46	2.10	0.80	0.03	0.72	1.23	4.38	3.91	0.32	0.12	0.02	0.06	0.52	0.09	99.95
PLAGIOGRANITE	73.70	13.07	1.60	0.78	0.03	0.74	1.53	6.34	0.96	0.28	0.09	0.03	0.07	0.49	0.11	99.82
GRANODIORITE	66.41	15.13	2.79	2.04	0.08	0.71	2.38	5.28	2.64	0.62	0.18	0.00	0.07	0.59	0.14	99.07
DOLERITE	50.06	6.11	6.83	10.98	0.19	5.00	7.98	4.60	1.62	4.52	0.53	0.00	0.25	0.43	0.09	99.41
DIORITE	51.67	14.68	4.71	5.71	0.09	6.37	8.06	3.62	1.17	1.46	0.20	0.46	0.04	0.94	0.15	99.35
GABBRO	47.25	14.68	4.64	8.02	0.15	7.64	8.81	3.51	0.79	2.25	0.27	0.01	0.08	1.32	0.12	99.64
U-MAFIC	40.04	8.38	6.26	6.16	0.79	27.27	2.66	0.19	0.06	0.61	0.12	0.00	0.00	7.78	0.00	100.3

Table II-2 Chemical composition of SiO_2 - rich rocks within Paiuseni assemblage of the HBSZ

Major elements concentrations (%)

#	Field #	Location	SiO_2	Al_2O_3	Fe_2O_3	FeO	MnO	MgO	CaO	Na_2O	K_2O	TiO_2	P_2O_5	CO_2	S	Fe(S)	H_2O+	Total
Igneous texture																		
1	6	Cuvin Quarry	65.05	16.20	2.84	2.74	0.11	0.50	2.10	3.75	3.35	0.50	0.10	0.00	0.00	0.00	0.38	99.62
2	2	Cuvin Village	72.71	12.61	2.38	0.72	0.05	0.10	1.54	3.40	5.10	0.38	0.15	0.00	0.03	0.03	0.60	99.78
3	3752	Cladova M. Cree	76.99	10.90	1.13	0.65	0.02	0.51	0.52	4.05	0.97	0.68	0.08	0.00	0.38	0.31	1.72	99.47
4	3764	Cladovita Creek	74.84	10.30	1.86	1.30	0.02	0.90	1.37	4.85	0.77	0.58	0.04	0.00	0.32	0.28	1.87	99.38
5	2500	Livorecu Peak	74.63	13.60	0.77	0.52	0.00	0.10	0.50	3.80	5.66	0.16	0.06	0.00	0.19	0.17	0.61	100.77
6	2551	Ravna Creek	72.70	13.14	3.38	0.58	0.01	0.08	0.48	3.04	6.01	0.48	0.06	0.00	0.12	0.10	0.57	100.71
7	3816	Caseala Creek	73.24	13.10	1.12	0.58	0.00	0.77	0.24	3.52	4.28	0.20	0.01	0.00	0.20	0.17	1.98	99.41
8	3230	Chimerosa Cree	65.78	14.10	2.49	2.72	0.05	0.75	1.76	3.99	3.94	0.60	0.13	0.00	0.35	0.30	2.41	99.37
9	2977	Chimerosa Cree	68.87	13.88	3.86	1.20	0.01	0.65	0.65	4.60	4.72	0.23	0.12	0.23	0.00	0.00	0.09	99.51
10	3254	Chimerosa Cree	74.69	14.10	0.95	0.14	0.02	0.50	0.70	3.75	4.30	0.08	0.08	0.00	0.21	0.18	0.13	99.79
11	3162	Nadas Creek	76.29	13.88	0.70	0.20	0.02	0.50	0.39	3.70	2.60	0.13	0.07	0.33	0.00	0.00	0.84	99.65
12	4496	Nadas Creek	81.42	9.40	0.79	0.38	0.01	0.29	0.26	3.96	0.58	0.72	0.02	0.00	0.37	0.32	0.88	99.40
13	3143	Nadas Creek	74.62	12.90	0.23	0.33	0.00	0.20	0.16	4.37	3.85	0.00	0.23	0.00	0.33	0.29	1.88	99.39
14	4014	Pustacu Creek	74.51	13.60	0.80	0.46	0.00	0.53	0.10	4.80	1.73	0.24	0.03	0.00	0.39	0.34	1.80	99.35
15	2444	Meghies Creek	75.67	12.04	0.51	0.23	0.01	0.59	0.34	0.34	7.30	0.10	0.05	0.00	0.15	0.13	1.92	99.38
16	2713	Chimerosa Cree	71.82	14.40	1.51	0.56	0.00	0.80	0.12	0.50	6.40	0.28	0.14	0.00	0.32	0.28	2.59	99.72
		AVERAGE	73.36	13.15	1.58	0.83	0.02	0.50	0.71	3.57	3.85	0.33	0.08	0.04	0.21	0.18	1.25	99.67
"Metaconglomerate" texture																		
1	2167	Olcovac Hill	83.46	8.04	0.00	0.65	0.00	2.60	0.31	0.39	1.02	0.28	0.08	0.00	0.17	0.15	2.38	99.47
2	3834	Maira Creek	86.25	5.60	0.00	0.24	0.01	0.20	0.20	0.16	4.54	0.00	0.03	0.00	0.30	0.26	1.85	99.64
3	9	Sina Hill	84.43	3.34	2.44	0.57	0.04	0.80	1.12	3.75	0.85	0.80	0.08	0.00	0.05	0.04	1.83	99.74
4	3572	Sina Hill	80.09	9.75	2.05	0.14	0.02	1.00	1.40	0.80	1.35	1.38	0.05	0.00	0.13	0.11	1.78	99.81
5	2231	Batrina Hill	84.82	6.86	0.71	0.91	0.00	0.80	0.24	0.31	1.58	0.78	0.05	0.00	0.10	0.09	0.21	97.48
6	2024	Horlea edge	86.80	5.34	0.18	0.20	0.01	0.23	0.26	1.80	0.44	0.38	0.03	0.00	0.16	0.14	1.15	100.1
7	4181	Almas Creek	84.56	1.06	1.37	0.57	0.06	1.00	2.10	2.55	0.83	0.45	0.51	0.78	0.00	0.00	0.28	96.12
8	4551	Chiosora Peak	87.74	5.90	0.57	0.24	0.00	0.28	0.06	2.30	0.52	0.44	0.01	0.00	0.32	0.28	0.64	99.28
9	3818	Caseala	83.98	0.58	1.88	0.13	0.00	0.74	0.05	0.48	1.34	0.40	0.00	0.00	0.20	0.17	2.49	92.42
10	2681	Draut Creek	86.95	6.54	0.44	0.48	0.01	0.38	0.26	0.53	0.96	0.40	0.05	0.00	0.35	0.30	1.08	99.31
11	2641	Highis Peak	78.84	10.29	0.31	1.11	0.01	0.17	0.28	3.61	0.95	1.30	0.08	0.00	0.72	0.63	0.69	99.17
12	2849	Highis Peak	87.38	5.82	0.81	0.72	0.02	1.70	0.70	0.15	0.95	0.28	0.04	0.00	0.00	0.00	1.22	99.87
13	2828	Strugarita Hill	90.61	4.19	1.04	0.00	0.03	0.40	0.98	0.30	1.00	0.28	0.04	0.00	0.03	0.03	1.00	99.91
14	2455	Meghies Creek	71.62	13.89	2.07	0.42	0.03	1.11	0.22	1.20	5.94	0.40	0.03	0.00	0.14	0.12	2.23	99.42
15	2442	Meghies Creek	72.56	13.20	2.00	0.58	0.01	0.64	0.49	0.68	6.07	0.38	0.05	0.05	0.04	0.03	1.76	100.54
16	3070	Poiana-Biharia	82.12	9.08	2.09	0.00	0.03	0.20	1.12	0.30	2.45	0.28	0.04	0.00	0.04	0.03	1.73	100.09
		AVERAGE	83.45	6.66	1.17	0.44	0.02	0.76	0.81	1.19	2.04	0.50	0.07	0.06	0.17	0.15	1.44	98.94

Minor elements concentrations (ppm)

#	Field #	Location	Pb	Cu	Zn	Sn	Ga	Ni	Co	Cr	V	Sc	Y	Yb	Zr	Nb	La	Ba	Sr
Igneous texture																			
1	6	Cuvin quarry	6	75	—	22	4	9	2	10	20	4	91	8.9	700	40	82	—	—
2	2	Cuvin village	75	12	—	26	3	8	2	10	20	4	90	8.6	700	34	82	—	—
3	3752	Cladova M. Cr	4	11	<30	10	2	36	6	32	33	7	27	2.7	540	10	42	410	80
4	3764	Cladovita Cr	42	23	32	16	2	95	7	96	76	7	17	1.8	260	10	30	75	100
5	2500	Livorecu Peak	2	27	<30	14	5	2	2	2	2	2	40	3.6	240	—	44	230	37
6	2551	Ravna Cr	15	14	<30	20	4	2	2	2	6	2	64	5.7	850	—	58	400	19
7	3816	Caseala Cr	11	90	34	15	13	11	3	4	15	6	43	4.8	130	10	30	560	14
8	3230	Chimerosa Cr	9	20	35	27	4	17	8	12	62	22	90	8	740	16	46	800	140
9	2977	Chimerosa Cr	2	30	32	14	3	21	5	10	19	9	74	8	360	11	30	600	70
10	3254	Chimerosa Cr	2	6	<30	12	2	7	2	5	8	2	74	8.8	290	14	65	200	20
11	3162	Nadas Cr	2	4	<30	15	3	7	2	6	4	2	40	4.1	100	10	30	380	35
12	4496	Nadas Cr	6	8	<30	8	2	8	2	14	30	4	24	2.8	620	10	68	100	22
13	3143	Nadas Cr	14	11	<30	18	9	4	2	2	5	3	32	3.8	90	10	30	480	20
14	4014	Pustacu Cr	8	17	<30	30	5	4	2	2	6	6	53	7.2	620	15	42	170	24
15	2444	Meghies Cr	21	35	<30	14	5	2	2	3	7	4	30	1.1	185	—	38	240	18
16	2713	Chimerosa Cr	2	7	<30	19	5	9	2	9	30	6	38	5.5	320	10	65	400	10
		AVERAGE	14	24	—	17	4	15	3	14	21	5	52	5.3	420	—	49	—	—
"Metaconglomerate" texture																			
1	2167	Olcovac Hill	5	6	<30	<2	6	8	3	5	11	2	10	1	90		<30	50	10
2	3834	Maira Creek	6	20	<30	<2	4	9	2	6	7	2	10	1	90	—	<30	600	22
3	9	Sina Hill	2	3	—	<2	23	38	34	44	270	30	80	4.7	330	—	<30	—	—
4	3572	Sina Hill	4	3	34	<2	2	15	4	23	43	17	80	704	160	—	<30	130	70
5	2231	Batrina Hill	8	3	<30	<2	7	9	3	17	30	9	30	2.3	250	—	44	125	75
6	2024	Horlea edge	3	6	<30	<2	2	10	3	6	11	3	10	1	100	—	<30	53	22
7	4181	Almas Creek	3	6	<30	<2	3	9	5	14	19	8	25	1.6	100	—	<30	140	40
8	4551	Chiosora Peak	2	22	<30	<2	4	10	2	6	12	2	10	1.4	170	—	<30	80	12
9	3818	Caseala	2	4	<30	<2	6	14	4	7	19	3	16	1.6	130	—	<30	190	14
10	2681	Draut Creek	2	3	<30	<2	5	10	2	7	8	3	15	1	115	—	<30	125	18
11	2641	Highis Peak	20	12	165	<2	7	11	2	37	80	7	15	1	260	—	<30	180	53
12	2849	Highis Peak	2	3	<30	<2	4	7	4	8	9	2	10	1	75	—	<30	65	10
13	2828	Strugarita Hill	2	4	<30	<2	4	7	4	5	5	2	10	1	60	—	<30	130	10
14	2455	Meghies Creek	6	6	<30	6	15	10	2	13	24	6	38	2.5	230	—	56	340	30
15	2442	Meghies Creek	6	20	<30	5	14	2	2	3	7	4	30	1.1	165	—	38	240	18
16	3070	Poiana-Biharia	2	4	36	<2	7	8	3	9	12	5	30	206	140	—	35	300	13
		AVERAGE	5	8	—	—	7	11	5	13	36	7	25	36.4	156	—	—	—	—

Table II-3. Chemical composition of the granitic rocks from HBSZ in the Biharia and Gilau mountains

Major elements concentrations (%)

#	Field #	Location	SiO2	Al2O3	Fe2O3	FeO	MnO	MgO	CaO	Na2O	K2O	TiO2	P2O5	CO2	S	Fe(S)	H2O+	Total
1	8003	Lazuri Creek	66.00	13.77	0.37	2.10	0.08	0.32	1.33	9.90	1.43	0.40	0.20	0.16	0.04	0.03	0.69	96.82
2	8001	Lazuri Creek	71.54	13.96	1.44	1.15	0.13	0.26	0.77	7.96	0.96	0.35	0.20	0.00	0.03	0.03	0.48	99.26
3	8000	Lazuri Creek	71.70	11.90	5.49	0.72	0.05	0.17	0.46	8.00	0.76	0.23	0.10	0.06	0.03	0.03	0.60	100.28
4	8010	Taul Mare Peak	67.78	15.63	3.81	2.30	0.02	1.00	0.70	6.15	0.25	0.56	0.13	0.00	0.00	0.00	1.27	99.39
5	8023	Draghita edge	75.44	13.15	0.46	0.43	0.02	0.74	0.18	7.63	0.00	0.25	0.75	0.00	0.09	0.08	0.27	99.49
6	8021	Draghita edge	75.93	10.67	3.62	0.43	0.01	0.40	1.40	6.00	1.06	0.10	0.11	0.00	0.05	0.04	0.88	99.70
7	8034	Dobrani Creek	74.68	13.99	0.41	0.72	0.03	0.97	0.12	6.65	0.30	0.34	0.70	0.32	0.12	0.10	0.23	99.48
8	8014	Neagra Creek	76.05	12.54	1.77	0.57	0.05	0.85	0.84	5.00	0.50	0.26	0.11	0.00	0.00	0.00	1.08	99.61
9	8038	Aries River	76.16	13.88	0.00	0.10	0.01	0.41	0.42	6.15	1.40	0.00	0.04	0.00	0.67	0.58	0.08	99.68
10	8043	Posaga Creek	75.00	12.96	0.69	0.86	0.03	1.56	0.44	6.05	0.25	0.40	0.36	0.86	0.13	0.11	0.47	99.87
11	8044	Posaga Creek	73.86	12.91	1.01	0.72	0.04	0.86	0.67	4.90	2.70	0.43	0.48	0.26	0.11	0.10	0.43	99.46
12	8045	Incesti Creek	74.00	12.87	0.97	0.86	0.04	1.30	0.67	4.50	2.15	0.46	0.57	0.75	0.07	0.06	0.32	99.59
13	8046	Urau Creek	74.96	12.65	1.43	0.86	0.05	0.81	1.50	3.85	1.44	0.46	0.50	0.65	0.11	0.10	0.39	99.46
14	8047	Urau Creek	73.64	12.95	0.99	1.44	0.06	1.17	0.84	6.55	0.21	0.46	0.37	0.23	0.09	0.08	0.41	99.49
15	8048	Urau Creek	74.61	12.75	0.87	1.44	0.07	0.98	1.62	4.10	1.61	0.58	0.42	0.42	0.10	0.09	0.71	100.47
16	8049	Sagagea Creek	71.90	12.98	1.12	1.73	0.07	1.00	1.88	4.45	1.96	0.68	0.47	0.65	0.10	0.09	0.34	99.42
17	8050	Posaga village	73.00	12.93	1.84	0.43	0.02	0.26	0.29	6.65	0.60	0.48	0.65	0.22	0.09	0.08	0.24	97.78
18	8051	Posaga village	77.45	12.29	0.68	0.43	0.02	0.12	0.14	5.96	0.83	0.46	0.43	0.15	0.11	0.10	0.30	99.48
19	8058	Pociovalistea Creek	78.23	10.91	1.51	0.82	0.06	0.36	1.56	4.27	1.27	0.12	0.00	0.00	0.06	0.04	0.74	99.64
20	8055	Belioara Creek	78.06	12.52	1.66	0.40	0.03	0.40	0.60	6.15	0.14	0.04	0.00	0.00	0.04	0.03	2.15	102.11
21	8052	Ocolis Creek	77.22	12.16	0.81	0.98	0.02	0.09	0.33	6.05	0.55	0.40	0.52	0.37	0.09	0.08	0.25	99.82
22	8054	Ocolis Creek	77.02	13.23	1.84	0.12	0.03	0.40	0.73	4.95	0.96	0.06	0.00	0.92	0.08	0.07	0.12	100.16
23	8057	Ierti Creek	77.79	12.16	1.64	0.99	0.06	0.84	0.41	4.61	1.00	0.08	0.00	0.00	0.07	0.06	1.03	100.44
24	8056	Posaga Creek	73.48	13.33	1.92	0.79	0.04	0.71	0.51	3.99	2.75	0.60	0.28	0.00	0.04	0.03	1.48	99.92
25	5957	Posaga Creek	75.42	15.45	1.42	0.06	0.03	0.12	0.11	5.76	0.23	0.08	0.00	0.00	0.04	0.03	1.48	100.22
26	5956	Posaga Creek	78.72	12.80	1.74	0.09	0.02	0.21	0.03	5.02	1.01	0.12	0.00	0.00	0.13	0.11	0.45	100.45
		AVERAGE	74.71	12.85	1.50	0.79	0.04	0.65	0.71	5.79	0.99	0.32	0.29	0.22	0.10	0.08	0.65	

Minor elements concentrations (ppm)

#	Field #	Location	Pb	Cu	Zn	Sn	Ga	Ni	Co	Cr	V	Sc	Y	Yb	Zr	Nb	La	U	Th	K	Cs
1	8003	Lazuri Creek	3	9	<30	<2	10	2	3	2	17	10	33	3.0	185	<10	<30				
2	8001	Lazuri Creek	<2	4	<30	<2	8	2	<2	2	6	5	23	2.2	130	<10	<30	1.2	3.01	0.73	0
3	8000	Lazuri Creek	<2	3	<30	<2	10	3	<2	3	4	5	35	3.4	200	<10	<30	—	—	—	—
4	8010	Taul Mare Peak	<2	2	<30	<2	19	3	4	1	8	13	66	5.5	400	<10	<30	1.44	7.91	1.15	893
5	8023	Draghita edge	<2	2	<30	<2	9	2	<2	4	16	4	14	1.9	90	<10	<30	0.04	4.7	0.12	0
6	8021	Draghita edge	<2	3	<30	<2	11	2	<2	7	20	9	45	5.9	180	<10	<30	1.85	10.1	1.03	583
7	8034	Dobrani Creek	<2	3	<30	<2	10	2	<2	3	12	4	19	3.0	120	<10	<30	—	—	—	—
8	8014	Neagra Creek	<2	4	<30	<2	8	2	<2	3	19	6	15	1.6	140	<10	<30	1.17	3.69	0.33	0
9	8038	Aries River	<2	2	<30	<2	14	2	<2	4	14	5	26	4.0	110	<10	<30	—	—	—	—
10	8043	Posaga Creek	<2	2	<30	<2	12	2	<2	5	17	4	38	4.4	170	<10	<30	—	—	—	—
11	8044	Posaga Creek	<2	3	<30	<2	9	3	<2	4	8	3	37	4.0	160	<10	<30	—	—	—	—
12	8045	Incesti Creek	4	3	<30	<2	17	4	<2	6	10	6	36	3.8	170	<10	<30	—	—	—	—
13	8046	Urau Creek	<2	3	<30	<2	6	2	<2	3	13	8	26	2.6	135	<10	<30	—	—	—	—
14	8047	Urau Creek	<2	7	<30	<2	6	5	<2	13	27	8	25	2.9	170	<10	<30	1.81	4.67	0.14	50
15	8048	Urau Creek	<2	3	<30	<2	11	3	<2	8	21	8	40	3.8	185	<10	<30	—	—	—	—
16	8049	Sagagea Creek	<2	2	<30	<2	10	3	<2	4	20	8	35	3.4	185	<10	<30	1.86	5.43	1.33	239
17	8050	Posaga village	<2	2	<30	<2	9	2	<2	5	9	6	32	4.2	160	<10	<30	—	—	—	—
18	8051	Posaga village	<2	2	<30	<2	7	3	<2	6	11	6	17	2.4	175	<10	<30	—	—	—	—
19	8058	Pociovalistea Creek	<2	4	<30	<2	9	3	<2	5	18	7	36	3.6	200	<10	<30	—	—	—	—
20	8055	Belioara Creek	<2	3	<30	<2	9	2	<2	5	12	7	23	3.0	230	<10	<30	1.91	3.96	0.3	460
21	8052	Ocolis Creek	<2	10	<30	<2	12	2	<2	4	10	6	75	6.5	100	<10	<30	1.9	16.4	0.51	1006
22	8054	Ocolis Creek	<2	12	<30	<2	11	2	<2	5	17	8	38	4.2	170	<10	<30	2.73	6.51	0.49	334
23	8057	Ierti Creek	<2	5	35	<2	10	3	<2	5	14	7	16	2.1	190	<10	<30	—	—	—	—
24	8056	Posaga Creek	3	9	<30	3	12	5	3	12	30	7	23	1.7	260	<10	<30	—	—	—	—
25	5957	Posaga Creek	4	2	<30	<2	12	2	<2	4	11	7	20	3.6	110	<10	<30	1.11	6.19	0.47	0
26	5956	Posaga Creek	<2	2	<30	<2	8	4	<2	7	12	7	14	2.8	140	<10	<30	—	—	—	—
		AVERAGE	—	4	—	—	10	3	—	5	14	7	31	4	171	—	—	—	—	—	—

Table II-4. Chemical composition of mafic rocks within Paiuseni assemblage of the HBSZ, Highis Mountains

Major elements concentrations (%)

#	Field #	Location	SiO2	Al2O3	Fe2O3	FeO	MnO	MgO	CaO	Na2O	K2O	TiO2	P2O5	CO2	S	Fe(S)	H2O+	Total
Igneous texture																		
1	2156	Olcovac Hill	46.60	13.95	8.52	5.18	0.17	4.86	11.09	2.65	0.13	1.10	0.15	1.38	0.00	0.00	1.96	97.69
2	4100	Gurghiului Peak	45.66	13.18	12.96	0.86	0.18	6.18	10.50	3.35	0.40	1.22	0.50	1.06	0.00	0.00	2.06	98.11
3	2134	Olcovac Hill	41.32	2.82	19.26	8.02	0.44	11.50	4.47	2.30	0.40	1.48	0.55	3.55	0.00	0.00	1.90	98.11
4	384	Cladova Creek	44.40	7.30	18.71	1.57	0.32	6.66	8.12	3.35	0.60	1.82	0.87	1.06	2.07	1.80	1.44	100.31
5	3602	Cladova Creek	49.94	16.20	2.69	5.59	0.12	7.51	9.00	3.86	0.27	0.86	0.20	1.33	0.25	0.22	2.63	100.69
6	5037	Miadin Peak	45.96	17.60	2.79	6.54	0.25	8.10	9.21	1.75	1.63	2.16	0.21	0.00	0.36	0.31	2.54	99.41
7	4548	Miadin Creek(m-d)	44.78	15.95	5.41	7.79	0.32	6.16	7.91	0.90	1.54	3.44	0.34	1.86	0.24	0.21	2.99	99.84
8	2416	Coasca Varnitei Hill	43.66	16.86	6.29	7.66	0.20	4.82	8.54	4.03	0.25	2.85	0.40	0.88	0.00	0.00	1.60	98.04
9	2488	Velicu Creek	41.46	14.33	13.43	1.14	0.16	5.86	12.74	3.98	0.48	2.60	0.37	1.10	0.00	0.00	2.16	99.83
2	2471	Velicu Creek	44.30	12.95	8.69	5.73	0.21	7.93	11.06	3.40	0.18	0.48	0.28	0.96	0.00	0.00	1.94	98.11
10	3020	Jernova Creek(b)	49.08	23.36	4.65	3.49	0.14	3.70	3.50	4.10	4.15	1.00	0.22	0.00	0.00	0.00	2.36	99.74
11	2619	Highis Creek	48.84	14.43	3.60	6.74	0.15	5.00	10.36	4.95	0.30	1.30	0.35	0.80	0.00	0.00	1.58	98.40
12	4484	Draut Creek	46.76	16.92	4.32	6.70	0.24	5.30	8.12	3.55	0.45	3.20	0.38	0.00	0.15	0.13	3.95	100.17
13	4011	Pustaciu Creek	45.21	15.90	7.21	6.59	0.20	8.15	2.25	3.25	0.60	3.12	0.24	0.00	0.37	0.32	6.03	99.44
14	10	Siria Hill	50.38	15.28	4.19	6.66	0.18	4.80	7.28	3.60	0.65	2.70	0.50	0.00	0.00	0.00	2.26	98.49
15	3852	Meira Creek	50.66	15.80	4.26	7.28	0.23	3.63	5.42	4.21	1.12	2.78	0.34	0.00	0.30	0.26	3.09	99.36
16	2218	Bodroc Creek	44.48	16.85	4.62	6.80	0.17	6.86	5.32	2.73	2.25	1.00	0.61	2.92	0.00	0.00	3.52	98.12
17	2200	Bodroc Creek	51.10	10.45	8.92	7.30	0.23	4.37	6.66	3.43	1.73	1.85	0.92	0.66	0.00	0.00	0.98	99.80
		AVERAGE	46.37	14.46	7.82	5.65	0.22	6.20	7.87	3.30	0.95	1.94	0.41	0.96	0.21	0.18	2.50	99.04
Metamorphic texture (sheared / retrogressed mafic igneous rocks)																		
1	2059	Cheresa Creek	40.02	20.36	4.88	7.74	0.12	12.73	2.22	0.43	0.13	1.76	0.55	2.62	0.06	0.06	4.30	97.58
2	2299	Agrisu Creek	46.46	15.15	3.78	7.45	0.25	5.24	8.66	2.80	0.13	1.30	0.46	1.34	2.41	2.10	2.84	100.36
3	2541	Ravna Creek	48.64	17.49	5.25	6.78	0.16	6.44	3.34	3.02	0.06	2.18	0.31	0.80	0.00	0.00	3.45	99.92
4	4494	Draut Creek	41.96	18.05	1.51	12.09	0.10	11.10	2.38	1.50	0.20	2.75	0.28	0.00	0.22	0.19	6.00	99.93
5	2929	Sicut Creek	46.96	13.99	3.01	9.90	0.24	6.70	7.14	1.75	0.00	2.40	0.15	2.15	0.00	0.00	4.11	98.50
7	2908	Sicut Creek	44.83	15.07	2.16	9.03	0.23	6.50	6.40	2.50	0.00	2.64	0.21	3.74	0.41	0.36	2.57	98.65
6	4370	Mitova-Dud Creek	51.67	16.26	1.76	7.50	0.09	7.20	3.06	2.30	0.36	2.75	0.32	1.41	0.17	0.15	4.07	100.00
8	2972	Chimerosa Creek	54.56	16.90	4.53	5.27	0.12	3.90	5.83	3.62	1.77	0.82	0.26	0.99	0.00	0.00	1.04	99.60
9	2437	Meghiea Creek	45.02	16.77	14.93	1.57	0.14	6.95	5.60	3.25	0.48	1.30	0.30	1.14	0.00	0.00	2.00	99.45
10	4411	Lugoj Creek	51.06	17.25	1.67	6.26	0.15	7.00	5.04	2.95	1.35	2.10	0.26	0.00	0.13	0.11	4.54	99.77
		AVERAGE	47.58	16.01	4.89	7.27	0.16	6.64	5.63	2.76	0.74	2.02	0.36	1.25	0.26	0.22	3.34	99.16

Minor elements concentrations (ppm)

#	Field #	Location	Pb	Cu	Zn	Sn	Ga	Ni	Co	Cr	V	Sc	Y	Yb	Zr	Nb	La	Ba	Sr
Igneous texture																			
1	2156	Olcovac Hill	2	20	80	<2	17	20	21	14	135	24	44	3.5	230	<10	<30	330	120
2	4100	Gurghiului Peak	6	25	100	<2	18	27	22	100	230	33	36	2.8	90	<10	<30	180	300
3	2134	Olcovac Hill	2	23	90	<2	17	34	30	110	250	40	37	2.8	80	<10	<30	20	200
4	384	Cladova Creek	12	15	110	3	16	23	28	17	220	27	60	4.4	300	<10	<30	90	360
5	3602	Cladova Creek	3	16	40	<2	13	75	35	220	300	48	24	2.5	10	<10	<30	34	220
6	5037	Miadin Peak	22	260	65	4	22	110	34	370	260	29	40	3.2	330	<10	34	220	300
7	4548	Miadin Creek(m-d)	38	55	140	3	22	42	34	75	250	34	50	5.7	300	<10	<30	270	260
8	2416	Coasca Varnitei Hill	7	17	85	<2	18	22	29	27	380	44	45	2.5	140	<10	<30	60	290
9	2488	Velicu Creek	9	40	110	3	17	37	40	100	360	40	42	4	140	40	<30	86	370
2	2471	Velicu Creek	10	27	120	<2	13	65	34	110	170	27	26	2	100	<10	<30	40	420
10	3020	Jernova Creek(b)	7	2	73	5	26	47	18	100	105	25	32	1.9	87	—	53	680	370
11	2619	Highis Creek	4	40	90	<2	16	27	30	85	220	34	36	2.8	150	12	<30	85	440
12	4484	Draut Creek	44	12	120	<2	29	40	41	65	300	42	52	4.6	270	<10	<30	45	500
13	4011	Pustaciu Creek	8	50	90	<2	26	26	34	90	320	42	44	3.4	240	<10	<30	28	78
14	10	Siria Hill	3	40	—	<2	23	38	34	44	270	30	60	4.7	330	20	<30	—	—
15	3852	Meira Creek	5	32	80	<2	23	32	24	37	280	30	7	500	10	300	66	230	48
16	2218	Bodroc Creek	6	20	80	<2	17	20	21	14	135	24	44	3.5	230	<10	<30	330	120
17	2200	Bodroc Creek	4	30	100	<2	22	12	21	10	170	26	55	4.4	340	20	45	400	250
		AVERAGE	11	40	93	—	20	38	29	88	242	33	41	31	186	—	—	196	270
Metamorphic texture (sheared / retrogressed mafic igneous rocks)																			
1	2059	Cheresa Creek	2	5	120	<2	13	53	32	110	200	34	50	3.6	160	12	<30	25	10
2	2299	Agrisu Creek	5	15	120	<2	18	26	29	65	280	36	50	4.4	170	10	<30	32	340
3	2541	Ravna Creek	5	42	135	<2	15	42	46	43	280	36	36	2.6	220	—	<30	12	170
4	4494	Draut Creek	3	200	170	<2	34	65	55	135	270	48	25	2.4	175	10	<30	17	16
5	2929	Sicut Creek	2	65	75	<2	18	50	40	135	330	67	44	2.6	100	—	<30	27	96
7	2908	Sicut Creek	3	46	84	<2	15	46	38	90	330	60	40	3.3	120	—	<30	26	40
6	4370	Mitova-Dud Creek	2	46	30	<2	27	20	30	58	250	32	53	5.7	300	10	40	26	35
8	2972	Chimerosa Creek	3	8	45	<2	22	24	18	110	180	25	50	4.6	240	10	33	270	220
9	2437	Meghiea Creek	15	3	120	<2	12	75	25	180	140	22	30	2.1	120	10	<30	130	540
10	4411	Lugoj Creek	2	19	40	<2	23	75	31	200	225	35	37	4.7	300	10	<30	290	200
		AVERAGE	4	45	94	—	20	46	34	113	249	40	42	4	191	—	—	96	167

Table II-5. Chemical compositions of the sheared mafic rocks from HBSZ in the Biharia and Gilau mountains

Major elements concentrations (%)

#	Field #	Location	SiO2	Al2O3	Fe2O3	FeO	MnO	MgO	CaO	Na2O	K2O	TiO2	P2O5	CO2	S	Fe(S)	H2O+	Total
1	8011	Taul Mare Peak	46.94	18.99	3.76	4.32	0.13	7.85	11.20	2.30	0.35	0.60	0.16	0.00	0.00	0.00	2.91	99.51
2	8007	Taul Mare Peak	48.58	13.95	4.41	7.00	0.21	7.21	11.85	1.98	0.12	1.26	0.20	0.96	0.04	0.03	1.66	99.44
3	8006	Taul Mare Peak	45.86	16.83	2.70	6.18	0.18	8.69	7.86	4.31	0.09	0.60	0.25	2.83	0.03	0.03	3.00	99.44
4	8005	Taul Mare Peak	44.96	13.94	4.14	5.46	0.21	6.61	11.79	2.42	0.27	1.16	0.21	6.99	0.06	0.05	1.40	99.67
5	8013	Aries River	48.04	17.61	3.47	7.20	0.20	6.26	7.70	3.70	0.00	1.75	0.11	0.00	0.00	0.00	3.35	99.59
6	8029	Arieseul Mic Creek	45.35	16.39	5.44	7.63	0.19	5.58	9.27	3.38	0.41	2.57	0.83	0.67	0.14	0.12	2.44	100.41
7	8028	Arieseul Mic Creek	44.90	17.11	3.72	7.34	0.22	6.25	11.47	3.07	0.67	2.23	0.52	0.54	0.12	0.10	2.11	100.37
8	8026	Arieseul Mic Creek	40.80	14.80	6.00	8.64	0.21	7.36	8.56	3.03	0.25	2.57	0.75	2.25	0.06	0.05	5.06	100.38
9	8025	Draghita edge	42.95	17.64	5.20	4.14	0.14	8.20	14.25	1.98	0.51	0.76	0.47	1.75	0.03	0.03	1.65	99.70
10	8024	Draghita edge	49.27	18.48	2.52	5.47	0.10	7.04	9.38	4.00	0.35	0.85	0.07	0.00	0.00	0.00	2.28	99.81
11	8022	Draghita edge	50.14	18.85	5.69	2.88	0.14	6.54	7.42	4.00	0.00	0.90	0.07	0.61	0.00	0.00	2.64	99.88
12	8020	Draghita edge	47.57	21.52	1.88	3.45	0.10	7.16	11.76	2.75	0.37	0.35	0.06	0.00	0.00	0.00	2.49	99.46
13	8019	Draghita edge	47.31	18.38	2.59	6.33	0.19	8.53	9.38	2.32	0.00	0.96	0.10	0.17	0.00	0.00	3.22	99.47
14	8035	Dobrani Creek	48.26	17.92	4.51	6.76	0.19	4.49	5.88	5.75	0.25	2.20	0.17	1.18	0.31	0.27	1.36	99.50
15	8033	Dobrani Creek	46.76	21.99	1.69	6.05	0.11	4.67	6.30	6.15	0.25	1.15	0.17	1.05	0.18	0.16	2.79	99.47
16	8015	Neagra Creek	47.07	18.74	0.00	8.44	0.18	7.26	7.14	3.00	0.00	1.75	0.15	0.35	1.13	0.98	2.96	99.15
17	8016	Neagra Creek	48.17	18.09	5.42	6.62	0.20	5.29	8.54	2.30	0.00	1.25	0.13	0.39	0.00	0.00	3.08	99.48
18	8037	Dobra Creek	48.59	17.74	4.12	7.20	0.24	4.21	5.32	4.56	0.00	1.25	0.15	2.72	0.00	0.00	3.31	99.41
19	8039	Posaga Creek	49.27	18.15	2.54	5.33	0.14	7.56	9.24	2.60	0.37	0.35	0.05	0.88	0.00	0.00	3.07	99.55
20	8053	Ocolis Creek	52.91	16.04	3.72	5.58	0.18	6.08	7.02	4.16	0.14	1.50	0.00	0.00	0.00	0.00	2.30	99.63
		AVERAGE	47.19	17.67	3.68	6.10	0.17	6.64	9.07	3.39	0.22	1.30	0.23	1.17	0.11	0.09	2.55	

Minor elements concentrations (ppm)

#	Field #	Location	Pb	Cu	Zn	Sn	Ga	Ni	Co	Cr	V	Sc	Y	Yb	Zr	Nb	U	Th	K	Ce
1	8011	Taul Mare Peak	5	56	30	<2	14	85	32	370	280	44	19	1.0	85	<10	0.01	1.02	0.30	0
2	8007	Taul Mare Peak	2	17	30	<2	14	67	42	280	420	53	19	1.3	57	<10	—	—	—	—
3	8006	Taul Mare Peak	2	2	30	<2	19	60	32	460	320	60	27	2.0	57	<10	—	—	—	—
4	8005	Taul Mare Peak	3	65	30	<2	19	60	32	460	320	60	27	2.0	57	<10	0.00	0.14	0.28	329
5	8013	Aries River	4	44	38	<2	20	34	36	160	410	54	40	4.4	180	<10	0.58	1.02	0.02	0
6	8029	Arieseul Mic Creek	8	80	44	<2	21	13	23	45	250	32	36	4.4	160	<10	—	—	—	—
7	8028	Arieseul Mic Creek	3	65	44	<2	20	42	30	170	280	29	42	5.0	250	<10	0.46	0.27	0.64	0
8	8026	Arieseul Mic Creek	3	65	60	<2	21	54	31	200	360	41	40	2.0	220	<10	—	—	—	—
9	8025	Draghita edge	18	10	30	<2	15	105	43	280	185	40	11	1.0	25	<10	—	—	—	—
10	8024	Draghita edge	3	2	30	<2	14	85	35	250	380	44	30	3.6	105	<10	0.20	0.00	0.10	0
11	8022	Draghita edge	24	100	32	<2	26	50	40	170	310	40	33	4.0	160	<10	—	—	—	—
12	8020	Draghita edge	10	7	30	<2	17	47	25	40	260	38	20	1.8	57	<10	0.16	0.93	0.33	0
13	8019	Draghita edge	7	50	32	<2	17	120	40	400	370	45	26	2.3	100	<10	—	—	—	—
14	8035	Dobrani Creek	3	80	48	<2	26	16	30	28	360	39	60	7.0	250	<10	—	—	—	—
15	8033	Dobrani Creek	10	5	50	<2	31	13	23	45	250	32	36	4.4	160	<10	0.79	3.80	0.10	431
16	8015	Neagra Creek	6	30	44	<2	21	115	48	300	370	42	36	4.0	185	<10	—	—	—	—
17	8016	Neagra Creek	17	55	48	<2	21	22	28	70	620	52	21	2.3	78	<10	—	—	—	—
18	8037	Dobra Creek	8	37	48	<2	22	16	26	43	450	44	24	2.3	85	<10	—	—	—	—
19	8039	Posaga Creek	2	10	32	<2	14	33	27	190	260	44	15	1.0	53	<10	0.09	1.17	0.26	0
20	8053	Ocolis Creek	2	2	30	<2	14	7	25	45	260	41	15	1.0	53	<10	0.09	0.90	0.23	1047
		AVERAGE	7	39	38	—	19	51	32	199	336	44	29	3	119	—	0.12	0.46	0.11	90

Table II-6. Chemical compositions of rocks within the "Black Series"

Major elements concentrations (%)

#	Field #	Location	SiO2	Al2O3	Fe2O3	FeO	MnO	MgO	CaO	Na2O	K2O	TiO2	P2O5	CO2	S	Fe(S)	H2O+	Total
Igneous texture																		
1	5037	Miadin Peak	45.96	17.6	2.79	6.54	0.25	8.1	9.21	1.75	1.63	2.16	0.21	0	0.36	0.31	2.54	99.41
2	4548	Miadin Creek(m-d)	44.78	15.95	5.41	7.79	0.32	6.16	7.91	0.90	1.54	3.44	0.34	1.86	0.24	0.21	2.99	99.84
3	3020	Jernova Creek(b)	49.08	23.36	4.65	3.49	0.14	3.70	3.50	4.10	4.15	1.00	0.22	0.00	0.00	0.00	2.35	99.74
		AVERAGE	46.61	18.97	4.28	5.94	0.24	5.99	6.87	2.25	2.44	2.20	0.26	0.62	0.20	0.17	2.63	99.66
Hornfels texture - black massive																		
4	3712	Cuvin village	54.39	20.14	5.27	2.50	0.13	3.41	2.27	3.39	4.03	1.10	0.10	0.00	0.24	0.21	2.37	99.55
5	7	Cuvin village	55.62	19.51	4.57	1.73	0.08	2.40	3.36	2.65	6.40	0.74	0.25	0.00	0.06	0.05	2.03	99.45
6	389	Cladova Creek	61.20	15.25	1.55	4.84	0.15	2.97	3.00	3.54	1.16	1.12	0.21	1.04	0.34	0.30	3.01	99.68
7	379	Cladova Creek	53.90	15.85	7.31	2.00	0.07	2.74	4.90	3.70	5.38	0.82	0.40	1.24	0.00	0.00	0.66	98.97
8	3769	Cladovita Creek	50.69	20.34	6.15	1.62	0.12	4.25	3.60	4.36	4.19	0.72	0.12	0.00	0.34	0.30	1.69	98.49
9	3780	Cladovita Creek(viole	49.66	20.74	6.16	1.50	0.10	4.03	3.90	5.27	3.94	0.84	0.11	0.00	0.32	0.28	2.51	99.36
10	3031	Jernova Creek	49.54	21.28	3.69	4.07	0.16	3.30	6.02	4.50	3.50	1.00	0.24	0.00	0.00	0.00	2.16	99.46
11	2740	Chimercea Creek	67.85	14.00	4.42	1.06	0.04	1.15	1.11	4.37	4.02	0.53	0.18	0.47	0.00	0.00	0.63	99.82
12	2748	Chimercea Creek	53.53	19.03	6.60	0.73	0.10	3.20	5.60	4.30	4.00	1.10	0.21	0.00	0.20	0.17	1.19	99.96
13	4477	Nadas Creek	47.86	20.90	5.63	3.10	0.15	4.50	2.90	4.26	5.75	1.04	0.31	0.00	0.18	0.16	2.86	99.60
14	4429	Nadas Creek	48.92	21.90	5.24	3.97	0.10	3.71	4.29	4.66	4.11	3.04	0.17	0.00	0.34	0.30	2.14	102.89
15	3122	Nadas Creek	47.10	22.24	6.98	3.18	0.13	4.37	2.44	4.42	4.84	0.92	0.24	0.00	0.33	0.29	3.10	100.58
		AVERAGE	53.36	19.27	5.30	2.63	0.11	3.34	3.62	4.12	4.28	1.08	0.21	0.23	0.20	0.17	2.03	99.82
Phyllonite - black																		
16	4547	Miadin Creek	51.76	23.10	3.31	2.05	0.11	3.58	2.08	3.81	5.43	0.92	0.10	0.00	0.22	0.19	3.06	99.72
17	4049	Pustaciu CreeK	54.76	15.50	5.26	4.83	0.24	3.00	3.34	5.59	0.18	3.04	0.74	0.00	0.38	0.33	3.50	100.69
18	4590	Chiodia Creek	45.30	15.60	0.73	6.04	0.11	9.67	1.40	5.05	3.26	2.56	0.21	0.00	0.12	0.10	3.31	93.46
		AVERAGE	50.61	18.07	3.10	4.31	0.15	5.42	2.27	4.82	2.96	2.17	0.35	0.00	0.24	0.21	3.29	97.96
Hornfels texture - grey massive																		
19	5	Cuvin village	55.74	18.03	4.85	2.02	0.11	2.30	3.36	4.60	5.35	1.04	0.21	0.00	0.00	0.00	1.75	99.36
20	3767	Cladovita Creek	55.04	20.04	5.54	1.13	0.10	2.74	4.01	4.82	4.05	0.76	0.11	0.00	0.34	0.30	1.67	100.65
21	2981	Chimercea Creek	50.82	21.96	2.94	3.78	0.10	3.80	5.04	4.65	3.25	1.24	0.25	0.00	0.16	0.14	1.67	99.80
22	3002	Chimercea Creek	53.43	20.05	4.38	2.03	0.11	2.90	4.34	5.50	3.00	1.24	0.12	0.00	0.15	0.13	2.69	100.07
		AVERAGE	53.76	20.02	4.43	2.24	0.11	2.94	4.19	4.89	3.91	1.07	0.17	0.00	0.16	0.14	1.85	99.97
Phyllonite - grey																		
23	1	Cuvin village	53.68	22.11	5.27	1.29	0.07	2.40	3.04	4.00	4.00	1.04	0.18	0.00	0.03	0.03	1.88	99.22
24	3574	Cuvin village	53.53	16.20	1.54	4.55	0.11	9.83	0.56	0.12	3.19	0.80	0.12	0.00	0.37	0.32	7.75	98.99
25	4553	Chiodia Creek	49.84	22.60	7.32	0.80	0.08	3.24	1.26	4.87	5.14	0.96	0.13	0.00	0.30	0.26	3.26	100.06
		AVERAGE	52.42	20.30	4.71	2.21	0.09	5.16	1.62	3.00	4.11	0.93	0.14	0.00	0.23	0.20	4.30	99.42
Biharia																		
26	3077	Poiana	49.99	22.05	6.39	1.53	0.13	3.90	4.90	3.30	3.56	1.24	0.05	0.00	0.14	0.12	0.55	97.85
27	3071	Baita	63.15	12.64	3.01	0.72	0.09	2.00	8.82	1.70	3.10	0.74	0.07	0.00	0.03	0.03	3.75	99.85
Layered phyllonite																		
28	3570	Highis Creek	57.59	20.17	6.61	0.73	0.02	2.15	0.91	4.10	3.70	0.49	0.18	0.71	0.00	0.00	2.25	99.61
29	379	Cladova Creek	57.86	16.63	8.57	0.86	0.04	2.40	1.54	5.13	3.00	1.20	0.14	1.28	0.01	0.01	0.56	99.23
30	2732	Chimercea Creek	66.56	17.20	6.02	0.26	0.00	1.30	0.28	1.67	3.20	0.43	0.14	0.00	0.00	0.00	2.21	99.25
31	4366	Dud Creek	66.60	17.63	4.83	0.66	0.01	1.25	0.26	1.82	3.32	0.46	0.11	0.23	0.00	0.00	2.55	99.73
		AVERAGE	62.15	17.91	6.51	0.63	0.02	1.78	0.74	3.18	3.31	0.65	0.14	0.56	0.00	0.00	1.89	99.46

Minor elements concentrations (ppm)

#	Field #	Location	Pb	Cu	Zn	Sn	Ga	Ni	Co	Cr	V	Sc	Y	Yb	Zr	Nb	La	Ba	Sr
Igneous texture																			
1	5037	Miadin Peak	22	260	65	4	22	110	34	370	260	29	40	3.2	330	<10	34	220	300
2	4548	Miadin Creek(m-d)	38	55	140	3	22	42	34	75	250	34	50	5.7	300	<10	30	270	260
3	3020	Jernova Creek(b)	7	2	73	5	26	47	18	100	105	25	32	1.9	87	—	53	880	370
		AVERAGE	22	106	93	4	23	66	29	182	205	29	41	3.6	239	—	39	457	310
Hornfels texture - black massive																			
4	3712	Cuvin village	16	2	53	6	30	58	22	80	140	19	44	3.9	200	12	52	300	190
5	7	Cuvin village	2	5		2	13	70	18	150	180	19	43	2.8	190	18	60	—	—
6	389	Cladova Creek	10	65	48	2	20	37	22	140	185	19	33	3.6	200	<10	30	250	210
7	379	Cladova Creek	2	2	30	2	19	55	10	90	110	12	12	1.8	85	<10	38	300	50
8	3769	Cladovita Creek	16	6	52	3	26	46	17	125	145	16	28	2.7	170	<10	55	570	230
9	3780	Cladovita Creek(viole	13	26	52	4	25	65	19	190	210	18	36	3.0	180	<10	67	900	900
10	3031	Jernova Creek	24	2	105	4	29	48	18	120	120	25	30	2.2	105	—	45	390	260
11	2740	Chimercea Creek	2	4	32	2	12	27	7	64	70	11	27	3.6	250	<10	40	450	75
12	2748	Chimercea Creek	15	3	55	4	21	40	16	100	90	17	36	4.4	200	<10	55	630	310
13	4477	Nadas Creek	7	7	110	5	27	60	16	120	160	19	40	3.2	130	<10	50	1200	310
14	4429	Nadas Creek	10	24	70	4	28	50	19	140	170	15	32	3.4	160	<10	55	620	270
15	3122	Nadas Creek	75	17	95	4	30	78	22	180	200	22	38	3.0	200	15	75	1050	300
		AVERAGE	16	13	64	3	23	53	17	125	148	18	33	3.1	173	—	52	—	—
Phyllonite - black																			
16	4547	Miadin Creek	15	42	80	4	20	67	18	110	140	17	32	2.1	90	<10	42	850	280
17	4049	Pustaciu CreeK	10	38	72	2	26	15	16	4	150	22	80	6.8	440	<10	46	28	120
18	4590	Chiodia Creek	3	8	140	4	24	42	27	150	210	35	40	2.8	75	<10	30	160	75
		AVERAGE	9	29	97	3	23	41	20	88	167	25	51	3.9	202	—	39	346	158
Hornfels texture - grey massive																			
19	5	Cuvin village	3	5	—	2	20	60	18	130	150	17	42	3.0	170	18	34	—	—
20	3767	Cladovita Creek	19	22	55	3	23	44	2	95	160	13	35	2.2	210	<10	56	680	300
21	2981	Chimercea Creek	3	2	63	2	20	43	19	100	100	16	23	28.0	70	<10	40	220	280
22	3002	Chimercea Creek	9	2	35	2	20	46	14	95	82	13	18	2.4	125	<10	50	350	70
		AVERAGE	8	8	51	2	21	48	13	105	123	15	30	8.9	144	—	46	417	217
Phyllonite - grey																			
23	1	Cuvin village	4	4	—	2	19	70	20	150	180	20	38	2.9	120	12	34	—	—
24	3574	Cuvin village	2	25	65	2	23	67	23	130	130	13	24	3.2	190	11	30	280	10
25	4553	Chiodia Creek	9	2	74	6	29	55	12	120	135	20	38	2.5	150	<10	66	960	190
		AVERAGE	5	10	70	3	24	64	18	133	148	18	33	2.9	153	—	43	620	100
Biharia																			
26	3077	Poiana	15	2	180	4	20	66	20	130	130	20	30	3.5	110	10	45	350	130
27	3071	Baita	9	2	58	4	15	16	7	46	42	13	39	3.6	120		34	260	130
Layered phyllonite																			
28	3570	Highis Creek	4	2	45	2	18	38	10	75	70	11	100	1.8	15	—	38	60	540
29	379	Cladova Creek	11	4	30	2	20	46	12	110	80	13	85	2.4	18	—	40	50	350
31	4366	Dud Creek	3	3	30	2	18	26	6	65	53	9	260	2.4	14	—	45	40	280
		AVERAGE	6	3	35	2	19	36	10	83	68	11	148	2.2	16		41	50	390

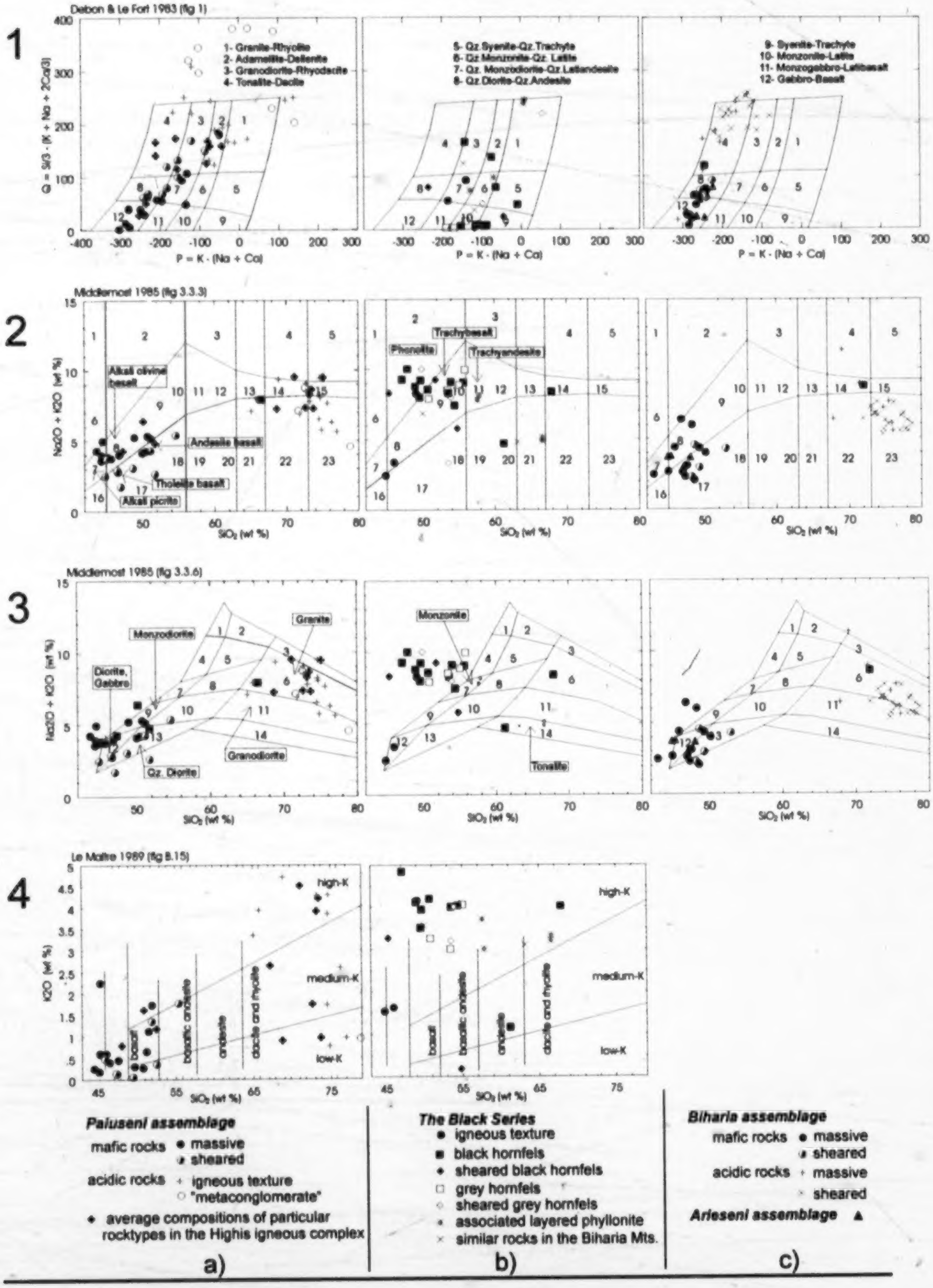

Fig. II-1. Major elements discrimination plots for the igneous and metamorphic rocks of the Highis-Biharia shear zone; a) Paiuseni assemblage, Highis Mountains; b) "the Black Series"; c) Biharia and Arieseni assemblages, Biharia and southern Gilau mountains.

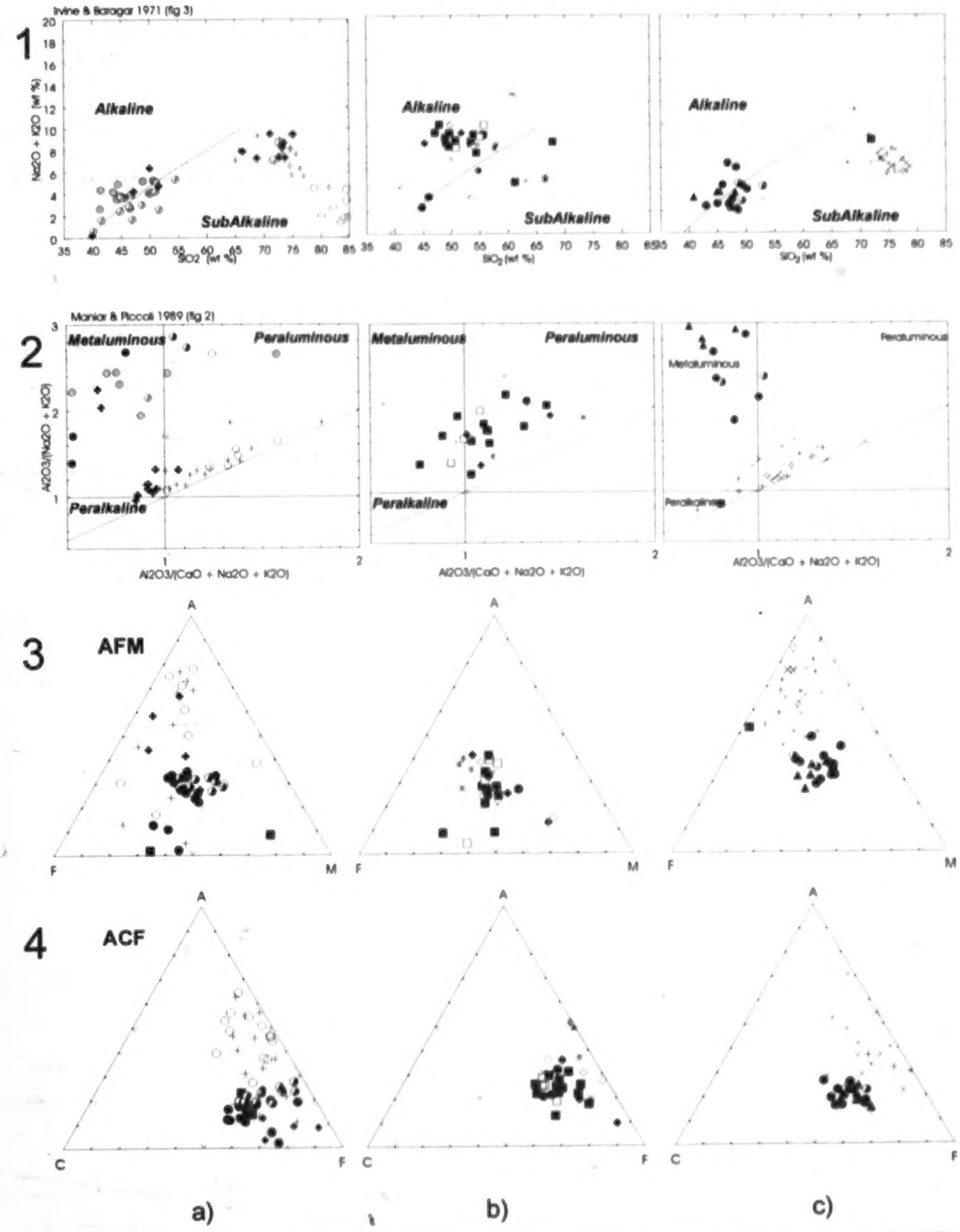

Fig. II-2. General petrochemical characteristics of the igneous and metamorphic rocks within the Highis-Biharia Shear zone; a) the Paiuseni assemblage, Highis Mountains; b) "the Black Series"; c) Biharia and Arieseni assemblages, Biharia and southern Gilau mountains. Symbols as in Fig. II-1.

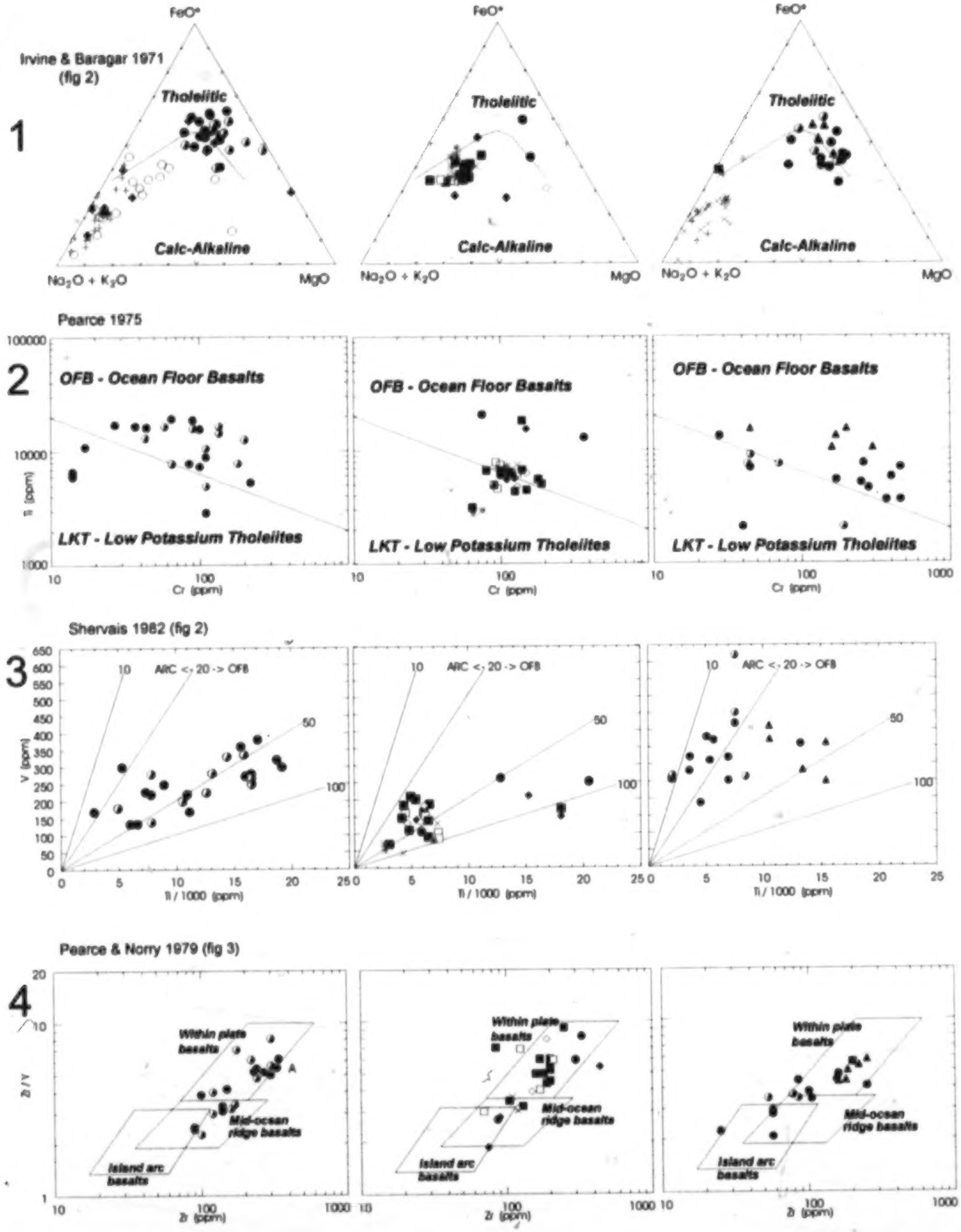

a) b) c)

Fig. II-3. Trace elements - tectonic discrimination plots for rocks of the Highis-Biharia shear zone; a) Paiuseni assemblage,Highis Mountains; b) "the Black Series"; c) Biharia and Arieseni assemblages, Biharia and southern Gilau mountains. Symbols as in Fig. II-1.

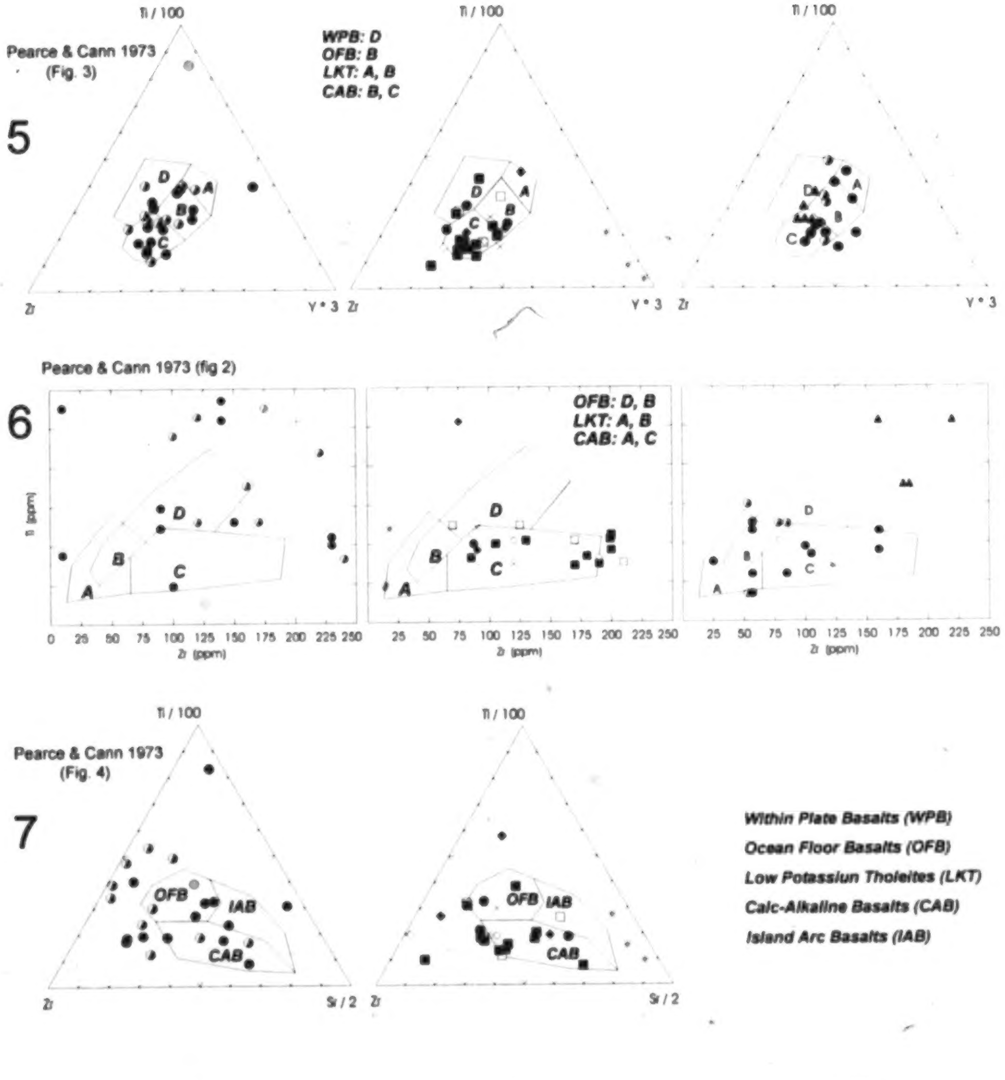

a) b) c)

Fig. II-3 (continued). Trace elements - tectonic discrimination plots for rocks of the Highis-Biharia shear zone; a) Paiuseni assemblage, Highis Mountains; b) "the Black Series"; c) Biharia and Arieseni assemblages, Biharia and southern Gilau mountains. Symbols as in Fig. II-1.

DISCUSSION

In an attempt to reconstruct the pre-Alpine tectonic framework of the region, the geochemical study has addressed two problems: 1. the tectonic significance of the igneous belt separating the two gneissic assemblages; 2. the nature of protolith within the low-grade assemblages of the HBSZ.

85 samples from the igneous pods and 74 samples of metamorphic rocks have been analysed for major and trace elements at the Chemical Analysis Laboratory of the Geological Survey of Romania. Chemical analysis for SiO_2-rich rocks are presented in Table II-2 (Highiş Mountains) and Table II-3 (Biharia and Gilău mountains) and for mafic rocks in Table II-4 (Highiş Mountains) and II-5 (Biharia and Gilău mountains). Average chemical compositions for the most common igneous rocks of the unsheared igneous complex in the Highiş Mountains (Tatu et al. 1993, unpublished report) are presented for comparison in Table II-1.

1. The tectonic significance of the igneous belt

The chemical compositions of igneous rocks from the Highiş Mountains are spread over the gabbro-diorite-monzodiorite and tonalite-granite fields (Fig. II-1.1.a). Most acidic samples fall in the narrow adamellite field. In contrast, igneous rocks from the Biharia-Gilău mountains are well grouped in the gabbro-quartz diorite and tonalite (trondhjemite) fields suggesting bimodal magmatism (Fig. II-1.1.c). The SiO_2 vs. K_2O diagrams emphasize the wide range of K concentrations of the late acidic intrusions in the Highiş Mountains. The alkali vs. silica diagram (Figs. II-1.2 and II-1.3) indicates a gap between acidic and mafic compositions better expressed in the Biharia and Gilău mountains. Mafic rocks show a transitional tholeiitic/calc-alkaline character (Fig. II-3.1). Rocks from the western segment of the HBSZ with a more pronounced tholeiitic affinity show V-Ti ratios indicative for "ocean floor" (Fig. II-3.3a), whilst rocks from the eastern segment evenly distributed between the tholeiitic and calc-alkaline fields (Fig. II-4.1c) are spread over the "ocean floor" and "arc" fields (Fig. II-3.3c). In the Zr/Y-Zr diagrams samples from the western HBSZ are spread over the "within plate" and "mid-ocean ridge" fields (Fig. II-3.4a) whilst samples from the eastern segment plot mainly in the "within plate" and "island arc" fields (Fig. II-3.4c). Most samples have Y-Nb ratios higher than 3, indicative for ocean floor basalts (Pearce and Cann, 1973) and Ti-Cr ratios of ocean floor basalts (Fig. II-3.2). In the Ti-Zr-Y diagrams (Fig. II-3.5), most samples plot outside the "within plate" field. Further discrimination using Ti-Zr (Fig. II-3.6) and Ti-Zr-Sr (Fig. II-3.7) diagrams is not possible as the same samples plot on different diagrams in different fields or outside the diagram. The mafic rocks from the HBSZ show ambiguous chemical characteristics inconsistent with the classical patterns constrained for major tectonic settings. We suggest that the tholeiitic and "ocean floor" character of some rocks all along the Highiş-Biharia igneous belt is the evidence for an extensional tectonic setting and that the calc-alkaline (Fig. II-3.5c and II-3.6c), "within plate" (Fig. II-3.4), and "island arc" (Fig. II-3.3c and Fig. II-3.4c) affinities only indicate different degrees of differentiation and/or larger participation of continental crust. The wider igneous complex from the Highiş Mountains with stronger tholeiitic and "mid-ocean ridge" character of the mafic rocks suggests more advanced extension across the western segment the Highiş-Biharia igneous belt. The narrower igneous belt from the southern Gilău with more prominent calc-alkaline chemical characteristics suggest that extension across the eastern segment was less advanced.

2. The nature of protolith within the low-grade assemblages of the HBSZ

The wide belt of low-grade assemblages contains a variety of sheared, partly re-equilibrated igneous rocks as well as pods of massive igneous rocks. Rock types completely re-equilibrated under low-grade conditions have been traditionally considered metamorphosed clastic sediments, and were defined based on their inferred original grain-size. The interpretation is questionable since all low-grade rocks record a large component of non-coaxial strain accompanied by extensive hydration reactions. For some of these rocks an igneous protolith could be traced by detailed sampling. Nevertheless, for several other rock types the nature of the protolith remains uncertain. The original chemical characteristics of the low-grade metamorphic rocks from the HBSZ have been altered to various degrees either by diagenetic and metamorphic processes or only by the shear zone metamorphism. For comparison metamorphic and igneous rocks are plotted on the same diagrams. One of the most characteristic metamorphic rocks within the HBSZ mainly exposed in the Highiş Mountains, is a quartz-clast bearing schist interpreted either as a "metaconglomerate" (e.g., Giuşcă, 1979; Dimitrescu, 1985;) or as a secondary quartz-clast phyllonite derived from igneous rocks (Pană and Ricman, 1988). Chemical analyses on SiO_2 - rich rocks are presented in Table II-2. Both massive (igneous) and sheared rocks of acidic composition are plotted in the discrimination diagrams of column a) in Figs. II-2 and II-3. All diagrams indicate an intriguing partial overlapping between the field of igneous acidic rocks and that of the quartz-clast bearing schist ("metaconglomerate") samples. Most quartz-clast bearing schists plot outside the field of igneous rocks; this does not necessarily indicate a sedimentary origin. Quartz veining, a common process in extensional shear zones, may have drastically altered the bulk whole rock composition (see chapter 5 Fig. 5-3 and 5-4). The quartz-clast bearing schists occupy large areas and do not correlate along strike. They may represent the locus of intense crack-seal processes in acidic protoliths within the wide HBSZ.

Controversial interpretations also exist for an association of black to gray massive rocks and their sheared equivalents. Initially mapped in a limited area near the western extremity of the Highiş Mountains, the rocks were considered black quartzite and shale (Giuşcă, 1979) and interpreted to represent a post-Variscan Carboniferous (Permian?) sedimentary cover named the "Black Series"(BS). Similar rocks, later described from additional locations were shown to be low temperature hornfelses up to biotite isograd, spatially and genetically related to the Highiş igneous complex (Savu, 1965; Pană and Ricman, 1988). Commonly, a very fine grained mesh of mica-quartz-albite-magnetite with epidote nests overprints and obscures the original texture. Behind this veil at several locations, basaltic and aplitic textures have been noticed. The chemical analysis on these controversial rocks are presented in

Table II-4 and in discrimination diagrams of column b) in Figures II-2, II-3 and II-4. Most samples of the "Black Series" plot in the latibasalt and trachyte fields. Spatially associated igneous rocks partly overprinted by similar hornfels texture are quartz-latiandesite and trachyte. Completely hornfelsed rocks show a more alkali character than the associated igneous rocks (Fig. II-1.1b). The particular alkaline character of the "BS" could not result from mixing of sediments originating in the acidic and mafic end members from the adjacent igneous rocks (Fig. II-1.2c). Although diagenetic K-rich clay minerals may eventually cause the shift, we note that all massive and sheared hornfels samples plot around one of the igneous subvolcanic rocks in the phonolite-trachybasalt fields, and outside the fields of their plutonic equivalents. The SiO_2 vs. K_2O diagrams emphasise a continuous transition between the "BS" and the high-K rhyolite of the late acidic intrusions in the Highiş Mountains . The field occupied by most "BS" samples corresponds to the high-K basalt and basaltic andesite and includes again the spatially associated aplitic rock. Whilst in the alkali vs. SiO_2 diagrams the "BS" occupies a separate field (Figs. II-1.1; II-1.2; and II-2.1), in diagrams that consider also the Al concentration (Fig. II-2.2) the "BS" rocks occupy an intermediate field between the essentially peraluminous acidic rocks and the mainly metaluminous mafic rocks. The AFM and ACF diagrams (Figs. II-2.3 and II-2.4) suggest a closer chemical affinity to the mafic suit. Ti/Cr ratios for most mafic rocks correspond to the ocean floor basalts (Figs. II-3.2.a and II-3.2.c) while most of the hornfelses show an intermediate character between ocean floor basalts and low potassium tholeiites (Fig. II-3.2.b). In the Zr/Y vs. Zr diagrams most rocks fall in the within plate basalt and MORB fields.

The geochemical data allow the following general conclusions:

a) the Highiş-Biharia igneous belt plugged a pre-Alpine transtensional setting separating two gneissic assemblages. The zone of crustal thinning favoured the development of the wide HBSZ during the Alpine tectonism.

b) the interlayered highly sheared rocks show chemical affinities with the adjacent igneous rocks. They may be interpreted either as low-grade mylonites or as proximal epiclastic deposits in a narrow basin following the igneous lineament. The lack of volcanic rocks in the unsheared domains and the presence of plutonic and subvolcanic pods throughout the low-grade metamorphic assemblages dominated by non-coaxial deformation favours the first interpretation.

c) the hornfels rocks of the "Black Series" most probably represent a subvolcanic differentiate of the mafic suit (phonolite/trachybasalt/trachyandesite), thermally affected by the late granitic intrusions.

APPENDIX III

$^{40}Ar/^{39}Ar$ ANALYTICAL DATA

Table III-1. $^{40}Ar/^{39}Ar$ analytical data for incremental-heating experiments on hornblende concentrates from structural units comprising the Apuseni Mountains, Romania

Release temp (°C)	$(^{40}Ar/^{39}Ar)^*$	$(^{36}Ar/^{39}Ar)^*$	$(^{37}Ar/^{39}Ar)^c$	^{39}Ar % of total	%^{40}Ar non-atmos.+	$^{36}Ar_{Ca}$ %	Apparent Age (Ma) **		
				BAIA DE ARIES ASSEMBLAGE					
Sample 15: J = 0.010122 (amphibolite)									
620	77.45	0.22316	5.204	1.76	15.39	0.63	206.2	±	3.0
720	21.68	0.04067	4.566	1.88	46.24	3.05	174.8	±	1.0
755	12.01	0.00429	5.906	1.53	93.35	37.43	194.6	±	0.4
780	10.27	0.01131	7.777	3.63	73.50	18.70	133.5	±	0.6
800	9.20	0.00809	7.719	6.63	80.70	25.96	131.3	±	0.2
820	8.25	0.00773	7.753	9.72	79.79	27.27	116.9	±	0.2
835	7.13	0.00411	8.107	12.44	92.01	53.60	116.6	±	0.2
850	7.16	0.00399	7.867	15.91	92.30	53.69	117.4	±	0.1
865	7.71	0.00455	7.753	13.33	90.57	46.35	123.7	±	0.3
880	7.21	0.00396	7.731	9.74	92.29	53.05	118.2	±	0.2
895	7.69	0.00576	7.412	14.65	85.51	34.97	116.7	±	0.2
915	7.98	0.00697	6.937	2.96	81.14	27.20	15.0	±	0.9
940	8.98	0.00997	7.554	3.44	73.90	20.61	117.8	±	1.3
Fusion	9.02	0.00243	6.843	2.38	98.09	76.74	155.4	±	2.3
Total	9.38	0.01004	7.577	100.00	85.34	40.71	124.2	±	0.4
Total without 620-800°C, fusion				82.20			118.2	±	0.3
Sample 17: J = 0.010144 (amphibolite)									
620	139.52	0.43586	4.409	1.22	7.94	0.28	192.4	±	11.5
720	28.99	0.03808	3.225	2.06	62.06	2.30	302.9	±	0.8
755	19.34	0.01332	3.719	4.10	81.15	7.59	267.0	±	0.8
780	10.13	0.00273	5.494	3.21	96.32	54.65	170.8	±	0.5
795	7.93	0.00350	5.561	13.68	92.53	43.23	130.0	±	0.1
815	7.02	0.00357	5.471	7.07	91.16	41.71	113.8	±	0.2
830	7.16	0.00355	5.517	10.63	91.46	42.29	116.3	±	0.1
850	7.45	0.00316	5.565	15.31	93.39	47.88	123.4	±	0.2
870	7.15	0.00315	5.639	15.69	93.25	48.73	118.5	±	0.1
885	7.09	0.00308	5.678	9.85	93.51	50.11	117.7	±	0.2
900	7.31	0.00332	5.607	15.07	92.65	45.90	120.3	±	0.1
Fusion	9.85	0.00766	5.385	2.10	81.35	19.12	141.4	±	1.7
Total	10.03	0.00980	5.438	100.00	90.44	42.71	133.4	±	0.4
Total without 620-795°C, fusion				73.62			119.0	±	0.1

Table III-1 (continued)

Sample 18: J = 0.010045 (amphibolite)

620	35.67	0.08177	3.390	6.22	33.02	1.13	202.1	±	0.4
720	15.37	0.01735	5.275	8.64	69.36	8.27	184.1	±	0.6
755	14.31	0.01964	10.302	4.14	65.18	14.27	162.5	±	0.9
770	14.59	0.01332	7.460	5.73	77.10	15.24	194.0	±	0.5
790	13.79	0.00841	4.401	8.18	84.50	14.23	200.2	±	0.5
805	10.86	0.00849	7.312	9.97	82.26	23.42	155.8	±	0.3
820	10.26	0.00657	7.761	13.47	87.09	32.12	155.7	±	0.3
835	10.38	0.00673	7.544	11.97	86.63	30.49	156.8	±	0.5
850	9.90	0.00579	8.182	6.19	89.31	38.44	154.3	±	0.3
865	9.70	0.00505	7.730	6.31	90.96	41.63	154.0	±	0.4
885	9.97	0.00565	6.920	4.14	88.78	33.33	154.3	±	0.7
910	9.56	0.00443	7.113	5.67	91.31	43.65	154.0	±	2.0
940	11.44	0.00833	7.244	6.35	84.20	23.64	154.8	±	1.0
Fusion	11.12	0.00925	6.693	3.02	80.21	19.69	155.4	±	2.9
Total	13.03	0.01336	6.904	100.00	80.26	24.68	167.2	±	0.7
Total without 620-790°C				67.09			155.5	±	0.4

CODRU ASSEMBLAGE

Sample 22: J = 0.009744 (amphibolite)

500	161.74	0.46107	6.905	0.56	16.10	0.41	409.4	±	2.9
550	100.36	0.22413	4.232	0.25	34.34	0.51	523.3	±	4.4
580	53.43	0.09179	1.399	0.33	49.44	0.41	413.4	±	2.7
610	58.41	0.09903	6.421	0.14	50.77	1.76	459.4	±	5.3
640	40.43	0.04048	4.175	0.22	71.23	2.81	447.1	±	3.2
670	37.83	0.04159	2.022	0.29	67.93	1.32	403.4	±	3.7
700	29.63	0.01706	5.710	0.37	84.51	9.10	395.0	±	2.5
740	31.06	0.04046	6.808	0.55	63.25	4.58	317.1	±	1.5
780	34.43	0.02788	7.128	0.84	77.72	6.96	419.5	±	0.9
820	27.76	0.01028	8.358	2.24	91.46	22.12	400.6	±	0.3
860	26.07	0.00812	9.253	17.87	93.63	31.01	386.8	±	0.3
900	24.04	0.00764	9.559	8.26	93.78	34.05	360.2	±	0.2
950	23.31	0.00509	9.409	29.60	96.76	50.26	360.3	±	0.2
1000	23.65	0.00459	10.056	31.70	97.66	59.65	368.2	±	0.2
Fusion	25.51	0.00934	9.705	6.79	92.21	28.25	374.2	±	0.1
Total	25.57	0.01020	9.458	100.00	94.46	44.69	371.1	±	0.3

Table III-1 (continued)

Sample 25: J = 0.008811 (amphibolite)

620	69.39	0.08898	4.971	1.80	62.68	1.52	586.7	±	3.5
700	25.46	0.02341	2.621	3.84	73.63	3.05	276.1	±	0.3
730	32.68	0.01512	4.812	2.81	87.49	8.66	406.4	±	0.5
755	51.83	0.02037	8.436	1.82	89.68	11.26	622.0	±	1.9
775	44.64	0.01217	5.528	2.86	92.93	12.36	563.6	±	0.4
790	37.28	0.01581	4.766	3.90	88.48	8.20	461.4	±	2.6
805	29.93	0.00503	4.317	6.66	96.17	23.35	408.7	±	0.5
820	29.27	0.00434	4.754	12.30	96.91	29.83	403.5	±	0.2
835	29.52	0.00424	5.054	17.49	97.11	32.43	407.4	±	0.4
850	29.02	0.00397	5.196	19.17	97.38	35.64	402.2	±	0.3
865	28.94	0.00304	5.432	12.89	98.38	48.56	405.0	±	0.3
880	24.93	0.00455	4.825	7.71	96.14	28.86	346.6	±	0.2
895	24.11	0.00306	7.282	3.06	98.65	64.65	344.7	±	1.3
910	24.01	0.00103	3.415	1.95	99.85	89.97	346.4	±	2.0
Fusion	24.76	0.01143	5.276	1.74	88.05	12.56	317.9	±	1.7
Total	30.43	0.00769	5.028	100.00	94.72	31.43	405.0	±	0.6
Total without 620-790°C, 880°C - fusion				68.51			404.9	±	0.3

Sample 24: J = 0.009322 (amphibolite)

600	198.92	0.55472	12.197	0.75	18.18	0.60	525.1	±	4.0
700	37.50	0.02694	1.457	4.43	79.07	1.47	440.5	±	0.4
750	30.53	0.01627	1.381	6.27	84.60	2.31	389.4	±	0.7
800	41.07	0.04769	10.121	3.01	67.65	5.77	417.8	±	0.9
850	38.01	0.03474	6.883	9.44	74.43	5.39	423.9	±	0.2
875	27.35	0.00659	5.296	10.09	94.41	21.86	390.2	±	0.4
900	25.11	0.00256	5.261	32.71	98.65	56.00	375.9	±	0.1
925	24.74	0.00158	4.118	3.26	99.43	71.00	373.2	±	0.3
950	24.68	0.00261	5.782	10.74	98.73	60.16	370.4	±	0.2
975	24.38	0.00111	5.835	9.17	100.56	143.25	372.5	±	0.2
1000	25.48	0.00611	7.997	6.22	95.42	35.61	370.2	±	0.1
Fusion	25.56	0.00339	7.604	3.90	98.45	61.09	381.7	±	0.3
Total	29.15	0.01355	5.537	100.00	92.65	47.94	386.8	±	0.3
Total without 600-875°C, fusion				62.11			373.7	±	0.2

Table III-1 (continued)

Sample 23: J = 0.008985 (amphibolite)

610	138.53	0.35533	4.746	1.11	24.47	0.36	431.0	±	0.5
710	3.09	0.00068	0.040	1.20	93.44	1.60	46.2	±	0.5
740	28.86	0.04425	1.372	1.82	55.06	0.84	241.0	±	0.3
770	27.05	0.02913	3.703	1.43	69.26	3.46	281.3	±	0.3
800	48.45	0.06398	13.132	0.24	63.14	5.58	441.4	±	2.8
830	48.30	0.05094	10.416	0.82	70.56	5.56	484.7	±	0.4
855	39.72	0.00999	6.891	1.21	93.95	18.76	523.6	±	0.2
880	31.50	0.00725	5.242	5.96	94.51	19.66	428.9	±	0.3
905	27.96	0.01032	4.976	20.73	90.51	13.12	370.7	±	0.3
930	25.73	0.00419	4.884	26.26	96.69	31.72	365.0	±	0.3
965	24.67	0.00081	5.007	15.59	100.63	167.56	364.3	±	0.4
1000	25.62	0.00321	5.281	8.99	97.93	44.70	367.9	±	0.2
1050	25.17	0.00190	5.360	6.66	99.46	76.94	367.2	±	0.2
Fusion	25.50	0.00443	5.145	7.97	96.47	31.61	361.3	±	0.2
Total	27.78	0.01045	4.980	100.00	93.85	30.38	367.1	±	0.3
Total without 610-880°C				86.20			366.4	±	0.3

SOMES ASSEMBLAGE

Sample 28: J = 0.009654 (amphibolite)

620	17.52	0.03376	7.021	11.42	46.25	5.66	136.4	±	3.0
720	13.81	0.01077	2.480	8.94	78.35	6.26	179.5	±	0.1
770	15.84	0.00749	5.569	12.33	88.82	20.23	230.4	±	0.2
800	19.69	0.00520	9.253	11.73	95.94	48.36	303.7	±	0.1
820	20.07	0.00595	10.722	17.18	95.50	48.98	308.1	±	0.2
835	20.02	0.00549	10.013	3.77	95.89	49.65	308.4	±	0.2
850	20.39	0.00697	10.093	5.42	93.85	39.40	307.5	±	1.4
865	20.77	0.00908	8.924	5.35	90.51	26.75	302.4	±	1.1
890	21.46	0.01166	11.093	6.91	88.07	25.88	304.2	±	[illegible]
920	20.65	0.00819	11.022	7.28	92.54	36.60	307.3	±	2.4
950	20.44	0.00759	11.329	4.93	93.67	40.62	307.5	±	0.7
Fusion	20.50	0.00620	8.679	4.74	94.43	38.05	310.5	±	2.1
Total	18.92	0.01051	8.579	100.00	86.36	31.49	266.8	±	1.0
Total without 620-770°C				67.01			306.1	±	0.8

Table III-2. $^{36}Ar/^{40}Ar$ vs. $^{40}Ar/^{39}Ar$ plateau isotope-correlations for hornblende concentrates from structural units comprising the Apuseni Mountains, Romania.

Sample	Isotope Correlation Age (Ma)*	$^{40}Ar/^{36}Ar$ Intecept**	MSWD	Increments Included'	% of total ^{39}Ar	Calculated $^{40}Ar/^{39}Ar$ Plateau Age (Ma)
BAIA DE ARIES ASSEMBLAGE						
15	117.2 ± 0.4	296.5 ± 3.8	1.23	820-940	82.20	118.2 ± 0.3
17	115.8 ± 0.3	367.2 ± 12.9	1.98	815-900	73.62	119.0 ± 0.1
18	151.6 ± 1.2	334.1 ± 8.4	1.15	805-fusion	67.09	155.5 ± 0.4
CODRU ASSEMBLAGE						
23	400.8 ± 1.2	366.1 ± 17.3	1.66	805-865	68.51	404.9 ± 0.3
24	372.2 ± 0.3	298.1 ± 8.3	1.03	900-1000	62.11	373.7 ± 0.2
25	364.4 ± 0.3	331.8 ± 2.9	1.11	905-fusion	86.20	366.4 ± 0.3
SOMES ASSEMBLAGE						
28	300.4 ± 1.0	376.5 ± 12.1	1.87	800-fusion	67.01	306.1 ± 0.8
30	313.6 ± 1.0	314.5 ± 3.1	1.36	720-920	87.62	316.7 ± 0.5

Calculated using the inverse abscissa intercept ($^{40}Ar/^{39}Ar$ ratio) in the age equation.

*Inverse ordinate intercept.

** Table III-1

°C.

Table III-3. ^{40}Ar/^{39}Ar analytical data for incremental-heating experiments on muscovite concentrates from structural units comprising the Apuseni Mountains, Romania.

Release temp (°C)	(^{40}Ar/^{39}Ar)*	(^{36}Ar/^{39}Ar)*	(^{37}Ar/^{39}Ar)^{c}	^{39}Ar % of total	%^{40}Ar non-atmos.+	^{36}Ar$_{Ca}$ %	Apparent Age (Ma) **		
				HIGHIS-BIHARIA SHEAR ZONE					
Sample 3: J = 0.010045 (mylonitic metaconglomerate)									
380	40.18	0.10500	1.133	0.46	22.98	0.29	160.1	±	1.2
420	12.09	0.00127	0.080	1.63	96.91	1.71	200.7	±	0.8
455	12.89	0.00436	0.146	2.73	90.06	0.91	199.1	±	0.3
490	14.55	0.00188	0.051	3.23	96.18	0.74	237.2	±	0.2
525	15.86	0.00032	0.027	5.04	99.37	2.27	265.1	±	0.2
560	17.50	0.00356	0.014	6.78	93.95	0.11	275.8	±	0.2
595	18.13	0.00059	0.056	11.88	99.03	2.59	299.1	±	0.3
630	18.39	0.00070	0.074	13.48	98.87	2.86	302.6	±	0.2
665	18.40	0.00139	0.056	15.74	97.77	1.11	299.7	±	0.2
700	18.21	0.00095	0.096	12.03	98.47	2.76	298.8	±	0.2
735	17.81	0.00020	0.050	7.46	99.66	6.97	296.0	±	0.2
770	17.87	0.00021	0.073	5.40	99.65	9.37	296.9	±	0.2
810	18.15	0.00107	0.037	4.58	98.25	0.95	297.2	±	0.1
850	18.43	0.00094	0.040	4.11	98.48	1.17	302.1	±	0.2
890	18.18	0.00223	0.184	2.89	96.43	2.25	292.7	±	0.1
Fusion	18.53	0.00389	0.196	2.55	93.85	1.37	290.5	±	0.1
Total	17.79	0.00172	0.073	100.00	97.51	2.62	288.6	±	0.2
Total without 380-560°C, 890°C - fusion				74.68			299.4	±	0.2

Table III-1 (continued)

Sample 30: J= 0.009233 (amphibolite)

620	38.68	0.05833	7.637	10.11	57.01	3.56	335.7	±	0.2
720	22.28	0.00690	3.302	16.32	92.02	13.02	313.2	±	0.7
745	25.66	0.01755	5.756	15.47	81.57	8.92	319.7	±	0.3
770	24.04	0.01305	6.371	9.29	86.06	13.28	316.4	±	0.5
785	23.20	0.01161	10.882	11.41	88.96	25.50	316.6	±	0.3
800	22.81	0.01008	10.089	11.91	90.47	27.23	316.3	±	0.4
815	21.80	0.00603	10.282	7.48	95.59	46.40	319.3	±	0.4
830	22.39	0.00874	9.828	3.80	91.96	30.57	315.7	±	1.5
920	22.34	0.00823	11.485	11.95	98.51	73.88	315.8	±	0.3
Fusion	20.54	0.01498	7.189	2.26	81.24	13.06	259.5	±	1.9
Total	24.73	0.01510	7.914	100.00	86.57	25.01	319.6	±	0.5
Total without 620, fusion				87.62			316.7	±	0.5

[*] measured.

[c] corrected for post-irradiation decay of ^{37}Ar (35.1 day 1/2-life).

[+] [$^{40}Ar_{tot.}$ - ($^{36}Ar_{atmos.}$) (295.5)] / $^{40}Ar_{tot.}$.

[**] calculated using correction factors of Dalrymple et al. (1981); two sigma, intralaboratory errors.

Table III-3 (continued).

Sample 5: J = 0.009160 (mylonitic granite)

500	8.67	0.01033	0.033	3.71	64.74	0.09	90.4	±	0.1
550	6.11	0.00006	0.067	4.53	99.70	30.82	98.0	±	0.1
580	6.81	0.00148	0.016	10.34	93.53	0.29	102.3	±	0.1
610	6.76	0.00015	0.007	8.38	99.26	1.30	107.6	±	0.1
640	6.58	0.00032	0.007	12.58	98.50	0.63	104.1	±	0.1
670	7.00	0.00051	0.008	13.82	97.76	0.42	109.7	±	0.2
700	7.27	0.00018	0.004	13.75	99.19	0.64	115.4	±	0.1
740	7.62	0.00003	0.002	13.84	99.80	2.00	121.4	±	0.1
780	7.85	0.00101	0.012	7.41	96.12	0.32	120.6	±	0.2
820	7.78	0.00019	0.003	3.87	99.21	0.46	123.3	±	0.2
860	8.12	0.00041	0.035	4.03	98.45	2.31	127.6	±	0.1
900	8.46	0.00148	0.019	2.15	94.77	0.35	127.9	±	0.1
Fusion	8.89	0.00594	0.194	1.60	80.35	0.89	114.4	±	0.1
Total	7.25	0.00092	0.015	100.00	96.50	2.20	111.7	±	0.1

Sample 7: J = 0.010095 (mylonitic schist)

500	11.67	0.01521	0.096	1.75	61.51	0.17	126.2	±	1.3
550	11.21	0.00357	0.142	3.55	90.64	1.08	176.1	±	0.2
585	11.20	0.00022	0.019	4.11	99.38	2.37	192.1	±	0.2
620	12.22	0.00077	0.031	6.91	98.11	1.10	206.0	±	0.2
650	12.91	0.00041	0.045	5.99	99.05	2.99	219.0	±	0.2
685	13.75	0.00029	0.020	7.34	99.34	1.90	233.1	±	0.2
715	15.16	0.00038	0.020	16.92	99.22	1.42	255.0	±	0.1
750	15.66	0.00055	0.021	15.58	98.94	1.06	262.2	±	0.1
785	16.42	0.00062	0.021	14.67	98.85	0.91	273.7	±	0.2
820	16.95	0.00041	0.025	13.51	99.27	1.68	283.1	±	0.1
850	17.66	0.00069	0.084	5.20	98.85	3.32	292.9	±	0.2
880	18.23	0.00367	0.095	3.31	94.06	0.70	288.1	±	0.2
Fusion	18.40	0.00887	0.257	1.16	85.83	0.79	266.8	±	0.2
Total	15.13	0.00106	0.037	100.00	97.75	1.50	251.1	±	0.2

Table III-3 (continued).

Sample 9: J = 0.008902 (mylonitic granite)

500	14.04	0.02247	0.045	1.49	52.68	0.05	115.0	±	0.1
550	11.91	0.00162	0.012	3.38	95.93	0.21	174.6	±	0.2
580	12.72	0.00303	0.011	4.50	92.91	0.09	180.4	±	0.1
610	12.42	0.00078	0.003	3.24	98.09	0.11	185.7	±	0.2
640	12.83	0.00082	0.002	4.54	98.07	0.08	191.5	±	0.1
670	15.72	0.01012	0.004	6.53	80.94	0.01	193.5	±	0.3
700	14.67	0.00071	0.012	8.10	98.55	0.47	218.4	±	0.2
740	15.27	0.00069	0.002	15.62	98.63	0.08	227.0	±	0.2
780	14.74	0.00065	0.003	19.98	98.66	0.14	219.6	±	0.3
820	14.06	0.00068	0.009	18.89	98.53	0.37	209.8	±	0.4
860	13.58	0.00041	0.031	8.46	99.09	2.10	204.1	±	0.2
900	13.10	0.00046	0.024	4.01	98.93	1.44	197.0	±	0.1
Fusion	13.28	0.00013	0.124	1.26	99.75	26.89	201.1	±	0.1
Total	14.21	0.00173	0.011	100.00	96.44	0.74	207.4	±	0.2

Sample 10: J = 0.009782 (mylonitic granite)

500	22.87	0.03114	0.056	1.34	59.76	0.05	226.3	±	0.2
550	16.60	0.00068	0.015	0.65	98.77	0.60	268.3	±	0.1
580	17.11	0.00304	0.009	1.80	94.73	0.08	265.5	±	0.2
610	18.05	0.00614	0.012	1.61	89.91	0.05	265.8	±	0.2
670	18.35	0.00144	0.009	2.71	97.65	0.18	291.4	±	0.2
700	18.83	0.00221	0.007	7.20	96.50	0.08	295.2	±	0.2
740	19.77	0.00166	0.007	7.40	97.49	0.12	311.6	±	0.2
780	20.16	0.00113	0.009	1.20	98.32	0.22	319.8	±	0.1
820	20.65	0.00088	0.006	20.47	98.71	0.18	327.9	±	0.1
860	20.80	0.00135	0.008	28.17	98.05	0.17	328.2	±	0.2
900	21.09	0.00122	0.011	18.20	98.26	0.23	333.0	±	0.2
950	21.32	0.00068	0.012	6.91	99.03	0.47	338.7	±	0.3
Fusion	21.36	0.00033	0.043	2.34	99.53	3.58	340.9	±	0.1
Total	20.47	0.00175	0.010	100.00	97.47	0.27	321.4	±	0.1

Table III-3 (continued).

BAIA DE ARIES ASSEMBLAGE

Sample 14: J = 0.009802 (schist)

500	11.38	0.02147	0.054	0.94	44.24	0.07	86.9	±	0.1
550	9.30	0.00762	0.004	1.06	75.71	0.01	120.4	±	0.2
580	7.75	0.00175	0.031	2.05	93.28	0.49	123.6	±	0.1
610	7.59	0.00101	0.028	1.62	96.00	0.76	124.4	±	0.1
640	7.44	0.00185	0.018	2.33	92.58	0.27	117.9	±	0.1
670	7.34	0.00172	0.005	8.77	93.01	0.08	116.9	±	0.1
700	7.05	0.00105	0.002	17.51	95.52	0.06	115.3	±	0.1
740	7.04	0.00073	0.002	25.55	96.84	0.07	116.6	±	0.1
780	7.49	0.00179	0.007	6.34	92.88	0.11	119.0	±	0.1
820	7.31	0.00123	0.021	6.23	94.96	0.47	118.8	±	0.2
860	7.20	0.00098	0.020	6.64	95.94	0.56	118.2	±	0.1
900	7.03	0.00103	0.006	7.96	95.61	0.16	115.1	±	0.1
950	7.15	0.00073	0.005	11.87	96.90	0.19	118.5	±	0.1
Fusion	7.40	0.00315	0.002	1.12	87.36	0.02	110.8	±	0.2
Total	7.24	0.00136	0.008	100.00	94.74	0.17	116.9	±	0.1
Total without 500-610°C, 900°C-fusion				73.37			116.9	±	0.1

Sample 16: J = 0.009185 (mylonitic gneiss)

510	10.95	0.00973	0.552	1.51	74.10	1.54	129.7	±	1.6
560	12.87	0.00793	0.498	1.76	82.07	1.71	167.1	±	0.9
595	7.33	0.00220	0.013	3.86	91.07	0.16	107.4	±	0.2
630	7.59	0.00219	0.048	4.35	91.46	0.60	111.5	±	0.1
665	7.42	0.00177	0.066	6.54	92.96	1.02	110.8	±	0.1
695	7.14	0.00103	0.038	14.98	95.69	0.99	109.8	±	0.1
25	7.37	0.00165	0.112	21.46	93.44	1.86	110.6	±	0.2
755	7.21	0.00119	0.014	10.52	95.07	0.31	110.1	±	0.1
785	7.08	0.00040	0.016	9.54	98.28	1.11	111.7	±	0.1
825	7.12	0.00072	0.009	5.90	96.92	0.32	110.8	±	0.1
865	7.09	0.00071	0.037	8.57	97.01	1.40	110.5	±	0.1
Fusion	7.07	0.00038	0.014	11.01	98.35	0.97	111.8	±	0.1
Total	7.38	0.00140	0.062	100.00	94.76	1.09	111.9	±	0.2
Total without 510-595°C				92.87			110.7	±	0.1

Table III-3 (continued).

CODRU ASSEMBLAGE

Sample 20: J = 0.009645 (schist)

500	29.75	0.03588	0.072	1.12	64.37	0.05	305.8	±	0.4
550	18.77	0.00284	0.002	1.97	95.50	0.02	287.7	±	0.1
580	20.43	0.00366	0.005	2.83	94.68	0.04	308.6	±	0.2
610	20.14	0.00287	0.022	2.66	95.76	0.21	307.7	±	0.2
640	20.99	0.00115	0.004	.76	98.35	0.10	327.6	±	0.2
670	21.48	0.00057	0.004	5.92	99.19	0.18	337.2	±	0.2
700	21.79	0.00175	0.001	10.24	97.59	0.02	336.5	±	0.2
740	21.82	0.00128	0.003	13.05	98.24	0.06	339.1	±	0.2
780	21.86	0.00141	0.002	8.34	98.07	0.05	339.0	±	0.3
820	21.84	0.00124	0.006	14.17	98.30	0.14	339.5	±	0.2
860	21.98	0.00149	0.003	14.48	97.97	0.05	340.4	±	0.2
900	22.14	0.00139	0.005	14.31	98.12	0.09	343.1	±	0.2
Fusion	21.98	0.00093	0.004	7.15	98.72	0.13	342.8	±	0.1
Total	21.80	0.00184	0.005	100.00	97.61	0.08	336.3	±	0.2
Total without 510-580°C, 840°C and fusion				87.67			339.9	±	0.2

Sample 21: J = 0.009432 (schist)

500	19.29	0.03144	0.062	1.10	51.84	0.05	162.6	±	0.3
550	15.40	0.00201	0.049	1.88	96.13	0.66	235.7	±	0.1
580	17.88	0.01167	0.056	0.97	80.71	0.13	230.2	±	0.3
610	17.96	0.00345	0.001	1.97	94.28	0.01	267.2	±	0.3
640	19.38	0.00209	0.006	2.68	96.78	0.07	293.9	±	0.2
670	21.03	0.00242	0.007	4.66	96.57	0.07	316.1	±	0.2
700	21.51	0.00280	0.002	4.14	96.12	0.02	321.4	±	0.2
740	21.99	0.00208	0.008	15.48	97.18	0.11	331.2	±	0.2
780	22.01	0.00130	0.002	18.87	98.23	0.03	334.7	±	0.2
820	21.98	0.00138	0.004	12.96	98.12	0.09	333.9	±	0.2
860	22.03	0.00129	0.003	19.10	98.24	0.06	335.0	±	0.3
900	22.34	0.00111	0.004	9.34	98.51	0.09	340.1	±	0.1
950	22.20	0.00031	0.005	5.54	99.56	0.41	341.6	±	0.2
Fusion	21.96	0.00034	0.041	1.32	99.54	3.35	338.1	±	0.2
Total	21.64	0.00197	0.007	100.00	97.17	0.14	326.4	±	0.2
Total without 500-700°C, 950°C-fusion				75.74			334.6	±	0.2

Table III-3 (continued).

SOMES ASSEMBLAGE

Sample 26: J = 0.009202 (retrogressed schist)

550	10.22	0.00356	0.029	2.13	89.66	0.22	146.1	±	0.2
580	11.99	0.00707	0.007	2.02	82.52	0.03	157.1	±	0.2
610	11.38	0.00083	0.011	5.23	97.79	0.37	175.8	±	0.3
640	12.04	0.00036	0.001	3.45	99.07	0.11	187.8	±	0.2
670	12.80	0.00110	0.009	5.77	97.42	0.23	195.9	±	0.1
700	13.75	0.00111	0.002	7.66	97.56	0.05	210.0	±	0.1
740	15.89	0.00066	0.004	13.50	98.73	0.16	243.2	±	0.4
780	17.43	0.00095	0.003	15.39	98.36	0.09	264.2	±	0.2
820	18.68	0.00079	0.004	17.83	98.73	0.12	282.8	±	0.2
860	19.41	0.00056	0.003	18.37	99.12	0.14	294.0	±	0.2
900	19.75	0.00097	0.005	7.54	98.52	0.14	297.1	±	0.2
Fusion	19.98	0.00033	0.004	1.11	99.48	0.34	303.0	±	0.2
Total	16.70	0.00098	0.005	100.00	98.01	0.14	253.0	±	0.2

Sample 27: J = 0.009973 (micaceous quartzite)

510	17.53	0.01402	0.057	2.50	76.37	0.11	226.1	±	0.8
540	18.09	0.01147	0.047	4.07	81.25	0.11	246.7	±	0.4
580	16.44	0.00104	0.030	4.29	98.11	0.80	269.0	±	0.1
615	17.27	0.00154	0.067	6.90	97.37	1.19	279.6	±	0.2
650	17.94	0.00094	0.025	7.02	98.43	0.71	292.5	±	0.2
680	18.45	0.00028	0.020	8.30	99.53	1.98	303.3	±	0.3
710	18.44	0.00042	0.014	10.97	99.30	0.91	302.5	±	0.3
740	18.30	0.00022	0.027	11.25	99.63	3.43	301.3	±	0.3
765	18.43	0.00068	0.019	10.89	98.89	0.75	301.2	±	0.2
795	18.35	0.00060	0.015	6.66	99.01	0.67	300.3	±	0.1
825	18.75	0.00150	0.058	6.84	97.63	1.06	302.4	±	0.2
860	19.00	0.00173	0.084	8.07	97.32	1.33	305.3	±	0.2
895	18.89	0.00154	0.044	7.92	97.58	0.77	304.3	±	0.1
930	19.51	0.00090	0.090	3.10	98.64	2.72	316.7	±	0.1
Fusion	19.05	0.00230	0.600	1.21	96.65	7.10	304.1	±	1.0
Total	18.32	0.00166	0.045	100.00	97.28	1.36	295.1	±	0.2
Total without 510-650°C, 930°C -fusion				70.92			302.5	±	0.2

Table III-3 (continued).

Sample 29: J = 0.009695 (retrogressed gneiss)

510	20.89	0.01544	0.014	1.41	78.13	0.03	265.0	±	1.0
560	19.39	0.00424	0.053	3.18	93.52	0.34	292.2	±	0.2
595	18.76	0.00010	0.017	6.55	99.82	4.62	300.9	±	0.2
630	19.80	0.00082	0.076	8.86	98.78	2.52	313.3	±	0.2
665	19.92	0.00082	0.019	17.88	98.76	0.62	314.9	±	0.2
695	19.96	0.00058	0.013	16.56	99.12	0.61	316.6	±	0.3
725	19.73	0.00074	0.055	9.25	98.88	2.00	312.6	±	0.3
755	19.68	0.00064	0.056	7.24	99.03	2.36	312.3	±	0.1
785	19.72	0.00047	0.047	7.53	99.28	2.72	313.5	±	0.2
815	19.60	0.00047	0.032	7.85	99.28	1.84	311.7	±	0.3
850	19.61	0.00050	0.061	7.50	99.23	3.28	311.8	±	0.3
885	19.76	0.00088	0.024	5.19	98.67	0.74	312.4	±	0.2
Fusion	19.38	0.00432	0.077	0.98	93.41	0.49	291.7	±	0.6
Total	19.73	0.00099	0.037	100.00	98.52	1.74	311.4	±	0.3
Total without 510-595°C, and fusion				87.88			313.8	±	0.2

Sample 31: J = 0.010025 (Muntele Mare granite)

510	11.70	0.01762	0.354	2.09	55.71	0.55	114.3	±	1.2
560	13.08	0.01334	0.326	3.59	70.03	0.67	158.5	±	0.3
595	9.74	0.00026	0.127	3.00	99.25	13.25	166.9	±	0.3
630	10.13	0.00198	0.053	6.09	94.21	0.73	164.8	±	0.1
665	10.48	0.00098	0.047	6.20	97.23	1.32	175.5	±	0.2
695	11.16	0.00010	0.016	9.81	99.69	4.29	190.7	±	0.3
725	11.64	0.00141	0.033	11.28	96.38	0.63	192.2	±	0.2
755	11.44	0.00122	0.062	10.61	96.85	1.39	190.1	±	0.1
785	11.53	0.00112	0.074	10.75	97.13	1.80	191.9	±	0.2
815	11.75	0.00200	0.058	9.88	94.96	0.79	191.4	±	0.1
845	12.33	0.00150	0.047	7.81	96.39	0.86	203.1	±	0.2
880	12.62	0.00085	0.085	5.55	98.01	2.70	210.8	±	0.1
915	12.90	0.00180	0.084	7.72	95.88	1.28	210.8	±	0.3
Fusion	13.18	0.00282	0.081	5.62	93.68	0.78	210.5	±	0.2
Total	11.69	0.00211	0.074	100.00	94.81	1.83	189.8	±	0.2
Total without 510-665°C, 845°C-fusion				52.33			191.3	±	0.2

Table III-3 (continued).

Sample 32: J = 0.009295 (retrogressed gneiss)

510	25.92	0.06609	0.621	1.35	24.83	0.26	104.9	±	0.9
560	10.54	0.01091	0.022	3.59	69.39	0.06	118.7	±	0.3
595	7.65	0.00664	0.047	6.74	74.35	0.19	93.0	±	0.1
630	7.74	0.00051	0.070	9.09	98.06	3.76	112.9	±	0.2
665	7.66	0.00017	0.042	15.48	99.31	6.71	123.2	±	0.2
695	7.76	0.00092	0.073	12.60	96.51	2.16	121.5	±	0.1
725	8.08	0.00152	0.078	8.84	94.44	1.40	123.7	±	0.3
755	8.04	0.00149	0.149	6.46	94.59	2.71	123.3	±	0.1
785	8.19	0.00185	0.077	6.61	93.34	1.13	123.9	±	0.2
815	8.04	0.00621	0.086	5.90	77.19	0.38	101.2	±	0.3
850	7.60	0.00420	0.152	6.57	83.74	0.99	103.7	±	0.3
885	7.29	0.00247	0.139	6.89	90.07	1.53	106.9	±	0.2
920	7.34	0.00176	0.219	3.63	93.06	3.38	111.1	±	0.5
955	7.40	0.00081	0.212	3.95	96.93	7.16	116.4	±	0.4
Fusion	7.33	0.00047	0.093	2.30	98.12	5.37	116.8	±	0.8
Total	8.09	0.00319	0.099	100.00	90.64	2.77	116.0	±	0.2
Total without 510-595°C, 815°C-fusion				59.08			122.9	±	0.2

Sample 33: J = 0.008882 (retrogressed mylonitic gneiss)

510	17.74	0.04636	0.251	0.48	22.88	0.15	63.9	±	0.4
560	8.89	0.00814	0.063	3.26	72.92	0.21	100.9	±	0.3
595	6.70	0.00254	0.077	5.05	88.79	0.83	92.9	±	0.3
630	6.72	0.00174	0.026	6.36	92.31	0.40	96.7	±	0.3
665	6.69	0.00096	0.037	8.72	95.70	1.04	99.8	±	0.2
695	6.59	0.00024	0.020	14.51	98.85	2.23	101.5	±	0.1
725	6.63	0.00080	0.027	13.61	96.38	0.91	99.5	±	0.2
755	6.90	0.00122	0.068	14.74	94.77	1.52	101.8	±	0.2
785	6.94	0.00166	0.046	9.84	92.90	0.75	100.4	±	0.2
815	6.80	0.00126	0.033	8.29	94.49	0.72	100.1	±	0.2
850	6.25	0.00032	0.023	6.38	98.44	1.97	96.0	±	0.1
885	6.74	0.00020	0.064	5.06	99.09	8.47	103.9	±	0.1
Fusion	6.32	0.00020	0.026	3.69	99.02	3.65	97.6	±	0.1
Total	6.82	0.00144	0.042	100.00	94.55	1.66	99.6	±	0.2
Total without 510-630°C, 850°C-fusion				69.71			100.6	±	0.2

[*] measured.

[c] corrected for post-irradiation decay of ^{37}Ar (35.1 day 1/2-life).

[+] $[^{40}Ar_{tot.} - (^{36}Ar_{atmos.})\,(295.5)] / ^{40}Ar_{tot.}$.

[**] calculated using correction factors of Dalrymple et al. (1981); two sigma, intralaboratory errors.

Table III-4. ^{40}Ar/^{39}Ar analytical data for incremental-heating experiments on whole-rock samples of slate/phyllite or phyllonite from structural units comprising the Apuseni Mountains, Romania.

Release temp (°C)	(^{40}Ar/^{39}Ar)*	(^{36}Ar/^{39}Ar)*	(^{37}Ar/^{39}Ar)^{c}	^{39}Ar % of total	%^{40}Ar non-atmos.+	^{36}Ar$_{Ca}$ %	Apparent Age (Ma) **		
HIGHIS-BIHARIA SHEAR ZONE									
Sample 1: J = 0.009625 (phyllonite)									
420	8.44	0.01279	0.070	1.59	55.25	0.15	79.2	±	0.2
455	7.89	0.00656	0.031	2.59	75.38	0.05	100.4	±	0.1
490	7.64	0.00117	0.037	2.14	95.42	0.85	122.3	±	0.1
525	7.55	0.00264	0.045	3.06	89.63	0.46	113.8	±	0.1
560	7.08	0.00008	0.038	3.48	99.62	2.70	114.0	±	0.1
595	7.19	0.00082	0.037	4.58	96.58	1.23	116.7	±	0.1
630	7.13	0.00100	0.010	24.96	95.78	0.28	114.9	±	0.1
665	7.08	0.00127	0.026	7.88	94.66	0.57	112.8	±	0.1
700	6.90	0.00062	0.018	9.26	97.30	0.81	112.9	±	0.1
735	6.85	0.00018	0.019	9.81	99.17	2.87	114.3	±	0.1
770	6.83	0.00042	0.012	7.69	98.12	0.79	112.8	±	0.3
810	6.82	0.00042	0.044	3.02	98.14	2.87	112.7	±	0.2
850	7.49	0.00080	0.040	7.41	96.78	0.36	121.6	±	0.1
890	7.22	0.00015	0.044	7.66	99.35	7.94	120.5	±	0.1
Fusion	7.16	0.00267	0.035	4.86	88.95	0.36	107.4	±	0.3
Total	7.16	0.00119	0.022	100.00	95.23	1.46	114.4	±	0.1
Total without 420-560°C, 850°C-fusion				67.20			114.1	±	0.1

Table III-4 (continued).

Sample 2: J = 0.009655 (phyllonite)

400	8.16	0.01010	0.068	1.47	63.44	0.18	88.0	±	0.1
440	7.70	0.00455	0.088	2.40	82.47	0.05	107.3	±	0.1
475	8.35	0.00318	0.172	2.41	90.04	1.47	101.0	±	0.2
550	7.94	0.00777	0.068	2.54	71.08	0.24	95.7	±	0.4
590	7.20	0.00641	0.087	3.22	73.62	0.03	90.1	±	0.1
600	6.94	0.00478	0.061	3.72	79.62	0.35	93.8	±	0.2
625	6.92	0.00329	0.021	13.75	85.88	0.17	100.7	±	0.2
650	6.41	0.00165	0.026	6.84	92.32	0.43	100.2	±	0.2
675	7.58	0.00563	0.035	8.50	78.01	0.17	100.2	±	0.1
700	7.43	0.00531	0.043	5.21	78.82	0.06	99.2	±	0.2
725	7.58	0.00606	0.052	8.58	76.35	0.23	98.1	±	0.3
750	7.64	0.00619	0.122	5.87	76.08	0.54	98.5	±	0.6
775	7.52	0.00552	0.068	7.00	78.32	0.34	99.8	±	0.3
800	8.04	0.00311	0.038	9.11	88.53	0.33	119.9	±	0.2
825	8.40	0.00146	0.016	13.01	94.91	0.30	133.8	±	0.1
840	8.68	0.01024	0.032	3.25	65.10	0.08	95.8	±	0.3
Fusion	9.15	0.01147	0.150	3.13	63.03	0.36	97.8	±	0.6
Total	7.66	0.00467	0.045	100.00	82.07	0.29	106.1	±	0.2
Total without 400-600°C, 800°C-fusion				55.76			99.7	±	0.3

Sample 4: J = 0.009601 (phyllonitic granite)

430	8.05	0.00444	0.085	0.44	83.70	0.52	113.1	±	0.4
500	12.46	0.02650	0.017	0.87	37.11	0.02	78.3	±	0.4
575	6.86	0.00132	0.087	2.92	94.34	1.79	108.7	±	0.2
600	6.40	0.00004	0.015	4.54	99.74	10.01	107.3	±	0.1
635	6.36	0.00009	0.013	8.03	99.50	3.84	106.4	±	0.1
650	6.44	0.00027	0.006	12.20	98.69	0.65	106.9	±	0.1
680	6.55	0.00034	0.006	16.28	98.39	0.50	108.3	±	0.1
700	6.57	0.00039	0.007	11.61	98.17	0.63	108.3	±	0.1
720	6.92	0.00169	0.006	11.40	92.70	0.10	107.9	±	0.1
750	7.13	0.00232	0.015	10.09	90.30	0.18	108.1	±	0.6
780	7.49	0.00003	0.014	3.79	99.82	13.40	125.1	±	0.3
800	7.69	0.00006	0.019	7.73	99.70	8.09	128.2	±	0.1
830	7.83	0.00227	0.009	7.40	91.37	0.10	119.9	±	0.2
Fusion	7.89	0.00591	0.056	2.69	77.85	0.26	103.4	±	0.3
Total	6.94	0.00119	0.014	100.00	95.45	2.23	110.5	±	0.2
Total without 430-500°C, 780°C-fusion				77.07			107.7	±	0.2

Table III-4 (continued).

Sample 6: J = 0.009375

510	8.20	0.00460	0.096	0.94	83.44	0.56	112.1	±	0.3
580	6.57	0.00602	0.089	2.06	72.94	0.40	79.2	±	0.2
600	12.21	0.02551	0.095	1.85	38.23	0.02	77.3	±	0.4
630	8.39	0.00344	0.169	1.26	89.25	1.33	86.5	±	0.3
650	8.96	0.01008	0.212	0.95	66.89	0.57	98.7	±	0.5
670	8.85	0.00546	0.093	2.48	81.71	0.06	118.4	±	0.6
700	8.76	0.00337	0.065	10.91	88.62	0.52	126.8	±	0.3
720	12.44	0.00248	0.092	7.58	94.11	1.00	187.9	±	0.4
740	13.38	0.00292	0.063	8.34	93.54	0.58	200.2	±	0.2
765	14.14	0.00199	0.050	8.95	95.82	0.69	215.7	±	0.2
780	13.78	0.00066	0.047	10.94	98.58	1.94	216.3	±	0.2
800	13.77	0.00057	0.038	6.37	98.76	1.81	216.5	±	0.2
820	13.67	0.00030	0.041	9.47	99.34	3.73	216.2	±	0.3
840	14.34	0.00248	0.027	14.29	94.87	0.29	216.5	±	0.2
Fusion	14.47	0.00276	0.069	13.60	94.36	0.68	217.2	±	0.2
Total	12.84	0.00276	0.056	100.00	92.84	1.10	192.2	±	0.3
Total without 510-740°C				63.63			216.5	±	0.2

Sample 8: J = 0.009655

510	54.63	0.00843	1.528	0.38	95.66	4.93	737.5	±	7.9
580	91.38	0.28145	0.379	0.38	17.99	0.04	292.6	±	9.8
610	16.87	0.01852	0.275	1.14	67.66	0.40	188.7	±	1.0
640	17.95	0.01927	0.082	7.04	84.72	0.09	207.1	±	0.3
675	17.59	0.01649	0.098	4.04	72.32	0.16	209.0	±	0.4
700	18.78	0.02138	0.137	5.71	66.39	0.17	205.1	±	0.4
720	17.50	0.01445	0.128	5.59	75.62	0.24	216.9	±	0.4
775	18.26	0.00065	0.110	10.70	98.96	4.59	290.1	±	0.3
800	16.82	0.00251	0.031	12.89	95.57	0.33	260.3	±	0.3
820	11.45	0.00015	0.041	6.68	99.58	7.27	188.4	±	0.2
850	11.83	0.00232	0.058	6.51	94.27	1.86	184.5	±	0.4
875	11.75	0.00126	0.067	9.71	96.83	1.45	188.0	±	0.2
900	11.30	0.00015	0.070	13.30	99.62	12.99	186.2	±	0.2
Fusion	11.23	0.00036	0.086	15.92	99.06	6.51	184.0	±	0.2
Total	14.90	0.00541	0.090	100.00	92.24	4.10	217.3	±	0.3
Total without 510-800°C				52.13			185.9	±	0.2

Table III-4 (continued).

BAIA DE ARIES ASSEMBLAGE

Sample 11: J = 0.008845 (phyllite)

450	52.74	0.02606	1.526	0.24	85.62	1.59	606.7	±	7.4
510	20.78	0.04514	0.326	1.01	35.89	0.20	115.3	±	2.1
580	10.65	0.01467	0.267	1.45	59.44	0.50	98.3	±	0.7
600	7.57	0.00171	0.097	1.77	93.34	1.54	109.4	±	0.3
630	9.13	0.00577	0.092	2.27	81.36	0.44	114.8	±	0.6
650	9.01	0.00348	0.089	2.38	89.05	1.47	107.6	±	0.3
675	7.48	0.00468	0.059	2.80	81.51	0.34	94.8	±	0.5
700	6.76	0.00160	0.053	5.75	92.98	0.89	97.6	±	0.2
725	6.69	0.00039	0.026	3.66	98.24	1.83	101.9	±	0.3
760	8.69	0.00037	0.013	10.96	98.70	1.00	131.9	±	0.1
780	9.43	0.00142	0.022	7.15	95.52	0.42	138.3	±	0.3
810	9.70	0.00030	0.026	11.18	99.06	2.35	147.1	±	0.1
840	10.27	0.00124	0.029	13.15	96.42	0.86	151.5	±	0.4
860	10.96	0.00066	0.019	22.33	98.18	0.78	164.1	±	0.3
Fusion	11.43	0.00103	0.022	13.91	97.30	0.59	169.3	±	0.5
Total	10.00	0.00184	0.043	100.00	95.12	0.99	144.5	±	0.3

Sample 12: J = 0.009625 (phyllonitic orthogneiss)

510	51.82	0.02797	1.426	0.45	84.26	1.39	633.5	±	7.4
580	10.49	0.01636	0.279	2.65	54.06	0.46	95.9	±	0.8
610	7.57	0.00171	0.099	3.26	93.34	1.58	118.7	±	0.4
640	9.04	0.00529	0.093	4.18	82.72	0.48	125.4	±	0.7
675	20.81	0.04934	0.088	0.86	30.30	0.57	136.4	±	2.5
710	14.87	0.00982	0.097	4.15	80.65	1.13	197.1	±	0.7
740	18.45	0.02375	0.205	4.46	47.89	0.23	208.5	±	0.4
775	16.00	0.00047	0.094	10.82	99.15	5.48	256.3	±	0.2
790	13.65	0.00093	0.298	6.96	98.11	8.67	218.8	±	0.3
815	14.17	0.01075	0.347	8.46	77.73	0.88	181.8	±	0.4
840	10.87	0.00261	0.521	7.22	93.23	5.43	167.9	±	0.3
875	11.08	0.00292	0.231	14.49	92.32	2.15	169.4	±	0.1
900	10.95	0.00259	0.087	17.29	93.02	0.92	168.7	±	0.2
Fusion	11.04	0.00300	0.284	14.76	92.13	2.57	168.5	±	0.1
Total	12.32	0.00525	0.244	100.00	87.97	2.66	177.5	±	0.3
Total without 510-815°C				53.77			168.7	±	0.2

Table III-4 (continued).

Sample 13: J = 0.009103 (phyllonitic orthogneiss)

430	8.14	0.01139	0.096	4.48	58.70	0.23	76.8	±	0.3
510	10.14	0.00839	0.125	1.48	83.23	0.09	82.4	±	1.8
580	8.30	0.00247	0.146	2.28	95.26	1.60	102.6	±	1.2
600	7.43	0.00095	0.091	4.47	96.23	2.61	113.7	±	0.3
620	9.46	0.00233	0.321	4.27	92.93	3.75	138.8	±	0.2
650	9.27	0.00226	0.322	4.28	93.00	3.87	136.2	±	0.2
670	9.34	0.00349	0.186	6.04	89.05	1.45	131.6	±	0.3
690	8.56	0.00025	0.176	5.06	99.14	8.27	134.2	±	1.2
720	9.32	0.00460	0.158	6.77	85.48	0.93	126.2	±	0.7
750	9.45	0.00591	0.381	10.53	81.77	1.75	122.6	±	0.1
775	10.33	0.00832	0.359	9.26	76.42	1.17	125.2	±	0.3
800	8.43	0.00168	0.221	15.54	94.23	3.57	125.9	±	0.1
820	11.35	0.01235	0.268	21.36	67.99	0.59	122.4	±	0.3
Fusion	9.60	0.00413	0.118	4.18	87.31	0.78	132.6	±	0.8
Total	10.75	0.00889	0.245	100.00	82.08	2.07	128.6	±	0.4
Total without 430-690°C, fusion				63.45			124.1	±	0.3

Sample 19: J = 0.009406 (phyllonite)

380	54.54	0.16797	0.053	0.96	8.99	0.01	81.3	±	0.4
420	9.12	0.01773	0.231	0.88	42.73	0.35	64.9	±	0.3
455	6.63	0.00587	0.073	3.41	73.85	0.34	81.2	±	0.2
490	8.31	0.00038	0.081	1.41	98.65	5.73	134.0	±	0.2
525	7.91	0.00018	0.058	4.27	99.31	8.71	128.5	±	0.1
560	6.66	0.00074	0.052	7.19	96.67	1.89	106.0	±	0.1
600	7.18	0.00032	0.069	5.34	98.69	5.90	116.3	±	0.1
640	7.14	0.00027	0.074	11.73	98.89	7.53	116.0	±	0.2
680	6.84	0.00035	0.068	21.47	98.50	5.35	110.8	±	0.2
700	6.85	0.00053	0.060	11.20	97.71	3.10	110.1	±	0.1
740	6.93	0.00167	0.047	9.55	92.85	0.77	106.0	±	0.1
775	7.86	0.00142	0.069	3.14	95.25	1.32	117.7	±	0.2
800	7.18	0.00017	0.065	7.22	99.28	10.20	116.9	±	0.1
850	7.11	0.00111	0.130	8.90	95.45	3.18	111.5	±	0.1
Fusion	7.37	0.00060	0.433	3.31	98.00	19.73	118.6	±	0.2
Total	7.56	0.00256	0.083	100.00	95.30	5.09	111.8	±	0.1

Table III-4 (continued).

TRIASSIC COVER - CODRU ASSEMBLAGE

Sample 34: J = 0.009672

450	8.43	0.01279	0.076	3.25	55.15	0.16	79.3	±	0.2
500	7.71	0.00490	0.082	1.77	81.16	0.07	105.9	±	0.1
600	6.98	0.00116	0.092	0.64	95.73	2.15	108.6	±	0.3
625	5.91	0.00114	0.106	0.95	94.21	0.15	94.7	±	0.1
640	6.87	0.00749	0.242	1.04	62.56	0.88	93.0	±	0.2
675	5.90	0.00009	0.038	1.39	99.51	11.59	99.6	±	0.2
700	6.05	0.00086	0.019	2.57	95.73	0.27	98.4	±	0.1
720	6.09	0.00021	0.016	2.23	98.88	2.02	102.2	±	0.2
750	6.94	0.00369	0.044	3.26	81.90	0.32	98.4	±	0.3
775	6.38	0.00217	0.053	3.43	89.87	0.16	97.3	±	0.4
810	9.74	0.01230	0.080	2.44	53.05	0.18	106.2	±	0.3
850	6.99	0.00010	0.014	12.40	99.49	3.71	117.5	±	0.2
875	7.07	0.00038	0.007	30.42	98.33	0.49	117.3	±	0.0
900	6.94	0.00008	0.016	17.41	99.58	5.12	116.7	±	0.1
Fusion	7.01	0.00017	0.046	16.81	99.27	7.54	117.5	±	0.1
Total	6.96	0.00129	0.025	100.00	94.75	3.03	111.1	±	0.1
Total without 450-810°C				77.03			117.2	±	0.1

---

[*] measured.

[c] corrected for post-irradiation decay of ^{37}Ar (35.1 day 1/2-life).

$[^{40}Ar_{tot} - (^{36}Ar_{atmos})(295.5)] / {}^{40}Ar_{tot}$.

[**] calculated using correction factors of Dalrymple et al. (1981); two sigma, intralaboratory errors.

APPENDIX IV

MICROPROBE DATA

SAMPLE 11110 – SLIDE 1

CALCITE

grain 1	wt%	norm wt%	Ox stoich	X–MgCO3
CaO	55.52	97.29	2.8975	
MgO	1.24	2.17	0.0899	0.030093
FeO	0.18	0.32	0.0075	
MnO	0.12	0.22	0.0051	
Total	57.07			
grain 2				
CaO	55.35	96.85	2.8779	
MgO	1.55	2.71	0.1118	0.037395
FeO	0.13	0.22	0.0051	
MnO	0.12	0.22	0.0051	
Total	57.15			
grain 3 – large vein				
CaO	56.02	98.4	2.9375	
MgO	0.78	1.38	0.0572	0.019100
FeO	0	0	0	
MnO	0.13	0.23	0.0053	
Total	56.93			
grain 4 – same vein				
CaO	57.14	98.25	2.9342	
MgO	0.79	1.36	0.0567	0.018957
FeO	0.09	0.15	0.0038	
MnO	0.14	0.23	0.0055	
Total	58.16			
grain 5 – same vein				
CaO	55.91	98.34	2.9392	
MgO	0.69	1.21	0.0503	0.016825
FeO	0.15	0.27	0.0062	
MnO	0.1	0.18	0.0044	
Total	56.85			
grain 6 – same vein				
CaO	55.48	97.99	2.9252	
MgO	0.86	1.52	0.0632	0.021148
FeO	0.07	0.12	0.0029	
MnO	0.21	0.37	0.0088	
Total	56.62			

DOLOMITE

grain 1	wt%	norm wt%	Ox stoich	X–MgCO3
CaO	33.35	60.28	1.5655	
MgO	21.93	39.64	1.4324	0.477801
FeO	0	0.01	0.0002	
MnO	0.05	0.09	0.0019	
Total	55.34			
grain 2				
CaO	32.61	59.35	1.5396	
MgO	22.09	40.2	1.4511	0.485171
FeO	0.12	0.22	0.0046	
MnO	0.12	0.22	0.0045	
Total	54.94			
grain 3				
CaO	33.29	60.06	1.5609	
MgO	21.96	39.62	1.4325	0.478552
FeO	0.16	0.28	0.0057	
MnO	0.02	0.04	0.0009	
Total	55.44			
grain 4				
CaO	32.8	59.32	1.5368	
MgO	22.39	40.5	1.4595	0.487100
FeO	0.02	0.03	0.0006	
MnO	0.08	0.015	0.003	
Total	55.28			
grain 5				
CaO	32.76	59.07	1.529	
MgO	22.59	40.73	1.4669	0.489635
FeO	0.11	0.2	0.004	
MnO	0	0	0	
Total	55.46			
grain 6				
CaO	32.58	59.07	1.531	
MgO	22.33	40.49	1.4599	0.488113
FeO	0.13	0.24	0.0048	
MnO	0.11	0.21	0.0042	
Total	55.16			

Calcite limb

T = A*x + B/x^2 + C*x^2 +D*x^0.5 + E

A	B	C	D	E	X–MgCO3	T,(K)		T,(C)
−2360	−0.01345	2620	2608	334	0.037395	744.1228	273	471.1228
−2360	−0.01345	2620	2608	334	0.030093	702.9194	273	429.9194
−2360	−0.01345	2620	2608	334	0.021148	634.4535	273	361.4535
−2360	−0.01345	2620	2608	334	0.019101	613.4551	273	340.4551
−2360	−0.01345	2620	2608	334	0.018957	611.8571	273	338.8571
−2360	−0.01345	2620	2608	334	0.016825	585.8085	273	312.8085

Dolomite limb

X–MgCO3	,(C) graph.
0.477801	
0.478552	
0.485171	
0.487101	
0.488113	
0.489635	

SAMPLE 11110 – SLIDE 2

CALCITE				
grain 1	wt%	norm wt%	Ox stoich	X–MgCO3
CaO	56.3	98.43	2.9426	
MgO	0.65	1.13	0.047	0.015721
FeO	0.11	0.19	0.0043	
MnO	0.15	0.26	0.0061	
Total	57.2			
grain 2				
CaO	56.59	98.56	2.9467	
MgO	0.62	1.07	0.0447	0.014942
FeO	0.08	0.013	0.0031	
MnO	0.13	0.23	0.0054	
Total	57.41			
grain 3				
CaO	57	98.46	2.942	
MgO	0.7	1.21	0.0504	0.016842
FeO	0	0	0	
MnO	0.19	0.32	0.0076	
Total	57.89			
grain 4				
CaO	55.84	97.89	2.9228	
MgO	0.87	1.53	0.0634	0.021230
FeO	0.12	0.21	0.005	
MnO	0.21	0.37	0.0088	
Total	57.04			
grain 5				
CaO	57.82	98.55	2.9479	
MgO	0.59	1	0.0417	0.013948
FeO	0.18	0.31	0.0073	
MnO	0.08	0.13	0.0031	
Total	58.67			

DOLOMITE				
grain 1	wt%	norm wt%	Ox stoich	X–MgCO3
CaO	33.65	60.83	1.5886	
MgO	21.26	38.43	1.3963	0.467787
FeO	0.28	0.51	0.0105	
MnO	0.13	0.23	0.0047	
Total	55.32			
grain 2				
CaO	32.5	59.33	1.5405	
MgO	21.95	40.07	1.4474	0.484420
FeO	0.21	0.38	0.0078	
MnO	0.12	0.21	0.0044	
Total	54.78			
grain 3				
CaO	31.97	59.05	1.5284	
MgO	22.07	40.76	1.4677	0.489870
FeO	0.07	0.13	0.0026	
MnO	0.04	0.07	0.0013	
Total	54.14			
grain 4				
CaO	32.67	59.56	1.5488	
MgO	21.77	39.69	1.436	0.481104
FeO	0.28	0.52	0.0105	
MnO	0.13	0.23	0.0047	
Total	54.85			
grain 5				
CaO	32.92	59.65	1.5519	
MgO	21.84	39.58	1.4325	0.479995
FeO	0.23	0.41	0.0083	
MnO	0.2	0.35	0.0073	
Total	55.18			

Calcite limb

T = A*x + B/x^2 + C*x^2 +D*x^0.5 + E

A	B	C	D	E	X–MgCO3	T,(K)		T,(C)
-2360	-0.01345	2620	2608	334	0.021231	635.2450	273	362.2450
-2360	-0.01345	2620	2608	334	0.016842	586.0366	273	313.0366
-2360	-0.01345	2620	2608	334	0.015721	570.1254	273	297.1254
-2360	-0.01345	2620	2608	334	0.014942	557.8744	273	284.8744
-2360	-0.01345	2620	2608	334	0.013948	540.4664	273	267.4664

Dolomite limb

X–MgCO3 ,(C) graph.

0.467787
0.479995
0.481104
0.484421
0.48987

SAMPLE 11020 SLIDE 1

CALCITE				
grain 1/1	wt%	norm wt%	Ox stoich	X-MgCO3
CaO	57.86	98.16	2.9266	
MgO	0.99	1.69	0.0699	0.023327
FeO	0.02	0.04	0.0008	
MnO	0.07	0.11	0.0027	
Total	58.95			
grain 1/2				
CaO	56.7	98.3	2.9293	
MgO	0.98	1.7	0.0707	0.023566
FeO	0	0	0	
MnO	0	0	0	
Total	57.68			
grain 2/1				
CaO	59.56	98.74	2.9485	
MgO	0.73	1.21	0.0503	0.016773
FeO	0	0	0	
MnO	0.03	0.05	0.0012	
Total	60.32			
grain 2/2				
CaO	57.74	98.68	2.9462	
MgO	0.74	1.26	0.0525	0.017507
FeO	0	0	0	
MnO	0.03	0.05	0.0013	
Total	58.51			
grain 3/1				
CaO	56.65	98.7	2.9464	
MgO	0.74	1.28	0.0533	0.017768
FeO	0	0	0	
MnO	0.01	0.01	0.0003	
Total	57.39			
grain 3/2				
CaO	57.28	98.73	2.9473	
MgO	0.74	1.27	0.0527	0.017566
FeO	0	0	0	
MnO	0	0	0	
Total	58.01			
grain 4/1				
CaO	56.88	98.22	2.9272	
MgO	0.99	1.72	0.0712	0.023745
FeO	0	0	0	
MnO	0.04	0.07	0.0016	
Total	57.91			
grain 4/2				
CaO	57.12	98.36	2.9341	
MgO	0.88	1.52	0.0631	0.021052
FeO	0.07	0.12	0.0028	
MnO	0	0	0	
Total	58.07			
grain 5				
CaO	56.46	98.56	2.9404	
MgO	0.82	1.43	0.0593	0.019768
FeO	0	0	0	
MnO	0.01	0.01	0.0003	
Total	57.28			

DOLOMITE				
grain 1/1	wt%	norm wt%	Ox stoich	X-MgCO3
CaO	33.71	59.78	1.5515	
MgO	22.55	39.98	1.4437	0.482004
FeO	0.13	0.24	0.0048	
MnO	0	0	0	
Total	56.39			
grain 1/2				
CaO	33.34	59.87	1.5526	
MgO	22.33	40.11	1.4469	0.482380
FeO	0.01	0.02	0.0005	
MnO	0	0	0	
Total	55.68			
grain 2				
CaO	33.41	60.13	1.5615	
MgO	22.09	39.76	1.4363	0.479118
FeO	0.04	0.07	0.0014	
MnO	0.02	0.04	0.0009	
Total	55.57			
grain 3/1				
CaO	32.88	57.77	1.55	
MgO	22.09	40.15	1.4483	0.483040
FeO	0.05	0.08	0.0017	
MnO	0	0	0	
Total	55.02			
grain 3/2				
CaO	33.16	59.88	1.5543	
MgO	22.12	39.94	1.442	0.481260
FeO	0.1	0.17	0.0035	
MnO	0	0.01	0.0001	
Total	55.38			
grain 3/3				
CaO	33.16	59.35	1.5374	
MgO	22.64	40.53	1.4602	0.487123
FeO	0.07	0.12	0.0024	
MnO	0	0	0	
Total	55.86			
grain 4				
CaO	32.87	59.36	1.5382	
MgO	22.39	40.42	1.4572	0.486479
FeO	0.12	0.22	0.0044	
MnO	0	0.01	0.0001	
Total	55.36			

Calcite limb

`T = A*x + B/x^2 + C*x^2 +D*x^0.5 + E`

A	B	C	D	E	X-MgCO3	T,(K)		T,(C)
-2360	-0.01345	2620	2608	334	0.023745	657.4615	273	384.4615
-2360	-0.01345	2620	2608	334	0.023566	655.9804	273	382.9804
-2360	-0.01345	2620	2608	334	0.023327	653.9809	273	380.9809
-2360	-0.01345	2620	2608	334	0.021052	633.5327	273	360.5327
-2360	-0.01345	2620	2608	334	0.019768	620.6339	273	347.6339
-2360	-0.01345	2620	2608	334	0.017768	597.9288	273	324.9288
-2360	-0.01345	2620	2608	334	0.017566	595.4196	273	322.4196
-2360	-0.01345	2620	2608	334	0.017507	594.6782	273	321.6782
-2360	-0.01345	2620	2608	334	0.016773	585.1084	273	312.1084

Dolomite limb

X-MgCO3
0.479118
0.481261
0.482004
0.482381
0.483041
0.486479
0.487123

SAMPLE 11020–SLIDE 2

CALCITE

grain 1/1	wt%	norm wt%	Ox stoich	X–MgCO3
CaO	56.38	97.62	2.9039	
MgO	1.3	2.25	0.0931	0.031064
FeO	0	0	0	
MnO	0.07	0.13	0.0031	
Total	57.75			
grain 1/2				
CaO	56.53	97.66	2.9069	
MgO	1.28	2.14	0.0884	0.029512
FeO	0.05	0.08	0.0019	
MnO	0.07	0.12	0.0028	
Total	59.93			
grain 2 – v veinlet				
CaO	56.42	98.89	2.9539	
MgO	0.63	1.11	0.0461	0.015366
FeO	0	0	0	
MnO	0	0	0	
Total	57.05			
grain 3 – veinlet				
CaO	56.22	98.5	2.9409	
MgO	0.76	1.33	0.0551	0.018391
FeO	0	0	0	
MnO	0.1	0.17	0.0041	
Total	57.08			
grain 4 – smaller vein				
CaO	56.8	98.62	2.9466	
MgO	0.67	1.16	0.048	0.016028
FeO	0.03	0.05	0.0012	
MnO	0.1	0.18	0.0042	
Total	57.6			
grain 5 – same vein				
CaO	56.02	98.86	2.9525	
MgO	0.65	1.14	0.0475	0.015833
FeO	0	0	0	
MnO	0	0	0	
Total	56.67			

DOLOMITE

grain 1	wt%	norm wt%	Ox stoich	X–MgCO3
CaO	32.69	59.62	1.5455	
MgO	22.08	40.27	1.4521	0.484420
FeO	0.06	0.11	0.0022	
MnO	0	0.01	0.0001	
Total	54.83			
grain 2				
CaO	33.02	59.69	1.5491	
MgO	22.15	40.04	1.4456	0.482719
FeO	0.13	0.24	0.0048	
MnO	0.02	0.03	0.0006	
Total	55.31			
grain 3				
CaO	32.6	59.32	1.5366	
MgO	22.27	40.53	1.4603	0.487270
FeO	0.08	0.15	0.0031	
MnO	0	0	0	
Total	54.96			
grain 4				
CaO	33.49	60.18	1.5646	
MgO	21.99	39.51	1.4291	0.477369
FeO	0.14	0.26	0.0052	
MnO	0.03	0.06	0.0012	
Total	55.65			
grain 5				
CaO	33.29	60.27	1.5666	
MgO	21.83	39.52	1.4291	0.477050
FeO	0.11	0.21	0.0042	
MnO	0	0.01	0.0001	
Total	55.23			
grain 6				
CaO	33.53	60.01	1.5585	
MgO	22.23	39.79	1.4376	0.479823
FeO	0.07	0.12	0.0024	
MnO	0.04	0.07	0.0015	
Total	55.86			

Calcite limb

T = A*x + B/x^2 + C*x^2 +D*x^0.5 + E

A	B	C	D	E	X–MgCO3	T,(K)		T,(C)
–2360	–0.01345	2620	2608	334	0.031064	708.9384	273	435.9384
–2360	–0.01345	2620	2608	334	0.029512	699.2206	273	426.2206
–2360	–0.01345	2620	2608	334	0.018391	605.3972	273	332.3972
–2360	–0.01345	2620	2608	334	0.016028	574.6686	273	301.6686
–2360	–0.01345	2620	2608	334	0.015833	571.8003	273	298.8003
–2360	–0.01345	2620	2608	334	0.015366	564.6776	273	291.6776

Dolomite limb

X–MgCO3	,(C) graph.
0.477051	
0.477369	
0.479823	
0.482719	
0.484421	
0.48727	

Sample 9947 v.lara

CALCITE

Grain I

point 1	core			
FeO	0.03	0.06	0.0013	
MnO	0.08	0.14	0.0032	
MgO	2.55	4.39	0.1801	0.060125
CaO	55.46	95.42	2.8153	
Total	58.12			
point 2				
FeO	0.03	0.05	0.0012	
MnO	0.03	0.06	0.0013	
MgO	2.16	3.76	0.1546	0.051576
CaO	55.15	96.13	2.8429	
Total	57.37			
point 3				
FeO	0.02	0.03	0.0007	
MnO	0.04	0.07	0.0017	
MgO	2.46	4.4	0.1807	0.060283
CaO	53.25	95.49	2.8166	
Total	55.76			

Grain III

point 1				
FeO	0	0	0	
MnO	0.04	0.08	0.0018	
MgO	0.6	1.06	0.0442	0.014741
CaO	56.18	98.86	2.9541	
Total	56.83			
point 2				
FeO	0	0	0	
MnO	0.02	0.04	0.001	
MgO	0.8	1.42	0.0589	0.019639
CaO	55.48	98.54	2.9401	
Total	56.3			
point 3				
FeO	0	0	0	
MnO	0.06	0.1	0.0024	
MgO	1.55	2.76	0.1141	0.038063
CaO	54.56	97.14	2.8835	
Total	56.17			

Grain II

point 1				
FeO	0	0	0.0001	
MnO	0	0	0	
MgO	2.62	4.59	0.1881	0.062702
CaO	54.45	95.41	2.8118	
Total	57.07			
point 2				
FeO	0.07	0.12	0.0027	
MnO	0.01	0.02	0.0006	
MgO	1.32	2.35	0.097	0.032368
CaO	54.97	97.51	2.8997	
Total	56.37			
point 3				
FeO	0	0	0	
MnO	0.01	0.02	0.0006	
MgO	2	3.6	0.1482	0.049408
CaO	53.5	96.38	2.8513	
Total	55.51			
point 4	at contact	with Dol		
FeO	0.12	0.21	0.0048	
MnO	0.1	0.17	0.004	
MgO	2.51	4.48	0.184	0.061515
CaO	53.21	95.13	2.8071	
Total	55.94			

X MgCO3:	T C (graf)	
0.062702	~580	573
0.061515	575	569
0.060283	570	565
0.060125	570	564
0.051576	545	533
0.049408	540	525
0.038063	485	474
0.032368	460	444
0.019639	350	346
0.014741	305	282

Coef.	Value
A	-2360
B	-0.01345
C	2620
D	2608
E	334

T K(calc)	273	T C(calc)
845.9556		572.9556
842.0264		569.0264
837.8839		564.8839
837.3477		564.3477
806.4797		533.4797
797.9871		524.9871
747.4976		474.4976
716.7267		443.7267
619.2730		346.2730
554.5275		281.5275

Sample 9947 v.lara

DOLOMITE

Grain I

point 1	wt%	norm wt%	Ox stoich	X MgCO3
FeO	0.16	0.3	0.006	
MnO	0.04	0.07	0.0014	
MgO	22.33	41.13	1.4796	0.494419
CaO	31.76	58.51	1.513	
Total	54.29			
point 2				
FeO	0.11	0.2	0.004	
MnO	0.05	0.09	0.0019	
MgO	22.39	41.09	1.4781	0.493687
CaO	31.95	58.62	1.5159	
Total	54.5			
point 3				
FeO	0.12	0.23	0.0047	
MnO	0.02	0.03	0.0006	
MgO	22.11	41.09	1.4781	0.493555
CaO	31.56	58.65	1.5167	
Total	53.82			
point 4				
FeO	0.15	0.28	0.0056	
MnO	0.06	0.1	0.0021	
MgO	22.52	41.63	1.4952	0.499682
CaO	31.36	57.99	1.4971	
Total	54.09			

Grain II

point 1				
FeO	0.09	0.16	0.0032	
MnO	0.01	0.03	0.0005	
MgO	22.38	41.69	1.4966	0.499482
CaO	31.19	58.12	1.4997	
Total	53.67			
point 2				
FeO	0.08	0.15	0.0031	
MnO	0	0.01	0.0001	
MgO	22.62	41.91	1.5031	0.501551
CaO	31.27	57.94	1.4938	
Total	53.97			
point 3				
FeO	0.08	0.15	0.0029	
MnO	0.11	0.21	0.0044	
MgO	22.09	41.58	1.4936	0.499081
CaO	30.84	58.06	1.4991	
Total	53.12			
point 4				
FeO	0.13	0.24	0.0047	
MnO	0.07	0.14	0.0028	
MgO	22.17	41.38	1.4868	0.496842
CaO	31.24	58.27	1.5057	
Total	53.61			

Grain III

point 1	near Cc	contact		
FeO	0.11	0.2	0.004	
MnO	0.05	0.09	0.0019	
MgO	22.3	41.28	1.4841	0.495691
CaO	31.57	58.43	1.5099	
Total	54.03			
point 2	away from	Cc contact		
FeO	0.15	0.28	0.0056	
MnO	0.06	0.12	0.0024	
MgO	22.44	41.42	1.4886	0.497543
CaO	31.53	58.18	1.5033	
Total	54.18			
point 3				
FeO	0.11	0.2	0.004	
MnO	0.05	0.1	0.0019	
MgO	22.64	41.82	1.5009	0.501302
CaO	31.33	57.88	1.4931	
Total	54.13			
point 4				
FeO	0.12	0.22	0.0045	
MnO	0.05	0.1	0.0021	
MgO	22.35	41.76	1.4989	0.500718
CaO	31	57.92	1.4946	
Total	53.52			
point 5	near opposite		edge	
FeO	0.14	0.25	0.0051	
MnO	0.04	0.08	0.0016	
MgO	22.1	41.23	1.4827	0.495356
CaO	31.32	58.43	1.5105	
Total	53.6			
point 6	at oppo .	edge		
FeO	0.13	0.024	0.0049	
MnO	0.06	0.1	0.0021	
MgO	22.53	41.62	1.4948	0.499432
CaO	31.42	58.03	1.4982	
Total	54.14			

		Grain IV	Dol incl.	in Cc
FeO	0.11	0.21	0.0042	
MnO	0.05	0.08	0.0017	
MgO	21.99	40.32	1.4544	0.485755
CaO	32.38	59.39	1.5397	
Total	54.53			

X MgCO3:	T C, graph.
0.485755	~550
0.493555	425
0.493687	420
0.494419	400
0.495356	380
0.495691	375
0.496842	355
0.497543	350
0,499081	~ 300
0.499432	< 300
0.499482	< 300
0.499682	< 300

Coef.	Value
A	−2360
B	−0.01345
C	2620
D	2608
E	334

SAMPLE 11091-SLIDE 2

CALCITE				
grain 1	wt%	norm wt%	Ox stoich	X-MgCO3
CaO	54.78	97.62	2.9026	
MgO	1.3	2.32	0.0961	0.032047
FeO	0	0	0	
MnO	0.03	0.06	0.0013	
Total	56.11			
grain 2				
CaO	55.17	97.42	2.8959	
MgO	1.38	2.44	0.1009	0.033669
FeO	0	0	0	
MnO	0.08	0.014	0.0032	
Total	56.63			
grain 3				
CaO	54.85	97.24	2.8877	
MgO	1.5	2.66	0.11	0.036694
FeO	0.06	0.1	0.0023	
MnO	0	0	0	
Total	56.4			
grain 4				
CaO	56.48	97.65	2.9049	
MgO	1.29	2.23	0.0921	0.030730
FeO	0.02	0.04	0.001	
MnO	0.05	0.09	0.002	
Total	57.84			
grain 5				
CaO	55.9	97.34	2.8948	
MgO	1.38	2.4	0.0994	0.033197
FeO	0.13	0.23	0.0053	
MnO	0.02	0.03	0.0006	
Total	57.43			

DOLOMITE				
grain 1	wt%	norm wt%	Ox stoich	X-MgCO3
CaO	32.18	58.88	1.5282	
MgO	22.02	40.3	1.455	0.487731
FeO	0.42	0.76	0.0157	
MnO	0.03	0.05	0.001	
Total	54.65			
grain2				
CaO	32.13	58.6	1.5221	
MgO	22.07	40.25	1.4546	0.488661
FeO	0.62	1.13	0.0229	
MnO	0.01	0.02	0.0004	
Total	54.84			
grain 3				
CaO	32.49	59.24	1.5406	
MgO	21.82	39.79	1.4396	0.483054
FeO	0.5	0.91	0.0186	
MnO	0.03	0.06	0.0012	
Total	54.85			
grain 4				
CaO	32.76	58.8	1.531	
MgO	22.14	39.73	1.4391	0.484529
FeO	0.8	1.44	0.0293	
MnO	0.02	0.03	0.0006	
Total	55.72			
grain 5				
CaO	32.27	58.78	1.5269	
MgO	22.07	40.2	1.4526	0.487531
FeO	0.54	0.99	0.02	
MnO	0.02	0.03	0.0006	
Total	54.89			

Calcite limb

T = A*x + B/x^2 + C*x^2 + D*x^.5 + E

A	B	C	D	E	X-MgCO3	T,(K)		T, (C)
-2360	-0.01345	2620	2608	334	0.036694	740.5207	273	467.5207
-2360	-0.01345	2620	2608	334	0.033669	724.1912	273	451.1912
-2360	-0.01345	2620	2608	334	0.033197	721.5165	273	448.5165
-2360	-0.01345	2620	2608	334	0.032047	714.8392	273	441.8392
-2360	-0.01345	2620	2608	334	0.030731	706.8963	273	433.8963

Dolomite limb

X-MgCO3	T, (C) graph
0.483054	
0.484529	
0.487531	
0.487731	
0.488661	

SAMPLE 11091–SLIDE 1

CALCITE

grain 1	wt%	norm wt%	Ox stoich	X–MgCO3
CaO	55.57	97.37	2.8925	
MgO	1.46	2.56	0.1058	0.035286
FeO	0.03	0.05	0.0014	
MnO	0.01	0.01	0.0003	
Total	57.6			
grain 2				
CaO	55.69	97.43	2.8961	
MgO	1.39	2.44	0.1009	0.033667
FeO	0.07	0.12	0.0027	
MnO	0.01	0.01	0.0003	
Total	57.16			
grain 3				
CaO	55.89	97.23	2.8893	
MgO	1.47	2.56	0.106	0.035388
FeO	0.12	0.2	0.0047	
MnO	0	0	0	
Total	57.48			
grain 4	darker phase			
CaO	56	97.62	2.9052	
MgO	1.25	2.18	0.0901	0.030080
FeO	0.06	0.11	0.0025	
MnO	0.05	0.09	0.0021	
Total	57.36			
grain 5:	calcite at contact with dolomite			
CaO	55.04	97.98	2.9179	
MgO	1.09	1.93	0.0801	0.026717
FeO	0	0	0	
MnO	0.05	0.08	0.002	
Total	56.17			
grain 6				
CaO	60.93	98.18	2.9265	
MgO	1.06	1.71	0.0708	0.023621
FeO	0.07	0.12	0.0027	
MnO	0	0	0	
Total	62.07			
grain 7				
CaO	55.53	97.78	2.911	
MgO	1.17	2.06	0.0853	0.028468
FeO	0.09	0.16	0.0037	
MnO	0	0	0	
Total	56.79			

DOLOMITE

grain 1	wt%	norm wt%	Ox stoich	X–MgCO3
CaO	33.55	58.5	1.5168	
MgO	23.3	40.63	1.4655	0.491399
FeO	0.46	0.8	0.0161	
MnO	0.04	0.08	0.0016	
Total	57.36			
grain 2				
CaO	32.86	59.68	1.5517	
MgO	21.84	39.67	1.435	0.480463
FeO	0.36	0.66	0.0133	
MnO	0	0	0	
Total	55.06			
grain 3/1				
CaO	31.96	58.45	1.5157	
MgO	22.22	40.64	1.4659	0.491646
FeO	0.44	0.81	0.0164	
MnO	0.05	0.1	0.002	
Total	54.68			
grain 3/2				
CaO	32.38	59.04	1.5367	
MgO	21.77	39.7	1.4376	0.483340
FeO	0.62	1.14	0.0231	
MnO	0.07	0.013	0.0026	
Total	54.84			
grain 4				
CaO	32.37	58.61	1.521	
MgO	22.32	40.41	1.4591	0.489614
FeO	0.5	0.91	0.0184	
MnO	0.04	0.07	0.0015	
Total	55.23			
grain 5				
CaO	32.91	58.94	1.5306	
MgO	22.43	40.17	1.4511	0.486668
FeO	0.44	0.79	0.016	
MnO	0.06	0.11	0.0023	
Total	55.85			

Calcite limb of solvus

T = A*x + B/x^2 + C*x^2 + D*x^.5 + E

A	B	C	D	E	X–MgCO3	T,K		T,C
-2360	-0.01345	2620	2608	334	0.035388	733.6343	273	460.6343
-2360	-0.01345	2620	2608	334	0.035286	733.0864	273	460.0864
-2360	-0.01345	2620	2608	334	0.033667	724.1800	273	451.1800
-2360	-0.01345	2620	2608	334	0.030081	702.8437	273	429.8437
-2360	-0.01345	2620	2608	334	0.028468	692.3764	273	419.3764
-2360	-0.01345	2620	2608	334	0.026717	680.2615	273	407.2615
-2360	-0.01345	2620	2608	334	0.023621	656.4370	273	383.4370

Dolomite limb of solvus

X–MgCO3	T,C (graph)
0.480463	
0.483341	
0.486668	
0.489614	
0.491648	
0.491399	